MSC SIGNALING IN REGENERATIVE MEDICINE

EDITED BY: Wolfgang Holnthoner, Sandra Hofmann and Martin James Stoddart
PUBLISHED IN: Frontiers in Bioengineering and Biotechnology

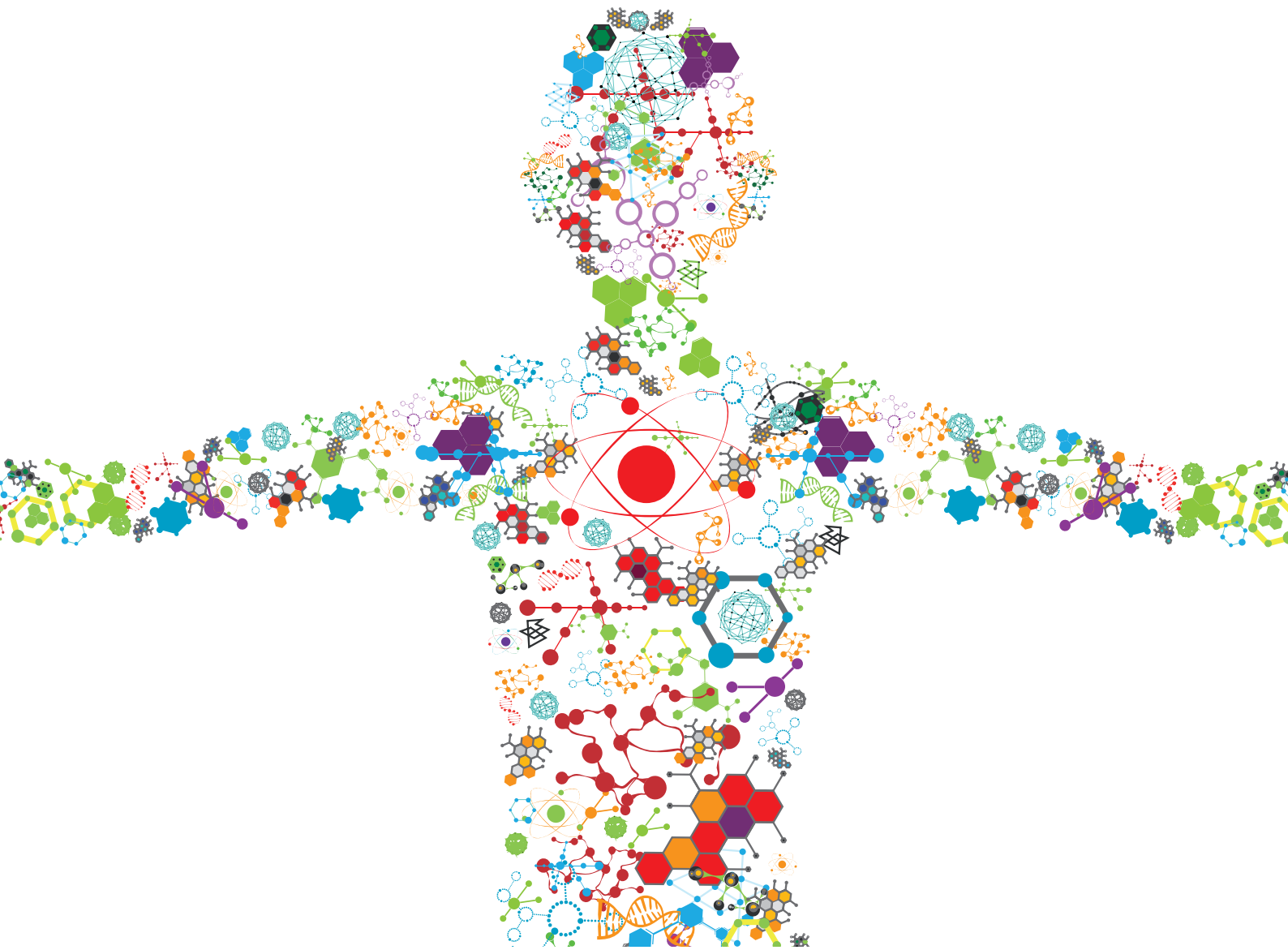

frontiers Research Topics

frontiers

ISSN 1664-8714
ISBN 978-2-88966-320-0
DOI 10.3389/978-2-88966-320-0

About Frontiers

Frontiers is more than just an open-access publisher of scholarly articles: it is a pioneering approach to the world of academia, radically improving the way scholarly research is managed. The grand vision of Frontiers is a world where all people have an equal opportunity to seek, share and generate knowledge. Frontiers provides immediate and permanent online open access to all its publications, but this alone is not enough to realize our grand goals.

Frontiers Journal Series

The Frontiers Journal Series is a multi-tier and interdisciplinary set of open-access, online journals, promising a paradigm shift from the current review, selection and dissemination processes in academic publishing. All Frontiers journals are driven by researchers for researchers; therefore, they constitute a service to the scholarly community. At the same time, the Frontiers Journal Series operates on a revolutionary invention, the tiered publishing system, initially addressing specific communities of scholars, and gradually climbing up to broader public understanding, thus serving the interests of the lay society, too.

Dedication to Quality

Each Frontiers article is a landmark of the highest quality, thanks to genuinely collaborative interactions between authors and review editors, who include some of the world's best academicians. Research must be certified by peers before entering a stream of knowledge that may eventually reach the public - and shape society; therefore, Frontiers only applies the most rigorous and unbiased reviews.
Frontiers revolutionizes research publishing by freely delivering the most outstanding research, evaluated with no bias from both the academic and social point of view. By applying the most advanced information technologies, Frontiers is catapulting scholarly publishing into a new generation.

What are Frontiers Research Topics?

Frontiers Research Topics are very popular trademarks of the Frontiers Journals Series: they are collections of at least ten articles, all centered on a particular subject. With their unique mix of varied contributions from Original Research to Review Articles, Frontiers Research Topics unify the most influential researchers, the latest key findings and historical advances in a hot research area! Find out more on how to host your own Frontiers Research Topic or contribute to one as an author by contacting the Frontiers Editorial Office: researchtopics@frontiersin.org

MSC SIGNALING IN REGENERATIVE MEDICINE

Topic Editors:
Wolfgang Holnthoner, Ludwig Boltzmann Institute for Experimental and Clinical Traumatology, Austria
Sandra Hofmann, Eindhoven University of Technology, Netherlands
Martin James Stoddart, AO Research Institute, Switzerland

Citation: Holnthoner, W., Hofmann, S., Stoddart, M. J., eds. (2021). MSC Signaling in Regenerative Medicine. Lausanne: Frontiers Media SA.
doi: 10.3389/978-2-88966-320-0

Table of Contents

05 ***Editorial: MSC Signaling in Regenerative Medicine***
Martin J. Stoddart, Sandra Hofmann and Wolfgang Holnthoner

07 ***Pediatric Mesenchymal Stem Cells Exhibit Immunomodulatory Properties Toward Allogeneic T and B Cells Under Inflammatory Conditions***
Virginia Palomares Cabeza, Martin Johannes Hoogduijn, Rens Kraaijeveld, Marcella Franquesa, Janneke Witte-Bouma, Eppo B. Wolvius, Eric Farrell and Pieter A. J. Brama

17 ***Hypoxia Conditioned Mesenchymal Stem Cell-Derived Extracellular Vesicles Induce Increased Vascular Tube Formation*** **in vitro**
Ciarra Almeria, René Weiss, Michelle Roy, Carla Tripisciano, Cornelia Kasper, Viktoria Weber and Dominik Egger

29 ***Bone Marrow Mesenchymal Stem Cells' Secretome Exerts Neuroprotective Effects in a Parkinson's Disease Rat Model***
Bárbara Mendes-Pinheiro, Sandra I. Anjo, Bruno Manadas, Jorge D. Da Silva, Ana Marote, Leo A. Behie, Fábio G. Teixeira and António J. Salgado

42 ***Targeting the Immune System With Mesenchymal Stromal Cell-Derived Extracellular Vesicles: What is the Cargo's Mechanism of Action?***
Jorge Diego Martin-Rufino, Natalia Espinosa-Lara, Lika Osugui and Fermin Sanchez-Guijo

51 ***Influence of Platelet Lysate on 2D and 3D Amniotic Mesenchymal Stem Cell Cultures***
Markus Pasztorek, Eva Rossmanith, Christoph Mayr, Fabian Hauser, Jaroslaw Jacak, Andreas Ebner, Viktoria Weber and Michael B. Fischer

68 ***Impact of Fibronectin Knockout on Proliferation and Differentiation of Human Infrapatellar Fat Pad-Derived Stem Cells***
Yiming Wang, Yawen Fu, Zuoqin Yan, Xiao-Bing Zhang and Ming Pei

81 ***Mesenchymal Stromal Cell-Based Bone Regeneration Therapies: From Cell Transplantation and Tissue Engineering to Therapeutic Secretomes and Extracellular Vesicles***
Darja Marolt Presen, Andreas Traweger, Mario Gimona and Heinz Redl

101 ***Unraveling the Molecular Signature of Extracellular Vesicles From Endometrial-Derived Mesenchymal Stem Cells: Potential Modulatory Effects and Therapeutic Applications***
Federica Marinaro, María Gómez-Serrano, Inmaculada Jorge, Juan Carlos Silla-Castro, Jesús Vázquez, Francisco Miguel Sánchez-Margallo, Rebeca Blázquez, Esther López, Verónica Álvarez and Javier G. Casado

120 ***Extracellular Vesicles Derived From Mesenchymal Stem Cells (MSC) in Regenerative Medicine: Applications in Skin Wound Healing***
Antonio Casado-Díaz, José Manuel Quesada-Gómez and Gabriel Dorado

139 ***Current Status and Future Prospects of Genome-Scale Metabolic Modeling to Optimize the Use of Mesenchymal Stem Cells in Regenerative Medicine***
Þóra Sigmarsdóttir, Sarah McGarrity, Óttar Rolfsson, James T. Yurkovich and Ólafur E. Sigurjónsson

161 ***Angiogenic Potential of Tissue Engineered Cartilage From Human Mesenchymal Stem Cells is Modulated by Indian Hedgehog and Serpin E1***
Yannick Nossin, Eric Farrell, Wendy J. L. M. Koevoet, Rodrigo A. Somoza, Arnold I. Caplan, Bent Brachvogel and Gerjo J. V. M. van Osch

174 ***Enhanced Chondrogenic Capacity of Mesenchymal Stem Cells After TNFα Pre-treatment***
Chantal Voskamp, Wendy J. L. M. Koevoet, Rodrigo A. Somoza, Arnold I. Caplan, Véronique Lefebvre, Gerjo J. V. M. van Osch and Roberto Narcisi

186 ***Comparative Effect of MSC Secretome to MSC Co-culture on Cardiomyocyte Gene Expression Under Hypoxic Conditions* in vitro**
Nina Kastner, Julia Mester-Tonczar, Johannes Winkler, Denise Traxler, Andreas Spannbauer, Beate M. Rüger, Georg Goliasch, Noemi Pavo, Mariann Gyöngyösi and Katrin Zlabinger

frontiers in Bioengineering and Biotechnology

EDITORIAL
published: 06 November 2020
doi: 10.3389/fbioe.2020.614561

Editorial: MSC Signaling in Regenerative Medicine

Martin J. Stoddart[1]*, *Sandra Hofmann*[2] and *Wolfgang Holnthoner*[3]

[1] Regenerative Orthopaedics Program, AO Research Institute Davos, Davos, Switzerland, [2] Department of Biomedical Engineering, Institute for Complex Molecular Systems, Eindhoven University of Technology, Eindhoven, Netherlands, [3] Allgemeine Unfallversicherungsanstalt Research Centre, Ludwig Boltzmann Institute for Experimental and Clinical Traumatology, Vienna, Austria

Keywords: exosomes, microvesicles, secretome, mesenchymal stem cells, signaling

Editorial on the Research Topic

MSC Signaling in Regenerative Medicine

Originally designated mesenchymal stem cells (MSCs), decades of research have expanded the number of functions MSCs possess, in turn leading to various proposals as to what "MSC" should signify. While the earlier research focused on MSC ability to differentiate into various cell types, more recently their ability to control other cells by way of secreted molecules has been the subject of intense focus. This special issue brought together a collection of articles exploring the signaling aspects of MSCs. The review article from Marolt Presen et al. highlighted the wide functional range of MSCs, from cell transplantation to secretome, and their potential therapeutic use for bone regeneration. To enable clinical use, the ability to characterize the cells effectively will be crucial. Understanding the metabolic changes that underlie the MSC phenotype offers an opportunity to better monitor expansion and differentiation, as discussed in the review article from Sigmarsdóttir et al.. Pasztorek et al. investigated MSC phenotype after stimulating amniotic derived cells with platelet lysate instead of FBS. A detailed analysis of stress fiber formation and mitochondrial distribution demonstrated differences between the human platelet lysate and FBS. Similarly, changes in human infrapatellar fat pad-derived stem cell (IPFSC) phenotype were observed when the cells were cultured in the absence of fibronectin. CRISPR/Cas9 knockout cells, or IPFSCs grown on ECM deposited by knockout cells, displayed increased cell growth, but decreased differentiation.

The recent advent of extracellular vesicles (EV) led to a rise in publications focusing on the biology, characterization, isolation, and therapeutic possibilities. In the review article from Martin-Rufino et al., the ability of MSC-derived EV's to regulate the immune system was highlighted and potential mechanisms were discussed. Casado-Díaz et al. report in their review article on EVs derived from MSCs and their therapeutic potential for skin regeneration. They point out the feasibility of MSC-EVs, especially as a cell-free alternative aiming at skin wound healing. In the study of Mendes-Pinheiro et al., the secretome of bone marrow MSCs have been found to have neuroprotective effects in a rat model of Parkinson's disease and the authors suggest this is a feasible alternative to stem cell transplantation therapies. The study of Kastner et al. provided *in vitro* evidence that the MSC-derived secretome has the potential to aid the survival and regeneration of human cardiomyocytes that have been stressed under hypoxic conditions. Marinaro et al. report on the biological properties of EVs derived from endometrial MSCs, which are involved in regeneration and repair of the endometrium. They characterized the proteome and the microRNAome and found candidates involved in the immune regulation, apoptosis, and different signaling pathways, among others. With regards to angiogenesis, the study by Almeria et al. points out that EVs derived from MSCs cultured under hypoxic conditions appear to be functionally more potent to induce vascular tube formation than EVs derived from MSCs under normoxic conditions or the soluble factors in the media.

Edited and reviewed by:
Ranieri Cancedda, Independent Researcher, Genova, Italy

***Correspondence:**
Martin J. Stoddart
martin.stoddart@aofoundation.org

Specialty section:
This article was submitted to Tissue Engineering and Regenerative Medicine, a section of the journal Frontiers in Bioengineering and Biotechnology

Received: *06 October 2020*
Accepted: *12 October 2020*
Published: *06 November 2020*

Citation:
Stoddart MJ, Hofmann S and Holnthoner W (2020) Editorial: MSC Signaling in Regenerative Medicine. Front. Bioeng. Biotechnol. 8:614561. doi: 10.3389/fbioe.2020.614561

In another study by Nossin et al., the aim was to do the opposite, namely to inhibit blood vessel invasion in regenerating cartilage in an attempt to stabilize tissue engineered cartilage constructs for tissue repair and replacement. They investigated how chondrogenically differentiated BMSCs could be prevented from maturing into bone through the endochondral pathway by investigating the pro-angiogenic potential of the secretome. Their results suggest that the endochondral ossification process could be prevented by inhibiting specific pro-angiogenic factors such as Indian Hedgehog and Serpin E1. The effect of soluble mediators can also be seen during the MSC expansion phase. Voskamp et al. demonstrated an increased chondrogenic potential of MSCs that were exposed to TNFα during cell expansion, even when the TNFα was still present during the differentiation phase. This offers a potential mechanism to improve chondrogenesis in inflamed sites.

Palomares Cabeza et al. studied the potential of MSCs derived from pediatric patients over MSCs from adults to modulate the immune response. They successfully showed that pediatric MSCs show immunomodulatory effects on allogeneic T- and B-cells and that those properties can be potentiated by inflammatory stimuli. All in all, this could have important implications in implant engraftment and the avoidance of a strong immune reaction.

AUTHOR CONTRIBUTIONS

All authors listed have made a substantial, direct and intellectual contribution to the work, and approved it for publication.

ACKNOWLEDGMENTS

The editors would like to thank all the authors that contributed to the Research Topic.

Conflict of Interest: The authors declare that the research was conducted in the absence of any commercial or financial relationships that could be construed as a potential conflict of interest.

frontiers in Bioengineering and Biotechnology

ORIGINAL RESEARCH
published: 12 June 2019
doi: 10.3389/fbioe.2019.00142

Pediatric Mesenchymal Stem Cells Exhibit Immunomodulatory Properties Toward Allogeneic T and B Cells Under Inflammatory Conditions

Virginia Palomares Cabeza[1,2,3], *Martin Johannes Hoogduijn*[2], *Rens Kraaijeveld*[2], *Marcella Franquesa*[4], *Janneke Witte-Bouma*[1], *Eppo B. Wolvius*[1], *Eric Farrell*[1]* *and Pieter A. J. Brama*[3]

[1] *Department of Oral and Maxillofacial Surgery, Erasmus University Medical Center, Rotterdam, Netherlands,* [2] *Nephrology and Transplantation, Department of Internal Medicine, Erasmus University Medical Center, Rotterdam, Netherlands,* [3] *School of Veterinary Medicine, University College Dublin, Dublin, Ireland,* [4] *REMAR Group and Nephrology Service, Germans Trias i Pujol Health Science Institute and University Hospital, Badalona, Spain*

OPEN ACCESS

Edited by:
Sandra Hofmann, Eindhoven University of Technology, Netherlands

Reviewed by:
Cecilia Götherström, Karolinska Institute (KI), Sweden
Guenther Eissner, University College Dublin, Ireland

***Correspondence:**
Eric Farrell
e.farrell@erasmusmc.nl

Specialty section:
This article was submitted to Tissue Engineering and Regenerative Medicine, a section of the journal Frontiers in Bioengineering and Biotechnology

Received: *19 March 2019*
Accepted: *28 May 2019*
Published: *12 June 2019*

Citation:
Palomares Cabeza V, Hoogduijn MJ, Kraaijeveld R, Franquesa M, Witte-Bouma J, Wolvius EB, Farrell E and Brama PAJ (2019) Pediatric Mesenchymal Stem Cells Exhibit Immunomodulatory Properties Toward Allogeneic T and B Cells Under Inflammatory Conditions. Front. Bioeng. Biotechnol. 7:142. doi: 10.3389/fbioe.2019.00142

Mesenchymal stem cells from pediatric patients (pMSCs) are an attractive cell source in regenerative medicine, due to their higher proliferation rates and better differentiation abilities compared to adult MSCs (aMSCs). We have previously characterized the immunomodulatory abilities of pMSCs on T cells under co-culture. It has also been reported that aMSCs can inhibit B cell proliferation and maturation under inflammatory conditions. In this study, we therefore aimed to clarify the immunomodulatory effect of pMSCs toward T and B cells in an inflammatory microenvironment. Bone marrow derived pMSCs were primed to simulate inflammatory conditions by exposure with 50 ng/mL of IFN-γ for 3 days. To analyze the interaction between pMSCs and T cells, CD3/CD28 stimulated peripheral blood mononuclear cells (PBMCs) were co-cultured with primed or unprimed pMSCs. To investigate B cell responses, quiescent B cells obtained from spleens by CD43 negative selection were stimulated with anti-IgM, anti-CD40, IL-2, and co-cultured with either IFN-γ primed or unprimed pMSC. pMSC phenotype, B and T cell proliferation, and B cell functionality were analyzed. Gene expression of indoleamine 2,3-dioxygenease (IDO), as well as the expression of HLA-ABC, HLA-DR and the co-stimulatory molecules CD80 and CD86 was upregulated on pMSCs upon IFN-γ priming. IFN-γ did not alter the immunomodulatory abilities of pMSCs upon $CD4^+$ nor $CD8^+$ stimulated T cells compared to unprimed pMSCs. IFN-γ primed pMSCs but not unprimed pMSCs strongly inhibited naïve ($CD19^+CD27^-$), memory ($CD19^+CD27^+$), and total B cell proliferation. Antibody-producing plasmablast ($CD19^+CD27^{high}CD38^{high}$) formation and IgG production were also significantly inhibited by IFN-γ primed pMSCs compared to unprimed pMSCs. Collectively, these results show that pMSCs have immunomodulatory effects upon the adaptive immune response which can be potentiated by inflammatory stimuli. This knowledge is useful in regenerative medicine and allogeneic transplantation applications toward tailoring pMSCs function to best modulate the immune response for a successful implant engraftment and avoidance of a strong immune reaction.

Keywords: mesenchymal stem cell, immunomodulation, allogeneic, T cell, B cell, inflammatory microenvironment

INTRODUCTION

Mesenchymal stem cells (MSCs) are a source of self-renewing multipotent stem cells that are capable of differentiating along adipogenic, osteogenic, and chondrogenic lineages (Chamberlain et al., 2007; Bianco et al., 2008). MSCs are also known to exert potent immunomodulatory effects upon a wide range of immune cells, both of the innate and the adaptive immune system (Gao et al., 2016). This effect seems to be dependent upon the inflammatory conditions of the micro-environment in which these MSCs are found (Krampera et al., 2006; Cuerquis et al., 2014). Particularly for the adaptive immune response, pro-inflammatory cytokines, such as IFN-γ, seem to potentiate the anti-proliferative effect of MSC on T cells by inducing an increase in the activity of the enzyme indoleamine 2,3-dioxygenease (IDO) (Meisel et al., 2004). Regarding their interaction with B cells, MSCs have been described to suppress B cell proliferation through soluble factors (Corcione et al., 2006) and abrogate plasmablast formation independently of T cells (Franquesa et al., 2015). It has also been shown that upon IFN-γ stimulation, MSCs significantly inhibit B cell proliferation and maturation by upregulating IDO expression (Luk et al., 2017).

Due to their multipotent differentiation and immune modulation properties, MSCs have been successfully investigated for their use in several diseases such as ischemia (Cortez-Toledo et al., 2018), autoimmune diseases (Gerdoni et al., 2007; González et al., 2009), as well as in solid organ transplantation (Benseler et al., 2014). Other applications of MSCs include their potential use in tissue engineering and regenerative medicine (Barry and Murphy, 2013; Shao et al., 2015). In particular in this field, bone marrow derived MSCs (BM-MSCs) have been successfully differentiated toward a chondrogenic phenotype and used for *in vivo* bone formation following the process of endochondral ossification (Farrell et al., 2011; van der Stok et al., 2014). Nevertheless, the high variability between BM-MSC donors as a result of age and disease status has been shown to have an increasing importance by negatively influencing their bone formation potential in the case of elderly donors (Stolzing, 2006; Ganguly et al., 2017). Hence, a source of BM-MSCs with less age related variations are potentially more promising candidates for these applications (Stolzing, 2006). Pediatric BM-MSCs (pMSCs) obtained from iliac crest bone chips from individuals between 7 and 13 years old have increased differentiation and proliferation capacities compared to adult BM-MSCs (aMSCs) (Knuth et al., 2018). pMSCs have been described to maintain an immunophenotype identical to aMSCs and are significantly less senescent (Knuth et al., 2018).

In the context of an allogeneic transplantation, the adaptive immune response plays an important role in determining the outcome of the engraftment of the allograft (Cozzi et al., 2017). Naïve and memory $CD4^+$ and $CD8^+$ alloreactive T cells mediate rejection and graft-vs.-host disease processes (Cozzi et al., 2017; DeWolf and Sykes, 2017). The cross-talk between B and T cells is critical in these immune responses, since B cells are known to be the mediators of humoral rejection by producing donor-specific human leukocyte antigen (HLA) antibodies upon activation by T cells (Larsen et al., 2006).

We have previously shown that pMSCs can exert an immunomodulatory effect on T cells by reducing their proliferation rates in an *in vitro* co-culture model (Knuth et al., 2018). Since in an allogeneic transplantation setting pMSCs might be subjected to an inflammatory microenvironment their immune properties might also be altered, affecting their success for clinical uses. Hence, to characterize how the inflammatory microenvironment can affect their immune status, in this study we investigated the effect of IFN-γ priming of a novel source of pMSCs on their immunomodulatory functionality toward B and T cells.

METHODS

Isolation and Culture of Human Pediatric Bone Marrow Derived MSCs (pMSCs)

pMSCs were isolated from leftover iliac crest bone chips of pediatric patients undergoing alveolar bone graft surgery. Written consent was not required according to institutional guidelines for the use of waste surgical material but an opt out was available. This was approved by the Erasmus Medical Ethical Committee (MEC-2014-16). The age of the patients ranged between 9 and 13 years old Detailed information about age and sex of the donors can be found in **Table 1**.

Briefly, pMSCs were obtained by washing the iliac crest chips twice with 10 mL of αMEM expansion medium supplemented with 10% heat inactivated fetal bovine serum, 1.5 μg/mL Amphotericin B, 25 μg/mL L-ascorbic acid 2-phosphate, 50 μg/mL gentamycin (all from Invitrogen) and 1 ng/mL fibroblast growth factor-2 (BioRad). The medium from the two washes containing the pMSCs was then plated in T75 flasks which were washed twice 24 h after with phosphate-buffered saline (PBS) supplemented with 2% v/v heat inactivated fetal bovine serum to remove non-adherent dead cells. Viable pMSCs were at all times cultured at 37°C and 5% carbon dioxide (CO_2) in a humidified atmosphere. Expansion medium was replaced at least twice a week and the cells were firstly passaged when several visible colonies were detected using 0.05% trypsin-EDTA (Invitrogen). Upon the second passage, cells were always trypsinized at 70–80% of confluency. The cells showed an MSC characteristic morphology and were used between passages three and five for all experiments. Their phenotypic characteristics were previously extensively described by our group (Knuth et al., 2018).

TABLE 1 | Details of age and sex of the pMSC donors used in the study.

Donor	Age (years)	Sex
Donor 1	12	Male
Donor 2	12	Female
Donor 3	10	Female
Donor 4	10	Male
Donor 5	Between 9 and 13	Male
Donor 6	9	Male

Isolation of PBMCs From Peripheral Blood

Peripheral blood from healthy male donors was obtained from Sanquin Bloedvoorziening (Rotterdam, the Netherlands). Samples were centrifuged at 388 g for 7 min to remove the top layer of plasma and washed at a 1:2 dilution in wash medium (RPMI-1640 supplemented with 1.5 μg/mL Amphotericin B and 50 μg/mL gentamycin). The remaining cell suspension was then transferred to Ficoll-Paque PLUS (density 1.077 g/mL; GE Healthcare) containing tubes and centrifuged at 690 g for 20 min with the brake turned off. The plasma was removed and the layers above the filter were then washed with wash medium up to a total volume of 50 mL. Samples were then washed three times in wash medium as in the previous step, and then finally cells were counted and resuspended in human serum conditioned medium (PBMC medium) composed of RPMI-1640 medium with 1% v/v GlutaMAX, 1.5 μg/mL Amphotericin B, 50 μg/mL gentamycin and 10% v/v heat inactivated human serum (Sigma-Aldrich). Cells were then resuspended in PBMC medium supplemented with a 10% of dimethylsulphoxide in appropriate numbers for optimal conservation and stored in liquid nitrogen until used for the experiments.

IFN-γ Pre-stimulation of pMSCs

Based on previous optimization experiments, pMSCs were pre-treated for 3 days using IFN-γ (50 ng/mL, Peprotech) prior to co-cultures (Luk et al., 2017). Twenty four hours before the co-culture day, cells were detached with 0.05% w/v trypsin-EDTA, washed with PBS and seeded in a 96 well plate at a density of 0.2×10^6 cells per well in either 100 μL of Iscove's Modified Dulbecco's Medium (IMDM, Lonza) supplemented with a 10% v/v heat inactivated FBS (for B cell co-cultures), or in 100 μL of PBMC medium (for PBMC co-cultures).

Quantitative Real-Time Reverse Transcription Polymerase Chain Reaction (qRT-PCR)

After 3 days of IFN-γ stimulation, 0.3×10^6 pMSCs were placed in 300 μL of RLT buffer and snap frozen. RNA was isolated using a RNeasy micro kit (QIAGEN), and complementary cDNA was synthetized using a first strand cDNA kit (RevertAid cDNA kit, Thermo Scientific). qRT-PCR was performed using a 2x TaqMan Universal PCR master mix (Applied Biosystems), according to manufacturer's instructions and assay on demand primers (Thermoscientific) for IDO (Hs 00158027.m1) and for GAPDH (forward: 5′-ATGGGGAAGGTGAAGGTCG-3′, reverse: 5′-TAAAAGCAGCCCTGGTGACC-3′, probe (FAM-TAMRA): 5′ CGCCCAATACGACCAAATCCGTTGAC-3′). TAQ DNA polymerase (Hot Start) was activated for 10 min at 95°C, then DNA was amplified following 40 cycles of 15 s at 95°C, and 1 min at 60°C. TAQman was analyzed on a CFX-96 thermal cycler (BioRad). Results are expressed as relative copy number of PCR products in respect to the housekeeper GAPDH.

pMSC Phenotyping by Flow Cytometry

pMSCs were immunophenotypically analyzed with and without IFN-γ pre-stimulation by assessing the expression of surface markers: HLA-ABC FITC, HLA-DR PerCP (clone G46.6), CD80 PE-Cy7 (clone L307.4), CD86 PE (clone 2331 FUN-1), all from BD Biosciences, San Jose, CA, USA by Flow Cytometry (FACS Jazz, BD Biosciences, San Jose, CA, USA). A total of $N = 3$ different pMSC donors in triplicates were analyzed.

T Cell Proliferation Analysis

Isolated PBMCs were thawed in 10 mL of pre-warmed PBMC medium and centrifuged at 248 g for 8 min. Cells were counted and in order to track proliferation, they were resuspended to a concentration of 10^7 cells/mL, and 20 μL of carboxyfluorescein succinimidyl ester (CFSE, 5 μM) were added per 0.980 μL of cell suspension for 7 min at 37°C. After that time, cell suspensions were topped up to a 10 mL volume of cold PBMC medium, and centrifuged 10 min at 690 g. T cell proliferation was stimulated using antibodies against CD3 and CD28 (1 mg/mL, 1 μL each per 10^6 cells, BD Biosciences) and a Goat linker antibody (0.5 mg/mL, 2 μL per 10^6 cells, BD Biosciences). Stimulated PBMCs were then added at 1:2.5, 1:5, 1:10 and 1:20 ratios to previously seeded pMSCs and co-cultured for 5 days.

PBMCs were removed by careful aspiration from the wells and washed with FACSflow. Cells were resuspended in 100 μL of FACSflow containing antibodies and fixed overnight in 4.6% paraformaldehyde. Prior to the analysis, samples were washed and resuspended in 100 μL of FACSflow. To identify T cells and specific subsets, antibodies against CD3 PerCP (clone SK7), CD4 APC (SK3) and CD8 PE-Cy7 (SK1) were used (all from BD Biosciences, San Jose, CA, USA). T cell proliferation was tracked by flow cytometry using FACS Jazz. Samples were analyzed using the software FlowJo V10.07 (BD Biosciences). $N = 3$ different pMSC donors with $N = 3$ different PBMC donors in triplicates were analyzed.

Isolation of B Cells From Spleens

Human splenocytes were obtained from the spleens of deceased kidney donors [The Netherlands Law of organ donation (Wet op Orgaandonatie, WOD), article 13]. Ficoll-Paque (Amersham Pharmacia Biotech, Uppsala, Sweden) density gradient separation was performed on spleens segments that were previously mechanically disrupted and filtered with a 70 μM cell strainer. Mononuclear cells were stored at −150°C until the date of use. On the co-culture day, quiescent B cells were isolated from thawn splenocytes by using anti-CD43 magnetic beads (Miltenyi Biotec GmbH, Bergisch Gladbach, Germany). $CD19^+$ purity was determined on the $CD43^-$ fraction by flow cytometry (FACS Canto II, BD Biosciences, San Jose, CA, USA) and cells suspensions with a >97% purity were used.

B Cell Proliferation and Subset Analysis

Purified $CD43^-$ quiescent B cells were labeled with CFSE (Molecular Probes Invitrogen, Karlsruhe, Germany) as described previously for PBMC proliferation for 7 min at 37°C. After labeling, B cells were resuspended in IMDM with 10% v/v heat inactivated FBS supplemented with a cocktail to mimic T cell activation, composed of 1,000 UI/mL IL-2 (Proleukin, Novartis, Prometheus laboratories Inc., San Diego, CA, USA), 10 μg/mL Goat anti-human IgM (Jackson Immunoresearch, Cambridgeshire, UK), and 5 μg/mL soluble recombinant human

CD40L (Biolegend, San Diego, CA, USA). One hundred microliter per well of the previously described cell suspension were added to the previously seeded pMSCs at a 1:5 MSC:B cell ratio and co-cultured for 7 days.

B cell proliferation was characterized by flow cytometry (FACS Canto II) and analyzed with FlowJo V10.07 (BD Biosciences). Samples were collected by careful aspiration and centrifuged for 5 min at 690 g, and supernatants were stored at −80°C for IgG quantification. Cells were stained using the following flow cytometry antibodies: CD19-BV512 (clone HIB19), CD27 PE-Cy7 (clone 0323), CD38-PE (clone HB7), Viaprobe (BD Biosciences, San Jose, CA, USA). A total of $N = 3$ different B cell donors co-cultured with one pMSC donor in duplicates or triplicates were analyzed.

IgG ELISA

Human IgG present in the supernatants was quantified by using a Human total IgG Ready SET Go ELISA kit (Thermofisher) following the manufacturer's instructions. Briefly, ELISA plates were coated overnight in coating buffer. The next day, samples were thawed in ice and diluted 1:2 in Assay buffer. Plates were washed twice with 400 μL per well of Wash Buffer, and blocked with 250 μL of Blocking buffer. One hundred microliter of either 1:2 diluted samples or standard IgG were added to the wells and incubated at room temperature for 2 hours with 400 rpm agitation. Upon incubation, wells were washed four times and 100 μL of detection antibody was added for 1 h at 400 rpm. After 4 washes, 100 μL per well of substrate solution were added and incubated for 15 min, upon when the reaction was stopped by pipetting 100 μL of stop solution to each well. Absorbance was read at 450 nm using a Versamax plate reader.

Statistical Analysis

Data is expressed as mean ± Standard Deviation (SD), $n = 3$ (experimental replicates) in duplicates or triplicates unless otherwise stated, where $p < 0.05$ values were considered as statistically significant. For all B and T cell proliferation analysis, $N = 3$ PBMC/B cell donors and a minimum of $N = 1$ pMSC donors were used. Statistical analysis was performed by the software IBM SPSS Version 24 using a linear mixed model with Bonferroni post-correction test for all figures, except for **Figure 1A** for which a Mann-Whitney test was used. *P*-values are represented as $^{***}p < 0.001$, $^{**}p < 0.01$, $^{*}p < 0.05$.

RESULTS

IFN-γ Pre-treatment Upregulates the Expression of IDO and Immune Related Markers on pMSCs

To study the effect of IFN-γ on the expression of immunomodulatory and co-stimulatory molecules on pMSCs, 50 ng/mL of IFN-γ was added to undifferentiated pMSCs for 3 days. After that time, the expression of IDO was quantified by qRT-PCR, and CD80, CD86, HLA-ABC, and HLA-DR surface levels were measured by FACS (**Figure 1**). Stimulation of pMSCs with IFN-γ significantly upregulated the gene expression levels of IDO (**Figure 1A**). Unprimed pMSC of all donors were highly positive for HLA-ABC, whereas for the rest of markers (CD80, CD86, and HLA-DR levels) unprimed cells expressed <50% of positive cells. Upon IFN-γ stimulation the percentage of positive cells of CD80, CD86, and HLA-DR was increased for all donors. We also found an increase in the expression levels per cell, expressed as the Mean Fluorescence Intensity (MFI) of HLA-ABC and HLA-DR for all donors (**Figures 1B,C**).

These results imply that IFN-γ pre-conditioning increases the expression of the immunomodulatory related enzyme IDO, but also the levels of HLA and co-stimulatory molecules involved in the activation of B and T cells on pMSCs.

IFN-γ Pre-treatment on pMSCs Does Not Affect Their Immunomodulatory Properties Upon T Cells

To assess the immunomodulatory abilities of pMSCs toward T cells under inflammatory conditions, IFN-γ primed or unprimed pMSCs were co-cultured with stimulated PBMCs (+CD3/CD28 antibodies) at 1:2.5, 1:5, 1:10, and 1:20 pMSC:PBMC for 5 days (**Figure 2**). The proliferation of $CD4^+$ and $CD8^+$ T cells was tracked using CFSE. The reduction in T cell proliferation for both $CD4^+$ (**Figure 2B**) and $CD8^+$ (**Figure 2C**) T cell subsets induced by pMSCs was dose dependent for IFN-γ primed or unprimed pMSCs co-cultures. However, there was not a significant difference between the IFN-γ primed or unprimed conditions for any of the doses tested. Hence, we concluded that pMSCs are able to exert their immunomodulatory abilities toward T cells regardless of the addition of IFN-γ.

IFN-γ Primed pMSCs Significantly Reduce the Proliferation Rates of B Cells

To examine whether inflammatory conditions could influence the anti-proliferative capacities of pMSCs on B cells, we co-cultured IFN-γ primed pMSCs with stimulated B cells for 7 days. We hypothesized that IFN-γ primed pMSCs would have similar immunomodulatory capacities on B cells compared to aMSCs (Luk et al., 2017).

B cells were stimulated with anti-CD40, anti-IgM, and IL-2 to mimic T cell activation in the absence of T cells. Viable B cells ($Viaprobe^-$ $CD19^+$) were analyzed by FACS and classified into $CD27^+$ (memory) and $CD27^-$ (naïve) B cells or plasmablasts ($CD27^{high}$ $CD38^{high}$) (**Figure 3A**).

Co-culture of unprimed pMSCs with B cells did not reduce proliferation rates of total B cells, naïve or memory B cells, but a tendency toward an increased proliferation was observed compared to stimulated B cells on their own. However, IFN-γ pre-conditioning of pMSCs decreased the proliferation rates of naïve, memory and total B cells in co-cultures compared to stimulated B cells. Moreover, IFN-γ primed pMSCs significantly decreased the proliferation rates of all B cell subsets when compared to unprimed pMSCs (**Figure 3B**).

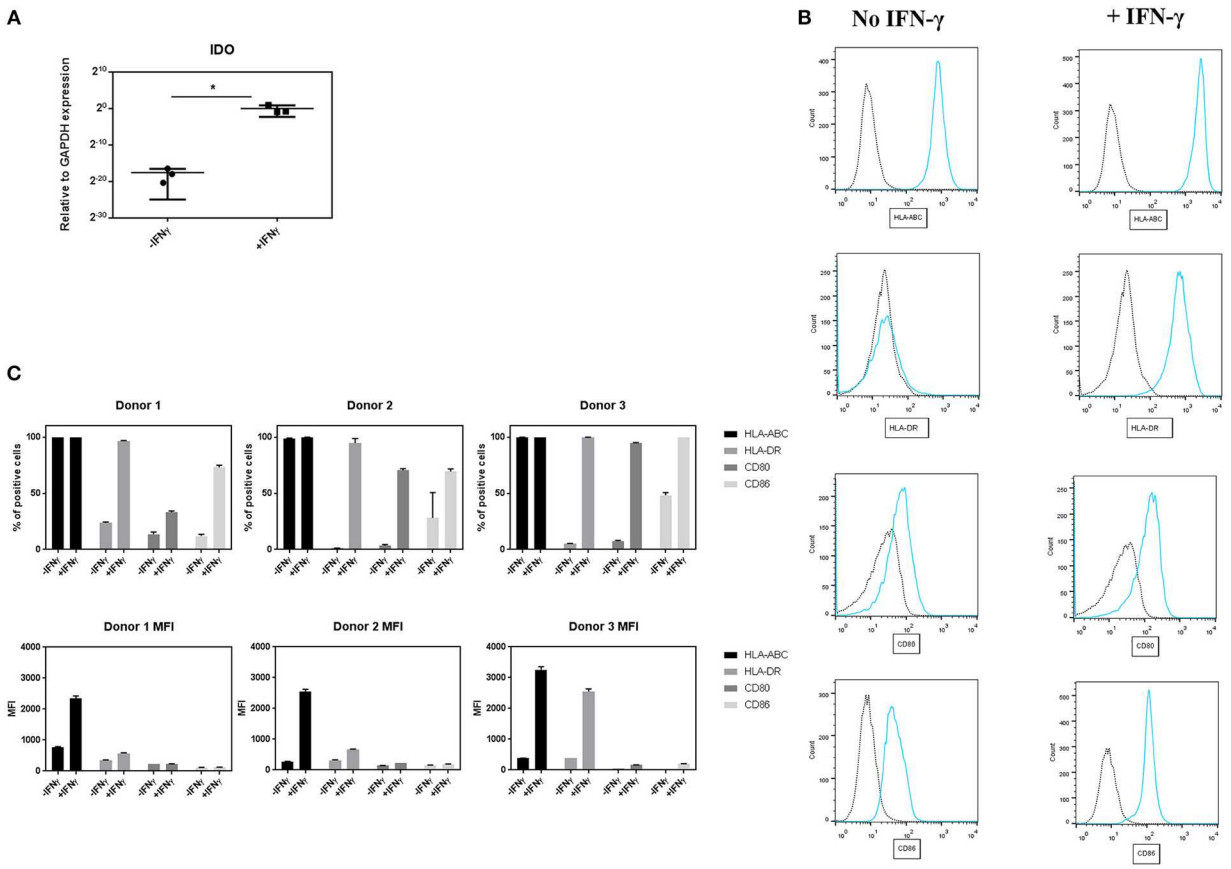

FIGURE 1 | Effect of IFN-γ on the expression of immune regulatory and co-stimulatory markers on pMSCs upon IFN-γ stimulation. pMSCs treated with 50 ng/mL IFN-γ for 3 days or unprimed (-IFN-γ) pMSCs were analyzed for IDO gene expression by qRT-PCR, and stained for HLA-ABC, HLA-DR, CD80, and CD86 expression and analyzed by FACS. **(A)** Expression of gene encoding for IDO relative to GAPDH. $N = 3$ pMSCs donors, single replicates. **(B)** Representative flow cytometry histograms of HLA-DR, HLA-ABC, CD80, and CD86 expression (blue line) on pMSCs based on the unstained control (dot line) with and without the addition of IFN-γ. **(C)** Percentage of positive cells and Mean Fluorescence Intensity (MFI) for HLA-ABC, HLA-DR, CD80, and CD86 markers. $N = 3$ different pMSC donors in triplicates. Results are shown as means ± SD. $^*p < 0.05$.

IFN-γ Primed pMSCs Abrogate Plasmablast Differentiation and IgG Production

After 7 days of co-culture with IFN-γ primed or unprimed pMSCs, we determined the frequencies of $CD19^+CD27^{high}CD38^{high}$ plasmablast cells by FACS (**Figure 3A**). In order to characterize B cell functionality, we quantified the amount of antibody released by B cells by measuring the IgG production in the supernatants of the co-cultures by ELISA.

Unprimed pMSCs did not significantly reduce the number of plasmablasts when co-cultured together with stimulated B cells (**Figure 4A**). However, there was a statistically significant reduction in the percentage of plasmablasts detected when co-cultured with IFN-γ primed pMSCs (8.9% of plasmablasts vs. 1.8%, respectively). A significant reduction in the amount of IgG present in the supernatants was also found when B cells were co-cultured with IFN-γ primed pMSCs compared to unprimed pMSCs, from 43 to 14 ng/mL (**Figure 4B**).

DISCUSSION

The immunomodulatory abilities of MSCs upon the adaptive immune response have been previously investigated in a number of studies (Bartholomew et al., 2002; Su et al., 2013; Franquesa et al., 2015; Luk et al., 2017). Moreover, MSCs immunomodulatory properties upon T and B cells have been shown to be highly influenced by the local inflammatory microenvironment (Krampera et al., 2006). These studies have reported some promising alternatives to tailor the immunosuppressive abilities of MSCs, by subjecting them to certain pro-inflammatory cytokines such as IFN-γ (Tipnis et al., 2010; Luk et al., 2017). However, they were performed using MSCs derived from diverse sources of aMSC donors, which can lead to high variability and unpredictable results due to a large age and origin variation among donors (Bruna et al., 2016), as well as reduced immunomodulatory abilities associated to age (Wu et al., 2014). We have previously established that the use of a potent source of pMSCs with enhanced multilineage differentiation and expansion abilities, as well as

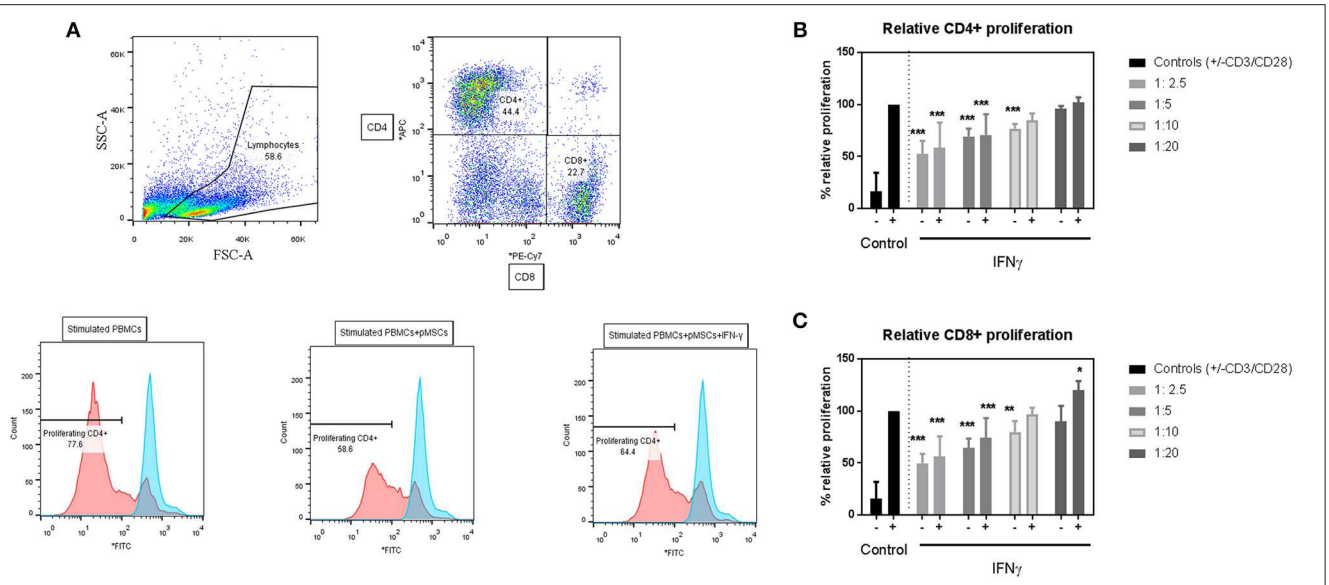

FIGURE 2 | pMSCs are immunomodulatory toward T cells in a dose-dependent manner. CD3/CD28 stimulated PBMCs were co-cultured with IFN-γ primed (+IFN-γ) or unprimed (-IFN-γ) pMSCs at 1:2.5, 1:5, 1:10, and 1:20 pMSCs:PBMCs ratios. Flow cytometric analysis was performed after 5 days of co-culture, and $CD4^+$ and $CD8^+$ proliferating T cells were detected by CFSE. **(A)** Representative FACS plots and histograms showing the gating strategy for stimulated $CD4^+$ and $CD8^+$ T cells alone or in co-culture with unprimed or IFN-γ primed pMSCs. **(B)** $CD4^+$ and **(C)** $CD8^+$ T cell proliferation in co-culture with unprimed or IFN-γ primed pMSCs. Results are expressed as the relative proliferation measured as the 1/Mean Fluorescence Intensity (MFI) of CFSE normalized to the (+CD3/CD28) stimulated control. $N = 3$ different pMSC donors with $N = 3$ different PBMC donors in triplicates. Results are represented as means ± SD. * $p < 0.05$, ** $p < 0.01$, *** $p < 0.001$.

reduced senescence, could make them attractive candidates for regenerative medicine (Knuth et al., 2018). Moreover, in the same study pMSCs were shown to reduce T cell proliferation in an allogeneic *in vitro* co-culture model. Here, we aimed to further investigate the immunomodulatory abilities of pMSCs toward T and B cells under inflammatory conditions as a promising MSC source for regenerative medicine and allogeneic transplantation with more consistent differentiation abilities and increased expansion properties.

Inflammatory signals have been suggested to alter the immunomodulatory functionality of MSCs toward B cells (Krampera et al., 2006). Luk et al. (2017) previously showed that IFN-γ primed adipose derived aMSCs inhibited naïve ($CD19^+CD27^-$) and memory ($CD19^+CD27^+$) B cell proliferation. In this study we clarified the immunomodulatory abilities of pMSCs upon stimulated B cells. Our findings suggest that IFN-γ priming is crucial for pMSCs in order to exert their immunomodulatory functionality upon B cells. IFN-γ primed pMSCs but not unprimed pMSCs showed a significant reduction in B cell proliferation for all different B cell subsets.

Franquesa et al. (2015) previously reported that in the presence of adipose-derived MSCs, antibody producing plasmablast ($CD19^+CD27^{high}CD38^{high}$) formation was inhibited. Hence, we hypothesized that pMSCs would also reduce plasmablast differentiation and that this effect would be enhanced by IFN-γ pre-priming. Our results showed that pMSCs reduced the numbers of plasmablasts only upon priming them with IFN-γ. We also showed that antibody production was significantly decreased when IFN-γ primed pMSCs were present and not in the presence of unprimed pMSCs. Since plasmablasts possess an antibody-producing functionality, these results suggest that in the case of an inflammatory microenvironment pMSCs significantly suppress humoral responses mediated by B cells. Moreover, since IFN-γ can be produced by T cells upon activation, these results suggest that the cross-talk between B and T cells might be of importance as a potential source of IFN-γ that can promote pMSC's immunosuppressive mechanisms upon B cells. In the situation of an allogeneic transplant, these properties of pMSCs might be advantageous to avoid allo-antibody formation against the allograft, one of the principal consequences of rejection and graft vs. host disease (GvHD) (Young et al., 2012). This knowledge might also be useful in the clinical context where an acute or chronic B cell mediated inflammation is present, such as autoimmune diseases or osteoarthritis.

MSCs are also well known to express major histocompatibility complex (MHC) class I molecules on their surface, but to have a minimal expression of MHC class II (Le Blanc et al., 2003) and co-stimulatory molecules such as CD80 and CD86 (Chamberlain et al., 2007). Addition of IFN-γ has been reported to enhance the expression of MHC class I and II (Majumdar et al., 2003), but it does not seem to increase the levels of CD80 and CD86 (Chinnadurai et al., 2014). Here, we show that unprimed pMSCs express high levels of MHC class I (HLA-ABC) and low levels of MHC class II (HLA-DR), CD80 and CD86. However, IFN-γ stimulation upregulated the levels of HLA-DR and both co-stimulatory molecules on pMSCs. This increase could mean that pMSCs would be more prone to act as

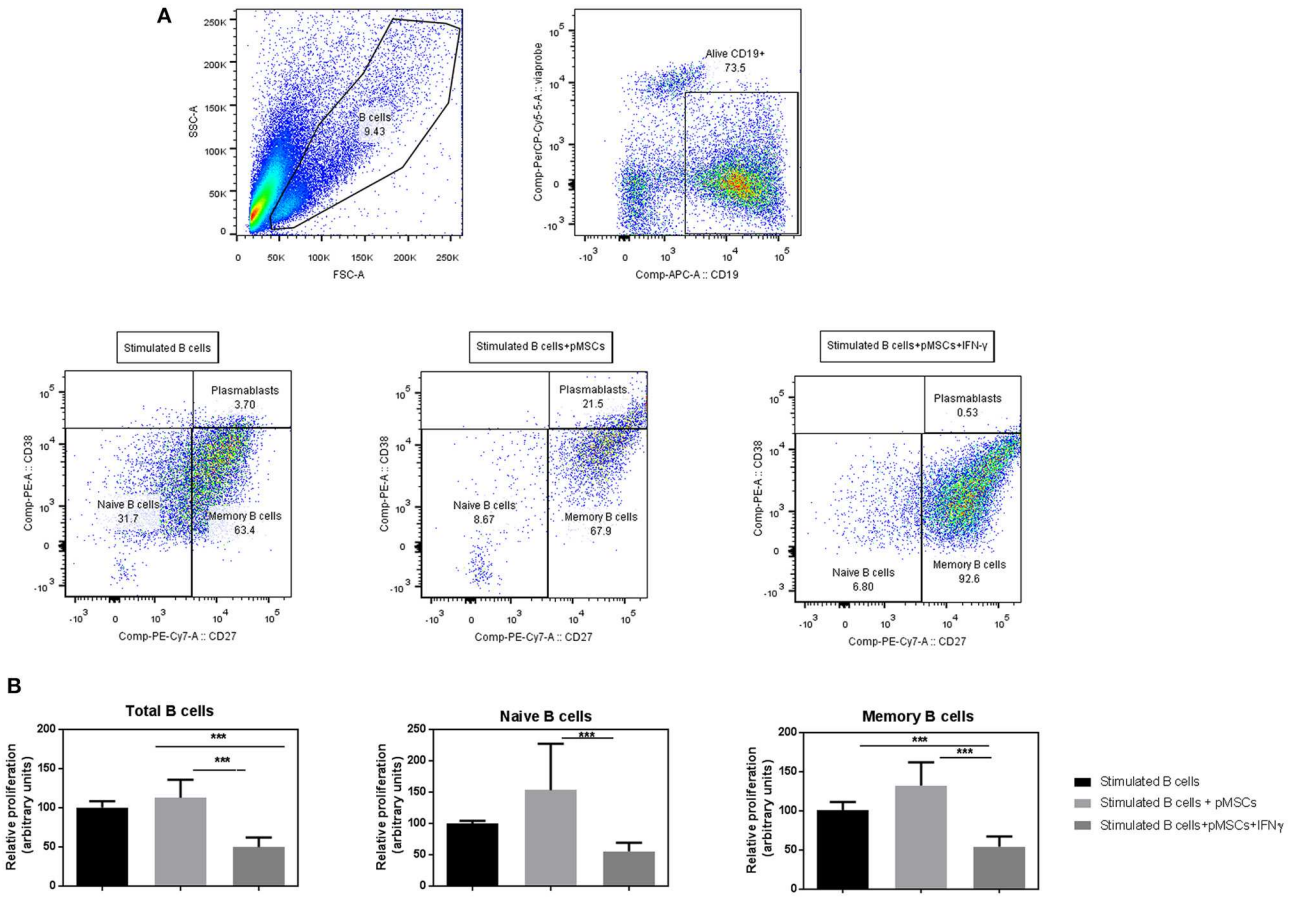

FIGURE 3 | IFN-γ primed pMSCs significantly reduce the proliferation rates on naïve, memory and total numbers of B cells compared to unprimed cells. Stimulated (+anti-CD40, anti-IgM, and IL-2) B cells were co-cultured with either IFN-γ primed or unprimed pMSCs. B cells were retrieved and analyzed by flow cytometry after 7 days. **(A)** FACS gating strategy of viable $CD19^+$ B cells that were classified according to the expression of CD27 into memory ($CD27^+$), naïve ($CD27^-$) B cells, or plasmablasts ($CD27^{high}$ $CD38^{high}$). **(B)** Relative proliferation of B cells when co-cultured with IFN-γ primed or unprimed pMSCs. Results are shown as the 1/MFI (CFSE) of $CD19^+$ viable cells (total B cells), $CD27^+$ cells (memory), and $CD27^-$ cells (naïve) relative to the B cell stimulated condition. $N = 3$ B cell donors co-cultured with 1 pMSC donor in duplicates or triplicates. Figures show means ± SD. *** $p < 0.001$.

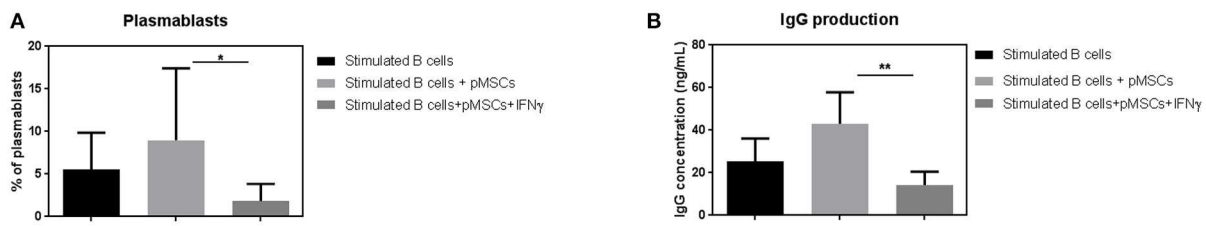

FIGURE 4 | IFN-γ primed pMSCs but not unprimed significantly decrease plasmablast differentiation and IgG production. **(A)** Plasmablast frequencies were measured upon 7 days of co-culture of stimulated B cells with IFN-γ primed or unprimed pMSCs. Results are expressed as the % of viable $CD19^+$ $CD27^{high}$ $CD38^{high}$ cells. **(B)** IgG concentration (ng/mL) was detected in the supernatants of stimulated B cells and IFN-γ primed or unprimed pMSCs by ELISA. $N = 3$ different B cell donors co-cultured with 1 pMSC donor Results are shown as means ± SD. * $p < 0.05$; ** $p < 0.01$.

antigen presenting cells and activate T cells under inflammatory conditions (Lim et al., 2012). Many studies have discussed the crucial role of IFN- γ on MSCs immunomodulatory abilities toward T cells (Krampera et al., 2006; Ryan et al., 2007). Since an increased immunosuppressive effect from MSCs upon T cells under inflammatory conditions has been linked to a higher IDO activity (Meisel et al., 2004), we examined the gene expression of IDO on pre-primed pMSCs. Our results showed that, in contrast to previous studies (Ryan et al., 2007; Wobma et al., 2018), IFN-γ priming did not affect pMSCs immunomodulatory

abilities upon T cells. However, IFN-γ significantly upregulated the gene expression of IDO in all pMSCs donors. Therefore, it is possible that the upregulation of HLA-DR, CD80, and CD86 triggered by IFN-γ on pMSCs counteracted the IDO mediated enhancement on their immunomodulatory abilities upon T cells. The extent of this upregulation was observed to be donor dependent. This indicates that intrinsic variation among pMSCs donors might impact the immunomodulatory abilities of pMSCs toward T cells according to the degree of expression of co-stimulatory molecules in an inverse manner. Despite this, under inflammatory conditions, pMSCs were still able to suppress T cell proliferation in a similar trend than unprimed pMSCs. Previous studies have reported as well that the immunomodulatory potency of MSCs is highly related to the inflammatory milieu created by T cells (Kronsteiner et al., 2011). Hence, the cytokine profile of T cells might in turn affect the immunomodulatory effect of MSCs on immune cells.

Differences in the immunomodulatory abilities of IFN- γ primed pMSCs compared to other sources of aMSCs may depend on multifactorial pathways that have been described to play a role in the degree of immunomodulation on MSCs toward T and B cells. Luk et al. (2017) previously reported that upon IFN-γ addition, MSCs inhibited B cell proliferation as well as IgG production and regulatory B cells (Breg) formation through the tryptophan depleting activity of the enzyme IDO. Some studies have reported the involvement of other immunomodulatory mechanisms, such as Galectin-9 (Gal-9) which significantly reduced IgG titers in an *in vivo* murine model (Ungerer et al., 2014). The Cyclooxygenase 2 (COX-2) pathway has also been indicated to play a role in Breg suppression through IL-10 depletion (Hermankova et al., 2016). Signaling pathways involving the release of metalloproteinase-processed CC-chemokine ligand 2 (CCL-2) by MSCs controlled by the downregulation of olfactory 1/early B cell factor–associated zinc-finger protein (OAZ) have been proposed as a mechanism of MSC inhibition of IgG synthesis on B cells (Feng et al., 2014).

Moreover, it is also important to remark that different extents in the increase of co-stimulatory molecules on pMSCs surface, which seems to be donor-dependent as presented in this study, might entail as well differences in IFN- γ primed pMSCs immunomodulatory abilities. This is due to the fact that a higher upregulation of these co-stimulatory molecules, such as CD80 and CD86, in certain donors may negatively impact the immunosuppressive potential of IFN- γ primed pMSCs. Hence, this intrinsic donor variability on the immune profile of pMSCs needs to be taken into account when considering using pMSCs for immune therapies.

Together, we show that IFN-γ priming exerts an impact on the expression of immune markers and co-stimulatory molecules on a novel source of pediatric MSCs. In this context, pMSCs maintain their immunomodulatory abilities upon T cells, significantly suppress B cell proliferation, as well as plasmablast differentiation and antibody production. *In vivo*, this might mean that upon receiving certain inflammatory signals, such as IFN-γ produced by activated T cells, pMSCs safeguard their immunomodulatory status toward T cells, and gain anti-proliferative abilities upon B cells, avoiding an allo-antibody immune response. This knowledge is useful for the design of novel immunotherapies in several types of diseases where a chronic inflammation is present, as well as in the areas of regenerative medicine and solid organ transplantation by using a novel MSC source with enhanced differentiation abilities and an immune privileged condition.

DATA AVAILABILITY

The datasets generated for this study are available on request to the corresponding author.

AUTHOR CONTRIBUTIONS

VP: conception and design, collection of data, data analysis and interpretation, and manuscript writing. MH: conception and design, data analysis and interpretation, and manuscript writing. RK: collection of data and final approval of manuscript. MF: conception and design, data analysis and interpretation, and final approval of manuscript. JW-B: collection of data and final approval of manuscript. EW: conception, manuscript writing, and final approval of manuscript. EF: conception and design, data analysis and interpretation, and manuscript writing. PB: conception, data analysis and interpretation, manuscript writing, and final approval of manuscript.

FUNDING

This research was supported by the AO Foundation, Switzerland (AOCMF-15-27F). MF is funded by the Catalan Health Department (Generalitat de Catalunya) contract PERIS (SLT002/16/00069).

ACKNOWLEDGMENTS

We would like to thank Dr. Roberto Narcisi at the Erasmus MC for his assistance with the statistical analysis.

REFERENCES

Barry, F., and Murphy, M. (2013). Mesenchymal stem cells in joint disease and repair. *Nat. Rev. Rheumatol.* 9, 584–594. doi: 10.1038/nrrheum.2013.109

Bartholomew, A., Sturgeon, C., Siatskas, M., Ferrer, K., McIntosh, K., Patil, S., et al. (2002). Mesenchymal stem cells suppress lymphocyte proliferation *in vitro* and prolong skin graft survival *in vivo*. *Exp. Hematol.* 30, 42–48. doi: 10.1016/S0301-472X(01)00769-X

Benseler, V., Obermajer, N., Johnson, C. L., Soeder, Y., Dahlke, M. D., and Popp, F. C. (2014). MSC-based therapies in solid organ transplantation. *Hepatol. Int.* 8, 179–184. doi: 10.1007/s12072-013-9509-1

Bianco, P., Robey, P. G., and Simmons, P. J. (2008). Mesenchymal stem cells: revisiting history, concepts, and assays. *Cell Stem Cell* 2, 313–319. doi: 10.1016/j.stem.2008.03.002

Bruna, F., Contador, D., Conget, P., Erranz, B., Sossa, C. L., and Arango-Rodríguez, M. L. (2016). Regenerative potential of mesenchymal stromal cells: age-related changes. *Stem Cells Int.* 2016:1461648. doi: 10.1155/2016/1461648

Chamberlain, G., Fox, J., Ashton, B., and Middleton, J. (2007). Concise review: mesenchymal stem cells: their phenotype, differentiation capacity, immunological features, and potential for homing. *Stem Cells* 25, 2739–2749. doi: 10.1634/stemcells.2007-0197

Chinnadurai, R., Copland, I. B., Patel, S. R., and Galipeau, J. (2014). IDO-independent suppression of T cell effector function by IFN-γ-licensed human mesenchymal stromal cells. *J. Immunol.* 2014:1301828. doi: 10.4049/jimmunol.1301828

Corcione, A., Benvenuto, F., Ferretti, E., Giunti, D., Cappiello, V., Cazzanti, F., et al. (2006). Human mesenchymal stem cells modulate B-cell functions. *Blood* 107:367. doi: 10.1182/blood-2005-07-2657

Cortez-Toledo, E., Rose, M., Agu, E., Dahlenburg, H., Yao, W., Nolta, J. A., et al. (2018). Enhancing retention of mesenchymal stem cells with pro-survival factors promotes angiogenesis in a mouse model of limb ischemia. *Stem Cells Dev.* 28, 114–119. doi: 10.1089/scd.2018.0090

Cozzi, E., Colpo, A., and De Silvestro, G. (2017). The mechanisms of rejection in solid organ transplantation. *Transfus Apher. Sci.* 56, 498–505. doi: 10.1016/j.transci.2017.07.005

Cuerquis, J., Romieu-Mourez, R., François, M., Routy, J. P., Young, Y. K., Zhao, J., et al. (2014). Human mesenchymal stromal cells transiently increase cytokine production by activated T cells before suppressing T-cell proliferation: effect of interferon-gamma and tumor necrosis factor-alpha stimulation. *Cytotherapy* 16, 191–202. doi: 10.1016/j.jcyt.2013.11.008

DeWolf, S., and Sykes, M. (2017). Alloimmune T cells in transplantation. *J. Clin. Invest.* 127, 2473–2481. doi: 10.1172/JCI90595

Farrell, E., Both, S. K., Odörfer, K. I., Koevoet, W., Kops, N., O'Brien, F. J., et al. (2011). *In-vivo* generation of bone via endochondral ossification by *in-vitro* chondrogenic priming of adult human and rat mesenchymal stem cells. *BMC Musculoskelet. Disord.* 12:31. doi: 10.1186/1471-2474-12-31

Feng, X., Che, N., Liu, Y., Chen, H., Wang, D., Li, X., et al. (2014). Restored immunosuppressive effect of mesenchymal stem cells on B cells after olfactory 1/early B cell factor–associated zinc-finger protein down-regulation in patients with systemic lupus erythematosus. *Arthritis Rheumatol.* 66, 3413–3423. doi: 10.1002/art.38879

Franquesa, M., Mensah, F. K., Huizinga, R., Strini, T., Boon, L., Lombardo, E., et al. (2015). Human adipose tissue-derived mesenchymal stem cells abrogate plasmablast formation and induce regulatory B cells independently of T helper cells. *Stem Cells* 33, 880–891. doi: 10.1002/stem.1881

Ganguly, P., El-Jawhari, J. J., Giannoudis, P. V., Burska, A. N., Ponchel, F., and Jones, E. A. (2017). Age-related changes in bone marrow mesenchymal stromal cells: a potential impact on osteoporosis and osteoarthritis development. *Cell Transplant.* 26, 1520–1529. doi: 10.1177/0963689717721201

Gao, F., Chiu, S. M., Motan, D. A., Zhang, Z., Chen, L., Ji, H. L., et al. (2016). Mesenchymal stem cells and immunomodulation: current status and future prospects. *Cell Death Dis.* 7:e2062. doi: 10.1038/cddis.2015.327

Gerdoni, E., Gallo, B., Casazza, S., Musio, S., Bonanni, I., Pedemonte, E., et al. (2007). Mesenchymal stem cells effectively modulate pathogenic immune response in experimental autoimmune encephalomyelitis. *Ann. Neurol.* 61, 219–227. doi: 10.1002/ana.21076

González, M. A., Gonzalez-Rey, E., Rico, L., Büscher, D., and Delgado, M. (2009). Adipose-derived mesenchymal stem cells alleviate experimental colitis by inhibiting inflammatory and autoimmune responses. *Gastroenterology* 136, 978–989. doi: 10.1053/j.gastro.2008.11.041

Hermankova, B., Zajicova, A., Javorkova, E., Chudickova, M., Trosan, P., Hajkova, M., et al. (2016). Suppression of IL-10 production by activated B cells via a cell contact-dependent cyclooxygenase-2 pathway upregulated in IFN-γ-treated mesenchymal stem cells. *Immunobiology* 221, 129–136. doi: 10.1016/j.imbio.2015.09.017

Knuth, C. A., Kiernan, C. H., Palomares Cabeza, V., Lehmann, J., Witte-Bouma, J., Ten Berge, D., et al. (2018). Isolating pediatric mesenchymal stem cells with enhanced expansion and differentiation capabilities. *Tissue Eng. Part C Methods* 24, 313–321. doi: 10.1089/ten.tec.2018.0031

Krampera, M., Cosmi, L., Angeli, R., Pasini, A., Liotta, F., Andreini, A., et al. (2006). Role for interferon-gamma in the immunomodulatory activity of human bone marrow mesenchymal stem cells. *Stem Cells* 24, 386–398. doi: 10.1634/stemcells.2005-0008

Kronsteiner, B., Wolbank, S., Peterbauer, A., Hackl, C., Redl, H., van Griensven, M., et al. (2011). Human mesenchymal stem cells from adipose tissue and amnion influence T-cells depending on stimulation method and presence of other immune cells. *Stem Cells Dev.* 20, 2115–2126. doi: 10.1089/scd.2011.0031

Larsen, C. P., Knechtle, S. J., Adams, A., Pearson, T., and Kirk, A. D. (2006). A new look at blockade of T-cell costimulation: a therapeutic strategy for long-term maintenance immunosuppression. *Am. J. Transplant.* 6 (5 Pt 1), 876–83. doi: 10.1111/j.1600-6143.2006.01259.x

Le Blanc, K., Tammik, C., Rosendahl, K., Zetterberg, E., and Ringdén, O. (2003). HLA expression and immunologic propertiesof differentiated and undifferentiated mesenchymal stem cells. *Exp. Hematol.* 31, 890–896. doi: 10.1016/S0301-472X(03)00110-3

Lim, T. S., Goh, J. K., Mortellaro, A., Lim, C. T., Hämmerling, G. J., and Ricciardi-Castagnoli, P. (2012). CD80 and CD86 differentially regulate mechanical interactions of T-cells with antigen-presenting dendritic cells and B-cells. *PLoS ONE* 7:e45185. doi: 10.1371/journal.pone.0045185

Luk, F., Carreras-Planella, L., Korevaar, S. S., de Witte, S. F. H., Borràs, F. E., Betjes, M. G. H., et al. (2017). Inflammatory conditions dictate the effect of mesenchymal stem or stromal cells on B cell function. *Front. Immunol.* 8:1042. doi: 10.3389/fimmu.2017.01042

Majumdar, M. K., Keane-Moore, M., Buyaner, D., Hardy, W. B., Moorman, M. A., McIntosh, K. R., et al. (2003). Characterization and functionality of cell surface molecules on human mesenchymal stem cells. *J. Biomed. Sci.* 10, 228–241. doi: 10.1007/BF02256058

Meisel, R., Zibert, A., Laryea, M., Göbel, U., Däubener, W., and Dilloo, D. (2004). Human bone marrow stromal cells inhibit allogeneic T-cell responses by indoleamine 2,3-dioxygenase-mediated tryptophan degradation. *Blood* 103, 4619–4621. doi: 10.1182/blood-2003-11-3909

Ryan, J. M., Barry, F., Murphy, J. M., and Mahon, B. P. (2007). Interferon-gamma does not break, but promotes the immunosuppressive capacity of adult human mesenchymal stem cells. *Clin. Exp. Immunol.* 149, 353–363. doi: 10.1111/j.1365-2249.2007.03422.x

Shao, J., Zhang, W., and Yang, T. (2015). Using mesenchymal stem cells as a therapy for bone regeneration and repairing. *Biol. Res.* 48:62. doi: 10.1186/s40659-015-0053-4

Stolzing, S. (2006). Aging of mesenchymal stem cells. *Ageing Res Rev.* 5:91. doi: 10.1016/j.arr.2005.10.001

Su, J., Chen, X., Huang, Y., Li, W., Li, J., Cao, K., et al. (2013). Phylogenetic distinction of iNOS and IDO function in mesenchymal stem cell-mediated immunosuppression in mammalian species. *Cell Death Differentiation* 21:388. doi: 10.1038/cdd.2013.149

Tipnis, S., Viswanathan, C., and Majumdar, A. S. (2010). Immunosuppressive properties of human umbilical cord-derived mesenchymal stem cells: role of B7-H1 and IDO. *Immunol. Cell Biol.* 88, 795–806. doi: 10.1038/icb.2010.47

Ungerer, C., Quade-Lyssy, P., Radeke, H. H., Henschler, R., Königs, C., Köhl, U., et al. (2014). Galectin-9 is a suppressor of T and B cells and predicts the immune modulatory potential of mesenchymal stromal cell preparations. *Stem Cells Dev.* 23, 755–766. doi: 10.1089/scd.2013.0335

van der Stok, J., Koolen, M. K., Jahr, H., Kops, N., Waarsing, J. H., Weinans, H., et al. (2014). Chondrogenically differentiated mesenchymal stromal cell pellets stimulate endochondral bone regeneration in critical-sized bone defects. *Eur. Cell Mater.* 27, 137–148. doi: 10.22203/eCM.v027a11

Wobma, H. M., Kanai, M., Ma, S. P., Shih, Y., Li, H. W., Duran-Struuck, R., et al. (2018). Dual IFN-γ/hypoxia priming enhances immunosuppression of mesenchymal stromal cells through regulatory proteins and metabolic mechanisms. *J. Immunol. Regen. Med.* 1, 45–56. doi: 10.1016/j.regen.2018.01.001

Wu, L. W., Wang, Y. L., Christensen, J. M., Khalifian, S., Schneeberger, S., Raimondi, G., et al. (2014). Donor age negatively affects the immunoregulatory properties of both adipose and bone marrow derived mesenchymal stem cells. *Transplant. Immunol.* 30, 122–127. doi: 10.1016/j.trim.2014.03.001

Young, J. S., Wu, T., Chen, Y., Zhao, D., Liu, H., Yi, T., et al. (2012). Donor B cells in transplants augment clonal expansion and survival of pathogenic $CD4^+$ T cells that mediate autoimmune-like chronic graft-versus-host disease. *J. Immunol.* 189:222. doi: 10.4049/jimmunol.1200677

Conflict of Interest Statement: The authors declare that the research was conducted in the absence of any commercial or financial relationships that could be construed as a potential conflict of interest.

The reviewer GE declared a shared affiliation, with no collaboration, with several of the authors, VP and PB, to the handling editor at the time of review.

frontiers in Bioengineering and Biotechnology

ORIGINAL RESEARCH
published: 23 October 2019
doi: 10.3389/fbioe.2019.00292

Hypoxia Conditioned Mesenchymal Stem Cell-Derived Extracellular Vesicles Induce Increased Vascular Tube Formation *in vitro*

Ciarra Almeria[1†], René Weiss[2†], Michelle Roy[1], Carla Tripisciano[2], Cornelia Kasper[1], Viktoria Weber[2] and Dominik Egger[1]*

[1] Department of Biotechnology, University of Natural Resources and Life Science, Vienna, Austria, [2] Christian Doppler Laboratory for Innovative Therapy Approaches in Sepsis, Department for Biomedical Research, Danube University Krems, Krems, Austria

OPEN ACCESS

Edited by:
Sandra Hofmann,
Eindhoven University of Technology, Netherlands

Reviewed by:
Andreina Schoeberlein,
University of Bern, Switzerland
Vincenzo Cantaluppi,
University of Piemonte Orientale, Italy

***Correspondence:**
Dominik Egger
dominik.egger@boku.ac.at

[†]These authors have contributed equally to this work

Specialty section:
This article was submitted to Tissue Engineering and Regenerative Medicine, a section of the journal Frontiers in Bioengineering and Biotechnology

Received: 29 July 2019
Accepted: 09 October 2019
Published: 23 October 2019

Citation:
Almeria C, Weiss R, Roy M, Tripisciano C, Kasper C, Weber V and Egger D (2019) Hypoxia Conditioned Mesenchymal Stem Cell-Derived Extracellular Vesicles Induce Increased Vascular Tube Formation in vitro. Front. Bioeng. Biotechnol. 7:292. doi: 10.3389/fbioe.2019.00292

Mesenchymal stem/stromal cells (MSCs) display a variety of therapeutically relevant effects, such as the induction of angiogenesis, particularly under hypoxic conditions. It is generally recognized that MSCs exert their effects by secretion of paracrine factors and by stimulation of host cells. Furthermore, there is increasing evidence that some therapeutically relevant effects of MSCs are mediated by MSC-derived extracellular vesicles (EVs). Since our current knowledge on MSC-derived EVs released under hypoxic conditions is very limited, we aimed to characterize MSC-derived EVs from normoxic vs. hypoxic conditions (5% O_2). Adipose-derived MSCs were grown under normoxic and hypoxic conditions, and EVs were analyzed by flow cytometry using lactadherin as a marker for EVs exposing phosphatidylserine, CD63 and CD81 as EV markers, as well as CD73 and CD90 as MSC surface markers. Particle concentration and size distribution were measured by nanoparticle tracking analysis (NTA), and the EV surface antigen signature was characterized using bead-based multiplex flow cytometry. Furthermore, we evaluated the potential of MSC-derived EVs obtained under hypoxic conditions to support angiogenesis using an *in vitro* assay with an hTERT-immortalized human umbilical vein endothelial cell (HUVEC) line. Proliferation and viability of MSCs were increased under hypoxic conditions. EV concentration, size, and surface signature did not differ significantly between normoxic and hypoxic conditions, with the exception of CD44, which was significantly upregulated on normoxic EVs. EVs from hypoxic conditions exhibited increased tube formation as compared to normoxic EVs or to the corresponding supernatants from both groups, indicating that tube formation is facilitated by EVs rather than by soluble factors. In conclusion, hypoxia conditioned MSC-derived EVs appear to be functionally more potent than normoxic MSC-derived EVs regarding the induction of angiogenesis.

Keywords: mesenchymal stem cells, extracellular vesicles, hypoxia, angiogenesis, tube formation, therapeutic potential

INTRODUCTION

The application potential of mesenchymal stem cells (MSCs) in regenerative cell-based therapies has been gaining substantial interest (Squillaro et al., 2016; Mastrolia et al., 2019). Advances in MSC research have provided evidence that the therapeutic effects are largely independent of the physical proximity of administered MSCs to their target tissues, but can rather be attributed to trophic effects provided by MSCs upon secretion of EVs as well as soluble factors, such as cytokines and growth factors (Gnecchi et al., 2008; Karp and Teol, 2009; Wagner et al., 2009; Williams and Hare, 2011).

EVs are released by almost all cell types. Three EV subgroups have been discriminated according to their size, and biogenesis: (i) apoptotic bodies (>1,000 nm) released during early apoptosis; (ii) microvesicles (100 to 1,000 nm) formed via outward budding of the plasma membrane; and (iii) exosomes (40 to 100 nm) secreted after fusion of multivesicular bodies with the plasma membrane (Cocucci and Meldolesi, 2015). Since these subgroups can overlap in size, and as markers for their unambiguous discrimination are lacking, the generic term extracellular vesicles is used to describe both exosomes and MVs in the context of this study (Thery et al., 2018).

The heterogeneity of EVs mandates a combination of methods for their characterization (Yeo et al., 2013; Thery et al., 2018). Flow cytometry enables the detection and characterization of EVs with regard to the expression of EV markers (Thery et al., 2009; Wyss et al., 2014; Dragovic et al., 2015) and cellular origin (Weiss et al., 2018). Nanoparticle tracking analysis (NTA), commonly used to determine the average size distribution and number of particles in suspension based on their Brownian motion, has been adapted for the characterization of EVs. While NTA is well suited for screening purposes, it fails to provide information on EV-specific molecular properties (Dragovic et al., 2011; Sokolova et al., 2011). Genomic and proteomic profiling has demonstrated that EVs carry host-specific cargo, including mRNAs, miRNAs, lipids and proteins (Théry et al., 2002; Subra et al., 2007; Simpson et al., 2008), which can be transferred to recipient cells and alter their phenotype (Valadi et al., 2007). Multiplex bead-based flow cytometry has recently been introduced to characterize the surface marker profile of EVs, which mediates the interaction of EVs with their target cells (Wiklander et al., 2018) and is relevant to understand the molecular content and related functions of subsets of EVs and to identifying potential EV subsets with a defined therapeutic activity.

Previous reports have convincingly shown that the quality and therapeutic function of human MSCs are impacted by the isolation methods and culture conditions, as well as by the age and genetic traits of the donors (Dufrane, 2017; Liu et al., 2017). Several *in vitro* studies have demonstrated a significantly higher proliferative activity of MSCs cultured under hypoxia (1–10% O_2) as compared to normoxia (21% O_2) (Nekanti et al., 2010). Hypoxic preconditioning of MSCs generates distinctive changes in stem cell characteristics and influences the secretion of cytokines and growth factors (Kinnaird et al., 2004). It has therefore been suggested that the biological activity of MSC-derived EVs differs depending on the cell source and culture parameters, such as medium composition, oxygen content, duration of culture, as well as shear stress (Patel et al., 2017). Along this line, EV release from several human cancer cell lines was enhanced in hypoxia (1% O_2) (Salomon et al., 2013; Endzelins et al., 2018; Kilic et al., 2018). Similar findings were reported for the release of EVs from hypoxic MSCs cultured in serum-free media (Lo Sicco et al., 2017), which was accompanied by an increased hypoxia-inducible factor 1-alpha (HIF-1-alpha) activation. It is therefore recognized that the cargo incorporated into EVs is regulated by hypoxic preconditioning, which ultimately affects their angiogenic potential, as well as their immunomodulatory and regenerative properties (King et al., 2012; Yu et al., 2012; Bian et al., 2014). Likewise, the EV surface protein profile may vary with the culture conditions, but studies on changes of EV surface proteins under normoxic/hypoxic conditions are lacking to date. Since EV surface molecules are crucial in mediating the interaction of EVs with their target cells, we characterized the surface signature of EVs from adipose-derived MSC culture supernatants generated under normoxic (21% O_2) and hypoxic (5% O_2) conditions and further investigated whether EVs derived from a hypoxic environment can increase vascular tube formation in HUVECs.

Abbreviations: EVs, Extracellular vesicles; HUVECs, human umbilical vein endothelial cells; LA, lactadherin; MFI, median fluorescence intensity; MSCs, mesenchymal stem cells; NTA, nanoparticle tracking analysis; PS, phosphatidylserine; VEGF, vascular endothelial growth factor.

MATERIALS AND METHODS

Cell Culture

The use of human tissue was approved by the ethics committee of the Medical University Vienna, Austria (EK Nr. 957/2011, 30 January 2013), and all donors gave written consent. Human MSCs were isolated within 8 h after surgery as previously described (Egger et al., 2017). MSCs from 6 donors (aged 20–70) were cultivated in standard medium composed of MEM alpha (Thermo Fisher Scientific, Waltham, MA, USA), 0.5% gentamycin (Lonza, Basel, Switzerland), 2.5% human platelet lysate (PL BioScience, Aachen, Germany; filtered through 0.2 µm filters according to the data sheet provided by the manufacturer; **Supplementary Figure 1**) and 1 IU/ml heparin (Ratiopharm, Ulm, Germany) in humidified atmosphere at 37°C, 5% CO_2 and 21% or 5% O_2, and cryo-preserved in liquid nitrogen as previously described (Neumann et al., 2014). Upon use, MSCs were thawed and subcultivated once, resulting in passage 2. Cells intended for cultivation at 5% O_2 were isolated and subcultivated at 5% O_2 until seeding. To characterize MSC-derived EVs, MSCs (passage 2) were seeded at a density of 3,000 cells/cm^2 into 12-well plates (TPP, Trasadingen, Switzerland) ($n = 4$ each) and cultivated in 2 ml standard medium at 21 or 5% O_2 for 6 days. The medium was completely exchanged every second day, and medium without cells served as control. The supernatants were stored at −20°C until further use.

Viability Assay

MSCs were seeded into a 96-well plate at a density of 3,000 cells/cm^2 and incubated at 21 or 5% O_2 for 6 days. Viability was assessed using the resazurin-based TOX8 kit (Sigma Aldrich) according to the manufacturer's instructions. Fluorescence intensity at 560/590 nm was determined using a plate reader (Tecan, Männedorf, Switzerland) after 2 h incubation at 37°C (5 or 21% O_2) with gentle shaking. The cell number was calculated based on a calibration curve.

Isolation of Extracellular Vesicles

MSCs were cultured as described above. MSC supernatants were centrifuged at 500 g for 5 min and at 1,500 g for 15 min at room temperature (RT) in order to remove cells and debris. The resulting supernatant was stored at −20°C until further characterization by flow cytometry and NTA. EVs isolated from the supernatant of MSCs cultured for 72 h in vesicle-depleted standard medium under normoxic and hypoxic conditions were subjected to an additional centrifugation step at 100,000 g, 4°C for 90 min using a Sorvall WX 80 ultracentrifuge with SW 32 Ti rotor (Beckman Coulter Inc., CA). The resulting pellet was resuspended in 1 ml phosphate buffered saline (PBS; Thermo Fisher Scientific) and stored at −20°C prior to use in tube formation assays (**Figure 1**).

Flow Cytometric Characterization of Stem Cell-Derived Extracellular Vesicles

Lactadherin was used as a marker for cell-surface derived EVs (Tripisciano et al., 2017; Weiss et al., 2018), since the large majority of the EV population that can be detected by flow cytometry (i.e., EVs larger than 250 nm) expose phosphatidylserine (PS). Cell culture supernatants were stained with FITC-conjugated lactadherin (LA) to detect PS, as well as with the following MSC surface markers: CD73-PE (Beckman Coulter, Brea, CA), CD90-APC-AF750 (Beckman Coulter), CD63-AF647 (Biolegend, San Diego, CA, USA) and CD81-PerCPCy 5.5 (Biolegend). CD41-PC7 (Beckman Coulter) was used as a marker for platelet-derived EVs. All antibodies used in this study and their respective fluorochromes are specified in **Supplementary Table 1**. Staining was performed for 15 min in the dark, and antibodies were centrifuged at 17,000 g for 10 min before use. Stained samples were diluted 5-fold in PBS, and analyzed on a Gallios flow cytometer (Beckman Coulter) equipped with 405, 488, and 638 nm lasers. Fluorescent-green silica particles (1.0, 0.5, 0.3 μm; excitation/emission 485/510 nm; Kisker Biotech, Steinfurt, Germany) were used for calibration, the triggering signal was set to forward scatter/size, and the EV gate was set below the 1 μm bead cloud as previously described (Tripisciano et al., 2017; Weiss et al., 2018) and as shown in **Figure 3A**. Data were acquired for 3 min at a flow rate of 10 μl/min and analyzed using the Kaluza Software (Beckman Coulter). EVs were identified as LA-positive events in the EV gate. To confirm that the signals in the EV fraction were indeed dependent on the presence of intact EVs, a detergent lysis control was included by treatment of the MSC supernatant with 0.25% TritonX-100 to lyse vesicles. Buffer controls, isotype controls, and single stainings of specific monoclonal antibodies are shown in **Supplementary Figure 2**.

Nanoparticle Tracking Analysis

The particle concentration and size distribution of MSC-derived EVs was determined in cell culture supernatants using nanoparticle tracking analysis (NTA; Zeta View, Particle Metrix, Inning, Germany). Measurements were performed at RT using the following instrument settings: 80 (sensitivity), 1,000 (maximal area), 5 (minimal area), and 25 (brightness). Data were acquired in one cycle of measurement over 11 positions and were analyzed using the software ZetaView version 8.04.02.

Bead-Based Multiplex Exosome Flow Cytometry Assay

MSCs were seeded at 3,000 cells/cm^2 in passage 2 and cultivated for 72 h. The cell culture supernatants were subjected to bead-based multiplex EV analysis by flow cytometry (MACSPlex Exosome Kit, human; Miltenyi Biotec, Bergisch Gladbach, Germany). To obtain samples for EV characterization, supernatants were pre-cleared according to manufacturer's recommendation. Pre-cleared cell culture supernatants were incubated with 15 μl of MACSPlex Exosome Capture Beads containing 39 different antibody-coated bead subsets and with 15 μl MACSPlex Exosome Detection Reagent containing APC-conjugated CD9, CD63, and CD81 for 1 h with gentle agitation

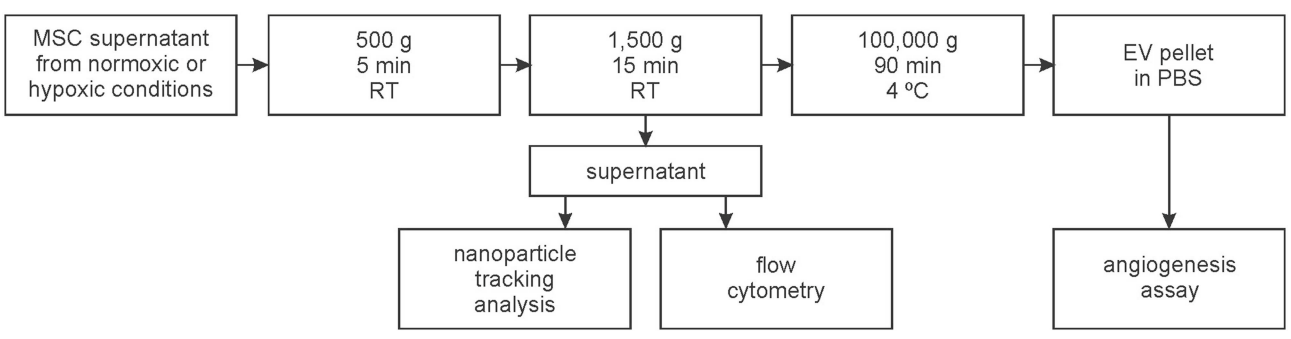

FIGURE 1 | Workflow for the isolation and characterization of extracellular vesicles (EVs). EVs were isolated from the supernatant of mesenchymal stem cells (MSCs) which were cultivated at 21% O_2 (normoxic) or at 5% O_2 (hypoxic).

at RT. Beads were washed with 1 ml of MACSPlex Buffer prior to flow cytometric analysis (CytoFLEX LX, Beckman Coulter). Raw APC median fluorescence intensity (MFI) for all surface epitope capture bead subsets was corrected by subtracting the corresponding MFI values obtained for isotype control beads. All antibodies and the respective fluorochromes are specified in **Supplementary Table 1.**

Angiogenesis Assay

MSCs from one donor (female, 28) were cultured in standard medium for 72 h under normoxic or hypoxic conditions at 37°C and 5% CO_2 ($n = 5$). As EV fractions were normalized regarding their protein content (see below), the medium was centrifuged at 100,000 g for 14 h at 4°C prior to use in order to deplete any non-MSC-derived protein components derived from medium supplements. Culture supernatants were collected and subjected to serial centrifugation at 500 g for 5 min, for 1,500 g for 15 min, and for 90 min at 100,000 g at 4°C (Sorvall WX 80 ultracentrifuge, SW 32 Ti rotor, Beckman Coulter) to pellet EVs. The EV pellet was resuspended in PBS. For the tube formation assay, immortalized HUVECs (Schiller et al., 2009) were seeded at a density of 3.5×10^5 cells/ml onto growth factor reduced Matrigel (Corning, New York, USA) in an ibidi µ-plate Angiogenesis 96 Well (Ibidi, Gräfelfing, Germany). HUVECs were treated with EVs (corresponding to 100 µg/ml protein), with EV-depleted supernatant (100 µg/ml protein; both from normoxic or hypoxic culture), with 100 ng/ml vascular endothelial growth factor (VEGF) in endothelial cell growth medium (EGM-2; Lonza) as positive control, and with PBS as negative control. Cells were incubated for 16 h and stained with calcein acetoxymethyl ester (calcein-AM, Sigma Aldrich). Fluorescence images were obtained at excitation/emission wavelengths of 490/515 nm with an inverted fluorescence microscope (DM IL LED by Leica, Wetzlar, Germany). The tube characteristics were analyzed and quantified using the Angiogenesis Analyzer toolset in ImageJ (version 1.52, NIH, Baltimore, MD, USA) (Carpentier, 2012).

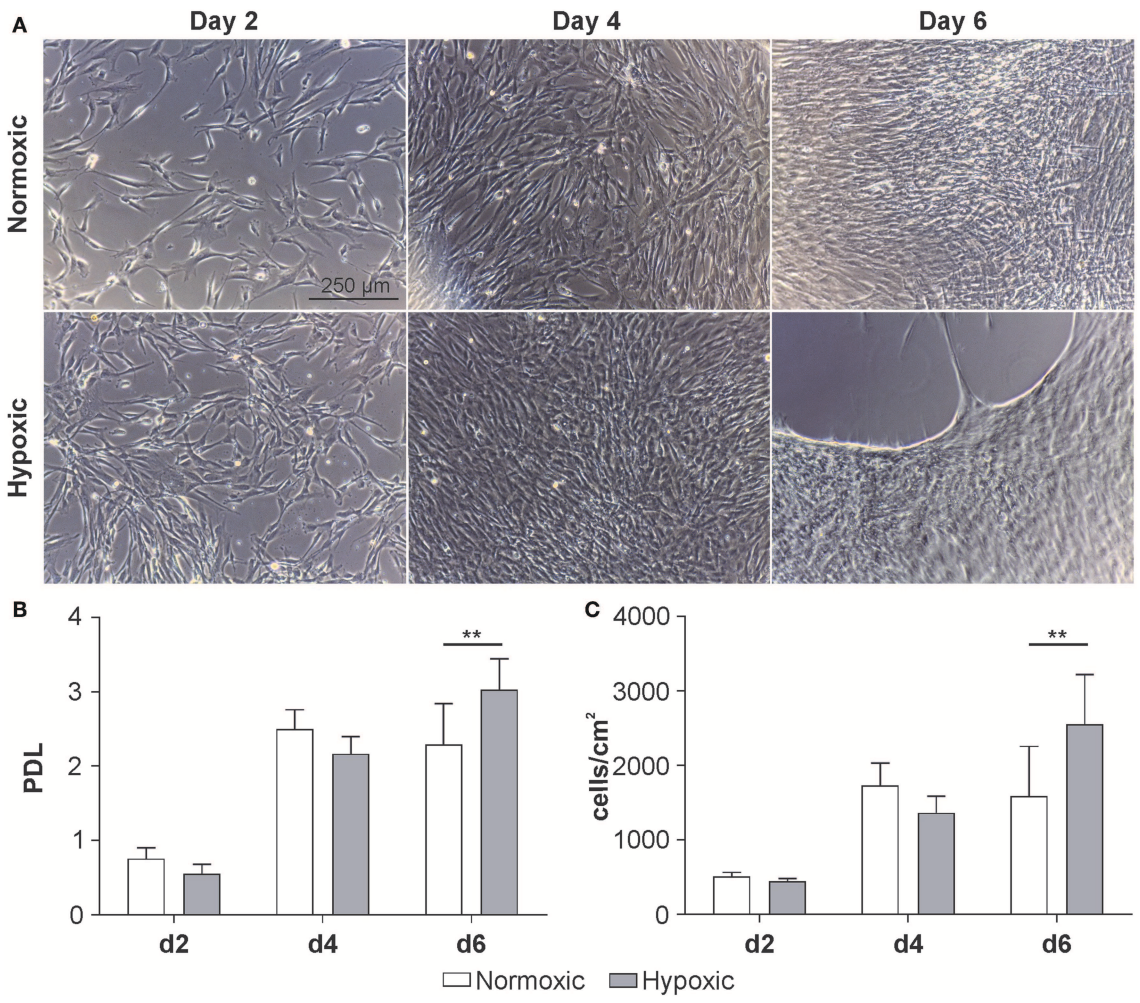

FIGURE 2 | Growth kinetics of MSCs at passage 3 cultivated at 21 % O_2 (normoxic) or 5 % O_2 (hypoxic). **(A)** Representative micrographs, **(B)** population doubling level (PDL) and **(C)** cellular concentration at day 2, 4 and 6. Cell number was determined using a resazurin-based viability assay as described in Materials and Methods. Data are given as mean ± SD ($n = 6$) $^{**}p < 0.01$.

Statistical Analysis

Statistical analysis was performed using GraphPad Prism version 7.02 (La Jolla, CA, USA). Data are presented as mean ± standard deviation (SD). For multiple comparisons, repeated measures two-way ANOVA followed by Tukey's multiple comparisons test was used to assess the increase/decrease within one group over time (time effect), while Bonferroni's multiple comparisons test was used to assess the difference between normoxic/hypoxic conditions at a given time point (group effect). Significance was accepted at $p \leq 0.05$.

RESULTS

Cultivation of MSCs Under Normoxic and Hypoxic Conditions

MSCs were grown under normoxic or hypoxic conditions for 6 days. Micrographs of the cells suggest a higher proliferation rate of MSCs under hypoxic conditions. After reaching confluence on day 4, the cells started to detach by day 6 (**Figure 2A**). Both, the population doubling level (PDL) (normoxic 2.3 ± 0.5 vs. hypoxic 3.0 ± 0.4; **Figure 2B**) and the cell density were

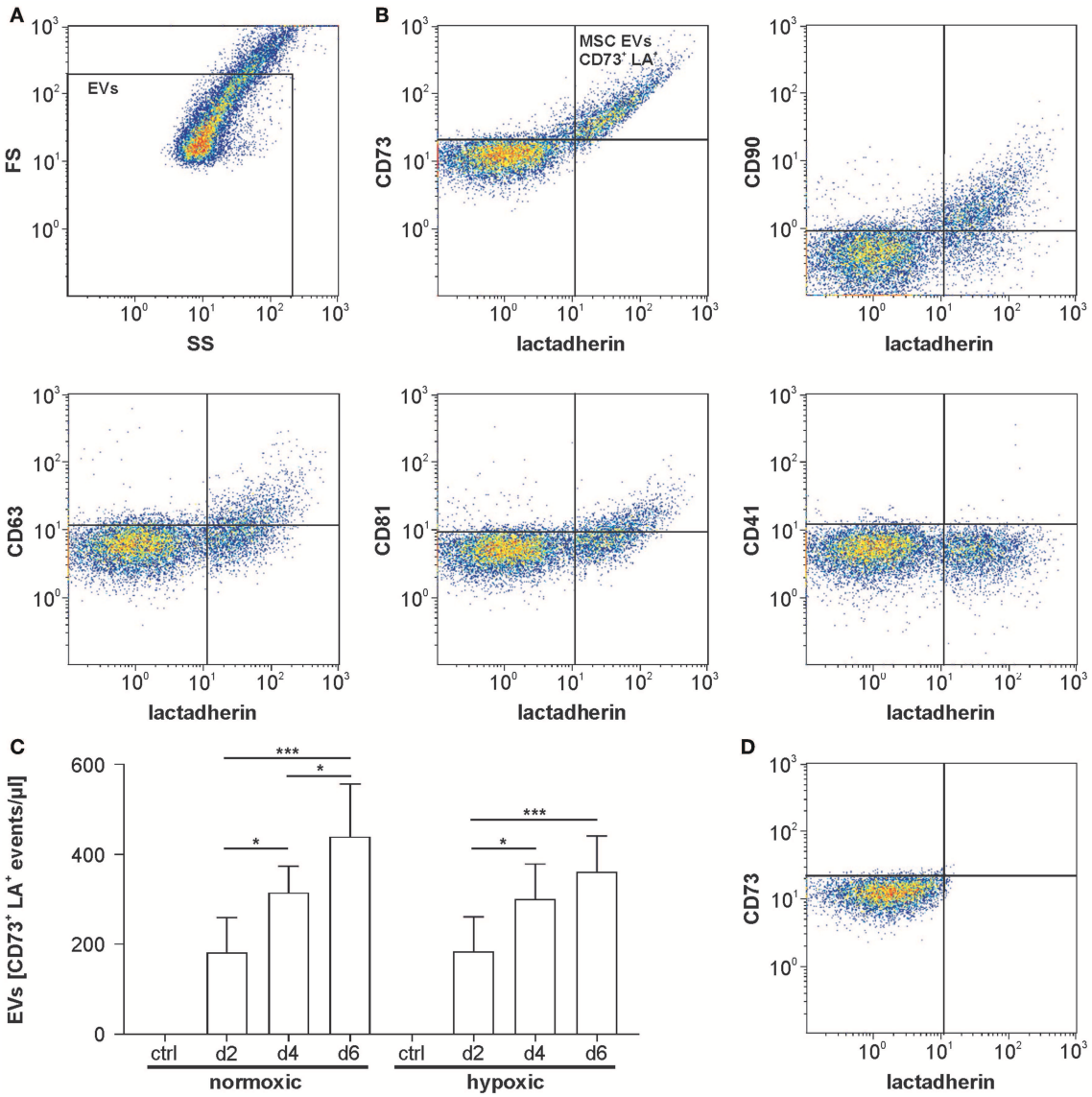

FIGURE 3 | Flow cytometric characterization of MSC-derived EVs. **(A)** Flow cytometric characterization was performed with fluorescent-green silica particles, and the EV gate was set below the 1 µm bead cloud. A forward scatter vs. side scatter (FS vs. SS) dot plot for MSC supernatant is shown as example. **(B)** MSC supernatants were stained with FITC-conjugated lactadherin as marker of phosphatidylserine-exposing EVs as well as with the general EV markers CD63 and CD81 and with the MSC markers CD73 and CD90. CD41 was used as a negative marker to label platelet-derived EVs potentially derived from human platelet lysate used as medium supplement. Lactadherin vs. surface marker plots are shown. **(C)** Release of MSC-derived EVs under normoxic or hypoxic conditions over time ($n = 6$). **(D)** MSC supernatant was treated with 0.25% TritonX-100 during staining as detergent lysis control, abolishing all signals in the EV gate and confirming the presence of vesicles. Data are given as mean ± SD. *$p < 0.05$; ***$p < 0.001$.

significantly higher under hypoxic conditions (normoxic $1.6 \times 10^5 \pm 3.4 \times 10^4$ vs. hypoxic $2.2 \times 10^5 \pm 7.3 \times 10^4$ cells/cm^2; **Figure 2C**).

Flow Cytometric Characterization of MSC-Derived EVs Under Normoxic and Hypoxic Conditions

According to flow cytometry, 100 and 75% of all EVs were positive for the MSC markers CD73 and CD90, respectively, while 35 and 40% were positive for the tetraspanins CD63 or CD81. Staining with CD41, which was included as control, did not provide evidence for the presence of EVs derived from the platelet lysate used as medium supplement (**Figure 3B**). Detergent lysis by treatment of MSC culture supernatants with 0.25% Triton X-100 abolished all signals in the EV gate, confirming the presence of intact vesicles (**Figure 3D**). Increased release of EVs was observed over time with a maximum after 6 days of cultivation. Supernatants from MSCs grown under normoxic or hypoxic conditions did not differ regarding the EV concentration (**Figure 3C**).

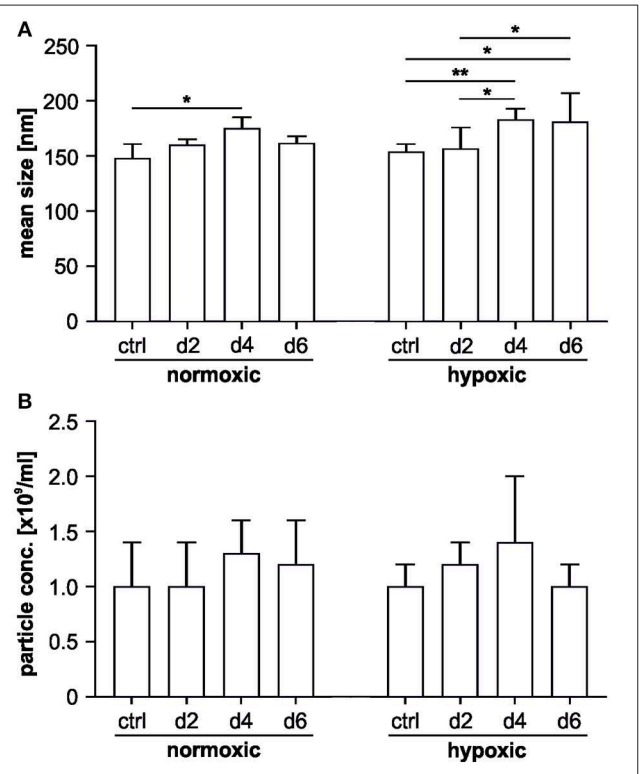

FIGURE 4 | Nanoparticle tracking analysis of MSC-derived EVs. The characterization was performed in scatter mode as described in Materials and Methods. **(A)** Mean particle sizes of MSC-derived EVs under normoxic or hypoxic conditions on day 2, 4 and 6; **(B)** mean number of particles/ml in MSC supernatants under normoxic or hypoxic conditions on day 2, 4, and 6. Data are presented as mean ± SD ($n = 6$; $^*p < 0.05$; $^{**}p < 0.01$).

Characterization of MSC-Derived EVs by Nanoparticle Tracking Analysis

According to NTA, supernatants from MSCs grown under normoxic and hypoxic conditions did not differ with regard to mean particle size and concentration. Mean particle size increased over time for both groups, while we failed to detect an increase in total particle concentration over time for the individual groups (**Figure 4**).

Detection of EV Surface Signatures

The bead-based multiplex assay used to characterize EV surface signatures comprises 37 labeled capture bead populations, each of them coated with different monoclonal antibodies against individual EV surface antigens. Individual bead populations can be identified and gated based on their respective fluorescence intensity (**Figure 5A**). After incubation with MSC culture supernatants, bead-captured EVs are detected by counterstaining with APC-labeled antibodies targeting the EV tetraspanins CD9, CD63 and CD81.

Platelet markers including CD49e (integrin α-5), CD9 (tetraspanin 29), CD62p (P-selectin), CD42a (glycoprotein IX) and CD29 (integrin β-1) were detected in the control medium containing 2.5% human platelet lysate. The MSC markers CD105 (endoglin, a receptor for transforming growth factor beta, TGF-β), CD63 and CD81 (tetraspanins), as well as CD146 (melanoma cell adhesion molecule) were detected at intermediate-positive APC fluorescence intensity for both, normoxic and hypoxic EVs. CD29 was present at high-positive APC fluorescence intensity on EVs from both, normoxic and hypoxic conditions. CD44, a surface glycoprotein involved in cell adhesion and migration, was expressed at significantly higher levels under normoxic as compared to hypoxic conditions (**Figure 5B**).

Characterization of Angiogenic Properties of MSC-Derived EVs From Normoxic and Hypoxic Conditions

We used a HUVEC tube formation assay to investigate the capacity of MSC-derived EVs to induce vascular tube formation. We employed an immortalized HUVEC cell line to increase the reproducibility, and seeded HUVECs onto growth factor-reduced Matrigel to avoid induction of tube formation by growth factors. The total tube length (length of all branches and loops), the number of branches, branching points, and loops was significantly increased ($p < 0.01$) after incubation with EVs from hypoxic conditions, as compared to EVs from normoxic conditions, and as compared to the EV-depleted supernatants from normoxic and hypoxic conditions (**Figure 6**). A rearrangement of HUVECs was observed for the EV-depleted supernatants, but without formation of complete tubes. Still, the tube formation parameters were higher than in the negative control.

DISCUSSION

A number of beneficial effects has been observed upon cultivation of MSCs under hypoxic conditions, usually at 1–10 % O_2

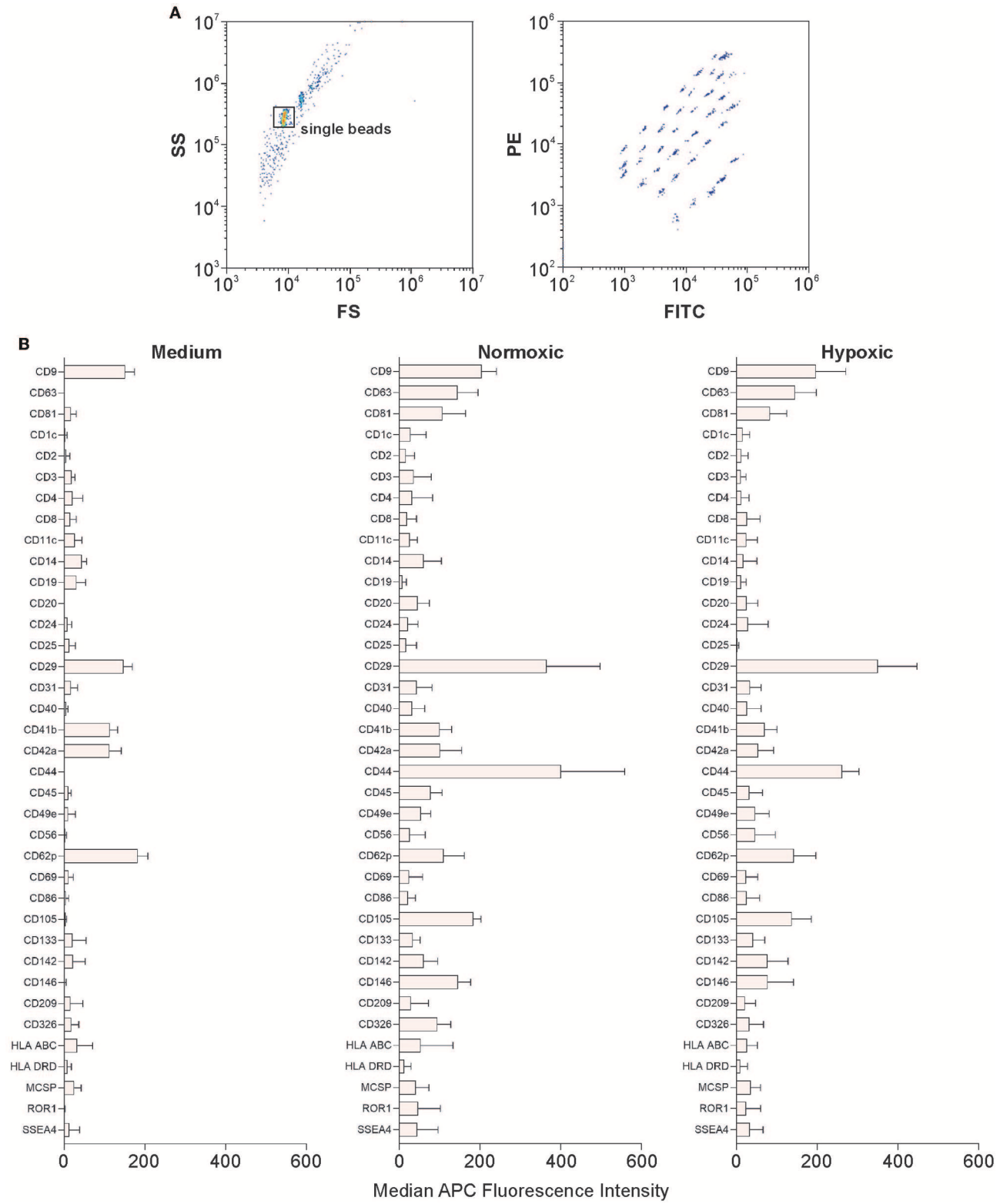

FIGURE 5 | Characterization of EVs using multiplex bead-based flow cytometry. Analysis was performed using a CytoFLEX LX flow cytometer as described in Materials and Methods. **(A)** Gating strategy to identify single beads and discrimination of differently labeled bead populations identified by their fluorescence in the FITC vs. PE channel. **(B)** Identification of EV surface signatures in MSC culture supernatants from normoxic or hypoxic conditions; medium without cells served as a control. A representative quantification of the median APC fluorescence values for all 37 surface epitope bead populations after isotype correction is shown. The difference in expression between normoxic and hypoxic conditions was statistically significant only for CD44. Data are given as mean ± SD ($n = 4$).

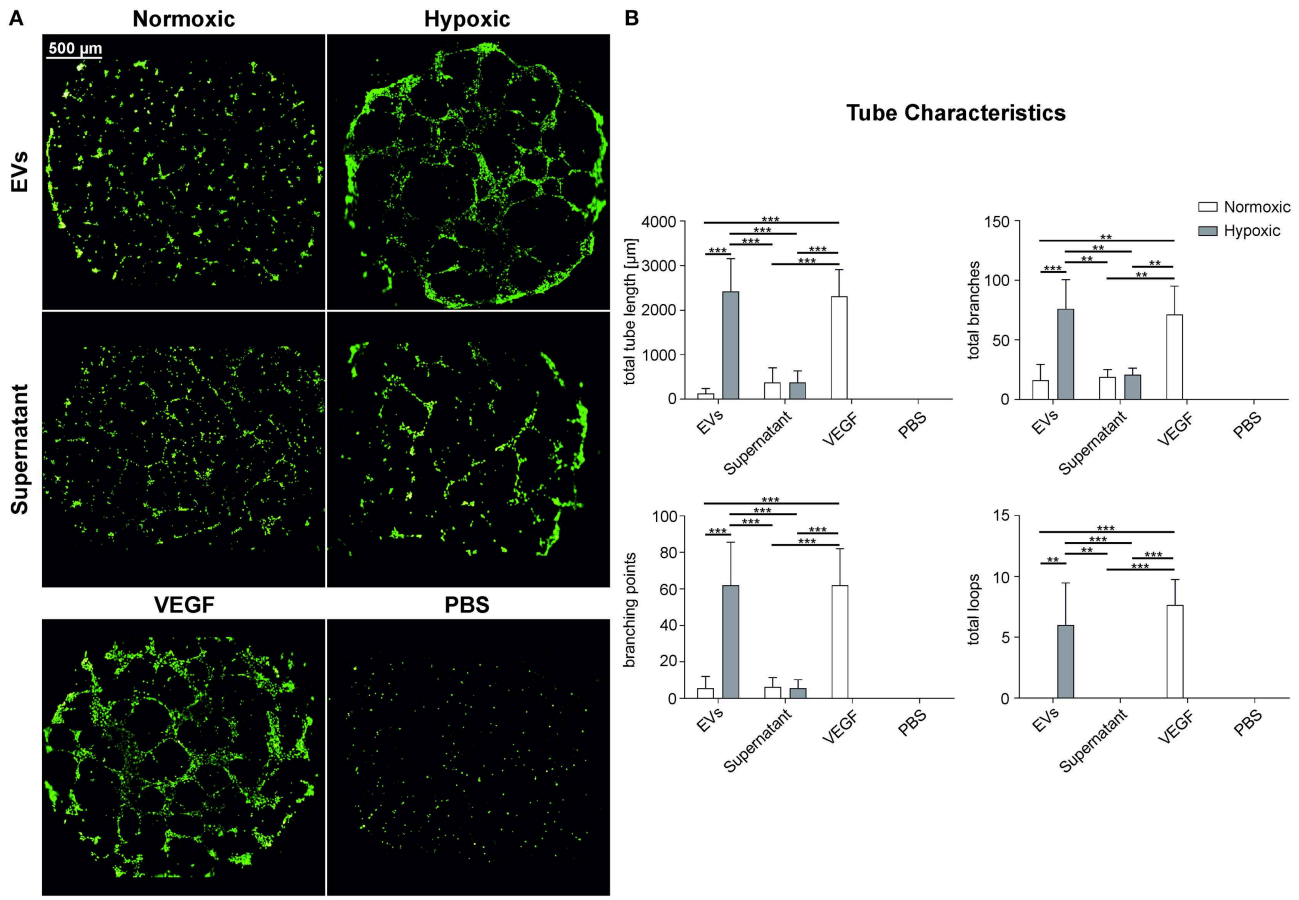

FIGURE 6 | Angiogenic properties of MSC-derived EVs obtained under normoxic and hypoxic conditions. HUVECs on growth factor reduced Matrigel were incubated with EVs derived from MSCs grown under normoxic and hypoxic conditions (100 µg protein/ml) as well as with EV-depleted supernatant. **(A)** HUVECs stained with calcein-AM and **(B)** tube characteristics of HUVECs after 16 h of incubation with the EV preparation, the corresponding supernatant, 100 ng/ml VEGF in EGM-2 (VEGF, positive control) and PBS (negative control). Data are given as mean ± SD ($n = 3$; $^{**}p < 0.01$; $^{***}p < 0.001$).

(Lavrentieva et al., 2010). Furthermore, the therapeutic potential of MSC-derived EVs has been shown in the field of kidney, heart, lung, as well as brain diseases (Börger et al., 2017; Phinney and Pittenger, 2017).

Our current understanding is that MSC-derived EVs can mediate their effects mainly by horizontal transfer of mRNAs, miRNAs, and proteins to their target cells, and that this cargo is affected by cell culture conditions (Phan et al., 2018). Next to the EV cargo, EV surface signatures are crucial for mediating the function of EVs, since they determine the interaction of EVs with their specific target cells.

In this study, we therefore aimed to characterize EVs derived from MSCs under normoxic and hypoxic conditions. We focused on potential differences regarding EV surface signatures as well as on differences related to angiogenesis, since enhanced angiogenesis of human umbilical vein endothelial cells has been previously described upon stimulation with exosome-like vesicles (Dai et al., 2017).

We used a combination of markers for the flow cytometric characterization of MSC-derived EVs. Lactadherin served as a marker for EVs, since the large majority of EVs detectable in flow cytometry are known to be derived from the cell surface and to expose phospatidylserine. The tetraspanins CD63 and CD81 were used as additional EV markers, complemented by the MSC markers CD73 and CD90. CD41 was added as a marker for EVs potentially derived from the human platelet lysate that served as medium supplement. We found that, while the large majority of PS-exposing EVs were $CD73^+$ or $CD90^+$, <50% of all PS-exposing EVs were $CD63^+$ or $CD81^+$, most likely because the tetraspanins CD63 and CD81 are mainly associated with exosomes. Since the current detection limit for EVs in flow cytometry is about 250 nm (Saunderson et al., 2008; Crescitelli et al., 2013; Willms et al., 2018), smaller $CD63^+$ or $CD81^+$ EVs, including the majority of exosomes, remain undetected. Flow cytometry did not provide evidence for platelet-derived $CD41^+$ EVs in a size range above 250 nm, consistent with the fact that human platelet lysate was filtered (0.2 µm) prior to use.

With the flow cytometry protocol used in this study, the concentration of MSC-derived EVs ($LA^+CD73^+CD90^+CD63^+CD41^-$) was in the range of 2–4

$\times 10^5$ EVs/ml. Other studies have reported EV concentrations ranging from 1×10^8 to 1×10^{11} EVs/ml, depending on the EV source, as well as the isolation and flow cytometry protocols used (Tripisciano et al., 2017; Endzelins et al., 2018; Reis et al., 2018; Weiss et al., 2018). The release of EVs in our study increased over time, correlating with the increasing cell number, in agreement with previous reports that frequent collection of cell culture supernatant enhances the yield of EVs (Patel et al., 2017). Moreover, there is evidence that both, EV release and cell growth are reduced at higher initial seeding densities, supporting the notion that EVs are released to support intercellular communication in the culture environment (Patel et al., 2017; Ohyashiki et al., 2018).

Complementing flow cytometry, we used NTA to determine particle concentrations in MSC culture supernatants. Analysis in scatter mode yielded particle concentrations in the range of 1×10^9 EVs/ml, more than 3 orders of magnitude higher as compared to flow cytometry. While this difference can be partly attributed to enhanced detection of smaller EVs using NTA, it also reflects the presence of non-vesicular particulate material derived from the cell culture medium (Lane et al., 2017), since NTA in scatter mode detects any light scattering event and thus is considerably less specific than flow cytometry. NTA also revealed a significant increase in the particle mean size over time. The particle size was comparable to previously published studies with a mean size ranging from 50 to 200 nm (Reis et al., 2018; Valandani et al., 2018; Li et al., 2019; Witwer et al., 2019).

Bead-based multiplex flow cytometry used to characterize EV surface signatures (Wiklander et al., 2018) did not indicate differences for vesicular (CD63, CD81) or MSC markers under normoxic vs. hypoxic conditions. As an exception, CD44, an MSC glycoprotein involved in cell-cell interaction, cell adhesion, and migration (Ramos et al., 2016), was significantly upregulated on EVs obtained under normoxic as compared to hypoxic conditions. CD44 expression on MSC-derived EVs has been previously shown to be required for their uptake by target cells (Bruno et al., 2009; Monsel et al., 2015). Moreover, CD44 expressing EVs have been recently implicated in anti-inflammatory effects, since the prevention of $CD44^+$ EV uptake by monocyte-derived macrophages (MDM) using an anti-CD44 antibody abrogated the ability of MSC-conditioned medium (and thus of MSC-derived EVs) to reduce macrophage TNF secretion (Morrison et al., 2017). However, based on our current data, we are not able to link the enhanced CD44 expression on normoxic EVs to the observed differences in angiogenesis induced by normoxic vs. hypoxic EVs.

Bead-based multiplex flow cytometry also revealed the presence of platelet-derived markers, specifically CD62p, in MSC culture supernatants, likely due to the use of human platelet lysate as cell culture supplement. While filtered (0.2 μm) platelet lysate was used, which did not contain detectable amounts of EVs in a size range above 250 nm according to flow cytometry, smaller platelet-derived EVs (or even soluble CD62p) remained undetected in flow cytometry, but were caught by beads coated with anti-CD62p and therefore detected in bead-based flow cytometry.

To investigate potential functional differences for normoxic and hypoxic MSC-derived EVs, we focused on their ability to support angiogenesis. MSCs and MSC-conditioned cell culture supernatants are known to induce vascular tube formation of HUVECs (Sorrell et al., 2009). Apparently, this paracrine effect is not only caused by soluble growth factors, such as fibroblast growth factor (FGF) and VEGF, or by cytokines, but also by specific factors associated with EVs (Nakamura et al., 2015; Merino-Gonzalez et al., 2016). MSC-derived EVs are known to stimulate angiogenesis (Lopatina et al., 2014) despite their low levels of VEGF (Nakamura et al., 2015). Furthermore, it is known that MSCs and MSC culture supernatants from hypoxic conditions promote angiogenic effects, which are commonly assessed by the tube formation of HUVECs (Stubbs et al., 2012; Hsiao et al., 2013). Still, it has not been previously addressed whether similar effects are induced by MSC-derived EVs obtained under hypoxic conditions. Incubation of HUVECs with purified MSC-derived EVs or the corresponding EV-depleted MSC culture supernatants significantly increased vascular tube formation for EVs from hypoxic conditions. The induction was comparable to the positive control, 100 ng/ml VEGF in EGM-2 containing a mixture of growth factors including FGF, epidermal growth factor (EGF) and insulin-like growth factor (IGF). MSC-derived EVs from normoxic conditions, in contrast, induced the formation of only a small number of branches, but no intact loops, which is not consistent with a previous study in which normoxic EVs significantly increased tube formation as compared to the EV-depleted MSC culture supernatant (Lopatina et al., 2014; Nakamura et al., 2015).

Overall, hypoxic conditioning of MSCs appears to increase vascular tube formation induced by MSC-derived EVs, suggesting that the induction of vascular tube formation by MSC-derived EVs is mainly mediated by EVs and to a lesser extent by soluble growth factors or cytokines present in the culture supernatant. This is in line with recent findings that angiogenic effects are mainly promoted by the transfer of miRNAs, such as miR-21, miR-23a, miR-125a, miR-126, and miR-130a (Liang et al., 2016; Gong et al., 2017; Zimta et al., 2019).

While our data indicate that hypoxic preconditioning of MSCs can promote the ability of the corresponding MSC-derived EVs to induce vascular tube formation, further effects of hypoxic preconditioning remain to be elucidated. Hypoxic preconditioning might also increase other effects that are usually enhanced in MSCs from hypoxic conditions, such as chondrogenesis (Malladi et al., 2006), immunosuppressive properties (Roemeling-van Rhijn et al., 2013), or the expression of regenerative growth factors (Wei et al., 2012; Chang et al., 2013).

Our findings highlight the relevance of culture conditions for the generation and composition of MSC-derived EVs, which has already been subject of a number of studies (Phan et al., 2018). MSCs were shown to produce more EVs when cultivated as 3D aggregates as compared to 2D cultivation, and these EVs displayed enhanced angiogenic and neurogenic potential. These effects were further promoted by cultivation of 3D aggregates under dynamic conditions (Cha et al., 2018), and the generation

of EVs was elevated when MSCs were grown on a 3D collagen matrix (Tao et al., 2017). Apparently, physiological culture conditions can increase both, the therapeutic potential of MSCs and the potency of MSC-derived EVs. In this context, bioreactor systems for the expansion of MSCs in 3D aggregates under hypoxic conditions (Egger et al., 2017) are suited to generate and control physiological culture conditions. While the efficiency and the potency of EVs produced in these systems need to be subject of future studies, bioreactor systems will probably play key roles in the stable, large-scale production of MSC-EVs under physiologic conditions (Egger et al., 2018).

CONCLUSIONS

In this study, we characterized MSC-derived EVs from hypoxic conditions in comparison to normoxic MSC-EVs. We found that hypoxia conditioned MSC-EVs induced significantly increased epithelial tube formation when compared to normoxic EVs. This effect was largely mediated by EVs and not by other soluble factors, suggesting that hypoxic conditioning might be used to increase the therapeutic potential of MSC-EVs.

DATA AVAILABILITY STATEMENT

The raw data supporting the conclusions of this manuscript will be made available by the authors, without undue reservation, to any qualified researcher.

ETHICS STATEMENT

The studies involving human participants were reviewed and approved by Ethics committee of the Medical University Vienna, Austria. The patients/participants provided their written informed consent to participate in this study.

AUTHOR CONTRIBUTIONS

CA performed cell culture experiments and tube formation assays and wrote the manuscript. RW designed and performed flow cytometry experiments, interpreted the data, and wrote the manuscript. MR performed cell culture experiments. CT performed NTA measurements and contributed to interpretation of the data and to writing the manuscript. CK and VW designed the study and reviewed the manuscript. DE designed the cell culture experiments, interpreted the data, and wrote the manuscript. All authors read and approved the final manuscript.

FUNDING

This work was funded by the Christian Doppler Society (Christian Doppler Laboratory for Innovative Therapy Approaches in Sepsis).

ACKNOWLEDGMENTS

We are grateful to Prof. Hannes Stockinger from the Medical University of Vienna for providing the immortalized HUVEC cell line.

SUPPLEMENTARY MATERIAL

The Supplementary Material for this article can be found online at: https://www.frontiersin.org/articles/10.3389/fbioe.2019.00292/full#supplementary-material

REFERENCES

Bian, S. Y., Zhang, L. P., Duan, L. F., Wang, X., Min, Y., and Yu, H. P. (2014). Extracellular vesicles derived from human bone marrow mesenchymal stem cells promote angiogenesis in a rat myocardial infarction model. *J. Mol. Med.* 92, 387–397. doi: 10.1007/s00109-013-1110-5

Börger, V., Bremer, M., Ferrer-Tur, R., Gockeln, L., Stambouli, O., Becic, A., et al. (2017). Mesenchymal stem/stromal cell-derived extracellular vesicles and their potential as novel immunomodulatory therapeutic agents. *Int. J. Mol. Sci.* 18:E1450. doi: 10.3390/ijms18071450

Bruno, S., Grange, C., Deregibus, M. C., Calogero, R. A., Saviozzi, S., Collino, F., et al. (2009). Mesenchymal stem cell-derived microvesicles protect against acute tubular injury. *J. Am. Soc. Nephrol.* 20, 1053–1067. doi: 10.1681/ASN.2008070798

Carpentier, G. (2012). *Angiogenesis Analyzer for ImageJ*. Available online at: http://imagej.nih.gov/ij/macros/toolsets/Angiogenesis%20Analyzer.txt

Cha, J. M., Shin, E. K., Sung, J. H., Moon, G. J., Kim, E. H., Cho, Y. H., et al. (2018). Efficient scalable production of therapeutic microvesicles derived from human mesenchymal stem cells. *Sci. Rep.* 8:1171. doi: 10.1038/s41598-018-19211-6

Chang, C. P., Chio, C. C., Cheong, C. U., Chao, C. M., Cheng, B. C., and Lin, M. T. (2013). Hypoxic preconditioning enhances the therapeutic potential of the secretome from cultured human mesenchymal stem cells in experimental traumatic brain injury. *Clin. Sci.* 124, 165–176. doi: 10.1042/CS20120226

Cocucci, E., and Meldolesi, J. (2015). Ectosomes and exosomes: shedding the confusion between extracellular vesicles. *Trends Cell Biol.* 25, 364–372. doi: 10.1016/j.tcb.2015.01.004

Crescitelli, R., Lässer, C., Szabó, T. G., Kittel, A., Eldh, M., Dianzani, I., et al. (2013). Distinct RNA profiles in subpopulations of extracellular vesicles: apoptotic bodies, microvesicles and exosomes. *J. Extracell Vesicles* 2:20677. doi: 10.3402/jev.v2i0.20677

Dai, M., Yu, M., Zhang, Y., and Tian, W. (2017). Exosome-like vesicles derived from adipose tissue provide biochemical cues for adipose tissue regeneration. *Tissue Eng. Part A* 23, 1221–1230. doi: 10.1089/ten.tea.2017.0045

Dragovic, R., Collett, G., Hole, P., Ferguson, D., Redman, C., Sargent, I., et al. (2015). Isolation of syncytiotrophoblast microvesicles and exosomes and their characterisation by multicolour flow cytometry and fluorescence Nanoparticle Tracking Analysis. *Methods* 87, 64–74. doi: 10.1016/j.ymeth.2015.03.028

Dragovic, R. A., Gardiner, C., Brooks, A. S., Tannetta, D. S., Ferguson, D. J., Hole, P., et al. (2011). Sizing and phenotyping of cellular vesicles using Nanoparticle Tracking Analysis. *Nanomed. Nanotechn. Biol. Med.* 7, 780–788. doi: 10.1016/j.nano.2011.04.003

Dufrane, D. (2017). Impact of age on human adipose stem cells for bone tissue engineering. *Cell Transplant.* 26, 1496–1504. doi: 10.1177/0963689717721203

Egger, D., Schwedhelm, I., Hansmann, J., and Kasper, C. (2017). Hypoxic three-dimensional scaffold-free aggregate cultivation of mesenchymal stem cells in a stirred tank reactor. *Bioengineering* 4:E47. doi: 10.3390/bioengineering4020047

Egger, D., Tripisciano, C., Weber, V., Dominici, M., and Kasper, C. (2018). Dynamic cultivation of mesenchymal stem cell aggregates. *Bioengineering* 5:E48. doi: 10.3390/bioengineering5020048

Endzelins, E., Abols, A., Buss, A., Zandberga, E., Palviainen, M., Siljander, P., et al. (2018). Extracellular vesicles derived from hypoxic colorectal cancer cells

confer metastatic phenotype to non-metastatic cancer cells. *Anticancer Res.* 38, 5139–5147. doi: 10.21873/anticanres.12836

Gnecchi, M., Zhang, Z. P., Ni, A. G., and Dzau, V. J. (2008). Paracrine mechanisms in adult stem cell signaling and therapy. *Circ. Res.* 103, 1204–1219. doi: 10.1161/CIRCRESAHA.108.176826

Gong, M., Yu, B., Wang, J. C., Wang, Y. G., Liu, M., Paul, C., et al. (2017). Mesenchymal stem cells release exosomes that transfer miRNAs to endothelial cells and promote angiogenesis. *Oncotarget* 8, 45200–45212. doi: 10.18632/oncotarget.16778

Hsiao, S. T., Lokmic, Z., Peshavariya, H., Abberton, K. M., Dusting, G. J., Lim, S. Y., et al. (2013). Hypoxic conditioning enhances the angiogenic paracrine activity of human adipose-derived stem cells. *Stem Cells Dev.* 22, 1614–1623. doi: 10.1089/scd.2012.0602

Karp, J. M., and Teol, G. S. L. (2009). Mesenchymal stem cell homing: the devil is in the details. *Cell Stem Cell* 4, 206–216. doi: 10.1016/j.stem.2009.02.001

Kilic, T., Valinhas, A. T. D., Wall, I., Renaud, P., and Carrara, S. (2018). Label-free detection of hypoxia-induced extracellular vesicle secretion from MCF-7 cells. *Sci. Rep.* 8:9402. doi: 10.1038/s41598-018-27203-9

King, H. W., Michael, M. Z., and Gleadle, J. M. (2012). Hypoxic enhancement of exosome release by breast cancer cells. *BMC Cancer* 12:421. doi: 10.1186/1471-2407-12-421

Kinnaird, T., Stabile, E., Burnett, M., Lee, C., Barr, S., Fuchs, S., et al. (2004). Marrow-derived stromal cells express genes encoding a broad spectrum of arteriogenic cytokines and promote *in vitro* and *in vivo* arteriogenesis through paracrine mechanisms. *Circ. Res.* 94, 678–685. doi: 10.1161/01.RES.0000118601.37875.AC

Lane, R. E., Korbie, D., Trau, M., and Hill, M. M. (2017). "Purification protocols for extracellular vesicles," in *Extracellular Vesicles. Methods in Molecular Biology*, Vol. 1660, eds W. Kuo and S. Jia (New York, NY: Springer; Humana Press), 111–130. doi: 10.1007/978-1-4939-7253-1_10

Lavrentieva, A., Majore, I., Kasper, C., and Hass, R. (2010). Effects of hypoxic culture conditions on umbilical cord-derived human mesenchymal stem cells. *Cell Commun. Signal.* 8:18. doi: 10.1186/1478-811X-8-18

Li, X., Liu, L. L., Yao, J. L., Wang, K., and Ai, H. (2019). Human umbilical cord mesenchymal stem cell-derived extracellular vesicles inhibit endometrial cancer cell proliferation and migration through delivery of exogenous miR-302a. *Stem Cells Int.* 2019:8108576. doi: 10.1155/2019/8108576

Liang, X., Zhang, L., Wang, S., Han, Q., and Zhao, R. C. (2016). Exosomes secreted by mesenchymal stem cells promote endothelial cell angiogenesis by transferring miR-125a. *J. Cell Sci.* 129, 2182–2189. doi: 10.1242/jcs.170373

Liu, M., Lei, H., Dong, P., Fu, X., Yang, Z., Yang, Y., et al. (2017). Adipose-derived mesenchymal stem cells from the elderly exhibit decreased migration and differentiation abilities with senescent properties. *Cell Transplant.* 26, 1505–1519. doi: 10.1177/0963689717721221

Lo Sicco, C., Reverberi, D., Balbi, C., Ulivi, V., Principi, E., Pascucci, L., et al. (2017). Mesenchymal stem cell-derived extracellular vesicles as mediators of anti-inflammatory effects: endorsement of macrophage polarization. *Stem Cells Transl. Med.* 6, 1018–1028. doi: 10.1002/sctm.16-0363

Lopatina, T., Bruno, S., Tetta, C., Kalinina, N., Porta, M., and Camussi, G. (2014). Platelet-derived growth factor regulates the secretion of extracellular vesicles by adipose mesenchymal stem cells and enhances their angiogenic potential. *Cell Commun. Signal.* 12:26. doi: 10.1186/1478-811X-12-26

Malladi, P., Xu, Y., Chiou, M., Giaccia, A. J., and Longaker, M. T. (2006). Effect of reduced oxygen tension on chondrogenesis and osteogenesis in adipose-derived mesenchymal cells. *Am. J. Physiol. Cell Physiol.* 290, C1139–1146. doi: 10.1152/ajpcell.00415.2005

Mastrolia, I., Foppiani, E. M., Murgia, A., Candini, O., Samarelli, A. V., Grisendi, G., et al. (2019). Concise review: challenges in clinical development of mesenchymal stromal/stem cells. *Stem Cells Transl. Med.* doi: 10.1002/sctm.19-0044. [Epub ahead of print].

Merino-Gonzalez, C., Zuniga, F. A., Escudero, C., Ormazabal, V., Reyes, C., Nova-Lamperti, E., et al. (2016). Mesenchymal stem cell-derived extracellular vesicles promote angiogenesis: potencial clinical application. *Front. Physiol.* 7:24. doi: 10.3389/fphys.2016.00024

Monsel, A., Zhu, Y.-g., Gennai, S., Hao, Q., Hu, S., Rouby, J.-J., et al. (2015). Therapeutic effects of human mesenchymal stem cell–derived microvesicles in severe pneumonia in mice. *Am. J. Respir. Crit. Care Med.* 192, 324–336. doi: 10.1164/rccm.201410-1765OC

Morrison, T. J., Jackson, M. V., Cunningham, E. K., Kissenpfennig, A., McAuley, D. F., O'Kane, C. M., et al. (2017). Mesenchymal stromal cells modulate macrophages in clinically relevant lung injury models by extracellular vesicle mitochondrial transfer. *Am. J. Respir. Crit. Care Med.* 196, 1275–1286. doi: 10.1164/rccm.201701-0170OC

Nakamura, Y., Miyaki, S., Ishitobi, H., Matsuyama, S., Nakasa, T., Kamei, N., et al. (2015). Mesenchymal-stem-cell-derived exosomes accelerate skeletal muscle regeneration. *FEBS Lett.* 589, 1257–1265. doi: 10.1016/j.febslet.2015.03.031

Nekanti, U., Dastidar, S., Venugopal, P., Totey, S., and Ta, M. (2010). Increased proliferation and analysis of differential gene expression in human Wharton's jelly-derived mesenchymal stromal cells under hypoxia. *Int. J. Biol. Sci.* 6:499. doi: 10.7150/ijbs.6.499

Neumann, A., Lavrentieva, A., Heilkenbrinker, A., Loenne, M., and Kasper, C. (2014). Characterization and application of a disposable rotating bed bioreactor for mesenchymal stem cell expansion. *Bioengineering* 1, 231–245. doi: 10.3390/bioengineering1040231

Ohyashiki, J. H., Umezu, T., and Ohyashiki, K. (2018). Extracellular vesicle-mediated cell-cell communication in haematological neoplasms. *Philos. Trans. Roy. Soc. B Biol. Sci.* 372:1737. doi: 10.1098/rstb.2016.0484

Patel, D. B., Gray, K. M., Santharam, Y., Lamichhane, T. N., Stroka, K. M., and Jay, S. M. (2017). Impact of cell culture parameters on production and vascularization bioactivity of mesenchymal stem cell-derived extracellular vesicles. *Bioeng. Trans. Med.* 2, 170–179. doi: 10.1002/btm2.10065

Phan, J., Kumar, P., Hao, D., Gao, K., Farmer, D., and Wang, A. J. (2018). Engineering mesenchymal stem cells to improve their exosome efficacy and yield for cell-free therapy. *J. Extracell Vesicles* 7:1522236. doi: 10.1080/20013078.2018.1522236

Phinney, D. G., and Pittenger, M. F. (2017). Concise review: MSC-derived exosomes for cell-free therapy. *Stem Cells* 35, 851–858. doi: 10.1002/stem.2575

Ramos, T. L., Sanchez-Abarca, L. I., Muntion, S., Preciado, S., Puig, N., Lopez-Ruano, G., et al. (2016). MSC surface markers (CD44, CD73, and CD90) can identify human MSC-derived extracellular vesicles by conventional flow cytometry. *Cell Commun. Signal.* 14:2. doi: 10.1186/s12964-015-0124-8

Reis, M., Mavin, E., Nicholson, L., Green, K., Dickinson, A. M., and Wang, X. N. (2018). Mesenchymal stromal cell-derived extracellular vesicles attenuate dendritic cell maturation and function. *Front. Immunol.* 9:2538. doi: 10.3389/fimmu.2018.02538

Roemeling-van Rhijn, M., Mensah, F. K., Korevaar, S. S., Leijs, M. J., van Osch, G. J., Ijzermans, J. N., et al. (2013). Effects of hypoxia on the immunomodulatory properties of adipose tissue-derived mesenchymal stem cells. *Front. Immunol.* 4:203. doi: 10.3389/fimmu.2013.00203

Salomon, C., Ryan, J., Sobrevia, L., Kobayashi, M., Ashman, K., Mitchell, M., et al. (2013). Exosomal signaling during hypoxia mediates microvascular endothelial cell migration and vasculogenesis. *PLoS ONE* 8:e68451. doi: 10.1371/journal.pone.0068451

Saunderson, S. C., Schuberth, P. C., Dunn, A. C., Miller, L., Hock, B. D., MacKay, P. A., et al. (2008). Induction of exosome release in primary B cells stimulated via CD40 and the IL-4 receptor. *J. Immunol.* 180, 8146–8152. doi: 10.4049/jimmunol.180.12.8146

Schiller, H. B., Szekeres, A., Binder, B. R., Stockinger, H., and Leksa, V. (2009). Mannose 6-phosphate/insulin-like growth factor 2 receptor limits cell invasion by controlling alpha V beta 3 integrin expression and proteolytic processing of urokinase-type plasminogen activator receptor. *Mol. Biol. Cell* 20, 745–756. doi: 10.1091/mbc.e08-06-0569

Simpson, R. J., Jensen, S. S., and Lim, J. W. (2008). Proteomic profiling of exosomes: current perspectives. *Proteomics* 8, 4083–4099. doi: 10.1002/pmic.200800109

Sokolova, V., Ludwig, A.-K., Hornung, S., Rotan, O., Horn, P. A., Epple, M., et al. (2011). Characterisation of exosomes derived from human cells by nanoparticle tracking analysis and scanning electron microscopy. *Coll. Surf. B Biointerfaces* 87, 146–150. doi: 10.1016/j.colsurfb.2011.05.013

Sorrell, J. M., Baber, M. A., and Caplan, A. I. (2009). Influence of adult mesenchymal stem cells on *in vitro* vascular formation. *Tissue Eng. Part A* 15, 1751–1761. doi: 10.1089/ten.tea.2008.0254

Squillaro, T., Peluso, G., and Galderisi, U. (2016). Clinical trials with mesenchymal stem cells: an update. *Cell Transplant.* 25, 829–848. doi: 10.3727/096368915X689622

Stubbs, S. L., Hsiao, S. T., Peshavariya, H. M., Lim, S. Y., Dusting, G. J., and Dilley, R. J. (2012). Hypoxic preconditioning enhances survival of human adipose-derived stem cells and conditions endothelial cells *in vitro*. *Stem Cells Dev.* 21, 1887–1896. doi: 10.1089/scd.2011.0289

Subra, C., Laulagnier, K., Perret, B., and Record, M. (2007). Exosome lipidomics unravels lipid sorting at the level of multivesicular bodies. *Biochimie* 89, 205–212. doi: 10.1016/j.biochi.2006.10.014

Tao, S. C., Guo, S. C., Li, M., Ke, Q. F., Guo, Y. P., and Zhang, C. Q. (2017). Chitosan wound dressings incorporating exosomes derived from MicroRNA-126-overexpressing synovium mesenchymal stem cells provide sustained release of exosomes and heal full-thickness skin defects in a diabetic rat model. *Stem Cells Transl. Med.* 6, 736–747. doi: 10.5966/sctm.2016-0275

Thery, C., Ostrowski, M., and Segura, E. (2009). Membrane vesicles as conveyors of immune responses. *Nat. Rev. Immunol.* 9, 581–593. doi: 10.1038/nri2567

Thery, C., Witwer, K. W., Aikawa, E., Alcaraz, M. J., Anderson, J. D., Andriantsitohaina, R., et al. (2018). Minimal information for studies of extracellular vesicles 2018 (MISEV2018): a position statement of the International Society for Extracellular Vesicles and update of the MISEV2014 guidelines. *J. Extracell Vesicles* 7:1535750. doi: 10.1080/20013078.2018.1535750

Théry, C., Zitvogel, L., and Amigorena, S. (2002). Exosomes: composition, biogenesis and function. *Nat. Rev. Immunol.* 2:569. doi: 10.1038/nri855

Tripisciano, C., Weiss, R., Eichhorn, T., Spittler, A., Heuser, T., Fischer, M. B., et al. (2017). Different potential of extracellular vesicles to support thrombin generation: contributions of phosphatidylserine, tissue factor, and cellular origin. *Sci. Rep.* 7:6522. doi: 10.1038/s41598-017-03262-2

Valadi, H., Ekström, K., Bossios, A., Sjöstrand, M., Lee, J. J., and Lötvall, J. O. (2007). Exosome-mediated transfer of mRNAs and microRNAs is a novel mechanism of genetic exchange between cells. *Nat. Cell Biol.* 9:654. doi: 10.1038/ncb1596

Valandani, H. M., Amirizadeh, N., Nikougoftar, M., Safa, M., Khalilabadi, R. M., and Kazemi, A. (2018). Effect of extracellular vesicles derived from mesenchymal stem cells on K-562 leukemia cell line. *Iran. Red Crescent Med. J.* 20:e64991. doi: 10.5812/ircmj.64991

Wagner, J., Kean, T., Young, R., Dennis, J. E., and Caplan, A. I. (2009). Optimizing mesenchymal stem cell-based therapeutics. *Curr. Opin. Biotechnol.* 20, 531–536. doi: 10.1016/j.copbio.2009.08.009

Wei, L., Fraser, J. L., Lu, Z. Y., Hu, X., and Yu, S. P. (2012). Transplantation of hypoxia preconditioned bone marrow mesenchymal stem cells enhances angiogenesis and neurogenesis after cerebral ischemia in rats. *Neurobiol. Dis.* 46, 635–645. doi: 10.1016/j.nbd.2012.03.002

Weiss, R., Gröger, M., Rauscher, S., Fendl, B., Eichhorn, T., Fischer, M. B., et al. (2018). Differential interaction of platelet-derived extracellular vesicles with leukocyte subsets in human whole blood. *Sci. Rep.* 8:6598. doi: 10.1038/s41598-018-25047-x

Wiklander, O. P., Bostancioglu, R. B., Welsh, J. A., Zickler, A. M., Murke, F., Corso, G., et al. (2018). Systematic methodological evaluation of a multiplex bead-based flow cytometry assay for detection of extracellular vesicle surface signatures. *Front. Immunol.* 9:1326. doi: 10.3389/fimmu.2018.01326

Williams, A. R., and Hare, J. M. (2011). Mesenchymal stem cells: biology, pathophysiology, translational findings, and therapeutic implications for cardiac disease. *Circ. Res.* 109, 923–940. doi: 10.1161/CIRCRESAHA.111.243147

Willms, E., Cabañas, C., Mäger, I., Wood, M. J., and Vader, P. (2018). Extracellular vesicle heterogeneity: subpopulations, isolation techniques, and diverse functions in cancer progression. *Front. Immunol.* 9:738. doi: 10.3389/fimmu.2018.00738

Witwer, K. W., Van Balkom, B. W. M., Bruno, S., Choo, A., Dominici, M., Gimona, M., et al. (2019). Defining mesenchymal stromal cell (MSC)-derived small extracellular vesicles for therapeutic applications. *J. Extracell. Vesicles* 8:1609206. doi: 10.1080/20013078.2019.1609206

Wyss, R., Grasso, L., Wolf, C., Grosse, W., Demurtas, D., and Vogel, H. (2014). Molecular and dimensional profiling of highly purified extracellular vesicles by fluorescence fluctuation spectroscopy. *Anal. Chem.* 86, 7229–7233. doi: 10.1021/ac501801m

Yeo, R. W. Y., Lai, R. C., Tan, K. H., and Lim, S. K. (2013). Exosome: a novel and safer therapeutic refinement of mesenchymal stem cell. *Exosomes Microvesicles* 1:7. doi: 10.5772/57460

Yu, X., Deng, L. Y., Wang, D., Li, N., Chen, X., Cheng, X., et al. (2012). Mechanism of TNF-alpha autocrine effects in hypoxic cardiomyocytes: Initiated by hypoxia inducible factor 1 alpha, presented by exosomes. *J. Mol. Cell. Cardiol.* 53, 848–857. doi: 10.1016/j.yjmcc.2012.10.002

Zimta, A. A., Baru, O., Badea, M., Buduru, S. D., and Berindan-Neagoe, I. (2019). The role of angiogenesis and pro-angiogenic exosomes in regenerative dentistry. *Int. J. Mol. Sci.* 20:406. doi: 10.3390/ijms20020406

Conflict of Interest: The authors declare that the research was conducted in the absence of any commercial or financial relationships that could be construed as a potential conflict of interest.

frontiers in Bioengineering and Biotechnology

ORIGINAL RESEARCH
published: 01 November 2019
doi: 10.3389/fbioe.2019.00294

Bone Marrow Mesenchymal Stem Cells' Secretome Exerts Neuroprotective Effects in a Parkinson's Disease Rat Model

Bárbara Mendes-Pinheiro[1,2], Sandra I. Anjo[3], Bruno Manadas[3], Jorge D. Da Silva[1,2], Ana Marote[1,2], Leo A. Behie[4], Fábio G. Teixeira[1,2†] and António J. Salgado[1,2†]*

[1] Life and Health Sciences Research Institute (ICVS), School of Medicine, University of Minho, Campus de Gualtar, Braga, Portugal, [2] ICVS/3B's-PT Government Associate Laboratory, Braga/Guimarães, Portugal, [3] CNC-Center for Neuroscience and Cell Biology, University of Coimbra, Coimbra, Portugal, [4] Canada-Research Chair in Biomedical Engineering (Emeritus), Schulich School of Engineering, University of Calgary, Calgary, AB, Canada

OPEN ACCESS

Edited by:
Wolfgang Holnthoner, Ludwig Boltzmann Gesellschaft (LBG), Austria

Reviewed by:
Livia Visai, University of Pavia, Italy
Seyed Mahmoud Hashemi, Shahid Beheshti University of Medical Sciences, Iran

***Correspondence:**
António J. Salgado
asalgado@med.uminho.pt

[†]These authors share senior authorship

Specialty section:
This article was submitted to Tissue Engineering and Regenerative Medicine, a section of the journal Frontiers in Bioengineering and Biotechnology

Received: *19 July 2019*
Accepted: *09 October 2019*
Published: *01 November 2019*

Citation:
Mendes-Pinheiro B, Anjo SI, Manadas B, Da Silva JD, Marote A, Behie LA, Teixeira FG and Salgado AJ (2019) Bone Marrow Mesenchymal Stem Cells' Secretome Exerts Neuroprotective Effects in a Parkinson's Disease Rat Model. Front. Bioeng. Biotechnol. 7:294. doi: 10.3389/fbioe.2019.00294

Parkinson's disease (PD) is characterized by a selective loss of dopamine (DA) neurons in the human midbrain causing motor dysfunctions. The exact mechanism behind dopaminergic cell death is still not completely understood and, so far, no cure or neuroprotective treatment for PD is available. Recent studies have brought attention to the variety of bioactive molecules produced by mesenchymal stem cells (MSCs), generally referred to as the secretome. Herein, we evaluated whether human MSCs-bone marrow derived (hBMSCs) secretome would be beneficial in a PD pre-clinical model, when compared directly with cell transplantation of hBMSCs alone. We used a 6-hydroxydpomanie (6-OHDA) rat PD model, and motor behavior was evaluated at different time points after treatments (1, 4, and 7 weeks). The impact of the treatments in the recovery of DA neurons was estimated by determining TH-positive neuronal densities in the *substantia nigra* and fibers in the striatum, respectively, at the end of the behavioral characterization. Furthermore, we determined the effect of the hBMSCs secretome on the neuronal survival of human neural progenitors *in vitro*, and characterized the secretome through proteomic-based approaches. This work demonstrates that the injection of hBMSCs secretome led to the rescue of DA neurons, when compared to transplantation of hBMSCs themselves, which can explain the recovery of secretome-injected animals' behavioral performance in the staircase test. Moreover, we observed that hBMSCs secretome induces higher levels of *in vitro* neuronal differentiation. Finally, the proteomic analysis revealed that hBMSCs secrete important exosome-related molecules, such as those related with the ubiquitin-proteasome and histone systems. Overall, this work provided important insights on the potential use of hBMSCs secretome as a therapeutic tool for PD, and further confirms the importance of the secreted molecules rather than the transplantation of hBMSCs for the observed positive effects. These could be likely through normalization of defective processes in PD, namely proteostasis or altered gene transcription, which lately can lead to neuroprotective effects.

Keywords: Parkinson's disease, mesenchymal stem cells, secretome, dopamine neurons, neuroprotection

INTRODUCTION

Parkinson's disease (PD) represents the second most common neurodegenerative disorder after Alzheimer's disease, affecting ∼1% of the population worldwide over 65 years old (Vos et al., 2017). Its pathogenesis is characterized by the death of dopamine (DA) neurons in the *substantia nigra* pars compacta (SNpc), leading to a decrease of DA levels in the striatum, which consequently causes typical motor dysfunctions, such as tremor ate rest, rigidity, bradykinesia, among others (Przedborski, 2017; Axelsen and Woldbye, 2018). Another important hallmark feature of PD is the presence of Lewy bodies that are abnormal aggregates of proteins enriched in α-synuclein (Axelsen and Woldbye, 2018). Current therapies, such as the administration of DA analogs or deep brain stimulation, are only focused on reducing the symptoms but fail to stop disease progression or to rescue the cells and the neuronal circuit (Anisimov, 2009; Sethi, 2010). On the other hand, stem cell-based therapies have been providing great opportunities to develop innovative strategies for PD therapy (Mahla, 2016). Within a variety of promising cell sources, mesenchymal stem cells (MSCs) have stood out as a valid therapeutic option (Mendes-Pinheiro, 2016). The initial research claimed that the engraftment and differentiation capacity of MSCs was the main responsible mechanism of their therapeutical effects. However, recent studies brought attention to the bioactive molecules produced by MSCs, generally referred to as the secretome (Teixeira et al., 2013; Vizoso et al., 2017). Among these set of factors/molecules released by MSCs we can list the soluble proteins (e.g., cytokines, chemokines, and growth factors), lipids and the extracellular vesicles, that are known for the capacity of promoting cell survival and differentiation, prevent neuronal cell death, protect other cells from oxidative stress or even regulate inflammatory processes (Baraniak and McDevitt, 2010; Teixeira et al., 2013; Marques et al., 2018). Previously, we have already shown that human MSCs-bone marrow derived (hBMSCs) secretome potentiated the increase of tyrosine hydroxylase (TH)-positive in the SNpc and striatum, respectively, which supports the improvements observed in the Parkinsonian animals (Teixeira et al., 2017). In fact, the use of secretome *per se* presents numerous advantages when compared with more conventional stem-cell based applications, regarding manufacturing, storage, handling, their potential as a ready-to-use biologic product and lack of immunosuppression-based adjuvant therapies (Vizoso et al., 2017). For instance, the time and cost of expansion and maintenance of cultured MSCs could be significantly reduced, and the storage can be done for long periods without loss of product potency and quality (Bermudez et al., 2015, 2016; Vizoso et al., 2017). The production in large quantities is possible under controlled laboratory conditions and the biological product could be modified to desired cell-specific effects (McKee and Chaudhry, 2017; Vizoso et al., 2017). Importantly, the use of the secretome derivatives could bypass potential issues associated with cell transplantation including the number of available cells for transplantation and its survival after this procedure, immune compatibility, tumorigenicity, and infection transmission (Tran and Damaser, 2015).

In view of the above, the main objective of this work was to study the efficacy of hBMSCs secretome when compared to the traditional approach in the field, that is hBMSCs transplantation, particularly on DA neurons survival and motor function of a 6-hydroxydopamine (6-OHDA) rat PD model. Here, we demonstrate that hBMSCs secretome was able to minimize the loss of DA neurons and ameliorates the motor deficits of 6-OHDA-lesioned animals. Moreover, we also observed that hBMSCs were able to induce neuronal differentiation *in vitro* and highlighted possible proteins and mechanisms that could mediate the above referred actions.

MATERIALS AND METHODS

Human Bone Marrow Mesenchymal Stem Cells Preparation

hBMSCs (Lonza, Switzerland) were defreeze and plated into T-75 gelatin (0.1%, Sigma, USA)-coated culture flasks with serum-free growth medium (PPRF-msc6) that was prepared as described elsewhere in detail (Jung et al., 2010). The medium changes were done every 3 days, and after reached 80% of confluence, cells were harvested using 0.05% trypsin/EDTA (Invitrogen, USA) and plated again in gelatin-coated flasks at a density of 5,000 cells/cm^2. For all *in vitro* experiments, hBMSCs from three different donors were used. The hBMSCs used in this work were previously characterized by our lab (Teixeira et al., 2016), being positive for the standard hMSCs markers CD13, CD73, CD90, and CD105, and negative for CD34, CD45, and HLA-DR.

Secretome Collection and Concentration

The secretome of hBMSCs was collected under the form of conditioned medium in passage 5 (P5) according to protocols already established in our laboratory (Fraga et al., 2013; Teixeira et al., 2016). Briefly, cells were seeded at a density of 5,000 cells/cm^2 for the *in vivo* experiments and 12,000 cells/cm^2 for proteomic analysis. After 3 days in culture, the cells were washed three times with PBS without Ca^{2+}/Mg^{2+} (Invitrogen), and once with Neurobasal-A medium (TermoFisher Scientific, USA) supplemented with 1% kanamycin (Life Technologies, USA), being incubated with this medium during 24 h. In the next day, the medium comprising the elements secreted by hBMSCs was collected and centrifuged at 1,200 rpm (Megafuge 1.0R, Heraeus, Germany) for 10 min to remove any cell debris. Then, hBMSCs secretome was concentrated (100×) by centrifugation using a 5 kDa cut-off concentrator (Vivaspin, GE Healthcare, UK) and frozen at −80°C until used for proteomic analysis and surgical procedures, as previously described (Mendes-Pinheiro et al., 2018).

Neural Progenitor Cells Growth and Incubation With hBMSCs Secretome

For neuronal differentiation studies, pre-isolated and cryopreserved human neural progenitor cells (hNPCs) were thawed at 37°C and grew as neurospheres in serum-free medium PPRF-h2 (Baghbaderani et al., 2010; Mendes-Pinheiro, 2016). Cells were isolated in respect with the protocols and strict ethical guidelines previously established and approved by the Conjoint

Health Research Ethics Board (CHREB, University of Calgary, Canada; ID: E-18786) (Mendez et al., 2002, 2005; Baghbaderani et al., 2010). After 3 days, cells were mechanically triturated to form single cells and cultivated again in fresh medium. After 14–20 days of growth, hNPCs were enzymatically dissociated and plated on 24-well plates coated with poly-D-lysine (100 μg/mL; Sigma) and laminin (10 μg/mL; Sigma) using 50,000 cells per well. The cells were exposed for 5 days to hBMSCs secretome, and supplemented Neurobasal-A medium [differentiation media; 2% B27 (Gibco, USA), 0.05% basic fibroblast growth factor (bFGF; R&D Systems, USA), 1% kanamycin, and 0.5% GlutaMAX (Gibco)] was used as positive control, and Neurobasal-A medium only with 1% kanamycin (basal media) was used as negative control group (Mendes-Pinheiro, 2016).

Immunocytochemical Staining

hNPCs were fixed in 4% paraformaldehyde (PFA; Merck, Portugal) for 30 min at room temperature (RT), to retain the antigenicity of the target molecules and preserve cell morphology. The permeabilization was done in phosphate buffered saline (PBS) with 0.1% Triton X-100 (PBS-T; Sigma) for 5 min, followed by blockage of non-specific binding sites using PBS with 10% newborn calf serum (NBCS; Biochrom, Germany) for 1 h. hNPCs were then incubated with the following primary antibodies: anti-doublecortin (DCX, rabbit polyclonal IgG, 1:300; ab18723, Abcam, UK) for immature neurons and anti-microtubule associated protein-2 for mature neurons (MAP-2, mouse monoclonal IgG, 1:500; M4403, Sigma), diluted in PBS with 10% NBCS for 1 h at RT. After washing, cells were incubated with the secondary antibodies Alexa Fluor 488 goat anti-rabbit (1:1000; Life Technologies) or Alexa Fluor 594 goat anti-mouse (1:1000; Life Technologies) for 1 h at RT. Nuclei were stained with 4-6-diamidino-2-phenylindole-dhydrochloride (DAPI, 1:1000; Life Technologies) for 10 min at RT. Afterwards, coverslips were mounted on glass slides using immu-mount (Thermo Scientific, UK). Finally, samples were observed using fluorescence microscopy (BX61, Olympus, Germany), being 3 coverslips per condition and 10 representative fields chosen for quantification analysis. The overall proportions of DCX or MAP-2-positive cells in all experiments were pooled and used for comparison between groups, and the quantification was done under blind conditions.

Subjects and Surgical Procedures

All animal experimentation was performed with the consent to the Portuguese national authority for animal research, Direção Geral de Alimentação e Veterinária (ID: DGAV28421) and Ethical Subcommittee in Life and Health Sciences (SECVS; ID: SECVS-008/2013, University of Minho). We used 8-weeks old *Wistar-Han* male rats (260–300 g; Charles River, Spain) that were caged in pairs with food and water *ad libitum*, in a temperature/humidity controlled-room maintained on 12 h light/dark cycles.

All surgical procedures were performed as previously described by our group (Teixeira et al., 2017; Mendes-Pinheiro et al., 2018). Succinctly, the PD model was induced by a unilateral stereotaxic injection of 20 mM 6-OHDA dissolved in saline containing 0.2 mg/mL ascorbic acid. The 6-OHDA group was injected with 2 μL of 6-OHDA in the right medial forebrain bundle (MFB; $n = 15$), and the sham group ($n = 9$) received an equal volume of vehicle solution in the same brain region. Five weeks later, some animals received hBMSCs transplants and others hBMSCs secretome in the SNpc and striatum (four different sites), and the groups were divided as follows: 6-OHDA control group (Neurobasal-A medium; $n = 5$), Sham group (sterile saline; $n = 9$), hBMSCs transplants ($n = 4$), and hBMSCs secretome ($n = 6$). The 6-OHDA-control group received 4 μL of 100× concentrated Neurobasal-A medium in the SNpc and 2 μL in each coordinate of striatum. The same volumes and concentrations were injected in the animals that received hBMSCs secretome. Cell transplanted groups received 200,000 cells (suspended in serum-free medium) in SNpc and 200,000 cells in the striatum divided equally for each coordinate (Mendes-Pinheiro, 2016). The coordinates used in this work were done according to the rat brain atlas Paxinos and Watson (2007) as already reported (Teixeira et al., 2017; Mendes-Pinheiro et al., 2018).

Behavioral Testing

Three weeks after 6-OHDA injections, animals were submitted to a first behavioral analysis for PD model characterization. In order to address the impact of hBMSCs transplants or hBMSCs secretome injections on motor performance of the animals, behavioral assessment was performed at 1, 4, and 7 weeks after treatments (**Figure 1**). Firstly, rats were tested in the rotarod apparatus (3376-4R, TSE systems, USA) to evaluate their motor coordination and balance as previously described (Monville et al., 2006). Then, to assess the fine motor control, the staircase test was performed using the protocol developed by Montoya et al. (1991).

Last, in order to estimate the dopaminergic denervation and to select the animals that were truly lesioned upon 6-OHDA injections, the rotameter test using apomorphine was performed as previously described (Carvalho et al., 2013).

TH Immunohistochemistry and Quantification in SNpc and Striatum

To further evaluate the degree of dopaminergic preservation, immunohistochemical staining for TH was performed. For that, animals were sacrificed after 13 weeks (including lesion characterization and behavioral assessment after treatments) with sodium pentobarbital (Eutasil, 60 mg/kg, i.p.; Ceva Saúde Animal, Portugal) and perfused through the ascending aorta with 4% PFA in PBS. Brains were post-fixed in 4% PFA during 24 h, followed by 30% sucrose in PBS for 1 week. Coronal striatal and mesencephalon sections were obtained using a vibratome (VT1000S, Leica, Germany) with 50 μm of thickness. For TH staining, the endogenous peroxidases activity was stopped in the free-floating sections using 3% hydrogen peroxidase for 20 min at RT, followed by permeabilization in 0.1% PBS-T for 10 min (three times) and blockage in PBS 10% NBCS. After this, the sections were incubated with anti-TH (rabbit polyclonal IgG, 1:2,000; Merck Millipore) overnight at 4°C. In the next day, sections were incubated with a

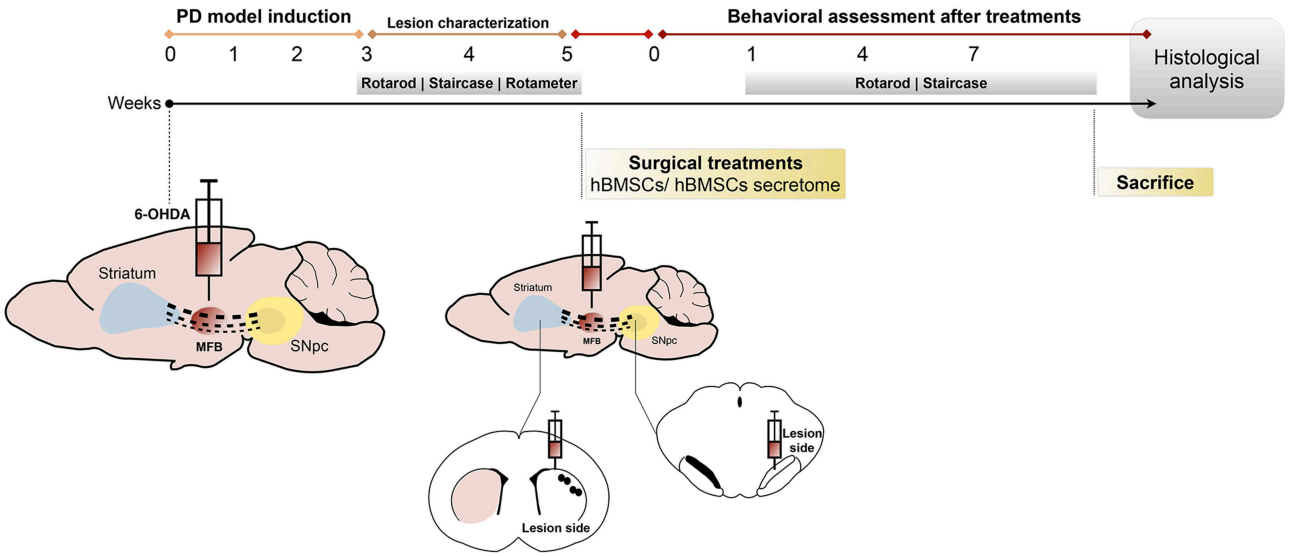

FIGURE 1 | Design of the *in vivo* experiments. The animals were unilaterally injected with 6-OHDA directly into the MFB. After 3 weeks, animals were behaviorally characterized (through rotarod, staircase and rotameter tests) to validate the model. At week 5, 6-OHDA-lesioned animals received hBMSCs transplants or hBMSCs secretome in the SNpc and striatum. Behavior analysis was performed 1, 4, and 7 weeks after treatments, using the rotarod and staircase tests, and posteriorly sacrificed to proceed with the histological analysis.

biotinylated secondary antibody (goat anti-polyvalent, TP-125-BN, ThermoFisher Scientific), followed by strepptavidine-peroxidase solution (TP-125-HR, ThermoFisher Scientific) for 30 min at RT. Antigen revelation was done using of 3,3′-diaminobenzidine tetrahydrochloride (DAB; D5905, Sigma) (25 mg DAB in 50 ml Tris–HCl 0.05 M with 12.5 µl H_2O_2, pH 7.6). Sections were mounted on slides, and after 24 h drying in the dark, they were counter-colored with thionin (Mendes-Pinheiro, 2016).

The estimation of the TH-positive cells' preservation was done by counting the total number of DA neurons in the SNpc and by densitometry analysis of the fibers in the striatum, in both hemispheres, as already described in detail (Teixeira et al., 2017). Four slices per animal were randomly chosen for evaluation and all the analysis was performed under blind conditions. Data is presented as the percentage (%) of remaining TH-positive cells in the lesioned side compared to the control side (intact side) for both regions.

Untargeted Mass Spectrometry Proteomic Analysis

In order to characterize the hBMSCs secretome we performed a non-targeted proteomic analysis based on a combined mass spectrometry (MS) approach as previously described (Mendes-Pinheiro et al., 2018). Only proteins with at least two confidently identified peptides were considered as positive identifications. Peptide's confidence was assessed by a False Discovery Analysis (FDR) and a minimum of 99% confidence (<1% FDR) was used to select the peptides. Three biological replicates of secretome were processed, and proteins that were just identified in a single biological replicate were not considered for analysis. The MS proteomics data have been deposited to the ProteomeXchange Consortium via the PRIDE (Perez-Riverol et al., 2019) partner repository with the dataset identifier PXD014887. The final list of proteins (**Supplementary Material**) was used for gene ontology characterization (levels 2 and 3) using PANTHER (Mi et al., 2013), regarding molecular function, protein class and signaling pathways. A levels 4 and 5 gene ontology analysis was performed through an over-representation analysis using the ConsensusPathDB (Kamburov et al., 2013), for molecular function. Protein complex-based gene sets were determined using the same software, and assuming a minimum complex size of 2, minimum overlap with input list of 2, and *p*-value cutoff of 1%. The two most represented protein complexes are shown, based on the *p*-value for association.

Statistics

A confidence interval of 95% was assumed for all statistical tests. The assumption of normality was tested for all continuous variables through evaluation of the frequency distribution histogram, the values of skewness and kurtosis and through the Shapiro-Wilk test. The assumption of homoscedasticity was tested through Levene's test. Both assumptions were met by all tested continuous variables. All continuous data is shown as the mean as mean ± SEM. For the comparison of proportions between different groups, a Chi-square test was performed, followed by a z-test for the comparison of independent proportions with the Bonferroni correction. For the comparison of means between two groups, a Student's *t*-test for independent samples was used, when data was continuous; for discrete data, a Mann-Whitney U test was

carried out. For the evaluation of mean differences in samples with one independent and one repeated measures variable, a mixed design ANOVA was carried out, with Tukey's *post-hoc* test for pairwise comparison of the independent variable. Statistical analysis was performed using IBM SPSS Statistics ver.24 (IBM Co., USA) and graphic representation using GraphPad Prism ver.7.0c (GraphPad Software; La Jolla, USA).

RESULTS

Effects of hBMSCs Secretome on Neuronal Differentiation *in vitro*

hNPCs grow as neurospheres in the presence of PPRF-h2 serum-free medium as previously described (Baghbaderani et al., 2010; Teixeira et al., 2015). Typically, upon removal of their growth medium hNPCs lose their neurosphere-like conformation, adhere and spontaneously start to differentiate. The differentiation of hNPCs was further confirmed by immunocytochemistry analysis for DCX and MAP-2, after 5 days in culture, staining for immature and early stage mature neurons, respectively. As expected, hNPCs with basal media (negative control) were unable to differentiate, while cells with differentiation medium (positive control) showed positive differentiation for both MAP-2 and DCX neurons (**Figures 2A–D**). Interestingly, the hBMSCs secretome was also able to increase the proportion of differentiated neurons, as shown by an increase in MAP-2 staining, similar to differentiation rates of standard neuronal differentiation media-treated cells (**Figures 2E–H**).

Injection of hBMSCs Secretome Attenuates the Fine Motor Deficits of 6-OHDA-Lesioned Animals

Three weeks after 6-OHDA injections into the MFB (**Figure 3A**), rats were behaviorally characterized in order to evaluate PD-like symptoms. To access the motor function of the animals, rotarod and the staircase tests were performed. Motor coordination and balance, assessed by the rotarod test, was found to be impaired in animals injected with 6-OHDA (**Figure 3B**). In the staircase test, performed to assess the forelimb use and skilled motor function, it was also observed that the 6-OHDA-injected animals were significantly affected when compared to sham animals (**Figure 3C**). To evaluate the level of DA depletion the rotameter test was performed at the end of rotarod and staircase tests, and an intense turning behavior after apomorphine administration was observed in 6-OHDA-injected animals when compared with sham group (**Figure 3D**) (Mendes-Pinheiro, 2016). Then, to address the effects of either hBMSCs transplants or hBMSCs secretome injections, as well as comparing both treatments, the motor performance of the animals was evaluated in three different time-points after treatments (1, 4, and 7 weeks) following the same timeline as previsouly reported elsewhere (Teixeira et al., 2017; Mendes-Pinheiro et al., 2018). Regarding the rotarod test, motor coordination and balance of the 6-OHDA-lesioned animals was unchanged upon hBMSCs cell transplantation or secretome administration (**Figure 4A**). On the other hand, in the staircase test, used to assess the fine motor movements, animals treated with hBMSCs secretome showed a significant increase in the success rate of eaten pellets when compared to the untreated group (**Figure 4B**). Moreover, the treatment with hBMSCs

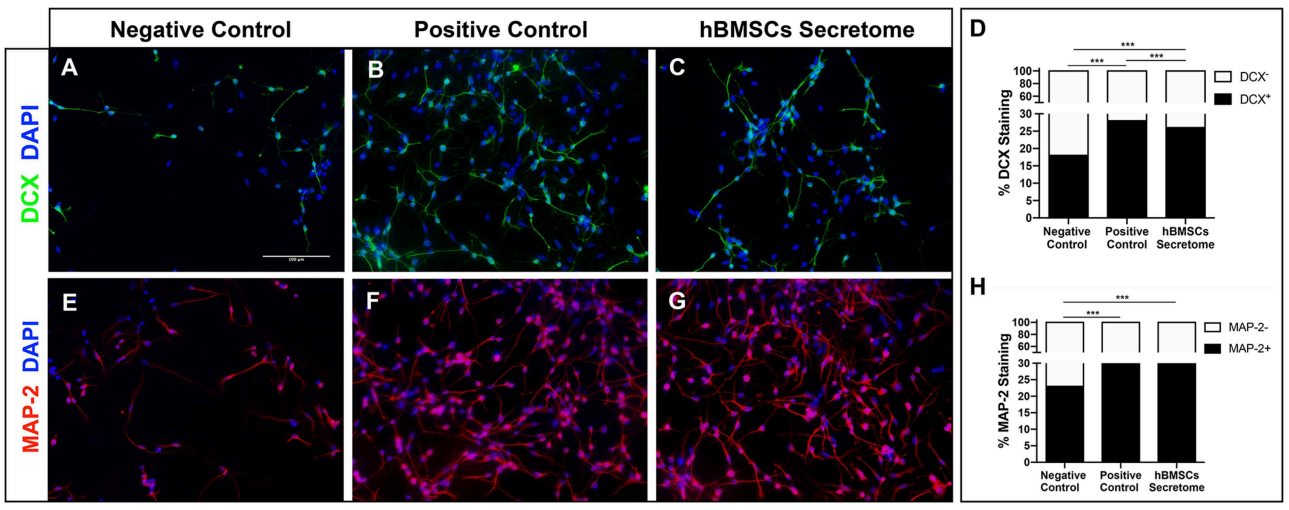

FIGURE 2 | Effect of hBMSCs secretome in the differentiation of hNPCs *in vitro*. **(A–C)** Representative microphotographs of DCX staining in hNPCs and **(D)** respective quantification of the proportion of stained cells, as marker of immature neurons [Chi-squared, $\chi^2_{(2)} = 79.862$, $p < 0.0001$]. A total number of 1,906 cells were scored for the negative control and a minimum of 13,000 for the other conditions, across two independent experiments. **(E–G)** Representative microphotographs of MAP-2 staining in hNPCs and **(H)** respective quantification of the proportion of stained cells, as a marker of mature neurons. A total number of 1,620 cells were scored for the negative control, and a minimum of 23,000 for the other conditions, across two independent experiments [Chi-squared, $\chi^2_{(2)} = 113.367$, $p < 0.0001$]. Nuclei were stained with DAPI. ***$p < 0.0001$ (Scale bar: 100 μm).

transplants was not able to improve the motor function of the animals in the staircase test when compared to the untreated group (**Figure 4B**).

Injection of hBMSCs Secretome Protects Against TH Damage in SNpc and Striatum

After histological analysis in the SNpc and striatum, we observed that the treatment with hBMSCs secretome was able to signifcantly minimize the dopaminergic loss upon 6-OHDA administration, which was not verified with hBMSCs transplanted group. In fact, TH staining revealed a significantly higher number of TH-positive cells in the SNpc when compared to the untreated group 6-OHDA (**Figures 5A–E**). Likewise, the same difference in the striatum was observed, by measuaring TH-positive fibers through densytometry analysis (**Figures 5F–J**). These finding are particularly important since they were obtained with a one-time administration of hBMSCs secretome, which produced effects over the course of the following 7 weeks. Moreover, it also important to highlight the differences obtained when compared to the hBMSCs cell transplanted group, which has been considered for many years one of the go-to strategies in stem cell base approaches for PD regenerative medicine.

Characterization of Protein Sets That Constitute the Secretome of hBMSCs Secretome

To identify potential therapeutic molecules in the hBMSCs secretome that could be involved in the strong response of the secretome-injected animals, the latter was characterized through a non-biased proteomic analysis based on a combined mass spectrometry (MS) approach (Mendes-Pinheiro, 2016). We were able to identify 279 proteins (according to the UniProtKB/Swiss-Prot classification) in the hBMSCs secretome, common to all replicates, from which 426 were detected based on 2 or more peptides, and therefore used in further analyses. An initial gene ontology analyses (levels 2 and 3) was carried out using PANTHER, in order to broadly characterize the protein types presented in the hBMSCs secretome. Regarding molecular function, more than 80% of identified proteins were either allocated in the binding or catalytic activity categories (**Figure 6A**), which is in accordance with the fact that this is a secreted media (Teixeira et al., 2016; Mendes-Pinheiro et al., 2018). In agreement, classification by protein class revealed that hydrolases and enzyme modulators were in the top three categories (**Figure 6B**). Regarding the signaling pathways that are mostly represented in the secretome, Parkinson's disease-related proteins was one of the top categories (**Figure 6C**), which suggests that the secretome contains protein elements that might be beneficial for PD context. A more detailed gene ontology analysis (levels 4 and 5) was then performed using the ConsensusPathDB. Interestingly, the most represented category of cellular components observed was extracellular exosomes (**Figure 6D**). When it comes to the mostly represented protein complexes, we identified elements from the proteasome (**Figure 6E**) and from histones (**Figure 6F**) as enriched in the secretome. This analysis provides interesting clues on the relevance of the composition of hBMSCs secretome in the context of PD.

DISCUSSION

The main goal of this study was to determine the impact of the injection of the secretome-derived from hBMSCs as a potential therapy for PD, when compared to what is considered the current gold standard in the field of cell-based therapies for regenerative medicine, that is the stem cell-based transplantation approaches.

PD is characterized by an extensive loss of DA neurons in the SNpc and their terminals in the striatum, resulting in debilitating motor problems (Przedborski, 2017). Therefore, in the *in vivo* experiments, in order to cause dopaminergic degeneration, was used a rat PD model induced by 6-OHDA injection into the MFB (Carvalho et al., 2013; Mendes-Pinheiro, 2016). As in line with previous reports (Teixeira et al., 2017; Mendes-Pinheiro et al., 2018), here we were able to successfully establish the model. As shown in the rotameter test (**Figure 3D**), 6-OHDA-lesioned animals displayed a strong turning behavior when compared to the sham group (injected with saline), indicating a clear magnitude of the lesion. We also verified that the motor function of these animals was affected, since they presented deficits in motor coordination and balance, as well as in the skilled motor function, addressed by the rotarod and staircase tests, respectively (**Figures 3B,C**). Regarding the effects of the treatments, we observed that neither the hBMSCs transplants nor secretome injections were able to improve the animals' motor coordination and balance in the rotarod test (**Figure 4A**). It is important to state that the rotarod test is commonly used in this context, however, it has also been described that is not the most sensitive test to use in models that present basal ganglia dysfunctions (Magen and Chesselet, 2010; Mann and Chesselet, 2014). Moreover, since we used the accelerating protocol during 4 consecutive days (4 trials per day), the fatigue of the animals could explain in part the results obtained. On the other hand, the fine motor skill task has been used in different models of PD, and it was shown to be very suitable to detect striatum/nigrostriatal bundle unilateral lesions (Baird et al., 2001). Indeed, when the forelimb reaching and grasping abilities were assessed using the staircase test, we observed that the injection of hBMSCs secretome improved the success rate of eaten pellets of the treated animals when compared to the untreated group 6-OHDA (**Figure 4B**). Additionally, rats injected with hBMSCs secretome showed better preservation in the number of TH-positive neurons in the SNpc, as well as an increase in the density of TH-positive fibers in the striatum (**Figure 5**). These histological outcomes nicely correlate with positive functional improvements that we observed in the fine motor movements for the animals treated with secretome. On the other hand, such evidences were not observed in hBMSCs-transplanted animals, probably due to the low survival rate of cells upon transplantation. We performed human nuclear antigen staining for hBMSCs detection (*data not shown*), and we were not able to observe the presence of the grafts on both SNpc and striatum. In fact, it has been shown that the MSCs survival

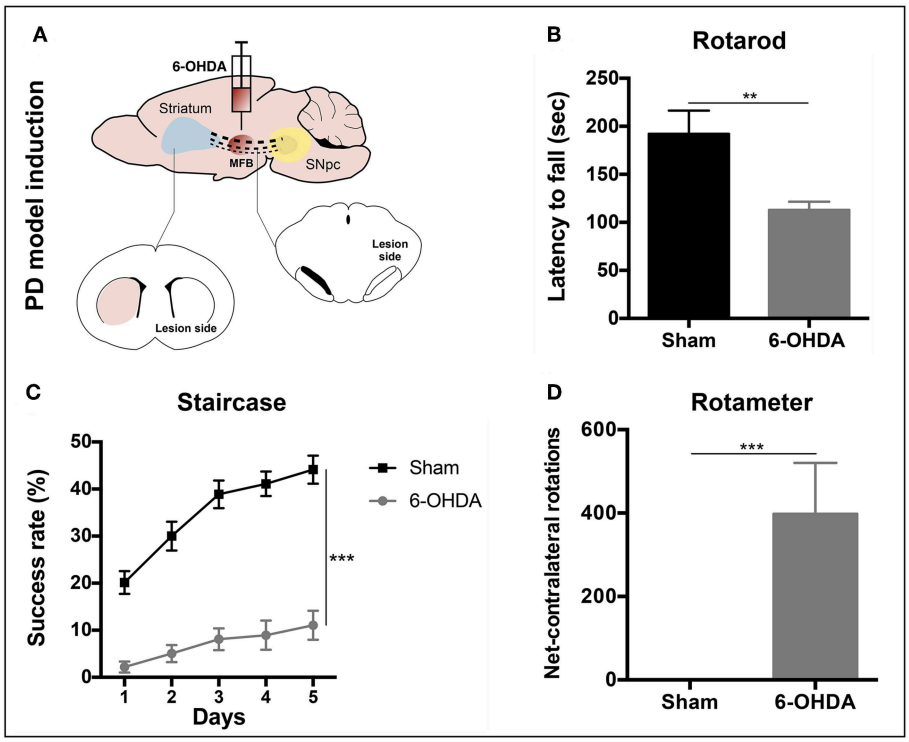

FIGURE 3 | PD model validation. **(A)** Animals received a unilateral injection of 6-OHDA into the MFB in order to induce PD-like symptoms. **(B)** Latency to fall was measured in the accelerating rotarod test, demonstrating that 6-OHDA-injected animals presented significant motor impairment in motor coordination and balance [Student's t-test, $t_{(19)} = 3.849$, $p < 0.01$, Sham: $n = 7$, 6-OHDA: $n = 14$]. **(C)** Deficits in forelimb use and skilled motor function were also observed after the staircase test evaluation [Mixed design ANOVA, $F_{group}(1,22) = 76.290$, $p < 0.0001$, Sham: $n = 9$, 6-OHDA: $n = 15$]. Data is presented as mean ± SEM. **(D)** Rotameter test revealed that 6-OHDA-injected animals exhibited an intense turning behavior, showing a clear decline of the dopaminergic system (Mann-Whitney, $U = 0$, $p < 0.0001$, Sham: $n = 9$, 6-OHDA: $n = 15$). Data is presented as median ± IQR. $^{**}p < 0.01$, $^{***}p < 0.001$.

is minimal and the implantation time of these cells is usually too short to have an effective impact (Vizoso et al., 2017).

In the past few years MSCs has been widely studied as therapeutical agents in different pathological conditions of the central nervous system (CNS), including PD (Teixeira et al., 2013; Salgado et al., 2015; Konala et al., 2016). Primary studies showed that transplanted MSCs were able to repair injured adult mesenchymal tissues; thereafter, some authors also reported the capacity of MSCs to transdifferentiate into ectodermal-derived cells (Donega et al., 2014; Takeda and Xu, 2015; Bagher et al., 2016). While these studies were accompanied with some controversy throughout the years, robust data have been demonstrating that the paracrine activity of MSCs could have a critical role in its beneficial effects. In fact, MSCs are able to secrete a wide spectrum of elements with strong immunomodulatory properties, which are also able to inhibit apoptosis, enhance angiogenesis and promote neuronal survival and differentiation (Marote et al., 2016). This is the first study comparing directly hBMSCs secretome injections with hBMSCs transplantation. Nonetheless, other authors correlated motor improvements and DA neurons' protection with the secretion and local increase of different growth factors after MSCs transplantation (Sadan et al., 2009; Cova et al., 2010; Wang et al., 2010; Cerri et al., 2015), supporting the secretome theory.

To explore the possible underlying mechanisms or key molecules behind the secretome effects, we characterized the latter using a MS proteomic approach. Interestingly, when we evaluated cellular components at a more detailed level, we observed a very large enrichment of proteins that are part of exosomes. Moreover, this category of proteins was clearly overrepresented when compared with the other top hits. In fact, some studies demonstrate that the administration of MSCs-derived exosomes was able to rescue tissue function in different disease/injury contexts and to induce beneficial *in vitro* effects, mainly mediated by exosomal-enclosed microRNAs (miRNAs) (Marote et al., 2016; Vilaça-Faria et al., 2019). For instance, Jarmalavičiute et al. (2015), using a 6-OHDA 3D culture model, showed that dental pulp MSCs-derived exosomes rescue DA neurons from cell death. Hence, the beneficial effects of the hBMSCs secretome that observed in this work could be mediated by a similar exosome-dependent mechanism. Additionally, other studies demonstrated the potential of exosomes produced by MSCs on neuronal differentiation. For instance, Lee et al. (2014) showed that BMSCs had the capacity to the deliver miRNAS, namely miR-124 and miR-145, to NPCs and astrocytes,

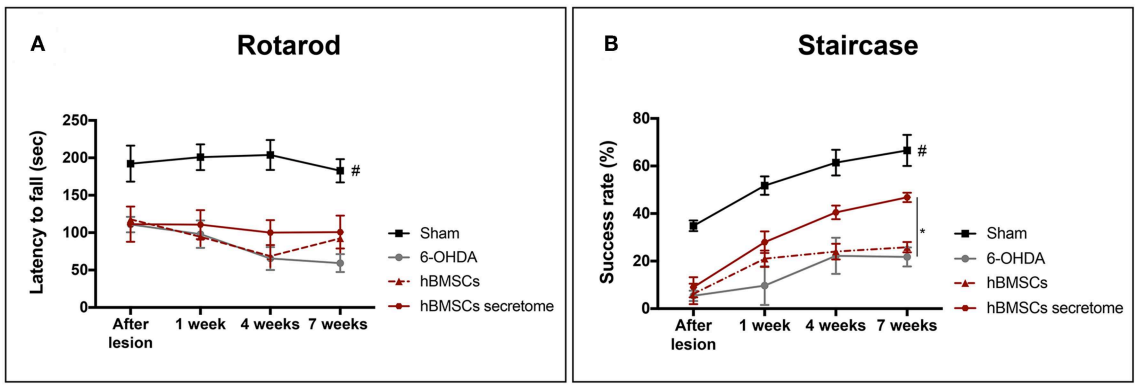

FIGURE 4 | Effects of hBMSCs transplants and hBMSCs secretome injections on the motor performance of 6-OHDA-lesioned animals at 1, 4, and 7 weeks after treatments. **(A)** No differences were found in the 6-OHDA-lesioned animals' motor coordination and balance after hBMSCs secretome administration [Mixed design ANOVA, $F_{Group}(3,17) = 28.875$, $p < 0.0001$, Sham: $n = 7$, 6-OHDA: $n = 5$, hBMSCs: $n = 4$, hBMSCs secretome: $n = 5$]. **(B)** In the staircase test, used to evaluate the fine motor movements, animals treated with hBMSCs secretome showed a significant increase in the success rate of eaten pellets when compared to the untreated group 6-OHDA [Mixed design ANOVA, $F_{Group}(3,20) = 22.804$, $p < 0.0001$, Sham: $n = 9$, 6-OHDA: $n = 5$, hBMSCs: $n = 4$, hBMSCs secretome: $n = 6$]. Data is presented as mean ± SEM. $^{*}p < 0.05$; Sham animals statistically different from all the other groups: $^{\#}p < 0.0001$.

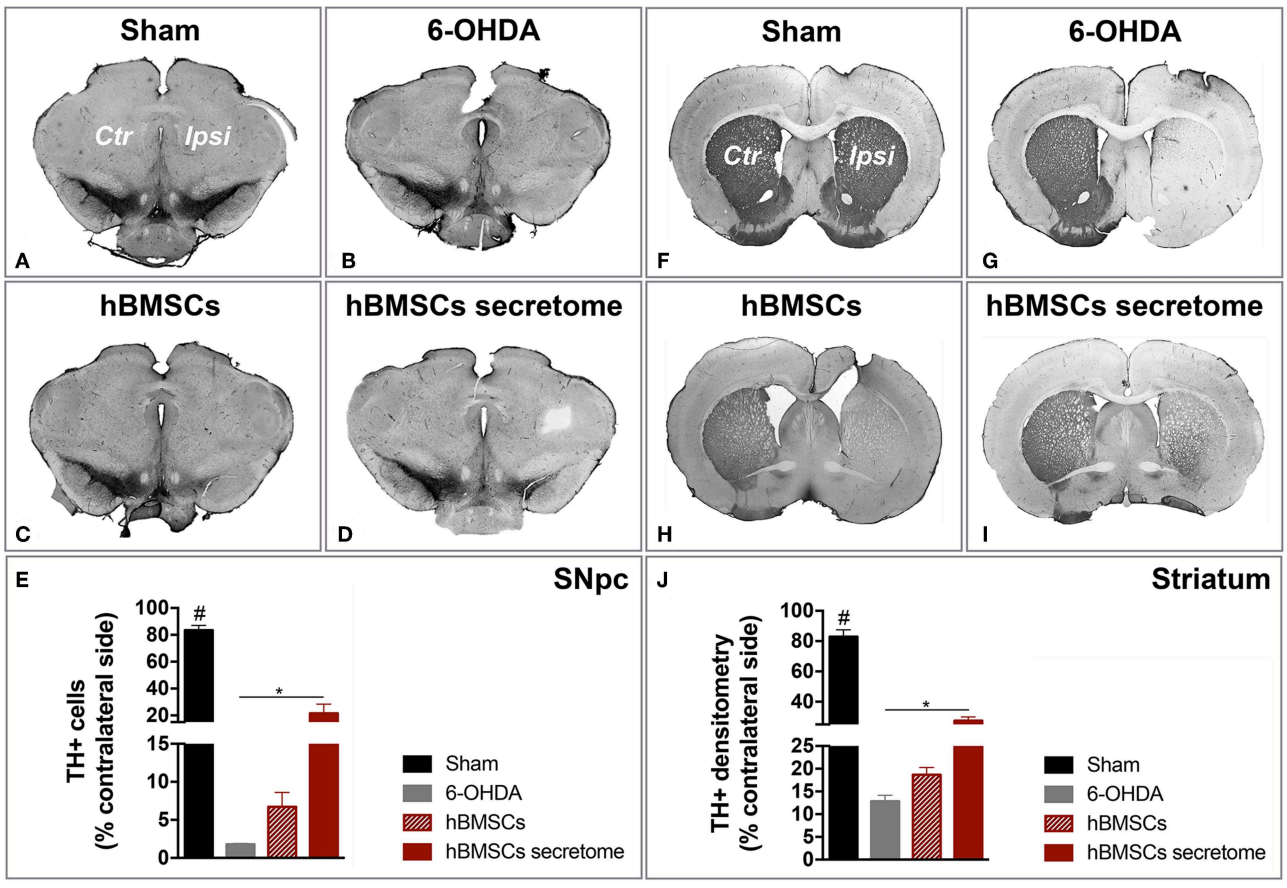

FIGURE 5 | Injection of hBMSCs secretome protects against DA neurons damage. **(A–E)** The TH-positive cells were counted in the entire SNpc, and we observed that hBMSCs secretome injections was able to minimize the TH loss when compared to the untreated group 6-OHDA [One-way ANOVA, $F_{(3, 23)} = 84.541$, $p < 0.0001$, Sham: $n = 9$, 6-OHDA: $n = 5$, hBMSCs: $n = 4$, hBMSCs secretome: $n = 6$]. **(F–J)** The same effect was also detected in the striatum, by measuring TH-positive fibers through densitometry analysis [One-way ANOVA, $F_{(3, 20)} = 110.564$, $p < 0.0001$, Sham: $n = 6$, 6-OHDA: $n = 5$, hBMSCs: $n = 4$, hBMSCs secretome: $n = 6$]. Data is presented as mean ± SEM. $^{*}p < 0.05$; Sham animals statistically different from all the other groups: $^{\#}p < 0.0001$.

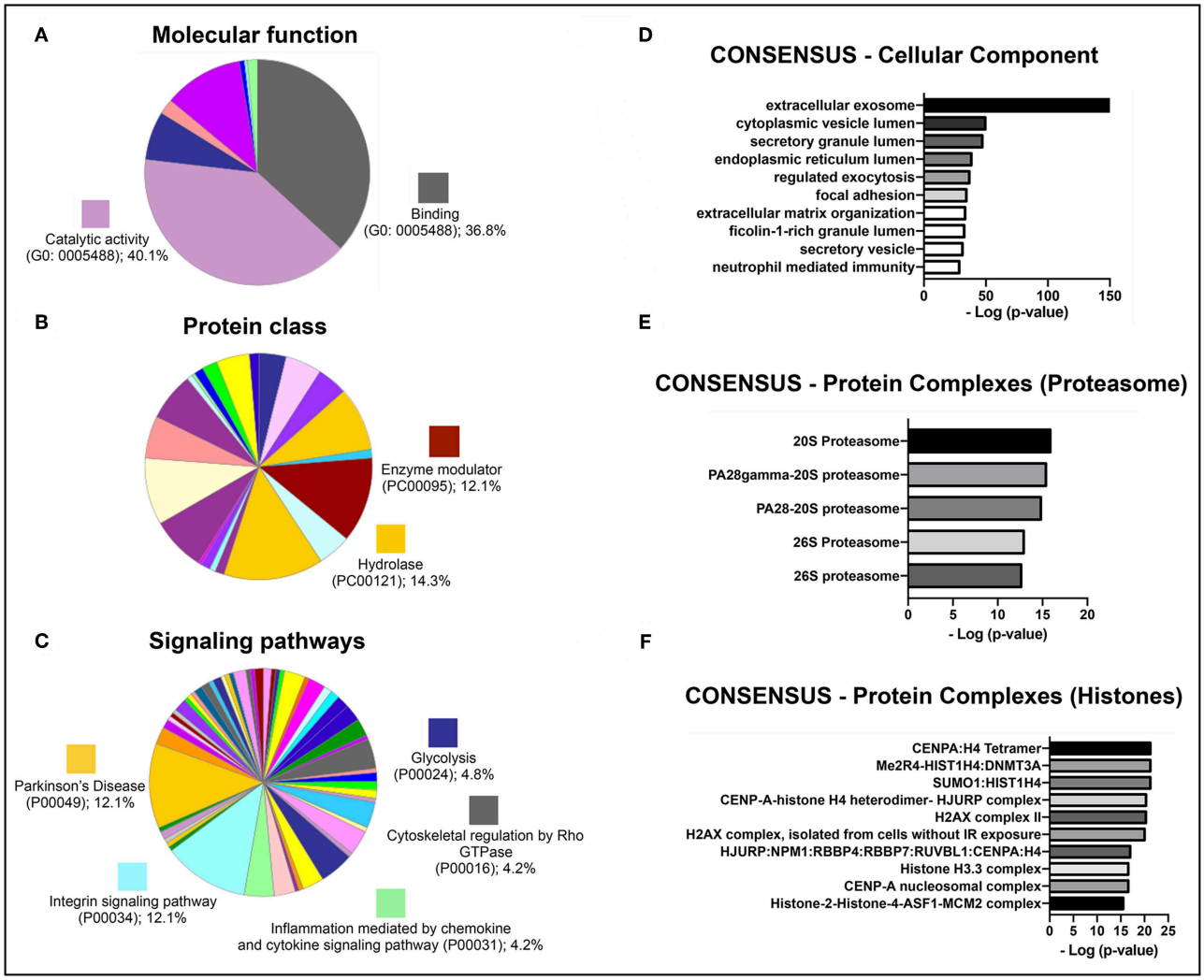

FIGURE 6 | Gene ontology analyses of the identified proteins in a proteomic analysis of the hBMSCs secretome from three independent donors. Categorization of the most represented **(A)** molecular functions, **(B)** protein classes, and **(C)** signaling pathways, using the PANTHER software (gene ontology levels 2 and 3). Results are shown as the percentage of proteins that are part of each individual GO category. Categorization of the enrichment of **(D)** cellular components, **(E)** elements of the proteasome and **(F)** elements of histones, using the ConsensusPathDB software (gene ontology levels 4 and 5). Results are shown as the –log of the *p*-value for the enrichment of each individual category.

impacting cell differentiation and increasing the expression of glutamate transporters. Another study, exposing cortical neurons to MSCs-derived exosomes, showed an improvement in neurite outgrowth, by increasing both neurite branch and total length, and attributing the effects to the transference of miR-133b to neural cells (Xin et al., 2012). Similarly, Lopez-Verrilli et al. (2016), showed that menstrual MSCs-derived and BMSCs exosomes promote neurite growth in cortical neurons and dorsal root ganglia neurons, respectively. This is also in line with our results, since secretome-treated hNPCs showed and increase proportion of MAP-2 staining. Moreover, another interesting study using a 6-OHDA mice PD model, reported that mimic-miR-124 increased neurogenesis in the subventricular zone (SVZ) which was correlated with significant behavioral improvements (Saraiva et al., 2016). Altogether, this evidence indicates that besides dopaminergic survival, the modulation of neurogenesis may also have influence in the recovery of PD, and could be one of the reasons behind the observed secretome-effects.

The precise cause of PD remains elusive, but compelling evidence spotlight the ubiquitin proteasome system (UPS) as a key feature in PD pathogenesis (Bentea et al., 2017). This connection was supported due to genetic mutations in the *PRKN* and UCHL1 genes, with critical roles in the UPS system, with familial parkinsonism (Kitada et al., 1998; Summers et al., 1998). In this follow up, McNaught et al. (2001) observed a significant decrease of proteasomal core subunits in the SN of sporadic PD brains. Furthermore, some studies showed that

proteasomal inhibitors like lactacystin and proteasome inhibitor 1 (PSI) leads to dopaminergic cell death *in vitro* and after brain injections (McNaught et al., 2002a,b; Matsui et al., 2010; Xie et al., 2010). Although it is not part of the UPS, overexpression of wild-type or mutant α-synuclein both *in vitro* and *in vivo* was also shown to impede proteasome function (Stefanis et al., 2001; Tanaka et al., 2001; Chen et al., 2006). With UPS dysfunction being one of the pathophysiological hallmarks of PD, and since one of more enriched protein networks in the hBMSCs secretome was the proteasome, we can speculate that the restoration of UPS-dependent proteostasis could be one of the main mechanism responsible for the phenotypical improvement we observed.

Finally, we also observed that histones are one of the mostly represented protein complexes in hBMSCs secretome. Indeed, histone modifications have been linked with the development, differentiation and maintenance of DA neurons (van Heesbeen et al., 2013). Park and co-workers (Park et al., 2016) demonstrated an increase of histone acetylation in DA neurons of PD patients when compared to healthy individuals. Besides that, using the MPTP model both *in vitro* and *in vivo*, the same authors showed a decrease of multiple histone deacetylases (HDACs), as well as in the midbrain tissues of human PD patients (Park et al., 2016). In cellular models, either dieldrin or paraquat were shown to induce histone acetylation (Song et al., 2010, 2011). In addition, Goers et al. (2003) showed in culture an interaction between histones and α-synuclein via complex formation, as well as, that α-synuclein fibrillation was intensely enhanced in the presence of histones. Another study, using two different PD models, demonstrated that DA reduction and following levodopa treatment were related with intense alterations in post-translational modifications histones in the striatum (Nicholas et al., 2008). Altogether, these findings suggest that chromatin remodeling may have an important role in PD pathogenesis.

Additionally, previous work from our already showed that hBMSCs is a source of numerous neuroregulatory molecules with neuroprotection character (Pires et al., 2016). For instance, similarly to the above referred work, we found in our proteomic analysis, important proteins known as anti-oxidant agents, such as DJ-1, TRXR1, and PRDX1 that have been shown to counteract dopaminergic cell death in different PD models as reviewed by Pires et al. (2016). Also PEDF, it is known for its neurotrophic properties but also for neuroprotective roles in different PD toxin models (Falk et al., 2009). This neuroprotective effects have been linked to the capacity for induce the activation of nuclear factor NF-κB signaling cascade, which in turn induces the expression of genes that are essential to neuronal protection and survival, such as BDNF and GDNF (Falk et al., 2010). Moreover, other proteins like Galactin-1 and Cystatin C have also been associated with anti-apoptotic effects in *in vitro* models of PD (Pires et al., 2016).

Although candidate molecules and possible mechanisms are under investigation, further detailed studies are needed to carefully define which players may be responsible for the hBMSCs secretome-mediated effects. In the future, we intend to conduct studies, both *in vitro* and *in vivo*, regarding the identification of some of these molecules and their roles in the context of PD. In conclusion, the present findings support hBMSCs secretome treatment as a novel therapeutic strategy for PD. Moreover, we have also shown that its application in a well-described rat model of PD is more effective than the traditional cell transplantation approaches, which have been considered one of the most preferred strategies in the field of stem cell-based PD regenerative medicine for several years. However, additional work is still necessary in order to improve the applicability of this approach.

DATA AVAILABILITY STATEMENT

The dataset PXD014887 for this study can be found in the ProteomeXchange Consortium via the PRIDE partner repository (http://www.ebi.ac.uk/pride).

ETHICS STATEMENT

The animal study was reviewed and approved by Direção Geral de Alimentação e Veterinária (ID: DGAV28421) and Ethical Subcommittee in Life and Health Sciences (SECVS; ID: SECVS-008/2013, University of Minho).

AUTHOR CONTRIBUTIONS

BM-P designed and performed most of the experiments, collected and analyzed the data, and drafted the manuscript. SA and BM performed and collected the data regarding the proteomic analysis. JD contributed to the proteomic and statistical analysis, and helped with the manuscript writing. AM helped with the animal experiments and with the manuscript writing. LB provided the study material and helped with the interpretation of the results. FT performed the stereotaxic surgeries, helped with the data interpretation, and with the manuscript writing. AS conceived and financially support the study, participated in its design and coordination, and critically read the manuscript. All authors read and approved the final manuscript.

FUNDING

This work was supported by Portuguese Foundation for Science and Technology: IF Development Grant (IF/00111/2013) to AS, Post-Doctoral Fellowship to FT (SFRH/BPD/118408/2016) and Doctoral Fellowship to BM-P (SFRH/BD/120124/2016); Canada Research Chair in Biomedical Engineering (LAB). This work was funded by FEDER, through the Competitiveness Internationalization Operational Programme (POCI), and by National funds, through the Foundation for Science and Technology (FCT), under the scope of the projects: POCI-01-0145-FEDER-029751; POCI-01-0145-FEDER-007038; POCI-01-0145-FEDER-032619; POCI-01-0145-FEDER-016428 (ref.: SAICTPAC/0010/2015), POCI-01-0145-FEDER-016795 (ref.: PTDC/NEU-SCC/7051/2014), POCI-01-0145-FEDER-029311

(ref.: PTDC/BTM-TEC/29311/2017), POCI-01-0145-FEDER-30943 (ref.: PTDC/MEC-PSQ/30943/2017) and PTDC/MED-NEU/27946/2017; UID/NEU/04539/2013 and POCI-01-0145-FEDER-007440. This article has also been developed under the scope of the project NORTE-01-0145-FEDER-000023, supported by the Northern Portugal Regional Operational Programme (NORTE 2020), under the Portugal 2020 Partnership Agreement, through the European Regional Development Fund (FEDER). Co-funded by the Programa Operacional Factores de Competitividade (QREN) and by The National Mass Spectrometry Network under the contract POCI-01-0145-FEDER-402-022125 (ref.: ROTEIRO/0028/2013).

ACKNOWLEDGMENTS

Some of the data presented in this work can be found in the master's thesis of the author BM-P and is available in the University of Minho repository (http://repositorium.sdum.uminho.pt/).

SUPPLEMENTARY MATERIAL

The Supplementary Material for this article can be found online at: https://www.frontiersin.org/articles/10.3389/fbioe.2019.00294/full#supplementary-material

REFERENCES

Anisimov, S. V. (2009). Cell-based therapeutic approaches for Parkinson's disease: progress and perspectives. *Rev. Neurosci.* 20, 347–381. doi: 10.1515/REVNEURO.2009.20.5-6.347

Axelsen, T. M., and Woldbye, D. P. D. (2018). Gene therapy for Parkinson's disease, an update. *J. Parkinsons Dis.* 8, 195–215. doi: 10.3233/JPD-181331

Baghbaderani, B. A., Mukhida, K., Sen, A., Kallos, M. S., Hong, M., Mendez, I., et al. (2010). Bioreactor expansion of human neural precursor cells in serum-free media retains neurogenic potential. *Biotechnol. Bioeng.* 105, 823–833. doi: 10.1002/bit.22590

Bagher, Z., Azami, M., Ebrahimi-Barough, S., Mirzadeh, H., Solouk, A., Soleimani, M., et al. (2016). Differentiation of Wharton's Jelly-derived mesenchymal stem cells into motor neuron-like cells on three-dimensional collagen-grafted nanofibers. *Mol. Neurobiol.* 53, 2397–2408. doi: 10.1007/s12035-015-9199-x

Baird, A. L., Meldrum, A., and Dunnett, S. B. (2001). The staircase test of skilled reaching in mice. *Brain Res. Bull.* 54, 243–250. doi: 10.1016/S0361-9230(00)00457-3

Baraniak, P. R., and McDevitt, T. C. (2010). Stem cell paracrine actions and tissue regeneration. *Regen. Med.* 5, 121–143. doi: 10.2217/rme.09.74

Bentea, E., Verbruggen, L., and Massie, A. (2017). The proteasome inhibition model of Parkinson's disease. *J. Parkinsons Dis.* 7, 31–63. doi: 10.3233/JPD-160921

Bermudez, M. A., Sendon-Lago, J., Eiro, N., Trevino, M., Gonzalez, F., Yebra-Pimentel, E., et al. (2015). Corneal epithelial wound healing and bactericidal effect of conditioned medium from human uterine cervical stem cells. *Invest. Ophthalmol. Vis. Sci.* 56, 983–992. doi: 10.1167/iovs.14-15859

Bermudez, M. A., Sendon-Lago, J., Seoane, S., Eiro, N., Gonzalez, F., Saa, J., et al. (2016). Anti-inflammatory effect of conditioned medium from human uterine cervical stem cells in uveitis. *Exp. Eye Res.* 149, 84–92. doi: 10.1016/j.exer.2016.06.022

Carvalho, M. M., Campos, F. L., Coimbra, B., Pego, J. M., Rodrigues, C., Lima, R., et al. (2013). Behavioral characterization of the 6-hydroxidopamine model of Parkinson's disease and pharmacological rescuing of non-motor deficits. *Mol. Neurodegener.* 8:14. doi: 10.1186/1750-1326-8-14

Cerri, S., Greco, R., Levandis, G., Ghezzi, C., Mangione, A. S., Fuzzati-Armentero, M.-T., et al. (2015). Intracarotid infusion of mesenchymal stem cells in an animal model of Parkinson's disease, focusing on cell distribution and neuroprotective and behavioral effects. *Stem Cells Transl. Med.* 4, 1073–1085. doi: 10.5966/sctm.2015-0023

Chen, L., Thiruchelvam, M. J., Madura, K., and Richfield, E. K. (2006). Proteasome dysfunction in aged human α-synuclein transgenic mice. *Neurobiol. Dis.* 23, 120–126. doi: 10.1016/j.nbd.2006.02.004

Cova, L., Armentero, M. T., Zennaro, E., Calzarossa, C., Bossolasco, P., Busca, G., et al. (2010). Multiple neurogenic and neurorescue effects of human mesenchymal stem cell after transplantation in an experimental model of Parkinson's disease. *Brain Res.* 1311, 12–27. doi: 10.1016/j.brainres.2009.11.041

Donega, V., Nijboer, C. H., Braccioli, L., Slaper-Cortenbach, I., Kavelaars, A., Van Bel, F., et al. (2014). Intranasal administration of human MSC for ischemic brain injury in the mouse: *in vitro* and *in vivo* neuroregenerative functions. *PLoS ONE* 9:e112339. doi: 10.1371/journal.pone.0112339

Falk, T., Gonzalez, R. T., and Sherman, S. J. (2010). The yin and yang of VEGF and PEDF: multifaceted neurotrophic factors and their potential in the treatment of Parkinson's Disease. *Int. J. Mol. Sci.* 11, 2875–2900. doi: 10.3390/ijms11082875

Falk, T., Zhang, S., and Sherman, S. J. (2009). Pigment epithelium derived factor (PEDF) is neuroprotective in two *in vitro* models of Parkinson's disease. *Neurosci. Lett.* 458, 49–52. doi: 10.1016/j.neulet.2009.04.018

Fraga, J. S., Silva, N. A., Lourenco, A. S., Goncalves, V., Neves, N. M., Reis, R. L., et al. (2013). Unveiling the effects of the secretome of mesenchymal progenitors from the umbilical cord in different neuronal cell populations. *Biochimie* 95, 2297–2303. doi: 10.1016/j.biochi.2013.06.028

Goers, J., Manning-Bog, A. B., McCormack, A. L., Millett, I. S., Doniach, S., Di Monte, D. A., et al. (2003). Nuclear localization of alpha-synuclein and its interaction with histones. *Biochemistry* 42, 8465–8471. doi: 10.1021/bi0341152

Jarmalavičiute, A., Tunaitis, V., Pivoraite, U., Venalis, A., and Pivoriunas, A. (2015). Exosomes from dental pulp stem cells rescue human dopaminergic neurons from 6-hydroxy-dopamine-induced apoptosis. *Cytotherapy* 17, 932–939. doi: 10.1016/j.jcyt.2014.07.013

Jung, S., Sen, A., Rosenberg, L., and Behie, L. A. (2010). Identification of growth and attachment factors for the serum-free isolation and expansion of human mesenchymal stromal cells. *Cytotherapy* 12, 637–657. doi: 10.3109/14653249.2010.495113

Kamburov, A., Stelzl, U., Lehrach, H., and Herwig, R. (2013). The ConsensusPathDB interaction database: 2013 update. *Nucleic Acids Res.* 41, 793–800. doi: 10.1093/nar/gks1055

Kitada, T., Asakawa, S., Hattori, N., Matsumine, H., Yamamura, Y., Minoshima, S., et al. (1998). Mutations in the parkin gene cause autosomal recessive juvenile parkinsonism. *Nature* 392, 605–608. doi: 10.1038/33416

Konala, V. B. R., Mamidi, M. K., Bhonde, R., Das, A. K., Pochampally, R., and Pal, R. (2016). The current landscape of the mesenchymal stromal cell secretome: a new paradigm for cell-free regeneration. *Cytotherapy* 18, 13–24. doi: 10.1016/j.jcyt.2015.10.008

Lee, H. K., Finniss, S., Cazacu, S., Xiang, C., and Brodie, C. (2014). Mesenchymal stem cells deliver exogenous miRNAs to neural cells and induce their differentiation and glutamate transporter expression. *Stem Cells Dev.* 23, 2851–2861. doi: 10.1089/scd.2014.0146

Lopez-Verrilli, M. A., Caviedes, A., Cabrera, A., Sandoval, S., Wyneken, U., and Khoury, M. (2016). Mesenchymal stem cell-derived exosomes from different sources selectively promote neuritic outgrowth. *Neuroscience* 320, 129–139. doi: 10.1016/j.neuroscience.2016.01.061

Magen, I., and Chesselet, M. F. (2010). Genetic mouse models of Parkinson's disease. The state of the art. in *Prog. Brain Res.* 184:53–87. doi: 10.1016/S0079-6123(10)84004-X

Mahla, R. S. (2016). Stem cells applications in regenerative medicine and disease therapeutics. *Int. J. Cell Biol.* 2016:6940283. doi: 10.1155/2016/6940283

Mann, A., and Chesselet, M. F. (2014). Techniques for motor assessment in rodents. *Mov. Disord.* 2015, 139–157. doi: 10.1016/B978-0-12-405195-9.00008-1

Marote, A., Teixeira, F. G., Mendes-Pinheiro, B., and Salgado, A. J. (2016). MSCs-derived exosomes: cell-secreted nanovesicles with regenerative potential. *Front. Pharmacol.* 7:231. doi: 10.3389/fphar.2016.00231

Marques, C. R., Marote, A., Mendes-Pinheiro, B., Teixeira, F. G., and Salgado, A. J. (2018). Cell secretome based approaches in Parkinson's disease regenerative medicine. *Expert Opin. Biol. Ther.* 18, 1235–1245. doi: 10.1080/14712598.2018.1546840

Matsui, H., Ito, H., Taniguchi, Y., Inoue, H., Takeda, S., and Takahashi, R. (2010). Proteasome inhibition in medaka brain induces the features of Parkinson's disease. *J. Neurochem.* 115, 178–187. doi: 10.1111/j.1471-4159.2010.06918.x

McKee, C., and Chaudhry, G. R. (2017). Advances and challenges in stem cell culture. *Colloids Surf. B Biointerfaces* 159, 62–77. doi: 10.1016/j.colsurfb.2017.07.051

McNaught, K. S. P., Björklund, L. M., Belizaire, R., Isacson, O., Jenner, P., and Olanow, C. W. (2002a). Proteasome inhibition causes nigral degeneration with inclusion bodies in rats. *Neuroreport* 13, 1437–1441. doi: 10.1097/00001756-200208070-00018

McNaught, K. S. P., Mytilin, C., JnoBaptiste, R., Yabut, J., Shashidharan, P., Jenner, P., et al. (2002b). Impairment of the ubiquitin-proteasome system causes dopaminergic cell death and inclusion body formation in ventral mesencephalic cultures. *J. Neurochem.* 81, 301–306. doi: 10.1046/j.1471-4159.2002.00821.x

McNaught, K. S. P., Olanow, C. W., Halliwell, B., Isacson, O., and Jenner, P. (2001). Failure of the ubiquitin proteasome system in Parkinson's disease. *Nat. Rev. Neurosci.* 2, 589–594. doi: 10.1038/35086067

Mendes-Pinheiro, B. (2016). Mesenchymal stem cells secretome in Parkinson's disease regenerative medicine. *Eur. Neuropsychopharmacol.* 27, S687–S688. doi: 10.1016/S0924-977X(17)31277-4

Mendes-Pinheiro, B., Teixeira, F. G., Anjo, S. I., Manadas, B., Behie, L. A., and Salgado, A. J. (2018). Secretome of undifferentiated neural progenitor cells induces histological and motor improvements in a rat model of Parkinson's disease. *Stem Cells Transl. Med.* 7, 829–838. doi: 10.1002/sctm.18-0009

Mendez, I., Dagher, A., Hong, M., Gaudet, P., Weerasinghe, S., McAlister, V., et al. (2002). Simultaneous intrastriatal and intranigral fetal dopaminergic grafts in patients with Parkinson disease: a pilot study. Report of three cases. *J. Neurosurg.* 96, 589–596. doi: 10.3171/jns.2002.96.3.0589

Mendez, I., Sanchez-Pernaute, R., Cooper, O., Vinuela, A., Ferrari, D., Bjorklund, L., et al. (2005). Cell type analysis of functional fetal dopamine cell suspension transplants in the striatum and substantia nigra of patients with Parkinson's disease. *Brain* 128, 1498–1510. doi: 10.1093/brain/awh510

Mi, H., Muruganujan, A., and Thomas, P. D. (2013). PANTHER in 2013: modeling the evolution of gene function, and other gene attributes, in the context of phylogenetic trees. *Nucleic Acids Res.* 41, 377–386. doi: 10.1093/nar/gks1118

Montoya, C. P., Campbell-Hope, L. J., Pemberton, K. D., and Dunnett, S. B. (1991). The "staircase test": a measure of independent forelimb reaching and grasping abilities in rats. *J. Neurosci. Methods* 36, 219–228. doi: 10.1016/0165-0270(91)90048-5

Monville, C., Torres, E. M., and Dunnett, S. B. (2006). Comparison of incremental and accelerating protocols of the rotarod test for the assessment of motor deficits in the 6-OHDA model. *J. Neurosci. Methods* 158, 219–223. doi: 10.1016/j.jneumeth.2006.06.001

Nicholas, A. P., Lubin, F. D., Hallett, P. J., Vattem, P., Ravenscroft, P., Bezard, E., et al. (2008). Striatal histone modifications in models of levodopa-induced dyskinesia. *J. Neurochem.* 106, 486–494. doi: 10.1111/j.1471-4159.2008.05417.x

Park, G., Tan, J., Garcia, G., Kang, Y., Salvesen, G., and Zhang, Z. (2016). Regulation of histone acetylation by autophagy in Parkinson disease. *J. Biol. Chem.* 291, 3531–3540. doi: 10.1074/jbc.M115.675488

Paxinos, G., and Watson, C. (2007). *The Rat Brain in Stereotaxic Coordinates. 6th Edn.* Amsterdam; Boston, MA: Elsevier.

Perez-Riverol, Y., Csordas, A., Bai, J., Bernal-Llinares, M., Hewapathirana, S., Kundu, D. J., et al. (2019). The PRIDE database and related tools and resources in 2019: improving support for quantification data. *Nucleic Acids Res.* 47, D442–D450. doi: 10.1093/nar/gky1106

Pires, A. O., Mendes-Pinheiro, B., Teixeira, F. G., Anjo, S. I., Ribeiro-Samy, S., Gomes, E. D., et al. (2016). Unveiling the differences of secretome of human bone marrow mesenchymal stem cells, adipose tissue-derived stem cells, and human umbilical cord perivascular cells: a proteomic analysis. *Stem Cells Dev.* 25, 1073–1083. doi: 10.1089/scd.2016.0048

Przedborski, S. (2017). The two-century journey of Parkinson disease research. *Nat. Rev. Neurosci.* 18, 251–259. doi: 10.1038/nrn.2017.25

Sadan, O., Bahat-Stromza, M., Barhum, Y., Levy, Y. S., Pisnevsky, A., Peretz, H., et al. (2009). Protective effects of neurotrophic factor-secreting cells in a 6-OHDA rat model of Parkinson disease. *Stem Cells Dev.* 18, 1179–1190. doi: 10.1089/scd.2008.0411

Salgado, A. J., Sousa, J. C., Costa, B. M., Pires, A. O., Mateus-Pinheiro, A., Teixeira, F. G., et al. (2015). Mesenchymal stem cells secretome as a modulator of the neurogenic niche: basic insights and therapeutic opportunities. *Front. Cell Neurosci.* 9:249. doi: 10.3389/fncel.2015.00249

Saraiva, C., Paiva, J., Santos, T., Ferreira, L., and Bernardino, L. (2016). MicroRNA-124 loaded nanoparticles enhance brain repair in Parkinson's disease. *J. Control. Release* 235, 291–305. doi: 10.1016/j.jconrel.2016.06.005

Sethi, K. D. (2010). The impact of levodopa on quality of life in patients with Parkinson disease. *Neurologist* 16, 76–83. doi: 10.1097/NRL.0b013e3181be6d15

Song, C., Kanthasamy, A., Anantharam, V., Sun, F., and Kanthasamy, A. G. (2010). Environmental neurotoxic pesticide increases histone acetylation to promote apoptosis in dopaminergic neuronal cells: relevance to epigenetic mechanisms of neurodegeneration. *Mol. Pharmacol.* 77, 621–632. doi: 10.1124/mol.109.062174

Song, C., Kanthasamy, A., Jin, H., Anantharam, V., and Kanthasamy, A. G. (2011). Paraquat induces epigenetic changes by promoting histone acetylation in cell culture models of dopaminergic degeneration. *Neurotoxicology* 32, 586–595. doi: 10.1016/j.neuro.2011.05.018

Stefanis, L., Larsen, K. E., Rideout, H. J., Sulzer, D., and Greene, L. A. (2001). Expression of A53T mutant but not wild-type alpha-synuclein in PC12 cells induces alterations of the ubiquitin-dependent degradation system, loss of dopamine release, and autophagic cell death. *J. Neurosci.* 21, 9549–60. doi: 10.1523/JNEUROSCI.21-24-09549.2001

Summers, A. P., Koob, T. J., Brainerd, E. L., Leroy, E., Boyer, R., Auburger, G., et al. (1998). The ubiquitin pathway in Parkinson's disease. *Nature* 395, 451–452. doi: 10.1038/26652

Takeda, Y. S., and Xu, Q. (2015). Neuronal differentiation of human mesenchymal stem cells using exosomes derived from differentiating neuronal cells. *PLoS ONE* 10:e0135111. doi: 10.1371/journal.pone.0135111

Tanaka, Y., Engelender, S., Igarashi, S., Rao, R. K., Wanner, T., Tanzi, R. E., et al. (2001). Inducible expression of mutant alpha-synuclein decreases proteasome activity and increases sensitivity to mitochondria-dependent apoptosis. *Hum. Mol. Genet.* 10, 919–926. doi: 10.1093/hmg/10.9.919

Teixeira, F. G., Carvalho, M. M., Neves-Carvalho, A., Panchalingam, K. M., Behie, L. A., Pinto, L., et al. (2015). Secretome of mesenchymal progenitors from the umbilical cord acts as modulator of neural/glial proliferation and differentiation. *Stem Cell Rev.* 11, 288–297. doi: 10.1007/s12015-014-9576-2

Teixeira, F. G., Carvalho, M. M., Panchalingam, K. M., Rodrigues, A. J., Mendes-Pinheiro, B., Anjo, S., et al. (2017). Impact of the secretome of human mesenchymal stem cells on brain structure and animal behavior in a rat model of Parkinson's disease. *Stem Cells Transl. Med.* 6, 634–646. doi: 10.5966/sctm.2016-0071

Teixeira, F. G., Carvalho, M. M., Sousa, N., and Salgado, A. J. (2013). Mesenchymal stem cells secretome: a new paradigm for central nervous system regeneration? *Cell Mol. Life Sci.* 70, 3871–3882. doi: 10.1007/s00018-013-1290-8

Teixeira, F. G., Panchalingam, K. M., Assuncao-Silva, R., Serra, S. C., Mendes-Pinheiro, B., Patricio, P., et al. (2016). Modulation of the mesenchymal stem cell secretome using computer-controlled bioreactors: impact on neuronal cell proliferation, survival and differentiation. *Sci. Rep.* 6:27791. doi: 10.1038/srep27791

Tran, C., and Damaser, M. S. (2015). Stem cells as drug delivery methods: application of stem cell secretome for regeneration. *Adv. Drug Deliv. Rev.* 82–83, 1–11. doi: 10.1016/j.addr.2014.10.007

van Heesbeen, H. J., Mesman, S., Veenvliet, J. V., and Smidt, M. P. (2013). Epigenetic mechanisms in the development and maintenance of dopaminergic neurons. *Development* 140, 1159–1169. doi: 10.1242/dev.089359

Vilaça-Faria, H., Salgado, A. J., and Teixeira, F. G. (2019). Mesenchymal stem cells-derived exosomes: a new possible therapeutic strategy for Parkinson's disease? *Cells* 8:118. doi: 10.3390/cells8020118

Vizoso, F. J., Eiro, N., Cid, S., Schneider, J., and Perez-Fernandez, R. (2017). Mesenchymal stem cell secretome: toward cell-free therapeutic strategies in regenerative medicine. *Int. J. Mol. Sci.* 18:1852. doi: 10.3390/ijms18091852

Vos, T., Abajobir, A. A., Abbafati, C., Abbas, K. M., Abate, K. H., Abd-Allah, F., et al. (2017). Global, regional, and national incidence, prevalence, and years lived with disability for 328 diseases and injuries for 195 countries, 1990–2016: a systematic analysis for the Global Burden of Disease Study 2016. *Lancet* 390, 1211–1259. doi: 10.1016/S0140-6736(17)32154-2

Wang, F., Yasuhara, T., Shingo, T., Kameda, M., Tajiri, N., Yuan, W. J., et al. (2010). Intravenous administration of mesenchymal stem cells exerts therapeutic effects on parkinsonian model of rats: focusing on neuroprotective effects of stromal cell-derived factor-1alpha. *BMC Neurosci.* 11:52. doi: 10.1186/1471-2202-11-52

Xie, W., Li, X., Li, C., Zhu, W., Jankovic, J., and Le, W. (2010). Proteasome inhibition modeling nigral neuron degeneration in Parkinson's disease. *J. Neurochem.* 115, 188–199. doi: 10.1111/j.1471-4159.2010.06914.x

Xin, H., Li, Y., Buller, B., Katakowski, M., Zhang, Y., Wang, X., et al. (2012). Exosome-mediated transfer of miR-133b from multipotent mesenchymal stromal cells to neural cells contributes to neurite outgrowth. *Stem Cells* 30, 1556–1564. doi: 10.1002/stem.1129

Conflict of Interest: The authors declare that the research was conducted in the absence of any commercial or financial relationships that could be construed as a potential conflict of interest.

frontiers in Bioengineering and Biotechnology

MINI REVIEW
published: 05 November 2019
doi: 10.3389/fbioe.2019.00308

Targeting the Immune System With Mesenchymal Stromal Cell-Derived Extracellular Vesicles: What Is the Cargo's Mechanism of Action?

Jorge Diego Martin-Rufino[1,2], *Natalia Espinosa-Lara*[1], *Lika Osugui*[1] *and Fermin Sanchez-Guijo*[1,2,3]*

[1] Unidad de Terapia Celular, Servicio de Hematología, IBSAL-Hospital Universitario de Salamanca, Salamanca, Spain, [2] Facultad de Medicina, Universidad de Salamanca, Salamanca, Spain, [3] Centro en Red de Medicina Regenerativa y Terapia Celular de Castilla y León, Salamanca, Spain

OPEN ACCESS

Edited by:
Martin James Stoddart, AO Research Institute, Switzerland

Reviewed by:
Maurizio Muraca, University of Padova, Italy
Karen Bieback, Universität Heidelberg, Germany

***Correspondence:**
Fermin Sanchez-Guijo
ferminsg@usal.es

Specialty section:
This article was submitted to Tissue Engineering and Regenerative Medicine, a section of the journal Frontiers in Bioengineering and Biotechnology

Received: *02 July 2019*
Accepted: *17 October 2019*
Published: *05 November 2019*

Citation:
Martin-Rufino JD, Espinosa-Lara N, Osugui L and Sanchez-Guijo F (2019) Targeting the Immune System With Mesenchymal Stromal Cell-Derived Extracellular Vesicles: What Is the Cargo's Mechanism of Action? Front. Bioeng. Biotechnol. 7:308. doi: 10.3389/fbioe.2019.00308

The potent immunomodulatory activities displayed by mesenchymal stromal cells (MSCs) have motivated their application in hundreds of clinical trials to date. In some countries, they have subsequently been approved for the treatment of immune disorders such as Crohn's disease and graft-versus-host disease. Increasing evidence suggests that their main mechanism of action *in vivo* relies on paracrine signaling and extracellular vesicles. Mesenchymal stromal cell-derived extracellular vesicles (MSC-EVs) play a prominent role in intercellular communication by allowing the horizontal transfer of microRNAs, mRNAs, proteins, lipids and other bioactive molecules between MSCs and their targets. However, despite the considerable momentum gained by MSC-EV research, the precise mechanism by which MSC-EVs interact with the immune system is still debated. Available evidence is highly context-dependent and fragmentary, with a limited number of reports trying to link their efficacy to specific active components shuttled within them. In this concise review, currently available evidence on the molecular mechanisms underlying the effects of MSC-EV cargo on the immune system is analyzed. Studies that pinpoint specific MSC-EV-borne mediators of immunomodulation are highlighted, with a focus on the signaling events triggered by MSC-EVs in target immune cells. Reports that study the effects of preconditioning or "licensing" in MSC-EV-mediated immunomodulation are also presented. The need for further studies that dissect the mechanisms of MSC-EV cargo in the adaptive immune system is emphasized. Finally, the major challenges that need to be addressed to harness the full potential of these signaling vehicles are discussed, with the ultimate goal of effectively translating MSC-EV treatments into the clinic.

Keywords: mesenchymal stromal cells, extracellular vesicles, immune system, cell therapy, regenerative medicine, stem cells, paracrine signaling, immunomodulation

MESENCHYMAL STROMAL CELLS, EXTRACELLULAR VESICLES, AND IMMUNOMODULATION

Mesenchymal stromal cells (MSCs) are a heterogeneous population of non-hematopoietic, fibroblast-like adult progenitor cells, which can be isolated from a variety of tissue sources (Hass et al., 2011; Samsonraj et al., 2017). MSCs can self-renew and are multipotent, given their ability to differentiate into adipocytes, chondrocytes, and osteocytes *in vitro* (Dominici et al., 2006). MSCs' ease of expansion, together with their tissue repair and immunotherapeutic capabilities, have motivated their application in hundreds of clinical trials to date and their subsequent approval in some countries as therapeutic agents for several immune disorders, such as Crohn's disease and graft-versus-host disease (Galderisi et al., 2016; Najar et al., 2016; Galipeau and Sensébé, 2018).

MSCs display potent immunosuppressive and anti-inflammatory activities, as well as low immunogenicity (Gao et al., 2016). They regulate the innate and adaptive immune systems, and target virtually all immune populations. MSCs suppress lymphocyte proliferation and activation, reduce cytokine secretion and cytotoxicity and induce peripheral tolerance and regulatory cell expansion (Di Nicola et al., 2002; Le Blanc et al., 2003; Zhao et al., 2016). They also hinder dendritic cell maturation and activation and polarize proinflammatory M1 toward anti-inflammatory M2 macrophages (Németh et al., 2009; Spaggiari et al., 2009).

Migration, engraftment and subsequent differentiation into target cells were initially considered the main mechanisms by which MSCs exert their therapeutic effects in regenerative applications. However, paracrine signaling is currently regarded as the primary mode of action of MSCs (Bi et al., 2007; Di Trapani et al., 2016; Vizoso et al., 2017; Ferreira et al., 2018). Indeed, the recent proposal to rename MSCs to "medicinal signaling cells" reflects the paradigm shift in the conception of their main mechanism of action *in vivo,* which is not multipotency but rather the production of trophic factors and bioactive molecules (Caplan, 2017). Furthermore, engraftment following infusion in recipient organisms is rare. It has been reported that MSCs are trapped in the lungs' microvasculature and are cleared within 24 h (Eggenhofer et al., 2012).

The secretome of MSCs encompasses a wide array of factors, including cytokines, chemokines, growth factors, and extracellular matrix proteins. Among the main candidates of MSCs' immunomodulatory effects are indoleamine 2,3-dioxygenase 1, prostaglandin E_2 (PGE_2), hepatocyte growth factor, transforming growth factor beta 1, TNF-alpha induced protein 6 (TSG-6) and major histocompatibility complex class I G (Di Nicola et al., 2002; Meisel et al., 2004; Aggarwal and Pittenger, 2005; Selmani et al., 2008; Choi et al., 2011). Extracellular vesicles (EVs)—bilipid membrane-enclosed vesicles ranging from 50 nm to a few μm in diameter—are also an important part of the MSC secretome (Lener et al., 2015). Mesenchymal stromal cell-derived extracellular vesicles (MSC-EVs) play a prominent role in intercellular communication by allowing the horizontal transfer of microRNAs (miRNAs), mRNAs, lncRNAs, proteins, lipids and other bioactive molecules between MSCs and target cells (Rani et al., 2015; Maas et al., 2017; van Niel et al., 2018).

So far, MSC-EVs have shown considerable therapeutic potential as cell-free surrogates of MSC immunomodulation in multiple disease models (Bruno et al., 2009; Lai et al., 2010). MSC-EVs have also been tested in a patient with graft-versus-host disease and in a patient cohort suffering from chronic kidney disease, although further evidence is still needed to support their widespread clinical use (Kordelas et al., 2014; Nassar et al., 2016). However, despite the considerable momentum gained by MSC-EV research, the precise mechanism by which MSC-EVs interact with the immune system is still debated, since available evidence is highly context-dependent and fragmentary, with a limited number of reports trying to link their efficacy to specific active components shuttled within them. An improved understanding of MSC-EVs' mechanism of action is therefore crucial to improve and standardize these therapies. Furthermore, by enriching MSC-EV cargo with certain bioactive molecules through specific preconditioning protocols tailored to each disease and patient, these strategies could potentially contribute to overcoming one of the major hurdles of MSC-based therapeutics, which is variable patient response (Wang et al., 2014a; Galipeau et al., 2016; Najar et al., 2018; Noronha et al., 2019).

In this work, the currently available evidence on the molecular mechanisms underlying MSC-EV cargo's immunomodulatory effects is reviewed. Although multiple reports have studied the effects of MSC-EVs on the immune system, this concise review selects and organizes studies that functionally validate and pinpoint specific MSC-EV-borne mediators of immunomodulation. The signaling events triggered by MSC-EVs in target immune cells are highlighted. Reports that study the effects of preconditioning in MSC-EV-mediated immunomodulation are also presented, as well as the major challenges that need to be addressed to harness the full potential of these signaling vehicles and effectively bring MSC-EV treatments to the clinic.

CHARACTERIZATION AND CARGO OF MESENCHYMAL STROMAL CELL-DERIVED EXTRACELLULAR VESICLES

MSC-EVs have been traditionally classified as exosomes, microvesicles, and apoptotic bodies (Giebel et al., 2017). However, physical separation of MSC-EVs by this biogenesis-based classification is not realistic given the current lack of unequivocally or universally specific makers for each subtype (Lötvall et al., 2014). For this reason, a recent position statement from the International Society for Extracellular Vesicles recommends to instead refer to EV subtypes using operational terms, such as size, density, biochemical composition, or descriptions of specific EV conditions or cell of origin (Théry et al., 2018).

MSC-EV characterization should comprise multiple, complementary techniques to rule out confounding factors and

assure that observed biological effects are not due to co-isolated materials (Théry et al., 2018). However, given the large number of MSC sources, culture conditions, preconditioning protocols, and EV isolation strategies, developing a one-size-fits-all solution to define MSC-EVs is not feasible. As a minimum prerequisite, MSC-EVs should derive from MSCs that meet the minimal criteria from the International Society for Cell and Gene Therapy (Dominici et al., 2006; Ramos et al., 2016; Witwer et al., 2019). MSC-EV characterization should also include assessment of MSC-EVs' lipid to protein or RNA ratios, purity, integrity, and cargo biological activity (Witwer et al., 2019).

Selective sorting mechanisms operate to enrich specific RNAs, proteins and lipids within EVs (Anand et al., 2019). Despite the aforementioned disparity of MSC-EV sources and preparation methods, a common specific MSC-EV proteomic signature has been recently proposed (Van Balkom et al., 2019). Comprehensive overviews of the miRNA and lipidomic profiles of MSC-EVs harvested from different tissue sources have also been published (Baglio et al., 2015; Fang et al., 2016; Ferguson et al., 2018; Kaur et al., 2018; Liu et al., 2019; Showalter et al., 2019). As the field of MSC-EV research grows, similar approaches will be crucial to understand and characterize the profile of EVs harvested from preconditioned MSCs.

MOLECULAR MEDIATORS OF THE CROSS-TALK BETWEEN MESENCHYMAL STROMAL CELL-DERIVED EXTRACELLULAR VESICLES AND THE IMMUNE SYSTEM

The majority of reports presented here focus on macrophages (**Figure 1**), underscoring the need for further studies that dissect these mechanisms in adaptive immunity. Interestingly, a recent paper reported that MSCs' immunomodulatory effects on B cells were not mediated by secreted MSC-EVs (Carreras-Planella et al., 2019). It is worth noting that the authors used size-exclusion chromatography to isolate EVs, in contrast with most of the works reviewed here, which rely on ultracentrifugation methods. Previous reports have also suggested that MSC-EVs are not as effective as their cellular counterparts (Conforti et al., 2014; Gouveia-de-Andrade et al., 2015). This highlights the necessity of greater standardization and reproducibility, given the variety of cell sources, isolation and functional assays available (Théry et al., 2018).

miRNAs

miRNAs are a subtype of small non-coding RNAs which interact with target mRNA molecules to induce their degradation and translational repression (O'Brien et al., 2018). miRNAs are selectively sorted into EVs, in which they remain protected from degradation (Li et al., 2012). Thus, miRNAs are delivered into target cells with high efficiency, in which they exert biological effects and regulate cell activity (Gallo et al., 2012; O'Brien et al., 2018). Several miRNAs have been singled out as mediators of the immunomodulatory effects of MSC-EVs on immune populations, and are briefly summarized below.

Toll like receptor 4 (TLR4) and the MYD88 innate immune signal transduction adaptor (MYD88)-dependent signaling pathway are the focus of a significant number of studies that analyze the effects of MSC-EV cargo on macrophage function. This signaling pathway mediates macrophage activation upon recognition of pathogen-associated molecular patterns such as bacterial lipopolysaccharide (LPS) (Lu et al., 2008; Park and Lee, 2013). Downstream signaling effectors converge to nuclear factor kappa B (NF-κB), which controls the expression of numerous proinflammatory molecules and drives macrophages into a M1 proinflammatory phenotype (Wang et al., 2014b). Several miRNAs presented in this and the preconditioning sections of the review target components of the TLR pathway. Among such miRNAs are miR-21, miR-146a, miR-182 or miR-223, to cite a few, which are enriched in MSC-EVs and act as negative regulators of this pathway (O'Neill et al., 2011; Qin et al., 2018; Curtale et al., 2019).

Murine MSC-EVs, enriched in miR-182-5p, have been shown to reduce TLR4, MyD88 and NF-κB levels in macrophages and induce polarization toward an M2 anti-inflammatory phenotype (Zhao et al., 2019). These effects were recapitulated by a miR-182 mimic and partially reversed upon miR-182 depletion in MSC-EVs. In an *in vivo* murine model of myocardial damage, the authors also showed that TLR4-deficient mice recapitulated MSC-EV-mediated dampening of myocardial inflammation and macrophages' phenotype shift.

An additional study focusing on macrophage polarization analyzed the role of MSC-EV-borne mir-223 (Wang et al., 2015). Through loss-of-function studies, it was shown that MSC-EVs from *Mir223* knockout mice failed to reduce LPS-induced cytokine production in macrophages. In turn, MSC-EVs from wild type mice carrying miR-223-5p and -3p inhibited this secretion. Furthermore, MSC-EVs dampened systemic inflammatory response, reduced cardiac dysfunction and increased survival in a murine model of polymicrobial sepsis, while injection of MSC-EVs from *Mir223* knockout mice failed to display these effects. Both miR-223-5p and -3p target numerous inflammatory mediators and have recently emerged as a critical factors in the pathogenesis of sepsis and inflammatory disease (Haneklaus et al., 2013).

In a report by Liu et al. (2018), mouse MSC-EVs also suppressed the secretion of proinflammatory mediators by impeding the activation of the nucleotide-binding and oligomerization domain-like receptor 3 (NLRP3) inflammasome in macrophages both *in vitro* and *in vivo*. Recently, several miRNAs have emerged as key regulators of the inflammasome, among which miR-17 is included (Zamani et al., 2019). Enriched in murine MSC-EVs, miR-17 was shown to reduce TXNIP levels, a key mediator of NLRP3 inflammasome activation. Disease amelioration and decreased NLRP3, caspase 1, IL-1ß and IL-18 levels were observed upon MSC-EV treatment. The observed *in vitro* and *in vivo* effects in macrophages were abrogated upon miR-17 knockdown in MSC-EVs.

miR-21-5p, highly enriched in human MSC-EVs, was pinpointed as a potential mediator of human MSC-EVs' impairment of dendritic cells' migration ability *in vitro* (Reis et al., 2018). MSC-EV-borne miR-21-5p decreased

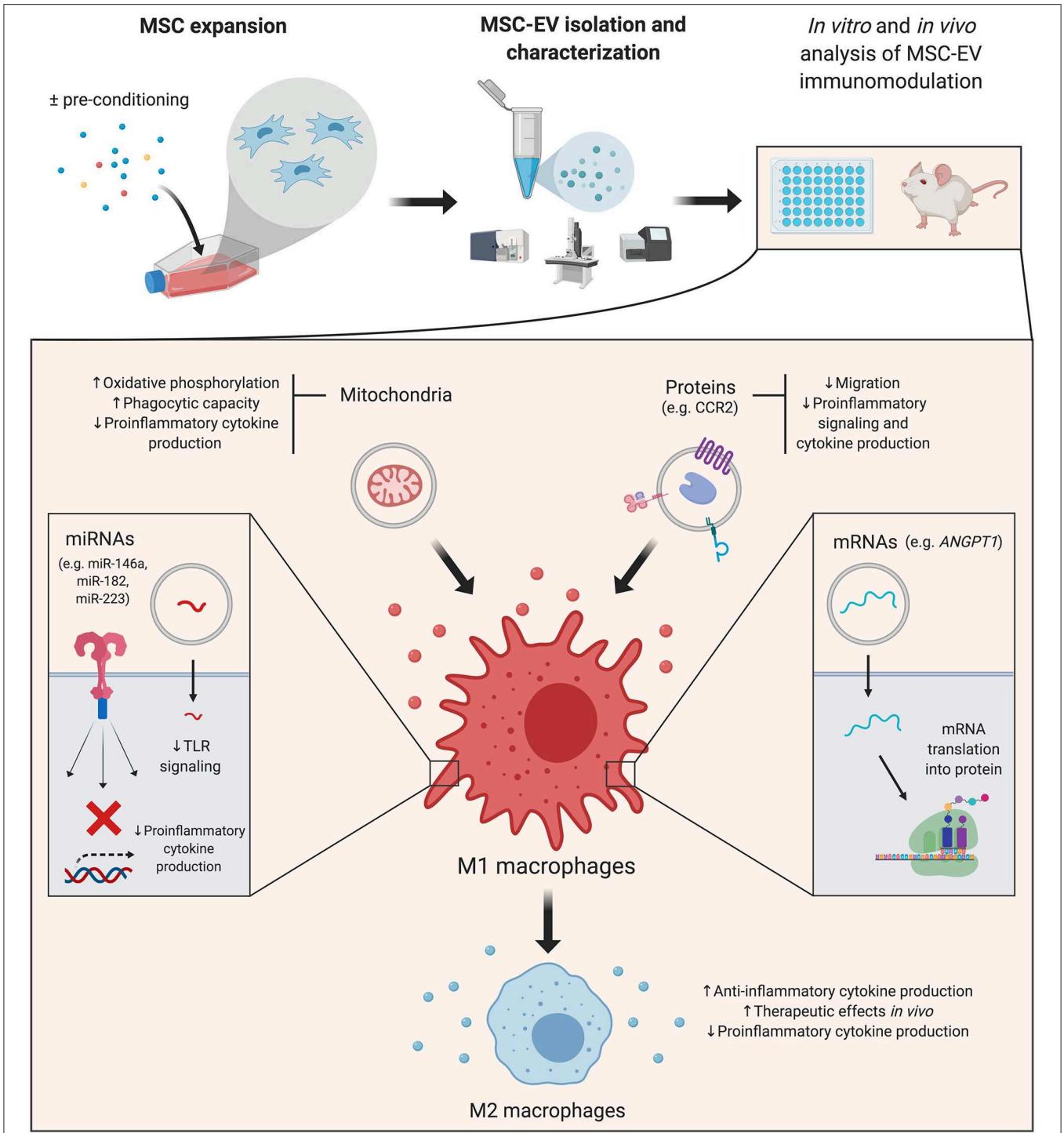

FIGURE 1 | Mesenchymal stromal cell-derived extracellular vesicles (MSC-EVs): cargo's effects on macrophages. A simplified overview of the main effects triggered by MSC-EV cargo in macrophages–which are the focus of the majority of reviewed studies–is presented. MSC-EVs are isolated from cultured cells, which can be pre-conditioned with different strategies to increase their immunomodulatory potential. Details of the effector molecules, signaling pathways and mediated immunological effects are presented in the main text. *ANGPT1*, angiopoietin 1; CCR2, membrane receptor chemokine (C-C motif) receptor 2; miRNA, microRNA; MSC, mesenchymal stromal cell; MSC-EV, mesenchymal stromal cell-derived extracellular vesicle; TLR, toll like receptor. Created with BioRender.com.

dendritic cells' CCR7 levels, a chemokine receptor with a crucial role in mature dendritic cell lymph node homing (Comerford et al., 2013). In this study, MSC-EVs also reduced antigen uptake in immature dendritic cells, limited their maturation and activation and increased anti-inflammatory cytokine production.

Corneal MSC-EVs were shown to reduce corneal neutrophil infiltration and fibrotic gene expression after wounding (Shojaati et al., 2019). However, MSC-EVs' regenerative capabilities were hampered following knockdown of Alix, a component of the miRNA EV-packaging system. This evidence, together with previous studies on liver fibrosis and inflammation, underscores the role of MSC-EV-borne miRNAs as mediators of MSC-EVs' interactions with the extracellular matrix, fibrosis, and scarring (Qiu et al., 2018).

mRNAs

Horizontal mRNA transfer mediated by MSC-EVs has recently emerged as a mechanism of paracrine exchange of genetic information by MSCs (Tomasoni et al., 2013; Ragni et al., 2017). These studies demonstrated effective horizontal mRNA transfer by MSC-EVs and subsequent translation in recipient cells, thus conferring new functionality. These findings are supported by the notion that MSC-EVs display a specific mRNA profile rather than just a random subset of expressed genes (Bruno et al., 2009; Ragni et al., 2017).

In a murine model of LPS-induced acute lung injury, experimental data suggested that human MSC-EV-transferred fibroblast growth factor 7 (*FGF7,* also known as keratinocyte growth factor) mRNA could mediate the therapeutic effects of MSCs. *FGF7* mRNA transfer and subsequent translation into human FGF7 protein contributed to a decrease in neutrophil influx and chemokine (C-X-C motif) ligand 2 (CXCL2) levels in the bronchoalveolar lavage fluid (BALF) (Zhu et al., 2014). It is worth noting that *FGF7* is one the most highly enriched mRNA in human MSC-EVs (Ragni et al., 2017). Indeed, the effects on acute lung injury were partially negated following MSC pretreatment with siRNA against *FGF7*. However, in this study, whether *FGF7* mRNA directly targeted the lung epithelium or inflammatory cells remained unanswered.

In the context of MSC-EVs' immunomodulatory effects on immune populations, a subsequent study by the same group demonstrated that angiopoietin 1 (*ANGPT1*) mRNA in MSC-EVs mediated an increase in IL-10 and a decrease in TNF-alpha in macrophages *in vitro* (Tang et al., 2017). This effect was lost in EVs derived from MSCs transfected with shRNA against *ANGPT1,* thus demonstrating a role for mRNA transfer in the crosstalk between MSC-EVs and immune cells. Reminiscent of the first study, MSC-EVs also reduced neutrophil influx and CXCL2 levels in the BALF of mice with LPS-induced acute lung injury. In contrast, *ANGPT1* mRNA-deficient MSC-EVs failed to do so.

Proteins

MSC-EVs are endorsed with functional surface proteins and may also modulate target cells by delivering intracellular proteins. Among the first group of molecules is the membrane receptor chemokine (C-C motif) receptor 2 (CCR2), enriched in murine MSC-EVs. It has been suggested that MSC-EV-borne CCR2 acts as a decoy to bind and reduce free extracellular C-C motif chemokine ligand 2 (CCL2) levels and function (Shen et al., 2016). MSC-EV treatment blocked CCL2 effects on macrophage recruitment, induction of NF-κB signaling and subsequent expression of proinflammatory cytokines.

TSG-6 was also validated as a one of the protein mediators of MSC-EV immunomodulation in a murine model of hyperoxia-induced lung injury. MSC-EV-induced decrease in neutrophil infiltration in BALF was negated by neutralizing anti-TSG-6 antibodies and by siRNA knockdown of TSG-6 within vesicles (Chaubey et al., 2018).

Inflammation-stimulated MSC-EVs were also found to be enriched in cyclooxygenase 2 (COX2), which might contribute to a local increase in PGE_2 (Harting et al., 2018). Moreover, MSC-EVs treated with COX2 inhibitors displayed reduced anti-inflammatory capabilities in an *in vitro* TNF-alpha production assay.

Mitochondria

Intriguingly, mitochondrial transfer to target cells has been recently identified as a mediator of MSCs' biological effects (Spees et al., 2006; Otsu et al., 2009; Islam et al., 2012; Konari et al., 2019). In particular, MSC-EV-mediated mitochondrial transfer enhanced oxidative phosphorylation in macrophages, which resulted in a reduction of their proinflammatory cytokine secretion and increased phagocytic capacity (Morrison et al., 2017). Phinney et al. (2015) provided further evidence that macrophages could engulf MSC-EV-borne mitochondria, which in turn enhanced macrophage bioenergetics. Collectively, these studies suggest a role for MSC-EV-mediated mitochondrial transfer in the modulation of the innate immune system.

PRECONDITIONING MODULATES MESENCHYMAL STROMAL CELL-DERIVED EXTRACELLULAR VESICLE CARGO AND IMPROVES ITS THERAPEUTIC EFFECTS

The immunosuppressive properties of MSCs are deeply influenced by the stimuli present in their local microenvironment, and the nature of these signals fundamentally determines the immunomodulatory effects of MSCs (Ren et al., 2008; Wang et al., 2014a; Najar et al., 2018). This context-dependency is endorsed by the fact that MSCs display increased efficacy in preclinical models of established inflammatory disease compared to their preventive administration before inflammation develops (Sudres et al., 2006; Shi et al., 2012). For this reason, several strategies have been proposed in order to precondition MSCs and improve their therapeutic potential, including proinflammatory cytokines, hypoxia, or chemical compounds (Najar et al., 2018; Noronha et al., 2019). These strategies aim to recapitulate the microenvironment to which MSCs are exposed upon infusion in patients with systemic inflammation or altered immune responses (Galipeau et al., 2016). As expected, the MSC secretome and MSC-EVs are also affected by preconditioning strategies, which

modulate their cargo and immunosuppressive properties (Domenis et al., 2018; Ferreira et al., 2018; Harting et al., 2018, Showalter et al., 2019).

Multiple studies have demonstrated that preconditioned MSC-EVs display an increased ability to induce an M2 anti-inflammatory phenotype in macrophages compared to basal MSC-EVs. As such, Domenis et al. (2018) reported that priming human MSCs with proinflammatory cytokines IFN-gamma and TNF-alpha favored this effect in MSC-EVs. Specific miRNAs involved in macrophage polarization were enriched in MSC-EVs following inflammatory preconditioning, among which stood miR-34a-5p, miR-146a-5p, and miR-21-5p. Interleukin 1 receptor associated kinase 1 (IRAK1), a signaling mediator of the MyD88 signaling pathway targeted by miR-146a, was strongly downregulated upon treatment with preconditioned MSC-EVs. Further functional studies will help understand the individual contribution of each identified miRNA to the observed effects.

Human MSC-EV-borne miR-146a was also the focus of Song et al. (2017), who observed that this miRNA was particularly enriched in IL-1ß-primed MSC-EVs. Primed MSC-EVs delivered miR-146a into macrophages, increased M2 markers IL-10 and *Arg1* mRNA, and decreased M1 markers TNF-alpha and *Nos2* (iNOS) mRNA in a greater extent that basal MSC-EVs. These effects were lost in IL-1ß-primed MSC-EVs previously transfected with miR-146a inhibitors, underscoring the role of miR-146a in M2 polarization by IL-1ß-primed MSC-EVs.

Increased M2 polarization capacity was also observed in EVs from LPS preconditioned MSCs. In this regard, the work from Ti et al. (2015) uncovered let-7b as the highest uniquely-expressed miRNA in human MSC-EVs with this priming strategy. let-7b regulated macrophage polarization through TLR4 and NF-κB subunit p65 downregulation and signal transducer and activator of transcription 3 (STAT3) and AKT upregulation.

Various studies focused on the influence of hypoxia in the mechanism of action of MSC-EV cargo. Lo Sicco et al. (2017) demonstrated that EVs from human MSCs cultured under hypoxic conditions displayed an increased ability to induce murine M2 anti-inflammatory macrophages compared to basal MSC-EVs. miR-223 and miR-146b stood out among over-expressed miRNAs in hypoxia-preconditioned MSC-EVs. Ren et al. (2019) provided further evidence that hypoxia-preconditioned human MSC-EVs favor human macrophage M2 polarization in comparison to their normoxic counterparts. In their study, they showed that miR-21-5p knockdown abrogated these effects, likely mediated by phosphatase and tensin homolog (PTEN) downregulation, which in turn released its blockage of AKT and STAT3 activation. These effects were maintained *in vivo* and partially mediated by miR-21-5p, which had been previously shown to be enriched in hypoxia-preconditioned murine MSC-EVs (Cui et al., 2018). Hypoxia is one of the hallmarks of tissue damage, and its use in MSC preconditioning might mimic the microenvironment to which MSCs are exposed *in vivo* (Ferreira et al., 2018).

CLOSING REMARKS: THE ROAD TOWARD CLINICAL-GRADE, CELL-FREE THERAPEUTICS

The generalized use of clinical-grade MSC-EVs is still far from becoming a reality, based on a number of challenges that need to be solved in the coming years. One of the main limitations for the use of EVs is the low yield of particles obtained with current technologies used for EV isolation and purification, resulting in insufficient EV numbers for clinical purposes (Haraszti et al., 2018; Paganini et al., 2019). The use of spinner-flasks containing different microcarriers that retain MSCs is one of the most extended options to increase MSC numbers, together with the use of hollow-fiber bioreactors, which can anchor up to 100-fold higher MSCs than conventional flasks (Lu et al., 2017; Cha et al., 2018; Phan et al., 2018). Alternative EV isolation techniques, some of which can be scalable and potentially GMP compatible, can potentially increase MSC-EV recovery (Watson et al., 2018, Paganini et al., 2019).

The multiple immunomodulatory signaling capabilities presented in the previous sections show MSC-EVs' immense potential for the treatment of immune disorders. MSC are considered advanced-therapy medical products (ATMP) by regulatory agencies (Lener et al., 2015). In contrast, given their cell-free nature, MSC-EVs are not subject to complex ATMP regulations and do not carry the risk of carcinogenic potential transformation. Due to their size, they are able to traverse the blood-brain barrier and other physiological interfaces. Finally, MSC-EVs are easily handled and stored and remain stable for extended periods of time (Rani et al., 2015; Maas et al., 2017; Sharma et al., 2017). Such potential advantages make MSC-EVs promising candidates for future therapeutic applications.

The studies summarized in this work support the claim that the fundamental mechanism of action of MSC-EVs lies in their ability to transmit biological information between cells. Although multiple candidates within MSC-EV cargo have been presented as mediators of their therapeutic effects, many operate through similar pathways and mechanisms of action, warranting further investigations that dissect their individual contribution. These studies are the starting point for the future development of engineered MSC-EVs and targeted preconditioning protocols, which could potentially enrich MSC-EVs with relevant immunomodulatory effectors and thus broaden their therapeutic capabilities in immune system disorders.

AUTHOR CONTRIBUTIONS

JM-R and FS-G conceptualized, designed and wrote the manuscript. JM-R drafted the manuscript, reviewed the literature and designed the figure. NE-L and LO revised and provided critical feedback on the manuscript.

FUNDING

FS-G was funded by Instituto de Salud Carlos III (PI16/01407), Consejería de Sanidad de Castilla y León (GRS1621/A/17) and Consejería de Educación de Castilla y León (CAS079P17). LO was also supported by Consejería de Educación de Castilla y León (CAS079P17). JM-R was supported by Fundación Científica de la Asociación Española contra el Cáncer (AECC). NE-L was funded by Sociedad Española de Hematología y Hemoterapia.

ACKNOWLEDGMENTS

We are grateful to Gaurav Agarwal for his comments on the manuscript.

REFERENCES

Aggarwal, S., and Pittenger, M. F. (2005). Human mesenchymal stem cells modulate allogeneic immune cell responses. *Blood* 105, 1815–1822. doi: 10.1182/blood-2004-04-1559

Anand, S., Samuel, M., Kumar, S., and Mathivanan, S. (2019). Ticket to a bubble ride: cargo sorting into exosomes and extracellular vesicles. *Biochim. Biophys. Acta* 26:140203. doi: 10.1016/j.bbapap.2019.02.005

Baglio, S. R., Rooijers, K., Koppers-Lalic, D., Verweij, F. J., Pérez Lanzón, M., Zini, N., et al. (2015). Human bone marrow- and adipose-mesenchymal stem cells secrete exosomes enriched in distinctive miRNA and tRNA species. *Stem Cell Res. Ther*. 6:127. doi: 10.1186/s13287-015-0116-z

Bi, B., Schmitt, R., Israilova, M., Nishio, H., and Cantley, L. G. (2007). Stromal cells protect against acute tubular injury via an endocrine effect. *J. Am. Soc. Nephrol.* 18, 2486–2496. doi: 10.1681/ASN.2007020140

Bruno, S., Grange, C., Deregibus, M. C., Calogero, R. A., Saviozzi, S., Collino, F., et al. (2009). Mesenchymal stem cell-derived microvesicles protect against acute tubular injury. *J. Am. Soc. Nephrol*. 20, 1053–1067. doi: 10.1681/ASN.2008070798

Caplan, A. I. (2017). Mesenchymal stem cells: time to change the name!. *Stem Cells Transl. Med*. 6, 1445–1451. doi: 10.1002/sctm.17-0051

Carreras-Planella, L., Monguió-Tortajada, M., Borràs, F. E., and Franquesa, M. (2019). Immunomodulatory effect of MSC on B cells is independent of secreted extracellular vesicles. *Front. Immunol*. 10:1288. doi: 10.3389/fimmu.2019.02413

Cha, J. M., Shin, E. K., Sung, J. H., Moon, G. J., Kim, E. H., Cho, Y. H., et al. (2018). Efficient scalable production of therapeutic microvesicles derived from human mesenchymal stem cells. *Sci. Rep*. 8:1171. doi: 10.1038/s41598-018-19211-6

Chaubey, S., Thueson, S., Ponnalagu, D., Alam, M. A., Gheorghe, C. P., Aghai, Z., et al. (2018). Early gestational mesenchymal stem cell secretome attenuates experimental bronchopulmonary dysplasia in part via exosome-associated factor TSG-6. *Stem Cell Res. Ther*. 9:173. doi: 10.1186/s13287-018-0903-4

Choi, H., Lee, R. H., Bazhanov, N., Oh, J. Y., and Prockop, D. J. (2011). Anti-inflammatory protein signaling in resident macrophages. *Blood* 118, 330–8. doi: 10.1182/blood-2010-12-327353

Comerford, I., Harata-Lee, Y., Bunting, M. D., Gregor, C., Kara, E. E., and McColl, S. R. (2013). A myriad of functions and complex regulation of the CCR7/CCL19/CCL21 chemokine axis in the adaptive immune system. *Cytokine Growth Factor Rev.* 24, 269–283. doi: 10.1016/j.cytogfr.2013.03.001

Conforti, A., Scarsella, M., Starc, N., Giorda, E., Biagini, S., Proia, A., et al. (2014). Microvescicles derived from mesenchymal stromal cells are not as effective as their cellular counterpart in the ability to modulate immune responses *in vitro*. *Stem Cells Dev*. 23, 2591–2599. doi: 10.1089/scd.2014.0091

Cui, G. H., Wu, J., Mou, F. F., Xie, W. H., Wang, F. B., Wang, Q. L., et al. (2018). Exosomes derived from hypoxia-preconditioned mesenchymal stromal cells ameliorate cognitive decline by rescuing synaptic dysfunction and regulating inflammatory responses in APP/PS1 mice. *FASEB J*. 32, 654–668. doi: 10.1096/fj.201700600R

Curtale, G., Rubino, M., and Locati, M. (2019). MicroRNAs as molecular switches in macrophage activation. *Front. Immunol.* 10:799. doi: 10.3389/fimmu.2019.00799

Di Nicola, M., Carlo-Stella, C., Magni, M., Milanesi, M., Longoni, P. D., Matteucci, P., et al. (2002). Human bone marrow stromal cells suppress T-lymphocyte proliferation induced by cellular or nonspecific mitogenic stimuli. *Blood*. 99, 3838–3843. doi: 10.1182/blood.V99.10.3838

Di Trapani, M., Bassi, G., Midolo, M., Gatti, A., Kamga, P. T., Cassaro, A., et al. (2016). Differential and transferable modulatory effects of mesenchymal stromal cell-derived extracellular vesicles on T, B and NK cell functions. *Sci. Rep*. 6:24120. doi: 10.1038/srep24120

Domenis, R., Cifù, A., Quaglia, S., Pistis, C., Moretti, M., Vicario, A., et al. (2018). Pro inflammatory stimuli enhance the immunosuppressive functions of adipose mesenchymal stem cells-derived exosomes. *Sci. Rep*. 8:13325. doi: 10.1038/s41598-018-31707-9

Dominici, M., Le Blanc, K., Mueller, I., Slaper-Cortenbach, I., Marini, F. C., Krause, D. S., et al. (2006). Minimal criteria for defining multipotent mesenchymal stromal cells. The international society for cellular therapy position statement. *Cytotherapy* 8, 315–317. doi: 10.1080/14653240600855905

Eggenhofer, E., Benseler, V., Kroemer, A., Popp, F. C., Geissler, E. K., Schlitt, H. J., et al. (2012). Mesenchymal stem cells are short-lived and do not migrate beyond the lungs after intravenous infusion. *Front. Immunol.* 3:297. doi: 10.3389/fimmu.2012.00297

Fang, S., Xu, C., Zhang, Y., Xue, C., Yang, C., Bi, H., et al. (2016). Umbilical cord-derived mesenchymal stem cell-derived exosomal MicroRNAs suppress myofibroblast differentiation by inhibiting the transforming growth factor-β/SMAD2 pathway during wound healing. *Stem Cells Transl. Med*. 5, 1425–1439. doi: 10.5966/sctm.2015-0367

Ferguson, S. W., Wang, J., Lee, C. J., Liu, M., Neelamegham, S., Canty, J. M., et al. (2018). The microRNA regulatory landscape of MSC-derived exosomes: a systems view. *Sci. Rep*. 8:1419. doi: 10.1038/s41598-018-19581-x

Ferreira, J. R., Teixeira, G. Q., Santos, S. G., Barbosa, M. A., Almeida-Porada, G., and Gonçalves, R. M. (2018). Mesenchymal stromal cell secretome: influencing therapeutic potential by cellular pre-conditioning. *Front. Immunol.* 9:2837. doi: 10.3389/fimmu.2018.02837

Galderisi, U., Squillaro, T., and Peluso, G. (2016). Clinical trials with mesenchymal stem cells: an update. *Cell Transplant*. 25, 829–848. doi: 10.3727/096368915X689622

Galipeau, J., Krampera, M., Barrett, J., Dazzi, F., Deans, R. J., DeBruijn, J., et al. (2016). International society for cellular therapy perspective on immune functional assays for mesenchymal stromal cells as potency release criterion for advanced phase clinical trials. *Cytotherapy* 18,151–159. doi: 10.1016/j.jcyt.2015.11.008

Galipeau, J., and Sensébé, L. (2018). Mesenchymal stromal cells: clinical challenges and therapeutic opportunities. *Cell Stem Cell* 22, 824–833. doi: 10.1016/j.stem.2018.05.004

Gallo, A., Tandon, M., Alevizos, I., and Illei, G. G. (2012). The majority of microRNAs detectable in serum and saliva is concentrated in exosomes. *PLoS ONE* 7:e30679. doi: 10.1371/journal.pone.0030679

Gao, F., Chiu, S. M., Motan, D. A., Zhang, Z., Chen, L., Ji, H. L., et al. (2016). Mesenchymal stem cells and immunomodulation: current status and future prospects. *Cell Death Dis*. 7:e2062. doi: 10.1038/cddis.2015.327

Giebel, B., Kordelas, L., and Börger, V. (2017). Clinical potential of mesenchymal stem/stromal cell-derived extracellular vesicles. *Stem Cell Investig.* 4:84. doi: 10.21037/sci.2017.09.06

Gouveia-de-Andrade, A. V., Bertolino, G., Riewaldt, J., Bieback, K., Karbanová, J., Odendahl, M., et al. (2015). Extracellular vesicles secreted by bone marrow- and adipose tissue-derived mesenchymal stromal cells fail to suppress lymphocyte proliferation. *Stem Cells Dev*. 24, 1374–1376. doi: 10.1089/scd.2014.0563

Haneklaus, M., Gerlic, M., O'Neill, L. A. J., and Masters, S. L. (2013). miR-223: infection, inflammation and cancer. *J. Intern. Med.* 274, 215–226. doi: 10.1111/joim.12099

Haraszti, R. A., Miller, R., Stoppato, M., Sere, Y. Y., Coles, A., Didiot, M. C., et al. (2018). Exosomes produced from 3D cultures of MSCs by tangential flow

filtration show higher yield and improved activity. *Mol. Ther.* 26, 2838–2847. doi: 10.1016/j.ymthe.2018.09.015

Harting, M. T., Srivastava, A. K., Zhaorigetu, S., Bair, H., Prabhakara, K. S., Toledano Furman, N. E., et al. (2018). Inflammation-stimulated mesenchymal stromal cell-derived extracellular vesicles attenuate inflammation. *Stem Cells* 36, 79–90. doi: 10.1002/stem.2730

Hass, R., Kasper, C., Böhm, S., and Jacobs, R. (2011). Different populations and sources of human mesenchymal stem cells (MSC): a comparison of adult and neonatal tissue-derived MSC. *Cell Commun. Signal.* 9:12. doi: 10.1186/1478-811X-9-12

Islam, M. N., Das, S. R., Emin, M. T., Wei, M., Sun, L., Westphalen, K., et al. (2012). Mitochondrial transfer from bone-marrow–derived stromal cells to pulmonary alveoli protects against acute lung injury. *Nat. Med.* 18, 759–765. doi: 10.1038/nm.2736

Kaur, S., Abu-Shahba, A. G., Paananen, R. O., Hongisto, H., Hiidenmaa, H., Skottman, H., et al. (2018). Small non-coding RNA landscape of extracellular vesicles from human stem cells. *Sci. Rep.* 8:15503. doi: 10.1038/s41598-018-33899-6

Konari, N., Nagaishi, K., Kikuchi, S., and Fujimiya, M. (2019). Mitochondria transfer from mesenchymal stem cells structurally and functionally repairs renal proximal tubular epithelial cells in diabetic nephropathy *in vivo*. *Sci. Rep.* 9:5184. doi: 10.1038/s41598-019-40163-y

Kordelas, L., Rebmann, V., Ludwig, A. K., Radtke, S., Ruesing, J., Doeppner, T. R., et al. (2014). MSC-derived exosomes: a novel tool to treat therapy-refractory graft-versus-host disease. *Leukemia* 28,970–973. doi: 10.1038/leu.2014.41

Lai, R. C., Arslan, F., Lee, M. M., Sze, N. S., Choo, A., Chen, T. S., et al. (2010). Exosome secreted by MSC reduces myocardial ischemia/reperfusion injury. *Stem Cell Res.* 4, 214–222. doi: 10.1016/j.scr.2009.12.003

Le Blanc, K., Tammik, L., Sundberg, B., Haynesworth, S. E., and Ringden, O. (2003). Mesenchymal stem cells inhibit. *Immunology* 57, 11–20. doi: 10.1046/j.1365-3083.2003.01176.x

Lener, T., Gimona, M., Aigner, L., Börger, V., Buzas, E., Camussi, G., et al. (2015). Applying extracellular vesicles based therapeutics in clinical trials – an ISEV position paper. *J. Extracell Vesicles* 4:30087. doi: 10.3402/jev.v4.30087

Li, L., Zhu, D., Huang, L., Zhang, J., Bian, Z., Chen, X., et al. (2012). Argonaute 2 complexes selectively protect the circulating microRNAs in cell-secreted microvesicles. *PLoS ONE* 7:e46957. doi: 10.1371/journal.pone.0046957

Liu, T., Zhang, Q., Zhang, J., Li, C., Miao, Y., Lei, Q., et al. (2019). EVmiRNA: a database of miRNA profiling in extracellular vesicles. *Nucleic Acids Res.* (2019) 47:D89–93. doi: 10.1093/nar/gky985

Liu, Y., Lou, G., Li, A., Zhang, T., Qi, J., Ye, D., et al. (2018). AMSC-derived exosomes alleviate lipopolysaccharide/d-galactosamine-induced acute liver failure by miR-17-mediated reduction of TXNIP/NLRP3 inflammasome activation in macrophages. *EBioMedicine*. 36, 140–150. doi: 10.1016/j.ebiom.2018.08.054

Lo Sicco, C., Reverberi, D., Balbi, C., Ulivi, V., Principi, E., Pascucci, L., et al. (2017). Mesenchymal stem cell-derived extracellular vesicles as mediators of anti-inflammatory effects: endorsement of macrophage polarization. *Stem Cells Transl. Med.* 6, 1018–1028. doi: 10.1002/sctm.16-0363

Lötvall, J., Hill, A. F., Hochberg, F., Buzás, E. I., Di Vizio, D., Gardiner, C., et al. (2014). Minimal experimental requirements for definition of extracellular vesicles and their functions: a position statement from the International Society for Extracellular Vesicles. *J. Extracell Vesicles* 3:26913. doi: 10.3402/jev.v3.26913

Lu, M., Xing, H., Yang, Z., Sun, Y., Yang, T., Zhao, X., et al. (2017). Recent advances on extracellular vesicles in therapeutic delivery: challenges, solutions, and opportunities. *Eur. J. Pharm. Biopharm.* 119, 381–395. doi: 10.1016/j.ejpb.2017.07.010

Lu, Y. C., Yeh, W. C., and Ohashi, P. S. (2008). LPS/TLR4 signal transduction pathway. *Cytokine* 42, 145–51. doi: 10.1016/j.cyto.2008.01.006

Maas, S. L. N., Breakefield, X. O., and Weaver, A. M. (2017). Extracellular vesicles: Unique intercellular delivery vehicles. *Trends Cell Biol.* 27, 172–88. doi: 10.1016/j.tcb.2016.11.003

Meisel, R., Zibert, A., Laryea, M., Göbel, U., Däubener, W., Dilloo, D., et al. (2004). Human bone marrow stromal cell responses by indoleamine 2,3-dioxygenase-mediated tryptophan degradation. *Blood* 103, 4619–21. doi: 10.1182/blood-2003-11-3909

Morrison, T. J., Jackson, M., Cunningham, E. K., Kissenpfennig, A., McAuley, D. F., O'Kane, C. M., et al. (2017). Mesenchymal stromal cells modulate macrophages in clinically relevant lung injury models by extracellular vesicle mitochondrial transfer. *Am. J. Respir. Crit. Care Med.* 196, 1275–1286. doi: 10.1164/rccm.201701-0170OC

Najar, M., Krayem, M., Merimi, M., Burny, A., Meuleman, N., Bron, D., et al. (2018). Insights into inflammatory priming of mesenchymal stromal cells: functional biological impacts. *Inflamm. Res.* 67, 467–477. doi: 10.1007/s00011-018-1131-1

Najar, M., Raicevic, G., Fayyad-Kazan, H., Bron, D., Toungouz, M., and Lagneaux, L. (2016). Mesenchymal stromal cells and immunomodulation: a gathering of regulatory immune cells. *Cytotherapy* 18, 160–171. doi: 10.1016/j.jcyt.2015.10.011

Nassar, W., El-Ansary, M., Sabry, D., Mostafa, M. A., Fayad, T., Kotb, E., et al. (2016). Umbilical cord mesenchymal stem cells derived extracellular vesicles can safely ameliorate the progression of chronic kidney diseases. *Biomater Res.* 20:21. doi: 10.1186/s40824-016-0068-0

Németh, K., Leelahavanichkul, A., Yuen, P. S., Mayer, B., Parmelee, A., Doi, K., et al. (2009). Bone marrow stromal cells attenuate sepsis via prostaglandin E2–dependent reprogramming of host macrophages to increase their interleukin-10 production. *Nat. Med.* 15, 42–49. doi: 10.1038/nm.1905

Noronha, N. C., Mizukami, A., Caliári-Oliveira, C., Cominal, J. G., Rocha, J. L. M., Covas, D. T., et al. (2019). Priming approaches to improve the efficacy of mesenchymal stromal cell-based therapies. *Stem Cell Res. Ther.* 10:131. doi: 10.1186/s13287-019-1224-y

O'Brien, J., Hayder, H., Zayed, Y., and Peng, C. (2018). Overview of microRNA biogenesis, mechanisms of actions, and circulation. *Front. Endocrinol.* 9:402. doi: 10.3389/fendo.2018.00402

O'Neill, L. A., Sheedy, F. J., and McCoy, C. E. (2011). MicroRNAs: the fine-tuners of Toll-like receptor signalling. *Nat. Rev. Immunol.* 11, 163–175. doi: 10.1038/nri2957

Otsu, K., Das, S., Houser, S. D., Quadri, S. K., Bhattacharya, S., and Bhattacharya, J. (2009). Concentration-dependent inhibition of angiogenesis by mesenchymal stem cells. *Blood* 113, 4197–4205. doi: 10.1182/blood-2008-09-176198

Paganini, C., Palmiero, U., Pocsfalvi, G., Touzet, N., Bongiovanni, A., Arosio, P., et al. (2019). Scalable production and isolation of extracellular vesicles: available sources and lessons from current industrial bioprocesses. *Biotech. J.* 14:e1800528. doi: 10.1002/biot.201800528

Park, B. S., and Lee, J. O. (2013). Recognition of lipopolysaccharide pattern by TLR4 complexes. *Exp. Mol. Med.* 45:e66. doi: 10.1038/emm.2013.97

Phan, J., Kumar, P., Hao, D., Gao, K., Farmer, D., Wang, A., et al. (2018). Engineering mesenchymal stem cells to improve their exosome efficacy and yield for cell-free therapy. *J. Extracell. Vesicles* 7:1522236. doi: 10.1080/20013078.2018.1522236

Phinney, D. G., Di Giuseppe, M., Njah, J., Sala, E., Shiva, S., St Croix, C. M., et al. (2015). Mesenchymal stem cells use extracellular vesicles to outsource mitophagy and shuttle microRNAs. *Nat. Commun.* 6:8472. doi: 10.1038/ncomms9472

Qin, S. B., Peng, D. Y., Lu, J. M., and Ke, Z. P. (2018). 182-5p inhibited oxidative stress and apoptosis triggered by oxidized low-density lipoprotein via targeting toll-like receptor. *J. Cell Physiol.* 233, 6630–6637. doi: 10.1002/jcp.26389

Qiu, G., Zheng, G., Ge, M., Wang, J., Huang, R., Shu, Q., et al. (2018). Mesenchymal stem cell-derived extracellular vesicles affect disease outcomes via transfer of microRNAs. *Stem Cell Res. Ther.* 9:320. doi: 10.1186/s13287-018-1069-9

Ragni, E., Banfi, F., Barilani, M., Cherubini, A., Parazzi, V., Larghi, P., et al. (2017). Extracellular vesicle-shuttled mRNA in mesenchymal stem cell communication. *Stem Cells* 35, 1093–1105. doi: 10.1002/stem.2557

Ramos, T., Sánchez-Abarca, L. I., Muntión, S., Preciado, S., Puig, N., López-Ruano, G., et al. (2016). MSC surface markers (CD44, CD73, and CD90) can identify human MSC-derived extracellular vesicles by conventional flow cytometry. *Cell Commun Signal.* 14:2. doi: 10.1186/s12964-015-0124-8

Rani, S., Ryan, A. E., Griffin, M. D., and Ritter, T. (2015). Mesenchymal stem cell-derived extracellular vesicles: toward cell-free therapeutic applications. *Mol. Ther.* 23:812–823. doi: 10.1038/mt.2015.44

Reis, M., Mavin, E., Nicholson, L., Green, K., Dickinson, A. M., and Wang, X. (2018). Mesenchymal stromal cell-derived extracellular vesicles attenuate dendritic cell maturation and function. *Front. Immunol.* 9:2538. doi: 10.3389/fimmu.2018.02538

Ren, G., Zhang, L., Zhao, X., Xu, G., Zhang, Y., Roberts, A. I., et al. (2008). Mesenchymal stem cell-mediated immunosuppression occurs via

concerted action of chemokines and nitric oxide. *Cell Stem Cell* 2, 141–150. doi: 10.1016/j.stem.2007.11.014

Ren, W., Hou, J., Yang, C., Wang, H., Wu, S., Wu, Y., et al. (2019). Extracellular vesicles secreted by hypoxia pre-challenged mesenchymal stem cells promote non-small cell lung cancer cell growth and mobility as well as macrophage M2 polarization via miR-21-5p delivery. *J. Exp. Clin. Cancer Res.* 38:62. doi: 10.1186/s13046-019-1027-0

Samsonraj, R. M., Raghunath, M., Nurcombe, V., Hui, J. H., van Wijnen, A. J., and Cool, S. M. (2017). Concise review: multifaceted characterization of human mesenchymal stem cells for use in regenerative medicine. *Stem Cells Transl. Med.* 6, 2173–2185. doi: 10.1002/sctm.17-0129

Selmani, Z., Naji, A., Zidi, I., Favier, B., Gaiffe, E., Obert, L., et al. (2008). Human leukocyte antigen-G5 secretion by human mesenchymal stem cells is required to suppress T lymphocyte and natural killer function and to induce $CD4^{+}CD25^{high}FOXP3^{+}$ regulatory T cells. *Stem Cells* 26, 212–222. doi: 10.1634/stemcells.2007-0554

Sharma, J., Hampton, J. M., Valiente, G. R., Wada, T., Steigelman, H., Young, M. C., et al. (2017). Therapeutic development of mesenchymal stem cells or their extracellular vesicles to inhibit autoimmune-mediated inflammatory processes in systemic lupus erythematosus. *Front. Immunol.* 8:526. doi: 10.3389/fimmu.2017.00526

Shen, B., Liu, J., Zhang, F., Wang, Y., Qin, Y., Zhou, Z., et al. (2016). CCR2 positive exosome released by mesenchymal stem cells suppresses macrophage functions and alleviates ischemia/reperfusion-induced renal injury. *Stem Cells Int.* 2016, 1–9. doi: 10.1155/2016/1240301

Shi, Y., Su, J., Roberts, A. I., Shou, P., Rabson, A. B., and Ren, G. (2012). How mesenchymal stem cells interact with tissue immune responses. *Trends Immunol.* 33, 136–143. doi: 10.1016/j.it.2011.11.004

Shojaati, G., Khandaker, I., Funderburgh, M. L., Mann, M. M., Basu, R., Stolz, D. B., et al. (2019). Mesenchymal stem cells reduce corneal fibrosis and inflammation via extracellular vesicle-mediated delivery of miRNA. *Stem Cells Trans. Med.* 8, 1192–201. doi: 10.1002/sctm.18-0297

Showalter, M. R., Wancewicz, B., Fiehn, O., Archard, J. A., Clayton, S., Wagner, J., et al. (2019). Primed mesenchymal stem cells package exosomes with metabolites associated with immunomodulation. *Biochem. Biophys. Res. Commun.* 512, 729–735. doi: 10.1016/j.bbrc.2019.03.119

Song, Y., Dou, H., Li, X., Zhao, X., Li, Y., Liu, D., et al. (2017). Exosomal miR-146a contributes to the enhanced therapeutic efficacy of interleukin-1β-primed mesenchymal stem cells against sepsis. *Stem Cells* 35, 1208–1221. doi: 10.1002/stem.2564

Spaggiari, G. M., Abdelrazik, H., Becchetti, F., and Moretta, L. (2009). MSCs inhibit monocyte-derived maturation and function by selectively interfering with the generation of immature DCs: central role of MSC derived prostaglandin E2. *Blood* 113, 6576–683. doi: 10.1182/blood-2009-02-203943

Spees, J. L., Olson, S. D., Whitney, M. J., and Prockop, D. J. (2006). Mitochondrial transfer between cells can rescue aerobic respiration. *Proc. Natl. Acad. Sci. U.S.A.* 103, 1283–1288. doi: 10.1073/pnas.0510511103

Sudres, M., Norol, F., Trenado, A., Gregoire, S., Charlotte, F., Levacher, B., et al. (2006). Bone marrow mesenchymal stem cells suppress lymphocyte proliferation *in vitro* but fail to prevent graft-versus-host disease in mice. *J. Immunol.* 176, 7761–7767. doi: 10.4049/jimmunol.176.12.7761

Tang, X. D., Shi, L., Monsel, A., Li, X. Y., Zhu, H. L., Zhu, Y. G., et al. (2017). Mesenchymal stem cell microvesicles attenuate acute lung injury in mice partly mediated by Ang-1 mRNA. *Stem Cells* 35, 1849–1859. doi: 10.1002/stem.2619

Théry, C., Witwer, K. W., Aikawa, E., Alcaraz, M. J., Anderson, J. D., Andriantsitohaina, R., et al. (2018). Minimal information for studies of extracellular vesicles 2018 (MISEV2018): a position statement of the International Society for Extracellular Vesicles and update of the MISEV2014 guidelines. *J. Extracell Vesicles* 7:1535750. doi: 10.1080/20013078.2018.1535750

Ti, D., Hao, H., Tong, C., Liu, J., Dong, L., Zheng, J., et al. (2015). LPS-preconditioned mesenchymal stromal cells modify macrophage polarization for resolution of chronic inflammation via exosome-shuttled let-7b. *J. Transl. Med.* 13:308. doi: 10.1186/s12967-015-0642-6

Tomasoni, S., Longaretti, L., Rota, C., Morigi, M., Conti, S., Gotti, E., et al. (2013). Transfer of growth factor receptor mRNA via exosomes unravels the regenerative effect of mesenchymal stem cells. *Stem Cells Dev.* 22, 772–780. doi: 10.1089/scd.2012.0266

Van Balkom, B. W. M., Gremmels, H., Giebel, B., and Lim, S. K. (2019). Proteomic signature of mesenchymal stromal cell-derived small extracellular vesicles. *Proteomics* 19:e1800163. doi: 10.1002/pmic.201800163

van Niel, G., D'Angelo, G., and Raposo, G. (2018). Shedding light on the cell biology of extracellular vesicles. *Nat. Rev. Mol. Cell Biol.* 19, 213–228. doi: 10.1038/nrm.2017.125

Vizoso, F. J., Eiro, N., Cid, S., Schneider, J., and Perez-Fernandez, R. (2017). Mesenchymal stem cell secretome: toward cell-free therapeutic strategies in regenerative medicine. *Int. J. Mol. Sci.* 18:1852. doi: 10.3390/ijms18091852

Wang, N., Liang, H., and Zen, K. (2014b). Molecular mechanisms that influence the macrophage m1-m2 polarization balance. *Front. Immunol.* 5:614. doi: 10.3389/fimmu.2014.00614

Wang, X., Gu, H., Qin, D., Yang, L., Huang, W., Essandoh, K., et al. (2015). Exosomal miR-223 contributes to mesenchymal stem cell-elicited cardioprotection in polymicrobial sepsis. *Sci. Rep.* 5:13721. doi: 10.1038/srep13721

Wang, Y., Chen, X., Cao, W., and Shi, Y. (2014a). Plasticity of mesenchymal stem cells in immunomodulation: pathological and therapeutic implications. *Nat. Immunol.* 15, 1009–1016. doi: 10.1038/ni.3002

Watson, D. C., Yung, B. C., Bergamaschi, C., Chowdhury, B., Bear, J., Stellas, D., et al. (2018). Scalable, cGMP-compatible purification of extracellular vesicles carrying bioactive human heterodimeric IL-15/lactadherin complexes. *J Extracell Vesicles* 7:1442088. doi: 10.1080/20013078.2018.1442088

Witwer, K. W., Van Balkom, B. W., Bruno, S., Choo, A., Dominici, M., Gimona, M., et al. (2019). Defining mesenchymal stromal cell (MSC)-derived small extracellular vesicles for therapeutic applications. *J. Extracell Vesicles.* 8:1609206. doi: 10.1080/20013078.2019.1609206

Zamani, P., Oskuee, R. K., Atkin, S. L., Navashenaq, J. G., and Sahebkar, A. (2019). MicroRNAs as important regulators of the NLRP3 inflammasome. *Prog. Biophys. Mol. Biol.* S0079–6107:30289–X. doi: 10.1016/j.pbiomolbio.2019.05.004

Zhao, J., Li, X., Hu, J., Chen, F., Qiao, S., Sun, X., et al. (2019). Mesenchymal stromal cell-derived exosomes attenuate myocardial ischaemia-reperfusion injury through miR-182-regulated macrophage polarization. *Cardiovasc Res.* 115, 1205–1216. doi: 10.1093/cvr/cvz040

Zhao, Q., Ren, H., and Han, Z. (2016). Mesenchymal stem cells: Immunomodulatory capability and clinical potential in immune diseases. *J. Cell Immunother.* 2, 3–20. doi: 10.1016/j.jocit.2014.12.001

Zhu, Y. G., Feng, X. M., Abbott, J., Fang, X. H., Hao, Q., Monsel, A., et al. (2014). Human mesenchymal stem cell microvesicles for treatment of *Escherichia coli* Endotoxin-induced acute lung injury in mice. *Stem Cells* 32, 116–125. doi: 10.1002/stem.1504

Conflict of Interest: The authors declare that the research was conducted in the absence of any commercial or financial relationships that could be construed as a potential conflict of interest.

frontiers in Bioengineering and Biotechnology

ORIGINAL RESEARCH
published: 15 November 2019
doi: 10.3389/fbioe.2019.00338

Influence of Platelet Lysate on 2D and 3D Amniotic Mesenchymal Stem Cell Cultures

*Markus Pasztorek[1], Eva Rossmanith[1], Christoph Mayr[2], Fabian Hauser[3], Jaroslaw Jacak[3], Andreas Ebner[2], Viktoria Weber[1,4] and Michael B. Fischer[1,4]**

[1] Department for Biomedical Research, Center of Experimental Medicine, Danube University Krems, Krems an der Donau, Austria, [2] Department of Applied Experimental Biophysics, Institute of Biophysics, Johannes Kepler University Linz, Linz, Austria, [3] School of Medical Engineering and Applied Social Sciences, University of Applied Sciences Upper Austria, Linz, Austria, [4] Christian Doppler Laboratories, Department for Biomedical Research, Danube University Krems, Krems an der Donau, Austria

The mechanobiological behavior of mesenchymal stem cells (MSCs) in two- (2D) or three-dimensional (3D) cultures relies on the formation of actin filaments which occur as stress fibers and depends on mitochondrial dynamics involving vimentin intermediate filaments. Here we investigate whether human platelet lysate (HPL), that can potentially replace fetal bovine serum for clinical-scale expansion of functional cells, can modulate the stress fiber formation, alter mitochondrial morphology, change membrane elasticity and modulate immune regulatory molecules IDO and GARP in amnion derived MSCs. We can provide evidence that culture supplementation with HPL led to a reduction of stress fiber formation in 2D cultured MSCs compared to a conventional growth medium (MSCGM). 3D MSC cultures, in contrast, showed decreased actin concentrations independent of HPL supplementation. When stress fibers were further segregated by their binding to focal adhesions, a reduction in ventral stress fibers was observed in response to HPL in 2D cultured MSCs, while the length of the individual ventral stress fibers increased. Dorsal stress fibers or transverse arcs were not affected. Interestingly, ventral stress fiber formation did not correlate with membrane elasticity. 2D cultured MSCs did not show differences in the Young's modulus when propagated in the presence of HPL and further cultivation to passage 3 also had no effect on membrane elasticity. In addition, HPL reduced the mitochondrial mass of 2D cultured MSCs while the mitochondrial mass in 3D cultured MSCs was low initially. When mitochondria were segregated into punctuate, rods and networks, a cultivation-induced increase in punctuate and network mitochondria was observed in 2D cultured MSCs of passage 3. Finally, mRNA and protein expression of the immunomodulatory molecule IDO relied on stimulation of 2D culture MSCs with pro-inflammatory cytokines IFN-γ and TNF-α with no effect upon HPL supplementation. GARP mRNA and surface expression was constitutively expressed and did not respond to HPL supplementation or stimulation with IFN-γ and TNF-α. In conclusion, we can say that MSCs cultivated in 2D and 3D are sensitive to medium supplementation with HPL with changes in actin filament formation, mitochondrial dynamics and membrane elasticity that can have an impact on the immunomodulatory function of MSCs.

Keywords: mesenchymal stem cells, stress fibers, mitochondrial dynamics, platelet lysate, membrane elasticity

OPEN ACCESS

Edited by:
Martin James Stoddart, AO Research Institute, Switzerland

Reviewed by:
Kar Wey Yong, University of Calgary, Canada
Luca Pierelli, Sapienza University of Rome, Italy

***Correspondence:**
Michael B. Fischer
michael.fischer@donau-uni.ac.at

Specialty section:
This article was submitted to Tissue Engineering and Regenerative Medicine, a section of the journal Frontiers in Bioengineering and Biotechnology

Received: *26 July 2019*
Accepted: *30 October 2019*
Published: *15 November 2019*

Citation:
Pasztorek M, Rossmanith E, Mayr C, Hauser F, Jacak J, Ebner A, Weber V and Fischer MB (2019) Influence of Platelet Lysate on 2D and 3D Amniotic Mesenchymal Stem Cell Cultures. Front. Bioeng. Biotechnol. 7:338. doi: 10.3389/fbioe.2019.00338

INTRODUCTION

For clinical-scale expansion of functional mesenchymal stem cells (MSCs) the use of xeno-based serum products are prohibited, but human platelet lysate (HPL) can potentially replace fetal bovine serum (FBS) the most widely used medium supplement in the past (Henschler et al., 2019). According to the European Medicines Agency and the European Commission (regulation number 1394/2007), MSCs belong to advanced-therapy medicinal products (ATMPs) that need to be produced under good manufacturing practice (GMP) conditions. FBS was banned because xeno-proteins can be taken up by MSCs and remained internalized during culture with a peri-nuclear localization (Spees et al., 2004) and patients developed antibodies against bovine antigens after receiving cell transplantation with MSCs expanded in FBS containing medium (Antoninus et al., 2015). Certain FBS lots, in addition, possess endotoxin content and can be a source of microbial contaminations, including viruses, bacteria, fungi, and prions. Therefore, human-derived FBS alternatives were developed such as HPLs and thrombin-induced or TRAP-induced platelet releasate (secretome) but MSCs were shown to be sensitive to medium supplementation during expansion, which can result in distinct supportive signaling by MSCs in processes of tissue regeneration or immune modulation.

An important issue for cultivation and expansion of MSCs, next to the culture medium selection, is the mechanobiological effect of 2D cultivation (the adherence of MSCs to coated plastic surfaces) or 3D cultivation (MSCs grown in spherical aggregate where cells produce autologous matrix components) (Dominici et al., 2006; Zhou et al., 2017). Depend on 2D or 3D cultivation, MSCs assemble actin filaments differently, which occur as branched stress fibers (SF) (Tojkander et al., 2012; Burridge and Wittchen, 2013; Burridge and Guilluy, 2016). They can be segregated into ventral and dorsal SFs or transverse arcs according to their appearance within the cell and their coupling to integrin-containing focal adhesions (FAs) (Tojkander et al., 2012; Xia and Kanchanawong, 2017). Ventral SFs are typically located at the ventral surface of the cell anchored at both ends to FAs, are several micrometers long and span the entire length of the cell. Dorsal SFs, in contrast, are usually shorter, appear radial to the cell and anchored at just one end to a FA. Transverse arcs are not bound to FAs at all. FAs are multi-protein subcellular structures comprising of talin, alpha-actinin, filamin, vinculin, paxillin, focal adhesion kinase, and tensin linking actin filaments to integrins on the cell surface to facilitate adhesion (Atherton et al., 2016). Proteins of FAs are in a continuous flux within the cytoplasm of MSCs with proteins constantly associating and dissociating in particular during cells in motion (Holle et al., 2013; Bays et al., 2014). Under static conditions, cell-generated forces can be transmitted across integrin-containing FAs to the surrounding extracellular matrix (ECM) network (Holle et al., 2013; Bays et al., 2014). In a reciprocal manner the ECM can influence actin filament formation, thereby controlling cell shape, regulate the balance between cell growth, differentiation and death (Zeiger et al., 2012; Yang et al., 2016). Considerations on the effect of the cell-matrix environment can help to solve the performance gap between physiological stem cell niches and engineered artificial environments for specific applications ranging from basic science to stem cell therapies (Gattazzo et al., 2014; Mullen et al., 2014; LeBlon et al., 2015).

Due to the potential of MSC application in regenerative medicine, the role of mitochondrial metabolism during cultivation in different culture media, have received substantial attention from life scientists and clinicians (Hsu et al., 2016). Intracellular organelles, including mitochondria are mechanoresponsive and undergo dynamic remodeling during MSC cultivation (Jackson and Krasnodembskaya, 2017). Mitochondria are the powerhouse of the cell and besides energy generation, they participate in calcium signaling, redox homeostasis and apoptosis (Rodriguez et al., 2018; Li C. et al., 2019). Mitochondrial accumulation at sites of high-energy demand, within the cytoplasm, is required to achieve local ATP production essential for virtually all cellular functions. Furthermore, stationary mitochondria serve as calcium buffers to avoid harmful intracellular calcium peaks. Mitochondrial fusion and fission dynamics involve vimentin intermediate filaments (IF). Binding of mitochondria to vimentin IFs is tightly regulated by GTPase Rac1 that acts through its effector PAK1 kinase and causes the phosphorylation of vimentin on Ser-55 modifying the mitochondria-binding site (Shankar et al., 2013). Consequently, released mitochondria can acquire the higher motility and the reduced mitochondrial membrane potential (MMP). Differences in vimentin IF formation can have influence on MSC function, as the timely delivery and distributions of mitochondria in the cytoplasm is crucial in particular for a fine-tuned mitochondrial fusion and fission process (Gruenbaum and Aebi, 2014; Pérez-Sala et al., 2015). MSCs are reliant on low levels of stress signals in the stem cell niche and intact mitochondrial metabolism for sufficient ATP production to maintain stemness (Zhou et al., 2017). In addition to stemness, the immunomodulatory characteristics of 3D cultured MSCs was enhanced as defined by gene expression profile analysis at mRNA and protein level as compared to 2D cultured MSCs, but a link between immunomodulatory function of MSCs with SF formation, mitochondrial morphology and membrane elasticity was not described in detail (Li et al., 2018).

Here we investigated the actin filament formation and mitochondrial morphology in 2D and 3D MSC cultures by flow cytometry or laser scanning confocal microscopy (LSM) in response to HPL, applied an MSC migration assay, studied force-distance profiles by atomic force microscopy (AFM) and analyzed the expression of immunomodulatory molecules GARP or IDO following pro-inflammatory stimulation with a combination of IFN-γ and TNF-α by RT-PCR and western blotting (Probst-Kepper and Buer, 2010; Shi et al., 2011; Carrillo-Galvez et al., 2015; Pérez-Sala et al., 2015; Niu et al., 2017; Najar et al., 2018; Li H. et al., 2019).

MATERIALS AND METHODS

Isolation, Culturing, Three-Lineage Differentiation, and Migration of MSCs

The study was approved by the ethic commission of the Medical University Vienna (EK791/2008, EK1192/2015), the University

Hospital of Lower Austria (GS1-EK-4/312-2015) and the Danube University Krems (Nr. 821/2009). The placenta was obtained from healthy delivering woman in accordance with the Austrian Hospital Act (KAG 1982) after written informed consent was signed. The amnion was separated from the placenta and cut in 3 × 3 cm squares. The slices were washed in physiological NaCl and digested with dispase (2.5 CU/ml, Becton Dickinson, Franklin Lakes, NJ) for 9 min at 37°C (Soncini et al., 2007). The fragments were incubated in a mix of collagenase A (1 mg/ml) and DNase I (0.01 mg/ml, both Roche, Basel, Switzerland) for 2 h at 37°C. For the separation of the cells from the tissue, the mix was centrifuged at 180 g for 5 min and the supernatant strained with a 100 μm cell-strainer. The cell suspension was centrifuged at 360 g for 10 min and amnion cells were adhered to plastic surfaces to propagate MSCs in 2D within MSCGM™- medium (Lonza Group Ltd., Basel, Switzerland) or MSCBM™ with 8% HPL (MacoPharma, Mouvaux, France), supplemented with 100 U/ml penicillin, 100 μg/ml streptomycin and 250 ng/ml amphotericin B (all from Gibco, Thermo Fisher Scientific, Waltham, MA) at 37°C in 5% CO_2 humidified environment (Stericycle, Thermo Fisher Scientific). Every 3 to 4 days medium was changed and MSCs were passaged at 80% confluence. For each experiment amnion-derived stromal cells were characterized by flow cytometry. Three-lineage differentiation of MSCs into chondrogenic, osteogenic, and adipogenic lineage (**Supplementary Figure 2C**) was performed using standard protocols (Walzer et al., 2019). For the migration assay, P3 MSCs (30 000 cells/well) were grown in 6 well plates with 2 well biocompatible silicone inserts with a defined 500 μm cell-free gap according to the manufacturer's instructions (Ibidi, Gräfelfing, Germany) and the analysis was performed according to a previous publication (Jonkman et al., 2014).

Preparation of MSC Spheroids

Adherent amnion derived stromal cells in passage 0 (P0) were grown to 80% confluence and the monolayers rinsed with PBS. Accutase (Gibco, Thermo Fisher Scientific) was added, incubated at 37°C until cells detach and stopped by adding 5 ml of PBS. The cells were centrifuged at 300 g for 5 min and counted. Five thousand cells/25 μl drop were pipetted on a lid from a 100 mm petri dish (Greiner Bio-One, Kremsmünster, Austria) and incubated as hanging drops at 37°C in 5% CO_2 humidified environment. The aggregate formation was monitored by a stereo microscope (Olympus IMT2) and spheroids were collected after 2 days and forwarded to characterization by flow cytometry.

Flow Cytometry Analysis of MSCs

Living MSCs (Live/Dead Cell Assay, Invitrogen, Thermo Fisher Scientific) from 2D cultures or spheroids in P1 were characterized for the expression of ecto-5'-nucleotidase (APC CD73), Thy-1 a glycophosphatidyl-inositol (GPI) anchored conserved cell surface protein (FITC CD90), endoglin a component of the receptor complex of TGF-β (PE-Cy7 CD105) and for glycoprotein A repetitions predominant (eFluor660® GARP) mAb (1 μg/ml, all from eBioscience, Thermo Fisher Scientific) on a Gallios 10/3 flow cytometer (Beckman Coulter GmbH, Krefeld, Germany). Actin and mitochondria quantification was performed using a AlexaFluor® 594 labeled phalloidin (1 U/ml) or MitoTracker™ Green FM (100 nM, both from Molecular Probes, Thermo Fisher Scientific) and size measurements were performed with silica beads [1.5 μm (Kisker Biotech, Steinfurt, Germany), 30 and 65 μm (Beckman Coulter GmbH)].

High Resolution Imaging of MSCs by Scanning Electron Microscopy

Spherical MSC aggregates or a suspension of 1 × 10^6 MSCs/ml were incubated in 24 well plates (Nunc, Thermo Fisher Scientific) on Nunc™Thermanox™ coverslips (Nunc, Thermo Fisher Scientific) for 16 h at 37°C in 5% CO_2 humidified environment. After three times washing with PBS, the coverslips were fixed with 2.5% glutaraldehyde (Sigma-Aldrich, St. Louis, MO) for 20 min at 4°C, washed two times again and dehydrated by stepwise alcohol extraction from 50 to 100%. The coverslips were mounted on EM-Tec CT12 conductive double side adhesive carbon tabs (Micro to Nano V.O.F., Haarlem, Netherlands) with a diameter of 12 mm and then surface sputtered with gold using a QuorumTech Q150T ES (Quorum Tech Ltd., Laughton, UK) for better resolution. For the scanning electron micrographs of spherical MSC aggregates and single adherent MSCs a FlexSEM 1,000 scanning electron microscope (Hitachi Ltd. Corp., Tokyo, Japan) with SEM MAP camera in SEM mode was used.

Stimulation of MSCs With Pro-inflammatory Cytokines

MSCs in P1 in 2D or 3D cultures were stimulated with 50 ng/ml TNF-α and 50 ng/ml 313 IFN-γ (both from PeproTech, Rocky Hill, NJ) in MSCGM™ - 314 medium or MSCBM™ with 8% HPL for 24 and 48 h.

Confocal Laser Scanning Microscopy for Investigating the Cyto-Architecture of Cultured MSCs

MSCs were grown in chamber slides for 72 h or alternatively MSC spherical aggregates were adhered to plastic surface for 16 h. The cells were fixed with fixation and permeabilization reagent (eBioscience, Thermo Fisher Scientific) and incubated either with vinculin (2 μg mouse mAb/ml, clone 7F9, Santa Cruz Biotechnology, Dallas, TX), with paxillin (2 μg mouse mAb/ml, clone B2 Santa Cruz Biotechnology) to reveal FA, with vimentin (3.6 μg mouse mAb/ml, clone 1/9, Dako Products, Agilent, Santa Clara, CA) to label the IFs, or with the MitoTracker™ Red CMX Ros (100 nM, Molecular Probes, Thermo Fisher Scientific) to reveal mitochondria. Chamber slides were incubated with the second ab, a goat-anti-rabbit polyclonal Fab fragment Ab labeled with AF-488 (3 μg/ml, Jackson Laboratories, Bar Harbor, MN) after two times of washing with PBS. For the labeling of f-actin MSCs were counterstained with AF-488 or AF-594 phalloidin (0.1 U/ml, Molecular Probes, Thermo Fisher Scientific) and finally nuclei were stained with DAPI (Sigma-Aldrich). The slides were mounted with Fluoromount-G™ (Southern Biotechnology, Thermo Fisher Scientific) and analyzed with an alpha-Plan-Apochromat 63x objective and a Leica TCS SP8 confocal microscope (Leica Microsystem GmbH, Wetzlar, Germany).

Serial dilutions of each primary and secondary antibody were tested to minimize non-specific adsorption, assure separation of the fluorescent signals, and optimize fluorophore concentration to preclude self-quenching.

TissueGnostics Technology for a Context-Based Actin Evaluation of Cultured MSCs

MSCs were grown, stained and scanned according to the "confocal microscopy" part. The presence of dorsal or ventral SFs as well as transverse arcs was analyzed by using the analysis software StrataQuest (TissueGnostics, Vienna, Austria). Context based quantitative analysis of fluorescence images on an automatic interface segregated dorsal SFs anchored only at one end to FAs, from ventral SFs spanning f-actin filament bundles from two FAs, and from transverse arcs that are not at all anchored to FAs but instead connected to intracellular structures.

Atomic Force Microscopy Topographical Imaging and Elasticity Mapping of Cultured MSCs

All samples were prepared in ibidi 35 mm μ-dishes (Ibidi). First of all, the μ-dishes were coated with 5 $\mu g/cm^2$ fibronectin (Sigma-Aldrich). The coating was done by covering the surface with a fibronectin solution and incubation for 60 min at 37°C. Thereafter, the remaining solution was discarded. MSCs were put on the fibronectin coated surface and incubated for 24 h at 37°C in 5% CO_2 air humidified environment and subsequently immobilized on the surface with 4% formaldehyde (Thermo Fisher Scientific). After immobilization the formaldehyde was discarded, and the μ-dish was filled with 1 ml PBS. A 6000 ILM AFM combination (Keysight, Santa Rosa, CA) was used for all measurements. This system consisted of an inverted microscope (Zeiss Observer D1), a motorized AFM stage (Keysight 6000) and the AFM head itself (N9583A model). The implemented camera was a Hamamatsu C11440. Noise cancellation was done using an Accurion Halcyonics Vario active vibration isolating system combined with an Accurion acoustic damping hood. Calculation of the Young's moduli was done with PicoView 1.18.2 software (Keysight). Further image processing (flattening, statistical evaluation, multilayer images) was performed using Gwyddion 2.45 and PicoImage 5.1.1 software (Keysight). The surface topography of immobilized MSCs was investigated using Bruker MSCT cantilever (Bruker AFM probes, Camarillo, CA). Images were taken in PBS and recorded in contact or tapping mode with 0.5 lines per second. For each sample at least three different cells were measured. The elasticity of immobilized MSCs was investigated by using Bruker MSCT cantilever and by performing force volume measurements in PBS. For most measurements a grid of 32 × 32 points was used. On each measurement point one force distance cycle was performed and the Young's modulus was simultaneously calculated using the Hertz model (Hertz, 1882; Sneddon, 1965; Butt and Jaschke, 1995; Haase and Pelling, 2015; Melzak and Toca-Herrera, 2015). The cycles were done by using a scan rate of 20 μm/s and a scan range of 5 to −5 μm. The maximum force was set to 5 V, which yielded a maximum force exerted on the cells of <2 nN. For each sample three cells were measured in total. For the calculation of the Young's moduli the exact spring constant of the cantilever was evaluated using thermal tune method.

Western Blotting to Semi-quantify Cellular IDO in Stimulated and Unstimulated MSCs

MSCs were lysed with 1% protease phosphatase inhibitor in RIPA extraction buffer and, total protein was measured using a Agilent Protein 230 kit (Agilent Technologies). Protein was loaded on precast 4–12% polyacrylamide Bis-Tris gels in a NuPage MOPS-buffer and SDS-PAGE western blotting was performed using a XCell SureLock™ Mini-Cell and a PowerEase 500 W power supply. For the transfer on nitrocellulose membranes with a 0.2 μm pore size a XCell II blot™ module was used (Invitrogen, Thermo Fisher Scientific). Membranes were subsequently blocked with non-fat dry milk (Biorad, Hercules, CA). A primary anti-IDO Ab (0.2 mg, clone H-11, Santa Cruz Biotechnology) was detected with HRP conjugate and Clarity Max Western ECL blotting substrate (Biorad) and the chemiluminescent signal was recorded with a Chemi-Doc documentation system (Biorad) for semi-quantification. For internal control, purified IDO protein (Bio-Techne, R&D Systems, Minneapolis, MN) was used at a total concentration of 25–200 ng.

Human Cytokine Array for HPL Characterization

Human Cytokine profiling was performed with a Proteome Profiler Human XL Cytokine Array Kit (R&D Systems, Minneapolis, MN). MSCBM™- medium (Lonza Group Ltd.) with 8% HPL (MacoPharma) and 3 μl Heparin (5,000 IU/ml, Gilvasan Pharma, Vienna, Austria) was used as sample, the procedure was performed according to the manufacturer's instructions. The chemiluminescent signal was recorded with a Chemi-Doc documentation system (Biorad).

Semi-quantitative RT-PCR Analysis for IDO and GARP Characterization

Total RNA was extracted from MSCs cultivated in 2D and 3D with and without addition of 50 ng/ml TNF-α and 50 ng/ml IFN-γ using an RNeasy Mini Kit (Qiagen, Venlo, Netherlands) according to the manufacturer's manual. RNA quality was assessed, and the quantity was measured by an RNA 6000 Nano assay (Agilent Technologies). RNA was adjusted to the same concentration for each sample after measuring the RNA concentration. Then, RNA samples were used for cDNA synthesis with the High-Capacity cDNA Transcription Kit (Applied Biosystems, Thermo Fisher Scientific) in a 20 μl reaction mixture according to the manufacturer's protocol. Primers (Metabion—International AG, Planegg, Germany) for HPRT (Toegel et al., 2007), PPIA (Li et al., 2015), IDO (fw: GGAGCAGACTACAAGAAT, rev: TAGCAATGAACATCCAGT) and GARP (Carrillo-Galvez et al., 2015), were used for the qRT-PCR reactions. The qRT-PCR reactions were performed with the SensiMix™ SYBR® Hi-ROX

Kit (Bioline, London, UK) according to the manufacturer's protocol. PCR amplification and analyzation were investigated with the LightCycler® 96 Instrument (Roche).

Mitochondrial 3D dSTORM Analysis

Cultivated MSCs were prepared in 8-well Lab-Tek™ chambers (Nunc, Thermo Fisher Scientific) with two different cultivation media. The cytoskeleton buffer with sucrose (CBS) (Symons and Mitchison, 1991) was used to improve the staining quality, to increase resolution of single molecule signals and to promote mitochondrial staining. MSCs were then fixed using 4% paraformaldehyde, permeabilized with 0.5% Triton X-100 and unspecific binding was blocked with 10 mg/ml albumin from chicken egg white (Sigma-Aldrich). Mitochondria were stained with anti-mitochondria mAb conjugated with AlexaFluor® 488 (5 μg/ml, clone 113-1, Merck Millipore, Darmstadt, Germany) for 60 min in CBS with blocking solution. Fluorescence Microscope images were acquired using a modified Olympus IX81 inverted epifluorescence microscope with an oil-immersion objective (UApo N 60x/1.49 NA, Olympus, Vienna, Austria) and additional tube-lens with a magnification of 1.6x. The signals were detected using an Andor iXonEM+ 897 (back-illuminated) EMCCD camera (16 μm pixel size, Andor Technology, Belfast, Northern Ireland). This results in an image pixel size of 166.667 nm/pixel and a total magnification of 96x. Fluorescence-labeled samples were excited using a 488 nm solid-state laser (diode-pumped, iBeam Smart, Toptica Photonics, Gräfelfing, Germany) and under certain conditions, fluorophores were additional recovered from dark state with a 405 nm diode laser (iPulse, Toptica Photonics). An additional cylindrical lens (f = 500 mm, Thorlabs, Newton, NJ) was introduced in the pathway between camera and the microscope's side port for 3D Super-Resolution microscopy. The fluorescent emission was additionally filtered by a 525/50 nm emission bandpass filter (AHF, Tübingen, Germany). For optimized photo-switching of the rhodamine dye AlexaFluor® 488 a buffer containing EC-Oxyrase® (Sigma-Aldrich), 60% LD-Lactate, 50 mM cystermine and PBS as described (Nahidiazar et al., 2016) has been used. For 3D STORM experiment, a ROI of about 256 × 256 pixels was chosen (depending on cell size) and between 10,000 and 20,000 frames were acquired. The fluorophores were illuminated with 20–30 ms at each frame and an optional 20 ms UV illumination during the readout time of the CCD could be added. Each frames were then analyzed using a custom written analysis software (3D dSTORM-Tools) (Mayr et al., 2018; Sage et al., 2019) and all fitted single molecules were used to reconstruct a 3D Super-Resolution image. Further analysis is based on the 3D point cloud data of the analyzed single molecules. Prior to each experiment, a calibration for the single molecule axial position localization, compensating the axial point spread function distortion, was performed using TetraSpeck (Thermo Fisher Scientific) beads.

Statistical Analysis

Data were expressed as mean ± standard deviation unless otherwise stated. Mann-Whitney test or unpaired *t*-test were performed for unpaired analysis and paired *t*-test or Wilcoxon test for paired analysis like described in the figure legend. Statistical analysis was performed by the GraphPad Prism software 8.

RESULTS

Effect of HPL on MSCs Cultured in Adherent to Plastic Surfaces or in Spheroids

Three batches of HPL from MacoPharma, used for all experiments, were analyzed with a Proteome Profiler Human XL Cytokine Array with 102 cytokines and results are given in a heat map (**Supplementary Figure 1A**). The analysis of the batches showed largely the same results with certain variations in individual cytokines.

Amnion derived MSCs propagated in adherence to plastic surface and analyzed in passage (P)1 or MSCs from spherical aggregates were positive for MSC specific markers CD73, CD90, and CD105 when cultivated in MSCGM™- medium or MSCBM™ with 8% HPL, and showed a size of ∼30–60 μm in diameter (**Supplementary Figures 2A,B**) compared to silica beads with similar refraction index. Only adherent P1 MSCs cultivated in 8% HPL showed a reduction in size (**Supplementary Figure 2B**). Images from scanning electron microscopy were provided to show that there is no morphological difference between MSCs grown in adherence to plastic surface or MSCs from spherical aggregates cultured with or without HPL (**Supplementary Figure 1B**). Furthermore, actin filament formation and mitochondrial mass determined by flow cytometry showed that culture supplementation with HPL could reduce the amount of f-actin in adherent P1 MSCs, while this effect could not be observed in MSCs from spherical aggregates (**Figure 1A**). Of note, actin can occur in MSCs either as g (globular)-actin or as f (filamentous)-actin, but phalloidin can only stain f-actin. Interestingly, mitochondrial mass followed the dynamics of f-actin. Lower quantities of mitochondria were found in adherent MSCs cultivated in HPL (**Figure 1B**).

Stress Fiber Formation and Mitochondrial Dynamics

SF formation in response to HPL was investigated by Laser Scanning Microscopy in single 2D adherent P1 MSCs or MSCs that emanated from 3D spherical aggregates (**Figures 1C,D**). In order to scan single MSCs, 3D spherical MSC aggregates harboring 3,000 to 5,000 cells were adhered to glass slides and during a period of 16 h MSCs were allowed to emerge from the aggregate and remain adhered in the immediate surrounding eligible for scanning (**Figure 1D**). Here we can show, that MSCs grown in adherence to plastic surfaces formed thick and well-defined bundles of SFs compared to MSCs that emerged from spherical aggregates that showed only thin f-actin filaments (**Figure 1C**). Within the aggregates MSCs assembled only few SFs confirming previous results favoring aggregate cultures for stress reduced cultivation (**Figure 1D**). SFs are attached to the FA complexes, in which vinculin and paxillin are prominent proteins that are involved in facilitate the binding of FAs to integrins that bind to the underlying matrix. Here we can show that FAs

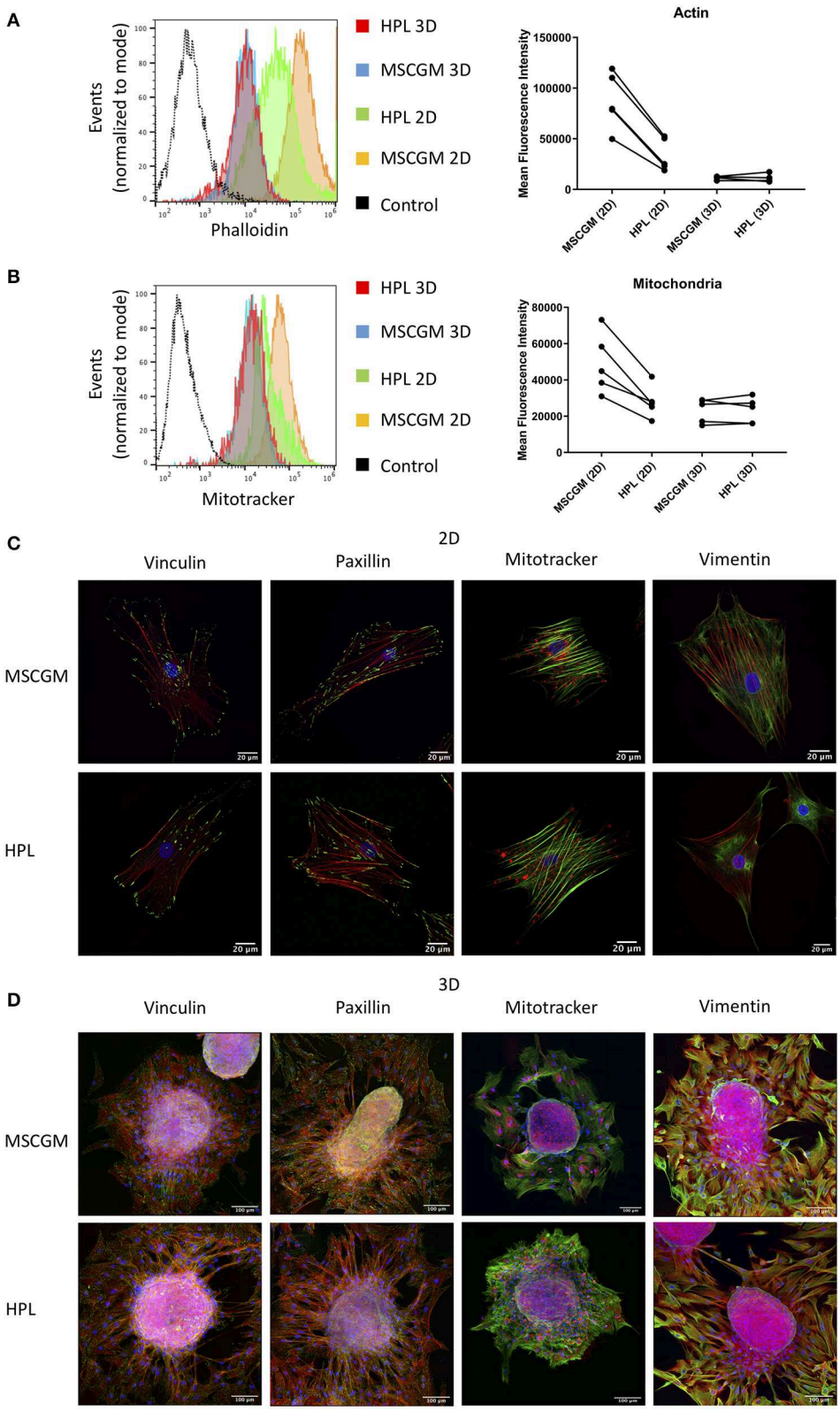

FIGURE 1 | Effect of HPL on 2D and 3D cultures. **(A)** Actin measurements with phalloidin of living CD90^{+} MSCs in 2D vs. 3D cultured in MSCGM^{TM} or MSCBM^{TM} with 8% HPL determined by flow cytometry. Dot plot of the mean fluorescence intensity of four different batches for 3D MSCs and five batches for 2D

(Continued)

FIGURE 1 | MSCs of 4,000 cells per batch, one representative flow cytometry histogram is shown. **(B)** Mitochondria measurements with MitoTracker™ of living CD73$^+$ MSCs in 2D vs. 3D cultured in MSCGM™ or MSCBM™ with 8% HPL determined by flow cytometry. Dot plot of the mean fluorescence intensity of five different batches, 2,000 MSCs were investigated per batch, one representative flow cytometry histogram is shown. **(C)** Images of passage 1 MSCs cultured in MSCGM™ or MSCBM™ with 8% HPL stained with the specific focal adhesion proteins vinculin and paxillin in green as well as stress fibers (f-actin) in red and nuclei in blue. Mitochondria were stained with MitoTracker™ in red, stress fibers in green and nuclei in blue. Type-3 intermediate filaments are given by staining vimentin in green, stress fibers in red and nuclei in blue. **(D)** Images of MSC spheroids, the staining corresponds to those described in **(A)**. The entire MSC spheroid is a maximal intensity projection of a stitched z-stack 3-channel overlay, magnification was 63x.

behaved the same as SFs and remained expressed intensely after MSCs emerged from the spherical aggregates or when MSCs were cultivated in adherence to plastic surface (**Figures 1C,D**). The cultivation supplementation with HPL had no effect on the FA composition involving vinculin and paxillin under the conditions applied.

Mitochondrial distribution in single adherent MSCs showed that mitochondria were found in areas of high cytoplasmic activity and appeared condensed to rods and networks, according to fusion and fission dynamics (**Figure 1C**). MSCs that emerged from the spherical aggregates showed condensed mitochondria (**Figure 1D**) while MSCs in the cellular aggregate had a more punctuated morphology (data not shown). Interestingly, mitochondrial condensation did not appear perinuclear in adherent MSCs. The type II IF vimentin is important to support anchoring mitochondria at positions of high activity. Here we can show that vimentin distribution was higher in adherence to plastic surface, which goes hand in hand with the observations of the mitochondria distribution (**Figures 1C,D**).

Influence of the Culture Media on the Occurrence of Stress Fiber Variants and Migratory Capability

Context-based analysis of confocal images allowed us the quantification of the SFs and the segregation of SFs in ventral SFs, dorsal SFs, and transverse arcs according to their connection with FAs (**Figure 2A**). Ventral SFs were segregated by their capability to anchor at both sides to FAs, dorsal SFs only bind one FA at one side, while the other side remained fixed to cytoplasmic organelles. Transverse arcs, in contrast do not bind to FAs at all but organize the tension within the cell. Here we can show an increase of the total number of SFs in thirty analyzed adherent P1 MSCs cultured in MSCGM™- medium (**Figure 2B**, left). This increase of actin fibers is comparable with the higher amount of actin determined in **Figure 1A**. Ventral SFs showed a response of cultivation where the number of ventral SFs decreased during cultivation of MSCs in HPL, while the length increased, dorsal SFs remained numerically constant. Transverse arcs, in contrast, remained constant both in number and length (**Figures 2B,C**). Perinuclear actin cap consists of SFs positioned above the nucleus that are mechanotransducers to convey force from the cell environment to the nucleus was not found in our system. When the migratory capability of P3 MSCs was investigated in a commercially available wound healing assay, where a 500 µm cell-free gap was introduced with a biocompatible silicone insert, we found an approximately 50% closure after 12 h and more than 90% after 24 h. No difference, however, was observed when P3 MSCs were cultivated either in MSCGM™- or in HPL supplemented medium (**Supplementary Figures 3A–C**).

Topographic Imaging and Elasticity Measurements of MSCs Dependent on Culture Media

Topographic images, to identify sub-membrane cytoskeletal structures in adherent P1 and P3 MSCs were performed by the AFM in deflection mode. MSCs showed a flat and spread morphology size (**Figure 3A**, left). Elasticity mapping and the calculation of Young's moduli of three MSCs of two batches were performed to investigate the effect of MSCGM™- medium or MSCBM™ with 8% HPL on the mechanical properties of P1 and P3 MSCs. Heat maps of 1,024 single measurements were carried out to show the stiffness or softness of the cultured MSCs (**Figure 3A**, middle). The individual data points were summarized in a histogram, the data points of the plastic substrate were excluded (**Figure 3A**, right). Young's moduli were presented in a boxplot for comparison to show that the change of the cellular compartment has no effect of the individual cell in influence of the media and passages on the elasticity and the mechanical characteristics (**Figure 3B**).

Pattern Analysis of the Mitochondria

We used an ImageJ macro tool (Valente et al., 2017) to further analyze mitochondrial morphology in response to HPL in single adherent P1 or P3 MSCs. Here we could distinguish between unbranched punctate, rods and branched structures (networks) with high precision, the images are single P3 MSCs stained with MitoTracker™ analyzed with high resolution confocal microscopy (**Figure 4A**) in living cells. Unbranched punctate and networks were shown to be increased in adherent P3 MSCs compared to adherent P1 MSCs cultivated in MSCGM™- medium. Interestingly, when P3 adherent MSCs were cultured in HPL, the cells showed the same mitochondrial morphology as P1 MSCs (**Figure 4B**). When networks were further analyzed for branching (length of branched mitochondrial structures) we found the highest values in P1 adherent MSCs cultured in MSCGM™- medium (**Figure 4C**). Finally, mitochondrial rods were found to be decreased in adherent P3 MSCs cultivated in HPL (**Figure 4B**).

Mitochondrial Imaging by dSTORM

MSCs were stained with an anti-mitochondria mAb, instead of MitoTracker™, to enable high resolution analysis of ATP5H mitochondrial synthase by a modified Olympus IX81 inverted

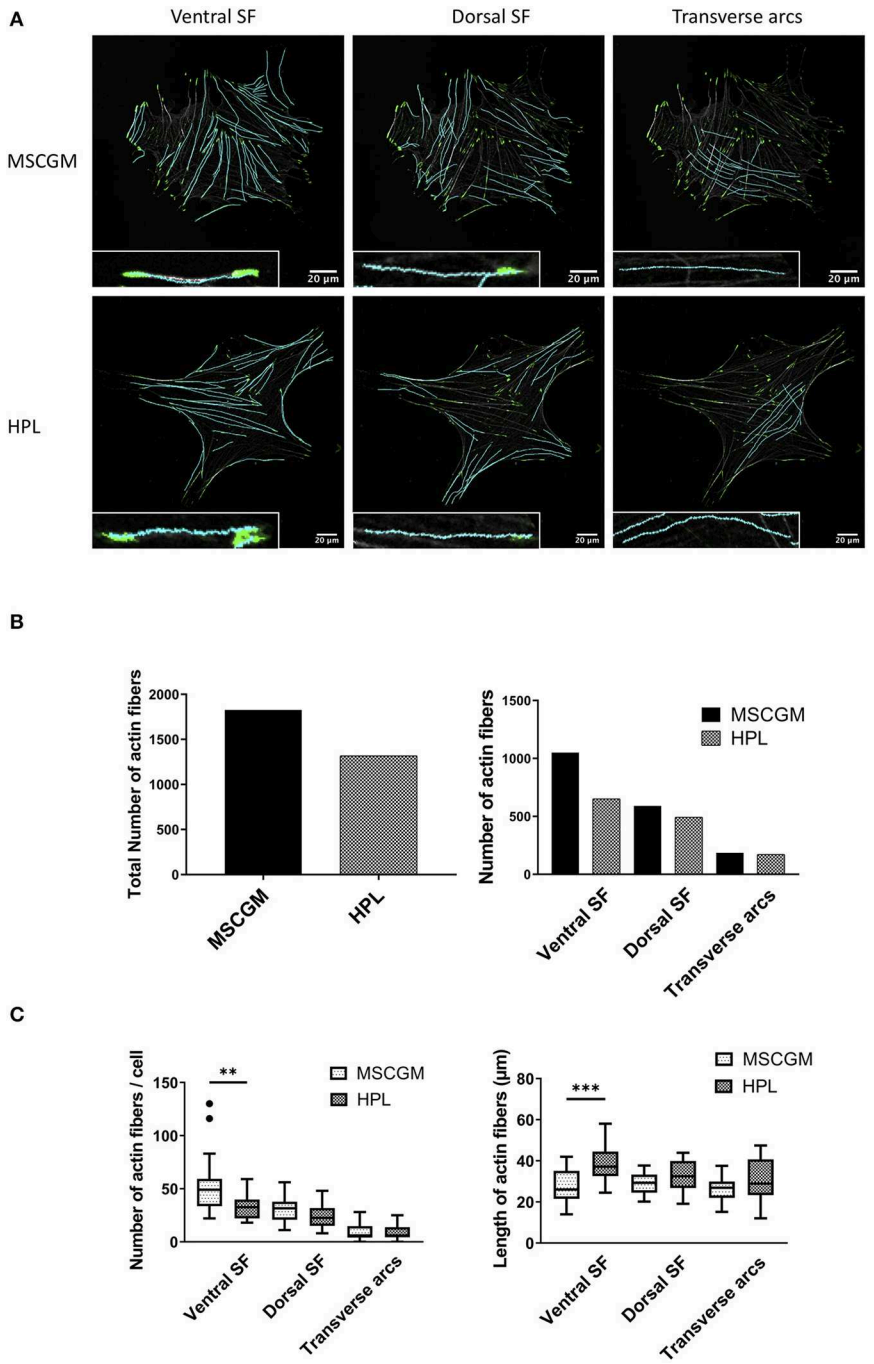

FIGURE 2 | Examination of cytoskeleton morphology. **(A)** Images of ventral, dorsal stress fibers and transverse arcs compared to the influence of MSCGM™ or MSCBM™ with 8% HPL. Higher magnification of the individual fibers is shown in the lower left corner. **(B)** Left: Total numbers of stress fibers. Right: Total number of stress fibers split in ventral, dorsal stress fibers and transverse arcs. **(C)** Left: Number of fibers per cells, Mann-Whitney test. Right: Median of the length per cell, unpaired *t*-test. The same 20 cells per media were compared in **(B,C)**. $^{**}p < 0.01$, $^{***}p < 0.001$.

epifluorescence microscope (**Figure 4D**). 3-D reconstructed high-resolution immunofluorescent images of 15 randomly selected single adherent permeabilized MSCs. When P3 adherent MSCs cultivated in MSCGM™- medium were compared with HPL and analyzed by the ImageJ macro tool, we found a trend toward a decrease in unbranched punctate mitochondria in P3. Interestingly, mitochondrial rods that count for the majority of mitochondrial structures and mitochondrial network structures showed no dependence on cultivation in HPL (**Figure 4E**).

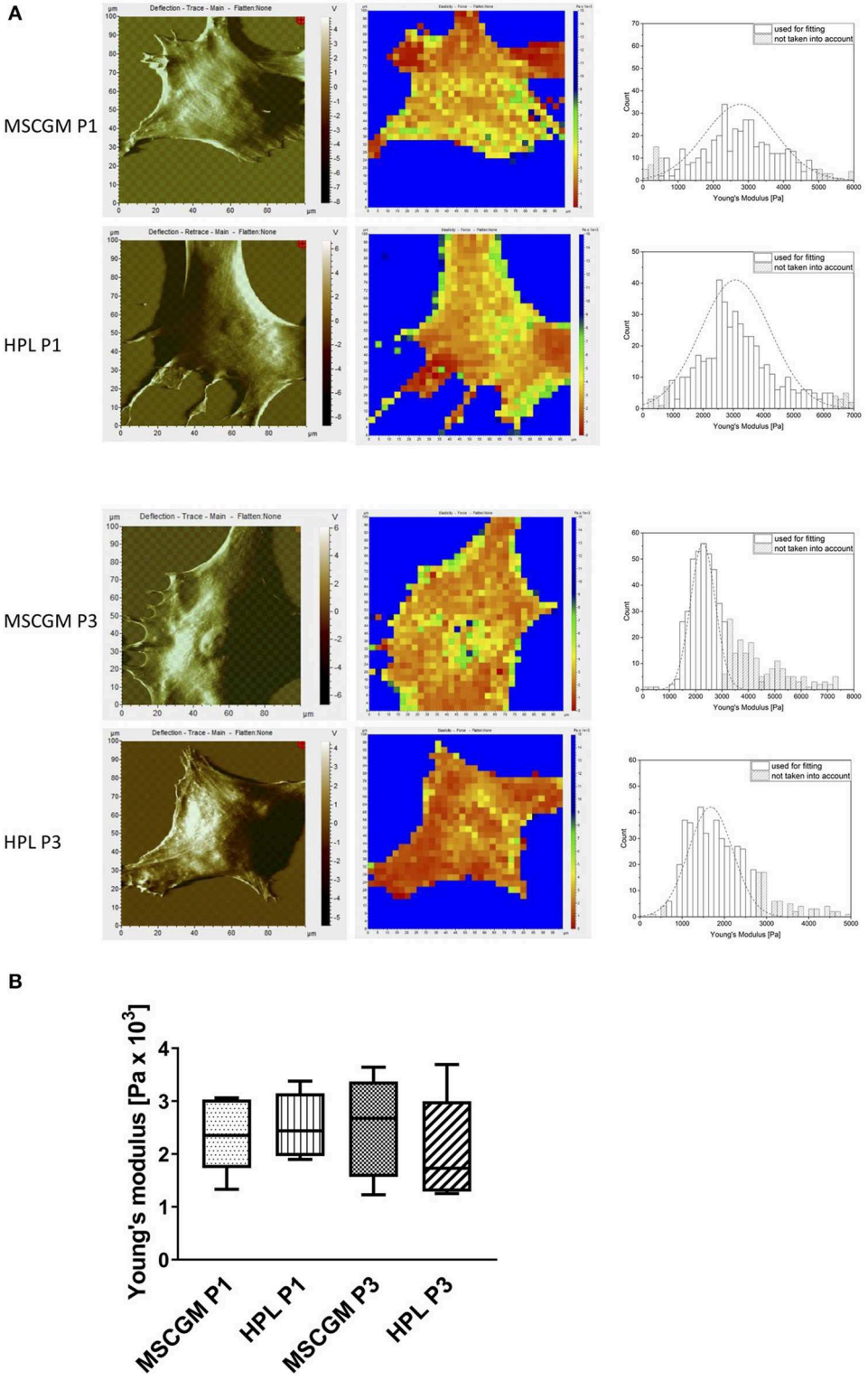

FIGURE 3 | Examination of elasticity. **(A)** Left: Topographic images of membrane structures from MSCs cultured in MSCGM™ or MSCBM™ with 8% HPL from passage 1 and 3 determined by atomic force microscopy. Middle: Elasticity mapping. Right: Surface elasticity measurements given by the Young's moduli shown in a histogram. **(B)** Comparison of 1,024 single surface elasticity measurements from individual MSCs shown in a box plot diagram ($n = 6$).

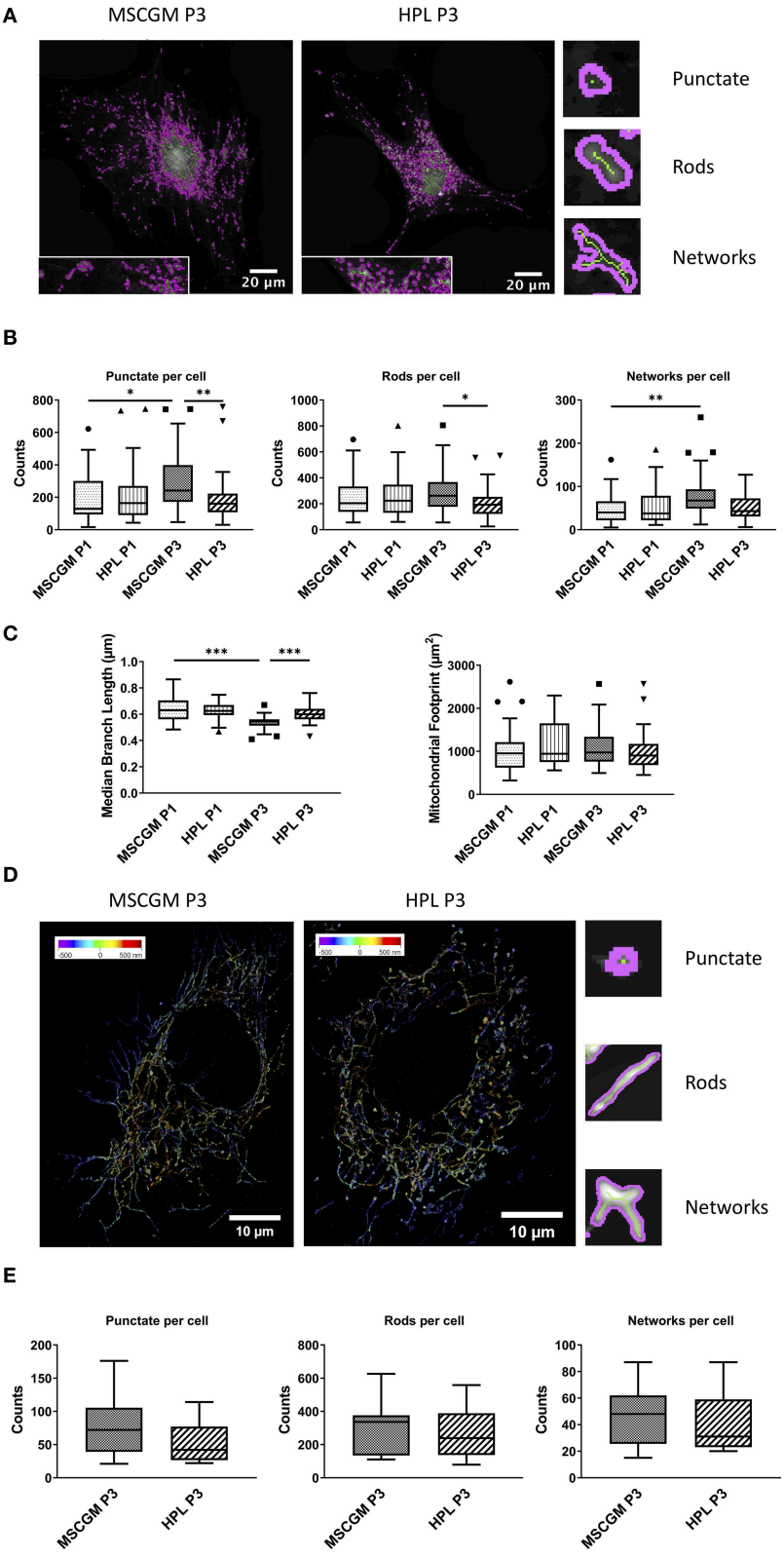

FIGURE 4 | Mitochondrial pattern analysis and super-resolution imaging. **(A)** Images of Mitochondrial Network Analysis (MiNA) from passage 3 MSCs cultured in MSCGM™ or MSCBM™ with 8% HPL stained with MitoTracker™ **(B)** Top: Numbers of punctate mitochondrial organelles per cell compared in different media and

(Continued)

FIGURE 4 | from passage 1 and 3, Wilcoxon and Mann Whitney test. Middle: Numbers of mitochondrial rods per cell, Mann Whitney test. Bottom: Numbers of mitochondrial networks per cell, Wilcoxon test. MiNA image interpretations are shown next to the diagrams. **(C)** Left: Median branch length of the mitochondrial networks in μm per cell, paired and unpaired *t*-test. Right: Mitochondrial footprint in μm^2 per cell. The same 30 cells per media or passage were compared in **(B,C)**. **(D)** Reconstructed fluorescence microscopy images (dSTORM) of mitochondria from passage 3 MSCs cultured in MSCGM™ or MSCBM™ with 8% HPL. **(E)** Numbers of punctate mitochondrial organelles as well as rods and networks per cell from passage 3 in different media. Data were calculated with Mitochondrial Network Analysis (MiNA), image interpretations are shown next to the diagrams. $^{*}p < 0.05$, $^{**}p < 0.01$, $^{***}p < 0.001$.

Determination of Immunological Molecules by Semi-quantitative RT-PCR

Gene and protein expression of immunological molecules that mediate MSC functions and might rely directly on the status of SF formation and mitochondrial activity like GARP and IDO were analyzed before and after the stimulation with pro-inflammatory cytokines IFN-γ and TNF-α in 2D and 3D cultivated MSCs. Gene as well as IDO protein expression could only be found after stimulation with pro-inflammatory cytokines TNF-α and IFN-γ and not in unstimulated cultures. Due to high variance in IDO RT-PCR the normalization to two housekeeping genes HPRT and PPIA showed no increase in MSCs cultured in MSCBM™ with 8% HPL after 24 and 48 h of stimulation (**Figure 5A**). Protein expression of IDO analyzed by western blot after 48 h stimulation with IFN-γ and TNF-α showed an increase depending on HPL cultivation (**Figure 5B**) but this difference could only be found in two of three investigated batches. When gene expression of GARP was analyzed by RT-PCR in unstimulated adherent MSCs or MSCs from spherical aggregates, we found decreased GARP mRNA in cultures supplemented with HPL (**Figure 6A**). GARP protein followed gene expression (**Figure 6C**). Unlike IDO, GARP was constitutively expressed and not responsive to stimulation with IFN-γ and TNF-α, neither in 2D nor in 3D cultivated MSCs (**Figures 6B,D**), after 24 or 48 h.

DISCUSSION

Extensive research is needed to understand the mechanism how MSCs contribute to organ repair in order to rescue damaged tissue. After application, MSCs can (1) repair connective tissue disease or trauma by integration and differentiation into the required organ specific mature cells at the target site. Furthermore, (2) a locally released secretome of the therapeutic MSCs within the disease milieu can further lead to recovery of damaged organ cells. Finally, (3) a transfer of mitochondria from MSCs to damaged cells in the immediate surroundings by tunneling nanotubes can also facilitate regeneration. The distribution and direct impact of the three different mechanisms of MSC-mediated tissue repair is currently under debate as well as the efficacy of MSC-induced regeneration without post-transplant integration just by the local release of the MSCs' secretome and mitochondrial transfer. Here we investigate the importance of culture medium composition involving HPL as human-derived FBS alternative for MSC expansion. In addition, we investigate the impact of 2D cultivation in adherence to plastic surfaces and 3D cultivation in MSC spherical aggregates generated by hanging drop technology. We found that MSCs grown in adherence to plastic surfaces showed higher levels of f-actin protein and formed thick and well-defined bundles of SFs, while MSCs from spherical aggregates showed lower amounts of f-actin protein which correlated with thinner and more delicate f-actin filaments. The application of HPL led to a reduction in f-actin protein in MSCs grown in adherence to plastic surface while HPL had no effect in MSCs grown in spherical aggregates. It seems likely that HPL has a direct effect on 2D cultured MSC reducing actin stress fiber formation and mitochondrial mass due to the spectrum of cytokines, chemokines, and growth factors provided in the HPL preparation. These human derived bioactive factors were shown to be capable to modulate resiliency of cultured MSCs stressed with palmitate and could lower overall variance in MSC performance between donors (Boland et al., 2019). In adherent MSCs SFs are attached to the FA complex, in which vinculin and paxillin are prominent proteins facilitating the binding of FAs to integrins. Here we can show that FAs behaved the same as SFs and remained expressed intensely after MSCs emerged from the spherical aggregates or when MSCs were cultivated in adherence to the plastic surface. The cultivation supplementation HPL, in contrast, had no effect on FA composition involving vinculin and paxillin when MSCs are adherent to plastic surfaces to facilitate binding via integrins. When SFs were further segregated in ventral SFs, dorsal SFs and transverse arcs according to their anchorage to FAs, ventral SFs showed a response to cultivation where the number of ventral SFs decreased during cultivation of MSCs in HPL, while the length increased, dorsal SFs remained numerically constant. Transverse arcs, in contrast, remained constant both in number and length. This has an effect on the inner tension force of adherent MSCs and eventually on deformability as well as membrane elasticity. These results gave clear evidence for HPL-induced reduction of SF formation in MSCs adherent to the plastic surface, a recommended technology to expand MSCs *ex vivo* (*in vitro*) by the ISCT (Dominici et al., 2006). Interestingly, HPL had no effect when cells were cultivated in 3D spherical aggregates where cells have contact with their autologous matrix. We found a mix of collagen type I, fibronectin, vitronectin, collagen type IV deposition in spherical aggregates of MSCs after 7 days of cultivation (Rossmanith, 2018) and this autologous matrix can facilitate mechanobiological effects of the surrounding environment important for MSC fate determination (Zeiger et al., 2012; Yang et al., 2016). It was shown previously that SF formation can determine the membrane topography of MSCs where bold SFs induce an imprint on the covering cell membrane and the inner tension can indirectly contribute to changes in membrane elasticity of MSCs when measured by AFM (Burridge and Wittchen, 2013; Burridge and Guilluy, 2016). Here we can show that the membrane elasticity determined by the Young's modulus did not change

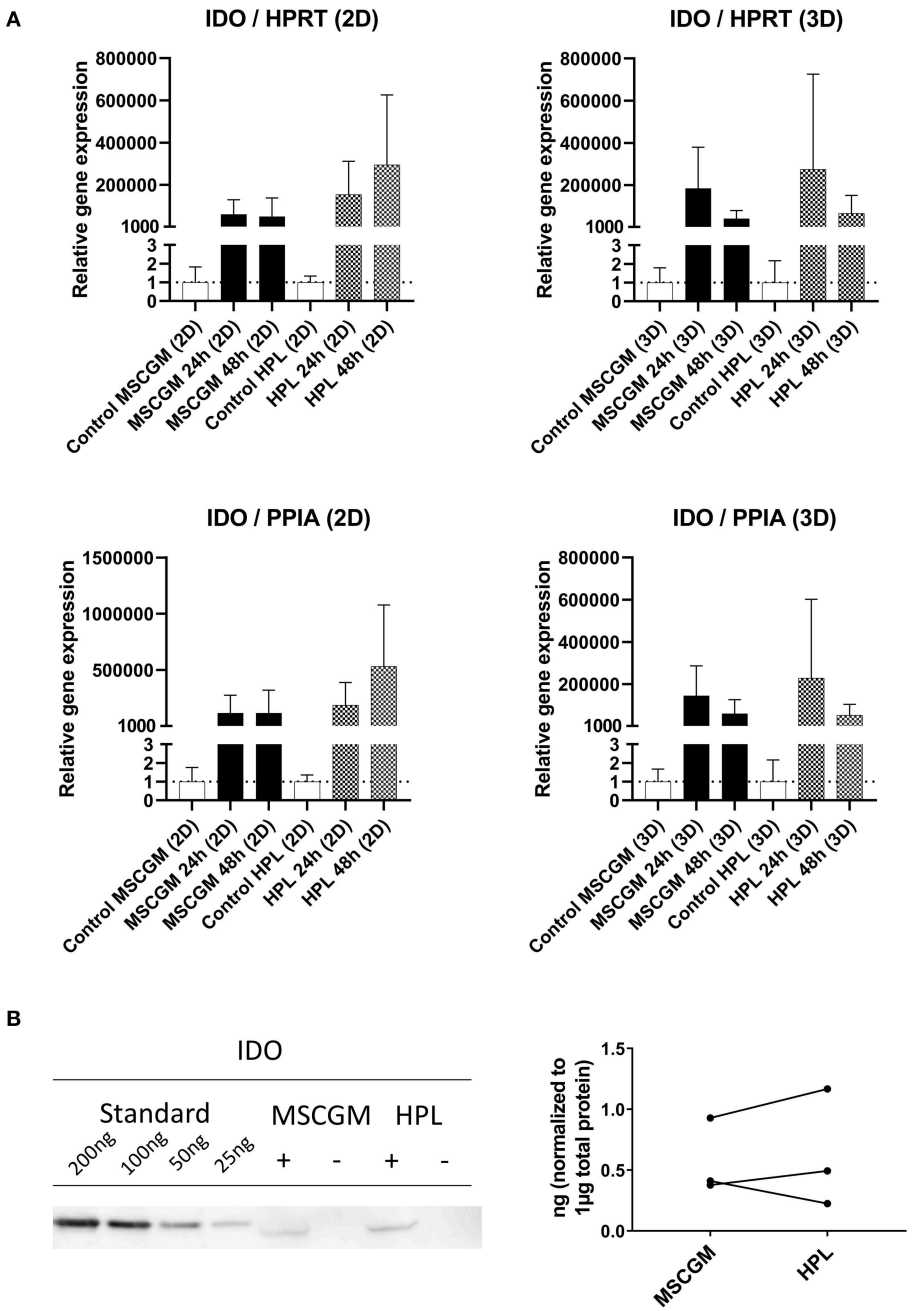

FIGURE 5 | Expression of the immunological molecule IDO. **(A)** RT-PCR analysis of IDO gene expression in 2D and 3D MSCs for 24 and 48 h stimulation with IFN-γ/TNF-α cultured in MSCGM™ or MSCBM™ with 8% HPL and a control with unstimulated cells. Top: Relative gene expression levels of IDO normalized to the housekeeping gene HPRT. Bottom: Normalized to the housekeeping gene PPIA (2D $n = 5$; 3D $n = 3$). **(B)** Left: Western blot analysis of IDO protein expression stimulated with IFN-γ/TNF-α (+) or unstimulated (–) after 48 h. An internal standard of IDO ranging from 25 to 200 ng was included. One representative blot of three independent experiments is shown. Right: Comparison of IDO protein expression in ng per 1 µg total protein of three IFN-γ/TNF-α stimulated batches.

upon the cultivation of adherent MSCs from P1 to P3 when 1024 single measurements were carried out. Due to high variance the decrease in membrane rigidity observed in adherent MSCs of P3 cultivated in the presence of HPL was not significant as compared to cultivation in MSCGM™- medium. Elasticity is a major biophysical property of a MSC and gives information on the resistance of the cell to deform under stress and can retune to its original shape when the strain is relieved. A relation between external force and force deformation exists (Carl and Schillers, 2008). When cell migration of adherent P3 MSCs was investigated in a commercially available wound healing assay no difference between P3 MSCs cultivated either in MSCGM™- or

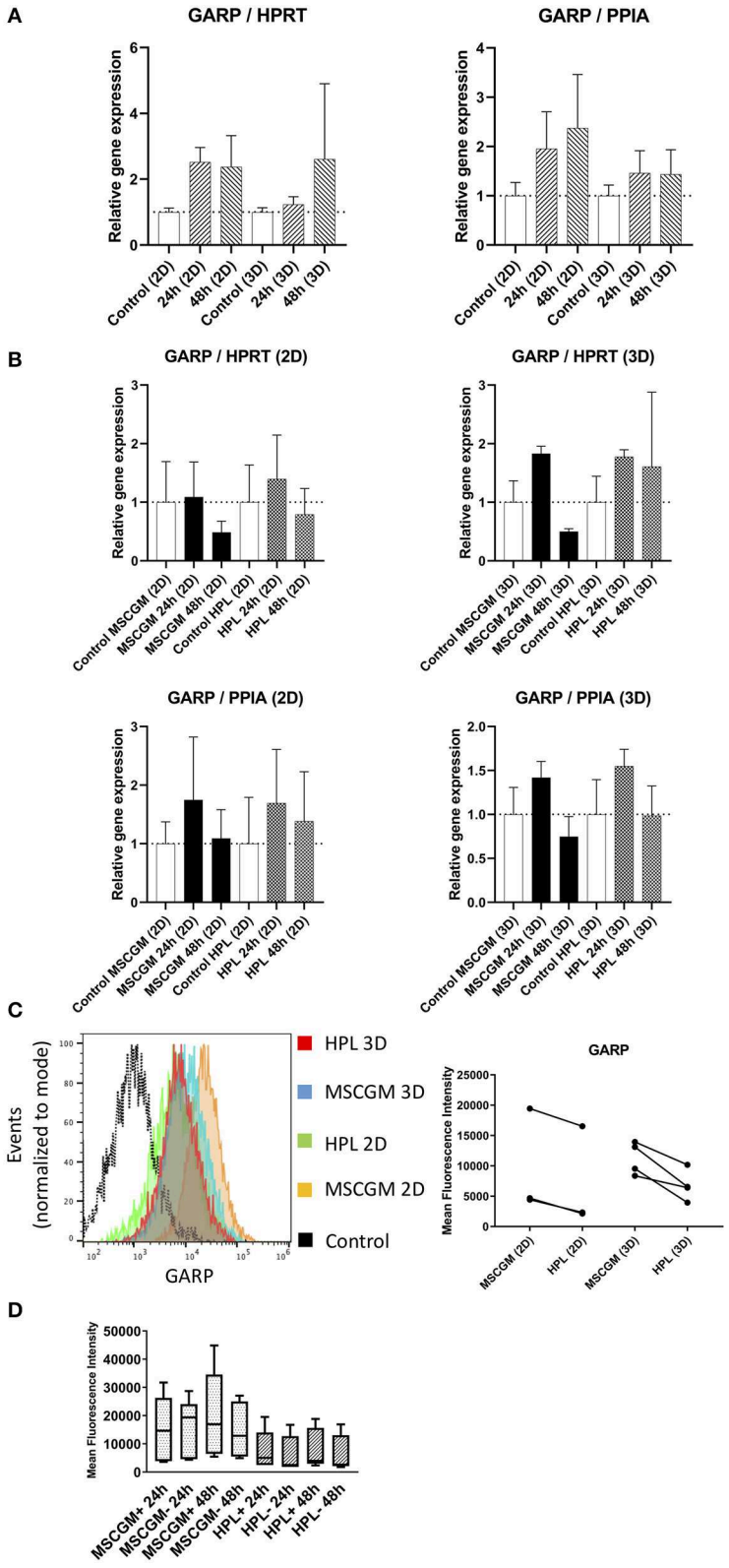

FIGURE 6 | Expression of the immunological molecule GARP. **(A)** Relative gene expression levels of GARP after 24 and 48 h cultivation with MSCGM™ or MSCBM™ with 8% HPL and a control and a control at the beginning of cultivation time. Left: Normalized to the housekeeping gene HPRT (2D $n = 5$; 3D $n = 3$). Right: Normalized to the housekeeping gene PPIA (2D $n = 5$; 3D $n = 3$). **(B)** RT-PCR analysis of GARP gene expression in 2D and 3D MSCs for 24 and 48 h stimulation

(Continued)

FIGURE 6 | with IFN-γ/TNF-α cultured in MSCGM™ or MSCBM™ with 8% HPL and a control with unstimulated cells. Top: Normalized to the housekeeping gene HPRT. Bottom: Normalized to the housekeeping gene PPIA (2D $n = 5$; 3D $n = 3$). **(C)** Left: GARP measurements of living $CD90^+$ MSCs in 2D vs. 3D cultured in different media determined by flow cytometry, 6,000 cells were compared. Right: Dot plot of the mean fluorescence intensity of three batches in 2D and four batches in 3D, 6,000 MSCs were investigated per batch. **(D)** Box plot of the mean fluorescence intensity of GARP protein expression of five batches unstimulated or stimulated with IFN-γ/TNF-α for 24 and 48 h.

in HPL supplemented medium (**Supplementary Figures 3A–C**) could be observed. Taken together, these results indicate that an adaptation to cultivation conditions that can alter membrane elasticity and deformability of MSCs as well as their migratory capability could not be observed in adherent P3 MSCs.

Mitochondria are the powerhouses of the cell producing the majority of ATP through respiration and oxidative phosphorylation (OXPHOS) but besides energy generation, mitochondria also participate in calcium signaling, redox homeostasis and apoptosis, thereby mitochondria metabolism can predetermine the fate of transplanted MSCs. It was shown previously that mitochondria accumulation at sites within the cytoplasm of high-energy demand where local ATP production is essential for virtually all cellular functions. Mitochondrial fusion and fission dynamics that involves transportation by IFs is therefore an indicator of MSC fitness. Here we can show that the mitochondrial mass increased during cultivation of adherent MSCs from P1 to P3 as determined by flow cytometry and HPL culture supplementation prevented this increase. Mitochondria were either determined by MitoTracker™, a vital fluorescent lipophilic cationic dye, or by a specific mAb that determines ATP5H mitochondrial synthase and analyzed by 3D reconstructed high resolution immunofluorescence microscopy. We could distinguish between unbranched punctate, rods, and branched structures (networks) with high precision in living MSCs. Unbranched punctate and networks were shown to be increased in adherent P3 MSCs compared to adherent P1 MSCs cultivated in MSCGM™-medium. When P3 adherent MSCs were cultured in HPL, cells showed the same mitochondrial morphology as P1 MSCs. When networks were analyzed for length of branched mitochondrial structures, we found the highest values in P1 adherent MSCs cultured in MSCGM™- medium. When P3 adherent MSCs cultivated in MSCGM™- medium were analyzed by dSTORM and calculated by ImageJ we found a trend toward a decrease in unbranched punctate mitochondria in P3 adherent cultivated in HPL, confirming previous experiments using the MitoTracker™. Interestingly, mitochondrial rods that count for the majority of mitochondrial structures found and mitochondrial network structures that appear as physically interconnected networks showed no dependence on cultivation in HPL when analyzed by dSTORM. dSTORM has the potential to examine mitochondrial reconstruction and semi-automated analysis of immunofluorescent images with high fidelity. It was shown previously that cultivation-induced mitochondrial remodeling involves mitochondrial fission that plays a crucial role in the segregation of aberrant mitochondrial fragments from the remaining tubular network as well as mitophagy. Mitochondria fission is regulated by cytoplasmic proteins Drp1 and Fis1 localized on the outer membrane of mitochondria, while NIX, BNIP3, FUNDC1, PINK (PTEN-induced putative kinase), and PARK2 (E3-ubiquitin ligase Parkin) dependent mechanisms are involved in determining damaged mitochondria and forward them for mitophagy (Bragoszewski et al., 2017; Bravo-San Pedro et al., 2017). Mitochondrial fusion, on the other hand, is induced by mitofusins (Mfn)1 and Mfn2 as well as optic atrophy protein (Opa)1. These outer mitochondrial membrane proteins mediate adhesion and fusion through their cytoplasmic exposed GTPase domain. This fusion mechanism promotes the formation of long tubular structured mitochondria with further interconnection into reticular structures as seen in adherent MSCs in P3. The deterioration of mitochondrial appearance in P3 MSCs was accompanied by nuclear budding as observed by DAPI-staining. A major component of maintaining cellular homeostasis is the recognition and removal of dysfunctional mitochondria, as mitochondria are an essential source of ATP for cellular function. We could further show, that MSCs grown in spherical hanging droplet cultures omitting adherence, in contrast, showed a mitochondrial network evenly distributed throughout the entire cytoplasm, indicating that this cultivation technique induced the least stress to the cultured MSCs.

MSCs facilitate immunomodulatory capabilities involving a network of regulatory pathways. These pathways need to be orchestrated both spatially and chronologically and rely on a dynamic cytoskeleton as well as energy in order to function properly, but the precise mechanism and the regulatory molecules involved are still an area of debate. Here we have selected two prominent immunomodulatory molecules indoleamine-2,3-dioxygenase (IDO), a tryptophan-catabolizing heme-containing enzyme that facilitates a rapid consumption of tryptophan from the local microenvironment and glycoprotein A repetitions predominant (GARP) a membrane receptor binding latency-associated peptide (LAP)/TGF-β1 to study their dependence on cultivation in 2D or 3D and the effect of HPL. IDO is of particular importance because removal of L-tryptophan by IDO starves the environment of this essential amino acid and stress-response pathways such as GCN2 and mTOR signaling pathways are sensitive to amino-acid withdrawal. The biologically active tryptophan catabolites such as kynurenine metabolites can contribute to a *de novo* induction of FoxP3. MSCs do not express IDO constitutively, but IDO can be induced by several factors, among which IFN-γ plays a prominent role (Ling et al., 2014; Rožman and Švajger, 2018). Here we can show that gene expression of IDO in MSCs was only found after stimulation with pro-inflammatory cytokines TNF-α and IFN-γ as IDO was not expressed in unstimulated MSCs. MSCs cultured with HPL supplementation showed no further increase of IDO mRNA due to high variance. IDO protein expression

was found only by western blotting, because IDO could not be investigated by flow cytometry because it remained cytoplasmic. An increase in protein expression of IDO in two of three batches analyzed by western blotting could be observed after 48 h of stimulation with TNF-α and IFN-γ when cultured in HPL compared to MSCGM^{TM}- medium. The second molecule GARP that was shown previously to be expressed by MSCs, activated FoxP3^{+} Tregs, and megakaryocytes/platelets co-localized with TGF-β1, thereby controlling immune regulatory molecules such as FoxP3 (Carrillo-Galvez et al., 2015). Unlike IDO, GARP was constitutively expressed and was found independent of stimulation with TNF-α and IFN-γ. Constitutive GARP expression on the surface of MSCs did not change when HPL was used as medium supplement.

In conclusion, we can say that cultivation in 3D is beneficial for MSCs to maintain low SF formation and physiological membrane elasticity as well as ensure adequate mitochondrial function and ATP supply. Cultivation in 2D, where MSCs adhere to the plastic surface, led to the intensive ventral SF formation where bold f-actin bundles span the entire length of the MSC and perinuclear mitochondrial accumulation. Ventral SFs anchored at two sides to FA can set up an internal force of contraction which enhances membrane elasticity. Serum substitution with HPL could partially reverse this effect in 2D cultivated MSCs leading to lower levels of f-actin protein and mitochondrial mass. For a successful therapeutic application of MSCs in a clinical setting, clinicians need to understand the complex regulatory pathways influencing MSC cyto-architecture, since generation of inner forces induced by ventral SF formation has an effect on membrane elasticity, deformability, and ability of MSCs to migrate. These physical properties of MSCs combined with mitochondrial dynamics can determine the immunomodulatory function of MSCs. Here we can show that IDO was not expressed in unstimulated MSCs and relayed on stimulation with IFN-γ in both 2D and 3D MSC cultures. The immune regulatory molecule GARP was found to be constitutively expressed independent of 2D or 3D cultivation with no additional upregulation upon stimulation with IFN-γ and TNF-α. Interestingly, HPL had no effect on IDO or GARP expression in our 2D or 3D MSC culture systems. This knowledge is relevant because MSCs, upon administration, can migrate to sites of injury, eventually engraft and differentiate into functional mature organ cells, but definitively secrete cytokines, chemokines, hormones and growth factors as well as extracellular vesicles at the target site. To perform combined investigations on SF formation, mitochondrial morphology and deformability of the MSC membrane and link these results with functional properties like the expression of immunomodulatory molecules is important prior to administration and a prerequisite to translate these results in a humanized animal model in the future.

DATA AVAILABILITY STATEMENT

The datasets generated for this study are available on request to the corresponding author.

ETHICS STATEMENT

The studies involving human participants were reviewed and approved by EK791/2008, EK1192/2015, GS1-EK-4/312-2015. The patients/participants provided their written informed consent to participate in this study.

AUTHOR CONTRIBUTIONS

MF conceived the presented idea and supervised the project as principle investigator. MP conducted the experiments and was responsible for acquisition, analysis, and interpretation of data for the work. MP drafted and MF contributed to the final version of the manuscript. VW revised the draft critically for important intellectual content. ER contributed at cell isolation, acquisition, and interpretation of data. CM and AE assisted with the atomic force microscopy and helped carry out the analysis. FH and JJ contributed the 3D dSTORM analysis.

FUNDING

This work was supported by the N F+B project (Nr: LS15-004) and INTERREG ATCZ 133 co-financed by Europäische Fonds für regionale Entwicklung (EFRE).

ACKNOWLEDGMENTS

The authors thank the company TissueGnostics for technical assistance and the Austrian Cluster for Tissue Regeneration for networking.

SUPPLEMENTARY MATERIAL

The Supplementary Material for this article can be found online at: https://www.frontiersin.org/articles/10.3389/fbioe.2019.00338/full#supplementary-material

REFERENCES

Antoninus, A. A., Widowati, W., Wijaya, L., Agustina, D., Puradisastra, S., Sumitro, S. B., et al. (2015). Human platelet lysate enhances the proliferation of Wharton's jelly-derived mesenchymal stem cells. *Biomarkers Genomic Med.* 7, 87–97. doi: 10.1016/j.bgm.2015.06.001

Atherton, P., Stutchbury, B., Jethwa, D., and Ballestrem, C. (2016). Mechanosensitive components of integrin adhesions: role of vinculin. *Exp. Cell Res.* 343, 21–27. doi: 10.1016/j.yexcr.2015.11.017

Bays, J. L., Peng, X., Tolbert, C. E., Guilluy, C., Angell, A. E., Pan, Y., et al. (2014). Vinculin phosphorylation differentially regulates mechanotransduction at cell-cell and cell-matrix adhesions. *J. Cell Biol.* 205, 251–263. doi: 10.1083/jcb.201309092

Boland, L. K., Burand, A. J., Boyt, D. T., Dobroski, H., Di, L., Liszewski, J. N., et al. (2019). Nature vs. nurture: defining the effects of mesenchymal stromal cell isolation and culture conditions on resiliency to palmitate challenge. *Front. Immunol.* 10:1080. doi: 10.3389/fimmu.2019.01080

Bragoszewski, P., Turek, M., and Chacinska, A. (2017). Control of mitochondrial biogenesis and function by the ubiquitin - proteasome system. *Open Biol.* 7:170007. doi: 10.1098/rsob.170007

Bravo-San Pedro, J. M., Kroemer, G., and Galluzzi, L. (2017). Autophagy and mitophagy in cardiovascular disease. *Circ. Res.* 120, 1812–1824. doi: 10.1161/CIRCRESAHA.117.311082

Burridge, K., and Guilluy, C. (2016). Focal adhesions, stress fibers and mechanical tension. *Exp. Cell Res.* 343, 14–20. doi: 10.1016/j.yexcr.2015.10.029

Burridge, K., and Wittchen, E. S. (2013). The tension mounts: stress fibers as force-generating mechanotransducers. *J. Cell Biol.* 200, 9–19. doi: 10.1083/jcb.201210090

Butt, H. J., and Jaschke, M. (1995). Calculation of thermal noise in atomic force microscopy. *Nanotechnology* 6:1–7. doi: 10.1088/0957-4484/6/1/001

Carl, P., and Schillers, H. (2008). Elasticity measurement of living cells with an atomic force microscope: data acquisition and processing. *Pflugers Arch. Eur. J. Physiol.* 457, 551–559. doi: 10.1007/s00424-008-0524-3

Carrillo-Galvez, A. B., Cobo, M., Cuevas-Ocana, S., Gutierrez-Guerrero, A., Sanchez-Gilabert, A., Bongarzone, P., et al. (2015). Mesenchymal stromal cells express GARP/LRRC32 on their surface: effects on their biology and immunomodulatory capacity. *Stem Cells* 33, 183–195. doi: 10.1002/stem.1821

Dominici, M., Le Blanc, K., Mueller, I., Slaper-Cortenbach, I., Marini, F. C., Krause, D. S., et al. (2006). Minimal criteria for defining multipotent mesenchymal stromal cells. The International Society for Cellular Therapy position statement. *Cytotherapy* 8, 315–317. doi: 10.1080/14653240600855905

Gattazzo, F., Urciuolo, A., and Bonaldo, P. (2014). Extracellular matrix: a dynamic microenvironment for stem cell niche. *Biochim. Biophys. Acta Gen. Subj.* 1840, 2506–2519. doi: 10.1016/j.bbagen.2014.01.010

Gruenbaum, Y., and Aebi, U. (2014). Intermediate filaments: a dynamic network that controls cell mechanics. *F1000Prime Rep.* 6:54. doi: 10.12703/P6-54

Haase, K., and Pelling, A. E. (2015). Investigating cell mechanics with atomic force microscopy. *J. R. Soc. Interface* 12:20140970. doi: 10.1098/rsif.2014.0970

Henschler, R., Gabriel, C., Schallmoser, K., Burnouf, T., and Koh, M. B. C. (2019). Human platelet lysate current standards and future developments. *Transfusion* 59, 1407–1413. doi: 10.1111/trf.15174

Hertz, H. (1882). Ueber die Berührung fester elastischer Körper. *J. Reine Angew. Math.* 1882, 156–171. doi: 10.1515/crll.1882.92.156

Holle, A. W., Tang, X., Vijayraghavan, D., Vincent, L. G., Fuhrmann, A., Choi, Y. S., et al. (2013). *In situ* mechanotransduction via vinculin regulates stem cell differentiation. *Stem Cells* 31, 2467–2477. doi: 10.1002/stem.1490

Hsu, Y.-C., Wu, Y.-T., Yu, T.-H., and Wei, Y.-H. (2016). Mitochondria in mesenchymal stem cell biology and cell therapy: from cellular differentiation to mitochondrial transfer. *Semin. Cell Dev. Biol.* 52, 119–131. doi: 10.1016/j.semcdb.2016.02.011

Jackson, M., and Krasnodembskaya, A. (2017). Analysis of mitochondrial transfer in direct co-cultures of human Monocyte-derived Macrophages (MDM) and Mesenchymal Stem Cells (MSC). *Bio Protoc.* 7:e2255. doi: 10.21769/BioProtoc.2255

Jonkman, J. E. N., Cathcart, J. A., Xu, F., Bartolini, M. E., Amon, J. E., Stevens, K. M., et al. (2014). An introduction to the wound healing assay using live-cell microscopy. *Cell Adhes. Migr.* 8, 440–451. doi: 10.4161/cam.36224

LeBlon, C. E., Casey, M. E., Fodor, C. R., Zhang, T., Zhang, X., and Jedlicka, S. S. (2015). Correlation between *in vitro* expansion-related cell stiffening and differentiation potential of human mesenchymal stem cells. *Differentiation* 90, 1–15. doi: 10.1016/j.diff.2015.08.002

Li, C., Cheung, M. K. H., Han, S., Zhang, Z., Chen, L., Chen, J., et al. (2019). Mesenchymal stem cells and their mitochondrial transfer: a double-edged sword. *Biosci. Rep.* 39:BSR20182417. doi: 10.1042/BSR20182417

Li, H., Shen, S., Fu, H., Wang, Z., Li, X., Sui, X., et al. (2019). Immunomodulatory functions of mesenchymal stem cells in tissue engineering. *Stem Cells Int.* 2019:9671206. doi: 10.1155/2019/9671206

Li, J., Chen, T., Huang, X., Zhao, Y., Wang, B., Yin, Y., et al. (2018). Substrate-independent immunomodulatory characteristics of mesenchymal stem cells in three-dimensional culture. *PLoS ONE* 13:e0206811. doi: 10.1371/journal.pone.0206811

Li, X., Yang, Q., Bai, J., Xuan, Y., and Wang, Y. (2015). Identification of appropriate reference genes for human mesenchymal stem cell analysis by quantitative real-time PCR. *Biotechnol. Lett.* 37, 67–73. doi: 10.1007/s10529-014-1652-9

Ling, W., Zhang, J., Yuan, Z., Ren, G., Zhang, L., Chen, X., et al. (2014). Mesenchymal stem cells use IDO to regulate immunity in tumor microenvironment. *Cancer Res.* 74, 1576–1587. doi: 10.1158/0008-5472.CAN-13-1656

Mayr, S., Hauser, F., Peterbauer, A., Tauscher, A., Naderer, C., Axmann, M., et al. (2018). Localization microscopy of actin cytoskeleton in human platelets. *Int. J. Mol. Sci.* 19:1150. doi: 10.3390/ijms19041150

Melzak, K. A., and Toca-Herrera, J. L. (2015). Atomic force microscopy and cells: indentation profiles around the AFM tip, cell shape changes, and other examples of experimental factors affecting modeling. *Microsc. Res. Tech.* 78, 626–632. doi: 10.1002/jemt.22522

Mullen, C. A., Vaughan, T. J., Voisin, M. C., Brennan, M. A., Layrolle, P., and McNamara, L. M. (2014). Cell morphology and focal adhesion location alters internal cell stress. *J. R. Soc. Interface* 11:20140885. doi: 10.1098/rsif.2014.0885

Nahidiazar, L., Agronskaia, A. V., Broertjes, J., Van Broek, B., Den, and Jalink, K. (2016). Optimizing imaging conditions for demanding multi-color super resolution localization microscopy. *PLoS ONE* 11:e0158884. doi: 10.1371/journal.pone.0158884

Najar, M., Fayyad-Kazan, M., Raicevic, G., Fayyad-Kazan, H., Meuleman, N., Bron, D., et al. (2018). Advanced glycation end-products-, C-type lectin- and cysteinyl/leukotriene-receptors in distinct mesenchymal stromal cell populations: differential transcriptional profiles in response to inflammation. *Cell J.* 20, 250–258. doi: 10.22074/cellj.2018.5104

Niu, J., Yue, W., Le-Le, Z., Bin, L., and Hu, X. (2017). Mesenchymal stem cells inhibit T cell activation by releasing TGF-β1 from TGF-β1/GARP complex. *Oncotarget* 8, 99784–99800. doi: 10.18632/oncotarget.21549

Pérez-Sala, D., Oeste, C. L., Martínez, A. E., Carrasco, M. J., Garzón, B., and Cañada, F. J. (2015). Vimentin filament organization and stress sensing depend on its single cysteine residue and zinc binding. *Nat. Commun.* 6:7287. doi: 10.1038/ncomms8287

Probst-Kepper, M., and Buer, J. (2010). FOXP3 and GARP (LRRC32): the master and its minion. *Biol. Direct* 5:8. doi: 10.1186/1745-6150-5-8

Rodriguez, A. M., Nakhle, J., Griessinger, E., and Vignais, M. L. (2018). Intercellular mitochondria trafficking highlighting the dual role of mesenchymal stem cells as both sensors and rescuers of tissue injury. *Cell Cycle* 17, 712–721. doi: 10.1080/15384101.2018.1445906

Rossmanith, E. (2018). Abstracts from the 45th ESAO Congress, 12-15 September 2018, Madrid, Spain. *Int. J. Artif. Organs* 41, 614–615. doi: 10.1177/0391398818785526

Rožman, P., and Švajger, U. (2018). The tolerogenic role of IFN-γ. *Cytokine Growth Factor Rev.* 41, 40–53. doi: 10.1016/j.cytogfr.2018.04.001

Sage, D., Pham, T. A., Babcock, H., Lukes, T., Pengo, T., Chao, J., et al. (2019). Super-resolution fight club: assessment of 2D and 3D single-molecule localization microscopy software. *Nat. Methods* 16, 387–395. doi: 10.1038/s41592-019-0364-4

Shankar, J., Kojic, L. D., St-Pierre, P., Wang, P. T. C., Fu, M., Joshi, B., et al. (2013). Raft endocytosis of AMF regulates mitochondrial dynamics through Rac1 signaling and the Gp78 ubiquitin ligase. *J. Cell Sci.* 126, 3295–3304. doi: 10.1242/jcs.120162

Shi, M., Liu, Z. W., and Wang, F. S. (2011). Immunomodulatory properties and therapeutic application of mesenchymal stem cells. *Clin. Exp. Immunol.* 164, 1–8. doi: 10.1111/j.1365-2249.2011.04327.x

Sneddon, I. N. (1965). The relation between load and penetration in the axisymmetric boussinesq problem for a punch of arbitrary profile. *Int. J. Eng. Sci.* 3, 47–57. doi: 10.1016/0020-7225(65)90019-4

Soncini, M., Vertua, E., Gibelli, L., Zorzi, F., Denegri, M., Albertini, A., et al. (2007). Isolation and characterization of mesenchymal cells from human fetal membranes. *J. Tissue Eng. Regen. Med.* 1, 296–305. doi: 10.1002/term.40

Spees, J. L., Gregory, C. A., Singh, H., Tucker, H. A., Peister, A., Lynch, P. J., et al. (2004). Internalized antigens must be removed to prepare hypoimmunogenic mesenchymal stem cells for cell and gene therapy. *Mol. Ther.* 9, 747–756. doi: 10.1016/j.ymthe.2004.02.012

Symons, M. H., and Mitchison, T. J. (1991). Control of actin polymerization in live and permeabilized fibroblasts. *J. Cell Biol.* 114, 503–513. doi: 10.1083/jcb.114.3.503

Toegel, S., Huang, W., Piana, C., Unger, F. M., Wirth, M., Goldring, M. B., et al. (2007). Selection of reliable reference genes for qPCR studies on chondroprotective action. *BMC Mol. Biol.* 8:13. doi: 10.1186/1471-2199-8-13

Tojkander, S., Gateva, G., and Lappalainen, P. (2012). Actin stress fibers - assembly, dynamics and biological roles. *J. Cell Sci.* 125, 1855–1864. doi: 10.1242/jcs.098087

Valente, A. J., Maddalena, L. A., Robb, E. L., Moradi, F., and Stuart, J. A. (2017). A simple ImageJ macro tool for analyzing mitochondrial network morphology in mammalian cell culture. *Acta Histochem.* 119, 315–326. doi: 10.1016/j.acthis.2017.03.001

Walzer, S. M., Toegel, S., Chiari, C., Farr, S., Rinner, B., Weinberg, A.-M., et al. (2019). A 3-dimensional *in vitro* model of zonally organized extracellular matrix. *Cartilage*. doi: 10.1177/1947603519865320. [Epub ahead of print].

Xia, S., and Kanchanawong, P. (2017). Nanoscale mechanobiology of cell adhesions. *Semin. Cell Dev. Biol.* 71, 53–67. doi: 10.1016/j.semcdb.2017.07.029

Yang, C., DelRio, F. W., Ma, H., Killaars, A. R., Basta, L. P., Kyburz, K. A., et al. (2016). Spatially patterned matrix elasticity directs stem cell fate. *Proc. Natl. Acad. Sci. U.S.A.* 113, E4439–4445. doi: 10.1073/pnas.1609731113

Zeiger, A. S., Loe, F. C., Li, R., Raghunath, M., and van Vliet, K. J. (2012). Macromolecular crowding directs extracellular matrix organization and mesenchymal stem cell behavior. *PLoS ONE* 7:e37904. doi: 10.1371/journal.pone.0037904

Zhou, Y., Chen, H., Li, H., and Wu, Y. (2017). 3D culture increases pluripotent gene expression in mesenchymal stem cells through relaxation of cytoskeleton tension. *J. Cell. Mol. Med.* 21, 1073–1084. doi: 10.1111/jcmm.12946

Conflict of Interest: The authors declare that the research was conducted in the absence of any commercial or financial relationships that could be construed as a potential conflict of interest.

frontiers in Bioengineering and Biotechnology

ORIGINAL RESEARCH
published: 15 November 2019
doi: 10.3389/fbioe.2019.00321

Impact of Fibronectin Knockout on Proliferation and Differentiation of Human Infrapatellar Fat Pad-Derived Stem Cells

Yiming Wang[1,2], *Yawen Fu*[3,4], *Zuoqin Yan*[2]*, *Xiao-Bing Zhang*[3,4]* and *Ming Pei*[1,5]*

[1] Stem Cell and Tissue Engineering Laboratory, Department of Orthopaedics, West Virginia University, Morgantown, WV, United States, [2] Department of Orthopaedics, Zhongshan Hospital, Fudan University, Shanghai, China, [3] State Key Laboratory of Experimental Hematology, Institute of Hematology and Blood Disease Hospital, Tianjin, China, [4] Department of Medicine, Loma Linda University, Loma Linda, CA, United States, [5] WVU Cancer Institute, Robert C. Byrd Health Sciences Center, West Virginia University, Morgantown, WV, United States

OPEN ACCESS

Edited by:
Martin James Stoddart,
AO Research Institute, Switzerland

Reviewed by:
Wei Seong Toh,
National University of Singapore, Singapore
Anna Lange-Consiglio,
University of Milan, Italy

***Correspondence:**
Zuoqin Yan
zuoqin_yan@163.com
Xiao-Bing Zhang
xzhang@llu.edu
Ming Pei
mpei@hsc.wvu.edu

Specialty section:
This article was submitted to Tissue Engineering and Regenerative Medicine, a section of the journal Frontiers in Bioengineering and Biotechnology

Received: 02 July 2019
Accepted: 28 October 2019
Published: 15 November 2019

Citation:
Wang Y, Fu Y, Yan Z, Zhang X-B and Pei M (2019) Impact of Fibronectin Knockout on Proliferation and Differentiation of Human Infrapatellar Fat Pad-Derived Stem Cells. Front. Bioeng. Biotechnol. 7:321. doi: 10.3389/fbioe.2019.00321

Fibronectin plays an essential role in tissue development and regeneration. However, the effects of fibronectin knockout (FN1-KO) on stem cells' proliferation and differentiation remain unknown. In this study, CRISPR/Cas9 generated FN1-KO in human infrapatellar fat pad-derived stem cells (IPFSCs) was evaluated for proliferation ability including cell cycle and surface markers as well as stemness gene expression and for differentiation capacity including chondrogenic and adipogenic differentiation. High passage IPFSCs were also evaluated for proliferation and differentiation capacity after expansion on decellularized ECM (dECM) deposited by FN1-KO cells. Successful FN1-KO in IPFSCs was confirmed by Sanger sequencing and Inference of CRISPR Edits analysis (ICE) as well as immunostaining for fibronectin expression. Compared to the GFP control, FN1-KO cells showed an increase in cell growth, percentage of cells in the S and G_2 phases, and CD105 and CD146 expression but a decrease in expression of stemness markers CD73, CD90, SSEA4, and mesenchymal condensation marker *CDH2* gene. FN1-KO decreased both chondrogenic and adipogenic differentiation capacity. Interestingly, IPFSCs grown on dECMs deposited by FN1-KO cells exhibited a decrease in cell proliferation along with a decline in *CDH2* expression. After induction, IPFSCs plated on dECMs deposited by FN1-KO cells also displayed decreased expression of both chondrogenic and adipogenic capacity. We concluded that FN1-KO increased human IPFSCs' proliferation capacity; however, this capacity was reversed after expansion on dECM deposited by FN1-KO cells. Significance of fibronectin in chondrogenic and adipogenic differentiation was demonstrated in both FN1-KO IPFSCs and FN(–) matrix microenvironment.

Keywords: fibronectin, infrapatellar fat pad-derived stem cell, proliferation, chondrogenic differentiation, adipogenic differentiation

INTRODUCTION

As a connective tissue, articular cartilage is susceptible to damage caused by trauma or osteoarthritis (OA). However, its healing response to injury is limited due to its avascular nature (Benedek, 2006). Despite many pre-clinical studies having been performed, the regeneration of functional articular cartilage for clinical use remains a challenge (Karnes et al., 2014). An increasing body of evidence indicates that mesenchymal stem cells (MSCs) have great potential for cartilage engineering and regeneration (Jones and Pei, 2012; Pizzute et al., 2015). After first being isolated from bone marrow (Friedenstein et al., 1976), MSCs have been found in a variety of tissues including infrapatellar fat pad (IPFP) (Sun et al., 2018a). IPFP-derived MSCs (IPFSCs) are easily accessible and have better chondrogenic potential than bone marrow-derived MSCs (BMSCs) (Hindle et al., 2017). IPFSCs from OA patients were shown to possess comparable chondrogenic potential as those from non-OA donors (Liu et al., 2014), supporting the feasibility of using patients' autologous cells for regeneration. However, MSCs including IPFSCs were reported to inevitably suffer from cell senescence due to *in vitro* expansion or donor age (Li and Pei, 2012; Lynch and Pei, 2014).

Recent studies indicate that microenvironment, provided by extracellular matrix (ECM), plays an important role in the regulation of stem cell stemness (Pei, 2017; Sun et al., 2018b). For instance, decellularized ECM (dECM) has been demonstrated to rejuvenate human IPFSCs (He and Pei, 2013), synovium-derived MSCs (SDSCs) (Li et al., 2014), and human BMSCs (Pei et al., 2011a). Fibronectin (FN), one of the major fibrillary components in ECM, is implicated in the proliferation and differentiation processes of MSCs (Chang et al., 2008; Kalkreuth et al., 2014). However, while most evidence relies on the effect of fibronectin ligands on cell behavior (Linask and Lash, 1988; Budd et al., 1990; Sapudom et al., 2015), with a few reports investigating the effect *via* fibronectin knockout (FN1-KO) (Liu et al., 2010; Lukjanenko et al., 2016), there is no evidence of the impact of FN1-KO on adult stem cells' chondrogenic capacity. Therefore, in this study, the FN1-KO approach was used to investigate the role of fibronectin in guiding IPFSCs' chondrogenic and adipogenic differentiation given the close relationship between these two lineages (Zhou et al., 2019) and in this specific type of stem cells (Sun et al., 2018a). Furthermore, the role of fibronectin on IPFSCs' proliferation and bi-lineage differentiation was evaluated *via* dECM deposited by FN1-KO IPFSCs, in other words, a three-dimensional FN(–) matrix microenvironment.

MATERIALS AND METHODS

IPFSC Harvest and Culture

Approval for this study was obtained from the Institutional Review Board. Human adult IPFPs were harvested from six young patients with acute meniscus or anterior crucial ligament tear (four male and two female, average 22 years old). These IPFPs were minced and sequentially digested with 0.1% trypsin (Roche, Indianapolis, IN) for 30 min and 0.1% collagenase P (Roche) for 2 h to separate cells. After filtration and centrifugation, obtained IPFSCs were pooled and cultured in growth medium [Minimum Essential Medium–Alpha Modification (αMEM) containing 10% fetal bovine serum (FBS), 100 U/ml penicillin, 100 μg/ml streptomycin, and 0.25 μg/ml fungizone (Invitrogen, Carlsbad, CA)] at 37°C in a humidified 21% O_2 and 5% CO_2 incubator. The medium was changed every 3 days.

Single-Guide RNA (sgRNA) Design, Plasmid Construction, and Virus Production

The CHOPCHOP website (https://chopchop.rc.fas.harvard.edu/) was consulted to design high-performance sgRNAs targeting FN1 (Zhang et al., 2016) sgFN1a (GCTGTAACCCAGACTTACGG) and sgFN1b (GCAAGCGTGAGTACTGACCG) were used in this study. Lentiviral vectors that express Cas9 (driven by the SFFV promoter) and sgRNA (driven by the U6 promoter) were constructed with a NEBuilder HiFi DNA Assembly Kit (New England Biolabs, Ipswich, MA). The vectors were verified by Sanger sequencing of the inserts. A standard calcium phosphate precipitation protocol was utilized for lentivirus production. The lentiviral vectors were condensed 100-fold by centrifugation at 6,000 × *g* for 24 h at 4°C to reach biological titers of ∼1 × 10 (Hindle et al., 2017)/ml.

Lentiviral CRISPR/Cas9 Mediated FN1-KO

Lentiviral CRISPR/Cas9 was used to generate FN1-KO in human IPFSCs according to a previous report (Zhang et al., 2017). Passage 1 human IPFSCs were transduced at a multiplicity of infection (MOI) of two with scramble sgRNA sequence-containing vector (green fluorescence protein control lentivirus particles, copGFP) or CRISPR/Cas9 vectors (sgFN1a and sgFN1b) in the presence of 4 μg/ml of protamine sulfate (MilliporeSigma, Burlington, MA). After 24 h, the medium was changed to αMEM with 10% FBS and 2 μg/ml of puromycin (MilliporeSigma) for selection. Five days after transduction and puromycin selection, DNA fragments surrounding the Cas9-sgRNA target sites were polymerase chain reaction (PCR) amplified. Sanger sequencing and Inference of CRISPR Edits (ICE) were used to evaluate the frameshift-induced knockout efficiency (Li et al., 2018). Meanwhile, immunofluorescence staining for fibronectin was also used to confirm transduction efficiency in the dECMs deposited by normal cells (normal ECM), Cas9-sgFN1a transduced cells (sgFN1a ECM), and Cas9-sgFN1b transduced cells (sgFN1b ECM).

dECM Preparation and Immunofluorescence Staining

The protocol to prepare dECM was detailed in a previous report (Li and Pei, 2018). Briefly, tissue culture plastic (TCP) was pre-coated with 0.2% gelatin (MilliporeSigma) at 37°C for 1 h, followed by treatment with 1% glutaraldehyde (MilliporeSigma) and 1 M ethanolamine (MilliporeSigma) at room temperature (RT) for 0.5 h, respectively. Passage 5 IPFSCs from the copGFP, sgFN1a, and sgFN1b groups were seeded on pre-coated TCP (6,000 cells/cm^2) until they reached 100% confluence, followed by addition of L-ascorbic acid

phosphate (Wako Chemicals, Richmond, VA) in the medium at a working concentration of 250 μM for an additional 7 days (Pizzute et al., 2016). Then, cells were incubated in 0.5% Triton X-100 (MilliporeSigma) containing 20 mM ammonium hydroxide (Sargent-Welch, Skokie, IL) at 37°C for 5 min. After the cells were removed, dECMs were rinsed with phosphate buffered solution (PBS) and stored in PBS containing 100 U/ml penicillin, 100 μg/ml streptomycin, and 0.25 μg/ml fungizone at 4°C until use.

dECMs were fixed in 4% paraformaldehyde, blocked with 1% bovine serum albumin (BSA), and incubated with primary antibody against human fibronectin (cat no. HFN 7.1; Developmental Studies Hybridoma Bank, Iowa City, IA). After rinsing with PBS, dECMs were incubated with secondary antibody [Donkey anti-Mouse IgG (H+L) Alexa Fluor 488, Invitrogen]. Fluorescence intensity was observed under a Zeiss Axiovert 40 CFL Inverted Microscope (Zeiss, Oberkochen, Germany).

Culture of IPFSCs on TCP and dECMs

Two experiments were designed as follows: (1) TCP culture regimen (Experiment 1), passage 5 IPFSCs from the copGFP, sgFN1a, and sgFN1b groups were expanded on TCP; and (2) dECM culture regimen (Experiment 2), high passage (passage 15) IPFSCs were expanded for 7 days on TCP and dECMs deposited by passage 5 IPFSCs from the copGFP, sgFN1a, and sgFN1b groups in terms of copGFP ECM, sgFN1a ECM, and sgFN1b ECM. Expanded cells were detached followed by incubation in a pellet culture system for chondrogenic induction or culture in T25 flasks for adipogenic induction.

Evaluation of Expanded Cells' Growth Rate, Surface Phenotypes, and Expression of Stemness Genes

Cell number was counted ($n = 8$ T175 flasks each group) and cell cycle was measured (the percentage of cells in the S and G_2 phases) to assess expanded cell growth. After a 7-day culture of seeded cells at 3,000 cells/cm^2, the harvested cells were counted using Countess® (Invitrogen). For cell cycle analysis, cells were fixed with 70% ethanol and stained with propidium iodide (MilliporeSigma). DNA contents were measured using FACS Calibur (BD Biosciences, San Jose, CA), and analyzed using FCS Express software package (*De Novo* Software, Los Angeles, CA).

Flow cytometry was used to evaluate surface phenotypes of expanded cells. The following primary antibodies were used: CD73-APC (cat no. 17-0739-42; eBioScience, Fisher Scientific, Waltham, MA), CD90-APC-Vio770 (cat no. 130-114-863; Miltenyi Biotec, San Diego, CA), CD105-PerCP-Vio700 (cat no. 130-112-170; Miltenyi Biotec), CD146-PE (cat no. 12-1469-42; eBioScience), and the stage-specific embryonic antigen 4-PE (SSEA4-PE; cat no. 330406; BioLegend, Dedham, MA). Samples of each 2×10^5 expanded cells were incubated in cold PBS containing 0.1% ChromPure Human IgG whole molecule (Jackson ImmunoResearch Laboratories, West Grove, PA) for 30 min, followed by binding with the primary antibodies at 4°C for 30 min. Fluorescence was examined by a FACS Calibur (BD Biosciences) using FCS Express software package (*De Novo* Software).

Total RNA was extracted from expanded cells ($n = 4$) using an RNase-free TRIzol® (Invitrogen). About 2 μg of mRNA was utilized for reverse transcription with a High-Capacity cDNA Reverse Transcription Kit (Applied Biosystems Inc., Foster, CA). Stemness genes [*NANOG* (assay ID: Hs02387400_g1), *SOX2* (SRY-box 2; assay ID: Hs01053049_s1), *KLF4* (Kruppel-like factor 4; assay ID: Hs00358836_m1), *BMI1* (B lymphoma Mo-MLV insertion region 1 homolog; assay ID: Hs00180411_m1), *MYC* (assay ID: Hs00153408_m1), *NOV* (nephroblastoma overexpressed; assay ID: Hs00159631_m1), *POU5F1* (POU class 5 homeobox 1; assay ID: Hs04260367_gH), and *NES* (nestin; assay ID: Hs04187831_g1)], senescent genes [*CDKN1A* (cyclin-dependent kinase inhibitor 1A; assay ID: Hs00355782_m1), *CDKN2A* (cyclin-dependent kinase inhibitor 2A; assay ID: Hs00923894_m1), and *TP53* (tumor protein p53; assay ID: Hs01034249_m1)], and the mesenchymal condensation gene [*CDH2* (cadherin 2; assay ID: Hs00983056_m1)] were customized by Applied Biosystems as part of the Custom TaqMan® Gene Expression Assays. *GAPDH* (glyceraldehyde-3-phosphate dehydrogenase; assay ID: Hs02758991_g1) was used as the endogenous control gene. Real-time quantitative PCR (qPCR) was performed using Applied Biosystems™ 7500 Fast Real-Time PCR System (Applied Biosystems). Relative transcript levels were calculated as $\chi = 2^{-\Delta\Delta Ct}$, in which $\Delta\Delta Ct = \Delta E - \Delta C$, $\Delta E = Ct_{exp} - Ct_{GAPDH}$, and $\Delta C = Ct_{ct1} - Ct_{GAPDH}$.

Chondrogenic Induction and Analysis

For chondrogenic induction, aliquots of 0.3×10^6 expanded cells were centrifuged at 500 *g* for 7 min in a 15-ml polypropylene tube to make a pellet. After overnight incubation (day 0), pellets were grown in a serum-free chondrogenic induction medium [high-glucose Dulbecco's modified Eagle's medium (DMEM) with 40 μg/ml proline (MilliporeSigma), 100 nM dexamethasone (MilliporeSigma), 100 U/ml penicillin, 100 μg/ml streptomycin, 0.1 mM ascorbic acid-2-phosphate, and 1× ITS™ Premix (BD Biosciences)] with the supplementation of 10 ng/ml transforming growth factor beta3 (TGFβ3; PeproTech, Rocky Hill, NJ) for up to 18 days. Chondrogenic differentiation was assessed using histology, immunohistochemistry, and qPCR.

Representative pellets ($n = 3$) were fixed in 4% paraformaldehyde at 4°C overnight, followed by dehydrating in a gradient ethanol series, clearing with xylene, and embedding in paraffin blocks. Five-micrometer-thick sections were stained with Alcian blue (MilliporeSigma) staining for sulfated glycosaminoglycan (GAG). For immunohistochemical staining (IHC), consecutive sections were incubated with primary antibody against type II collagen (cat no. II-II6B3; Developmental Studies Hybridoma Bank) followed by the secondary antibody of biotinylated horse anti-mouse IgG (Vector, Burlingame, CA). Immunoactivity was identified using Vectastain ABC reagent (Vector).

Total RNA was extracted from chondrogenically induced pellets ($n = 4$) using an RNase-free TRIzol® (Invitrogen). After reverse transcription, chondrogenic marker-related genes [*SOX9* (SRY-box 9; assay ID: Hs00165814_m1), *ACAN* (aggrecan;

assay ID: Hs00153936_m1), *COL2A1* (type II collagen; assay ID: Hs00156568_m1), and *PRG4* (proteoglycan 4; assay ID: Hs00981633_m1)] and hypertrophic marker genes [*COL10A1* (type X collagen; assay ID: Hs00166657_m1) and *MMP13* (matrix metallopeptidase 13; assay ID: Hs00233992_m1)] were customized by Applied Biosystems as part of the Custom TaqMan® Gene Expression Assays. *GAPDH* was used as the endogenous control gene. Each experiment was repeated three times.

Adipogenic Induction and Analysis

When cells reached 90% confluence in T25 flasks, they were cultured for 21 days in adipogenic medium (growth medium supplemented with 1 μM dexamethasone, 0.5 mM isobutyl-1-methyxanthine, 200 μM indomethacin, and 10 μM insulin). Cells in T25 flasks ($n = 3$) were fixed in 4% paraformaldehyde and stained with a 0.6% (w/v) Oil Red O (ORO) solution (60% isopropanol, 40% water) for 10 min. Intracellular lipid-filled droplet-bound staining was recorded under a Nikon TE300 phase-contrast microscope (Nikon, Tokyo, Japan).

Total RNA was extracted from adipogenically induced cells ($n = 4$) using an RNase-free TRIzol® (Invitrogen). After reverse transcription, adipogenic marker genes [*LPL* (lipoprotein lipase; assay ID: Hs00173425_m1), *PPARG* (peroxisome proliferator-activated receptor gamma; assay ID: Hs01115513_m1), *FABP4* (fatty acid-binding protein 4; assay ID: Hs01086177_m1), and *CEBPA* (CCAAT enhancer binding protein alpha; assay ID: Hs00269972_s1)] were customized by Applied Biosystems as part of the Custom TaqMan® Gene Expression Assays. *GAPDH* was used as the endogenous control gene. Each experiment was repeated three times.

Statistical Analysis

Mann–Whitney *U* test was used for pairwise comparison. All statistical analyses were conducted with SPSS 20.0 statistical software (SPSS Inc., Chicago, IL). $P < 0.05$ was considered statistically significant.

RESULTS

FN1-KO Cell Model and Influence on IPFSCs in Proliferation and Stemness

In this study, CRISPR/Cas9 was used to generate knockout FN1 in human IPFSCs. To confirm the success of FN1-KO, Sanger sequencing and ICE analysis were conducted and the results revealed 74% indels for sgFN1a (**Figure 1A**) and 96% indels for sgFN1b (**Figure 1B**). This result was in line with our immunofluorescence data (**Figure 1C**). We found that, compared to abundant expression of fibronectin in "normal ECM" deposited by non-transduced IPFSCs, "sgFN1a ECM" and "sgFN1b ECM" exhibited considerably less expression of fibronectin, particularly for the sgFN1b ECM group.

In order to determine whether fibronectin influences stem cell proliferation, cell increase was measured (**Figure 2A**) and cell cycle was monitored (**Figure 2B**) during cell expansion. We found that IPFSCs from both sgFN1a and sgFN1b groups grew faster than those from the copGFP group. This phenomenon was also supported by cell cycle data, in which both Cas9-sgFN1a and Cas9-sgFN1b transduced IPFSCs exhibited a higher percentage of cells in the S phase (%S). Our flow cytometry data suggested that FN1-KO decreased the expression of SSEA4 (**Figure 2C**) in both percentage and median and CD73 (**Figure 2D**) and CD90 (**Figure 2E**) in median but increased expression of CD105 (**Figure 2F**) in median and CD146 (**Figure 2G**) in both percentage and median in human IPFSCs.

To find out whether fibronectin affected stem cell stemness, a list of stemness genes was assessed using qPCR in FN1-KO IPFSCs and the control groups. Most stemness genes including *NANOG*, *SOX2*, *KLF4*, *BMI1*, and *MYC* were down-regulated in FN1-KO IPFSCs; however, some stemness genes, *NOV* and *POU5F1* (also known as *OCT4*), were down-regulated in the sgFN1a group but slightly up-regulated in the sgFN1b group (**Figure 2H**). Interestingly, *NES* was up-regulated in both sgFN1a and sgFN1b groups compared with the copGFP group (**Figure 2H**). We also found that all senescence-related genes were down-regulated in the FN1-KO IPFSCs, including *CDKN1A*, *CDKN2A*, and *TP53* (**Figure 2I**). Since fibronectin is linked with mesenchymal condensation, *CDH2*, a condensation marker, was also evaluated using qPCR. The data showed that *CDH2* expression in IPFSCs dramatically decreased in line with the extent of FN1-KO (**Figure 2J**).

Effects of FN1-KO on IPFSCs in Chondrogenic and Adipogenic Differentiation

To ascertain whether FN1-KO affected IPFSCs' differentiation capacity, chondrogenesis (**Figure 3**) and adipogenesis (**Figure 4**) were evaluated using histology, immunostaining, and qPCR. A pellet culture system was employed for chondrogenic induction. After an 18-day chondrogenic incubation, FN1-KO IPFSCs yielded pellets with a smaller size and incomplete (rough) surface compared to the copGFP group, particularly for the sgFN1b group. This discrepancy was observed in Alcian blue staining for sulfated GAGs and IHC for type II collagen, two typical chondrogenic markers. The pellets from FN1-KO IPFSCs were weakly stained for both GAGs and type II collagen (**Figure 3A**); these results were validated at the mRNA levels by qPCR analysis demonstrating that FN1-KO significantly decreased the expression of chondrogenesis-related genes including *SOX9*, *ACAN*, *COL2A1*, and *PRG4* but increased hypertrophy-related genes in terms of *COL10A1* and *MMP13* (**Figure 3B**).

After a 21-day adipogenic induction, Oil Red O staining showed that, compared to the copGFP group, FN1-KO significantly decreased lipid droplets in induced IPFSCs, particularly for the sgFN1b group (**Figure 4A**). The staining data were further confirmed by qPCR data for typical adipogenic genes. The data showed that, compared to the copGFP group, the sgFN1a group had significantly lower expression of *LPL*, *FABP4*, and *CEBPA* but not *PPARG*, whereas the sgFN1b group had remarkably lower expression of all of the four adipogenic genes (**Figure 4B**).

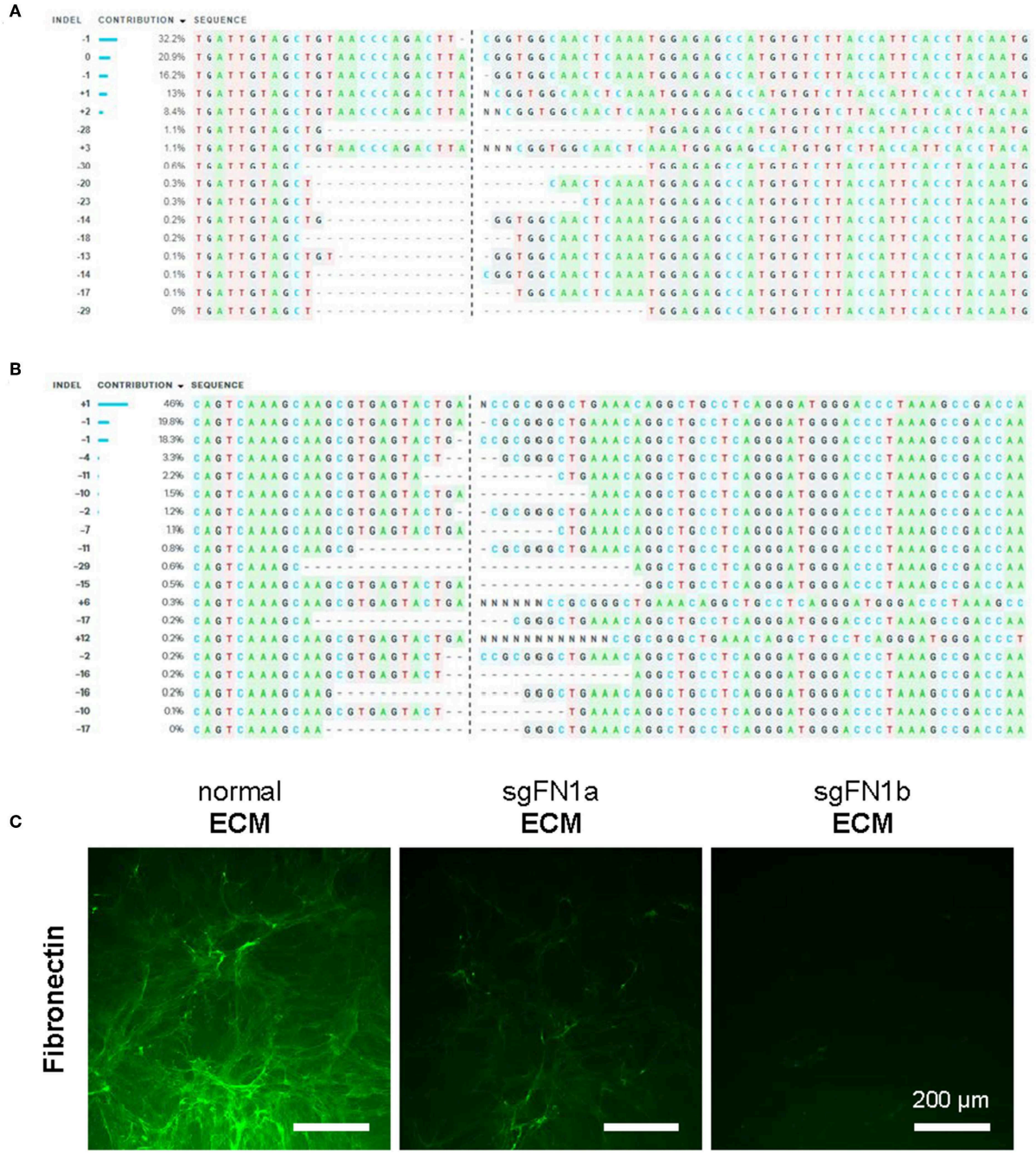

FIGURE 1 | Knockout of FN1 in IPFSCs. Human IPFSCs were transduced with scramble sgRNA sequence-containing vector (green fluorescence protein control lentivirus particles, copGFP) or CRISPR/Cas9 vectors (sgFN1a and sgFN1b). Five days after transduction, amplicons targeting the Cas9-sgFN1 cleavage sites were subject to Sanger sequencing and ICE analysis. Representative diagrams of indel mutations were induced by sgFN1a **(A)** and sgFN1b **(B)**. FN1-KO was also confirmed by immunofluorescence staining for fibronectin in the dECMs deposited by normal cells (normal ECM) and Cas9-sgFN1a/b transduced cells (sgFN1a ECM and sgFN1b ECM, respectively) **(C)**.

Impact of dECMs Deposited by FN1-KO Cells on IPFSCs in Proliferation and Stemness

In order to determine the influence of FN(–) matrix microenvironment on IPFSCs' proliferation, we compared passage 15 IPFSCs grown on sgFN1a ECM, sgFN1b ECM, copGFP ECM, and TCP. We found that all dECM groups exhibited higher cell increase (**Figure 5A**) and percentage of cells in the S and G_2 phases (**Figure 5B**). Compared to the copGFP ECM group, a decline in cell growth and percentage of

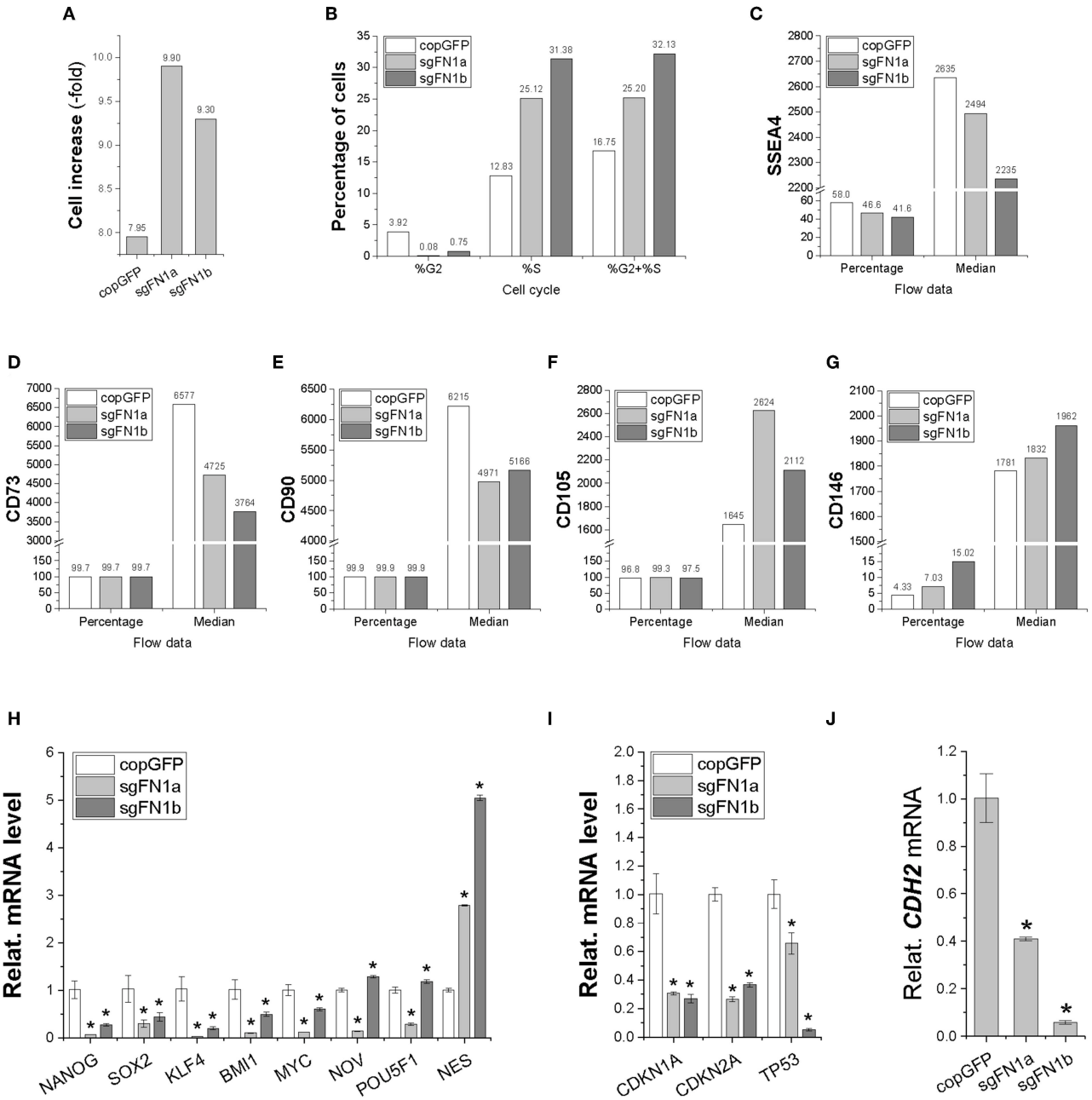

FIGURE 2 | Cell proliferation capacity in human IPFSCs after FN1-KO. FN1-KO cells were compared with copGFP in cell increase **(A)**, percentage of cells in the S and G_2 phases **(B)**, and surface markers [SSEA4 **(C)**, CD73 **(D)**, CD90 **(E)**, CD105 **(F)**, and CD146 **(G)**] by flow cytometry; stemness genes (*NANOG*, *SOX2*, *KLF4*, *BMI1*, *MYC*, *NOV*, *POU5F1*, and *NES*) **(H)**, senescent genes (*CDKN1A*, *CDKN2A*, and *TP53*) **(I)**, and the mesenchymal condensation gene (*CDH2*) **(J)** by qPCR. *GAPDH* was used as an endogenous control. Data are shown as bar charts. * indicates a significant difference compared to the corresponding copGFP group ($P < 0.05$).

cells in the S and G_2 phases was observed in the dECM groups deposited by FN1-KO IPFSCs. Our flow cytometry data also showed that, compared to the TCP group, all dECM-expanded cells exhibited increased expression of SSEA4 (**Figure 5C**) in both percentage and median but decreased expression of CD73 (**Figure 5D**) and CD90 (**Figure 5E**) in median and CD105 (**Figure 5F**) in both percentage and median, which were further strengthened in those grown on dECMs deposited by FN1-KO cells (**Figures 5C–F**).

To determine the effect of FN(–) matrix microenvironment on high passage IPFSCs' stemness, our qPCR data showed that, despite a dramatic up-regulation of all tested stemness genes including *NANOG*, *SOX2*, *KLF4*, *BMI1*, *MYC*, *NOV*, *POU5F1*, and *NES* in human IPFSCs grown on copGFP ECM

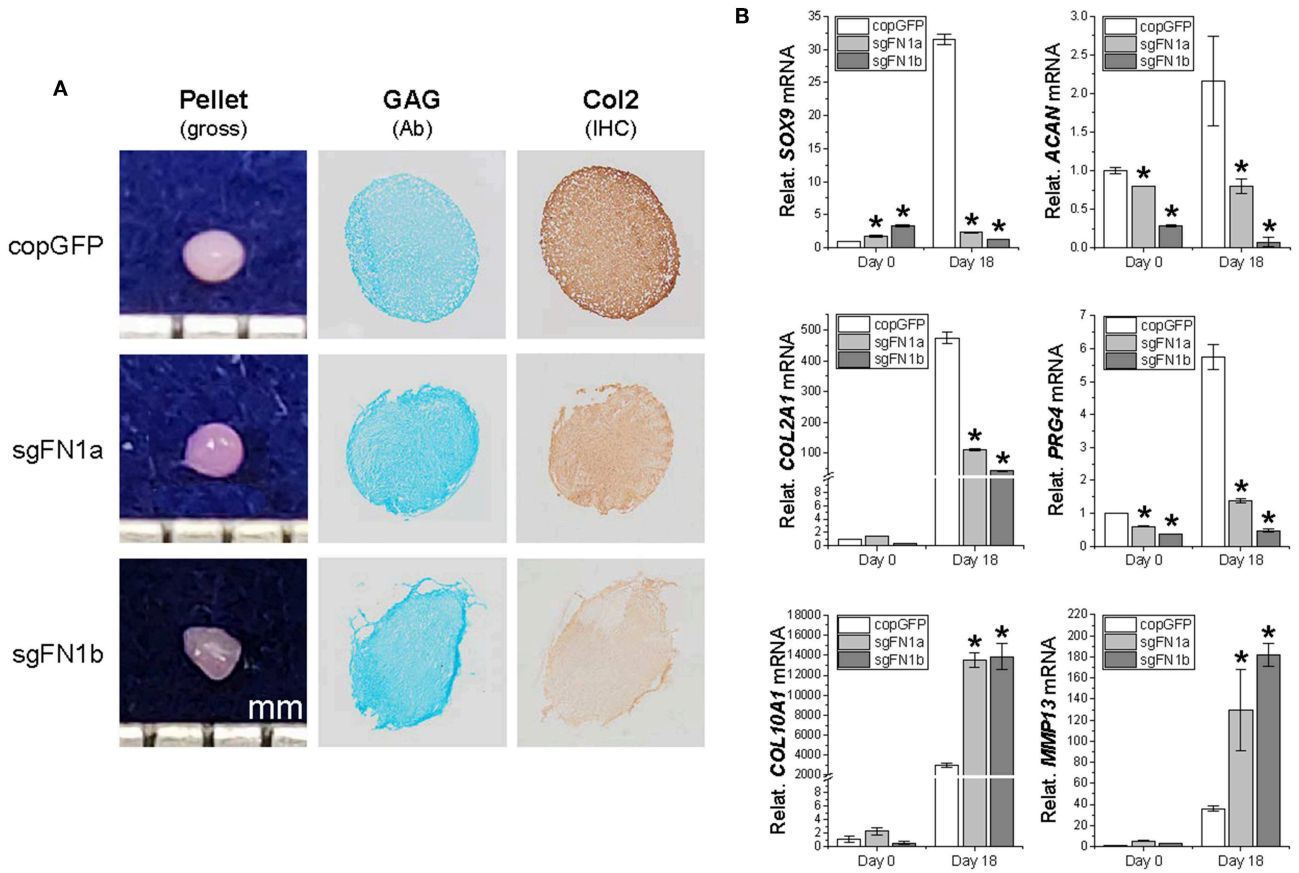

FIGURE 3 | Chondrogenic potential of human IPFSCs after FN1-KO. Human IPFSCs were chondrogenically induced in a pellet culture system for 18 days. The effect of fibronectin on chondrogenic capacity of human IPFSCs was evaluated using gross observation of 18-day pellets, Alcian blue staining (Ab) for sulfated GAGs and immunohistochemical staining (IHC) for type II collagen (Col2) **(A)**. qPCR was used to evaluate expression of chondrogenic marker genes (*SOX9*, *ACAN*, *COL2A1*, and *PRG4*) and hypertrophic marker genes (*COL10A1* and *MMP13*) **(B)**. *GAPDH* was used as an endogenous control. Data are shown as bar charts. *indicates a significant difference compared to the corresponding copGFP group ($P < 0.05$).

compared to TCP, up-regulation of most stemness genes was diminished in IPFSCs after expansion on dECMs deposited by FN1-KO IPFSCs (**Figure 5G**). Interestingly, the FN(–) matrix microenvironment yielded expanded IPFSCs with higher expression of *CDKN2A* and *TP53*, but lower expression of *CDKN1A* (**Figure 5H**). Not surprisingly, compared to those grown on TCP, expansion on copGFP ECM yielded IPFSCs with up-regulation of *CDH2* expression; however, dECMs deposited by FN1-KO cells produced expanded cells with significantly lowered expression of *CDH2* (**Figure 5I**).

Effects of dECMs Deposited by FN1-KO Cells on IPFSCs in Chondrogenic and Adipogenic Differentiation

We next wondered whether the FN(–) matrix microenvironment played a negative role in determining IPFSCs' differentiation preference. After chondrogenic induction, high passage IPFSCs grown on copGFP ECM yielded 18-day pellets with a larger size and more intensive staining of Alcian blue for sulfated GAGs and of IHC of type II collagen compared to those plated on TCP; however, this advantage of dECM expansion was diminished when high passage IPFSCs were expanded on dECMs deposited by FN1-KO cells (**Figure 6A**). These histological findings were supported by qPCR results showing that expansion on copGFP ECM yielded 18-day pellets with significantly higher expression of chondrogenic markers *SOX9*, *ACAN*, *COL2A1*, and *PRG4* as well as hypertrophic markers *COL10A1* and *MMP13*. However, expansion on dECMs deposited by FN1-KO cells yielded 18-day pellets with declining expression of these marker genes, particularly for the dECM deposited by Cas9-sgFN1b transduced cells (**Figure 6B**).

After adipogenic induction, we found that, compared to the TCP group, expansion on copGFP ECM yielded IPFSCs with less intensive staining of Oil Red O for lipid droplets, which further decreased if IPFSCs were pre-grown on dECMs deposited by FN1-KO cells (**Figure 7A**). This finding was consistent with qPCR data, in which expansion on TCP yielded IPFSCs with the highest expression of adipogenic marker genes *LPL*, *PPARG*, *FABP4*, and *CEBPA* after induction followed by expansion on

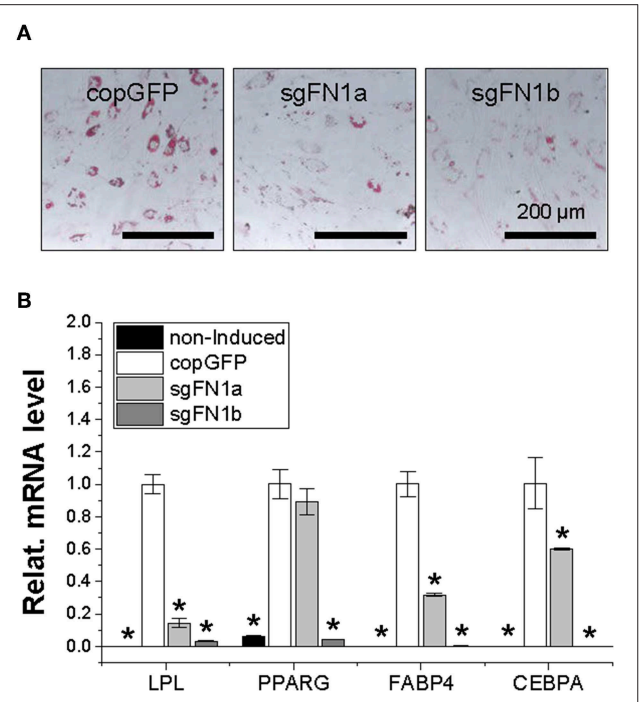

FIGURE 4 | Adipogenic potential of human IPFSCs after FN1-KO. Human IPFSCs were adipogenically induced in differentiation medium for 21 days. The effect of FN1-KO on adipogenic capacity of human IPFSCs was evaluated using Oil Red O staining for liquid droplets **(A)** and qPCR for adipogenic marker gene (*LPL*, *PPARG*, *FABP4*, and *CEBPA*) expression **(B)**. *GAPDH* was used as an endogenous control. Data are shown as bar charts. *indicates a significant difference compared to the corresponding copGFP group ($P < 0.05$).

copGFP ECM with the least expression in dECMs deposited by FN1-KO cells, particularly for the dECM deposited by Cas9-sgFN1b transduced cells (**Figure 7B**).

DISCUSSION

In this study, we used CRISPR/Cas9 technology to investigate the role of fibronectin in IPFSCs' proliferation and chondrogenic/adipogenic differentiation *via* direct FN1-KO in IPFSCs and indirect growth on dECMs deposited by FN1-KO IPFSCs. We found that FN1-KO increased IPFSCs' proliferation but decreased the proliferation of high passage IPFSCs grown on FN(–) dECM. Furthermore, FN1-KO had a negative effect on chondrogenic and adipogenic differentiation of IPFSCs, which was also reflected in high passage IPFSCs grown on FN(–) dECM.

The effect of fibronectin on stem cell proliferation remains controversial. Song et al. reported no effect of fibronectin on human BMSCs (Song et al., 2008); however, others reported that fibronectin promotes stem cell proliferation (Kalkreuth et al., 2014; Tao et al., 2018). In our study, we found that FN1-KO increased IPFSCs' proliferation, which was accompanied by up-regulation of CD105 and CD146 and down-regulation of senescence-associated genes. CD146, a putative surface marker of MSCs, is negatively linked with cellular senescence. For instance, CD146 expression was dramatically decreased in human umbilical cord blood-derived MSCs (UCB-MSCs) after long-term *in vitro* expansion; human UCB-MSCs with high CD146 expression exhibited a high rate of growth and telomerase activity as well as a notably lower expression of p16, p21, and p53 (Jin et al., 2016). Intriguingly, FN1-KO down-regulated most stemness genes except *NOV*, *POU5F1*, and *NES* in human IPFSCs. Interestingly, despite an increase of cell growth and percentage of cells in the S and G_2 phases and SSEA4 expression in all dECM groups, expansion on dECMs deposited by FN1-KO cells yielded IPFSCs with decreased cell growth and cell cycling. Similar to previous reports (Zhang et al., 2015a,b; Pizzute et al., 2016), dECM expansion decreased expression of CD73, CD90, and CD105 in IPFSCs, which was strengthened in the sgFN1b ECM group. We also found that, compared to the TCP group, expansion on dECM deposited by copGFP cells exhibited the highest levels of stemness gene expression, which were diminished if grown on dECMs deposited by FN1-KO cells including *POU5F1* and *NES*. Interestingly, *CDKN2A* and *TP53* were up-regulated in IPFSCs after expansion on dECMs deposited by FN1-KO cells. Since few reports are available on interpretation of the interconnection among stem cells and surface markers and stemness gene expression, more research is needed to clarify the correlation.

Fibronectin promoted chondrogenic differentiation of mouse chondrogenic progenitor cells when fibronectin was included in the culture medium (Tao et al., 2018) and of human embryonic stem cells when cells were cultured on fibronectin type III domain-coated substrates (Cheng et al., 2018). Fibronectin matrix assembly was reported to be critical for cell condensation during chondrogenesis (Singh and Schwarzbauer, 2014). Given that fibronectin treatment could significantly decrease *COL10A1* and *MMP13* expression (Tao et al., 2018), it is reasonable to detect a dramatic increase of these two hypertrophic marker gene levels in FN1-KO IPFSCs. Considering that CDH2, a mesenchymal condensation marker, could enhance stem cell aggregation and subsequent chondrogenic differentiation (Goldring et al., 2006), decreased expression of *CDH2* in FN1-KO IPFSCs in our study might be responsible for the down-regulation of chondrogenic markers and incomplete surface of chondrogenic pellets.

In accord with previous reports (Pei, 2017), dECM-expanded high passage IPFSCs exhibited an enhanced chondrogenic differentiation, perhaps due to the sequestration of TGFβ in ECM (Horiguchi et al., 2012), which promoted dECM-expanded IPFSCs' stemness and amplified TGFβ-mediated chondrogenesis (Pei et al., 2011b). Similar to the appearance of pellets from FN1-KO IPFSCs, we found a rough exterior in the pellets of IPFSCs grown on dECMs deposited by FN1-KO cells, suggesting that human IPFSCs' differentiation preference is markedly influenced by FN(–) matrix microenvironment. It was found that deletion of fibronectin from young generating muscles reproduced the aging phenotype (Lukjanenko et al., 2016). Since a young environment contributed to an improved revitalization effect on aged progenitor cells (Conboy et al., 2005), it is reasonable to speculate a compromised rejuvenation effect of dECM resulted from FN1-KO related

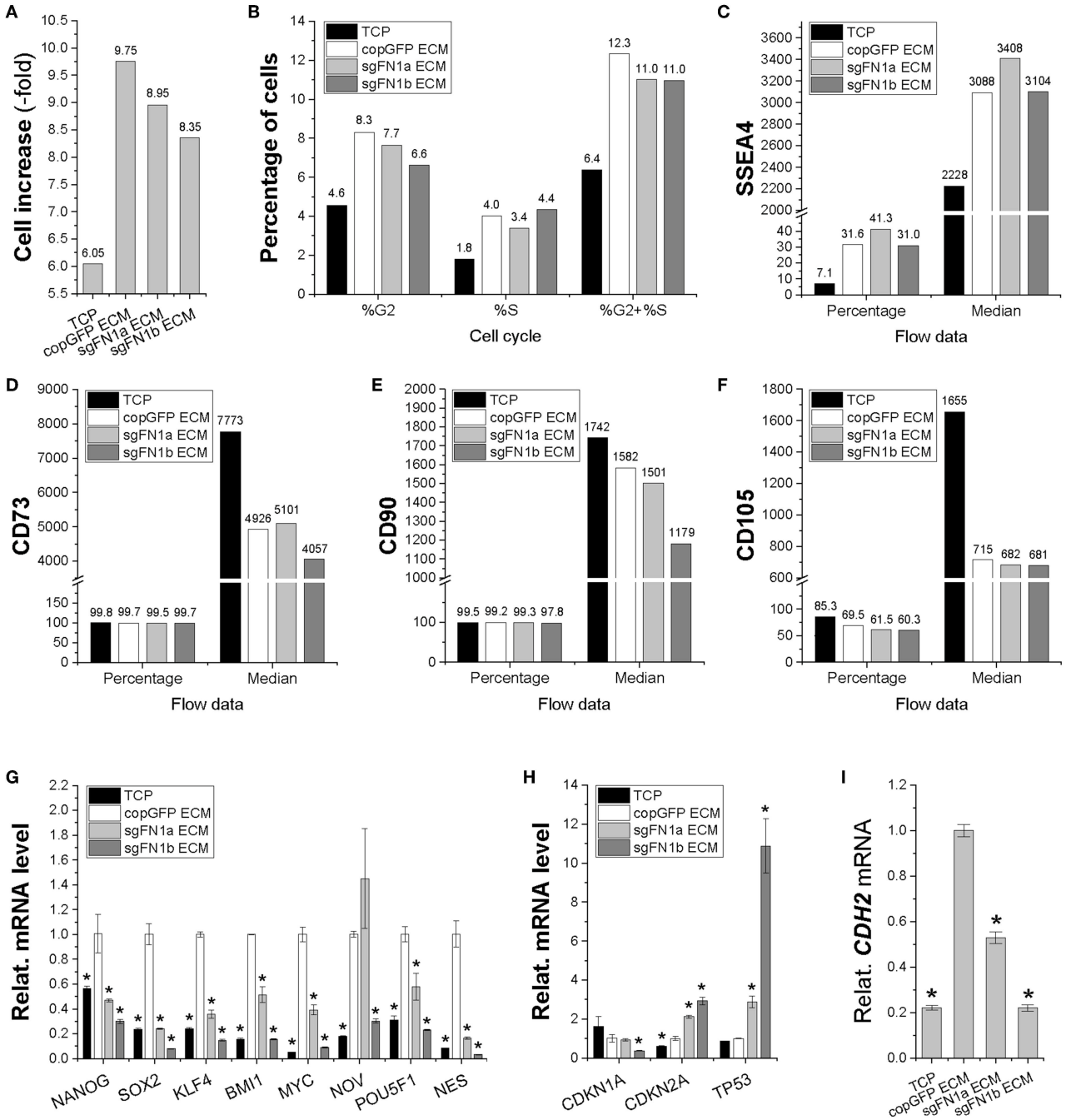

FIGURE 5 | Proliferation capacity of human IPFSCs after expansion on the dECMs deposited by FN1-KO cells. Passage 15 human IPFSCs were compared after expansion on dECMs deposited by Cas9-sgFN1a/b transduced cells (sgFN1a ECM and sgFN1b ECM, respectively) with those deposited by copGFP (copGFP ECM) and those grown on TCP (TCP) as controls in cell increase **(A)**, percentage of cells in the S and G_2 phases **(B)**, and surface markers [SSEA4 **(C)**, CD73 **(D)**, CD90 **(E)**, and CD105 **(F)**] by flow cytometry; stemness genes (*NANOG*, *SOX2*, *KLF4*, *BMI1*, *MYC*, *NOV*, *POU5F1*, and *NES*) **(G)**, senescence genes (*CDKN1A*, *CDKN2A*, and *TP53*) **(H)**, and the mesenchymal condensation gene (*CDH2*) **(I)** by qPCR. *GAPDH* was used as an endogenous control. Data are shown as bar charts. *indicates a significant difference compared to the corresponding copGFP group ($P < 0.05$).

cell aging. Interestingly, inconsistent with up-regulated expression of hypertrophic markers in FN1-KO cells, IPFSCs plated on dECMs deposited by FN1-KO cells exhibited a down-regulated expression of hypertrophic marker genes. The underlying mechanisms remain unknown and deserve further investigation.

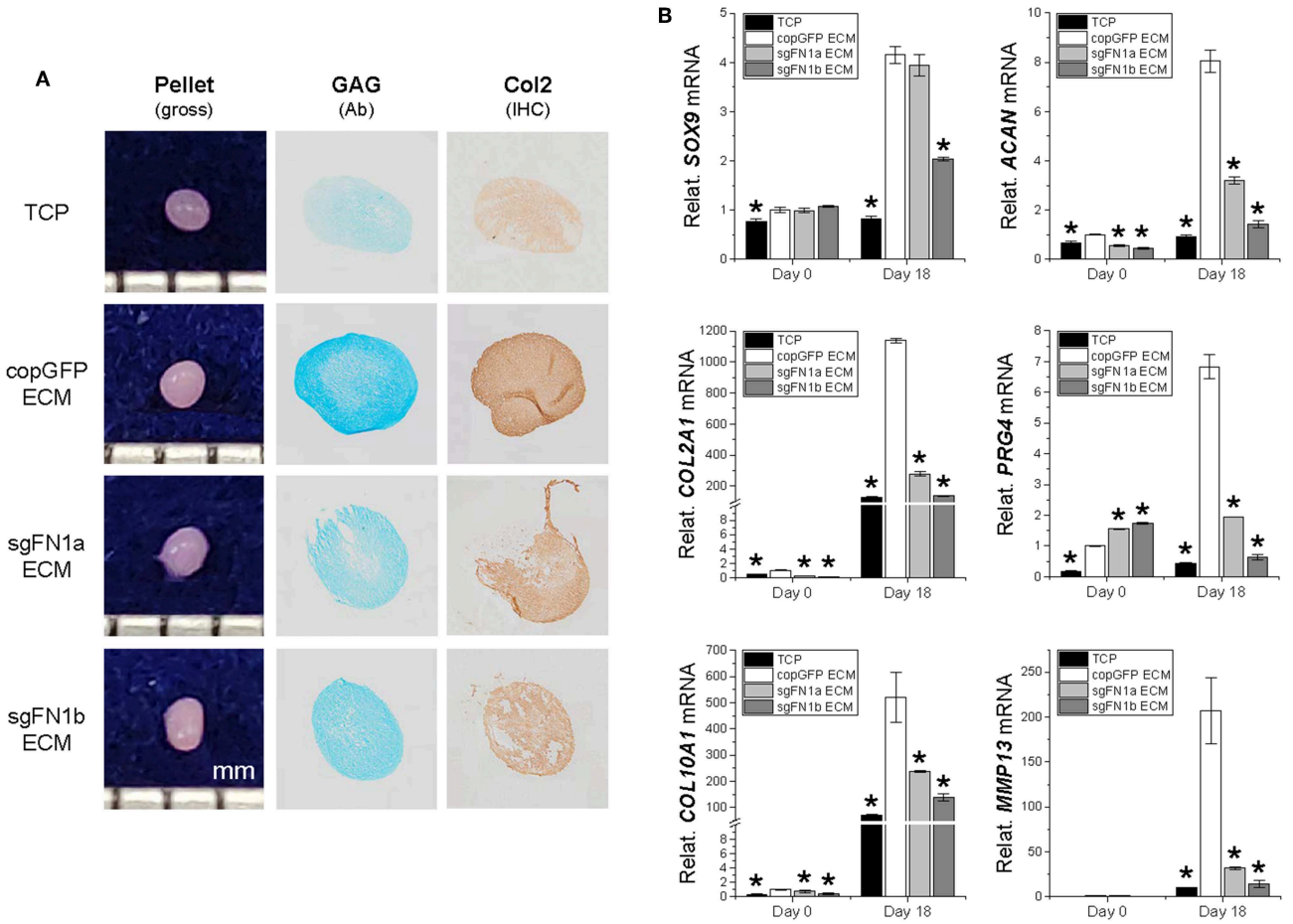

FIGURE 6 | Chondrogenic potential of human IPFSCs after expansion on dECMs deposited by FN1-KO cells. Passage 15 human IPFSCs in a pellet culture system were compared for chondrogenic capacity after expansion on dECMs deposited by Cas9-sgFN1a/b transduced cells (sgFN1a ECM and sgFN1b ECM, respectively) with those deposited by copGFP (copGFP ECM) and those grown on TCP (TCP) as controls including gross observation of 18-day pellets, Alcian blue staining (Ab) for sulfated GAGs, and IHC for type II collagen (Col2) **(A)**. qPCR was used to evaluate expression of chondrogenic marker genes (*SOX9*, *ACAN*, *COL2A1*, and *PRG4*) and hypertrophic marker genes (*COL10A1* and *MMP13*) **(B)**. *GAPDH* was used as an endogenous control. Data are shown as bar charts. *indicates a significant difference compared to the corresponding copGFP group ($P < 0.05$).

Despite adipogenesis being marked by a transformation from the fibronectin-rich stromal matrix (types I and III collagen, β1-integrin, and fibronectin) of the preadipocytes to the basement membrane (type IV collagen and entactin) of mature adipocytes (Gregoire et al., 1998; Selvarajan et al., 2001), we found that human IPFSCs after FN1-KO exhibited a dramatic decrease of adipogenic differentiation, as evidenced by Oil Red O staining for lipid droplets and qPCR for adipogenic marker genes, particularly for Cas9-sgFN1b transduced cells. This finding might be explained by the lack of fibronectin in human IPFSCs causing the failure of fibronectin fibrillogenesis, which is one of the crucial determinants for adipogenesis (Kamiya et al., 2002).

Many reports evaluated the effect of fibronectin on adipogenesis by using a fibronectin-coated surface or supplementing with fibronectin in the culture medium. For example, growth on fibronectin matrices inhibited adipogenesis of 3T3-F442A cells, which could be reversed by exposure to cytochalasin D that disrupted the actin cytoskeleton (Spiegelman and Ginty, 1983). Fukai et al. found that the addition of rat plasma fibronectin inhibited adipogenic differentiation of ST-13 preadipocytes; however, the thermolysin digest of fibronectin promoted adipocyte differentiation (Fukai et al., 1993). Considering potential sequestration and concentration of latent TGFβ by interaction with specific ECM components for future activation (Horiguchi et al., 2012), it seems reasonable that, compared to TCP culture, dECM expansion decreased IPFSCs' adipogenic differentiation because TGFβ is a potent inhibitor of adipogenic differentiation through promoting ECM synthesis including fibronectin (Gagnon et al., 1998). In this study, we also found that this unfavorable effect of dECM on adipogenic differentiation was further strengthened if dECMs

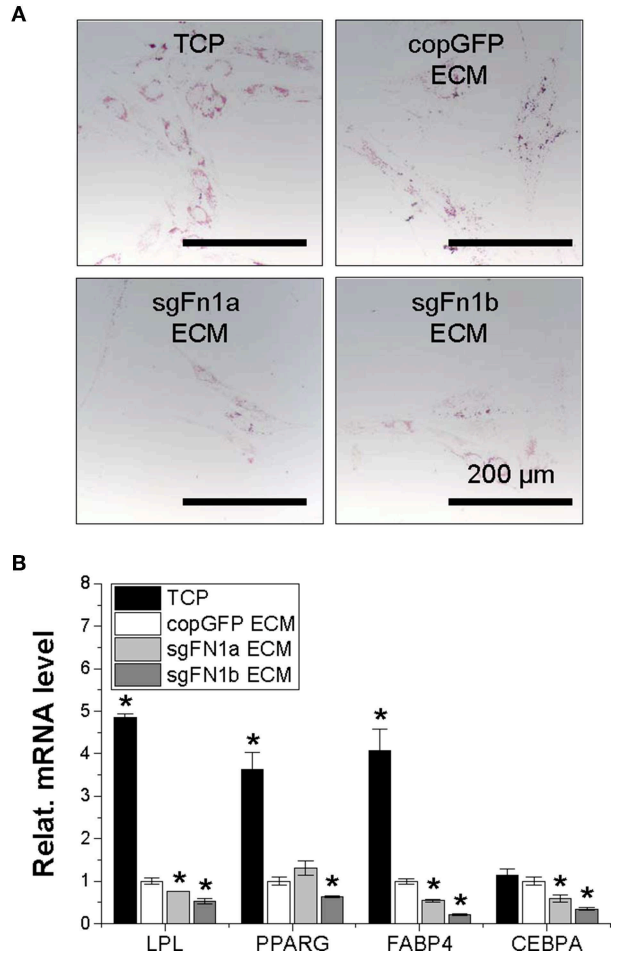

FIGURE 7 | Adipogenic potential of human IPFSCs after expansion on dECMs deposited by FN1-KO cells. Human IPFSCs were compared for adipogenic capacity after expansion on dECMs deposited by Cas9-sgFN1a/b transduced cells (sgFN1a ECM and sgFN1b ECM, respectively) with those deposited by copGFP (copGFP ECM) and those grown on TCP (TCP) as controls including Oil Red O staining for lipid droplets **(A)** and qPCR for adipogenic marker gene (*LPL*, *PPARG*, *FABP4*, and *CEBPA*) expression **(B)**. *GAPDH* was used as an endogenous control. Data are shown as bar charts. *indicates a significant difference compared to the corresponding copGFP group ($P < 0.05$).

were deposited by FN-KO cells. This effect might be explained by the influence of FN(–) matrix microenvironment on expanded human IPFSCs *via* mirror characters.

In summary, FN1-KO increased human IPFSCs' proliferation capacity; however, this capacity was reversed after expansion on dECMs deposited by FN1-KO cells. The importance of fibronectin in chondrogenic and adipogenic differentiation was demonstrated in both FN1-KO IPFSCs and the FN(–) matrix microenvironment, which might lay the foundation for fibronectin-mediated tissue engineering and regeneration.

DATA AVAILABILITY STATEMENT

The raw data supporting the conclusions of this manuscript will be made available by the authors, without undue reservation, to any qualified researcher.

AUTHOR CONTRIBUTIONS

YW: conception and design, acquisition of data, analysis and interpretation of the data, drafting the article, and final approval of the article. YF: acquisition of data, analysis and interpretation of the data, revising the article, and final approval of the article. ZY and X-BZ: conception and design, revising the article, and final approval of the article. MP: conception and design, analysis and interpretation of the data, drafting and revising the article, final approval of the article, and obtaining the funding.

FUNDING

Research reported in this publication was supported by the National Institute of Arthritis and Musculoskeletal and Skin Diseases of the National Institutes of Health under Award Number (AR067747-01A1) and the Musculoskeletal Transplant Foundation to MP, the National Natural Science Foundation of China (81871742) and Joint Project of Innovating Technology from Shanghai Shenkang Hospital Developing Center (SHDC12017107) to ZY, and the Loma Linda University School of Medicine GCAT grant (2017) to X-BZ. We also would like to acknowledge the WVU Flow Cytometry & Single Cell Core Facility and the grants that support the facility, TME CoBRE grant P20GM131322, and the WV CTS grant GM104942.

ACKNOWLEDGMENTS

We thank Suzanne Danley for editing the manuscript and Dr. Gerald Hobbs for assistance with statistics.

REFERENCES

Benedek, T. G. (2006). A history of the understanding of cartilage. *Osteoarthr. Cartil.* 14, 203–209. doi: 10.1016/j.joca.2005.08.014

Budd, J. S., Allen, K. E., Bell, P. R., and James, R. F. (1990). The effect of varying fibronectin concentration on the attachment of endothelial cells to polytetrafluoroethylene vascular grafts. *J. Vasc. Surg.* 12, 126–130. doi: 10.1016/0741-5214(90)90100-O

Chang, C. F., Hsu, K. H., Chiou, S. H., Ho, L. L., Fu, Y. S., and Hung, S. C. (2008). Fibronectin and pellet suspension culture promote differentiation of human mesenchymal stem cells into insulin producing cells. *J. Biomed. Mater. Res. Part A* 86, 1097–1105. doi: 10.1002/jbm.a.31767

Cheng, A., Cain, S. A., Tian, P., Baldwin, A. K., Uppanan, P., Kielty, C. M., et al. (2018). Recombinant extracellular matrix protein fragments support human embryonic stem cell chondrogenesis. *Tissue Eng. Part A* 24, 968–978. doi: 10.1089/ten.tea.2017.0285

Conboy, I. M., Conboy, M. J., Wagers, A. J., Girma, E. R., Weissman, I. L., and Rando, T. A. (2005). Rejuvenation of aged progenitor cells by exposure to a young systemic environment. *Nature* 433, 760–764. doi: 10.1038/nature 03260

Friedenstein, A. J., Gorskaja, J. F., and Kulagina, N. N. (1976). Fibroblast precursors in normal and irradiated mouse hematopoietic organs. *Exp. Hematol*. 4, 267–274.

Fukai, F., Iso, T., Sekiguchi, K., Miyatake, N., Tsugita, A., and Katayama, T. (1993). An amino-terminal fibronectin fragment stimulates the differentiation of ST-13 preadipocytes. *Biochemistry* 32, 5746–5751. doi: 10.1021/bi00073a004

Gagnon, A. M., Chabot, J., Pardasani, D., and Sorisky, A. (1998). Extracellular matrix induced by TGFbeta impairs insulin signal transduction in 3T3-L1 preadipose cells. *J. Cell Physiol.* 175, 370–378. doi: 10.1002/(SICI)1097-4652(199806)175:3<370::AID-JCP15>3.0.CO;2-9

Goldring, M. B., Tsuchimochi, K., and Ijiri, K. (2006). The control of chondrogenesis. *J. Cell Biochem*. 97, 33–44. doi: 10.1002/jcb.20652

Gregoire, F. M., Smas, C. M., and Sul, H. S. (1998). Understanding adipocyte differentiation. *Physiol. Rev*. 78, 783–809. doi: 10.1152/physrev.1998.78.3.783

He, F., and Pei, M. (2013). Extracellular matrix enhances differentiation of adipose stem cells from infrapatellar fat pad toward chondrogenesis. *J. Tissue Eng. Regen. Med*. 7, 73–84. doi: 10.1002/term.505

Hindle, P., Khan, N., Biant, L., and Péault, B. (2017). The infrapatellar fat pad as a source of perivascular stem cells with increased chondrogenic potential for regenerative medicine. *Stem Cells Transl. Med*. 6, 77–87. doi: 10.5966/sctm.2016-0040

Horiguchi, M., Ota, M., and Rifkin, D. B. (2012). Matrix control of transforming growth factor-β function. *J. Biochem*. 152, 321–329. doi: 10.1093/jb/mvs089

Jin, H. J., Kwon, J. H., Kim, M., Bae, Y. K., Choi, S. J., Oh, W., et al. (2016). Downregulation of melanoma cell adhesion molecule (MCAM/CD146) accelerates cellular senescence in human umbilical cord blood-derived mesenchymal stem cells. *Stem Cells Transl. Med*. 5, 427–439. doi: 10.5966/sctm.2015-0109

Jones, B. A., and Pei, M. (2012). Synovium-derived stem cells: a tissue-specific stem cell for cartilage tissue engineering and regeneration. *Tissue Eng. Part B Rev*. 18, 301–311. doi: 10.1089/ten.teb.2012.0002

Kalkreuth, R. H., Krüger, J. P., Lau, S., Niemeyer, P., Endres, M., Kreuz, P. C., et al. (2014). Fibronectin stimulates migration and proliferation, but not chondrogenic differentiation of human subchondral progenitor cells. *Regen. Med*. 9, 759–773. doi: 10.2217/rme.14.40

Kamiya, S., Kato, R., Wakabayashi, M., Tohyama, T., Enami, I., Ueki, M., et al. (2002). Fibronectin peptides derived from two distinct regions stimulate adipocyte differentiation by preventing fibronectin matrix assembly. *Biochemistry* 41, 3270–3277. doi: 10.1021/bi015660a

Karnes, J., Zhang, Y., and Pei, M. (2014). "Cell therapy for the creation of cartilage and related clinical trials," in *Gene and Cell Therapy: Therapeutic Mechanisms and Strategies, 4th Edn*, ed N. S. Templeton (Taylor & Francis/CRC Press), 1123–1135. doi: 10.1201/b18002-53

Li, J., Hansen, K. C., Zhang, Y., Dong, C., Dinu, C. Z., Dzieciatkowska, M., et al. (2014). Rejuvenation of chondrogenic potential by young stem cell microenvironment. *Biomaterials* 35, 642–653. doi: 10.1016/j.biomaterials.2013.09.099

Li, J., and Pei, M. (2012). Cell senescence: a challenge in cartilage engineering and regeneration. *Tissue Eng. Part B* 18, 270–287. doi: 10.1089/ten.teb.2011.0583

Li, J., and Pei, M. (2018). A protocol to prepare decellularized stem cell matrix for rejuvenation of cell expansion and cartilage regeneration. *Methods Mol. Biol*. 1577, 147–154. doi: 10.1007/7651_2017_27

Li, X. L., Li, G. H., Fu, J., Fu, Y. W., Zhang, L., Chen, W., et al. (2018). Highly efficient genome editing via CRISPR-Cas9 in human pluripotent stem cells is achieved by transient BCL-XL overexpression. *Nucleic Acids Res*. 46, 10195–10215. doi: 10.1093/nar/gky804

Linask, K. K., and Lash, J. W. (1988). A role for fibronectin in the migration of avian precardiac cells. I. Dose-dependent effects of fibronectin antibody. *Dev. Biol*. 129, 315–323. doi: 10.1016/0012-1606(88)90378-8

Liu, K., Cheng, L., Flesken-Nikitin, A., Huang, L., Nikitin, A. Y., and Pauli, B. U. (2010). Conditional knockout of fibronectin abrogates mouse mammary gland lobuloalveolar differentiation. *Dev. Biol*. 346, 11–24. doi: 10.1016/j.ydbio.2010.07.001

Liu, Y., Buckley, C. T., Almeida, H. V., Mulhall, K. J., and Kelly, D. J. (2014). Infrapatellar fat pad-derived stem cells maintain their chondrogenic capacity in disease and can be used to engineer cartilaginous grafts of clinically relevant dimensions. *Tissue Eng. Part A* 20, 3050–3062. doi: 10.1089/ten.tea.2014.0035

Lukjanenko, L., Jung, M. J., Hegde, N., Perruisseau-Carrier, C., Migliavacca, E., Rozo, M., et al. (2016). Loss of fibronectin from the aged stem cell niche affects the regenerative capacity of skeletal muscle in mice. *Nat. Med*. 22, 897–905. doi: 10.1038/nm.4126

Lynch, K., and Pei, M. (2014). Age associated communication between cells and matrix: a potential impact on stem cell-based tissue regeneration strategies. *Organogenesis* 10, 289–298. doi: 10.4161/15476278.2014.970089

Pei, M. (2017). Environmental preconditioning rejuvenates stem cells' chondrogenic potential. *Biomaterials* 117, 10–23. doi: 10.1016/j.biomaterials.2016.11.049

Pei, M., He, F., and Kish, V. L. (2011a). Expansion on extracellular matrix deposited by human bone marrow stromal cells facilitates stem cell proliferation and tissue-specific lineage potential. *Tissue Eng. Part A* 17, 3067–3076. doi: 10.1089/ten.tea.2011.0158

Pei, M., Li, J. T., Shoukry, M., and Zhang, Y. (2011b). A review of decellularized stem cell matrix: a novel cell expansion system for cartilage tissue engineering. *Eur. Cell Mater*. 22, 333–343. doi: 10.22203/eCM.v022a25

Pizzute, T., Lynch, K., and Pei, M. (2015). Impact of tissue-specific stem cells on lineage specific differentiation: a focus on musculoskeletal system. *Stem Cell Rev. Rep*. 11, 119–132. doi: 10.1007/s12015-014-9546-8

Pizzute, T., Zhang, Y., He, F., and Pei, M. (2016). Ascorbate-dependent impact on cell-derived matrix in modulation of stiffness and rejuvenation of infrapatellar fat derived stem cells toward chondrogenesis. *Biomed. Mater*. 11:045009. doi: 10.1088/1748-6041/11/4/045009

Sapudom, J., Rubner, S., Martin, S., Thoenes, S., Anderegg, U., and Pompe, T. (2015). The interplay of fibronectin functionalization and TGF-beta1 presence on fibroblast proliferation, differentiation and migration in 3D matrices. *Biomater. Sci*. 3, 1291–1301. doi: 10.1039/C5BM00140D

Selvarajan, S., Lund, L. R., Takeuchi, T., Craik, C. S., and Werb, Z. (2001). A plasma kallikrein-dependent plasminogen cascade required for adipocyte differentiation. *Nat. Cell Biol*. 3, 267–275. doi: 10.1038/35060059

Singh, P., and Schwarzbauer, J. E. (2014). Fibronectin matrix assembly is essential for cell condensation during chondrogenesis. *J. Cell Sci*. 127, 4420–4428. doi: 10.1242/jcs.150276

Song, G., Ju, Y., and Soyama, H. (2008). Growth and proliferation of bone marrow mesenchymal stem cells affected by type I collagen, fibronectin and bFGF. *Mater. Sci. Eng. C* 28, 1467–1471. doi: 10.1016/j.msec.2008.04.005

Spiegelman, B. M., and Ginty, C. A. (1983). Fibronectin modulation of cell shape and lipogenic gene expression in 3T3-adipocytes. *Cell* 35, 657–666. doi: 10.1016/0092-8674(83)90098-3

Sun, Y., Chen, S., and Pei, M. (2018a). Comparative advantage of infrapatellar fat pad: an emerging stem cell source for regeneration medicine. *Rheumatology* 57, 2072–2086. doi: 10.1093/rheumatology/kex487

Sun, Y., Yan, L., Chen, S., and Pei, M. (2018b). Functionality of decellularized matrix in cartilage regeneration: a comparison of tissue versus cell sources. *Acta Biomaterialia* 74, 56–73. doi: 10.1016/j.actbio.2018.04.048

Tao, T., Li, Y., Gui, C., Ma, Y., Ge, Y., Dai, H., et al. (2018). Fibronectin enhances cartilage repair by activating progenitor cells through integrin α5β1 receptor. *Tissue Eng. Part A* 24, 1112–1124. doi: 10.1089/ten.tea.2017.0322

Zhang, J. P., Li, X. L., Li, G. H., Chen, W., Arakaki, C., Botimer, G. D., et al. (2017). Efficient precise knockin with a double cut HDR donor after CRISPR/Cas9-mediated double-stranded DNA cleavage. *Genome Biol*. 18:35. doi: 10.1186/s13059-017-1164-8

Zhang, J. P., Li, X. L., Neises, A., Chen, W., Hu, L. P., Ji, G. Z., et al. (2016). Different effects of sgRNA length on CRISPR-mediated gene knockout efficiency. *Sci. Rep*. 6:28566. doi: 10.1038/srep28566

Zhang, Y., Li, J., Davis, M. E., and Pei, M. (2015a). Delineation of in vitro chondrogenesis of human synovial stem cells following

preconditioning using decellularized matrix. *Acta Biomaterialia* 20, 39–50. doi: 10.1016/j.actbio.2015.04.001

Zhang, Y., Pizzute, T., Li, J., He, F., and Pei, M. (2015b). sb203580 preconditioning recharges matrix-expanded human adult stem cells for chondrogenesis in an inflammatory environment – a feasible approach for autologous stem cell based osteoarthritic cartilage repair. *Biomaterials* 64, 88–97. doi: 10.1016/j.biomaterials.2015.06.038

Zhou, S., Chen, S., Jiang, Q., and Pei, M. (2019). Determinants of stem cell lineage differentiation toward chondrogenesis versus adipogenesis. *Cell Mol. Life Sci.* 76, 1653–1680. doi: 10.1007/s00018-019-03017-4

Conflict of Interest: The authors declare that the research was conducted in the absence of any commercial or financial relationships that could be construed as a potential conflict of interest.

frontiers in Bioengineering and Biotechnology

REVIEW
published: 27 November 2019
doi: 10.3389/fbioe.2019.00352

Mesenchymal Stromal Cell-Based Bone Regeneration Therapies: From Cell Transplantation and Tissue Engineering to Therapeutic Secretomes and Extracellular Vesicles

Darja Marolt Presen[1,2]*, *Andreas Traweger*[2,3], *Mario Gimona*[4] and *Heinz Redl*[1,2]

[1] Ludwig Boltzmann Institute for Experimental and Clinical Traumatology, AUVA Research Center, Vienna, Austria, [2] Austrian Cluster for Tissue Regeneration, Vienna, Austria, [3] Spinal Cord Injury & Tissue Regeneration Center Salzburg, Institute of Tendon and Bone Regeneration, Paracelsus Medical University, Salzburg, Austria, [4] GMP Unit, Spinal Cord Injury & Tissue Regeneration Center Salzburg, Paracelsus Medical University, Salzburg, Austria

OPEN ACCESS

Edited by:
Martin James Stoddart,
AO Research Institute, Switzerland

Reviewed by:
Antonio Salgado,
University of Minho, Portugal
Anna Lange-Consiglio,
University of Milan, Italy

***Correspondence:**
Darja Marolt Presen
darja.marolt@trauma.lbg.ac.at

Specialty section:
This article was submitted to Tissue Engineering and Regenerative Medicine, a section of the journal Frontiers in Bioengineering and Biotechnology

Received: 06 September 2019
Accepted: 06 November 2019
Published: 27 November 2019

Citation:
Marolt Presen D, Traweger A, Gimona M and Redl H (2019) Mesenchymal Stromal Cell-Based Bone Regeneration Therapies: From Cell Transplantation and Tissue Engineering to Therapeutic Secretomes and Extracellular Vesicles. Front. Bioeng. Biotechnol. 7:352. doi: 10.3389/fbioe.2019.00352

Effective regeneration of bone defects often presents significant challenges, particularly in patients with decreased tissue regeneration capacity due to extensive trauma, disease, and/or advanced age. A number of studies have focused on enhancing bone regeneration by applying mesenchymal stromal cells (MSCs) or MSC-based bone tissue engineering strategies. However, translation of these approaches from basic research findings to clinical use has been hampered by the limited understanding of MSC therapeutic actions and complexities, as well as costs related to the manufacturing, regulatory approval, and clinical use of living cells and engineered tissues. More recently, a shift from the view of MSCs directly contributing to tissue regeneration toward appreciating MSCs as "cell factories" that secrete a variety of bioactive molecules and extracellular vesicles with trophic and immunomodulatory activities has steered research into new MSC-based, "cell-free" therapeutic modalities. The current review recapitulates recent developments, challenges, and future perspectives of these various MSC-based bone tissue engineering and regeneration strategies.

Keywords: mesenchymal stromal cells, stem cells, MSCs, secretome, extracellular vesicles, cell therapy, bone tissue engineering, bone regeneration

INTRODUCTION

Regeneration of bone defects often presents significant challenges, particularly in patients with decreased tissue regeneration capacity due to extensive tissue damage, disease, advanced age, and confounding systemic and lifestyle factors (Gruber et al., 2006; Borrelli et al., 2012). Between 5 and 10% of all bone fractures, according to some reports even up to 50%, result in delayed or failed healing (Tzioupis and Giannoudis, 2007; Gómez-Barrena et al., 2015; Ekegren et al., 2018). To overcome these barriers, a number of research studies focused on enhancing bone regeneration by applying mesenchymal stromal cells (MSCs) derived from various connective tissues. *Ex vivo* processing and culture methods have been developed to obtain sufficient MSC numbers for therapy

(Schallmoser et al., 2009; Sensebé et al., 2013; Robey et al., 2015). Furthermore, MSCs have been combined with various scaffolds and signaling factors in order to tissue engineer viable "bone substitutes" recapitulating key features of autologous bone grafts and enhancing bone regeneration (Frohlich et al., 2008; Jakob et al., 2012). *In vitro* culture of these constructs in order to drive cell differentiation, bone-like matrix deposition, and increased mechanical properties has also been extensively studied (Marolt et al., 2006; Grayson et al., 2011; Bhumiratana et al., 2016; Vetsch et al., 2016; Mitra et al., 2017; Zhao et al., 2018). Recapitulation of mechanisms present during embryonic bone development was proposed as a "developmental (re)engineering" strategy for the preparation of intermediate grafts capable of forming fully functional bone (Jukes et al., 2008; Tonnarelli et al., 2014; Bernhard et al., 2017). Viable, large bone-like grafts in clinically relevant dimensions (several millimeters to centimeters in size) have been achieved using dynamic culture of scaffolds seeded with MSCs in bioreactors (Grayson et al., 2010, 2011; Güven et al., 2011; Sørensen et al., 2012; Bhumiratana et al., 2016). In addition, in some cases these grafts comprised rudimentary vascular networks. Bone marrow and adipose tissue MSCs were used in the majority of preclinical and clinical studies (Marolt et al., 2010; Robey, 2011; Grayson et al., 2015; Nancarrow-Lei et al., 2017) (**Table 1**). However, various other sources of MSCs have also been investigated, including skeletal muscle, bone, cartilage, tendon, dental pulp, perinatal tissues (e.g., Wharton's Jelly, umbilical vein/cord blood, amnion, placenta), embryonic stem cells and induced pluripotent stem cells. Due to the aging-related decline in tissue regeneration (Kassem and Marie, 2011; Marie, 2014; Baker et al., 2015; Bhattacharjee et al., 2019), involving both intra- as well as extra-cellular mechanisms, perinatal tissues and induced pluripotent stem cells have raised interest as potential sources of "young" MSCs with high regenerative properties (Kern et al., 2006; Baksh et al., 2007; Robey, 2011; De Peppo et al., 2013; Ghasemzadeh et al., 2018; Spitzhorn et al., 2019).

Despite this growing knowledge, the translation of MSC-based bone regeneration strategies from research studies to clinical use has been slow (Jakob et al., 2012; Grayson et al., 2015). Limited mechanistic understanding of MSC therapeutic actions and MSC fate following transplantation (Dupont et al., 2010; Manassero et al., 2016) has made the requirements for therapeutic preparations, such as optimal cell numbers, cell phenotype, maturity, and mechanical properties of tissue-engineered grafts difficult to define (Jakob et al., 2012; Oryan et al., 2017). Technical challenges and high costs related to manufacturing under good manufacturing practice (GMP) guidelines and procedures for regulatory approval of MSC therapies (e.g., under advanced therapy medicinal products (ATMP) classification) pose additional barriers for clinical translation (Sensebé et al., 2013). According to our recent search in one of the clinical trials databases (www.clinicaltrials.gov, July 2019, combinations of search terms "bone regeneration," "bone fracture," "alveolar bone," "maxilla," "osteonecrosis," and "stem cells"), a number of clinical trials (mostly phase I and I/II) employing MSCs to enhance bone regeneration have been registered. However, only for a few the research findings have been published (**Table 1**).

In recent years, a shift from the view of MSCs as being cells that directly contribute to new tissue formation toward seeing MSCs as "medicinal cell factories" that secrete a variety of bioactive molecules with trophic and immunomodulatory activities has steered the research into MSC secretome for bone regeneration (Hofer and Tuan, 2016; Caplan, 2017). MSCs also secrete various types of extracellular vesicles (EVs) which contain proteins, lipids, and nucleic acids with potential pro-regenerative properties (Marote et al., 2016; Börger et al., 2017; Turchinovich et al., 2019; van Balkom et al., 2019). Several recent studies in small animal models suggested the therapeutic potential of unfractionated MSC secretome as well as MSC-derived extracellular vesicles for bone regeneration (**Table 2**). In the current review, we recapitulate the recent developments in bone regeneration strategies employing MSC transplantation and MSC-based tissue engineering, as well as the use of MSC secretome and vesicular fractions (**Figure 1**). Finally, we discuss the challenges and future perspective of these various MSC-based bone regeneration strategies.

SOURCES AND CULTURE OF MSCs FOR BONE REGENERATION THERAPIES

According to a consensus position statement, the term MSCs is used to describe a population of multipotent mesenchymal stromal cells that: (1) can be isolated based on their ability to adhere and grow on tissue culture plastic surface, (2) exhibit a defined pattern of positive and negative surface markers, and (3) have the ability to undergo differentiation into osteogenic, chondrogenic, and adipogenic lineages under standard *in vitro* conditions (Dominici et al., 2006). The cells corresponding to this definition were initially isolated from the bone marrow (Friedenstein et al., 1987; Pittenger et al., 1999) and subsequently from many other fetal and adult tissues, including bone, adipose tissue, muscle, blood, dental pulp, placenta, amnion-amniotic fluid, umbilical cord/cord blood etc. (Sudo et al., 2007; Crisan et al., 2008). Importantly, the "stemness" of MSCs, i.e., their ability to self-renew *in vivo*, has only been shown for some MSC subpopulations from the bone marrow by serial transplantation assays (Sacchetti et al., 2007; Méndez-Ferrer et al., 2010). As a surrogate measure of stem cells present in cell preparations, a colony forming units (CFU) assay was commonly used (Robey, 2011) and this was suggested to correspond to the bone forming capacity *in vivo* (Braccini et al., 2007). Only recently, the identity of genuine, self-replicating skeletal stem cells has been described (Chan et al., 2018). Nevertheless, the possibility to relatively easily isolate, culture, and differentiate MSCs from various tissues, particularly those remaining as medical waste (e.g., lipoaspirate, perinatal tissues), has fueled the research into MSCs for bone regeneration therapies.

Abbreviations: ASCs, adipose stromal cells; ATMP, advanced therapy medicinal product; CFU, colony forming units; EV, extracellular vesicle; GMP, good manufacturing practice; hESCs, human embryonic stem cells; hiPSCs, human induced pluripotent stem cells; MNCs, mononuclear cells; MSCs, mesenchymal stromal cells; NO, nitric oxide; SVF, stromal vascular fraction; TE, tissue engineering.

TABLE 1 | Clinical studies using MSCs and isolated progenitors for bone regeneration.

Identifier	Phase	Completion	Condition	Cell type	Patients	Treatment groups	Masking	Main outcome (Reference)
SEARCH TERMS: "BONE FRACTURE, STEM CELLS"								
NCT03325504	III	Recruiting	Non-union	Autologous bone marrow MSCs (*in vitro* expanded)	Est. 108	Low dose stem cell application with biomaterial High dose stem cell application with biomaterial Control autologous bone graft	None	/
NCT02483364	II	Recruiting	Pseudoarthrosis	Autologous or allogeneic adipose MSCs	Est. 12	Allogeneic stem cell application with tricalcium phosphate Autologous stem cell application with tricalcium phosphate	None	/
NCT02815423	I/II	Not yet recruiting	Non-union	Umbilical cord MSCs	Est. 40	Stem cell injection Control placebo injection	None	/
NCT01842477	I/II	February 2016	Delayed union Non-union	Autologous bone marrow MSCs (cultured)	30	Application of stem cells with bone substitute	None	No severe adverse events and 26/28 treated patients radiologically healed at 1 year (Gómez-Barrena et al., 2019)
NCT01813188	II	December 2013	Pseudoarthrosis	Autologous bone marrow MNCs	5	Application of cells seeded on tricalcium phosphate	None	/
NCT01788059	II	November 2013	Non-union	Autologous bone marrow MSCs (Ficoll separated)	19	Stem cell injection	None	/
NCT01581892	I/II	January 2013	Non-union	Autologous bone marrow MNCs (Ficoll separated)	7	Stem cell injection	None	/
NCT02177565	NA	October 2011	Non-union	Autologous bone marrow MSCs (*in vitro* expanded)	35	Stem cell application with carrier Control carrier alone	Double	/
NCT01206179	I	March 2011	Non-union	Autologous bone marrow MSCs (*in vitro* expanded)	6	Stem cell injection	None	Stem cell injections were tolerated with evidence of union in 3/5 patients (Emadedin et al., 2017)
NCT00916981	I/II	June 2009	Non-union Pseudoarthrosis	Autologous bone marrow derived pre-osteoblastic cells	30	Pre-osteoblastic cell injection	None	/
NCT02140528	II	April 2016	Tibial fracture	Allogeneic adipose MSCs	40	Stem cell injection Control placebo injection	Double	/
NCT00512434	NA	September 2013	Tibial fracture, open fracture	Autologous bone marrow MNCs	85	Stem cell injection and osteosynthesis Control osteosynthesis only	None	/
NCT00250302	I/II	April 2011	Tibial fracture	Autologous bone marrow MSCs (isolated)	24	Stem cell implantation with autologous platelet rich plasma/demineralized bone carrier Control no treatment	None	Shorter time to union in stem cell group (1.5 months) compared to control group (3 months) (Liebergall et al., 2013)
NCT02755922	III	December 2010	Mandibular fracture	Autologous adipose MSCs (24 h post-isolation)	20	Stem cell application Control no application	Single	Ossification values in stem cell group were similar to control at 4 weeks and higher as control at 12 weeks (Castillo-Cardiel et al., 2017)

(Continued)

TABLE 1 | Continued

Identifier	Phase	Completion	Condition	Cell type	Patients	Treatment groups	Masking	Main outcome (Reference)
NCT01532076	III	September 2014 (terminated)	Osteoporotic fracture	Autologous stromal vascular fraction	8	Application of cell-seeded hydroxyapatite/fibrin gel graft Control acellular composite graft	Single	/
SEARCH TERMS: "BONE, STEM CELLS, MAXILLA, ALVEOLAR"								
NCT03766217	III	Not yet recruiting	Cleft lip and palate	Autologous MSCs from deciduous dental pulp (enzyme isolated)	Est. 62	Application of stem cells with collagen and hydroxyapatite Control autologous bone graft	None	/
NCT02751125	I	Recruiting by invitation	Bone atrophy	Autologous bone marrow MSCs (cultured)	13	Application of stem cells mixed with biphasic calcium phosphate	None	Treatment resulted in bone formation sufficient for dental implant placement after 4–6 months (Gjerde et al., 2018)
NCT03070275	I/II	December 2017	Implant therapy	Autologous alveolar bone marrow MSCs (*in vitro* expanded)	20	Application of stem cells with autologous fibrin glue in collagen scaffold	Single	/
NCT02449005	I/II	December 2016	Chronic periodontitis	Autologous alveolar bone marrow MSCs (*in vitro* expanded)	30	Application of stem cells with autologous fibrin glue in collagen scaffold Control fibrin glue with collagen scaffold alone Control no graft materials	Quadruple	/
NCT01389661	I/II	April 2016	Maxillary cyst Bone loss of substance	Autologous jaw bone marrow MSCs (cultured, pre-differentiated in osteogenic matrix)	11	Application of cells cultured in autologous plasma matrix	None	Treatment resulted in increased cyst density by CT and no adverse effects (Redondo et al., 2018)
NCT02859025	I	February 2016	Cleft of alveolar ridge	Autologous buccal fat pad MSCs (cultured on bovine bone mineral)	10	Cells cultured on bovine bone applied with autologous spongy bone and collagen membrane Cells cultured on bovine bone applied with autologous cortical bone Control autologous spongy bone with collagen membrane	None	Cell-therapy groups showed a trend of higher bone formation after 6 months (Khojasteh et al., 2017)
NCT01932164	NA	December 2015	Cleft lip and palate	Autologous MSCs from deciduous dental pulp (isolated, characterized, frozen)	5	Application of stem cells with collagen and hydroxyapatite	None	Bone formation closing the alveolar cleft after 6 months in all patients
SEARCH TERMS: "OSTEONECROSIS, STEM CELLS"								
NCT02448121	I/II	Active, not recruiting	Avascular necrosis of bone in sickle cell disease patients	Autologous bone marrow MNCs	Est. 100	Stem cell injection	None	/
NCT01605383	I/II	Active, not recruiting	Avascular necrosis of the femoral head	Autologous bone marrow MSCs (cultured)	Est. 24	Application of cells with allogeneic bone Control standard treatment only	None	/

(Continued)

TABLE 1 | Continued

Identifier	Phase	Completion	Condition	Cell type	Patients	Treatment groups	Masking	Main outcome (Reference)
NCT02065167	II	Active, not recruiting	Avascular necrosis of the femoral head	Autologous bone marrow MSCs (cultured)	26	Stem cell injection	None	/
NCT01700920	II	December 2015	Osteonecrosis of the femoral head	Autologous bone marrow MSCs (cultured)	3	Stem cell injection	None	/
NCT01643655	NA	March 2015	Avascular necrosis of the femoral head	Autologous adipose MSCs	15	Stem cell injection	None	/
NCT01198080	I	June 2013	Osteonecrosis of the femoral head	Autologous CD133 bone marrow cells	10	Stem cell injection	None	Treatment resulted in disease score improvement, reduced joint injuries and pain relief (Emadedin et al., 2019)
NCT01544712	NA	September 2010	Osteonecrosis of the femoral head	Autologous bone marrow aspirate concentrate	50	Bone marrow concentrate injection Control standard treatment only	Double	Cell therapy did not improve stage 3 osteonecrosis (Hauzeur et al., 2018)
NCT00821470	I	September 2008	Osteonecrosis of the femoral head	Autologous bone marrow aspirate	21	Bone marrow injection Control standard treatment only	Triple	/

Studies were searched in the Clinicaltrials.gov database (July 2019), using combinations of search terms "bone, bone fracture, stem cells, maxilla, alveolar, osteonecrosis." Registered studies with unknown status and terminated studies were excluded. Cell type designation in the table is according to the information provided for the specific clinical study in the database.

Bone Marrow-Derived MSCs

Bone marrow has been investigated in most studies as the standard source of MSCs/progenitors contributing to bone repair *in vivo* (Park et al., 2012; Zhou et al., 2014; Nancarrow-Lei et al., 2017). Bone marrow MSCs have been isolated from individuals of various ages and health backgrounds (Alves et al., 2012; Chadid et al., 2018; Tencerova et al., 2019). Bone marrow MSCs are relatively rare, comprising <0.01% of the isolated mononuclear cell (MNC) fraction (Pittenger et al., 1999). Numbers of isolated MSCs vary between individual patients as well as the site and technique used for tissue harvesting (Muschler et al., 1997; Pierini et al., 2013; Patterson et al., 2017; Herrmann et al., 2019). In order to increase MSC numbers for therapeutic use, protocols for *in vitro* expansion have been developed, employing standardized, animal-supplement-free culture conditions (Schallmoser et al., 2009; Fekete et al., 2012). Bone marrow MSCs can reach over 50 population doublings *in vitro* (Bianco et al., 2001). However, with increased chronological age of the patient and extended *in vitro* culture, bone marrow MSC proliferation and differentiation potentials can decline and the proportion of senescent cells can increase, limiting the therapeutic potential (Stolzing et al., 2008; Churchman et al., 2017; Ganguly et al., 2017).

Adipose Tissue-Derived MSCs

With the discovery of MSC-like cells in adipose tissue lipoaspirates (Zuk et al., 2001), many studies have turned to this waste tissue as a source for MSC isolation. Volumes of lipoaspirate remaining at plastic surgeries can range from milliliters to several liters and reportedly contain a relatively high proportion of MSCs (between 1 and 5% of the isolated nucleated cells) depending on the donor, harvesting procedure, and tissue harvesting site (Gimble et al., 2007; Jurgens et al., 2008; Dubey et al., 2018). Importantly, some properties of the stromal vascular fraction (SVF) cells isolated from adipose tissue change upon culture *in vitro* (e.g., expression of surface markers) (Gimble et al., 2007), and the cultured cells are subsequently termed adipose MSCs or adipose tissue stromal cells (ASCs) (Bourin et al., 2013). Adipose MSCs exhibit robust osteogenic differentiation potential *in vitro* using standard osteogenic supplements (dexamethasone, beta-glycerophosphate, and ascorbic acid) (Fröhlich et al., 2010; Brennan et al., 2017). However, *in vivo* studies using an ectopic transplantation model in nude mice demonstrated important functional differences between bone marrow and adipose MSCs. When culture-expanded (unprimed) MSCs were transplanted together with osteoinductive calcium phosphate biomaterial or with Matrigel, higher bone ossicle formation and the presence of bone marrow compartment were exclusively found with the bone marrow MSCs as compared to adipose MSCs and cells from other sources (Reinisch et al., 2015; Brennan et al., 2017). This limitation might be overcome by *in vitro* pre-induction of adipose MSCs via the endochondral ossification route (Osinga et al., 2016). On the other hand, adipose MSCs contain vasculogenic subpopulations, which might be an advantage for bone healing by promoting neovascularization (Hutton et al., 2014; Brennan et al., 2017). According to recent

TABLE 2 | Preclinical studies reporting the use of MSC-secretome and MSC-EVs for bone regeneration.

References	Cell source	*In vivo* model	Main outcome of secretome treatment
UNFRACTIONATED SECRETOME/CONDITIONED MEDIUM			
Osugi et al. (2012)	Human bone marrow MSCs	Rat calvarial bone defect	Enhanced bone formation (after 4 and 8 weeks), rat MSC migration into the defect
Katagiri et al. (2013)	Human bone marrow MSCs	Rat calvarial bone defect	Early bone regeneration (after 2 and 4 weeks)
Katagiri et al. (2017)	Human bone marrow MSCs	Rat calvarial bone defect	Vascular endothelial growth factor is crucial for angiogenesis and bone regeneration
Ando et al. (2014)	Human bone marrow MSCs Human skin fibroblasts	Mouse distraction osteogenesis model	Accelerated distraction osteogenesis through endogenous cell recruitment of MSC secretome Activity of MSC secretome similar to MSCs transplantation
Kawai et al. (2015)	Human bone marrow MSCs	Rat periodontal defect	Periodontal tissue regeneration (after 4 weeks) and increased presence of CD31, CD105, and Flk1 positive cells
Ogata et al. (2015)	Human bone marrow MSCs	Rat bisphosphonate-related osteonecrosis of the jaw model	Increased bone healing with complete soft tissue coverage; histology demonstrated new bone formation and the presence of osteoclasts
Ogata et al. (2018)	Human bone marrow MSCs Three cytokines mixture	Rat medication-related osteonecrosis of the jaw model	Increased bone healing with soft tissue coverage in conditioned medium and three cytokines mixture groups
Fujio et al. (2017)	Hypoxic human dental pulp cells	Mouse distraction osteogenesis model	Increased blood vessel density and higher bone formation (after 4 weeks)
Xu et al. (2016)	Human fetal bone marrow MSCs	Rat distraction osteogenesis model	Continuous secretome injection improved bone consolidation compared to controls
Wang et al. (2016)	Human fetal MSCs	Mouse ectopic bone formation model	Restored osteogenic capacity of senescent adult human MSCs
EXTRACELLULAR VESICLES SECRETOME FRACTION			
Furuta et al. (2016)	Human bone marrow MSCs	CD9 negative mouse fracture healing model	EV injections in the fracture site accelerated fracture healing
Qin et al. (2016)	Human bone marrow MSCs	Rat calvarial bone defect	EV hydrogel application promoted bone regeneration after 8 weeks
Zhang et al. (2016b)	Human ESC-MSCs	Rat osteochondral defect model	Restoration of cartilage and subchondral bone after 12 weeks
Qi et al. (2016)	Human iPSC-MSCs	Ovariectomized rat calvarial bone defect	EV application stimulated bone regeneration and angiogenesis
Li et al. (2018)	Human adipose MSCs	Mouse calvarial bone defect	Enhanced bone regeneration after 6 weeks
Zhang et al. (2019)	Human umbilical cord MSCs	Rat stabilized femoral fracture model	Enhanced angiogenesis and bone healing after 14 and 31 days

reports, regenerative properties of adipose MSCs might not be adversely influenced by age, as is often the case with bone marrow MSCs (Dufrane, 2017; Reumann et al., 2018).

MSCs Derived From Perinatal Tissues

In addition to bone marrow and adipose tissue, perinatal tissues including umbilical cord, cord blood, amniotic membrane, and placenta are of high interest for bone regenerative therapies, particularly as their collection does not require invasive harvesting procedures (Brown et al., 2019). While autologous use of MSCs from these sources might require cell banking for extended periods, the advantage may be in their younger "chronological" age and thus presumably higher regenerative potential compared to the MSCs from adult/elderly patients. Indeed, umbilical cord MSCs reportedly exhibited a higher proliferation capacity, similar or higher osteogenic differentiation, and absence of adipogenic differentiation as compared to bone marrow and adipose-derived MSCs (Kern et al., 2006; Zhang et al., 2011). Similarly, comparative studies indicated that amnion MSCs have higher proliferation rates and comparable or higher osteogenic differentiation compared to bone marrow and adipose MSCs (Topoluk et al., 2017; Ghasemzadeh et al., 2018), and umbilical cord MSCs exhibited higher proliferation and more rapid osteogenic differentiation compared to bone marrow MSCs (Baksh et al., 2007).

Induced Pluripotent Stem Cells-Derived MSCs

Populations similar to MSCs have been reported in many other adult and fetal tissues, and evidence of their perivascular location points to their role in responses to injury (Caplan, 2008; Crisan et al., 2008). However, practical aspects, such as quantity of tissue available for harvesting, donor site injury, and limited scientific knowledge might preclude their clinical use. In contrast, practically unlimited numbers of autologous MSC-like cells can be obtained by differentiation of human induced pluripotent stem cells (hiPSCs). hiPSCs are derived from the patient's adult somatic cells by nuclear reprogramming using cocktails of transcription factors (and small molecules) with key roles in

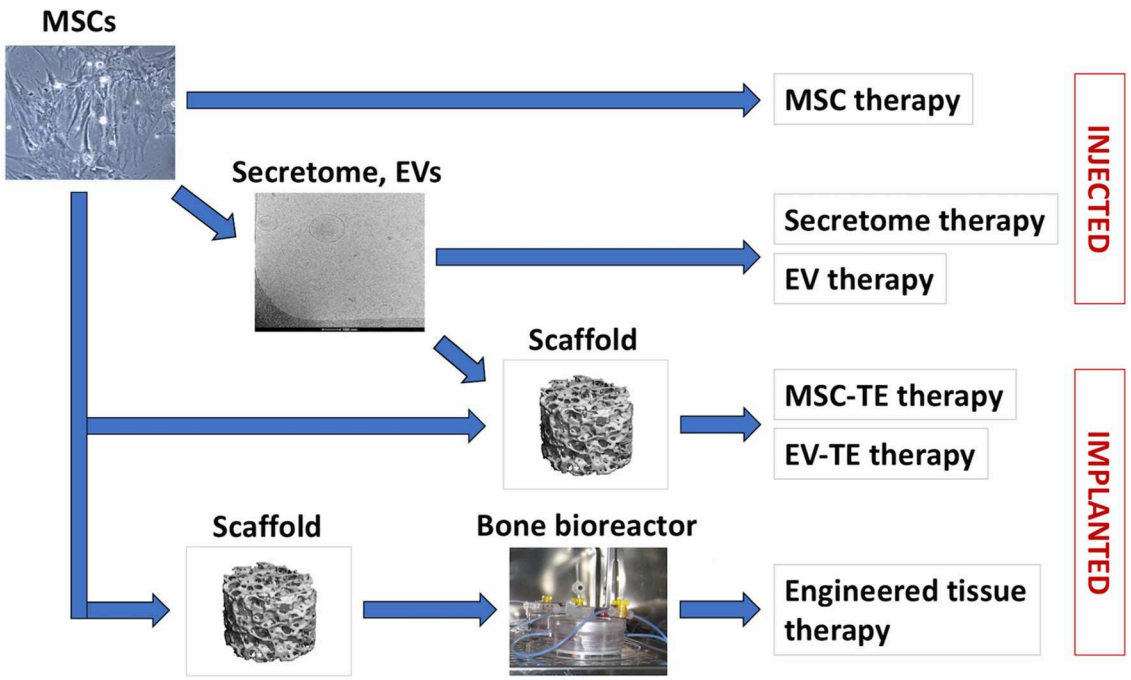

FIGURE 1 | MSC-based bone regeneration strategies. Cultured MSCs can be used for cell therapies or for therapeutic secretome/EVs production (arrow). In tissue engineering (TE) therapies, MSCs or MSC-EVs are applied in combination with biomaterial scaffolds. For certain indications, MSCs are seeded on biomaterial scaffolds and cultured *in vitro* in bioreactors, to support engineered tissue development and maturation prior to application.

the pluripotency regulation network (Takahashi et al., 2007; Zhu et al., 2010; Ma et al., 2013). hiPSCs largely resemble human embryonic stem cells (hESCs) in their pluripotency (i.e., ability to form differentiated tissues of all three germ layers, confirmed *in vivo* by teratoma assay) and differentiation potential (Bock et al., 2011; Bilic and Izpisua Belmonte, 2012). A number of studies reported the differentiation of hiPSCs into MSC-like progenitors (hiPSC-MSCs) and further into bone-like tissue *in vitro* and *in vivo* (reviewed in De Peppo and Marolt, 2013; Luzzani and Miriuka, 2017; Wu et al., 2017). hiPSC-MSCs largely resemble adult MSCs in surface antigen expression pattern, differentiation potential, and global gene expression and thus correspond to the definition of adult MSCs, though variations are observed between individual lines, similarly to adult MSCs (De Peppo et al., 2013). The procedure of their derivation via nuclear reprogramming of adult/aged somatic cells might be used to "rejuvenate" the regenerative potential of cells from elderly patients (Lapasset et al., 2011; Frobel et al., 2014; Spitzhorn et al., 2019). Further investigations into the hiPSC-MSCs phenotype, stability, safety, and *in vivo* development in preclinical models are needed (Jung et al., 2012; Levi et al., 2012; De Peppo et al., 2013; Phillips et al., 2014) prior to their consideration for potential clinical use. Nevertheless, hiPSCs offer a unique opportunity for engineering bone organoids containing various cell lineages from a single unlimited cell source, with broad applications in basic studies and translational applications.

Heterogeneity and Changes in MSC Properties During *in vitro* Culture

Notably, freshly isolated progenitors as well as cultured MSC populations are highly heterogeneous. Investigations are thus focused on defining the subpopulations endowed with the highest bone regenerative potential that can be procured with minimal manipulation (Caralla et al., 2013; Chung et al., 2015), as well as the development of fast screening methods to predict cell functionality (Li et al., 2016; Murgia et al., 2016). During *in vitro* culture, MSCs progressively lose their proliferation and differentiation potentials and the proportion of senescent cells increases (Stolzing et al., 2008; Churchman et al., 2017). This functional decline can be mitigated to some extent by the adjustment of culture conditions, including specific media supplements (e.g., the widely used basic fibroblast growth factor) (Martin et al., 1997; Chase et al., 2010) and culture on substrates containing extracellular matrix proteins (Mauney et al., 2004, 2006; Chase et al., 2010; Rakian et al., 2015). Such adaptations might not only preserve MSC biological properties, but also allow efficient MSC expansion for cell banking, repeated therapeutic applications, and the preparation of therapeutic secretome.

Taken together, MSCs isolated from different sources exhibit important differences in their availability, characteristics and regenerative potential. Therefore, the choice of cell source and subsequent isolation and manipulation techniques will depend on the requirements of specific research/clinical applications.

MSCs-BASED THERAPIES AND BONE TISSUE ENGINEERING

MSCs in Clinical Applications

Cell therapy approaches to regenerate bone were initially based on the premise that the transplanted MSCs would differentiate and form new bone tissue, thus substituting for the activity of endogenous cells compromised by the injury (Bruder and Fox, 1999; Stegemann et al., 2014; Marcucio et al., 2015). Based on the positive outcomes of preclinical studies (Bruder et al., 1998; Petite et al., 2000; Arinzeh et al., 2003; Granero-Moltó et al., 2009; Caralla et al., 2013; Chung et al., 2015), freshly isolated bone marrow mononuclear cells (MNCs) as well as culture-expanded MSCs from bone marrow, adipose tissue, and dental pulp were evaluated clinically in order to enhance the healing of bone fractures, non-unions, various jaw bone defects, and to prevent bone degradation in femoral head osteonecrosis (**Table 1**) (Stegemann et al., 2014). For fracture non-unions, fluoroscopy-controlled percutaneous injection of autologous MNCs, concentrated from bone marrow aspirates by centrifugation, i.e., the "Hernigou procedure," was reported (Hernigou et al., 2005). Successful bone union was obtained in 53 of 60 patients in whom a significantly higher concentration as well as total number of progenitor cells (evaluated by the CFU assay) were transplanted when compared to the 7 patients who did not achieve a bony union. A positive correlation was found between the total number and the concentration of transplanted CFUs and the volume of mineralized callus at 4 months, and a negative correlation was found between the time needed to obtain union and the concentration of CFUs in the graft (Hernigou et al., 2005). Similarly, Le Nail et al. analyzed a series of 43 patients with open tibial fractures with a risk of developing non-unions or presenting non-unions, some of whom received injections of concentrated bone marrow progenitors. They determined a threshold number of transplanted progenitors above which healing was 100% successful (Le Nail et al., 2014).

Quarto et al. first reported the application of culture-expanded bone marrow MSCs together with hydroxyapatite biomaterial for the treatment of large bone defects resulting from traumatic fractures and unsuccessful lengthening in three patients (Quarto et al., 2001). Abundant callus formation along the implants and good integration at the interfaces with the host bones 2 months after surgery were reported. There were no adverse reactions to the implants and all three patients recovered full limb function (Quarto et al., 2001). Several other registered clinical studies used autologous bone marrow MNCs, MSCs, or pre-osteoblasts, either injected or co-applied with bone substitute materials as carriers to treat delayed unions and non-unions of long bones (**Table 1**). Of these, Emadedin et al. reported that injections of cultured MSCs were safe and evidence of bone union was found in 3 of 5 treated patients (Emadedin et al., 2017). Furthermore, Gomez-Barrena et al. reported that surgical delivery of culture expanded bone marrow MSCs combined with bioceramic granules for the treatment of delayed unions and non-unions was safe and feasible, with 26 of 28 patients exhibiting radiologic healing 1 year after treatment (Gómez-Barrena et al., 2019). For the treatment of tibial, osteoporotic, and mandibular fractures, autologous bone marrow MNCs or MSCs, autologous adipose SVF and autologous or allogeneic adipose MSCs, injected or applied with biomaterials, were studied in comparison to non-cell-therapy controls (**Table 1**). Liebergall et al. reported that a prophylactic, minimally invasive intervention, involving injection of magnetically-separated bone marrow MSCs, mixed with platelet-rich plasma and demineralized bone matrix (study group, 12 patients), resulted in shorter time to union compared to control group with conventional fracture treatment (12 patients) (Liebergall et al., 2013). Castillo-Cardiel et al. similarly reported that the treatment of mandibular fractures with autologous adipose MSCs (12 patients) resulted in higher ossification rates at 12 weeks compared to the non-cell-therapy control group (12 patients) (Castillo-Cardiel et al., 2017).

Various jaw bone defects were also treated using MSC-therapies, with cells isolated and culture-expanded either from the jaw bone marrow, buccal fat pad, and dental pulp, and subsequently applied in combination with biomaterials (**Table 1**). Khojasteh et al. reported the treatment of human alveolar cleft defects with buccal fat pad-derived MSCs in combinations with biomaterials. The cell-therapy groups exhibited a trend of higher bone formation after 6 months (Khojasteh et al., 2017). Redondo et al. tested alveolar bone marrow MSCs, osteogenically pre-differentiated within an autologous serum-derived scaffolds *in vitro*, for the treatment of maxillary cysts in 9 patients. They found no adverse effects and an increased density of the cyst interior by computed tomography evaluation (Redondo et al., 2018). Gjerde et al. applied bone marrow MSCs with biphasic calcium phosphate for the treatment of severely atrophied mandibular bone in 13 patients and found no adverse events and sufficient bone regeneration for implant placement after 4–6 months (Gjerde et al., 2018).

Therapies involving autologous bone marrow MNCs or MSCs and adipose MSCs were also evaluated in several studies to treat osteonecrosis of the femoral head (**Table 1**) (Hernigou and Beaujean, 2002; Hernigou et al., 2018). Hernigou et al. reported that supplementation of the core decompensation procedure with concentrated bone marrow MNCs injections was effective in treating patients with earlier stages of the disease (resulting in less hip replacements), with better outcomes in patients who had greater numbers of progenitors transplanted (Hernigou and Beaujean, 2002). After 20–30 years follow-up, it was reported that core decompression with bone marrow cell injection improved the outcome of the disease (with less hip replacements) as compared with core decompression alone in the same patient group (Hernigou et al., 2018). Recently, injections of magnetically-separated CD133 positive bone marrow progenitors in 9 patients with femoral head osteonecrosis resulted in improved disease scores, less joint injuries, and provided clinically-relevant pain relief (Emadedin et al., 2019). In contrast, Hauzeur et al. reported that implantation of concentrated bone marrow MNCs after core decompression did not produce any improvement in the progression of stage 3 non-traumatic osteonecrosis of the femoral head (Hauzeur et al., 2018).

Taken together, published results of these various clinical studies and reports suggest the overall safety of MSC-based therapeutic approaches, as well as potential enhancement of bone healing compared to control groups. However, differences in

clinical indications, study designs and the absence of control groups preclude further mechanistic conclusions. Thus far, no MSC-based therapeutic product has become the standard of care for bone regeneration.

Systemic MSC delivery approaches were also investigated, e.g., for the treatment of osteoporosis (Phetfong et al., 2016), as well as novel therapeutic molecules that would enhance the mobility of endogenous MSCs toward the injured bone sites. In this regard, a biphasic small molecule that recruits osteogenic cells to the bone surfaces was reported to improve bone regeneration in a small animal fracture model (Guan et al., 2012; Yao et al., 2016). It was also reported that co-administration of PTH stimulated systemically administered MSCs to migrate to and regenerate spine injuries and vertebral fractures in preclinical models (Sheyn et al., 2016; Cohn Yakubovich et al., 2017). However, these advances have yet to be implemented and tested in the course of controlled clinical studies to Demonstrate enhanced bone regeneration.

Bone Tissue Engineering

More "advanced" bone tissue engineering approaches are predominantly in the preclinical research phase. These include various combinations of osteogenic cells, biomaterial scaffolds, signaling factors, and graft culture/maturation procedures (*in vitro* and *in vivo*) toward "functional" bone substitutes. Initially, most *in vitro* studies reported smaller bone constructs (up to several millimeters in size and <0.5 mm thick), since static culture limits new tissue development due to mass transport by diffusion only, as well as batch feeding regimes. Nevertheless, these smaller constructs allowed the evaluation of differences between various bone biomaterials, growth factor delivery regimes, cell differentiation pathways, and cell types to support new bone matrix deposition and mineralization (Meinel et al., 2006; Correia et al., 2012; Marcos-Campos et al., 2012; Chuenjitkuntaworn et al., 2016; Osinga et al., 2016; Rindone et al., 2019). In order to scale-up and standardize these bone tissue engineering strategies to sizes relevant for preclinical studies in large animal models and for clinical applications (beyond reconstruction of smaller jaw bone defects), research has focused on advanced scaffold manufacturing technologies (recently reviewed in Forrestal et al., 2017) and on dynamic tissue culture in bioreactor systems (Meinel et al., 2004, 2005; Marolt et al., 2006; Timmins et al., 2007; Grayson et al., 2008, 2011; Fröhlich et al., 2010; Woloszyk et al., 2014). Perfusion systems that support the interstitial flow of culture medium through bone scaffolds showed the most promise for bone tissue engineering from MSCs originating from adult tissues and pluripotent stem cells (De Peppo et al., 2013; Vetsch et al., 2016; Mitra et al., 2017; Sladkova et al., 2018). The appropriate biochemical milieu and biophysical stimulation provided to the osteogenic cells by the fluid shear force on the cells allowed increased cell numbers and enhanced the uniform cell distribution and the amount of new bone matrix (Sikavitsas et al., 2003; Grayson et al., 2011; Zhao et al., 2018). Grayson and colleagues were the first to report the bioreactor-based engineering of clinically sized, viable human, bone marrow MSCs-derived bone grafts, precisely fitting the complex anatomy of the temporomandibular joint condylar bone (Grayson et al., 2010). In following studies, several centimeter large ramus condyle grafts containing immature bone tissue were engineered from porcine adipose MSCs and evaluated *in vivo* in Yucatan minipigs (Bhumiratana et al., 2016). Six months after implantation, the engineered grafts maintained their anatomical structure, integrated with native tissues and generated greater volume of new bone and greater vascular infiltration than either non-seeded anatomical scaffolds or untreated defects (Bhumiratana et al., 2016). These advances are currently under way to be evaluated in a clinical phase-1 study. Sorensen et al. evaluated the effect of bone marrow MNCs pre-cultured on poly-lactic acid-coated bicalcium phosphate scaffolds in perfusion bioreactors on a spine fusion model in sheep (Sørensen et al., 2012). They found that bioreactor-generated, cell-based bone substitutes were as effective as autologous bone grafts and superior to cell-free bone substitutes in their bone fusion ability. However, bone structure was superior in autografts (Sørensen et al., 2012). In a following study, the bioreactor system was automated for the streamlined production of engineered osteogenic grafts (Ding et al., 2016).

Preclinical studies indicated that the survival of cells in engineered bone grafts can be severely limited after *in vivo* implantation (Giannoni et al., 2010; Becquart et al., 2012; Kaempfen et al., 2015; Manassero et al., 2016). As with autologous grafts, the transplanted tissue that is not immediately connected to the host vasculature is subject to oxygen deprivation and nutrient limitation and the interior portions of the graft undergo necrosis. Pre-vascularization strategies of the tissue-engineered bone grafts are thus an intense area of investigation (Barabaschi et al., 2015). For instance, Güven et al. reported that a 5-days perfusion bioreactor culture of adipose SVF within hydroxyapatite scaffolds resulted in capillary network formation, which anastomosed with the host vasculature already 1 week after ectopic nude rat implantation and promoted a faster tissue ingrowth and more abundant and uniform new bone tissue after 8 weeks, as compared to bone marrow or adipose MSC cultures (Güven et al., 2011). MSCs from different sources might also exhibit different sensitivity to hypoxic conditions. For instance, we previously found that hiPSC-derived MSC engineered bone constructs ($\sim$0.5 cm in size) remained viable for 12 weeks in a subcutaneous site, continued to develop, and functional blood vessels were found within the interior portions of the transplants (De Peppo et al., 2013). Furthermore, the application of tissue engineering protocols involving the endochondral differentiation pathway, which is predominant in the healing of long bones, might allow enhanced survival, vascularization, and remodeling of the transplanted hypertrophic cartilage grafts toward new bone regeneration (Bernhard et al., 2017; Epple et al., 2019).

MSC-DERIVED SECRETOME FOR BONE REGENERATION

The native process of bone healing proceeds through overlapping stages of inflammation, repair, and remodeling, which involve multiple signaling pathways acting in concert within the bone

defect and the surrounding soft tissues (Oryan et al., 2017). *In vivo* studies examining effects of transplanted MSCs on bone regeneration found limited numbers of transplanted cells surviving and engrafting in the defect sites, and the exact mechanisms of the contribution of exogenous MSCs to new tissue formation are not clear (Geuze et al., 2010; Bhumiratana et al., 2016; Manassero et al., 2016; Oryan et al., 2017). *In vitro* and *in vivo* studies suggested that the transplanted MSCs can have multiple paracrine effects on endogenous cell populations, including immune cell modulation, angiogenic activity, MSC and endothelial progenitor recruitment, cell proliferation, stem cell differentiation, anti-apoptotic effects, and wound healing (Ponte et al., 2007; Chen et al., 2008; Ando et al., 2014; Hofer and Tuan, 2016; Oryan et al., 2017). Depending on their source and manipulation (Oskowitz et al., 2011), MSCs produce a variety of signaling factors, including: purines, bone morphogenetic proteins, CCL2, Connexin 43, cyclooxygenase/prostaglandin, CD95/CD95 ligand, galectins, heme oxygenase-1, human leukocyte antigen-G, interleukin-3, interleukin-6, leukemia inhibitory factor, NO, transforming growth factor beta, vascular endothelial growth factor, hepatocyte growth factor, platelet derived growth factor, basic fibroblast growth factor, and others (Ponte et al., 2007; Chen et al., 2008; Ando et al., 2014; Hofer and Tuan, 2016). The growing understanding of MSC immunomodulatory and trophic activities has steered the research toward the potential of therapeutic MSC secretome, prepared by media conditioning on cultured MSCs, to enhance various stages of bone regeneration (Caplan and Dennis, 2006). In a sense, the use of therapeutic secretome mimics more closely the process of native bone healing by involving multiple signaling factors that work in synergy at low concentrations, rather than a single or a few signaling factors in super-physiologic concentrations (potentially leading to serious side effects, as reported for the high, clinically applied doses of recombinant bone morphogenetic protein therapies) (James et al., 2016). In addition, secretome-based cell-free therapeutic approaches present several significant advantages over current cell- and tissue-based therapies. The absence of replicating (allogeneic) cells in secretome fractions significantly improves the patient safety profile, the low metabolic activity allows for improved quality control and quality assurance, and the simplicity of storage provides the basis for cost-efficient shipping of this potentially off-the-shelf therapeutic substance.

A number of studies evaluated the potential of MSC secretome, either as unfractionated conditioned medium or the extracellular vesicles-enriched fraction, for bone regeneration (**Table 2**). Secretomes from human adult bone marrow MSCs (Osugi et al., 2012; Katagiri et al., 2013; Ando et al., 2014; Ogata et al., 2015), human dental pulp cells (Fujio et al., 2017), and human fetal MSCs (Wang et al., 2016; Xu et al., 2016) have been investigated. Human adult bone marrow MSC-conditioned media contained insulin-like growth factor-1, vascular endothelial growth factor, hepatocyte growth factor, transforming growth factor beta, monocyte chemoattractant proteins-1 and−3, interleukin-3, and interleukin 6, as determined by ELISA assays (Osugi et al., 2012; Katagiri et al., 2013; Ando et al., 2014; Kawai et al., 2015). Extended analysis of the bone marrow MSC-conditioned medium using a cytokine antibody array yielded 43 proteins with levels at least 1.5-times higher compared to a control medium background (Ando et al., 2014). In particular, serum-free conditioning of the bone marrow MSCs, as reported by most studies (**Table 2**), was shown to result in a highly angiogenic secretome (Oskowitz et al., 2011).

Osugi et al. reported the potential of human bone marrow MSC-conditioned medium to enhance bone healing in a rat calvarial defect model (Osugi et al., 2012). *In vitro*, this study demonstrated that conditioned medium from human bone marrow MSCs enhanced the migration, proliferation, and expression of osteogenic marker genes, such as osteocalcin and *RUNX2*, in rat bone marrow MSCs (Osugi et al., 2012). Application of the conditioned medium with agarose gel in calvarial defects resulted in higher bone regeneration compared to the agarose gel mixed with human bone marrow MSCs or vehicle controls (phosphate buffered saline or culture medium) after 4 and 8 weeks, presumably by enhancing rat MSC migration into the defect (Osugi et al., 2012). A related study by Katagiri et al. confirmed the *in vitro* findings of Osugi et al. and found that the conditioned medium soaked onto collagen sponges significantly increased early bone regeneration in calvarial defects (after 2 and 4 weeks) compared to the control group (Katagiri et al., 2013). A later study of angiogenesis in the newly regenerated bone suggested vascular endothelial growth factor to be the crucial component in the conditioned medium, promoting angiogenesis and migration of endogenous stem cells (Katagiri et al., 2017). Together, these studies suggested that bone marrow MSC-conditioned medium promotes angiogenesis and bone regeneration in a rat calvarial defect model, but also has the potential to mobilize endogenous MSCs.

Ando et al. demonstrated that repeated applications of human bone marrow MSC-conditioned medium accelerated callus formation in a high-speed mouse distraction osteogenesis model through multiple regenerative mechanisms, similar to the transplantation of bone marrow MSCs (Ando et al., 2014). Analysis of conditioned medium identified factors that recruit mouse bone MSCs, endothelial cells, and endothelial progenitors, inhibit inflammation and apoptosis, and promote osteoblast differentiation, angiogenesis, and cell proliferation. In particular, conditioned medium depleted of monocyte chemoattractant proteins-1 and−3 failed to recruit mouse bone marrow MSCs and callus formation (Ando et al., 2014). Further studies with human bone marrow MSC-conditioned medium showed the potential to enhance regeneration of rat periodontal defects and rat bisphosphonate-related osteonecrosis of the jaw (Kawai et al., 2015; Ogata et al., 2015). In periodontal defects, CD31, CD105, and Flk1 positive progenitors occurred more frequently in the conditioned medium group than controls after 2 weeks and regenerated periodontal tissue was found 4 weeks after implantation (Kawai et al., 2015). In the bisphosphonate-related osteonecrosis of the jaw model, conditioned medium resulted in the healing of open alveolar bone sockets in 63% of the rats (with complete soft tissue coverage and socket bones), compared to the exposed necrotic bone with inflamed soft tissue remaining in the control group (Ogata et al., 2015).

Histological analyses demonstrated new bone formation and appearance of osteoclasts with conditioned medium treatment, which was significantly higher compared to the non-treatment group, thus indicating that anti-apoptotic and anti-inflammatory effects of conditioned medium regulated the turnover of local bone (Ogata et al., 2015). A related *in vitro* study indicated that bone marrow MSCs release paracrine factors which directed osteo/odontogenic differentiation of dental pulp cells (Al-Sharabi et al., 2014). Further *in vitro* studies indicated that bone marrow MSC-conditioned medium promoted osteoclast differentiation and expression of master regulatory transcriptional factors for osteoclastogenesis, as well as showed maintenance of osteoclasts despite the presence of RANKL inhibitors (Ogata et al., 2017). Interestingly, a cytokine mixture composed of recombinant monocyte chemoattractant proteins-1, vascular endothelial growth factor, and insulin-like growth factor-1 in concentrations similar to those found in bone marrow MSC conditioned medium, promoted migration, proliferation, and osteogenic differentiation of rat MSCs *in vitro* similarly to conditioned medium, and intravenous application improved the healing of medication-related osteonecrosis of the jaw in a rat model (Ogata et al., 2018).

Fujio et al. studied conditioned media from human dental pulp cells cultured in normoxic and hypoxic conditions (Fujio et al., 2017). Significantly higher angiogenic potential of conditioned media from hypoxic compared to normoxic cultures and no enhancement of either conditioned media compared to controls on the mineralization of human fetal osteoblasts were found *in vitro*. In a mouse distraction osteogenesis model, repeated injections of conditioned medium resulted in increased blood vessel density and higher bone formation compared to the medium control group at 4 weeks (Fujio et al., 2017). In a comparative study of conditioned media from human fetal MSCs, human adult MSCs and rat MSCs, human fetal MSC-conditioned medium showed the highest osteogenic capacity and the lowest immunogenicity *in vitro*, as well as enhanced bone consolidation after repeated injections in the rat distraction osteogenesis model (Xu et al., 2016). A further *in vitro* study reported that the secretome of human fetal MSCs ameliorated replicative senescence and enhanced cell proliferation and the osteogenic differentiation potential of human adult MSCs (Wang et al., 2016). Concomitant activation of *SIRT1* and *FOXO3a* expression, upregulation of p21 gene expression, and downregulation of *BAX* and p53 gene expression were found, and the pre-treatment resulted in restored osteogenic ability of senescent human adult MSCs in a nude mouse ectopic bone formation model (Wang et al., 2016).

Based on the positive outcomes of studies in bone regeneration models, Katagiri et al. reported a first-in-human study and clinical case reports of alveolar bone regeneration using conditioned medium from human bone marrow MSCs (Katagiri et al., 2016). Human bone marrow MSC-conditioned medium was soaked on beta-tricalcium phosphate or on atelocollagen sponge and 8 patients with severe alveolar bone atrophy were treated prior to, or at the same time as dental implant placement. The patients experienced no systemic or local complications and showed early mineralization in the augmented bone according to radiographic evaluations. Calcium phosphate biomaterial structures gradually became indistinct from the surrounding bone 6 months after the surgeries, and biopsies confirmed new bone replacement of the resorbed biomaterial (Katagiri et al., 2016).

MSC-SECRETED EXTRACELLULAR VESICLES FOR BONE REGENERATION

Growing understanding of MSC intercellular communication via their secretome offers new options for tissue engineering strategies in bone regeneration (Lamichhane et al., 2015). Extracellular vesicles (EVs) are a heterogeneous group of small, lipid-bilayer enclosed, cell-derived particles, exerting effects on fundamental cellular processes in a pleiotropic manner (El Andaloussi et al., 2013). This mechanism is evolutionary conserved from bacteria to humans and plants (Schuh et al., 2019) and was initially considered a means of eliminating unneeded cellular compounds (Johnstone et al., 1987). However, in 1996, Raposo et al. demonstrated that EVs could modulate an adaptive immune response (Raposo et al., 1996) and research from the last two decades has shown that they facilitate intercellular communication, acting as mobile signaling platforms modulating fundamental biological processes in health and disease (Isola and Chen, 2016). Virtually every cell type secretes EVs and they act by the horizontal transfer of proteins, lipids, mRNAs, miRNAs, and other non-coding RNAs, altering the activity of a neighboring or distant target cell (Van Niel et al., 2018). Thereby, the lipid bilayer protects nucleic acids and proteins from degradation in the extracellular environment, allowing their efficient transport. Taken together, these findings have spurred a tremendous amount of effort to exploit EVs as potential therapeutics for immune response modulation and tissue regeneration.

Currently, the term "extracellular vesicles" refers to all types of secreted vesicles released by different cell types under different conditions (Araldi et al., 2012). Based on their biogenesis, two main categories of EVs can be envisioned for therapeutic use: exosomes and microvesicles. Exosomes are rather homogeneous in size (∼40–100 nm) and are generated in the endosome as intraluminal vesicles which subsequently mature to multivesicular endosomes. Cargo is sorted into exosomes by distinct mechanisms resulting in the formation of heterogeneous populations of intraluminal vesicles (Colombo et al., 2014). Sorting either involves ESCRT (endosomal sorting complex required for transport), Alix (or PDCD6IP; programmed cell death 6 interacting protein), and TSG101 (tumor susceptibility gene 101 protein) or takes place via an ESCRT-independent mechanism (reviewed in Van Niel et al., 2018). Finally, exosomes are released into the extracellular space upon fusion of the multivesicular endosomes with the cellular plasma membrane. Some of the commonly used markers to identify exosomes are various tetraspanins (CD63, CD81, and CD9), ALIX, TSG101 (tumor susceptibility gene 101 protein), and flotilin-1. However, a recent study demonstrated that classical tetraspanin-enriched exosomes contain a much more

limited repertoire of active molecules than has previously been assumed (Jeppesen et al., 2019), highlighting the necessity of suitable protocols for exosome characterization.

Microvesicles (often also referred to as ectosomes or shedding vesicles) represent a rather heterogeneous population of EVs generated by outward budding and subsequent fission of the plasma membrane. Both cargo sorting and subsequent Ca^{2+}-dependent vesicle shedding are regulated by various small GTPases, including members of the ARF (ARF6 and ARF1), Rab20, and Rho (Rac1 and RhoA) families (Tricarico et al., 2017). Microvesicles can range in size from ∼100 nm to ∼1 μm, are rich in phosphatidylserine and are often characterized by the presence of integrins, selectins, and CD40 ligand. Recently, annexin A1 has been proposed as a specific marker for microvesicles which are shed directly from the plasma membrane (Jeppesen et al., 2019). Once EVs are released into the extracellular environment, uptake into target cells takes place either by a receptor-mediated process, internalization by endocytic uptake, or by simple fusion of the cell and vesicle lipid bilayer. However, the unequivocal classification of EVs remains difficult, as the different types share overlapping characteristics and no unique markers are available. Further, current protocols used to purify EVs result in a heterogeneous vesicle population (Willms et al., 2016) and cannot fully exclude a soluble fraction within the purified product, which is why the term "vesicular secretome fraction" has been coined, encompassing both soluble and vesicular components (Gimona et al., 2017).

Several groups provided evidence that EVs are important regulators of stromal cell maintenance (Ratajczak et al., 2006; Quesenberry et al., 2015) and function (Weilner et al., 2016) and it is now widely accepted that much of the efficacy of stromal cell therapies comes from EVs and/or soluble factors (Caplan and Dennis, 2006; Caplan and Correa, 2011). In particular, EVs secreted by MSCs are considered promising candidates for future cell-free regenerative therapies. The paracrine action of MSCs was shown by Gnecchi et al., demonstrating that application of MSC-conditioned medium ameliorated tissue damage in a rodent model of acute myocardial infarction (Gnecchi et al., 2005). Later studies confirmed these results in both pig and mouse models using fractionated MSC secretome preparations (Timmers et al., 2008; Arslan et al., 2013). Since then, the regenerative and immunomodulatory capacity of MSC-derived EVs have been evaluated in several animal disease models, including e.g., kidney and liver injury, lung disease, cartilage repair, hind limb ischemia, ischemic brain injury, and spinal cord injury (reviewed in Harrell et al., 2019).

As MSCs secrete large amounts of EVs (Yeo et al., 2013), EV-based approaches to boost bone regeneration were soon evaluated. As pointed out earlier, in comparison with direct MSC transplantation, MSC-derived EVs appear *prima facie* safer, as they are devoid of viable cells. Further, systemically applied EV preparations are less likely to be trapped in the lung or liver and are most likely less immunogenic (Lai et al., 2013). Finally, they can be stored for an extended period of time, offering the possibility of an off-the-shelf product for restoration of bone defects (Webber and Clayton, 2013). Indeed, EVs purified from bone marrow MSCs, umbilical cord MSCs, endothelial progenitor cells, and iPSC-MSCs enhanced healing of bone in rodent models (Furuta et al., 2016; Qi et al., 2016; Jia et al., 2019; Zhang et al., 2019). Furuta et al. isolated EVs from human bone marrow MSC-conditioned medium and injected it into femoral fractures in a CD9 negative mouse strain (which produces low levels of EVs) and wild type mice (Furuta et al., 2016). Preparations of EVs contained low levels of bone-repair related cytokines. However, their application accelerated fracture healing compared to control (vehicle treated) animals (Furuta et al., 2016). Repeated injections of EVs prepared from human ESC-MSCs similarly promoted the regeneration of osteochondral defects in a rat femur model (Zhang et al., 2016b) and enhanced bone regeneration was found in a rat distraction osteogenesis model with injections of EVs prepared from rat endothelial progenitors (Jia et al., 2019).

More recently, MSC-EVs combined with various scaffold materials generated bone *in vivo* in ectopic sites (Xie et al., 2017) and successfully promoted bone repair in rodent calvarial bone defects (Qi et al., 2016; Qin et al., 2016; Li et al., 2018). Ideally, biocompatible scaffolds should degrade at an appropriate rate and facilitate the controlled release of the extracellular vesicles, as mere loading results in a burst release and might be less efficient in exerting pro-regenerative effects. Qi et al. showed in a calvarial defect model, established in osteoporotic rats, that treatment with tricalcium phosphate scaffolds loaded with EVs prepared from hiPSC-MSCs repaired bone defects through enhanced angiogenesis and osteogenesis (Qi et al., 2016). More recently, Li et al. reported that human adipose MSC-derived EVs immobilized onto poly-lactic-co-glycolic acid scaffolds exhibited a slow release profile *in vitro* and enhanced bone regeneration in mouse calvarial defects after 6 weeks (Li et al., 2018).

However, the molecular and cellular mechanisms underpinning the osteogenic effect of EVs remain poorly defined and they are certainly cell- and tissue context-dependent (Harrell et al., 2019). Potentially, they can be attributed to a protective effect in necrotic and ischemic environments (Liu et al., 2017), recruitment of endogenous MSCs (Osugi et al., 2012; Furuta et al., 2016), and HIF-1alpha-dependent pro-angiogenic activity (Qi et al., 2016; Zhang et al., 2019). In addition, MSC-EVs seem to directly promote osteogenic differentiation, in part by activating the PI3K/AKT signaling pathway (Zhang et al., 2016a) and via the activity of miRNA-196a released from the EVs (Qin et al., 2016). In general, MSC-derived extracellular vesicles have been shown to exert anti-inflammatory properties by inducing high levels of anti-inflammatory proteins, while concomitantly attenuating pro-inflammatory cytokines in THP-1 monocytes *in vitro* and inducing regulatory T cells *in vivo* (Zhang et al., 2014). Taken together, MSC-EVs elicit pleiotropic effects, promoting bone repair. However, it is important to note that the characteristics of the microenvironment influence the function of EVs produced by these cells (Huang and Feng, 2017). Along these lines, Zhu et al. demonstrated that the pro-angiogenic and osteogenic actions of bone marrow MSC-EVs are impaired in type-1 diabetes (Zhu et al., 2019). Therefore, it is imperative to choose appropriate cell sources for EV production for future therapeutic strategies. Taken together, EV-based, cell-free therapies appear to be a promising strategy to repair bone tissue.

However, to ensure comparability between preclinical studies and to allow future translation into the clinic, EV purification and characterization protocols urgently need to be harmonized (Witwer et al., 2019).

PRODUCTION OF MSCs, SECRETOME, AND EXTRACELLULAR VESICLES FOR CLINICAL USE

Production of MSCs for clinical use requires appropriate laboratory procedures adhering to GMP regulations. These procedures have been reported previously by several groups for bone marrow MSCs (Schallmoser et al., 2009; Fekete et al., 2012). Similarly, the manufacturing of MSC-derived therapeutic secretome and EVs for clinical testing requires GMP-compliant strategies, and several groups focused on establishing such protocols (Andriolo et al., 2018; Mendt et al., 2018; Rohde et al., 2019). Existing GMP protocols for MSC expansion can be largely adopted for the first step in secretome/EV production and standard operating procedures can be expanded by the concomitant processing steps of the conditioned medium. Overall, the therapeutic secretome/EV field benefits at this point from the experience gained from MSC manufacturing for clinical applications as well as from the ample experience available from virus-like particle enrichment. In an excellent overview on the current status of EV manufacturing, Whitford and Guterstam (2019) indicated that the technologies and knowledge for GMP-compliant EV production are at hand. However, some adaptation and fine tuning is still required. For instance, it should be noted that large scale production of therapeutic MSCs in order to obtain significant batch sizes of either cells or EVs for preclinical and clinical testing may alter the physiological state of the MSCs. The influence of cell passage number on the therapeutic potential of MSC-derived EVs has been questioned at least for adipose MSCs (Serra et al., 2018). Furthermore, the use of serum-free medium can cause changes in exosome biology and cargo sorting, and the use of coatings (e.g., fibronectin, gelatin) alters the profile of MSC adhesion and mechanotransduction and automatically violates a central requirement for defining MSCs, namely plastic adherence (Brindley et al., 2011; Whitford and Guterstam, 2019).

Bioreactor systems and associated analytical approaches have been studied for scale-up and a more efficient, reproducible, safe and cost-effective production of MSCs and secretome compared to static culture (Carmelo et al., 2015; Mizukami et al., 2019). Carmelo et al. developed a xeno-free microcarrier-based stirred culture system for scalable expansion of bone marrow and adipose MSCs. Their secretome analysis suggested a priming effect of stirred culture conditions toward potentially increased production of specific cytokines by MSCs (Carmelo et al., 2015). Similarly, a study by Teixeira et al. indicated that culture of bone marrow MSCs on microcarriers using computer-controlled suspension bioreactors enhanced the neuroregulatory profile of the secretome compared to static cultures (Teixeira et al., 2016). Secretory profiles of the MSCs can also be modulated by the surface structure of the microenvironment (Leuning et al., 2018), pointing further to the enhanced potential of engineered three-dimensional culture environment for optimizing MSC-derived therapeutic products.

FUTURE DIRECTIONS AND CHALLENGES FOR MSC-BASED BONE REGENERATION APPROACHES

Within the field of bone regeneration, there is a clear need for new cell-based or cell-free therapies for a number of conditions in which bone does not heal, resulting is significant morbidity and burden for the patients. At this time, several MSC-based therapies have reached the stage of clinical trials, but none of the approaches has been accepted in the clinic as the standard of care (Stegemann et al., 2014). Additional research is needed to advance our mechanistic understanding of various cell-, EV-, and tissue engineering-based therapies within specific clinical indications.

For MSC-based cell therapies, some of the currently registered clinical studies are starting to address the questions of dosing, the use of autologous vs. allogeneic cells, and efficacy compared to standard treatments using autologous bone grafts. However, many challenges remain in the standardization, quality control, and potency evaluation of MSC-based cell therapies, as well as in the scale-up, GMP manufacturing, and logistics, in particular when autologous MSCs are used. In addition to inter-patient variability due to age, health, and various risk factors, inherent differences between MSCs from various tissue sources present specific advantages and disadvantages, such as the potential to be harvested in high or low yields, surgical procedures and donor site morbidity, potential of use with minimal intra-surgical manipulation/preparation of the cells, the need for additional cell storage and culture of the cells to increase their numbers, co-application of signals to promote cell phenotype/differentiation, local vs. systemic delivery via injections or in combination with scaffolds (i.e., tissue-engineered therapies). For certain indications, e.g., complex facial bone defects, extended *in vitro* or *in vivo* engineering of viable bone substitutes might be required to provide appropriate architecture as well as mechanical properties for defect stabilization and loading, which are key for successful healing. For others, MSC injections or co-application with bone substitute materials might provide the critical components required for successful outcomes.

Due to these complexities with viable cells and tissue transplantation, a number of investigations have also focused on enhanced mobilization and homing of endogenous cells (which has not been extensively investigated in the clinic) (Yao and Lane, 2015; Karlsson et al., 2016; Yao et al., 2016) and on novel, secretome-based therapeutic approaches. Whereas clinical translation of the whole secretome might prove challenging as well, re-constitution of major secreted growth factor components (e.g., by using recombinant proteins) in concentrations similar to those in the MSC secretome might recapitulate the therapeutic effects, as was recently demonstrated (Ogata et al., 2018). Of note, repeated applications of conditioned media were used in several studies to achieve the therapeutic effects, in contrast to single

applications in the case of cell- and tissue-engineering-based therapeutic approaches. Surviving transplanted cells/tissues will be exposed to the effects of the local environment in the defect and might change their functions as a result. In contrast, preparation of therapeutic secretome might incorporate *in vitro* culture modifications to modulate the composition of released components.

Therapies based on EVs face similar problems as cell therapies in translating the promising research data into well-defined clinical trials and subsequent applications to patients. A central issue in the field is the standardization of manufacturing and analytic processes. A prerequisite for this advancement seems to be the awareness that any cell-derived EV product will always comprise of a heterogeneous mixture of extracellular vesicles and in most cases also of co-purifying soluble components. While this heterogeneity may be more of a concern for naive, unmanipulated MSC-EV preparations, loading and engineering of EV products to contain specific signals (Sutaria et al., 2017) might be less affected, with a greater focus on the characterization of the active component (e.g., siRNAs or engineered proteins) and its therapeutic potential.

Intuitively, the discussion on the best cell source for use in bone regeneration will always consider that cells that perform better in *in vitro* differentiation assays toward osteogenic lineage may be better suited for the manufacturing of EVs that support or enhance bone healing. It must be emphasized though, that these assays are highly artificial and the link between *in vitro* cell differentiation potential and the regenerative potential of cell-derived EVs must be further evaluated. Current efforts in the EV community are focused on determining the best producer cell source, on potential modes of action, and on standardization of physico-chemical assays and analytical devices for functional EV characterization. At the present time, analytical methods that are specifically tailored to characterize therapeutic EVs are largely missing. Nanoparticle tracking analysis is capable of determining the total number of particles in the heterogeneous (secretome) solution, but neither the particle size nor the particle number can currently predict the functionality of the product. Cell-based potency assays are difficult to establish to the level of GMP compliance and will have to be designed specifically for each clinical indication.

There is also no current consensus on the best method to expand the producer MSCs (two-dimensional vs. three-dimensional culture, batch-feed vs. stirred tank bioreactor, serum supplemented vs. serum free/defined medium) or to enrich/purify EVs or secretome. Therefore, application for clinical trials cannot rely on or reference to already approved investigational new drug/investigational medicinal products. This is well-reflected by the mere four interventional studies with EVs that are listed at clinicaltrials.gov. To some, the current classification of EV-containing therapeutic substances as biologicals by both EMA and FDA seems to be an advantage, since ATMP regulations do not apply. It remains to be seen, however, how the regulatory agencies deal with the application on a case-by-case basis in the absence of clear and binding regulations.

Finally, prospective manufacturers of EV therapeutics have to take into consideration that EV-based products for improved bone healing and regeneration aim, for the most part, at non-life-threatening medical indications. Irrespective of the considerable benefit for the patient and the health care system, this fact impacts the possible pricing of the product and thus the total manufacturing cost. For instance, the current financial requirement for available CAR-T cell therapy (430,000$ US) is an extreme example of the costs of cell-based therapy. Therapies based on EVs toward bone healing should look more at costs in the range of 1,000–2,000$ US to make the treatment both attractive and suitable for refund by the health insurance providers. This, however, will again demand precise calculations of the cost of goods and manufacturing costs, as well as for costs for testing, release, and storage. In this respect, batch size and dosing once again take center stage and must be considered in the development of a GMP-compliant manufacturing process for EV therapeutics and EV-enriched secretome.

In conclusion, further advancements in the science and translation of MSC-based therapies are required, and this growing body of knowledge, in conjunction with the improved identification of clinical indications and patients best suited for these treatments, will be key to creating therapies that will be consistently more successful than current treatments, while also being cost effective and marketable.

AUTHOR CONTRIBUTIONS

All authors listed have made a substantial, direct and intellectual contribution to the work, and approved it for publication.

FUNDING

This work was supported by the European Regional Development Fund Interreg V-A Italia–Austria 2014–2020 (Project EXOTHERA IT-AT 1036), the Project ExtraNeu from the State of Salzburg, Austria, and the project RejuvenateBone funding from the European Union's Horizon 2020 Research and Innovation Programme under the Marie Sklodowska-Curie grant agreement No. 657716.

ACKNOWLEDGMENTS

The authors would like to thank James Ferguson for the English language editing and Alain Brisson for the EV image acquisition.

REFERENCES

Al-Sharabi, N., Xue, Y., Fujio, M., Ueda, M., Gjerde, C., Mustafa, K., et al. (2014). Bone marrow stromal cell paracrine factors direct osteo/odontogenic differentiation of dental pulp cells. *Tissue Eng. Part A* 20, 3063–3072. doi: 10.1089/ten.tea.2013.0718

Alves, H., van Ginkel, J., Groen, N., Hulsman, M., Mentink, A., Reinders, M., et al. (2012). A mesenchymal stromal cell gene signature

for donor age. *PLoS ONE* 7:e42908. doi: 10.1371/journal.pone.0042908

Ando, Y., Matsubara, K., Ishikawa, J., Fujio, M., Shohara, R., Hibi, H., et al. (2014). Stem cell-conditioned medium accelerates distraction osteogenesis through multiple regenerative mechanisms. *Bone* 61, 82–90. doi: 10.1016/j.bone.2013.12.029

Andriolo, G., Provasi, E., Lo Cicero, V., Brambilla, A., Soncin, S., Torre, T., et al. (2018). Exosomes from human cardiac progenitor cells for therapeutic applications: development of a GMP-grade manufacturing method. *Front. Physiol.* 9:1169. doi: 10.3389/fphys.2018.01169

Araldi, E., Krämer-Albers, E.-M., 't Hoen, E. N., Peinado, H., Psonka-Antonczyk, K. M., Rao, P., et al. (2012). International Society for Extracellular Vesicles: first annual meeting, April 17–21, 2012: ISEV-2012. *J. Extracell. Vesicles* 1:19995. doi: 10.3402/jev.v1i0.19995

Arinzeh, T. L., Peter, S. J., Archambault, M. P., Van Den Bos, C., Gordon, S., Kraus, K., et al. (2003). Allogeneic mesenchymal stem cells regenerate bone in a critical-sized canine segmental defect. *J. Bone Jt. Surg.* 85, 1927–1935. doi: 10.2106/00004623-200310000-00010

Arslan, F., Lai, R. C., Smeets, M. B., Akeroyd, L., Choo, A., Aguor, E. N. E., et al. (2013). Mesenchymal stem cell-derived exosomes increase ATP levels, decrease oxidative stress and activate PI3K/Akt pathway to enhance myocardial viability and prevent adverse remodeling after myocardial ischemia/reperfusion injury. *Stem Cell Res.* 10, 301–312. doi: 10.1016/j.scr.2013.01.002

Baker, N., Boyette, L. B., and Tuan, R. S. (2015). Characterization of bone marrow-derived mesenchymal stem cells in aging. *Bone* 70, 37–47. doi: 10.1016/j.bone.2014.10.014

Baksh, D., Yao, R., and Tuan, R. S. (2007). Comparison of proliferative and multilineage differentiation potential of human mesenchymal stem cells derived from umbilical cord and bone marrow. *Stem Cells* 25, 1384–1392. doi: 10.1634/stemcells.2006-0709

Barabaschi, G. D. G., Manoharan, V., Li, Q., and Bertassoni, L. E. (2015). Engineering pre-vascularized scaffolds for bone regeneration. *Adv. Exp. Med. Biol.* 881, 79–94. doi: 10.1007/978-3-319-22345-2_5

Becquart, P., Cambon-Binder, A., Monfoulet, L. E., Bourguignon, M., Vandamme, K., Bensidhoum, M., et al. (2012). Ischemia is the prime but not the only cause of human multipotent stromal cell death in tissue-engineered constructs *in vivo*. *Tissue Eng. Part A* 18, 2084–2094. doi: 10.1089/ten.tea.2011.0690

Bernhard, J., Ferguson, J., Rieder, B., Heimel, P., Nau, T., Tangl, S., et al. (2017). Tissue-engineered hypertrophic chondrocyte grafts enhanced long bone repair. *Biomaterials* 139, 202–212. doi: 10.1016/j.biomaterials.2017.05.045

Bhattacharjee, A., Kuiper, J. H., Roberts, S., Harrison, P. E., Cassar-Pullicino, V. N., Tins, B., et al. (2019). Predictors of fracture healing in patients with recalcitrant nonunions treated with autologous culture expanded bone marrow-derived mesenchymal stromal cells. *J. Orthop. Res.* 37, 1303–1309. doi: 10.1002/jor.24184

Bhumiratana, S., Bernhard, J. C., Alfi, D. M., Yeager, K., Eton, R. E., Bova, J., et al. (2016). Tissue-engineered autologous grafts for facial bone reconstruction. *Sci. Transl. Med.* 8:343ra83. doi: 10.1126/scitranslmed.aad5904

Bianco, P., Riminucci, M., Gronthos, S., and Robey, P. G. (2001). Bone marrow stromal stem cells: nature, biology, and potential applications. *Stem Cells* 19, 180–192. doi: 10.1634/stemcells.19-3-180

Bilic, J., and Izpisua Belmonte, J. C. (2012). Concise review: induced pluripotent stem cells versus embryonic stem cells: close enough or yet too far apart? *Stem Cells* 30, 33–41. doi: 10.1002/stem.700

Bock, C., Kiskinis, E., Verstappen, G., Gu, H., Boulting, G., Smith, Z. D., et al. (2011). Reference maps of human es and ips cell variation enable high-throughput characterization of pluripotent cell lines. *Cell* 144, 439–452. doi: 10.1016/j.cell.2010.12.032

Börger, V., Bremer, M., Ferrer-Tur, R., Gockeln, L., Stambouli, O., Becic, A., et al. (2017). Mesenchymal stem/stromal cell-derived extracellular vesicles and their potential as novel immunomodulatory therapeutic agents. *Int. J. Mol. Sci.* 18:E1450. doi: 10.3390/ijms18071450

Borrelli, J., Pape, C., Hak, D., Hsu, J., Lin, S., Giannoudis, P., et al. (2012). Physiological challenges of bone repair. *J. Orthop. Trauma* 26, 708–711. doi: 10.1097/BOT.0b013e318274da8b

Bourin, P., Bunnell, B. A., Casteilla, L., Dominici, M., Katz, A. J., March, K. L., et al. (2013). Stromal cells from the adipose tissue-derived stromal vascular fraction and culture expanded adipose tissue-derived stromal/stem cells: a joint statement of the International Federation for Adipose Therapeutics and Science (IFATS) and the International So. *Cytotherapy* 15, 641–648. doi: 10.1016/j.jcyt.2013.02.006

Braccini, A., Wendt, D., Farhadi, J., Schaeren, S., Heberer, M., and Martin, I. (2007). The osteogenicity of implanted engineered bone constructs is related to the density of clonogenic bone marrow stromal cells. *J. Tissue Eng. Regen. Med.* 1, 60–65. doi: 10.1002/term.11

Brennan, M. A., Renaud, A., Guilloton, F., Mebarki, M., Trichet, V., Sensebé, L., et al. (2017). Inferior *in vivo* osteogenesis and superior angiogeneis of human adipose tissue: a comparison with bone marrow-derived stromal stem cells cultured in xeno-free conditions. *Stem Cells Transl. Med.* 6, 2160–2172. doi: 10.1002/sctm.17-0133

Brindley, D., Moorthy, K., Lee, J. H., Mason, C., Kim, H. W., and Wall, I. (2011). Bioprocess forces and their impact on cell behavior: implications for bone regeneration therapy. *J. Tissue Eng.* 2, 1–13. doi: 10.4061/2011/620247

Brown, C., McKee, C., Bakshi, S., Walker, K., Hakman, E., Halassy, S., et al. (2019). Mesenchymal stem cells: cell therapy and regeneration potential. *J. Tissue Eng. Regen. Med.* 13, 1738–1755. doi: 10.1002/term.2914

Bruder, S. P., and Fox, B. S. (1999). Tissue engineering of bone: cell based strategies. *Clin. Orthop. Relat. Res.* 367, S68–S83. doi: 10.1097/00003086-199910001-00008

Bruder, S. P., Kurth, A. A., Shea, M., Hayes, W. C., Jaiswal, N., and Kadiyala, S. (1998). Bone regeneration by implantation of purified, culture-expanded human mesenchymal stem cells. *J. Orthop. Res.* 16, 155–162. doi: 10.1002/jor.1100160202

Caplan, A. I. (2008). All MSCs are pericytes? *Cell Stem Cell* 3, 229–230. doi: 10.1016/j.stem.2008.08.008

Caplan, A. I. (2017). Mesenchymal stem cells: time to change the name! *Stem Cells Transl. Med.* 6, 1445–1451. doi: 10.1002/sctm.17-0051

Caplan, A. I., and Correa, D. (2011). The MSC: an injury drugstore. *Cell Stem Cell* 9, 11–15. doi: 10.1016/j.stem.2011.06.008

Caplan, A. I., and Dennis, J. E. (2006). Mesenchymal stem cells as trophic mediators. *J. Cell. Biochem.* 98, 1076–1084. doi: 10.1002/jcb.20886

Caralla, T., Joshi, P., Fleury, S., Luangphakdy, V., Shinohara, K., Pan, H., et al. (2013). *In vivo* transplantation of autogenous marrow-derived cells following rapid intraoperative magnetic separation based on hyaluronan to augment bone regeneration. *Tissue Eng. Part A* 19, 125–134. doi: 10.1089/ten.tea.2011.0622

Carmelo, J. G., Fernandes-Platzgummer, A., Diogo, M. M., da Silva, C. L., and Cabral, J. M. S. (2015). A xeno-free microcarrier-based stirred culture system for the scalable expansion of human mesenchymal stem/stromal cells isolated from bone marrow and adipose tissue. *Biotechnol. J.* 10, 1235–1247. doi: 10.1002/biot.201400586

Castillo-Cardiel, G., López-Echaury, A. C., Saucedo-Ortiz, J. A., Fuentes-Orozco, C., Michel-Espinoza, L. R., Irusteta-Jiménez, L., et al. (2017). Bone regeneration in mandibular fractures after the application of autologous mesenchymal stem cells, a randomized clinical trial. *Dent. Traumatol.* 33, 38–44. doi: 10.1111/edt.12303

Chadid, T., Morris, A., Surowiec, A., Robinson, S., Sasaki, M., Galipeau, J., et al. (2018). Reversible secretome and signaling defects in diabetic mesenchymal stem cells from peripheral arterial disease patients. *J. Vasc. Surg.* 68, 137S−151S.e2. doi: 10.1016/j.jvs.2018.05.223

Chan, C. K. F., Gulati, G. S., Sinha, R., Tompkins, J. V., Lopez, M., Carter, A. C., et al. (2018). Identification of the human skeletal stem cell. *Cell* 175, 43–56.e21. doi: 10.1016/j.cell.2018.07.029

Chase, L. G., Lakshmipathy, U., Solchaga, L. A., Rao, M. S., and Vemuri, M. C. (2010). A novel serum-free medium for the expansion of human mesenchymal stem cells. *Stem Cell Res. Ther.* 1:8. doi: 10.1186/scrt8

Chen, L., Tredget, E. E., Wu, P. Y. G., Wu, Y., and Wu, Y. (2008). Paracrine factors of mesenchymal stem cells recruit macrophages and endothelial lineage cells and enhance wound healing. *PLoS ONE* 3:e1886. doi: 10.1371/journal.pone.0001886

Chuenjitkuntaworn, B., Osathanon, T., Nowwarote, N., Supaphol, P., and Pavasant, P. (2016). The efficacy of polycaprolactone/hydroxyapatite scaffold in combination with mesenchymal stem cells for bone tissue engineering. *J. Biomed. Mater. Res.* 104, 264–271. doi: 10.1002/jbm.a.35558

Chung, C. G., James, A. W., Asatrian, G., Chang, L., Nguyen, A., Le, K., et al. (2015). Human perivascular stem cell-based bone graft

substitute induces rat spinal fusion. *Stem Cells Transl. Med.* 4, 538–538. doi: 10.5966/sctm.2014-0027erratum

Churchman, S. M., Boxall, S. A., McGonagle, D., and Jones, E. A. (2017). Predicting the remaining lifespan and cultivation-related loss of osteogenic capacity of bone marrow multipotential stromal cells applicable across a broad donor age range. *Stem Cells Int.* 2017:6129596. doi: 10.1155/2017/6129596

Cohn Yakubovich, D., Sheyn, D., Bez, M., Schary, Y., Yalon, E., Sirhan, A., et al. (2017). Systemic administration of mesenchymal stem cells combined with parathyroid hormone therapy synergistically regenerates multiple rib fractures. *Stem Cell Res. Ther.* 8:51. doi: 10.1186/s13287-017-0502-9

Colombo, M., Raposo, G., and Théry, C. (2014). Biogenesis, secretion, and intercellular interactions of exosomes and other extracellular vesicles. *Annu. Rev. Cell Dev. Biol.* 30, 255–289. doi: 10.1146/annurev-cellbio-101512-122326

Correia, C., Bhumiratana, S., Yan, L. P., Oliveira, A. L., Gimble, J. M., Rockwood, D., et al. (2012). Development of silk-based scaffolds for tissue engineering of bone from human adipose-derived stem cells. *Acta Biomater.* 8, 2483–2492. doi: 10.1016/j.actbio.2012.03.019

Crisan, M., Yap, S., Casteilla, L., Chen, C. W., Corselli, M., Park, T. S., et al. (2008). A perivascular origin for mesenchymal stem cells in multiple human organs. *Cell Stem Cell* 3, 301–313. doi: 10.1016/j.stem.2008.07.003

De Peppo, G. M., Marcos-Campos, I., Kahler, D. J., Alsalman, D., Shang, L., Vunjak-Novakovic, G., et al. (2013). Engineering bone tissue substitutes from human induced pluripotent stem cells. *Proc. Natl. Acad. Sci. U.S.A.* 110, 8680–8685. doi: 10.1073/pnas.1301190110

De Peppo, G. M., and Marolt, D. (2013). Modulating the biochemical and biophysical culture environment to enhance osteogenic differentiation and maturation of human pluripotent stem cell-derived mesenchymal progenitors. *Stem Cell Res. Ther.* 4:106. doi: 10.1186/scrt317

Ding, M., Henriksen, S. S., Wendt, D., and Overgaard, S. (2016). An automated perfusion bioreactor for the streamlined production of engineered osteogenic grafts. *J. Biomed. Mater. Res. B Appl. Biomater.* 104, 532–537. doi: 10.1002/jbm.b.33407

Dominici, M., Le Blanc, K., Mueller, I., Slaper-Cortenbach, I., Marini, F. C., Krause, D. S., et al. (2006). Minimal criteria for defining multipotent mesenchymal stromal cells. The International Society for Cellular Therapy position statement. *Cytotherapy* 8, 315–317. doi: 10.1080/14653240600855905

Dubey, N. K., Mishra, V. K., Dubey, R., Deng, Y. H., Tsai, F. C., and Deng, W. P. (2018). Revisiting the advances in isolation, characterization and secretome of adipose-derived stromal/stem cells. *Int. J. Mol. Sci.* 19:E2200. doi: 10.3390/ijms19082200

Dufrane, D. (2017). Impact of age on human adipose stem cells for bone tissue engineering. *Cell Transplant.* 26, 1496–1504. doi: 10.1177/0963689717721203

Dupont, K. M., Sharma, K., Stevens, H. Y., Boerckel, J. D., García, A. J., and Guldberg, R. E. (2010). Human stem cell delivery for treatment of large segmental bone defects. *Proc. Natl. Acad. Sci. U.S.A.* 107, 3305–3310. doi: 10.1073/pnas.0905444107

Ekegren, C. L., Edwards, E. R., de Steiger, R., and Gabbe, B. J. (2018). Incidence, costs and predictors of non-union, delayed union and mal-union following long bone fracture. *Int. J. Environ. Res. Public Health* 15:E2845. doi: 10.3390/ijerph15122845

El Andaloussi, S., Mäger, I., Breakefield, X. O., and Wood, M. J. A. (2013). Extracellular vesicles: Biology and emerging therapeutic opportunities. *Nat. Rev. Drug Discov.* 12, 347–357. doi: 10.1038/nrd3978

Emadedin, M., Karimi, S., Karimi, A., Labibzadeh, N., Niknejadi, M., Baharvand, H., et al. (2019). Autologous bone marrow–derived CD133 cells with core decompression as a novel treatment method for femoral head osteonecrosis: a pilot study. *Cytotherapy* 21, 107–112. doi: 10.1016/j.jcyt.2018.10.005

Emadedin, M., Labibzadeh, N., Fazeli, R., Mohseni, F., Hosseini, S. E., Moghadasali, R., et al. (2017). Percutaneous autologous bone marrow-derived mesenchymal stromal cell implantation is safe for reconstruction of human lower limb long bone atrophic nonunion. *Cell J.* 19, 159–165. doi: 10.22074/cellj.2016.4866

Epple, C., Haumer, A., Ismail, T., Lunger, A., Scherberich, A., Schaefer, D. J., et al. (2019). Prefabrication of a large pedicled bone graft by engineering the germ for *de novo* vascularization and osteoinduction. *Biomaterials* 192, 118–127. doi: 10.1016/j.biomaterials.2018.11.008

Fekete, N., Rojewski, M. T., Fürst, D., Kreja, L., Ignatius, A., Dausend, J., et al. (2012). GMP-compliant isolation and large-scale expansion of bone marrow-derived MSC. *PLoS ONE* 7:e43255. doi: 10.1371/journal.pone.0043255

Forrestal, D. P., Klein, T. J., and Woodruff, M. A. (2017). Challenges in engineering large customized bone constructs. *Biotechnol. Bioeng.* 114, 1129–1139. doi: 10.1002/bit.26222

Friedenstein, A. J., Chailakhyan, R. K., and Gerasimov, U. V. (1987). Bone marrow osteogenic stem cells: *in vitro* cultivation and transplantation in diffusion chambers. *Cell Prolif.* 20, 263–272. doi: 10.1111/j.1365-2184.1987.tb01309.x

Frobel, J., Hemeda, H., Lenz, M., Abagnale, G., Joussen, S., Denecke, B., et al. (2014). Epigenetic rejuvenation of mesenchymal stromal cells derived from induced pluripotent stem cells. *Stem Cell Rep.* 3, 414–422. doi: 10.1016/j.stemcr.2014.07.003

Frohlich, M., Grayson, W., Wan, L., Marolt, D., Drobnic, M., and Vunjak-Novakovic, G. (2008). Tissue engineered bone grafts: biological requirements, tissue culture and clinical relevance. *Curr. Stem Cell Res. Ther.* 3, 254–264. doi: 10.2174/157488808786733962

Fröhlich, M., Grayson, W. L., Marolt, D., Gimble, J. M., Kregar-Velikonja, N., and Vunjak-Novakovic, G. (2010). Bone grafts engineered from human adipose-derived stem cells in perfusion bioreactor culture. *Tissue Eng. Part A* 16, 179–189. doi: 10.1089/ten.tea.2009.0164

Fujio, M., Xing, Z., Sharabi, N., Xue, Y., Yamamoto, A., Hibi, H., et al. (2017). Conditioned media from hypoxic-cultured human dental pulp cells promotes bone healing during distraction osteogenesis. *J. Tissue Eng. Regen. Med.* 11, 2116–2126. doi: 10.1002/term.2109

Furuta, T., Miyaki, S., Ishitobi, H., Ogura, T., Kato, Y., Kamei, N., et al. (2016). Mesenchymal stem cell-derived exosomes promote fracture healing in a mouse model. *Stem Cells Transl. Med.* 5, 1620–1630. doi: 10.5966/sctm.2015-0285

Ganguly, P., El-Jawhari, J. J., Giannoudis, P. V., Burska, A. N., Ponchel, F., and Jones, E. A. (2017). Age-related changes in bone marrow mesenchymal stromal cells: a potential impact on osteoporosis and osteoarthritis development. *Cell Transplant.* 26, 1520–1529. doi: 10.1177/0963689717721201

Geuze, R. E., Prins, H. J., Öner, F. C., Van Der Helm, Y. J. M., Schuijff, L. S., Martens, A. C., et al. (2010). Luciferase labeling for multipotent stromal cell tracking in spinal fusion versus ectopic bone tissue engineering in mice and rats. *Tissue Eng. Part A* 16, 3343–3351. doi: 10.1089/ten.tea.2009.0774

Ghasemzadeh, M., Hosseini, E., Ahmadi, M., Kamalizad, M., and Amirizadeh, N. (2018). Comparable osteogenic capacity of mesenchymal stem or stromal cells derived from human amnion membrane and bone marrow. *Cytotechnology* 70, 729–739. doi: 10.1007/s10616-017-0177-1

Giannoni, P., Scaglione, S., Daga, A., Ilengo, C., Cilli, M., and Quarto, R. (2010). Short-time survival and engraftment of bone marrow stromal cells in an ectopic model of bone regeneration. in *Tissue Eng. Part A*, 489–499. doi: 10.1089/ten.tea.2009.0041

Gimble, J. M., Katz, A. J., and Bunnell, B. A. (2007). Adipose-derived stem cells for regenerative medicine. *Circ. Res.* 100, 1249–60. doi: 10.1161/01.RES.0000265074.83288.09

Gimona, M., Pachler, K., Laner-Plamberger, S., Schallmoser, K., and Rohde, E. (2017). Manufacturing of human extracellular vesicle-based therapeutics for clinical use. *Int. J. Mol. Sci.* 18:E1190. doi: 10.3390/ijms18061190

Gjerde, C., Mustafa, K., Hellem, S., Rojewski, M., Gjengedal, H., Yassin, M. A., et al. (2018). Cell therapy induced regeneration of severely atrophied mandibular bone in a clinical trial. *Stem Cell Res. Ther.* 9:213. doi: 10.1186/s13287-018-0951-9

Gnecchi, M., He, H., Liang, O. D., Melo, L. G., Morello, F., Mu, H., et al. (2005). Paracrine action accounts for marked protection of ischemic heart by Akt-modified mesenchymal stem cells [2]. *Nat. Med.* 11, 367–368. doi: 10.1038/nm0405-367

Gómez-Barrena, E., Rosset, P., Gebhard, F., Hernigou, P., Baldini, N., Rouard, H., et al. (2019). Feasibility and safety of treating non-unions in tibia, femur and humerus with autologous, expanded, bone marrow-derived mesenchymal stromal cells associated with biphasic calcium phosphate biomaterials in a multicentric, non-comparative trial. *Biomaterials* 196, 100–108. doi: 10.1016/j.biomaterials.2018.03.033

Gómez-Barrena, E., Rosset, P., Lozano, D., Stanovici, J., Ermthaller, C., and Gerbhard, F. (2015). Bone fracture healing: cell therapy in delayed unions and nonunions. *Bone* 70, 93–101. doi: 10.1016/j.bone.2014.07.033

Granero-Moltó, F., Weis, J. A., Miga, M. I., Landis, B., Myers, T. J., O'Rear, L., et al. (2009). Regenerative effects of transplanted mesenchymal stem cells in fracture healing. *Stem Cells* 27, 1887–1898. doi: 10.1002/stem.103

Grayson, W. L., Bhumiratana, S., Cannizzaro, C., Chao, P. H. G., Lennon, D. P., Caplan, A. I., et al. (2008). Effects of initial seeding density and fluid perfusion rate on formation of tissue-engineered bone. *Tissue Eng. Part A.* 14, 1809–1820. doi: 10.1089/ten.tea.2007.0255

Grayson, W. L., Bunnell, B. A., Martin, E., Frazier, T., Hung, B. P., and Gimble, J. M. (2015). Stromal cells and stem cells in clinical bone regeneration. *Nat. Rev. Endocrinol.* 11, 140–150. doi: 10.1038/nrendo.2014.234

Grayson, W. L., Fröhlich, M., Yeager, K., Bhumiratana, S., Chan, M. E., Cannizzaro, C., et al. (2010). Engineering anatomically shaped human bone grafts. *Proc. Natl. Acad. Sci. U.S.A.* 107, 3299–3304. doi: 10.1073/pnas.0905439106

Grayson, W. L., Marolt, D., Bhumiratana, S., Fröhlich, M., Guo, X. E., and Vunjak-Novakovic, G. (2011). Optimizing the medium perfusion rate in bone tissue engineering bioreactors. *Biotechnol. Bioeng.* 108, 1159–1170. doi: 10.1002/bit.23024

Gruber, R., Koch, H., Doll, B. A., Tegtmeier, F., Einhorn, T. A., and Hollinger, J. O. (2006). Fracture healing in the elderly patient. *Exp. Gerontol.* 41, 1080–1093. doi: 10.1016/j.exger.2006.09.008

Guan, M., Yao, W., Liu, R., Lam, K. S., Nolta, J., Jia, J., et al. (2012). Directing mesenchymal stem cells to bone to augment bone formation and increase bone mass. *Nat. Med.* 18, 456–462. doi: 10.1038/nm.2665

Güven, S., Mehrkens, A., Saxer, F., Schaefer, D. J., Martinetti, R., Martin, I., et al. (2011). Engineering of large osteogenic grafts with rapid engraftment capacity using mesenchymal and endothelial progenitors from human adipose tissue. *Biomaterials* 32, 5801–5809. doi: 10.1016/j.biomaterials.2011.04.064

Harrell, C. R., Fellabaum, C., Jovicic, N., Djonov, V., Arsenijevic, N., and Volarevic, V. (2019). Molecular mechanisms responsible for therapeutic potential of mesenchymal stem cell-derived secretome. *Cells* 8:467. doi: 10.3390/cells8050467

Hauzeur, J. P., De Maertelaer, V., Baudoux, E., Malaise, M., Beguin, Y., and Gangji, V. (2018). Inefficacy of autologous bone marrow concentrate in stage three osteonecrosis: a randomized controlled double-blind trial. *Int. Orthop.* 42, 1429–1435. doi: 10.1007/s00264-017-3650-8

Hernigou, P., and Beaujean, F. (2002). Treatment of osteonecrosis with autologous bone marrow grafting. *Clin. Orthop. Relat. Res.* 405, 14–23. doi: 10.1097/00003086-200212000-00003

Hernigou, P., Dubory, A., Homma, Y., Guissou, I., Flouzat Lachaniette, C. H., Chevallier, N., et al. (2018). Cell therapy versus simultaneous contralateral decompression in symptomatic corticosteroid osteonecrosis: a thirty year follow-up prospective randomized study of one hundred and twenty five adult patients. *Int. Orthop.* 42, 1639–1649. doi: 10.1007/s00264-018-3941-8

Hernigou, P., Poignard, A., Beaujean, F., and Rouard, H. (2005). Percutaneous autologous bone-marrow grafting for nonunions: influence of the number and concentration of progenitor cells. *J. Bone Jt. Surg. Am.* 87, 1430–1437. doi: 10.2106/JBJS.D.02215

Herrmann, M., Hildebrand, M., Menzel, U., Fahy, N., Alini, M., Lang, S., et al. (2019). Phenotypic characterization of bone marrow mononuclear cells and derived stromal cell populations from human iliac crest, vertebral body and femoral head. *Int. J. Mol. Sci.* 20:3454. doi: 10.3390/ijms20143454

Hofer, H. R., and Tuan, R. S. (2016). Secreted trophic factors of mesenchymal stem cells support neurovascular and musculoskeletal therapies. *Stem Cell Res. Ther.* 7:131. doi: 10.1186/s13287-016-0394-0

Huang, Z., and Feng, Y. (2017). Exosomes derived from hypoxic colorectal cancer cells promote angiogenesis through Wnt4-Induced β-catenin signaling in endothelial cells. *Oncol. Res.* 25, 651–661. doi: 10.3727/096504016X14752792816791

Hutton, D. L., Kondragunta, R., Moore, E. M., Hung, B. P., Jia, X., and Grayson, W. L. (2014). Tumor necrosis factor improves vascularization in osteogenic grafts engineered with human adipose-derived stem/stromal cells. *PLoS ONE* 9:e107199. doi: 10.1371/journal.pone.0107199

Isola, A., and Chen, S. (2016). Exosomes: the messengers of health and disease. *Curr. Neuropharmacol.* 15, 157–165. doi: 10.2174/1570159x14666160825160421

Jakob, M., Saxer, F., Scotti, C., Schreiner, S., Studer, P., Scherberich, A., et al. (2012). Perspective on the evolution of cell-based bone tissue engineering strategies. *Eur. Surg. Res.* 49, 1–7. doi: 10.1159/000338362

James, A. W., LaChaud, G., Shen, J., Asatrian, G., Nguyen, V., Zhang, X., et al. (2016). A review of the clinical side effects of bone morphogenetic protein-2. *Tissue Eng. Part B Rev.* 22, 284–297. doi: 10.1089/ten.teb.2015.0357

Jeppesen, D. K., Fenix, A. M., Franklin, J. L., Higginbotham, J. N., Zhang, Q., Zimmerman, L. J., et al. (2019). Reassessment of exosome composition. *Cell* 177, 428–445.e18. doi: 10.1016/j.cell.2019.02.029

Jia, Y., Zhu, Y., Qiu, S., Xu, J., and Chai, Y. (2019). Exosomes secreted by endothelial progenitor cells accelerate bone regeneration during distraction osteogenesis by stimulating angiogenesis. *Stem Cell Res. Ther.* 10:12. doi: 10.1186/s13287-018-1115-7

Johnstone, R. M., Adam, M., Hammond, J. R., Orr, L., and Turbide, C. (1987). Vesicle formation during reticulocyte maturation. Association of plasma membrane activities with released vesicles (exosomes). *J. Biol. Chem.* 262, 9412–9420.

Jukes, J. M., Both, S. K., Leusink, A., Sterk, L. M. T., Van Blitterswijk, C. A., and De Boer, J. (2008). Endochondral bone tissue engineering using embryonic stem cells. *Proc. Natl. Acad. Sci. U.S.A.* 105, 6840–6845. doi: 10.1073/pnas.0711662105

Jung, Y., Bauer, G., and Nolta, J. A. (2012). Concise review: induced pluripotent stem cell-derived mesenchymal stem cells: progress toward safe clinical products. *Stem Cells* 30, 42–47. doi: 10.1002/stem.727

Jurgens, W. J. F. M., Oedayrajsingh-Varma, M. J., Helder, M. N., ZandiehDoulabi, B., Schouten, T. E., Kuik, D. J., et al. (2008). Effect of tissue-harvesting site on yield of stem cells derived from adipose tissue: implications for cell-based therapies. *Cell Tissue Res.* 332, 415–426. doi: 10.1007/s00441-007-0555-7

Kaempfen, A., Todorov, A., Güven, S., Largo, R. D., Jaquiéry, C., Scherberich, A., et al. (2015). Engraftment of prevascularized, tissue engineered constructs in a novel rabbit segmental bone defect model. *Int. J. Mol. Sci.* 16, 12616–12630. doi: 10.3390/ijms160612616

Karlsson, J., Harmankaya, N., Palmquist, A., Atefyekta, S., Omar, O., Tengvall, P., et al. (2016). Stem cell homing using local delivery of plerixafor and stromal derived growth factor-1alpha for improved bone regeneration around Ti-implants. *J. Biomed. Mater. Res. Part A* 104, 2466–2475. doi: 10.1002/jbm.a.35786

Kassem, M., and Marie, P. J. (2011). Senescence-associated intrinsic mechanisms of osteoblast dysfunctions. *Aging Cell* 10, 191–197. doi: 10.1111/j.1474-9726.2011.00669.x

Katagiri, W., Kawai, T., Osugi, M., Sugimura-Wakayama, Y., Sakaguchi, K., Kojima, T., et al. (2017). Angiogenesis in newly regenerated bone by secretomes of human mesenchymal stem cells. *Maxillofac. Plast. Reconstr. Surg.* 39:8. doi: 10.1186/s40902-017-0106-4

Katagiri, W., Osugi, M., Kawai, T., and Hibi, H. (2016). First-in-human study and clinical case reports of the alveolar bone regeneration with the secretome from human mesenchymal stem cells. *Head Face Med.* 12:5. doi: 10.1186/s13005-016-0101-5

Katagiri, W., Osugi, M., Kawai, T., and Ueda, M. (2013). Novel cell-free regeneration of bone using stem cell–derived growth factors. *Int. J. Oral Maxillofac. Implants* 28, 1009–1016. doi: 10.11607/jomi.3036

Kawai, T., Katagiri, W., Osugi, M., Sugimura, Y., Hibi, H., and Ueda, M. (2015). Secretomes from bone marrow-derived mesenchymal stromal cells enhance periodontal tissue regeneration. *Cytotherapy* 17, 369–381. doi: 10.1016/j.jcyt.2014.11.009

Kern, S., Eichler, H., Stoeve, J., Klüter, H., and Bieback, K. (2006). Comparative analysis of mesenchymal stem cells from bone marrow, umbilical cord blood, or adipose tissue. *Stem Cells* 24, 1294–1301. doi: 10.1634/stemcells.2005-0342

Khojasteh, A., Kheiri, L., Behnia, H., Tehranchi, A., Nazeman, P., Nadjmi, N., et al. (2017). Lateral ramus cortical bone plate in alveolar cleft osteoplasty with concomitant use of buccal fat pad derived cells and autogenous bone: phase I clinical trial. *Biomed Res. Int.* 2017:6560234. doi: 10.1155/2017/6560234

Lai, R. C., Yeo, R. W. Y., Tan, K. H., and Lim, S. K. (2013). Exosomes for drug delivery–a novel application for the mesenchymal stem cell. *Biotechnol. Adv.* 31, 543–551. doi: 10.1016/j.biotechadv.2012.08.008

Lamichhane, T. N., Sokic, S., Schardt, J. S., Raiker, R. S., Lin, J. W., and Jay, S. M. (2015). Emerging roles for extracellular vesicles in tissue engineering and regenerative medicine. *Tissue Eng. Part B Rev.* 21, 45–54. doi: 10.1089/ten.teb.2014.0300

Lapasset, L., Milhavet, O., Prieur, A., Besnard, E., Babled, A., Ät-Hamou, N., et al. (2011). Rejuvenating senescent and centenarian human cells by

reprogramming through the pluripotent state. *Genes Dev.* 25, 2248–2253. doi: 10.1101/gad.173922.111

Le Nail, L. R., Stanovici, J., Fournier, J., Splingard, M., Domenech, J., and Rosset, P. (2014). Percutaneous grafting with bone marrow autologous concentrate for open tibia fractures: analysis of forty three cases and literature review. *Int. Orthop.* 38, 1845–1853. doi: 10.1007/s00264-014-2342-x

Leuning, D. G., Beijer, N. R. M., Du Fossé, N. A., Vermeulen, S., Lievers, E., Van Kooten, C., et al. (2018). The cytokine secretion profile of mesenchymal stromal cells is determined by surface structure of the microenvironment. *Sci. Rep.* 8:7716. doi: 10.1038/s41598-018-25700-5

Levi, B., Hyun, J. S., Montoro, D. T., Lo, D. D., Chan, C. K. F., Hu, S., et al. (2012). *In vivo* directed differentiation of pluripotent stem cells for skeletal regeneration. *Proc. Natl. Acad. Sci. U.S.A.* 109, 20379–20384. doi: 10.1073/pnas.1218052109

Li, B., Menzel, U., Loebel, C., Schmal, H., Alini, M., and Stoddart, M. J. (2016). Monitoring live human mesenchymal stromal cell differentiation and subsequent selection using fluorescent RNA-based probes. *Sci. Rep.* 6:26014. doi: 10.1038/srep26014

Li, W., Liu, Y., Zhang, P., Tang, Y., Zhou, M., Jiang, W., et al. (2018). Tissue-engineered bone immobilized with human adipose stem cells-derived exosomes promotes bone regeneration. *ACS Appl. Mater. Interfaces* 10, 5240–5254. doi: 10.1021/acsami.7b17620

Liebergall, M., Schroeder, J., Mosheiff, R., Gazit, Z., Yoram, Z., Rasooly, L., et al. (2013). Stem cell-based therapy for prevention of delayed fracture union: a randomized and prospective preliminary study. *Mol. Ther.* 21, 1631–1638. doi: 10.1038/mt.2013.109

Liu, X., Li, Q., Niu, X., Hu, B., Chen, S., Song, W., et al. (2017). Exosomes secreted from human-induced pluripotent stem cell-derived mesenchymal stem cells prevent osteonecrosis of the femoral head by promoting angiogenesis. *Int. J. Biol. Sci.* 13, 232–244. doi: 10.7150/ijbs.16951

Luzzani, C. D., and Miriuka, S. G. (2017). Pluripotent stem cells as a robust source of mesenchymal stem cells. *Stem Cell Rev. Rep.* 13, 68–78. doi: 10.1007/s12015-016-9695-z

Ma, T., Xie, M., Laurent, T., and Ding, S. (2013). Progress in the reprogramming of somatic cells. *Circ. Res.* 112, 562–574. doi: 10.1161/CIRCRESAHA.111.249235

Manassero, M., Paquet, J., Deschepper, M., Viateau, V., Retortillo, J., Bensidhoum, M., et al. (2016). Comparison of survival and osteogenic ability of human mesenchymal stem cells in orthotopic and ectopic sites in mice. *Tissue Eng. Part A* 22, 534–544. doi: 10.1089/ten.tea.2015.0346

Marcos-Campos, I., Marolt, D., Petridis, P., Bhumiratana, S., Schmidt, D., and Vunjak-Novakovic, G. (2012). Bone scaffold architecture modulates the development of mineralized bone matrix by human embryonic stem cells. *Biomaterials* 33, 8329–8342. doi: 10.1016/j.biomaterials.2012.08.013

Marcucio, R. S., Nauth, A., Giannoudis, P. V., Bahney, C., Piuzzi, N. S., Muschler, G., et al. (2015). Stem cell therapies in orthopaedic trauma. *J. Orthop. Trauma* 29, S24–S27. doi: 10.1097/BOT.0000000000000459

Marie, P. J. (2014). Bone cell senescence: mechanisms and perspectives. *J. Bone Miner. Res.* 29, 1311–1321. doi: 10.1002/jbmr.2190

Marolt, D., Augst, A., Freed, L. E., Vepari, C., Fajardo, R., Patel, N., et al. (2006). Bone and cartilage tissue constructs grown using human bone marrow stromal cells, silk scaffolds and rotating bioreactors. *Biomaterials* 27, 6138–6149. doi: 10.1016/j.biomaterials.2006.07.015

Marolt, D., Knezevic, M., and Novakovic, G. V. (2010). Bone tissue engineering with human stem cells. *Stem Cell Res. Ther.* 1:10. doi: 10.1186/scrt10

Marote, A., Teixeira, F. G., Mendes-Pinheiro, B., and Salgado, A. J. (2016). MSCs-derived exosomes: cell-secreted nanovesicles with regenerative potential. *Front. Pharmacol.* 7:231. doi: 10.3389/fphar.2016.00231

Martin, I., Muraglia, A., Campanile, G., Cancedda, R., and Quarto, R. (1997). Fibroblast growth factor-2 supports *ex vivo* expansion and maintenance of osteogenic precursors from human bone marrow. *Endocrinology* 138, 4456–4462. doi: 10.1210/endo.138.10.5425

Mauney, J. R., Kaplan, D. L., and Volloch, V. (2004). Matrix-mediated retention of osteogenic differentiation potential by human adult bone marrow stromal cells during *ex vivo* expansion. *Biomaterials* 25, 3233–3243. doi: 10.1016/j.biomaterials.2003.10.005

Mauney, J. R., Kirker-Head, C., Abrahamson, L., Gronowicz, G., Volloch, V., and Kaplan, D. L. (2006). Matrix-mediated retention of *in vitro* osteogenic differentiation potential and *in vivo* bone-forming capacity by human adult bone marrow-derived mesenchymal stem cells during *ex vivo* expansion. *J. Biomed. Mater. Res. Part A* 79, 464–475. doi: 10.1002/jbm.a.30876

Meinel, L., Fajardo, R., Hofmann, S., Langer, R., Chen, J., Snyder, B., et al. (2005). Silk implants for the healing of critical size bone defects. *Bone* 37, 688–698. doi: 10.1016/j.bone.2005.06.010

Meinel, L., Hofmann, S., Betz, O., Fajardo, R., Merkle, H. P., Langer, R., et al. (2006). Osteogenesis by human mesenchymal stem cells cultured on silk biomaterials: comparison of adenovirus mediated gene transfer and protein delivery of BMP-2. *Biomaterials* 27, 4993–5002. doi: 10.1016/j.biomaterials.2006.05.021

Meinel, L., Karageorgiou, V., Fajardo, R., Snyder, B., Shinde-Patil, V., Zichner, L., et al. (2004). Bone tissue engineering using human mesenchymal stem cells: effects of scaffold material and medium flow. *Ann. Biomed. Eng.* 32, 112–122. doi: 10.1023/B:ABME.0000007796.48329.b4

Méndez-Ferrer, S., Michurina, T. V., Ferraro, F., Mazloom, A. R., MacArthur, B. D., Lira, S. A., et al. (2010). Mesenchymal and haematopoietic stem cells form a unique bone marrow niche. *Nature* 466, 829–834. doi: 10.1038/nature09262

Mendt, M., Kamerkar, S., Sugimoto, H., McAndrews, K. M., Wu, C. C., Gagea, M., et al. (2018). Generation and testing of clinical-grade exosomes for pancreatic cancer. *JCI Insight* 3:99263. doi: 10.1172/jci.insight.99263

Mitra, D., Whitehead, J., Yasui, O. W., and Leach, J. K. (2017). Bioreactor culture duration of engineered constructs influences bone formation by mesenchymal stem cells. *Biomaterials* 146, 29–39. doi: 10.1016/j.biomaterials.2017.08.044

Mizukami, A., Thomé, C. H., Ferreira, G. A., Lanfredi, G. P., Covas, D. T., Pitteri, S. J., et al. (2019). Proteomic identification and time-course monitoring of secreted proteins during expansion of human mesenchymal stem/stromal in stirred-tank bioreactor. *Front. Bioeng. Biotechnol.* 7:154. doi: 10.3389/fbioe.2019.00154

Murgia, A., Veronesi, E., Candini, O., Caselli, A., D'Souza, N., Rasini, V., et al. (2016). Potency biomarker signature genes from multiparametric osteogenesis assays: will cGMP human bone marrow mesenchymal stromal cells make bone? *PLoS ONE* 11:e016362. doi: 10.1371/journal.pone.0163629

Muschler, G. F., Boehm, C., and Easley, K. (1997). Aspiration to obtain osteoblast progenitor cells from human bone marrow: the influence of aspiration volume. *J. Bone Jt. Surg. Am.* 79, 1699–1709. doi: 10.2106/00004623-199711000-00012

Nancarrow-Lei, R., Mafi, P., Mafi, R., and Khan, W. (2017). A systemic review of adult mesenchymal stem cell sources and their multilineage differentiation potential relevant to musculoskeletal tissue repair and regeneration. *Curr. Stem Cell Res. Ther.* 12, 601–610. doi: 10.2174/1574888X12666170608124303

Ogata, K., Katagiri, W., and Hibi, H. (2017). Secretomes from mesenchymal stem cells participate in the regulation of osteoclastogenesis *in vitro*. *Clin. Oral Investig.* 21, 1979–1988. doi: 10.1007/s00784-016-1986-x

Ogata, K., Katagiri, W., Osugi, M., Kawai, T., Sugimura, Y., Hibi, H., et al. (2015). Evaluation of the therapeutic effects of conditioned media from mesenchymal stem cells in a rat bisphosphonate-related osteonecrosis of the jaw-like model. *Bone* 74, 95–105. doi: 10.1016/j.bone.2015.01.011

Ogata, K., Matsumura, M., Moriyama, M., Katagiri, W., Hibi, H., and Nakamura, S. (2018). Cytokine mixtures mimicking secretomes from mesenchymal stem cells improve medication-related osteonecrosis of the jaw in a rat model. *JBMR Plus* 2, 69–80. doi: 10.1002/jbm4.10013

Oryan, A., Kamali, A., Moshirib, A., and Eslaminejad, M. B. (2017). Role of mesenchymal stem cells in bone regenerative medicine: what is the evidence? *Cells Tissues Organs* 204, 59–83. doi: 10.1159/000469704

Osinga, R., Di Maggio, N., Todorov, A., Allafi, N., Barbero, A., Laurent, F., et al. (2016). Generation of a bone organ by human adipose-derived stromal cells through endochondral ossification. *Stem Cells Transl. Med.* 5, 1090–1097. doi: 10.5966/sctm.2015-0256

Oskowitz, A., McFerrin, H., Gutschow, M., Carter, M. L., and Pochampally, R. (2011). Serum-deprived human multipotent mesenchymal stromal cells (MSCs) are highly angiogenic. *Stem Cell Res.* 6, 215–225. doi: 10.1016/j.scr.2011.01.004

Osugi, M., Katagiri, W., Yoshimi, R., Inukai, T., Hibi, H., and Ueda, M. (2012). Conditioned media from mesenchymal stem cells enhanced bone regeneration in rat calvarial bone defects. *Tissue Eng. Part A* 18, 1479–1489. doi: 10.1089/ten.tea.2011.0325

Park, D., Spencer, J. A., Koh, B. I., Kobayashi, T., Fujisaki, J., Clemens, T. L., et al. (2012). Endogenous bone marrow MSCs are dynamic, fate-restricted

participants in bone maintenance and regeneration. *Cell Stem Cell* 10, 259–272. doi: 10.1016/j.stem.2012.02.003

Patterson, T. E., Boehm, C., Nakamoto, C., Rozic, R., Walker, E., Piuzzi, N. S., et al. (2017). The efficiency of bone marrow aspiration for the harvest of connective tissue progenitors from the human iliac crest. *J. Bone Jt. Surg. Am.* 99, 1673–1682. doi: 10.2106/JBJS.17.00094

Petite, H., Viateau, V., Bensaïd, W., Meunier, A., De Pollak, C., Bourguignon, M., et al. (2000). Tissue-engineered bone regeneration. *Nat. Biotechnol.* 18, 959–963. doi: 10.1038/79449

Phetfong, J., Sanvoranart, T., Nartprayut, K., Nimsanor, N., Seenprachawong, K., Prachayasittikul, V., et al. (2016). Osteoporosis: the current status of mesenchymal stem cell-based therapy. *Cell. Mol. Biol. Lett.* 21:12. doi: 10.1186/s11658-016-0013-1

Phillips, M. D., Kuznetsov, S. A., Cherman, N., Park, K., Chen, K. G., McClendon, B. N., et al. (2014). Directed differentiation of human induced pluripotent stem cells toward bone and cartilage: *in vitro* versus *in vivo* assays. *Stem Cells Transl. Med.* 3, 867–878. doi: 10.5966/sctm.2013-0154

Pierini, M., Di Bella, C., Dozza, B., Frisoni, T., Martella, E., Bellotti, C., et al. (2013). The posterior iliac crest outperforms the anterior iliac crest when obtaining mesenchymal stem cells from bone marrow. *J. Bone Jt. Surg. Am.* 95, 1101–1107. doi: 10.2106/JBJS.L.00429

Pittenger, M. F., Mackay, A. M., Beck, S. C., Jaiswal, R. K., Douglas, R., Mosca, J. D., et al. (1999). Multilineage potential of adult human mesenchymal stem cells. *Science* 284, 143–147. doi: 10.1126/science.284.5411.143

Ponte, A. L., Marais, E., Gallay, N., Langonné, A., Delorme, B., Hérault, O., et al. (2007). The *in vitro* migration capacity of human bone marrow mesenchymal stem cells: comparison of chemokine and growth factor chemotactic activities. *Stem Cells* 25, 1737–1745. doi: 10.1634/stemcells.2007-0054

Qi, X., Zhang, J., Yuan, H., Xu, Z., Li, Q., Niu, X., et al. (2016). Exosomes secreted by human-induced pluripotent stem cell-derived mesenchymal stem cells repair critical-sized bone defects through enhanced angiogenesis and osteogenesis in osteoporotic rats. *Int. J. Biol. Sci.* 12, 836–849. doi: 10.7150/ijbs.14809

Qin, Y., Wang, L., Gao, Z., Chen, G., and Zhang, C. (2016). Bone marrow stromal/stem cell-derived extracellular vesicles regulate osteoblast activity and differentiation *in vitro* and promote bone regeneration *in vivo*. *Sci. Rep.* 6:21961. doi: 10.1038/srep21961

Quarto, R., Mastrogiacomo, M., Cancedda, R., Kutepov, S. M., Mukhachev, V., Lavroukov, A., et al. (2001). Repair of large bone defects with the use of autologous bone marrow stromal cells. *N. Engl. J. Med.* 344, 385–386. doi: 10.1056/NEJM200102013440516

Quesenberry, P. J., Aliotta, J., Deregibus, M. C., and Camussi, G. (2015). Role of extracellular RNA-carrying vesicles in cell differentiation and reprogramming. *Stem Cell Res. Ther.* 6:153. doi: 10.1186/s13287-015-0150-x

Rakian, R., Block, T. J., Johnson, S. M., Marinkovic, M., Wu, J., Dai, Q., et al. (2015). Native extracellular matrix preserves mesenchymal stem cell "stemness" and differentiation potential under serum-free culture conditions. *Stem Cell Res. Ther.* 6:235. doi: 10.1186/s13287-015-0235-6

Raposo, G., Nijman, H. W., Stoorvogel, W., Leijendekker, R., Harding, C. V., Melief, C. J. M., et al. (1996). B lymphocytes secrete antigen-presenting vesicles. *J. Exp. Med.* 183, 1161–1172. doi: 10.1084/jem.183.3.1161

Ratajczak, J., Miekus, K., Kucia, M., Zhang, J., Reca, R., Dvorak, P., et al. (2006). Embryonic stem cell-derived microvesicles reprogram hematopoietic progenitors: evidence for horizontal transfer of mRNA and protein delivery. *Leukemia* 20, 847–856. doi: 10.1038/sj.leu.2404132

Redondo, L. M., García, V., Peral, B., Verrier, A., Becerra, J., Sánchez, A., et al. (2018). Repair of maxillary cystic bone defects with mesenchymal stem cells seeded on a cross-linked serum scaffold. *J. Cranio Maxillofac. Surg.* 46, 222–229. doi: 10.1016/j.jcms.2017.11.004

Reinisch, A., Etchart, N., Thomas, D., Hofmann, N. A., Fruehwirth, M., Sinha, S., et al. (2015). Epigenetic and *in vivo* comparison of diverse MSC sources reveals an endochondral signature for human hematopoietic niche formation. *Blood* 125, 249–260. doi: 10.1182/blood-2014-04-572255

Reumann, M. K., Linnemann, C., Aspera-Werz, R. H., Arnold, S., Held, M., Seeliger, C., et al. (2018). Donor site location is critical for proliferation, stem cell capacity, and osteogenic differentiation of adipose mesenchymal stem/stromal cells: Implications for bone tissue engineering. *Int. J. Mol. Sci.* 19:E1868. doi: 10.3390/ijms19071868

Rindone, A. N., Kachniarz, B., Achebe, C. C., Riddle, R. C., O'Sullivan, A. N., Dorafshar, A. H., et al. (2019). Heparin-conjugated decellularized bone particles promote enhanced osteogenic signaling of PDGF-BB to adipose-derived stem cells in tissue engineered bone grafts. *Adv. Healthc. Mater.* 8:e1801565. doi: 10.1002/adhm.201801565

Robey, P. G. (2011). Cell sources for bone regeneration: the good, the bad, and the ugly (but promising). *Tissue Eng. Part B Rev.* 17, 423–430. doi: 10.1089/ten.teb.2011.0199

Robey, P. G., Kuznetsov, S. A., Ren, J., Klein, H. G., Sabatino, M., and Stroncek, D. F. (2015). Generation of clinical grade human bone marrow stromal cells for use in bone regeneration. *Bone* 70, 87–92. doi: 10.1016/j.bone.2014.07.020

Rohde, E., Pachler, K., and Gimona, M. (2019). Manufacturing and characterization of extracellular vesicles from umbilical cord–derived mesenchymal stromal cells for clinical testing. *Cytotherapy* 21, 581–592. doi: 10.1016/j.jcyt.2018.12.006

Sacchetti, B., Funari, A., Michienzi, S., Di Cesare, S., Piersanti, S., Saggio, I., et al. (2007). Self-renewing osteoprogenitors in bone marrow sinusoids can organize a hematopoietic microenvironment. *Cell* 131, 324–336. doi: 10.1016/j.cell.2007.08.025

Schallmoser, K., Rohde, E., Bartmann, C., Obenauf, A. C., Reinisch, A., and Strunk, D. (2009). Platelet-derived growth factors for GMP-compliant propagation of mesenchymal stromal cells. *Biomed. Mater. Eng.* 19, 271–276. doi: 10.3233/BME-2009-0591

Schuh, C. M. A. P., Cuenca, J., Alcayaga-Miranda, F., and Khoury, M. (2019). Exosomes on the border of species and kingdom intercommunication. *Transl. Res.* 210, 80–98. doi: 10.1016/j.trsl.2019.03.008

Sensebé, L., Gadelorge, M., and Fleury-Cappellesso, S. (2013). Production of mesenchymal stromal/stem cells according to good manufacturing practices: a review. *Stem Cell Res. Ther.* 4:66. doi: 10.1186/scrt217

Serra, S. C., Costa, J. C., Assunção-Silva, R. C., Teixeira, F. G., Silva, N. A., Anjo, S. I., et al. (2018). Influence of passage number on the impact of the secretome of adipose tissue stem cells on neural survival, neurodifferentiation and axonal growth. *Biochimie* 155, 119–128. doi: 10.1016/j.biochi.2018.09.012

Sheyn, D., Shapiro, G., Tawackoli, W., Jun, D. S., Koh, Y., Kang, K. B., et al. (2016). PTH induces systemically administered mesenchymal stem cells to migrate to and regenerate spine injuries. *Mol. Ther.* 24, 318–330. doi: 10.1038/mt.2015.211

Sikavitsas, V. I., Bancroft, G. N., Holtorf, H. L., Jansen, J. A., and Mikos, A. G. (2003). Mineralized matrix deposition by marrow stromal osteoblasts in 3D perfusion culture increases with increasing fluid shear forces. *Proc. Natl. Acad. Sci. U.S.A.* 100, 14683–14688. doi: 10.1073/pnas.2434367100

Sladkova, M., Alawadhi, R., Alhaddad, R. J., Esmael, A., Alansari, S., Saad, M., et al. (2018). Segmental additive tissue engineering. *Sci. Rep.* 8:10895. doi: 10.1038/s41598-018-29270-4

Sørensen, J. R., Koroma, K. E., Ding, M., Wendt, D., Jespersen, S., Juhl, M. V., et al. (2012). Effects of a perfusion bioreactor activated novel bone substitute in spine fusion in sheep. *Eur. Spine J.* 21, 1740–1747. doi: 10.1007/s00586-012-2421-x

Spitzhorn, L. S., Megges, M., Wruck, W., Rahman, M. S., Otte, J., Degistirici, Ö., et al. (2019). Human iPSC-derived MSCs (iMSCs) from aged individuals acquire a rejuvenation signature. *Stem Cell Res. Ther.* 10:100. doi: 10.1186/s13287-019-1209-x

Stegemann, J. P., Verrier, S., Gebhard, F., Laschke, M. W., Martin, I., Simpson, H., et al. (2014). Cell therapy for bone repair: narrowing the gap between vision and practice. *Eur. Cells Mater.* 27, 1–4. doi: 10.22203/eCM.v027sa01

Stolzing, A., Jones, E., McGonagle, D., and Scutt, A. (2008). Age-related changes in human bone marrow-derived mesenchymal stem cells: consequences for cell therapies. *Mech. Ageing Dev.* 129, 163–173. doi: 10.1016/j.mad.2007.12.002

Sudo, K., Kanno, M., Miharada, K., Ogawa, S., Hiroyama, T., Saijo, K., et al. (2007). Mesenchymal progenitors able to differentiate into osteogenic, chondrogenic, and/or adipogenic cells *in vitro* are present in most primary fibroblast-like cell populations. *Stem Cells* 25, 1610–1617. doi: 10.1634/stemcells.2006-0504

Sutaria, D. S., Badawi, M., Phelps, M. A., and Schmittgen, T. D. (2017). Achieving the promise of therapeutic extracellular vesicles: the devil is in details of therapeutic loading. *Pharm. Res.* 34, 1053–1066. doi: 10.1007/s11095-017-2123-5

Takahashi, K., Tanabe, K., Ohnuki, M., Narita, M., Ichisaka, T., Tomoda, K., et al. (2007). Induction of pluripotent stem cells from adult human fibroblasts by defined factors. *Cell* 131, 861–872. doi: 10.1016/j.cell.2007.11.019

Teixeira, F. G., Panchalingam, K. M., Assunção-Silva, R., Serra, S. C., Mendes-Pinheiro, B., Patrício, P., et al. (2016). Modulation of the mesenchymal stem cell secretome using computer-controlled bioreactors: impact on neuronal cell proliferation, survival and differentiation. *Sci. Rep.* 6:27791. doi: 10.1038/srep27791

Tencerova, M., Frost, M., Figeac, F., Nielsen, T. K., Ali, D., Lauterlein, J. J. L., et al. (2019). Obesity-associated hypermetabolism and accelerated senescence of bone marrow stromal stem cells suggest a potential mechanism for bone fragility. *Cell Rep.* 27, 2050–2062.e6. doi: 10.1016/j.celrep.2019.04.066

Timmers, L., Lim, S. K., Arslan, F., Armstrong, J. S., Hoefer, I. E., Doevendans, P. A., et al. (2008). Reduction of myocardial infarct size by human mesenchymal stem cell conditioned medium. *Stem Cell Res.* 1, 129–137. doi: 10.1016/j.scr.2008.02.002

Timmins, N. E., Scherberich, A., Früh, J. A., Heberer, M., Martin, I., and Jakob, M. (2007). Three-dimensional cell culture and tissue engineering in a T-CUP (tissue culture under perfusion). *Tissue Eng.* 13, 2021–2028. doi: 10.1089/ten.2006.0158

Tonnarelli, B., Centola, M., Barbero, A., Zeller, R., and Martin, I. (2014). Re-engineering development to instruct tissue regeneration. *Curr. Top. Dev. Biol.* 108, 319–338. doi: 10.1016/B978-0-12-391498-9.00005-X

Topoluk, N., Hawkins, R., Tokish, J., and Mercuri, J. (2017). Amniotic mesenchymal stromal cells exhibit preferential osteogenic and chondrogenic differentiation and enhanced matrix production compared with adipose mesenchymal stromal cells. *Am. J. Sports Med.* 45, 2637–2646. doi: 10.1177/0363546517706138

Tricarico, C., Clancy, J., and D'Souza-Schorey, C. (2017). Biology and biogenesis of shed microvesicles. *Small GTPases* 8, 220–232. doi: 10.1080/21541248.2016.1215283

Turchinovich, A., Drapkina, O., and Tonevitsky, A. (2019). Transcriptome of extracellular vesicles: state-of-the-art. *Front. Immunol.* 10:202. doi: 10.3389/fimmu.2019.00202

Tzioupis, C., and Giannoudis, P. V. (2007). Prevalence of long-bone non-unions. *Injury* 38:S3. doi: 10.1016/j.injury.2007.02.005

van Balkom, B. W. M., Gremmels, H., Giebel, B., and Lim, S. K. (2019). Proteomic signature of mesenchymal stromal cell-derived small extracellular vesicles. *Proteomics* 19:e1800163. doi: 10.1002/pmic.201800163

Van Niel, G., D'Angelo, G., and Raposo, G. (2018). Shedding light on the cell biology of extracellular vesicles. *Nat. Rev. Mol. Cell Biol.* 19, 213–228. doi: 10.1038/nrm.2017.125

Vetsch, J. R., Müller, R., and Hofmann, S. (2016). The influence of curvature on three-dimensional mineralized matrix formation under static and perfused conditions: an *in vitro* bioreactor model. *J. R. Soc. Interface* 13:2016042. doi: 10.1098/rsif.2016.0425

Wang, B., Lee, W. Y. W., Huang, B., Zhang, J. F., Wu, T. Y., Jiang, X., et al. (2016). Secretome of human fetal mesenchymal stem cell ameliorates replicative senescen. *Stem Cells Dev.* 25, 1755–1766. doi: 10.1089/scd.2016.0079

Webber, J., and Clayton, A. (2013). How pure are your vesicles? *J. Extracell. Vesicles* 2. doi: 10.3402/jev.v2i0.19861

Weilner, S., Schraml, E., Wieser, M., Messner, P., Schneider, K., Wassermann, K., et al. (2016). Secreted microvesicular miR-31 inhibits osteogenic differentiation of mesenchymal stem cells. *Aging Cell* 15, 744–754. doi: 10.1111/acel.12484

Whitford, W., and Guterstam, P. (2019). Exosome manufacturing status. *Future Med. Chem.* 11, 1225–1236. doi: 10.4155/fmc-2018-0417

Willms, E., Johansson, H. J., Mäger, I., Lee, Y., Blomberg, K. E. M., Sadik, M., et al. (2016). Cells release subpopulations of exosomes with distinct molecular and biological properties. *Sci. Rep.* 6:22519. doi: 10.1038/srep22519

Witwer, K. W., Van Balkom, B. W. M., Bruno, S., Choo, A., Dominici, M., Gimona, M., et al. (2019). Defining mesenchymal stromal cell (MSC)-derived small extracellular vesicles for therapeutic applications. *J. Extracell. Vesicles* 8:1609206. doi: 10.1080/20013078.2019.1609206

Woloszyk, A., Dircksen, S. H., Bostanci, N., Muöller, R., Hofmann, S., and Mitsiadis, T. A. (2014). Influence of the mechanical environment on the engineering of mineralised tissues using human dental pulp stem cells and silk fibroin scaffolds. *PLoS ONE* 9:e111010. doi: 10.1371/journal.pone.0111010

Wu, Q., Yang, B., Hu, K., Cao, C., Man, Y., and Wang, P. (2017). Deriving osteogenic cells from induced pluripotent stem cells for bone tissue engineering. *Tissue Eng. Part B Rev.* 23, 1–8. doi: 10.1089/ten.teb.2015.0559

Xie, H., Wang, Z., Zhang, L., Lei, Q., Zhao, A., Wang, H., et al. (2017). Extracellular vesicle-functionalized decalcified bone matrix scaffolds with enhanced pro-angiogenic and pro-bone regeneration activities. *Sci. Rep.* 7:45622. doi: 10.1038/srep45622

Xu, J., Wang, B., Sun, Y., Wu, T., Liu, Y., Zhang, J., et al. (2016). Human fetal mesenchymal stem cell secretome enhances bone consolidation in distraction osteogenesis. *Stem Cell Res. Ther.* 7:134. doi: 10.1186/s13287-016-0392-2

Yao, W., and Lane, N. E. (2015). Targeted delivery of mesenchymal stem cells to the bone. *Bone* 70, 62–65. doi: 10.1016/j.bone.2014.07.026

Yao, W., Lay, Y. A. E., Kot, A., Liu, R., Zhang, H., Chen, H., et al. (2016). Improved mobilization of exogenous mesenchymal stem cells to bone for fracture healing and sex difference. *Stem Cells* 34, 2587–2600. doi: 10.1002/stem.2433

Yeo, R. W. Y., Lai, R. C., Zhang, B., Tan, S. S., Yin, Y., Teh, B. J., et al. (2013). Mesenchymal stem cell: an efficient mass producer of exosomes for drug delivery. *Adv. Drug Deliv. Rev.* 65, 336–341. doi: 10.1016/j.addr.2012.07.001

Zhang, B., Yin, Y., Lai, R. C., Tan, S. S., Choo, A. B. H., and Lim, S. K. (2014). Mesenchymal stem cells secrete immunologically active exosomes. *Stem Cells Dev.* 23, 1233–1244. doi: 10.1089/scd.2013.0479

Zhang, J., Liu, X., Li, H., Chen, C., Hu, B., Niu, X., et al. (2016a). Exosomes/tricalcium phosphate combination scaffolds can enhance bone regeneration by activating the PI3K/Akt signaling pathway. *Stem Cell Res. Ther.* 7:136. doi: 10.1186/s13287-016-0391-3

Zhang, S., Chu, W. C., Lai, R. C., Lim, S. K., Hui, J. H. P., and Toh, W. S. (2016b). Exosomes derived from human embryonic mesenchymal stem cells promote osteochondral regeneration. *Osteoarthr. Cartil.* 24, 2135–2140. doi: 10.1016/j.joca.2016.06.022

Zhang, X., Hirai, M., Cantero, S., Ciubotariu, R., Dobrila, L., Hirsh, A., et al. (2011). Isolation and characterization of mesenchymal stem cells from human umbilical cord blood: reevaluation of critical factors for successful isolation and high ability to proliferate and differentiate to chondrocytes as compared to mesenchymal stem cells from bone marrow and adipose tissue. *J. Cell. Biochem.* 112, 1206–1218. doi: 10.1002/jcb.23042

Zhang, Y., Hao, Z., Wang, P., Xia, Y., Wu, J., Xia, D., et al. (2019). Exosomes from human umbilical cord mesenchymal stem cells enhance fracture healing through HIF-1α-mediated promotion of angiogenesis in a rat model of stabilized fracture. *Cell Prolif.* 52:e12570. doi: 10.1111/cpr.12570

Zhao, F., van Rietbergen, B., Ito, K., and Hofmann, S. (2018). Flow rates in perfusion bioreactors to maximise mineralisation in bone tissue engineering *in vitro*. *J. Biomech.* 79, 232–237. doi: 10.1016/j.jbiomech.2018.08.004

Zhou, B. O., Yue, R., Murphy, M. M., Peyer, J. G., and Morrison, S. J. (2014). Leptin-receptor-expressing mesenchymal stromal cells represent the main source of bone formed by adult bone marrow. *Cell Stem Cell* 15, 154–168. doi: 10.1016/j.stem.2014.06.008

Zhu, S., Li, W., Zhou, H., Wei, W., Ambasudhan, R., Lin, T., et al. (2010). Reprogramming of human primary somatic cells by OCT4 and chemical compounds. *Cell Stem Cell* 7, 651–655. doi: 10.1016/j.stem.2010.11.015

Zhu, Y., Jia, Y., Wang, Y., Xu, J., and Chai, Y. (2019). Impaired bone regenerative effect of exosomes derived from bone marrow mesenchymal stem cells in type 1 diabetes. *Stem Cells Transl. Med.* 8, 593–605. doi: 10.1002/sctm.18-0199

Zuk, P. A., Zhu, M., Mizuno, H., Huang, J., Futrell, J. W., Katz, A. J., et al. (2001). Multilineage cells from human adipose tissue: implications for cell-based therapies. *Tissue Eng.* 7, 211–228. doi: 10.1089/107632701300062859

Conflict of Interest: The authors declare that the research was conducted in the absence of any commercial or financial relationships that could be construed as a potential conflict of interest.

frontiers in Bioengineering and Biotechnology

ORIGINAL RESEARCH
published: 20 December 2019
doi: 10.3389/fbioe.2019.00431

Unraveling the Molecular Signature of Extracellular Vesicles From Endometrial-Derived Mesenchymal Stem Cells: Potential Modulatory Effects and Therapeutic Applications

Federica Marinaro[1†], *María Gómez-Serrano*[2,3,4†], *Inmaculada Jorge*[2,3*], *Juan Carlos Silla-Castro*[5], *Jesús Vázquez*[2,3], *Francisco Miguel Sánchez-Margallo*[1,2*], *Rebeca Blázquez*[1,2], *Esther López*[1], *Verónica Álvarez*[1] and *Javier G. Casado*[1,2]

[1] Stem Cell Therapy Unit, Jesús Usón Minimally Invasive Surgery Centre, Cáceres, Spain, [2] CIBER de Enfermedades Cardiovasculares, Madrid, Spain, [3] Laboratory of Cardiovascular Proteomics, Centro Nacional de Investigaciones Cardiovasculares, Madrid, Spain, [4] Center for Tumor Biology and Immunology, Institute of Molecular Biology and Tumor Research, Philipps University, Marburg, Germany, [5] Bioinformatics Unit, Centro Nacional de Investigaciones Cardiovasculares, Madrid, Spain

Endometrial-derived Mesenchymal Stem Cells (endMSCs) are involved in the regeneration and remodeling of human endometrium, being considered one of the most promising candidates for stem cell-based therapies. Their therapeutic effects have been found to be mediated by extracellular vesicles (EV-endMSCs) with pro-angiogenic, anti-apoptotic, and immunomodulatory effects. Based on that, the main goal of this study was to characterize the proteome and microRNAome of these EV-endMSCs by proteomics and transcriptomics approaches. Additionally, we hypothesized that inflammatory priming of endMSCs may contribute to modify the therapeutic potential of these vesicles. High-throughput proteomics revealed that 617 proteins were functionally annotated as *Extracellular exosome* (GO:0070062), corresponding to the 70% of the EV-endMSC proteome. Bioinformatics analyses allowed us to identify that these proteins were involved in adaptive/innate immune response, complement activation, antigen processing/presentation, negative regulation of apoptosis, and different signaling pathways, among others. Of note, multiplexed quantitative proteomics and Systems Biology analyses showed that IFNγ priming significantly modulated the protein profile of these vesicles. As expected, proteins involved in antigen processing and presentation were significantly increased. Interestingly, immunomodulatory proteins, such as CSF1, ERAP1, or PYCARD were modified. Regarding miRNAs expression profile in EV-endMSCs, Next-Generation Sequencing (NGS) showed that the preferred site of microRNAome targeting was the nucleus ($n = 371$ microTargets), significantly affecting *signal transduction* (GO:0007165), *cell proliferation* (GO:0008283), and *apoptotic processes* (GO:0006915), among others. Interestingly, NGS analyses highlighted that several miRNAs, such as hsa-miR-150-5p or hsa-miR-196b-5p, were differentially expressed in IFNγ-primed EV-endMSCs. These miRNAs have a functional involvement in glucocorticoid receptor signaling, IL-6/8/12 signaling, and in the role of macrophages.

OPEN ACCESS

Edited by:
Wolfgang Holnthoner, Ludwig Boltzmann Institute for Experimental and Clinical Traumatology, Austria

Reviewed by:
Benedetta Bussolati, University of Turin, Italy
Michela Pozzobon, University of Padova, Italy

***Correspondence:**
Inmaculada Jorge
inmaculada.jorge@cnic.es
Francisco Miguel Sánchez-Margallo
msanchez@ccmijesususon.com

[†]These authors have contributed equally to this work and share first authorship

Specialty section:
This article was submitted to Tissue Engineering and Regenerative Medicine, a section of the journal Frontiers in Bioengineering and Biotechnology

Received: *20 September 2019*
Accepted: *05 December 2019*
Published: *20 December 2019*

Citation:
Marinaro F, Gómez-Serrano M, Jorge I, Silla-Castro JC, Vázquez J, Sánchez-Margallo FM, Blázquez R, López E, Álvarez V and Casado JG (2019) Unraveling the Molecular Signature of Extracellular Vesicles From Endometrial-Derived Mesenchymal Stem Cells: Potential Modulatory Effects and Therapeutic Applications. Front. Bioeng. Biotechnol. 7:431. doi: 10.3389/fbioe.2019.00431

In summary, these results allowed us to understand the complexity of the molecular networks in EV-endMSCs and their potential effects on target cells. To our knowledge, this is the first comprehensive study based on proteomic and genomic approaches to unravel the therapeutic potential of these extracellular vesicles, that may be used as immunomodulatory effectors in the treatment of inflammatory conditions.

Keywords: mesenchymal stem cells, endometrial, proteomic analyses, next generation sequencing-NGS, interferon-γ, extracellular vesicles (EV), miRNA-microRNA, priming

INTRODUCTION

Mesenchymal Stem Cells (MSCs) obtained from endometrial tissue have become one of the most promising candidates in the field of stem cell therapies. They are involved in the dynamic remodeling and regeneration of human endometrium, being necessary for normal tissue self-renewal. In bibliography, different populations of endometrial stem cells have been described (Chan et al., 2004) and different names have been used for these cells, such as menstrual blood-derived stromal/mesenchymal cells, or endometrial-derived stromal/mesenchymal stem cells (endMSCs) (Kyurkchiev et al., 2010; Gargett et al., 2016). Additionally, different laboratory procedures have been established for *in vitro* isolation and expansion (Schüring et al., 2011; Wang et al., 2012; Rossignoli et al., 2013). Nowadays, menstrual blood-derived endMSCs can be easily isolated by a non-invasive method, without any painful procedure and their *in vitro* expansion can be achieved by simple, and reproducible methods (Sun et al., 2019).

The therapeutic potential of endMSCs have been described and reviewed for different diseases, such as myocardial infarction (Liu et al., 2019), and Parkinson disease (Bagheri-Mohammadi et al., 2019). Recent preclinical studies have also evaluated their therapeutic effects in murine models of pulmonary fibrosis (Zhao et al., 2018), and experimental colitis (Lv et al., 2014). In addition, a recent clinical trial using autologous menstrual blood-derived stromal cells have shown satisfactory results for the treatment of severe Asherman's syndrome (Tan et al., 2016).

The biological mechanisms underlying endMSCs function have been associated to their immunomodulatory capacity (Nikoo et al., 2012), which is mediated—at least in part—by indoleamine 2,3-dioxygenase-1, cyclooxygenase-2, IL-10, and IL-27 (Peron et al., 2012; Nikoo et al., 2014). Moreover, these cells have demonstrated a potent pro-angiogenic and anti-apoptotic effect mediated by HGF, IGF-1, and VEGF (Du et al., 2016). Similarly to other MSCs, such as adipose-derived MSCs, or bone marrow-derived MSCs, the therapeutic effect of endMSCs is mediated by the paracrine action of extracellular vesicles (EVs). EVs (including microvesicles, exosomes, and apoptotic bodies) act as carriers of bioactive molecules, such as proteins, microRNAs (miRNAs), and lipids (Doyle and Wang, 2019). In this sense, our group has recently revealed the presence of TGF-β in EVs derived from endMSCs (EV-endMSCs). The functional studies performed by TGF-β blockade demonstrated that this molecule is partially involved in the immunomodulatory effect of these vesicles (Álvarez et al., 2018). Apart from their immunomodulatory effects, EV-endMSCs have been used as co-adjuvants to improve the *in vitro* fertilization outcomes in murine models (Blázquez et al., 2018), and the proteomic analysis of these EVs revealed an abundant expression of proteins involved in embryo development (Marinaro et al., 2019).

These preliminary results opened several questions about the hypothetical biological mechanisms that may mediate the therapeutic effect of EV-endMSCs. In this regard, a profound characterization of proteins and miRNAs, as regulatory elements, may help us to identify protein or gene targets for the treatment of specific diseases, increasing the translational impact of this research.

On the other hand, an important issue in the field of EVs derived from MSCs relies in the enhancement of their therapeutic effect. Basically, the main goal is to get vesicles with more biologically relevant effector molecules. During the last years, the protocols for MSCs priming (also called "MSCs licensing"), to generate more immunosuppressive MSCs, are gaining interest. This idea has been studied by using Interferon gamma (IFNγ)-priming (DelaRosa et al., 2009; Chinnadurai et al., 2014; Liang et al., 2018), Toll-like receptors priming (Sangiorgi and Panepucci, 2016; Najar et al., 2017), and other inflammatory stimuli (Kim and Cho, 2016). This concept has been recently reviewed by Yin et al. (2019) and the idea of MSCs priming has been extrapolated to the production of licensed EVs. Several examples can be found in bibliography: exosomes from Interleukin 1β-primed MSCs expressed miR-146a to induce M2 polarization (Song et al., 2017); EVs from TNFα/IFNγ-primed MSCs were found to enhance the immunomodulatory activity of MSCs by altering the COX2/PGE2 pathway (Harting et al., 2018); furthermore, it was proved that exosomes from MSCs under low oxygen conditions produced exosomes with a higher pro-mitotic effect (Yuan et al., 2019), and immunomodulatory potential (Showalter et al., 2019).

Abbreviations: DMEM, Dulbecco's Modified Eagle's medium; endMSCs, Endometrial-derived stromal/Mesenchymal Stem Cells; EV-endMSCs, Extracellular Vesicles from Endometrial-derived stromal/Mesenchymal Stem Cells; EVs, Extracellular Vesicles; FDR, False Discovery Rate; GO, Gene Ontology; IFNγ/EV-endMSCs, Extracellular Vesicles from IFNγ-primed Endometrial-derived stromal/Mesenchymal Stem Cells; IFNγ, Interferon gamma; IPA, Ingenuity Pathway Analysis; iTRAQ, Isobaric Tags for Relative and Absolute Quantitation; LC-MS/MS, Liquid chromatographytandem mass spectrometry; MS, Mass spectrometry; MSCs, Mesenchymal Stem Cells; NGS, Next Generation Sequencing; PBS, Phosphate buffered saline; PCA, Principal Component Analysis; SBT, Systems Biology Triangle; TMM, Trimmed mean of M-values; TPM, Tags Per Million; UMI, Unique Molecular Index; WSPP, Weighted Spectrum, Peptide, Protein.

In this work, we hypothesized that IFNγ-primed endMSCs may produce EVs (IFNγ/EV-endMSCs) with therapeutic effects that may be applicable in different clinical settings. In order to explore this idea, a large-scale analysis of proteins and miRNAs was performed using high throughput proteomic screening and Next Generation Sequencing (NGS), respectively. Our results revealed the existence of a wide range of proteins and miRNAs involved in the immune process, apoptosis, or cell signaling, among others. Nowadays, bioinformatics resources, such as DAVID (https://david.ncifcrf.gov/), miRTargetLink (https://ccb-web.cs.uni-saarland.de/mirtargetlink/), and Ingenuity Pathway Analysis (IPA) (https://www.qiagenbioinformatics.com/products/ingenuity-pathway-analysis/) are available and effective tools to handle and filter the massive amount of data at the basis of *in silico* functional analyses. In our study, these tools allowed us to classify proteins and miRNAs according to their biological roles. In the case of high throughput proteomic analysis, some of the most significant differences were observed on immune-related proteins, being the increase of CSF-1 in IFNγ/EV-endMSCs especially relevant. Additionally, NGS for miRNA expression identified relevant miRNAs whose target genes are implicated in the functionality of macrophages, and IL6/IL8/IL12 signaling. These results suggest that IFNγ/EV-endMSCs may serve as important carriers for miRNAs and proteins with immunomodulatory effects.

MATERIALS AND METHODS

Human endMSCs Isolation, Culture, and Characterization

This study was performed in agreement with the ethical guidelines of the Minimally Invasive Surgery Centre Research Ethics Committee, which approved the study (approval number: 017/16). All menstrual blood donors provided written informed consent to participate in the study. The endMSCs were obtained from menstrual blood collected by four healthy pre-menopausal women (30–34 years of age). Cells were isolated according to previously described protocols (Álvarez et al., 2018; Marinaro et al., 2019). Briefly, the menstrual blood was diluted 1:2 in phosphate buffered saline (PBS) and centrifuged at 450 × g for 10 min. The pellets of cells were resuspended in Dulbecco's Modified Eagle's medium (DMEM) (containing 10% fetal bovine serum (Gibco, Thermo Fisher Scientific, Bremen, Germany), 1% penicillin/streptomycin, and 1% glutamine) and cultured at 37°C and 5% CO_2. Cell culture medium was removed after 24 h to eliminate non-adherent cells. The adherent endMSCs were cultured to 80% confluency, then detached using PBS containing 0.25% trypsin (Lonza, Gaithersburg, MD, USA) and seeded again into 175 cm^2 culture flasks at a density of 5,000 cells/cm^2, changing the cell culture medium every 4 days. endMSCs characterization was carried out by flow cytometry and differentiation assay, as previously mentioned (Álvarez et al., 2018; Marinaro et al., 2019). Briefly, the phenotypic analysis by flow cytometry was performed on 2 × 10^5 cells (passages 3–4), stained with human monoclonal antibodies against CD14, CD20, CD34, CD44, CD45, CD73, CD80, CD90, CD117, and HLA-DR, using the isotype-matched antibodies as negative controls. A FACScalibur cytometer (BD Biosciences, San Jose, CA, USA) and the CellQuest software (BD Biosciences) were used to analyze the cells. The differentiation of endMSCs toward the adipogenic, chondrogenic, and osteogenic lineages was carried out on cells at passages 3–4. After 21 days of culture in differentiation specific media (Gibco, Thermo Fisher Scientific), adipogenic, chondrogenic, and osteogenic differentiation were evidenced by Oil Red O, Alcian Blue, and Alizarin Red S stainings, respectively.

Human endMSCs Treatment With IFNγ and EV-endMSCs Purification and Characterization

in vitro expanded endMSCs at passages 5–6 were treated with 3 ng/ml human IFNγ Recombinant Protein (Invitrogen, Thermo Fisher Scientific) for 6 days. For EV-endMSCs isolation, the standard culture medium (for control EV-endMSCs), or the culture medium containing IFNγ (for IFNγ/EV-endMSCs) were removed, and replaced by DMEM containing 1% insulin–transferrin–selenium (ThermoFisher Scientific), after rinsing with PBS. After 4 days, the supernatants were collected and EVs isolated according to a previous optimized protocol (Álvarez et al., 2018; Marinaro et al., 2019). Briefly, supernatants were centrifuged at 1,000 × g for 10 min and 5,000 × g for 20 min at 4°C to eliminate dead cells and debris. The supernatants were then filtered using firstly 450 nm pore size sterile cellulose acetate filters, followed by 200 nm pore size filters (Corning, NY, USA). 3 kDa MWCO Amicon® Ultra devices (Merck-Millipore, MA, USA) were used to concentrate up to 15 ml filtered supernatants, by centrifugation at 4,000 × g for 60 min at 4°C. The obtained concentrated supernatants were collected, characterized, and stored at −20°C for the subsequent analyses. EV-endMSCs characterization was carried out as previously described our group (Álvarez et al., 2018). Briefly, the protein content of EV-endMSCs was quantified by a Bradford assay (BioRad Laboratories, CA, USA); the size of EV-endMSCs was determined by nanoparticle tracking analysis (Malvern Panalytical Ltd., Malvern, UK), and the particle-tracking analysis software package version 2.2 (Malvern Panalytical Ltd.); EV-endMSCs surface marker analysis was performed by flow cytometry in a FACScalibur cytometer (BD Biosciences) and with the CellQuest software (BD Biosciences), after incubation with aldehyde/sulfate latex beads (Molecular probes, Life Technologies, Thermo Fisher Scientific), and human monoclonal antibodies against CD9 and CD63 (BD Biosciences, San Jose, CA, USA).

Protein Analysis by High-Resolution Liquid Chromatography Coupled to Mass Spectrometry-Based Proteomics

The characterization of EV-endMSCs proteome from three different donors was performed by high-throughput multiplexed quantitative proteomics approach according to previously described protocols (Jorge et al., 2009; Navarro and Vázquez, 2009; Bonzon-Kulichenko et al., 2011; Navarro et al., 2014; García-Marqués et al., 2016). Protein extracts were incubated

with trypsin using the Filter Aided Sample Preparation (FASP) digestion kit (Expedeon, San Diego, CA), as previously described (Wiśniewski et al., 2011). The resulting peptides were labeled using 8plex-iTRAQ (isobaric Tags for Relative and Absolute Quantitation) reagents, according to manufacturer's instructions, and desalted on OASIS HLB extraction cartridges (Waters Corporation, Milford, MA, USA). Half of the tagged peptides were directly analyzed by liquid chromatography tandem mass spectrometry (LC-MS/MS) in different acquisition runs, and the remaining peptides were separated into three fractions using the high pH reversed-phase peptide fractionation kit (Thermo Fisher Scientific). Samples were analyzed using an Easy nLC 1000 nano-HPLC coupled to a QExactive mass spectrometer (Thermo Fisher Scientific). Peptides were injected onto a C18 reversed phase nano-column (75 μm I.D. and 50 cm, Acclaim PepMap100 from Thermo Fisher Scientific) in buffer A [0.1% formic acid (v/v)] and eluted with a 180 min lineal gradient of buffer B [90% acetonitrile, 0.1% formic acid (v/v)], at 200 nl/min. Mass spectrometry (MS) runs consisted of 140,000 enhanced FT-resolution spectra in the 390–1,500 m/z wide range and separated 390–700 m/z (range 1), 650–900 m/z (range 2), and 850–1,500 m/z (range 3) followed by data-dependent MS/MS spectra of the 15 most intense parent ions acquired along the chromatographic run. HCD fragmentation was performed at 30% of normalized collision energy. A total of 14 MS data sets, eight from unfractionated material and six from the corresponding fractions, were registered with 42 h total acquisition time. For peptide identification the MS/MS spectra were searched with the SEQUEST HT algorithm implemented in Thermo Fisher Proteome Discoverer version 2.1 using a Uniprot database containing human protein sequences (Dec-2017). For database searching, parameters were selected as follows: trypsin digestion with two maximum missed cleavage sites, precursor mass tolerance of 800 ppm, fragment mass tolerance of 0.02 Da. Variable methionine oxidation (+15.994915 Da) and fixed cysteine carbamidomethylation (+57.021 Da), and iTRAQ 8-plex labeling at lysine and N-terminal modification (+304.2054) were chosen.

Peptide Identification, Protein Quantification, and Statistical Analysis

Peptide identification from MS/MS data was performed using the probability ratio method (Martínez-Bartolomé et al., 2008) and the false discovery rate (FDR) of peptide identification was calculated based on the search results against a decoy database using the refined method (Navarro and Vázquez, 2009). Peptide and scan counting were performed assuming as positive events those with a FDR equal or lower than 1%.

Quantitative information of iTRAQ-8plex reporter ions was extracted from MS/MS spectra using an in-house developed program (SanXoT), as described (Trevisan-Herraz et al., 2019), and protein abundance changes were analyzed using the weighted spectrum, peptide and protein (WSPP) statistical model (Navarro et al., 2014). This model provides a standardized variable, Zq, defined as the mean-corrected $\log_2$– ratio expressed in units of standard deviation at the protein level. For the protein functional analysis, proteins were annotated based on Gene Ontology database (The Gene Ontology Consortium, 2017) and Systems Biology Triangle (SBT) model (García-Marqués et al., 2016). This algorithm estimates weighted functional category averages (Zc) from the protein values by performing the protein to category integration. Student *t*-test was used to compare Zq and Zc values from EV-endMSCs and IFNγ/EV-endMSCs, and the statistical significance was set at p-value < 0.05. Enrichment analysis of proteins was performed by DAVID bioinformatics tool (Huang et al., 2009a,b) and Benjamini-Hochberg FDR was used for multiple test correction (FDR < 0.05).

Principal Component Analysis (PCA) was performed on Zq values of 895 selected proteins (number of peptides, Np, >2 at 1% FDR) quantified after iTRAQ proteomics analysis, using Metaboanalyst software version 4.0 (https://www.metaboanalyst.ca/) (Chong et al., 2018).

Human M-CSF ELISA

Considering the biological relevance of M-CSF, the changes observed for this protein were analyzed by ELISA. The quantification of M-CSF (also called CSF-1) was performed using the Human M-CSF Pre-Coated ELISA Kit (Peprotech, UK) according to the manufacturer's instructions. Briefly, the EV-endMSCs and IFNγ/EV-endMSCs from four different donors were diluted 1:10 in dilution buffer and quantified. Median, mean, 25th percentile, and 75th percentile were calculated and paired *t*-test was used to compare the two groups.

miRNA Analysis by Next Generation Sequencing

All experiments, except IPA, PCA, miRTargetLink, and DAVID analyses, were performed at QIAGEN Genomic Services (Hilden, Germany). Total RNA was isolated from aliquots of 3–4 ml of concentrated EV-endMSCs, with an exoRNeasy Serum/Plasma Kit (QIAGEN) according to manufacturer's instructions. For NGS, the miRNA NGS library was generated by fragmentation and reverse transcription to cDNA, starting with 5 μl total RNA for each sample, and with the use of the QIAseq miRNA Library Kit (QIAGEN). Each individual RNA molecule was tagged with adapters containing a Unique Molecular Index (UMI), aimed to detect, quantify, and sequence unique RNA transcripts with high-resolution. The obtained cDNAs were amplified in 22 cycles of PCR and purified. Bioanalyzer 2100 or TapeStation 4200 (both from Agilent Technologies, Santa Clara, CA, USA) were used for library preparation QC. The libraries were pooled in equimolar ratios, according to quality and concentration of the inserts, and were submitted to qPCR for quantification. Next, the library pools were sequenced on a NextSeq500 sequencing instrument in accordance with manufacturer's indications. The bcl2fastq software (Illumina, San Diego, CA, USA) was used to obtain FASTQ files from raw data, and the FastQC tool (http://www.bioinformatics.babraham.ac.uk/projects/fastqc/) was adopted the check FASTQ data.

As previously mentioned, adapters and 12 nt-long UMI sequences were ligated to RNA molecules during processing.

Therefore, trimming and UMI correction were required before moving to the mapping of detected sequences. Cutadapt (1.11) (https://cutadapt.readthedocs.io/en/stable/) was used to rid the raw reads of adapter sequences and UMIs. Briefly, the raw FASTQ data were screened to detect adapters and UMI, filtering only the reads containing adapters and insert sequence length equal or larger than minimal insert length (default 16 nt). Raw data with UMI sequences shorter than 10 nt were discarded, while reads containing UMI (equal or longer than 10 nt) were classified in partial-UMI reads (equal or longer than 10 nt), and full-UMI reads (equal or longer than 12 nt). The last reads were combined and were submitted to the quality control (FastQC) and to the mapping process, that was carried out with the software Bowtie2 (2.2.2) in order to evaluate the quality of the samples. Reads were aligned to spike-ins, abundant sequence and miRBase_20 (http://www.mirbase.org/) (Kozomara et al., 2019) taking into consideration, as mapping criterion, the perfect match of the reads to the reference sequences. To map to the genome, not more than one mismatch was allowed in the first 32 bases of the read. No INDELs (small insertions and deletions) were allowed in mapping. Bowtie2 (2.2.2) was used to map the reads. UMI-corrected reads whose length was around 18–23 nucleotides and that were associated to relevant entries in mirbase_20, were selected for further analyses.

Mapped miRNAs with Tags Per Million (TPM) $\geq$ 10, belonging to EV-endMSCs samples, were processed by IPA (QIAGEN Inc.) (Ngwa et al., 2011) to determine the human targeted genes with *Experimentally observed* annotations. Enrichment analysis of EV-endMSCs microTargets was performed using DAVID bioinformatics tool. Only terms with p-value < 0.05 were considered statistically significant. For multiple test correction, Benjamini-Hochberg approach was used to control the FDR (FDR < 0.05).

PCA was performed on log-fold and absolute gene-wise changes in expression levels between samples (TMM normalization) (Robinson and Oshlack, 2010) of the 225 miRNAs, considering that each miRNA was detected in at least three of the four replicates from one group (EV-endMSCs and IFNγ/EV-endMSCs), and using Metaboanalyst software (version 4.0) (https://www.metaboanalyst.ca/) (Chong et al., 2018).

Differential expression analysis was performed using the EdgeR statistical software package (http://bioconductor.org/). For normalization, the trimmed mean of M-values method based on log-fold and absolute gene-wise changes in expression levels between samples (TMM normalization) was used. Using Benjamini-Hochberg FDR corrected p-values, miRNAs were considered differentially expressed at a significance level of 0.05 (FDR). IPA was performed to determine the microTargets of the significantly altered miRNAs between EV-endMSCs and IFNγ/EV-endMSCs samples.

In order to identify multiple query nodes among miRNAs in EV-endMSCs, the top-abundant miRNAs ($\geq$200 TPMs), were submitted to a miRTargetLink analysis. Only results with a strong experimental evidence were taken into consideration.

Macrophage Polarization Assay

Human monocytes from one healthy donor were isolated from peripheral blood collected in EDTA containing tubes. Blood was diluted in PBS, layered over Histopaque-1077 (Sigma, St. Louis, MO) and centrifuged at 900 × g for 20 min at room temperature. The peripheral blood mononuclear cells were carefully aspirated and washed twice with PBS. The peripheral blood mononuclear cells were resuspended in RPMI-1640 supplemented with 10% FBS. The cells were seeded in tissue culture plates and incubated for 3 h at 37°C and 5% CO_2. Non-adherent cells were removed by four washes with PBS. Adherent monocytes were stimulated with 50 ng/ml of Macrophages Colony-Stimulating Factor (M-CSF) (Gibco, Thermo Fisher Scientific) to promote the cell differentiation from monocytes to M2 macrophages. Simultaneously, adherent monocytes were stimulated with 50 ng/ml of Granulocyte-Macrophages Colony-Stimulating Factor (GM-CSF) (Gibco, Thermo Fisher Scientific) to promote cell differentiation from monocytes to M1 macrophages (Gao et al., 2018). Finally, EV-endMSCs and IFNγ/EV-endMSCs from four different donors were added to the adherent monocytes. At day 6, adherent cells were trypsinized with a 0.25% trypsin solution, washed, and counted for flow cytometry analysis.

For flow cytometry, adherent cells co-cultured with M-CSF, GM-CSF, EV-endMSCs, and IFNγ/EV-endMSCs were incubated for 30 min at 4°C with the following human monoclonal antibodies from BD Biosciences. PE-conjugated anti-CD14 was used as macrophage marker and APC-conjugated anti-CD206 was used as a M2-differentiation marker. Cells were analyzed on a FACScalibur cytometer (BD Biosciences) using FSC/SSC characteristics. Fluorescence was analyzed with CellQuest Pro software (BD Biosciences), using isotype-matched antibodies as negative controls. The percentage of CD206-positive cells on gated CD14 macrophages was represented. Median, mean, 25th percentile, and 75th percentile were calculated and paired t-test was used to compare EV-endMSCs and IFNγ/EV-endMSCs with GM-CSF.

For transcriptional analysis studies, total RNA from adherent cells co-cultured with EV-endMSCs ($n = 3$) and IFNγ/EV-endMSCs ($n = 3$) was isolated at day 6 using mirVana miRNA isolation kit (ThermoFisher Scientific), following the manufacturer's protocol for total RNA extraction. Quality and concentration of total RNAs were evaluated by spectrophotometry. The cDNA was synthesized from 55 ng of RNA in reverse transcription reactions performed with the iScript Reverse Transcription Supermix (BioRad, Hercules, CA, USA), according to manufacturer's instructions. 5.5 ng of cDNA for each sample were then amplified in qPCR reactions using TaqMan™ Fast Advanced Master Mix (Catalog number 4444964, ThermoFisher Scientific) and TaqMan® Gene Expression Assays probes (ThermoFisher Scientific) for the genes *TBP* (Assay ID: Hs00427620_m1), *IL1B* (Hs01555410_m1), *TNF* (Hs00174128_m1), *NOS2* (Hs01075529_m1), and *TGFB* (Hs00998133_m1). Samples were evaluated in triplicate and 2 μl of water replaced the cDNA templates in the three negative controls for each probe. All the reaction mixtures were prepared

following manufacturer's protocol, and the suggested thermal profile was used to carry out templates amplification in a QuantStudio 3 Real-Time PCR System (Applied Biosystems, Thermo Fisher Scientific Inc.). The qRT-PCR products were quantified by fluorescent method using the $2^{-\Delta Ct}$ expression. All samples were analyzed separately and normalized using TATA-Box Binding Protein (*TBP)* as endogenous control (Saleh et al., 2011).

RESULTS

Characterization of endMSCs and EV-endMSCs

The phenotypic analysis of endMSCs was performed by flow cytometry. The endMSCs ($n = 4$) were negative for CD14, CD20, CD34, CD45, CD80, and HLA-DR, while CD44, CD73, CD90, and CD117 markers were positively expressed. Microscopic analysis of Oil Red O, Alcian Blue, and Alizarin Red S stainings on endMSCs cultured in differentiation specific media proved their multipotency toward the adipogenic, chondrogenic, and osteogenic lineages. The nanoparticle tracking analysis of EV-endMSCs showed that their mean size was 153.5 ± 63.05 nm. Furthermore, CD9 and CD63 exosomal markers were positively expressed, in accordance with the Minimal information for studies of extracellular vesicles 2018 (MISEV2018) guidelines (Théry et al., 2018) (**Supplementary Figure 1**). An accurate explanation and the characterization of cells and vesicles can be found in our previous studies (Álvarez et al., 2018; Blázquez et al., 2018; Marinaro et al., 2019).

Characterization of EV-endMSCs Molecular Cargo

In order to elucidate the modulation of protein composition suffered by EV-endMSCs under IFNγ priming, we have resorted to a high-throughput quantitative proteomic approach performed using multiplex peptide stable isotope labeling (**Figure 1**). The datasets generated and analyzed for this study are available via ProteomeXchange (http://www.proteomexchange.org/) with identifier PXD015465 (https://www.ebi.ac.uk/pride/archive/projects/PXD015465). This strategy of data discovery gave us a reliable identification of 895 proteins (number of peptides, Np, >2 at 1% FDR) corresponding to 866 human genes (**Supplementary Table 1**). Of note, 71 proteins were included in the 100 top-identified proteins of ExoCarta database (http://www.exocarta.org/) (Keerthikumar et al., 2016), and 617 proteins were annotated as *Extracellular exosome* proteins (GO:0070062) in the Gene Ontology (GO) database (p-value < 0.001, 1% FDR) (**Figure 1**, **Supplementary Table 2**). These exosomal proteins corresponded to about 80% of the EV-endMSCs proteome composition in terms of absolute quantification (**Supplementary Table 1**). Regarding the subcellular origin of EV-endMSCs identified proteins, *Extracellular matrix* (GO:0031012), *Cytosol* (GO:0005829), and *Membrane* (GO:0016020) were the most representative categories (**Figure 2A**, **Supplementary Table 2**). *Mitochondrion* (GO:0005739), and *Cytoskeleton* (GO:0005856) terms were also significantly enriched (p-value < 0.001, 1% FDR). In contrast, no significant results were found for nuclear, or ribosomal proteins. Interestingly, *Immunological synapse* (GO:0001772) related proteins were also significantly represented in the EV-endMSCs proteome (enrichment p-value < 0.001, 1% FDR) (**Figure 2B**, **Supplementary Table 2**).

Since RNA species are also essential components of EV cargo (Abels and Breakefield, 2016), we performed NGS analysis to identify and quantify the presence of miRNAs in EV-endMSCs and IFNγ/EV-endMSCs (**Figure 1**). The datasets generated and analyzed for this study can be found in the European Nucleotide Archive (https://www.ebi.ac.uk/ena) with accession number PRJEB34442. On average 6.6 million UMI-corrected reads were obtained for each sample and the average percentage of mappable reads was 79.5%. Nearly 54% (on average) corresponded mostly to small RNA species (**Supplementary Figure 2**).

After mapping the data using miRBase 20 database, a total of 225 miRNAs were identified in at least three of the four replicates from each group (EV-endMSCs and IFNγ/EV-endMSCs). In order to predict the potential effects that these miRNAs may have on a target cell, we performed an Ingenuity Pathway Analysis (IPA). This analysis allowed us to elucidate a detailed regulatory network to identify those genes targeted by identified miRNAs (Ngwa et al., 2011). The microTargets with *Experimentally observed* annotations for these microRNAs were analyzed (**Supplementary Table 3**). A total of 48 miRNAs identified in EV-endMSCs (≥10 TPM) targeted 937 genes (**Supplementary Table 3A**). Of note, key intracellular signaling nodes, such as *PTEN* or *MYC* were highly targeted (8 and 4 miRNAs targeted these genes, respectively) (**Supplementary Table 3B**). In contrast to protein cargo, enrichment analysis showed that the preferred site for miRNAs targeting is the nucleus (n = 371 microTargets) (**Figure 2C**). Other over-represented subcellular targets were cytosol (n = 296 microTargets), plasma membrane (n = 250), and mitochondrion ($n = 101$), among others (**Figures 2C,D** and **Supplementary Table 4**). The miRTargetLink analysis (Wong and Wang, 2015; Liu and Wang, 2019) was performed to identify multiple query nodes among those miRNAs with more than or equal to 200 TPMs, on average: hsa-let-7a-5p, hsa-miR-143-3p, hsa-miR-21-5p, hsa-let-7b-5p, hsa-let-7f-5p, hsa-miR-16-5p, and hsa-miR-199a-3p (see **Supplementary Table 3A**). Our results revealed that *PTGS2*, *BCL2*, *KRAS*, *HRAS*, *EGFR*, *HMGA2*, *HMGA1*, *CDK6*, *TNFRSF10B*, *CCND1*, and *PRDM1* genes were targeted by at least three of these miRNAs with a strong experimental evidence and that *IGF1R* was the target of four out of seven top-abundant miRNAs in EV-endMSCs (hsa-miR-143-3p, hsa-miR-16-5p, hsa-miR-21-5p, and hsa-let-7b-5p) (**Supplementary Figure 3**).

Interestingly, enrichment analyses also showed the potential effect of molecular cargo on different biological processes (**Figure 3**). EV-endMSCs proteins were shown to be involved in several processes as the *extracellular matrix organization* (GO:0030198), the *unfolded protein response* (GO:0006986), and the *cell redox homeostasis* (GO:0045454) (p-value < 0.001, 1% FDR, **Figure 3A**, **Supplementary Table 2**). Besides, the

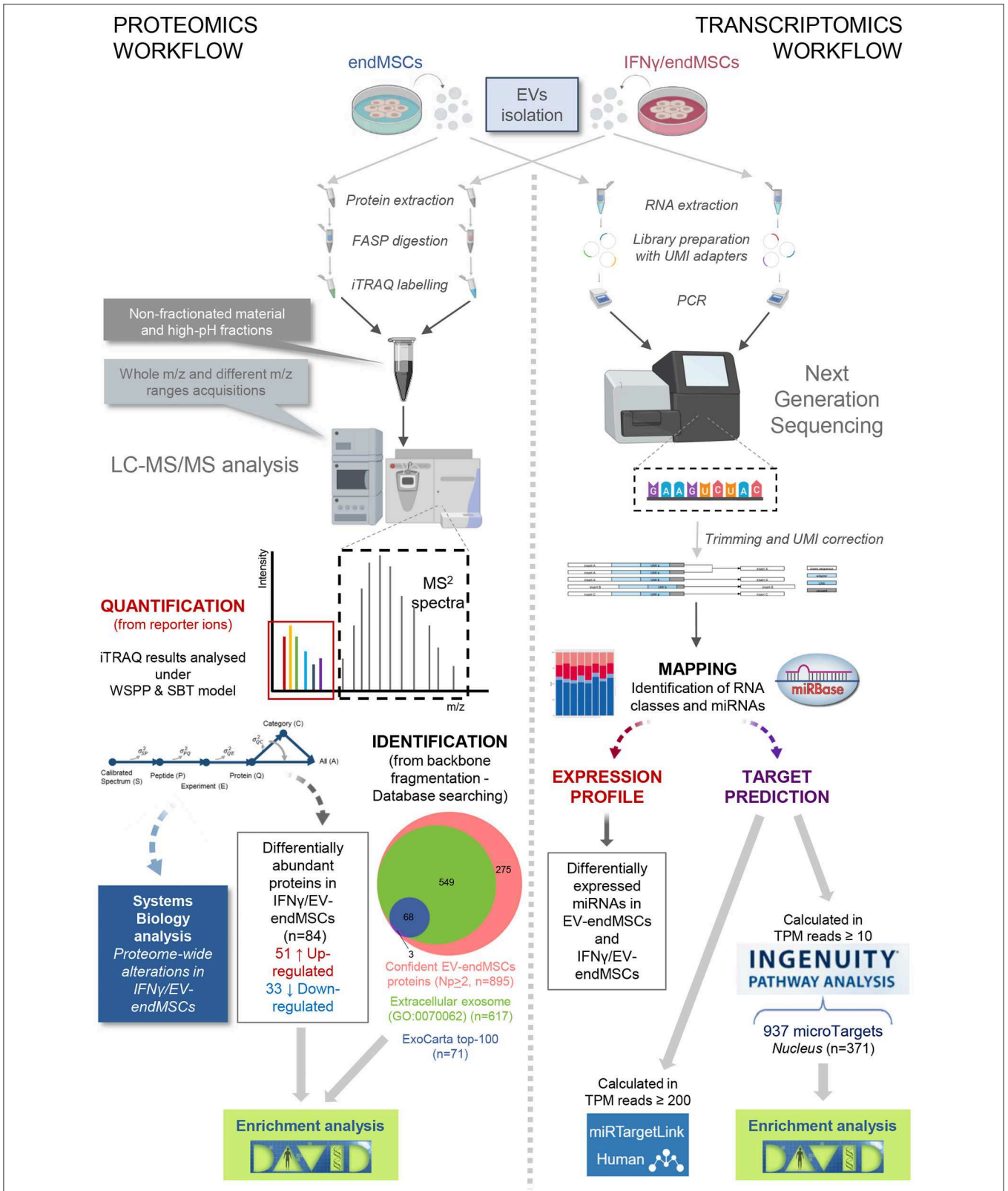

FIGURE 1 | Overview of the proteomic and transcriptomic approaches. For both studies, EV samples were obtained from endMSCs under two different conditions (IFNγ-treated and control cells). According to proteomic procedures (fully described in Materials and Methods section), iTRAQ technology allowed us to simultaneously obtain peptide identification and quantification from the MS2 spectra. We identified 895 confident proteins (at least two different peptide backbone

(Continued)

FIGURE 1 | fragmentation spectrum matched with reference sequences from database under 1% FDR). At the same time, quantification of peptide/protein levels were retrieved from the reporter ions (low m/z range in the MS2 spectra) being analyzed under the *WSPP* model (Navarro et al., 2014). In order to describe proteome-wide alterations, category analyses were performed based on the *SBT* model (García-Marqués et al., 2016). For the transcriptomics workflow, extracted total RNAs from EV samples were submitted to Next Generation sequencing. The UMI-corrected reads were aligned to miRBase (http://www.mirbase.org/) to discriminate the populations of RNAs in EVs cargo, and for the identification of the detected miRNAs in EV-endMSCs and IFNγ/EV-endMSCs. Human targeted genes were detected after an Ingenuity Pathway Analysis (IPA) on mapped microRNAs of control cells with TPM ≥ 10. Of the 937 identified microTargets, 371 were associated to the nucleus that may be the preferred site of EV-endMSCs targeting. miRTargetLink (https://ccb-web.cs.uni-saarland.de/mirtargetlink/) was used to identify multiple query nodes among identified miRNAs (TPM ≥ 200). Enrichment analyses of protein and microTarget lists were performed by DAVID software (https://david.ncifcrf.gov/) using Benjamini-Hochberg FDR for multiple test correction (FDR < 0.05). Images have been created with BioRender (https://app.biorender.com/), and BioVenn (http://www.biovenn.nl/). Two pictures in the trascriptomics workflow belong to the miRNA NGS Data Analysis Report from QIAGEN Genomic Services (Hilden, Germany). endMSCs, Endometrial-derived MSCs; EV, Extracellular Vesicles; EV-endMSCs, Extracellular Vesicles from Endometrial-derived stromal/Mesenchymal Stem Cells; FASP, Filter-Aided Sample Preparation; FDR, False Discovery Rate; HPLC-MS, High-Performance Liquid Chromatography coupled to Mass Spectrometry; IFNγ/EV-endMSCs, Extracellular Vesicles from IFNγ-primed Endometrial-derived stromal/Mesenchymal Stem Cells; IPA, Ingenuity Pathway Analysis; iTRAQ, Isobaric Tags for Relative and Absolute Quantitation; LC-MS/MS, Liquid chromatography tandem mass spectrometry; PCR, Polymerase Chain Reaction; SBT, Systems Biology Triangle; TPM, Tags Per Million; UMI, Unique Molecular Index; WSPP, Weighted Spectrum Peptide Protein.

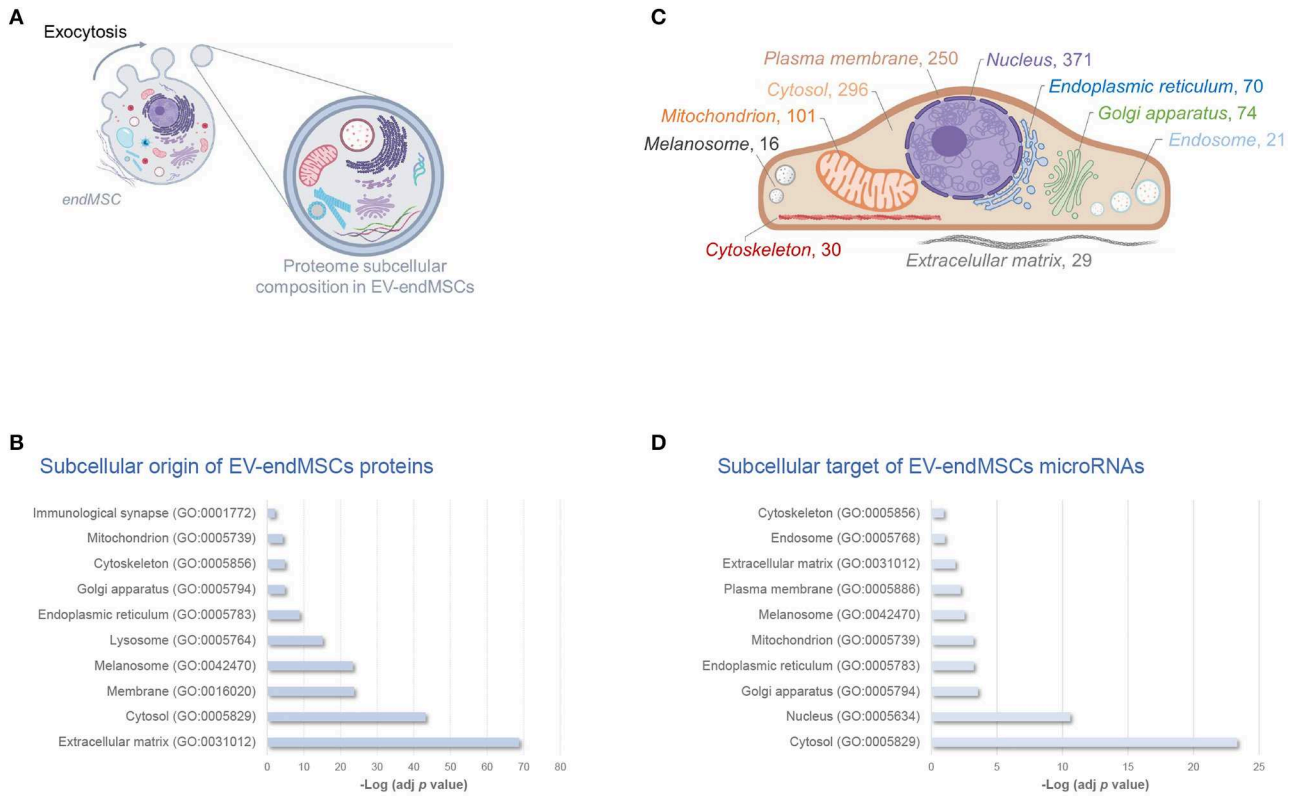

FIGURE 2 | Subcellular composition of EV-endMSCs molecular cargo. Schematic overview of subcellular origin of protein cargo **(A)**, and microRNA cellular targets **(C)** of EV-endMSCs. Subcellular organelles are highlighted according to over-represented protein annotations, and the number of microTargets, respectively. **(B)** Relative contribution of major subcellular components in the EV-endMSC proteome, and **(D)** microTargets. Graph bars represent adjusted enrichment *p*-values (-Log) from significantly represented GO annotations (only terms with an enrichment *p*-value adjusted by Benjamini-Hochberg FDR correction <0.01 were considered). See further information about enrichment analyses from EV-endMSC proteins and microTargets in **Supplementary Tables 2**, **4**, respectively. Images have been created with BioRender (https://app.biorender.com/). EV-endMSCs, Extracellular Vesicles derived from endometrial MSCs; FDR, False Discovery Rate; GO, Gene Ontology.

miRNA component was shown to affect *signaling transduction* (GO:0007165), *cell proliferation* (GO:0008283) and *apoptotic processes* (GO:0006915), among others (p-value < 0.001, 1% FDR, **Figure 3B**, **Supplementary Table 4**). Interestingly, *MAPK cascade* (GO:0000165), and *PI3K-Akt signaling* (hsa04151) pathways were also over-represented among microTargets (p-value < 0.001, 1% FDR) (**Figure 3B**), which in turn showed a significant enrichment within protein cargo (**Figure 3A**, **Supplementary Table 2**). Finally, results from tissue up-regulated gene annotations showed that microTargets were over-represented in brain (n = 427), placenta (n = 273 genes), epithelium (n = 232), liver (n = 147), and B-cells (n = 32) among others (p-value < 0.01, 1% FDR, **Supplementary Table 4**).

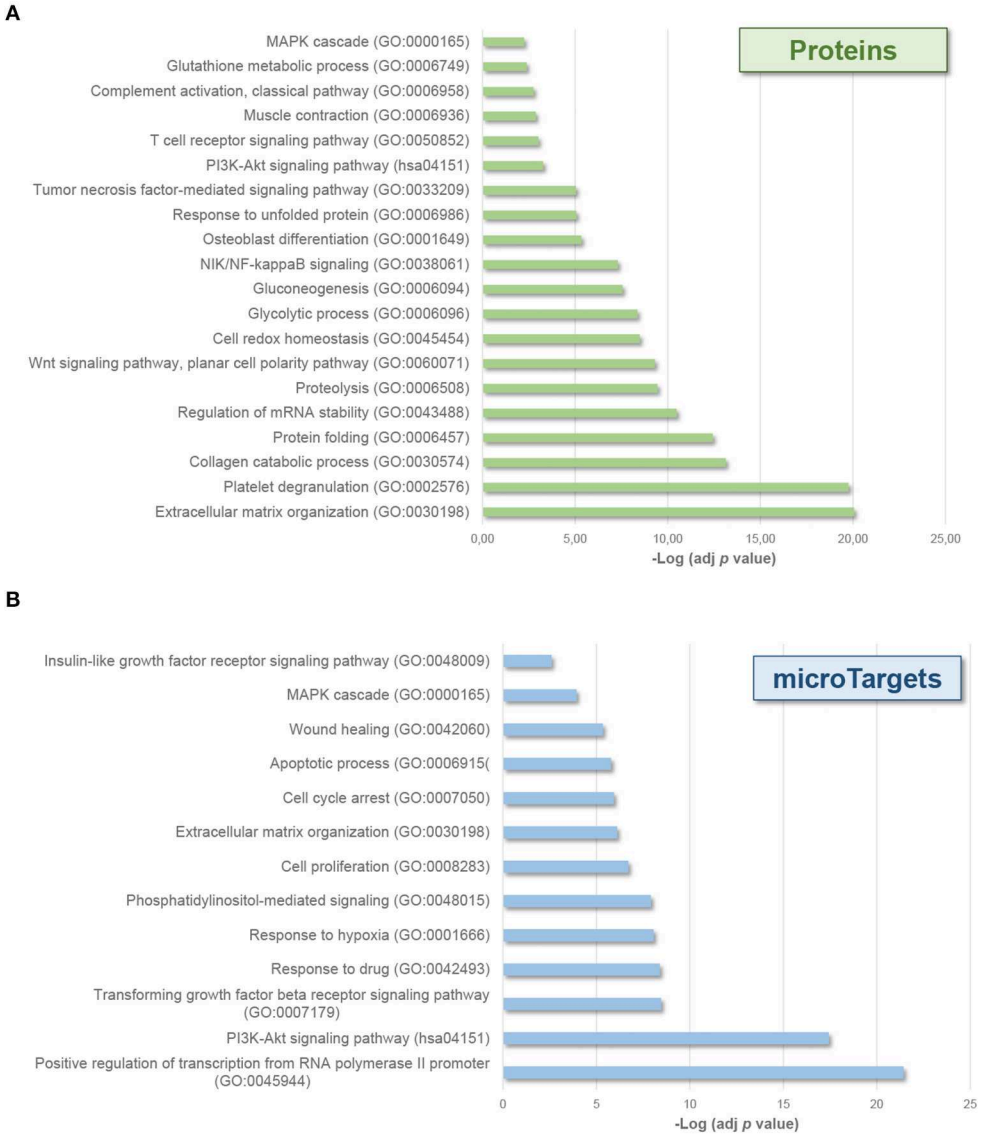

FIGURE 3 | Biological processes affected by EV-endMSCs molecular cargo. Graph bars represent adjusted enrichment *p*-values (–Log) of significantly enriched categories from proteins **(A)**, and microTargets **(B)**. Only terms with an enrichment *p*-value adjusted by Benjamini-Hochberg FDR correction <0.01 were considered. See further information about enrichment analyses from EV-endMSC proteins and microTargets in **Supplementary Tables 2**, **4**, respectively. EV-endMSCs, Extracellular Vesicles derived from endometrial MSCs; FDR, False Discovery Rate.

Effect of IFNγ Priming in the EV-endMSCs Proteome Signature

With the aim of studying the modulation of protein composition in EV-endMSCs under IFNγ treatment, a comparative analysis of the proteome from EV-endMSCs ($n = 3$) and IFNγ/EV-endMSCs ($n = 3$) was carried out (**Figure 1**). The multiplexed quantitative proteomics approach provided an extensive dynamic range and great proteome coverage, allowing the simultaneous identification and quantification of hundreds of proteins in the same experiment, which offers an invaluable advantage for the analysis of limited sample amounts (Edwards and Haas, 2016; Jylhä et al., 2018), as the case for EVs samples. In this study, protein abundance changes in each sample were calculated in relation to the average values of each protein corresponding to control samples [$\log_2$-ratio expressed in units of standard deviation (Zq), **Supplementary Table 5**]. We have applied a robust and rigorous *ad-hoc* statistical analysis based on the WSPP model (Navarro et al., 2014), which has been repeatedly validated for the treatment of quantitative proteomics data in several models (Ruiz-Meana et al., 2014; Gómez-Serrano et al., 2016; Binek et al., 2017; Martínez-López et al., 2019).

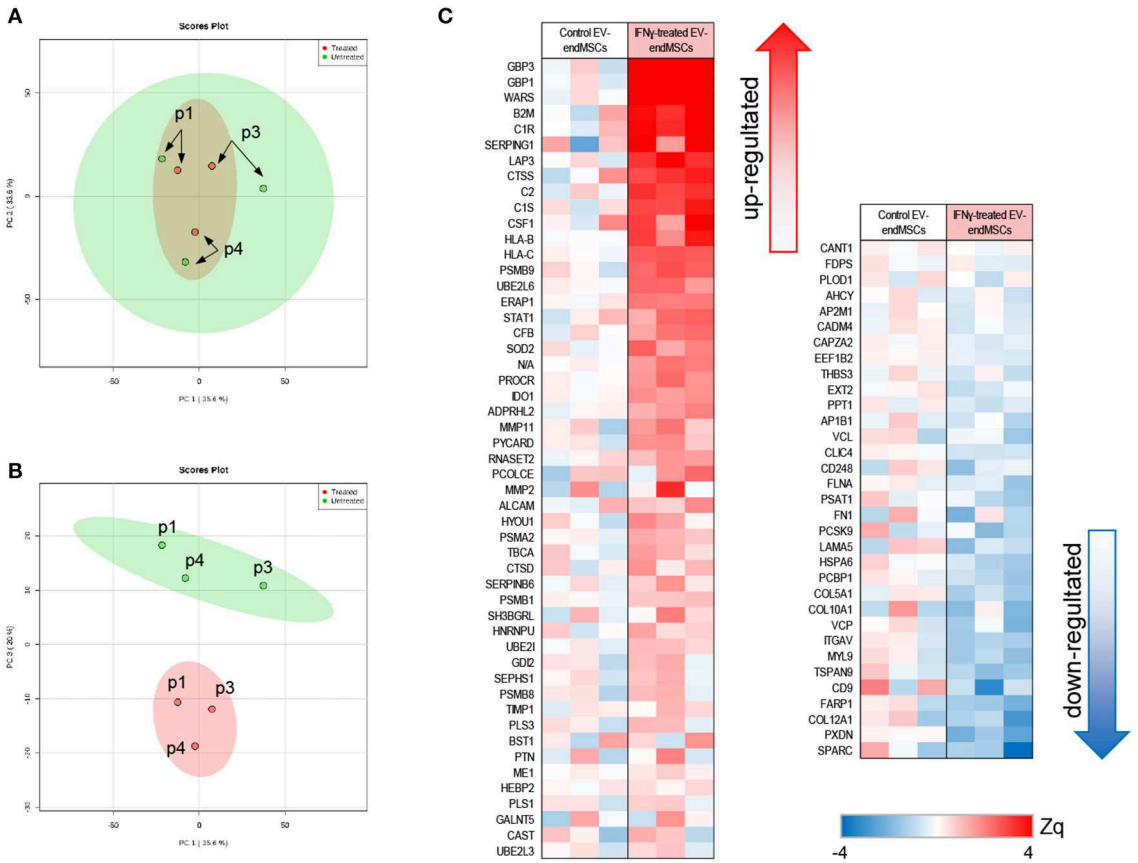

FIGURE 4 | Quantitative proteomic analysis of IFNγ/EV-endMSCs. A total of 895 proteins (number of peptides, Np, >2 at 1% FDR) quantified after iTRAQ proteomic approach were first subjected to Principal Component Analysis (PCA). **(A)** Score plot for PC1 (35.6% variance explained) vs. PC2 (33.6% variance explained). **(B)** Score plot for PC1 (35.6% variance explained) vs. PC3 (20% variance explained). Data display 95% confidence regions. Patient origin ($n = 3$) are indicated on the plots as p1, p3, and p4. IFNγ/EV-endMSCs (treated) and EV-endMSCs (untreated, control) samples are indicated in red and green, respectively. **(C)** Quantitative proteomics results. Protein profile changes were analyzed by WSPP model (Navarro et al., 2014) to identified significantly altered proteins comparing IFNγ/EV-endMSCs and EV-endMSCs samples. Protein values (Zq) are reported as the standardized variable, which is defined as the mean corrected $\log_2$-ratio expressed in units of standard deviation. Protein ratio of each sample was calculated against an internal standard (IS) based on the average of iTRAQ reporters from EV-endMSCs control samples. Statistical differences between Zq values of samples groups were evaluated by paired *t*-test. Significant protein abundance change was set at *p*-value <0.05. EV-endMSCs, Extracellular Vesicles derived from endometrial MSCs; IFNγ/EV-endMSCs, Extracellular Vesicles derived from IFNγ-primed endometrial MSCs; WSPP, Weighted Spectrum Peptide Protein.

The unsupervised study of proteomic results through PCA revealed substantial differences between EV-endMSCs and IFNγ/EV-endMSCs (**Figures 4A,B**, **Supplementary Figure 4**). Additionally, PCA analyses revealed that distribution of main protein components (PC1 *vs.* PC2) from the same individual behaved similarly, underlying a distinctive individual EV-endMSCs proteome background regardless of endMSCs treatment (**Figures 4A,B**). Despite inter-individual differences, IFNγ-priming of endMSCs caused an important effect on EVs proteome (**Figure 4B**). In order to evaluate the most representative candidates of this effect, differences in protein levels between samples groups were evaluated through paired *t*-test. A total of 84 proteins showed significant changes (*p*-value < 0.05) between EV-endMSCs and IFNγ/EV-endMSCs (51 and 33 proteins were up- and down-regulated, respectively) (**Figure 4C**, **Supplementary Table 5**). Notably, guanylate-binding proteins 1, and 3 (GBP1, GBP3) were highly up-regulated under IFNγ-treatment as well as proteins related to complement system, such as C1R (complement C1r subcomponent), C1S (complement C1s subcomponent), or SERPING1 (Plasma protease C1 inhibitor) (**Figure 4C**). Additionally, cytokines, such as CSF1 (also called M-CSF), cell adhesion molecules, like CD166 antigen—an important component of the immunological synapse (Kato et al., 2006; Gilsanz et al., 2013), and CD9 antigen—involved in platelet activation and aggregation (Worthington et al., 1990; Miao et al., 2001)—were also altered in IFNγ/EV-endMSCs. Enrichment analyses showed that IFNγ protein mediators were over-represented among differentially abundant proteins (*p*-value < 0.001, 5% FDR) (**Supplementary Table 6**). These analyses also pinpointed significant changes on proteins related to *angiogenesis* (GO:0001525), *collagen catabolism* (GO:0030574), *tumor necrosis factor signaling* (GO:0033209), *innate immune response*

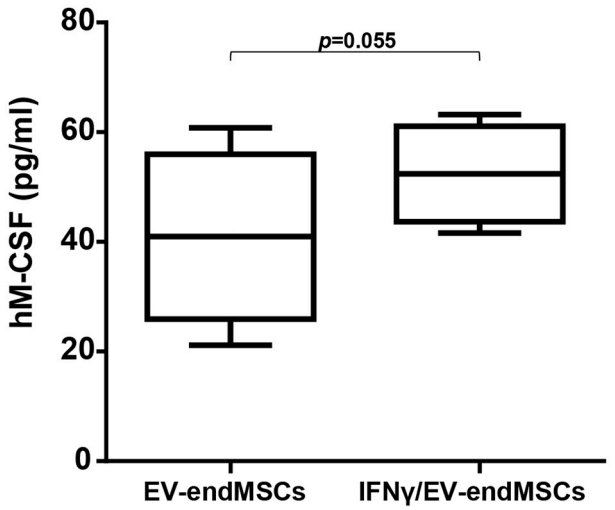

FIGURE 5 | Human M-CSF in extracellular vesicles derived from endometrial mesenchymal stem cells. The quantification of hM-CSF was performed by ELISA. EV-endMSCs from different donors were analyzed ($n = 4$). The lower boundary of the boxes indicates the 25th percentile and the upper boundary, the 75th percentile. Bars above and below the boxes indicate the 90th and 10th percentiles. The line within the boxes marks the median. A paired *t*-test was used to compare EV-endMSCs and IFNγ/EV-endMSCs.

(GO:0045087), and *proteasome core complex* (GO:0005839), among others.

Based on proteomic analyses and considering the biological relevance of human M-CSF on M1/M2 macrophage polarization, M-CSF was quantified by ELISA. EV-endMSCs and IFNγ/EV-endMSCs from different donors were analyzed ($n = 4$) and compared by a paired *t*-test. Human M-CSF levels appeared to be modified in IFNγ/EV-endMSCs, when compared to controls (**Figure 5**).

To study the impact of IFNγ-priming on protein functional dynamics, we additionally analyzed the normal distribution of protein quantifications predicted by the WSPP statistical model (Navarro et al., 2014) under the null hypothesis using the Systems Biology Triangle (SBT) algorithm (García-Marqués et al., 2016), which allows to detect alterations to protein function produced by the coordinated action of proteins in biological systems. Thus, a functional category was considered up- or down-regulated when the changes of its protein components fail to follow a normal distribution. In the comparison of protein profiles between EV-endMSCs and IFNγ/EV-endMSCs, a total of 117 functional categories were found significantly altered (p-value $<$ 0.05), considering categories containing more than ten proteins (**Supplementary Table 7**). As expected, one of the largest category clusters, comprising 10 categories related to *antigen processing and presentation* (i.e., GO:0019882; GO:0002480; GO:0042605; GO:0002479; GO:0002486; GO:0002474; GO:0002486; GO:0003823; hsa04612), was increased. The majority of the corresponding protein components were up-regulated (e.g., HLA class I histocompatibility antigens, proteasome subunits, beta-2-microglobulin and heat shock proteins). In agreement with the enrichment analysis, *innate immune response* (GO:0045087) was up-regulated, with a significant increase of B2M, SERPING1, CSF1, PYCARD, and HLA-B and C proteins, among others. In addition, *adaptive immune response* (GO:0002250) encompassing differentially abundant proteins, such as ERAP1, ALCAM, and CTSS were also up-regulated (**Figure 6A**, **Supplementary Table 8A**). Notably, *complement activation* (GO:0006958) composed of C1R, C1S, SERPING1, or C2 immune mediators (**Figure 6B**, **Supplementary Table 8B**) was significantly up-regulated. Finally, functional proteome profiling revealed that several cell signaling pathways were also altered (**Supplementary Table 7**). This cluster contained several proteins with statistically significant increased abundance when comparing EV-endMSCs and IFNγ/EV-endMSCs. Some remarkable examples are the *IFNγ-mediated signaling pathway* (GO:0060333) and *NIK/NF-kappaB signaling* (GO:0038061), *T cell receptor signaling pathway* (GO:0050852) and *MAPK cascade* (GO:0000165), mostly related to the *proteasome complex* (GO:0000502). This complex includes significantly up-regulated subunits, such as PSMB10, PSMB9, PSME1, and PSME2 (**Figure 6C**, **Supplementary Table 8C**).

microRNAome Alterations in EV-endMSCs Under IFNγ Priming

A comparative analysis of the miRNA expression profile was carried out in EV-endMSCs ($n = 4$) and IFNγ/EV-endMSCs ($n = 4$) (**Figure 1**). PCA analysis demonstrated that EV-endMSCs microRNAome does not discriminate as much as proteome does (**Supplementary Figure 5**).

The comparison of miRNA expression among EV-endMSCs and IFNγ/EV-endMSCs led to 18 significantly altered miRNAs (p-value < 0.05), four of them with an FDR < 0.05 (hsa-miR-196b-5p, hsa-miR-1246, hsa-miR-92a-3p, hsa-miR-150-5p) (**Table 1**, **Supplementary Table 9**). Next, we aimed to obtain a better understanding of the functional impact of these altered miRNAs at the cell, for which we performed IPA analysis to determine the potential microTargets.

According to IPA analysis, only two miRNAs (hsa-miR-150-5p and hsa-miR-196b-5p) showed *Experimentally observed* target annotation (**Figure 7**). The genes targeted by hsa-miR-150-5p are involved in acute-phase response and signaling in macrophages (*Akt, CEBPB*), IL signaling (*CSF1R*), adipogenesis (*EGR2*), inhibition of angiogeneisis (*VEGFA*), endocytosis, macropinocytosis (*PDGFB*), and glucocorticoid receptor signaling (*CEBPB*), among others. On the other hand, among the genes targeted by hsa-miR-196b-5p, there were *ANXA1* and *KRT5* (implicated in glucocorticoid receptor signaling), as well as *IKBKB* and *S100A9* (both associated to IL-mediated cell signaling). The full list of microTargets from the differentially expressed miRNAs and their functional pathways are described in **Supplementary Table 10**.

Macrophage Polarization Assay

Human monocytes were *in vitro* cultured and differentiated toward M1-macrophages and M2-macrophages using GM-CSF and M-CSF, respectively. Similarly, human monocytes were co-cultured with EV-endMSCs ($n = 4$) and IFNγ/EV-endMSCs (n

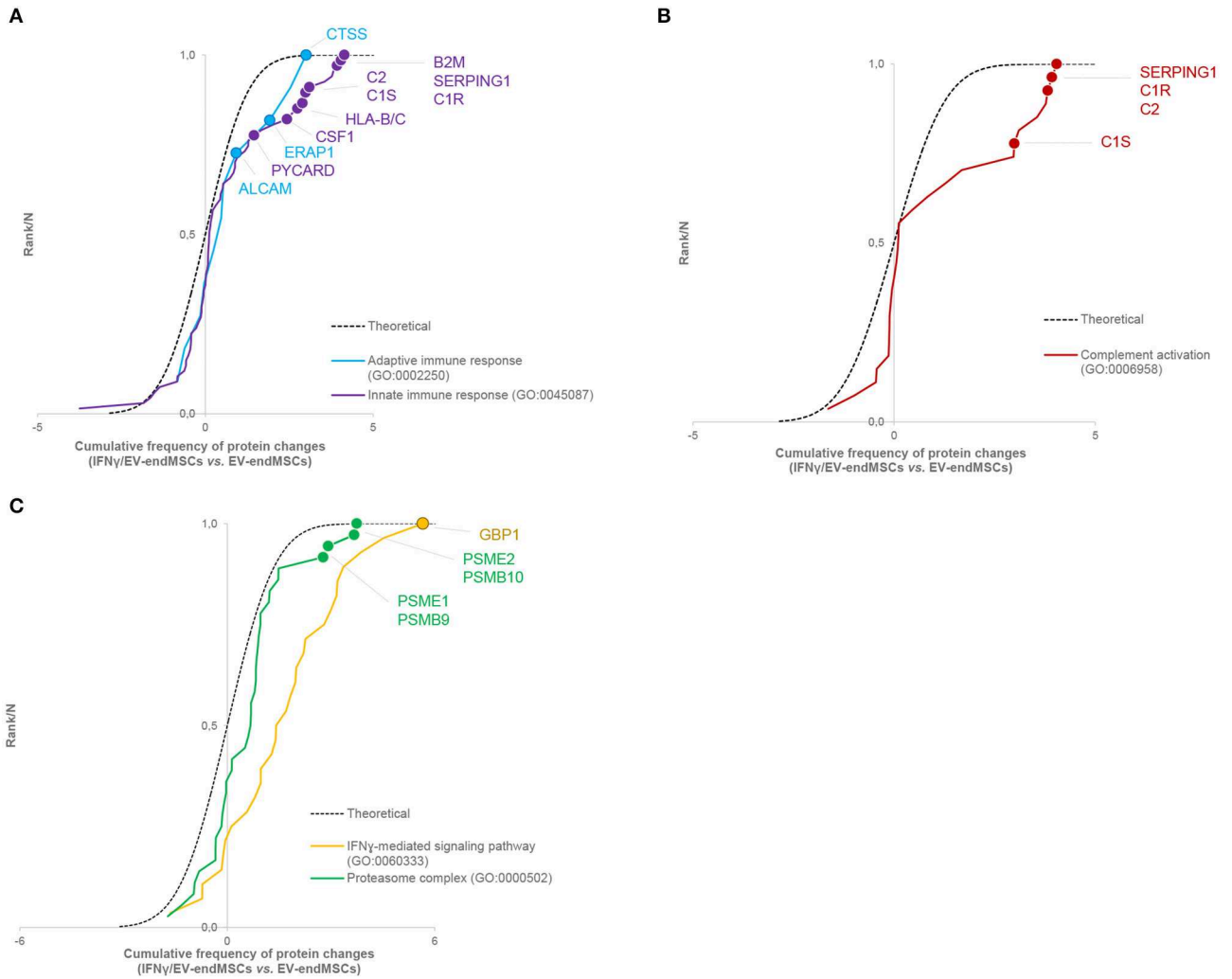

FIGURE 6 | Systems biology analysis of the IFNγ effect on EV-endMSC proteome. Quantitative proteomics results were analyzed using the Systems Biology Triangle (SBT) model (García-Marqués et al., 2016) to detect coordinated protein changes in the functional pathways. Functional categories were considered significantly changed at p-value <0.05. Results show the cumulative distribution of average difference of Zq values from proteins of interesting categories. A right-wards shift from the theoretical curve represents a global tendency of up-regulation in IFNγ/EV-endMSCs *vs*. EV-endMSCs. **(A)** *Innate immune response* (GO:0045087), and *adaptive immune response* (GO:0002250). **(B)** *Complement activation* (GO:0006958). **(C)** *IFNγ-mediated signaling pathway* (GO:0060333), and *proteasome complex* (GO:0000502). The complete sets of protein changes from each category are listed in **Supplementary Tables 8A–C**, respectively. EV-endMSCs, Extracellular Vesicles derived from endometrial MSCs; IFNγ/EV-endMSCs, Extracellular Vesicles derived from IFNγ-primed endometrial MSCs.

= 4). At day 6, the flow cytometry analysis of CD206 allowed us to quantify the monocyte-to-macrophage differentiation and polarization (**Figure 8**). Our results demonstrated that EV-endMSCs and IFNγ/EV-endMSCs triggered the macrophage differentiation toward M2 phenotype ($p < 0.05$). As expected, significant differences were found when we compared M1-differentiated cells and EVs-differentiated cells. However, our study did not reveal any significant difference between EV-endMSCs and IFNγ/EV-endMSCs.

Finally, for a more detailed characterization, *in vitro* differentiated monocytes co-cultured with EV-endMSCs and IFNγ/EV-endMSCs were also analyzed by qPCR. In this analysis, M1/M2 cytokines (*IL1b*, *TNF*, *TGFb,* and *NOS2)* did not reveal any conclusive result in terms of gene expression (**Supplementary Figure 6**).

DISCUSSION

The extracellular vesicles (EVs) derived from MSCs are gaining interest among researchers (Keshtkar et al., 2018), and a proof of that is the increasing number of related publications (Roy et al., 2018). MSCs can be isolated from very different sources, however, endometrial tissue-resident MSCs are especially attractive from a therapeutic point of view because of their remarkable proliferating capacity, effective regenerative, and angiogenic potential (Tempest et al., 2018).

TABLE 1 | Significantly expressed miRNAs in IFNγ/EV-endMSCs.

miRNA	logFC	*p*-value	FDR
hsa-miR-196b-5p	1.07	< 0.0001	**0.00019**
hsa-miR-1246	−1.12	< 0.0001	**0.00616**
hsa-miR-92a-3p	−1.34	0.0001	**0.01187**
hsa-miR-150-5p	−1.87	0.00023	**0.02956**
hsa-miR-299-5p	−4.32	0.00055	0.05749
hsa-miR-146a-5p	−1.88	0.00114	0.09818
hsa-miR-378a-3p	−1.45	0.00763	0.49394
hsa-miR-27a-5p	0.99	0.01104	0.61100
hsa-miR-484	−2.12	0.01614	0.61698
hsa-miR-409-3p	−0.80	0.01816	0.61698
hsa-miR-490-3p	1.15	0.01853	0.61698
hsa-miR-30c-5p	−0.87	0.02242	0.61698
hsa-miR-10b-5p	0.34	0.02252	0.61698
hsa-miR-574-5p	1.25	0.02263	0.61698
hsa-miR-486-5p	−1.25	0.02619	0.64869
hsa-miR-17-5p	1.20	0.02630	0.64869
hsa-miR-376c-3p	0.96	0.03618	0.67893
hsa-miR-146b-5p	−0.59	0.03790	0.67893

miRNA expression level is expressed as log fold change (logFC) between IFNγ/EV-endMSCs (n = 4), and EV-endMSCs groups (n = 4). The comparison of expression levels between groups led to 18 significantly altered microRNAs (p < 0.05), 4 of them presenting 5% FDR (bold highlighted) based on Benjamini-Hochberg FDR adjusted p-values. The full list of differentially expressed miRNAs is described in ***Supplementary Table 9****. EV-endMSCs: Extracellular Vesicles derived from endometrial MSCs; FDR: False Discovery Rate; IFNγ/EV-endMSCs: Extracellular Vesicles derived from IFNγ-primed endometrial MSCs.*

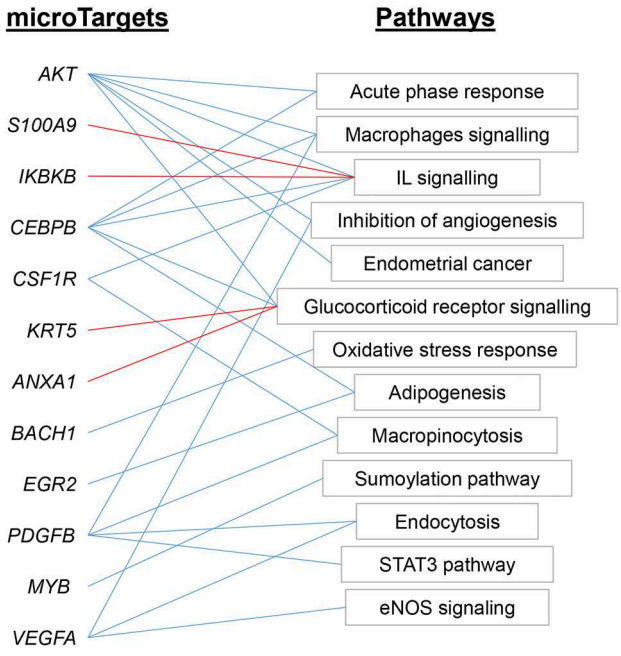

FIGURE 7 | Functional analysis of miRNAs expression profile EV-endMSCs. Ingenuity Pathway Analyses were performed to identify the microTargets of those miRNAs with *Experimentally observed* annotation. Figure shows interesting/representative pathways targeted by hsa-miR-196b-5p (red) and hsa-miR-150-5p (blue). Full lists of functional pathways involving *Experimentally observed* targeted genes (microTargets) are shown in **Supplementary Table 10**. EV-endMSCs, Extracellular Vesicles derived from endometrial MSCs.

The main objective of this study was focused on an exhaustive characterization of EVs released by menstrual blood-derived endMSCs (EV-endMSCs). Moreover, our interest was also focused on the biological consequences of IFNγ-priming on EV-endMSC, unraveling the proteome and microRNAome of these brand-new therapeutic tools (Murphy et al., 2019), and finding for them new and safe clinical applications.

As well as stem/stromal cells derived from placenta (Silini and Parolini, 2018), amniotic fluid (Ramasamy et al., 2018), and Wharton's jelly (Joerger-Messerli et al., 2016), MSCs from endometrial tissue can be easily expanded using standardized protocols, and without ethical concerns. This aspect is an important issue, since the simplicity of isolation protocols by non-invasive procedures and the robust expansion capacity of stem cells are crucial for a successful clinical translation of adult stem cells (Bunpetch et al., 2017).

From a methodological point of view, the *in vitro* isolation of EV-endMSCs was a simple and laborious procedure that required the collection of cell culture supernatants every 3 days and subsequent centrifugations, filtrations, and size-exclusion concentrations. Because of the complexity and variability of EVs released by *in vitro* cultured cells (exosomes, microvesicles, apoptotic bodies), and the variety of isolation protocols (ultracentrifugations, size-exclusion chromatography, field flow fractionation), the characterizations and isolations of released vesicles have been recently reviewed by the International Society for Extracellular Vesicles (Théry et al., 2018). In our study, the isolation/enrichment protocols for EV-endMSCs collection were developed according to previous studies from our group, after comparing different isolation protocols (Álvarez et al., 2015). The workflow for molecular characterization was performed using two strategies: high throughput proteomic analysis, and next generation sequencing (NGS) for miRNAs. In order to simplify and clarify the relevance of these results, the proteomic and miRNAs analyses will be separately discussed.

The study of EV-endMSCs proteome was performed with a high-throughput quantitative proteomic approach based on multiplex peptide stable isotope labeling, whose applicability on EV proteome profiling has been extensively studied and reviewed (Raimondo et al., 2011; Pocsfalvi et al., 2016; Greening et al., 2017). We considered more appropriate to characterize the untreated EV-endMSCs proteome (whose cells were not treated with IFNγ) before moving toward the absolute quantification of proteins due to IFNγ-priming. We found that the 69% of the entire EV-endMSCs proteome composition was associated to the GO term *Extracellular exosome* (GO:0070062), demonstrating the relatively high purity of the vesicles. Among these proteins, 71 were included in the 100 top-identified

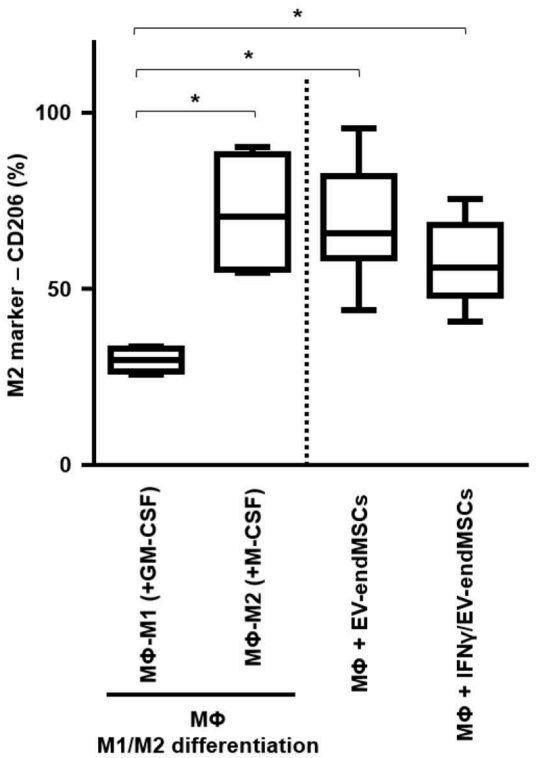

FIGURE 8 | *In vitro* M1/M2 Macrophage differentiation assay. Monocytes were firstly isolated from peripheral blood cells by plastic adherence. The M1 differentiation was performed in the presence of 50 ng/ml of human Granulocyte-Macrophages Colony-Stimulating Factor (GM-CSF). The M2 differentiation was performed in the presence of 50 ng/ml of human Macrophages Colony-Stimulating Factor (GM-CSF). M1-differentiated Macrophages (MΦ-M1) and M2-differentiated Macrophages (MΦ-M2) were analyzed at day 6 of differentiation. In parallel, EV-endMSCs and IFNγ/EV-endMSCs were added to monocytes at day 0 and *in vitro* cultured for 6 days. Similarly, monocytes were differentiated toward M1 Macrophages (MΦ-M1) in the presence of EV-endMSCs and IFNγ/EV-endMSCs. The macrophages were then trypsinized and the surface expression of CD206 (M2 marker) was determined by flow cytometry in $CD14^+$ cells. The lower boundary of the boxes indicates the 25th percentile and the upper boundary, the 75th percentile. Bars above and below the boxes indicate the 90th and 10th percentiles. The line within the boxes marks the median. No significant differences were observed between EV-endMSCs and IFNγ/EV-endMSCs. $^*p \leq 0.05$.

proteins in ExoCarta database. Since ExoCarta is one of the most reliable database about EVs biomolecules (Rosa-Fernandes et al., 2017) and it has been commonly used by several authors to characterize the proteomic profiles of EVs (Jeannin et al., 2018; Arab et al., 2019; Göran Ronquist, 2019), our results further confirmed the vesicular origin of identified proteins. Surprisingly, the first identified protein was serotransferrin (see **Supplementary Table 1**). However, serotransferrin should not be considered a component of the released EVs since its presence may be the consequence of using an insulin-transferrin-selenium solution for *in vitro* cell culture and EV collection, as previously described by other authors (Tauro et al., 2012; Garcia et al., 2015; Chen et al., 2017).

It is important to note that EVs are considered critical mediators of cell to cell communication through the exchange of different molecules, such as proteins, DNA, RNA species, and metabolites (Caruso Bavisotto et al., 2019). Remarkably, EVs cargo can be modulated by different stimuli to the source cell, exerting pleiotropic effects on the recipient cell (Yoon et al., 2014). Being EVs natural carriers of proteins, which are essential for organism function and homeostasis, we aimed to investigate the subcellular origins of the EV-carried proteins. In accordance with other authors (Raimondo et al., 2011; Yuan et al., 2019), the Gene Ontology analysis of the EV-endMSCs proteome demonstrated an enrichment of proteins classified by the terms *Cytosol* (GO:0005829), *Extracellular space* (GO:0005615), *Membrane* (GO:0016020), and *Extracellular matrix* (GO:0031012). The inclusion of our EV-proteins in these four categories is understandable, considering that they are necessary for EV biogenesis, release, and uptake (Abels and Breakefield, 2016; Mathieu et al., 2019). In addition, the proteins classified within these categories are involved in different biological processes, such as cellular migration (Sung et al., 2015), invasion (Mu et al., 2013), embryo implantation (Desrochers et al., 2016), tumor metastasis (Hoshino et al., 2015; Sedgwick et al., 2015), and neutrophils recruitment during inflammation (Majumdar et al., 2016), among others.

Furthermore, the EV-endMSCs proteome was composed by proteins classified in the significantly enriched GO term *Mitochondrion* (GO:0005739). Even though this category was not reported by the above mentioned authors describing EV proteomes (Raimondo et al., 2011; Yuan et al., 2019), recent studies have outlined the existence of a mitochondrial-endolysosomal axis (Soto-Heredero et al., 2017; Picca et al., 2019a), where mitochondrial molecules are carried by EVs and exert their effect in processes like mitochondrial quality control (Picca et al., 2019b), senescence (Eitan et al., 2017), and "inflamm-aging" (Prattichizzo et al., 2017).

The presence of several EV-endMSCs proteins related to the *Immunological synapse* (GO:0001772) confirmed the findings of other researchers, who already associated EVs to mechanisms like T cell-antigen presenting cell interaction (Choudhuri et al., 2014), antigen-specific T-cell activation induced by dendritic cell (Théry et al., 2002), MHC class-II mediated antigen presentation (Roche and Furuta, 2015), and T-helper 1 cells differentiation (Qazi et al., 2009). In contrast to other authors who detected the presence of nuclear (Raimondo et al., 2011; Yuan et al., 2019) and ribosomal EV proteins (Ung et al., 2014), the EV-endMSCs proteome was not significantly enriched in these components.

As previously mentioned, the comparative analysis between EV-endMSCs and IFNγ/EV-endMSCs has revealed statistically significant differences in a wide range of proteins with different biological functions. In an attempt to determine the most relevant results from this exhaustive analysis, we focused our interest on immunomodulatory proteins that may have a key role in the therapeutic efficacy of these EVs. Of course, we are aware that this selection is questionable and, for sure, many other proteins may deserve a proper discussion and further investigation.

The identification of CSF-1 (also called M-CSF), in EV-endMSCs, and the differential expression observed on IFNγ/EV-endMSCs, could be considered one of the most relevant results from this study. The changes observed for this protein were further confirmed by ELISA. The immunoassay corroborated the significant differences observed in the proteomic analysis between EV-endMSCs and IFNγ/EV-endMSCs. It is widely accepted that CSF-1 is a primary regulator for macrophages (Jones and Ricardo, 2013) and it has been associated with M2 polarization and shifts toward homeostatic/reparative state (Hamilton, 2008; Hamilton et al., 2014). Additionally, CSF-1 has been found to modulate inflammatory responses, promoting the expansion and viability of macrophages in patients with inflammatory-mediated diseases (Lenzo et al., 2012; Hamilton and Achuthan, 2013). In the context of stem cell-based therapies, preclinical studies in myocardial infarction have demonstrated the immunomodulatory capacity of MSCs promoting the shift from M1 to M2 macrophages (Cho et al., 2014). More recently, a deep analysis of MSCs-macrophages interactions have shown that MSCs triggered the proliferation/differentiation of macrophages toward M2 by cell-to-cell contact, and by soluble factors where CSF-1 has a key role (Takizawa et al., 2017). All these findings, together with the identification of CSF-1 in these vesicles, and its significant increase in EVs from IFNγ-primed cells, may suggest that EV-endMSCs promote a M2 polarization. In accordance with this idea, an *in vitro* functional assay was performed using EV-endMSCs and IFNγ/EV-endMSCs. These vesicles were co-cultured with peripheral blood monocytes and macrophage differentiation/polarization demonstrated that both control EV-endMSCs and IFNγ/EV-endMSCs favored macrophages differentiation toward M2. In agreement with these *in vitro* results, our research group has recently demonstrated that extracellular vesicles from cardiosphere-derived cells stimulate M2 differentiation in the acute phase of porcine myocardial infarction (López et al., accepted).

Another relevant protein that was found in the proteome of EV-endMSCs and that increased in IFNγ/EV-endMSCs was ERAP1 (an aminopeptidase). Considering that ERAP1 is directly involved in the MHC class I presentation process (Cifaldi et al., 2012), the upregulation of this molecule under IFNγ treatment is not surprising. ERAP-1 is also involved in numerous biological processes and the presence of this protein in EV-endMSCs may have some other consequences. Firstly, the presence of ERAP1 has been found to increase the shedding of cytokine receptors (Cui et al., 2002), and to modulate the overall innate immune response (Aldhamen et al., 2013). Therefore, it is expected that the presence of ERAP1 in EV-endMSCs may have an impact in the inflammatory signaling on target cells. Secondly, ERAP-1 is also involved in cell proliferation, migration and angiogenesis upon stimulation with VEGF (Miyashita et al., 2002; Reeves and James, 2017), so the presence of this molecule in EV-endMSCs may be responsible, at least in part, for the pro-angiogenic effects observed on endMSCs (Hayati et al., 2011; Zhang et al., 2016).

The third protein showing an increase on IFNγ/EV-endMSCs (and classified as immunomodulatory), was PYCARD (also called ASC). This protein is an adaptor for inflammasomes that activate caspase-1 (Taxman et al., 2011) which also regulate the transcription of cytokines through NF-κB activation pathway (Stehlik et al., 2002). Interestingly, PYCARD has been found to inhibit the NF-κB activation mediated by proinflammatory cytokines. Based on that, the presence of this protein in EV-endMSCs may reduce the susceptibility to inflammatory stimuli in target cells. In other words, the interactions between EV-endMSCs and inflammatory cells could modulate the intracellular signaling pathways toward a less inflammatory phenotype.

Together with proteins, miRNA species are essential components of EV cargo (Abels and Breakefield, 2016). For this reason, the characterization of the proteomic profile was followed by an NGS analysis to define the RNA signature of EV-endMSCs. Firstly, our results demonstrated that miRNAs in EV-endMSCs are underrepresented over other small RNAs, which is in agreement with other studies developed in exosomes (Jenjaroenpun et al., 2013; Baglio et al., 2015; Tosar et al., 2015; Sork et al., 2018). Ingenuity Pathways Analyses allowed us to understand the pathways and biological mechanisms of miRNAs dataset. These analyses revealed that, among the 937 miRNAs with more than 10 TPMs, the genes *PTEN*, *CDK6*, *BCL2*, *CCND1*, and *MET* were targeted by 5 to 8 different miRNAs. These genes are directly involved in intracellular signaling, and cell proliferation, so the internalization of the above-mentioned miRNAs in target cells would have a significant impact on these intracellular pathways. Additionally, the quantification of miRNAs revealed that hsa-let-7a-5p, hsa-miR-143-3p, hsa-miR-21-5p, hsa-let-7b-5p, hsa-let-7f-5p, hsa-miR-16-5p, and hsa-miR-199a-3p were abundantly expressed, having an average of more than 200 TPMs. A networks analysis to identify multiple query nodes was performed with miRTargetLink (Wong and Wang, 2015; Liu and Wang, 2019). According to this analysis, 4 of the top-abundant miRNAs (hsa-miR-143-3p, hsa-miR-16-5p, hsa-miR-21-5p, and hsa-let-7b-5p) showed a validated interaction with *IGF1R*. This result may indicate that different miRNAs from EV-endMSCs could inhibit the IGF1R signaling in target cells and, subsequently the IGF1R-related pathways to modulate proliferation, survival, cell adhesion, etc. (Girnita et al., 2014). Finally, miRNA expression profile of EV-endMSCs and IFNγ/EV-endMSCs samples showed four differentially expressed miRNAs (FDR $\leq$ 0.005). Moreover, the IPA analysis revealed that two *Experimentally observed* miRNAs, hsa-miR-150-5p and hsa-miR-196b-5p, target some genes involved in *Glucocorticoid Receptor Signaling*, *IL-6/8/12 Signaling*, and in the *Role of Macrophages*. However, when we tried to validate the expression by qPCR of hsa-mir-1246, hsa-mir-150-5p, hsa-mir-196b-5p, and hsa-mir-92a-3p, we did not obtain conclusive results. PCR amplification of low abundant miRNAs in extracellular vesicles can be a challenge. Unfortunately, the four differentially expressed miRNAs (FDR $<$ 0.05) that we tried to amplify by qPCR were between the least abundant detected by NGS. Hence, we could not validate these miRNAs, even using commercially available optimized probes.

In summary, our qualitative, quantitative, bioinformatics, and *in vitro* analyses of proteins and miRNAs have provided

some clues and hints to unravel the molecules involved in the biological effect of these vesicles. This result, together with proteomics and the macrophage polarization assay suggests that EV-endMSCs may have an immunomodulatory effect in inflammatory conditions.

DATA AVAILABILITY STATEMENT

The datasets generated and analyzed for this study can be found in the European Nucleotide Archive (https://www.ebi.ac.uk/ena) with accession number PRJEB34442 and via ProteomeXchange (http://www.proteomexchange.org/) with identifier PXD015465 (https://www.ebi.ac.uk/pride/archive/projects/PXD015465).

AUTHOR CONTRIBUTIONS

FM, MG-S, FS-M, IJ, and JC conceived and designed the experiments. FM, MG-S, JV, EL, VÁ, JS-C, and RB performed the experiments and analyzed the data. FM, MG-S, IJ, and JC wrote the manuscript.

FUNDING

This study was supported by competitive grants, such as: CIBER-CV (CB16/11/00494 grant to FS-M, CB16/11/00277 grant to JV); Miguel Servet I grant from Instituto de Salud Carlos III to JC (CP17/00021 and MS17/00021 co-financed by FEDER and FSE); Ayuda Grupos de Investigación de Extremadura. Consejería de Economía, Ciencia y Agenda Digital to FS-M (GR18199 cofinanced by FEDER); MAFRESA S.L. grant to FM; Instituto de Salud Carlos III grant to JC (PI18/0911 co-financed by FEDER); Junta de Extremadura to JC (IB16168 grant) co-financed by FEDER; Spanish Ministry of Science, Innovation and Universities to JV (BIO2015-67580-P grant and PGC2018-097019-B-I00 grant), through the Carlos III Institute of Health-Fondo de Investigación Sanitaria grant PRB3 to JV (IPT17/0019-ISCIII-SGEFI/ERDF, ProteoRed), Fundació MaratóTV3 to JV (grant 122/C/2015) and la Caixa Banking Foundation to JV (project code HR17-00247). CNIC was supported by Instituto de Salud Carlos III (ISCIII), Ministerio de Ciencia, Innovación y Universidades (MCNU) and the Pro CNIC Foundation, and it is a Severo Ochoa Center of Excellence (SEV-2015-0505). Sara Borrell grant (co-financed by FSE) to EL. Cell culture *in vitro* studies were performed at the ICTS Nanbiosis (Unit 14, Stem Cell Therapy). The funders had no role in study designs, data collection and analysis, decision to publish, or preparation of the manuscript.

ACKNOWLEDGMENTS

The authors acknowledge the contribution of Carlos Carrasco and Sara Pérez (Bachelor students from University of Extremadura) in the cell culture collection and extracellular vesicle isolations. Special thanks to our colleague Joaquín González for the technical support in figures handling.

SUPPLEMENTARY MATERIAL

The Supplementary Material for this article can be found online at: https://www.frontiersin.org/articles/10.3389/fbioe.2019.00431/full#supplementary-material

REFERENCES

Abels, E. R., and Breakefield, X. O. (2016). Introduction to extracellular vesicles: biogenesis, RNA cargo selection, content, release, and uptake. *Cell. Mol. Neurobiol.* 36, 301–312. doi: 10.1007/s10571-016-0366-z

Aldhamen, Y. A., Seregin, S. S., Rastall, D. P. W., Aylsworth, C. F., Pepelyayeva, Y., Busuito, C. J., et al. (2013). Endoplasmic reticulum aminopeptidase-1 functions regulate key aspects of the innate immune response. *PLoS ONE* 8:e69539. doi: 10.1371/journal.pone.0069539

Álvarez, V., Blázquez, R., Sánchez-Margallo, F. M., DelaRosa, O., Jorge, I., Tapia, A., et al. (2015). Comparative study of isolated human mesenchymal stem cell derived exosomes for clinical use. *Acta Bioquim. Clin. Latinoam.* 49, 311–320. Available online at: http://www.scielo.org.ar/scielo.php?script=sci_isoref&pid=S0325-29572015000300004&lng=en&tlng=es

Álvarez, V., Sánchez-Margallo, F. M., Macías-García, B., Gómez-Serrano, M., Jorge, I., Vázquez, J., et al. (2018). The immunomodulatory activity of extracellular vesicles derived from endometrial mesenchymal stem cells on $CD4^+$ T cells is partially mediated by TGFbeta. *J. Tissue Eng. Regen. Med.* 12, 2088–2098. doi: 10.1002/term.2743

Arab, T., Raffo-Romero, A., Van, C. C., Lemaire, Q., Le, F. M.-C., Drago, F., et al. (2019). Proteomic characterisation of leech microglia extracellular vesicles (EVs): comparison between differential ultracentrifugation and Optiprep™ density gradient isolation. *J. Extracell. Vesicles* 8:1603048. doi: 10.1080/20013078.2019.1603048

Bagheri-Mohammadi, S., Karimian, M., Alani, B., Verdi, J., Tehrani, R. M., and Noureddini, M. (2019). Stem cell-based therapy for Parkinson's disease with a focus on human endometrium-derived mesenchymal stem cells. *J. Cell. Physiol.* 234, 1326–1335. doi: 10.1002/jcp.27182

Baglio, S. R., Rooijers, K., Koppers-Lalic, D., Verweij, F. J., Pérez Lanzón, M., Zini, N., et al. (2015). Human bone marrow- and adipose-mesenchymal stem cells secrete exosomes enriched in distinctive miRNA and tRNA species. *Stem Cell Res. Ther.* 6:127. doi: 10.1186/s13287-015-0116-z

Binek, A., Fernández-Jiménez, R., Jorge, I., Camafeita, E., López, J. A., Bagwan, N., et al. (2017). Proteomic footprint of myocardial ischemia/reperfusion injury: longitudinal study of the at-risk and remote regions in the pig model. *Sci. Rep.* 7:12343. doi: 10.1038/s41598-017-11985-5

Blázquez, R., Sánchez-Margallo, F. M., Álvarez, V., Matilla, E., Hernández, N., Marinaro, F., et al. (2018). Murine embryos exposed to human endometrial MSCs-derived extracellular vesicles exhibit higher VEGF/PDGF AA release, increased blastomere count and hatching rates. *PLoS ONE* 13:e0196080. doi: 10.1371/journal.pone.0196080

Bonzon-Kulichenko, E., Pérez-Hernández, D., Núñez, E., Martínez-Acedo, P., Navarro, P., Trevisan-Herraz, M., et al. (2011). A robust method for quantitative high-throughput analysis of proteomes by 18O labeling. *Mol. Cell Proteomics* 10:M110.003335. doi: 10.1074/mcp.M110.003335

Bunpetch, V., Wu, H., Zhang, S., and Ouyang, H. (2017). From "Bench to Bedside": current advancement on large-scale production of mesenchymal stem cells. *Stem Cells Dev.* 26, 1662–1673. doi: 10.1089/scd.2017.0104

Caruso Bavisotto, C., Scalia, F., Marino Gammazza, A., Carlisi, D., Bucchieri, F., Conway de Macario, E., et al. (2019). Extracellular vesicle-mediated cell–cell communication in the nervous system: focus on neurological diseases. *Int. J. Mol. Sci.* 20:434. doi: 10.3390/ijms20020434

Chan, R. W. S., Schwab, K. E., and Gargett, C. E. (2004). Clonogenicity of human endometrial epithelial and stromal cells. *Biol. Reprod.* 70, 1738–1750. doi: 10.1095/biolreprod.103.024109

Chen, L., Xiang, B., Wang, X., and Xiang, C. (2017). Exosomes derived from human menstrual blood-derived stem cells alleviate fulminant hepatic failure. *Stem Cell Res. Ther.* 8:9. doi: 10.1186/s13287-016-0453-6

Chinnadurai, R., Copland, I. B., Patel, S. R., and Galipeau, J. (2014). IDO-independent suppression of T cell effector function by IFN-γ-licensed human mesenchymal stromal cells. *J. Immunol.* 192, 1491–1501. doi: 10.4049/jimmunol.1301828

Cho, D.-I., Kim, M. R., Jeong, H., Jeong, H. C., Jeong, M. H., Yoon, S. H., et al. (2014). Mesenchymal stem cells reciprocally regulate the M1/M2 balance in mouse bone marrow-derived macrophages. *Exp. Mol. Med.* 46:e70. doi: 10.1038/emm.2013.135

Chong, J., Soufan, O., Li, C., Caraus, I., Li, S., Bourque, G., et al. (2018). MetaboAnalyst 4.0: towards more transparent and integrative metabolomics analysis. *Nucleic Acids Res.* 46, W486–W494. doi: 10.1093/nar/gky310

Choudhuri, K., Llodrá, J., Roth, E. W., Tsai, J., Gordo, S., Wucherpfennig, K. W., et al. (2014). Polarized release of TCR-enriched microvesicles at the T cell immunological synapse. *Nature* 507:118. doi: 10.1038/nature12951

Cifaldi, L., Romania, P., Lorenzi, S., Locatelli, F., and Fruci, D. (2012). Role of endoplasmic reticulum aminopeptidases in health and disease: from infection to cancer. *Int. J. Mol. Sci.* 13, 8338–8352. doi: 10.3390/ijms13078338

Cui, X., Hawari, F., Alsaaty, S., Lawrence, M., Combs, C. A., Geng, W., et al. (2002). Identification of ARTS-1 as a novel TNFR1-binding protein that promotes TNFR1 ectodomain shedding. *J. Clin. Invest.* 110, 515–526. doi: 10.1172/JCI13847

DelaRosa, O., Lombardo, E., Beraza, A., Mancheño-Corvo, P., Ramirez, C., Menta, R., et al. (2009). Requirement of IFN-gamma-mediated indoleamine 2,3-dioxygenase expression in the modulation of lymphocyte proliferation by human adipose-derived stem cells. *Tissue Eng. Part A* 15, 2795–2806. doi: 10.1089/ten.TEA.2008.0630

Desrochers, L. M., Bordeleau, F., Reinhart-King, C. A., Cerione, R. A., and Antonyak, M. A. (2016). Microvesicles provide a mechanism for intercellular communication by embryonic stem cells during embryo implantation. *Nat. Commun.* 7:11958. doi: 10.1038/ncomms11958

Doyle, L. M., and Wang, M. Z. (2019). Overview of extracellular vesicles, their origin, composition, purpose, and methods for exosome isolation and analysis. *Cells* 8:E727. doi: 10.3390/cells8070727

Du, X., Yuan, Q., Qu, Y., Zhou, Y., and Bei, J. (2016). Endometrial mesenchymal stem cells isolated from menstrual blood by adherence. *Stem Cells Int.* 2016:3573846. doi: 10.1155/2016/3573846

Edwards, A., and Haas, W. (2016). Multiplexed quantitative proteomics for high-throughput comprehensive proteome comparisons of human cell lines. *Methods Mol. Biol.* 1394, 1–13. doi: 10.1007/978-1-4939-3341-9_1

Eitan, E., Green, J., Bodogai, M., Mode, N. A., Bæk, R., Jørgensen, M. M., et al. (2017). Age-related changes in plasma extracellular vesicle characteristics and internalization by leukocytes. *Sci. Rep.* 7:1342. doi: 10.1038/s41598-017-01386-z

Gao, J., Scheenstra, M. R., van Dijk, A., Veldhuizen, E. J. A., and Haagsman, H. P. (2018). A new and efficient culture method for porcine bone marrow-derived M1- and M2-polarized macrophages. *Vet. Immunol. Immunopathol.* 200, 7–15. doi: 10.1016/j.vetimm.2018.04.002

Garcia, N. A., Ontoria-Oviedo, I., González-King, H., Diez-Juan, A., and Sepúlveda, P. (2015). Glucose starvation in cardiomyocytes enhances exosome secretion and promotes angiogenesis in endothelial cells. *PLoS ONE* 10:e0138849. doi: 10.1371/journal.pone.0138849

García-Marqués, F., Trevisan-Herraz, M., Martínez-Martínez, S., Camafeita, E., Jorge, I., Lopez, J. A., et al. (2016). A novel systems-biology algorithm for the analysis of coordinated protein responses using quantitative proteomics. *Mol. Cell Proteomics* 15, 1740–1760. doi: 10.1074/mcp.M115.055905

Gargett, C. E., Schwab, K. E., and Deane, J. A. (2016). Endometrial stem/progenitor cells: the first 10 years. *Hum. Reprod. Update* 22, 137–163. doi: 10.1093/humupd/dmv051

Gilsanz, A., Sánchez-Martín, L., Gutiérrez-López, M. D., Ovalle, S., Machado-Pineda, Y., Reyes, R., et al. (2013). ALCAM/CD166 adhesive function is regulated by the tetraspanin CD9. *Cell. Mol. Life Sci.* 70, 475–493. doi: 10.1007/s00018-012-1132-0

Girnita, L., Worrall, C., Takahashi, S.-I., Seregard, S., and Girnita, A. (2014). Something old, something new and something borrowed: emerging paradigm of insulin-like growth factor type 1 receptor (IGF-1R) signaling regulation. *Cell. Mol. Life Sci.* 71, 2403–2427. doi: 10.1007/s00018-013-1514-y

Gómez-Serrano, M., Camafeita, E., García-Santos, E., López, J. A., Rubio, M. A., Sánchez-Pernaute, A., et al. (2016). Proteome-wide alterations on adipose tissue from obese patients as age-, diabetes- and gender-specific hallmarks. *Sci. Rep.* 6:25756. doi: 10.1038/srep25756

Göran Ronquist, K. (2019). Extracellular vesicles and energy metabolism. *Clin. Chim. Acta* 488, 116–121. doi: 10.1016/j.cca.2018.10.044

Greening, D. W., Xu, R., Gopal, S. K., Rai, A., and Simpson, R. J. (2017). Proteomic insights into extracellular vesicle biology–defining exosomes and shed microvesicles. *Expert Rev. Proteomics* 14, 69–95. doi: 10.1080/14789450.2017.1260450

Hamilton, J. A. (2008). Colony-stimulating factors in inflammation and autoimmunity. *Nat. Rev. Immunol.* 8, 533–544. doi: 10.1038/nri2356

Hamilton, J. A., and Achuthan, A. (2013). Colony stimulating factors and myeloid cell biology in health and disease. *Trends Immunol.* 34, 81–89. doi: 10.1016/j.it.2012.08.006

Hamilton, T. A., Zhao, C., Pavicic, P. G., and Datta, S. (2014). Myeloid colony-stimulating factors as regulators of macrophage polarization. *Front. Immunol.* 5:554. doi: 10.3389/fimmu.2014.00554

Harting, M. T., Srivastava, A. K., Zhaorigetu, S., Bair, H., Prabhakara, K. S., Toledano Furman, N. E., et al. (2018). Inflammation-stimulated mesenchymal stromal cell-derived extracellular vesicles attenuate inflammation. *Stem Cells* 36, 79–90. doi: 10.1002/stem.2730

Hayati, A.-R., Nur Fariha, M.-M., Tan, G.-C., Tan, A.-E., and Chua, K. (2011). Potential of human decidua stem cells for angiogenesis and neurogenesis. *Arch. Med. Res.* 42, 291–300. doi: 10.1016/j.arcmed.2011.06.005

Hoshino, A., Costa-Silva, B., Shen, T.-L., Rodrigues, G., Hashimoto, A., Tesic Mark, M., et al. (2015). Tumour exosome integrins determine organotropic metastasis. *Nature* 527, 329–335. doi: 10.1038/nature15756

Huang, D. W., Sherman, B. T., and Lempicki, R. A. (2009a). Bioinformatics enrichment tools: paths toward the comprehensive functional analysis of large gene lists. *Nucleic Acids Res.* 37, 1–13. doi: 10.1093/nar/gkn923

Huang, D. W., Sherman, B. T., and Lempicki, R. A. (2009b). Systematic and integrative analysis of large gene lists using DAVID bioinformatics resources. *Nat. Protoc.* 4, 44–57. doi: 10.1038/nprot.2008.211

Jeannin, P., Chaze, T., Giai Gianetto, Q., Matondo, M., Gout, O., Gessain, A., et al. (2018). Proteomic analysis of plasma extracellular vesicles reveals mitochondrial stress upon HTLV-1 infection. *Sci. Rep.* 8:5170. doi: 10.1038/s41598-018-23505-0

Jenjaroenpun, P., Kremenska, Y., Nair, V. M., Kremenskoy, M., Joseph, B., and Kurochkin, I. V. (2013). Characterization of RNA in exosomes secreted by human breast cancer cell lines using next-generation sequencing. *PeerJ* 1:e201. doi: 10.7717/peerj.201

Joerger-Messerli, M. S., Marx, C., Oppliger, B., Mueller, M., Surbek, D. V., and Schoeberlein, A. (2016). Mesenchymal stem cells from Wharton's jelly and amniotic fluid. *Best Pract. Res. Clin. Obstet. Gynaecol.* 31, 30–44. doi: 10.1016/j.bpobgyn.2015.07.006

Jones, C. V., and Ricardo, S. D. (2013). Macrophages and CSF-1: implications for development and beyond. *Organogenesis* 9, 249–260. doi: 10.4161/org.25676

Jorge, I., Navarro, P., Martínez-Acedo, P., Núñez, E., Serrano, H., Alfranca, A., et al. (2009). Statistical model to analyze quantitative proteomics data obtained by 18O/16O labeling and linear ion trap mass spectrometry: application to the study of vascular endothelial growth factor-induced angiogenesis in endothelial cells. *Mol. Cell Proteomics* 8, 1130–1149. doi: 10.1074/mcp.M800260-MCP200

Jylhä, A., Nättinen, J., Aapola, U., Mikhailova, A., Nykter, M., Zhou, L., et al. (2018). Comparison of iTRAQ and SWATH in a clinical study with multiple time points. *Clin. Proteomics* 15:24. doi: 10.1186/s12014-018-9201-5

Kato, Y., Tanaka, Y., Hayashi, M., Okawa, K., and Minato, N. (2006). Involvement of CD166 in the activation of human γδT cells by tumor cells sensitized with nonpeptide antigens. *J. Immunol.* 177, 877–884. doi: 10.4049/jimmunol.177.2.877

Keerthikumar, S., Chisanga, D., Ariyaratne, D., Al Saffar, H., Anand, S., Zhao, K., et al. (2016). ExoCarta: a web-based compendium of exosomal cargo. *J. Mol. Biol.* 428, 688–692. doi: 10.1016/j.jmb.2015.09.019

Keshtkar, S., Azarpira, N., and Ghahremani, M. H. (2018). Mesenchymal stem cell-derived extracellular vesicles: novel frontiers in regenerative medicine. *Stem Cell Res. Ther.* 9:63. doi: 10.1186/s13287-018-0791-7

Kim, N., and Cho, S.-G. (2016). Overcoming immunoregulatory plasticity of mesenchymal stem cells for accelerated clinical applications. *Int. J. Hematol.* 103, 129–137. doi: 10.1007/s12185-015-1918-6

Kozomara, A., Birgaoanu, M., and Griffiths-Jones, S. (2019). miRBase: from microRNA sequences to function. *Nucleic Acids Res.* 47, D155–D162. doi: 10.1093/nar/gky1141

Kyurkchiev, S., Shterev, A., and Dimitrov, R. (2010). Assessment of presence and characteristics of multipotent stromal cells in human endometrium and decidua. *Reprod. Biomed. Online* 20, 305–313. doi: 10.1016/j.rbmo.2009.12.011

Lenzo, J. C., Turner, A. L., Cook, A. D., Vlahos, R., Anderson, G. P., Reynolds, E. C., et al. (2012). Control of macrophage lineage populations by CSF-1 receptor and GM-CSF in homeostasis and inflammation. *Immunol. Cell Biol.* 90, 429–440. doi: 10.1038/icb.2011.58

Liang, C., Jiang, E., Yao, J., Wang, M., Chen, S., Zhou, Z., et al. (2018). Interferon-γ mediates the immunosuppression of bone marrow mesenchymal stem cells on T-lymphocytes *in vitro*. *Hematology* 23, 44–49. doi: 10.1080/10245332.2017.1333245

Liu, W., and Wang, X. (2019). Prediction of functional microRNA targets by integrative modeling of microRNA binding and target expression data. *Genome Biol.* 20:18. doi: 10.1186/s13059-019-1629-z

Liu, Y., Niu, R., Li, W., Lin, J., Stamm, C., Steinhoff, G., et al. (2019). Therapeutic potential of menstrual blood-derived endometrial stem cells in cardiac diseases. *Cell. Mol. Life Sci.* 76, 1681–1695. doi: 10.1007/s00018-019-03019-2

López, E., Blázquez, R., Marinaro, F., Álvarez, V., Blanco, V., Báez, C., et al. (accepted). The intrapericardial delivery of extracellular vesicles from cardiosphere-derived cells stimulates M2 polarization during the acute phase of porcine myocardial infarction. *Stem Cell Rev. Rep.*

Lv, Y., Xu, X., Zhang, B., Zhou, G., Li, H., Du, C., et al. (2014). Endometrial regenerative cells as a novel cell therapy attenuate experimental colitis in mice. *J. Transl. Med.* 12:344. doi: 10.1186/s12967-014-0344-5

Majumdar, R., Tameh, A. T., and Parent, C. A. (2016). Exosomes mediate LTB4 release during neutrophil chemotaxis. *PLoS Biol.* 14:e1002336. doi: 10.1371/journal.pbio.1002336

Marinaro, F., Macías-García, B., Sánchez-Margallo, F. M., Blázquez, R., Álvarez, V., Matilla, E., et al. (2019). Extracellular vesicles derived from endometrial human mesenchymal stem cells enhance embryo yield and quality in an aged murine model. *Biol. Reprod.* 100, 1180–1192. doi: 10.1093/biolre/ioy263

Martínez-Bartolomé, S., Navarro, P., Martín-Maroto, F., López-Ferrer, D., Ramos-Fernández, A., Villar, M., et al. (2008). Properties of average score distributions of SEQUEST: the probability ratio method. *Mol. Cell Proteomics* 7, 1135–1145. doi: 10.1074/mcp.M700239-MCP200

Martínez-López, D., Camafeita, E., Cedó, L., Roldan-Montero, R., Jorge, I., García-Marqués, F., et al. (2019). APOA1 oxidation is associated to dysfunctional high-density lipoproteins in human abdominal aortic aneurysm. *EBioMedicine* 43, 43–53. doi: 10.1016/j.ebiom.2019.04.012

Mathieu, M., Martin-Jaular, L., Lavieu, G., and Théry, C. (2019). Specificities of secretion and uptake of exosomes and other extracellular vesicles for cell-to-cell communication. *Nat. Cell. Biol.* 21, 9–17. doi: 10.1038/s41556-018-0250-9

Miao, W.-M., Vasile, E., Lane, W. S., and Lawler, J. (2001). CD36 associates with CD9 and integrins on human blood platelets. *Blood* 97, 1689–1696. doi: 10.1182/blood.V97.6.1689

Miyashita, H., Yamazaki, T., Akada, T., Niizeki, O., Ogawa, M., Nishikawa, S., et al. (2002). A mouse orthologue of puromycin-insensitive leucyl-specific aminopeptidase is expressed in endothelial cells and plays an important role in angiogenesis. *Blood* 99, 3241–3249. doi: 10.1182/blood.v99.9.3241

Mu, W., Rana, S., and Zöller, M. (2013). Host matrix modulation by tumor exosomes promotes motility and invasiveness. *Neoplasia* 15:875. doi: 10.1593/neo.13786

Murphy, D. E., de Jong, O. G., Brouwer, M., Wood, M. J., Lavieu, G., Schiffelers, R. M., et al. (2019). Extracellular vesicle-based therapeutics: natural versus engineered targeting and trafficking. *Exp. Mol. Med.* 51:32. doi: 10.1038/s12276-019-0223-5

Najar, M., Krayem, M., Meuleman, N., Bron, D., and Lagneaux, L. (2017). Mesenchymal stromal cells and toll-like receptor priming: a critical review. *Immune Netw.* 17, 89–102. doi: 10.4110/in.2017.17.2.89

Navarro, P., Trevisan-Herraz, M., Bonzon-Kulichenko, E., Núñez, E., Martínez-Acedo, P., Pérez-Hernández, D., et al. (2014). General statistical framework for quantitative proteomics by stable isotope labeling. *J. Proteome Res.* 13, 1234–1247. doi: 10.1021/pr4006958

Navarro, P., and Vázquez, J. (2009). A refined method to calculate false discovery rates for peptide identification using decoy databases. *J. Proteome Res.* 8, 1792–1796. doi: 10.1021/pr800362h

Ngwa, J. S., Manning, A. K., Grimsby, J. L., Lu, C., Zhuang, W. V., and Destefano, A. L. (2011). Pathway analysis following association study. *BMC Proc.* 5:S18. doi: 10.1186/1753-6561-5-S9-S18

Nikoo, S., Ebtekar, M., Jeddi-Tehrani, M., Shervin, A., Bozorgmehr, M., Kazemnejad, S., et al. (2012). Effect of menstrual blood-derived stromal stem cells on proliferative capacity of peripheral blood mononuclear cells in allogeneic mixed lymphocyte reaction. *J. Obstet. Gynaecol. Res.* 38, 804–809. doi: 10.1111/j.1447-0756.2011.01800.x

Nikoo, S., Ebtekar, M., Jeddi-Tehrani, M., Shervin, A., Bozorgmehr, M., Vafaei, S., et al. (2014). Menstrual blood-derived stromal stem cells from women with and without endometriosis reveal different phenotypic and functional characteristics. *Mol. Hum. Reprod.* 20, 905–918. doi: 10.1093/molehr/gau044

Peron, J. P. S., Jazedje, T., Brandão, W. N., Perin, P. M., Maluf, M., Evangelista, L. P., et al. (2012). Human endometrial-derived mesenchymal stem cells suppress inflammation in the central nervous system of EAE mice. *Stem Cell Rev.* 8, 940–952. doi: 10.1007/s12015-011-9338-3

Picca, A., Guerra, F., Calvani, R., Bucci, C., Lo Monaco, M. R., Bentivoglio, A. R., et al. (2019a). Mitochondrial dysfunction and aging: insights from the analysis of extracellular vesicles. *Int. J. Mol. Sci.* 20:E805. doi: 10.3390/ijms20040805

Picca, A., Guerra, F., Calvani, R., Bucci, C., Lo Monaco, M. R., Bentivoglio, A. R., et al. (2019b). Mitochondrial-derived vesicles as candidate biomarkers in Parkinson's disease: rationale, design and methods of the EXosomes in PArkiNson Disease (EXPAND) study. *Int. J. Mol. Sci.* 20:E2373. doi: 10.3390/ijms20102373

Pocsfalvi, G., Stanly, C., Vilasi, A., Fiume, I., Capasso, G., Turiák, L., et al. (2016). Mass spectrometry of extracellular vesicles. *Mass Spectrom. Rev.* 35, 3–21. doi: 10.1002/mas.21457

Prattichizzo, F., Micolucci, L., Cricca, M., De Carolis, S., Mensà, E., Ceriello, A., et al. (2017). Exosome-based immunomodulation during aging: a nano-perspective on inflamm-aging. *Mech. Ageing Dev.* 168, 44–53. doi: 10.1016/j.mad.2017.02.008

Qazi, K. R., Gehrmann, U., Domange Jordö, E., Karlsson, M. C. I., and Gabrielsson, S. (2009). Antigen-loaded exosomes alone induce Th1-type memory through a B-cell-dependent mechanism. *Blood* 113, 2673–2683. doi: 10.1182/blood-2008-04-153536

Raimondo, F., Morosi, L., Chinello, C., Magni, F., and Pitto, M. (2011). Advances in membranous vesicle and exosome proteomics improving biological understanding and biomarker discovery. *Proteomics* 11, 709–720. doi: 10.1002/pmic.201000422

Ramasamy, T. S., Velaithan, V., Yeow, Y., and Sarkar, F. H. (2018). Stem cells derived from amniotic fluid: a potential pluripotent-like cell source for cellular therapy? *Curr. Stem Cell Res. Ther.* 13, 252–264. doi: 10.2174/1574888X13666180115093800

Reeves, E., and James, E. (2017). Tumour and placenta establishment: The importance of antigen processing and presentation. *Placenta* 56, 34–39. doi: 10.1016/j.placenta.2017.02.025

Robinson, M. D., and Oshlack, A. (2010). A scaling normalization method for differential expression analysis of RNA-seq data. *Genome Biol.* 11:R25. doi: 10.1186/gb-2010-11-3-r25

Roche, P. A., and Furuta, K. (2015). The ins and outs of MHC class II-mediated antigen processing and presentation. *Nat. Rev. Immunol.* 15, 203–216. doi: 10.1038/nri3818

Rosa-Fernandes, L., Rocha, V. B., Carregari, V. C., Urbani, A., and Palmisano, G. (2017). A perspective on extracellular vesicles proteomics. *Front. Chem.* 5:102. doi: 10.3389/fchem.2017.00102

Rossignoli, F., Caselli, A., Grisendi, G., Piccinno, S., Burns, J. S., Murgia, A., et al. (2013). Isolation, characterization, and transduction of endometrial decidual tissue multipotent mesenchymal stromal/stem cells from menstrual blood. *Biomed. Res. Int.* 2013:901821. doi: 10.1155/2013/901821

Roy, S., Hochberg, F. H., and Jones, P. S. (2018). Extracellular vesicles: the growth as diagnostics and therapeutics; a survey.

J. Extracell. Vesicles 7:1438720. doi: 10.1080/20013078.2018.1438720

Ruiz-Meana, M., Núñez, E., Miro-Casas, E., Martínez-Acedo, P., Barba, I., Rodriguez-Sinovas, A., et al. (2014). Ischemic preconditioning protects cardiomyocyte mitochondria through mechanisms independent of cytosol. *J. Mol. Cell. Cardiol.* 68, 79–88. doi: 10.1016/j.yjmcc.2014.01.001

Saleh, L., Otti, G. R., Fiala, C., Pollheimer, J., and Knöfler, M. (2011). Evaluation of human first trimester decidual and telomerase-transformed endometrial stromal cells as model systems of *in vitro* decidualization. *Reprod. Biol. Endocrinol.* 9:155. doi: 10.1186/1477-7827-9-155

Sangiorgi, B., and Panepucci, R. A. (2016). Modulation of immunoregulatory properties of mesenchymal stromal cells by toll-like receptors: potential applications on GVHD. *Stem Cells Int.* 2016:9434250. doi: 10.1155/2016/9434250

Schüring, A. N., Schulte, N., Kelsch, R., Röpke, A., Kiesel, L., and Götte, M. (2011). Characterization of endometrial mesenchymal stem-like cells obtained by endometrial biopsy during routine diagnostics. *Fertil. Steril.* 95, 423–426. doi: 10.1016/j.fertnstert.2010.08.035

Sedgwick, A. E., Clancy, J. W., Balmert, M. O., and D'Souza-Schorey, C. (2015). Extracellular microvesicles and invadopodia mediate non-overlapping modes of tumor cell invasion. *Sci. Rep.* 5:14748. doi: 10.1038/srep14748

Showalter, M. R., Wancewicz, B., Fiehn, O., Archard, J. A., Clayton, S., Wagner, J., et al. (2019). Primed mesenchymal stem cells package exosomes with metabolites associated with immunomodulation. *Biochem. Biophys. Res. Commun.* 512, 729–735. doi: 10.1016/j.bbrc.2019.03.119

Silini, A. R., and Parolini, O. (2018). Placental cells and derivatives: advancing clinical translation. *Cell Transplant.* 27, 1–2. doi: 10.1177/0963689717745332

Song, Y., Dou, H., Li, X., Zhao, X., Li, Y., Liu, D., et al. (2017). Exosomal miR-146a contributes to the enhanced therapeutic efficacy of interleukin-1β-primed mesenchymal stem cells against sepsis. *Stem Cells* 35, 1208–1221. doi: 10.1002/stem.2564

Sork, H., Corso, G., Krjutskov, K., Johansson, H. J., Nordin, J. Z., Wiklander, O. P. B., et al. (2018). Heterogeneity and interplay of the extracellular vesicle small RNA transcriptome and proteome. *Sci. Rep.* 8, 1–12. doi: 10.1038/s41598-018-28485-9

Soto-Heredero, G., Baixauli, F., and Mittelbrunn, M. (2017). Interorganelle communication between mitochondria and the endolysosomal system. *Front. Cell Dev. Biol.* 5:95. doi: 10.3389/fcell.2017.00095

Stehlik, C., Fiorentino, L., Dorfleutner, A., Bruey, J.-M., Ariza, E. M., Sagara, J., et al. (2002). The PAAD/PYRIN-family protein ASC is a dual regulator of a conserved step in nuclear factor kappaB activation pathways. *J. Exp. Med.* 196, 1605–1615. doi: 10.1084/jem.20021552

Sun, Y., Ren, Y., Yang, F., He, Y., Liang, S., Guan, L., et al. (2019). High-yield isolation of menstrual blood-derived endometrial stem cells by direct red blood cell lysis treatment. *Biol. Open* 8:bio.038885. doi: 10.1242/bio.038885

Sung, B. H., Ketova, T., Hoshino, D., Zijlstra, A., and Weaver, A. M. (2015). Directional cell movement through tissues is controlled by exosome secretion. *Nat. Commun.* 6:7164. doi: 10.1038/ncomms8164

Takizawa, N., Okubo, N., Kamo, M., Chosa, N., Mikami, T., Suzuki, K., et al. (2017). Bone marrow-derived mesenchymal stem cells propagate immunosuppressive/anti-inflammatory macrophages in cell-to-cell contact-independent and -dependent manners under hypoxic culture. *Exp. Cell Res.* 358, 411–420. doi: 10.1016/j.yexcr.2017.07.014

Tan, J., Li, P., Wang, Q., Li, Y., Li, X., Zhao, D., et al. (2016). Autologous menstrual blood-derived stromal cells transplantation for severe Asherman's syndrome. *Hum. Reprod.* 31, 2723–2729. doi: 10.1093/humrep/dew235

Tauro, B. J., Greening, D. W., Mathias, R. A., Ji, H., Mathivanan, S., Scott, A. M., et al. (2012). Comparison of ultracentrifugation, density gradient separation, and immunoaffinity capture methods for isolating human colon cancer cell line LIM1863-derived exosomes. *Methods* 56, 293–304. doi: 10.1016/j.ymeth.2012.01.002

Taxman, D. J., Holley-Guthrie, E. A., Huang, M. T.-H., Moore, C. B., Bergstralh, D. T., Allen, I. C., et al. (2011). The NLR adaptor ASC/PYCARD regulates DUSP10, mitogen-activated protein kinase (MAPK), and chemokine induction independent of the inflammasome. *J. Biol. Chem.* 286, 19605–19616. doi: 10.1074/jbc.M111.221077

Tempest, N., Maclean, A., and Hapangama, D. K. (2018). Endometrial stem cell markers: current concepts and unresolved questions. *Int. J. Mol. Sci.* 19:E3240. doi: 10.3390/ijms19103240

The Gene Ontology Consortium (2017). Expansion of the gene ontology knowledgebase and resources. *Nucleic Acids Res.* 45, D331–D338. doi: 10.1093/nar/gkw1108

Théry, C., Duban, L., Segura, E., Véron, P., Lantz, O., and Amigorena, S. (2002). Indirect activation of naïve $CD4^+$ T cells by dendritic cell-derived exosomes. *Nat. Immunol.* 3, 1156–1162. doi: 10.1038/ni854

Théry, C., Witwer, K. W., Aikawa, E., Alcaraz, M. J., Anderson, J. D., Andriantsitohaina, R., et al. (2018). Minimal information for studies of extracellular vesicles 2018 (MISEV2018): a position statement of the International Society for Extracellular Vesicles and update of the MISEV2014 guidelines. *J. Extracell. Vesicles* 7:1535750. doi: 10.1080/20013078.2018.1535750

Tosar, J. P., Gámbaro, F., Sanguinetti, J., Bonilla, B., Witwer, K. W., and Cayota, A. (2015). Assessment of small RNA sorting into different extracellular fractions revealed by high-throughput sequencing of breast cell lines. *Nucleic Acids Res.* 43, 5601–5616. doi: 10.1093/nar/gkv432

Trevisan-Herraz, M., Bagwan, N., García-Marqués, F., Rodriguez, J. M., Jorge, I., Ezkurdia, I., et al. (2019). SanXoT: a modular and versatile package for the quantitative analysis of high-throughput proteomics experiments. *Bioinformatics* 35, 1594–1596. doi: 10.1093/bioinformatics/bty815

Ung, T. H., Madsen, H. J., Hellwinkel, J. E., Lencioni, A. M., and Graner, M. W. (2014). Exosome proteomics reveals transcriptional regulator proteins with potential to mediate downstream pathways. *Cancer Sci.* 105, 1384–1392. doi: 10.1111/cas.12534

Wang, J., Chen, S., Zhang, C., Stegeman, S., Pfaff-Amesse, T., Zhang, Y., et al. (2012). Human endometrial stromal stem cells differentiate into megakaryocytes with the ability to produce functional platelets. *PLoS ONE* 7:e44300. doi: 10.1371/journal.pone.0044300

Wiśniewski, J. R., Ostasiewicz, P., and Mann, M. (2011). High recovery FASP applied to the proteomic analysis of microdissected formalin fixed paraffin embedded cancer tissues retrieves known colon cancer markers. *J. Proteome Res.* 10, 3040–3049. doi: 10.1021/pr200019m

Wong, N., and Wang, X. (2015). miRDB: an online resource for microRNA target prediction and functional annotations. *Nucleic Acids Res.* 43, D146–D152. doi: 10.1093/nar/gku1104

Worthington, R. E., Carroll, R. C., and Boucheix, C. (1990). Platelet activation by CD9 monoclonal antibodies is mediated by the Fc gamma II receptor. *Br. J. Haematol.* 74, 216–222. doi: 10.1111/j.1365-2141.1990.tb02568.x

Yin, J. Q., Zhu, J., and Ankrum, J. A. (2019). Manufacturing of primed mesenchymal stromal cells for therapy. *Nat. Biomed. Eng.* 3, 90–104. doi: 10.1038/s41551-018-0325-8

Yoon, Y. J., Kim, O. Y., and Gho, Y. S. (2014). Extracellular vesicles as emerging intercellular communicasomes. *BMB Rep.* 47, 531–539. doi: 10.5483/BMBRep.2014.47.10.164

Yuan, O., Lin, C., Wagner, J., Archard, J. A., Deng, P., Halmai, J., et al. (2019). Exosomes derived from human primed mesenchymal stem cells induce mitosis and potentiate growth factor secretion. *Stem Cells Dev.* 28, 398–409. doi: 10.1089/scd.2018.0200

Zhang, Y., Lin, X., Dai, Y., Hu, X., Zhu, H., Jiang, Y., et al. (2016). Endometrial stem cells repair injured endometrium and induce angiogenesis via AKT and ERK pathways. *Reproduction* 152, 389–402. doi: 10.1530/REP-16-0286

Zhao, Y., Lan, X., Wang, Y., Xu, X., Lu, S., Li, X., et al. (2018). Human endometrial regenerative cells attenuate bleomycin-induced pulmonary fibrosis in mice. *Stem Cells Int.* 2018:3475137. doi: 10.1155/2018/3475137

Conflict of Interest: The authors declare that the research was conducted in the absence of any commercial or financial relationships that could be construed as a potential conflict of interest.

frontiers in Bioengineering and Biotechnology

REVIEW
published: 03 March 2020
doi: 10.3389/fbioe.2020.00146

Extracellular Vesicles Derived From Mesenchymal Stem Cells (MSC) in Regenerative Medicine: Applications in Skin Wound Healing

Antonio Casado-Díaz[1], José Manuel Quesada-Gómez[1] and Gabriel Dorado[2]*

[1] Unidad de Gestión Clínica de Endocrinología y Nutrición, CIBER de Fragilidad y Envejecimiento Saludable (CIBERFES), Instituto Maimónides de Investigación Biomédica de Córdoba (IMIBIC), Hospital Universitario Reina Sofía, Córdoba, Spain, [2] Dep. de Bioquímica y Biología Molecular, Campus Rabanales C6-1-E17, Campus de Excelencia Internacional Agroalimentario (ceiA3), Universidad de Córdoba, CIBERFES, Córdoba, Spain

The cells secrete extracellular vesicles (EV) that may have an endosomal origin, or from evaginations of the plasma membrane. The former are usually called exosomes, with sizes ranging from 50 to 100 nm. These EV contain a lipid bilayer associated to membrane proteins. Molecules such as nucleic acids (DNA, mRNA, miRNA, lncRNA, etc.) and proteins may be stored inside. The EV composition depends on the producer cell type and its physiological conditions. Through them, the cells modify their microenvironment and the behavior of neighboring cells. That is accomplished by transferring factors that modulate different metabolic and signaling pathways. Due to their properties, EV can be applied as a diagnostic and therapeutic tool in medicine. The mesenchymal stromal cells (MSC) have immunomodulatory properties and a high regenerative capacity. These features are linked to their paracrine activity and EV secretion. Therefore, research on exosomes produced by MSC has been intensified for use in cell-free regenerative medicine. In this area, the use of EV for the treatment of chronic skin ulcers (CSU) has been proposed. Such sores occur when normal healing does not resolve properly. That is usually due to excessive prolongation of the inflammatory phase. These ulcers are associated with aging and diseases, such as diabetes, so their prevalence is increasing with the one of such latter disease, mainly in developed countries. This has very important socio-economic repercussions. In this review, we show that the application of MSC-derived EV for the treatment of CSU has positive effects, including accelerating healing and decreasing scar formation. This is because the EV have immunosuppressive and immunomodulatory properties. Likewise, they have the ability to activate the angiogenesis, proliferation, migration, and differentiation of the main cell types involved in skin regeneration. They include endothelial cells, fibroblasts, and keratinocytes. Most of the studies carried out so far are preclinical. Therefore, there is a need to advance more in the knowledge about the conditions of production, isolation, and action mechanisms of EV. Interestingly, their potential application in the treatment of CSU opens the door for the design of new highly effective therapeutic strategies.

Keywords: exosomes, mesenchymal stem cells, skin, wound healing, regenerative medicine, extracellular vesicles

OPEN ACCESS

Edited by:
Wolfgang Holnthoner, Ludwig Boltzmann Institute for Experimental and Clinical Traumatology, Austria

Reviewed by:
Pavel Makarevich, Lomonosov Moscow State University, Russia
Roberta Tasso, University of Genoa, Italy

****Correspondence:***
Antonio Casado-Díaz
bb1cadia@uco.es

Specialty section:
This article was submitted to Tissue Engineering and Regenerative Medicine, a section of the journal Frontiers in Bioengineering and Biotechnology

Received: *09 December 2019*
Accepted: *12 February 2020*
Published: *03 March 2020*

Citation:
Casado-Díaz A, Quesada-Gómez JM and Dorado G (2020) Extracellular Vesicles Derived From Mesenchymal Stem Cells (MSC) in Regenerative Medicine: Applications in Skin Wound Healing. Front. Bioeng. Biotechnol. 8:146. doi: 10.3389/fbioe.2020.00146

INTRODUCTION

Extracellular Vesicles: Definition, Discovery, Classification, Isolation, and Characterization

The word "exosome" is ambiguous, requiring clarification. Thus, it may refer to the "exosome *complex*," being a proteic (enzymatic) macromolecular machinery, present in archaea and eukaryotic cells, being involved in RNA degradation. On the other hand, the "exosome *vesicle*" is an extracellular particle released from the endosomal compartment of most eukaryotic cells. This review deals with the latter only. The exosome vesicles are a type of extracellular vesicles (EV), which are defined as lipid-bilayer spheroid structures, without replicating capacity, that are released from cells, including both prokaryotes and eukaryotes. That includes from simple unicellular organisms to complex multicellular ones. These structures are involved in intercellular-communication mechanisms, being preserved by evolution. Their functionality has been observed not only between cells of the same organism, but also among cells from different organisms of the same or different species, even involving prokaryotes and eukaryotes (Kim et al., 2015; Gho and Lee, 2017). For instance, inter-kingdom communications have been found between the microbiota and the epithelial cells of the large intestine, contributing to maintain the intestinal homeostasis (Cañas et al., 2018).

The EV were first reported after observing procoagulant platelet-derived particles in normal blood plasma (Chargaff and West, 1946). Such particles were defined as "platelet dust" (Wolf, 1967). The release of vesicles generated after the formation of multi-vesicular bodies (MVB) in reticulocytes was independently reported by two research teams, at the beginning of the 1980s (Pan and Johnstone, 1983; Harding et al., 1984). Later on, the term exosome was coined for these endosomal vesicles (Johnstone et al., 1987). Since then, EV have been purified from different cellular types of mammals. In addition, they have been also found in other biological fluids, like urine, breast milk, blood serum (blood plasma without clotting factors), saliva, and semen (Yáñez-Mó et al., 2015). Interestingly, EV may contain ribonucleic acids (RNA), and in particular microRNA (miRNA) (Ratajczak et al., 2006; Valadi et al., 2007). That sparked the interest on such particles, as mediators or intercellular communications. Thus, research on the EV biology has exponentially increased in the last two decades, including their physiological and pathologic roles *in vivo*. Thus, the PubMed database[1] showed only four exosome vesicle hits in 1999, increasing to more than 11,000 in February 2020.

The EV have been traditionally classified into four types, mainly taking into account their origins and sizes: (i) endosomal exosomes (50–100 nm); (ii) microvesicles (MV) from the plasma membrane (20–1000 nm); (iii) membrane particles, also from the plasma membrane (50–600 nm); and (iv) apoptotic vesicles from the plasma membrane and endoplasmic reticulum, through apoptotic processes (1000–5000 nm) (**Figure 1**) (van der Pol et al., 2012). Other authors have classified them into just two types: exosomes, as previously described, and ectosomes (microparticles-MV). The latter ones are derived from the plasma membrane, ranging from 100 to 350 nm (Cocucci and Meldolesi, 2015). Due to the current lack of consensus about the classification and biochemical markers characterizing the different EV types, the International Society for Extracellular Vesicles stated the following in the "Minimal Information for Studies of Extracellular Vesicles 2018" (MISEV2018), in relation to the EV nomenclature: "EV is the preferred generic term for the subject of our investigations, and subtypes should be defined by physical and biochemical characteristics and/or conditions/sources. When other terms are used, careful definition is required" (Théry et al., 2018).

The traditional approach to isolate EV is differential ultracentrifugation. However, new methods have been developed in the last years, like density-gradient ultracentrifugation, allowing to isolate more specific EV populations. Likewise, other technologies have been applied to reduce the isolation time, without expensive specialized equipment. Such later methodologies include the following, among others: (i) exosome precipitation using polymers, like the ExoQuick family of reagents from System Biosciences[2] (Palo Alto, CA, United States); (ii) immunological methods, to capture and quantify exosomes from different fluids; (iii) size-exclusion chromatography; and (iv) magnetic-activated cell sorting (MACS) (Gurunathan et al., 2019).

Characterization of EV is fundamental to determine their biochemical properties and biological functions. That can be accomplished using different methodologies, allowing to determine size, shape, concentration, contents, and surface biochemical-markers. They include: (i) western blotting; (ii) identification and quantification of nucleic-acid contents, using polymerase chain-reaction (PCR), microarray and second-generation sequencing (SGS) and third-generation sequencing (TGS), sometimes known with the ambiguous name of "next"-generation sequencing (NGS); (iii) lipidomic approaches; (iv) nanoparticle-tracking analyses (NTA) or (v) tunable-resistive pulse sensing (TRPS), both for determination of the size and concentration of particles; (vi) dynamic-light scattering (DLS) or (vii) photon-correlation spectroscopy (PCS), both to measure exosome sizes; (viii) atomic-force microscopy (AFM) or (ix) transmission electron microscopy (TEM), both for visualization and characterization of their structure, morphology, and size; (x) flow cytometry, for the characterization of surface biochemical markers; and (xi) fixation for *in situ* imaging (Choi et al., 2013; Kreimer et al., 2015; Gupta et al., 2019; Gurunathan et al., 2019).

Biogenesis

The EV cargos depend on the vesicle types, as well as the cells from which they are derived, and their physiological conditions. The main components of the EV are proteins, lipids, and nucleic acids (**Figure 1**). EV may contain specific groups of cellular proteins, independently of the producing cell. Nevertheless others are secreting-cell-specific peptides.

[1] https://www.ncbi.nlm.nih.gov/pubmed

[2] https://systembio.com/products/exosome-research/exosome-isolation

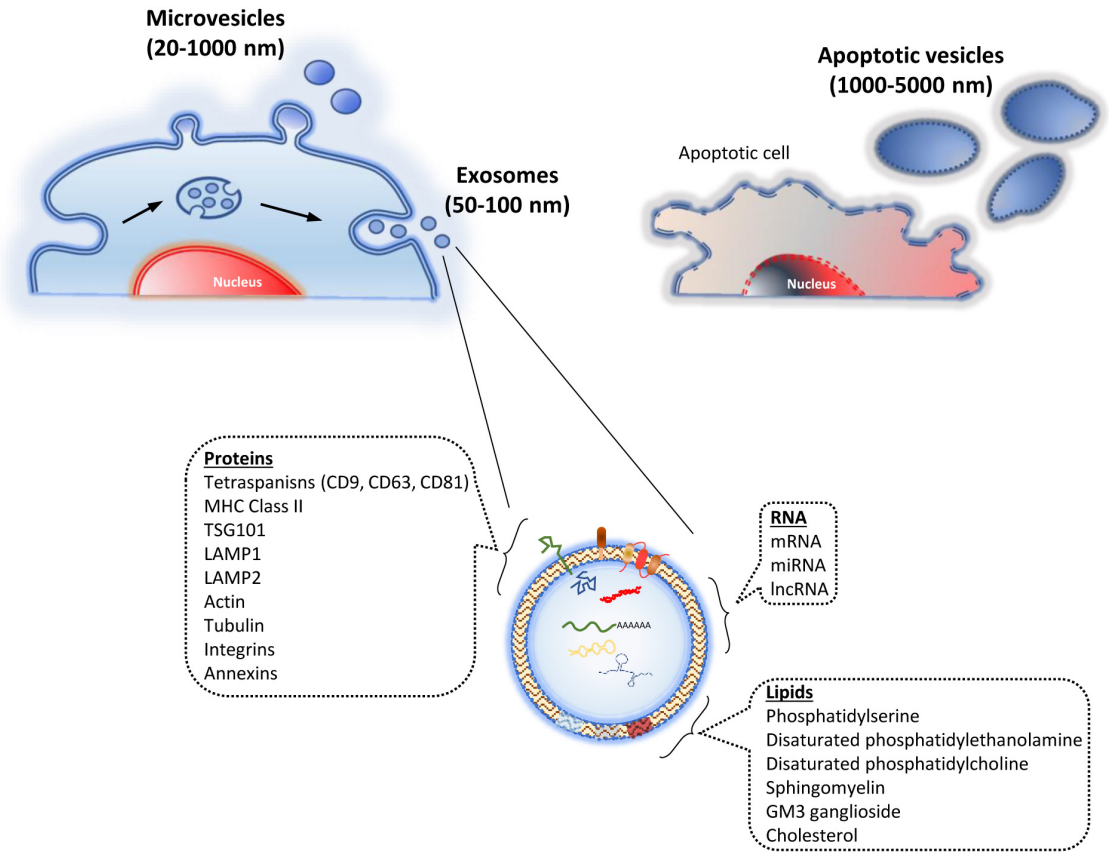

FIGURE 1 | Types of extracellular vesicles. They are classified taking into account their origin. Thus, they include the ones derived from endosomes (exosomes), evagination of the plasma membrane (microvesicles), and vesicles from apoptosis (apoptotic vesicles). The lower part shows the exosome structure, including its main cargo molecules.

The proteins found in the EV include the ones from the endosome itself, plasma membrane, and cytosol. The proteins from the nucleus, mitochondria, endoplasmic reticulum, and Golgi complex are usually absent in the EV. Interestingly, that shows a specific differential selection of proteins when generating such vesicles (Colombo et al., 2014).

On the other hand, the lipid composition of the EV depends on the cellular types from which they are derived. Their lipid bilayer mainly contains the components from the plasma membrane, but they may be enriched in some of them, including phosphatidylserine, disaturated phosphatidylethanolamine, disaturated phosphatidylcholine, sphingomyelin, GM3 ganglioside, and cholesterol (Choi et al., 2013).

Since the discovery that EV carry nucleic acids (Ratajczak et al., 2006; Valadi et al., 2007), numerous studies have described the presence of different RNA types in such particles. They include messenger RNA (mRNA), miRNA, and non-coding RNA (ncRNA). Again, as with proteins and lipids described above, the comparative analyses of nucleic acids between the cells and the EV generated from them may show differential contents.

The biogenesis of exosomes is due to exocytosis of multivesicular endosomes. Such MVB fuse with the plasma membrane, being released to the extracellular environment. Thus, the exosome biogenesis can be divided into three stages: (i) formation of endocytic vesicles, by invagination of the plasma membrane; (ii) formation of MVB, by inward budding of the endosomal membranes; and (iii) fusion of MVB with the plasma membrane and release of the exosomes (**Figure 2**) (Colombo et al., 2014).

In many instances, the contents of the MVB are degraded by hydrolases, if the former merge with lysosomes. But, in other instances, some MVB may fuse with the plasma membrane. That allows to release their contents to the extracellular environment (**Figure 2**). Specific MVB features include the presence of tetraspanins {membrane proteins associated to lysosomes, like lysosomal-associated membrane protein 1, 2, and 3 [LAMP-1, LAMP-2, and LAMP-3, respectively; also known as cluster of differentiation 107a, 107b, and 63 or 208 (CD-107a, CD-107b, and CD-63 or CD-208 antigen), respectively]}, besides other molecules generally present in the late endosomes [e.g., major histocompatibility complex (MHC) class II, in antigen-presenting cells] (Raposo et al., 1996; Colombo et al., 2014).

The best-known mechanism of MVB and exosome generation is the one carried out by the endosomal sorting complex required for transport (ESCRT). It is composed of approximately 30 proteins, generating four complexes (ESCRT-0, -I, -II, and

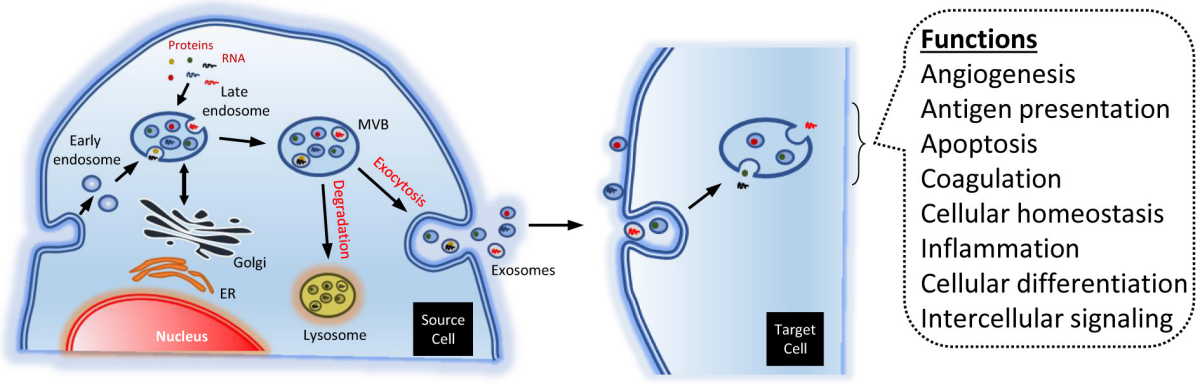

FIGURE 2 | Endosomal biogenesis of exosomes. The endosomes generate multi-vesicular bodies. The latter carry different types of molecules, like RNA and proteins. Such cargos are partially added in a specific way. The MVB may be degraded by the lysosomes, or merge with the plasma membrane, dumping contents to the extracellular space. The exosomes may bind and activate different membrane receptors in the target cells. Alternatively, they can be engulfed, releasing their cargos into the cell. The exosomes may modulate numerous physiological process, though such mechanisms.

-III) with associated proteins, such as vacuolar protein sorting-associated protein 4 (VPS4), vesicle trafficking 1 (VTA-1), and apoptosis-linked gene 2 (ALG-2)-interacting protein X (Alix), also called programmed cell-death 6 interacting protein (PDCD-6-IP) (Hanson and Cashikar, 2012). The ESCRT-0 complex recognizes and sequesters ubiquitinated proteins in the endosomal membrane. On the other hand, ESCRT-I and -II complexes are responsible for membrane deformation into buds, with sequestered cargos. Finally, ESCRT-III drives vesicle scission (Juan and Fürthauer, 2018). Besides such ESCRT-dependent pathways, other ESCRT-independent mechanisms for EV biogenesis have been described. They involve hydrolysis of sphingomyelin into ceramide, or proteins like tetraspanins, as CD-63 (Andreu and Yáñez-Mó, 2014; Colombo et al., 2014). Tetraspanins are also involved in cargo secretion of EV, as well as the process of uptake by receptor cells (Andreu and Yáñez-Mó, 2014).

Functions

Accumulating evidence suggests that the EV have a vital role, not only in the regulation of normal physiological processes, such as stem-cell maintenance, tissue repair, and immune modulation (Mistry et al., 2012; Basu and Ludlow, 2016; Chan et al., 2019), but also in the pathology underlying the occurrence of several diseases (El Andaloussi et al., 2013). The EV regulate physiological events and cellular behavior through several mechanisms. For instance, activating membrane receptors through proteic or lipidic ligands, as well as pouring their contents into receptor cells (**Figure 2**). This way, they can transfer transcription factors, oncogenes, miRNA, mRNA, and even infectious particles (Yáñez-Mó et al., 2015). Because of that, they have been considered signalosomes: multifunctional signaling complexes for controlling fundamental cellular and biological functions (El Andaloussi et al., 2013).

The biological processes involving EV include angiogenesis, antigen presentation, apoptosis, coagulation, cellular homeostasis, inflammation, cellular differentiation, and intercellular signaling. It has been found that the exosomes from progenitor cells stimulate migration, proliferation, and formation of blood vessels in endothelial cells (Yi et al., 2019). The exosome liberation may inhibit or activate apoptosis, depending on their cargos and the receptor-cell types (Xiao et al., 2016; Zhu et al., 2017). The functionality of EV as antigen-presenting helper T lymphocytes is known since the end of the last century. Thus, it has been reported that B lymphocytes secrete vesicles enriched in the MHC class II, with capacity to activate T lymphocytes (Raposo et al., 1996). The EV can work as pro-inflammatory (e.g., when they are produced by cancer cells, synovial fibroblasts, CD-4 + T cells, macrophages, or dendritic cells), or as anti-inflammatory [e.g., when derived from mesenchymal stem cells or mesenchymal stromal cells (MSC), dendritic cells, or T cells]. As a consequence, the EV may play an important role in the genesis or prevention of immunologic diseases, like bowel disease, sepsis, arthritis, diabetes, atherosclerosis, and neurodegenerative ones (Chan et al., 2019).

The physiological roles of the EV depend on their cargos and their capacity to transfer proteins, nucleic acids, and other molecules into the receptor cells. Fortunately, they can be intravenously given to patients, having the capacity to pass through the blood–brain barrier. Therefore, they have been recently considered as relevant therapeutic tools, with significant potential for the prognosis, diagnosis, and treatment of several pathologies (Gurunathan et al., 2019). This is due to several reasons, including that they can: (i) carry different biomolecules, reflecting the physiological condition of producing cells; (ii) be used as stable biomarkers of pathologies, like cancer (Fu et al., 2018); (iii) move through the body fluids; (iv) be identified from such body fluids, like cerebrospinal, urine, saliva, and blood, facilitating their detection and quantification by non-invasive techniques; (v) be used as therapeutic tools to transport and liberate drugs, including miRNA, short hairpin RNA (shRNA), small-interfering RNA (siRNA), as well as other compounds of pharmacological interest, for the treatment of diseases, like

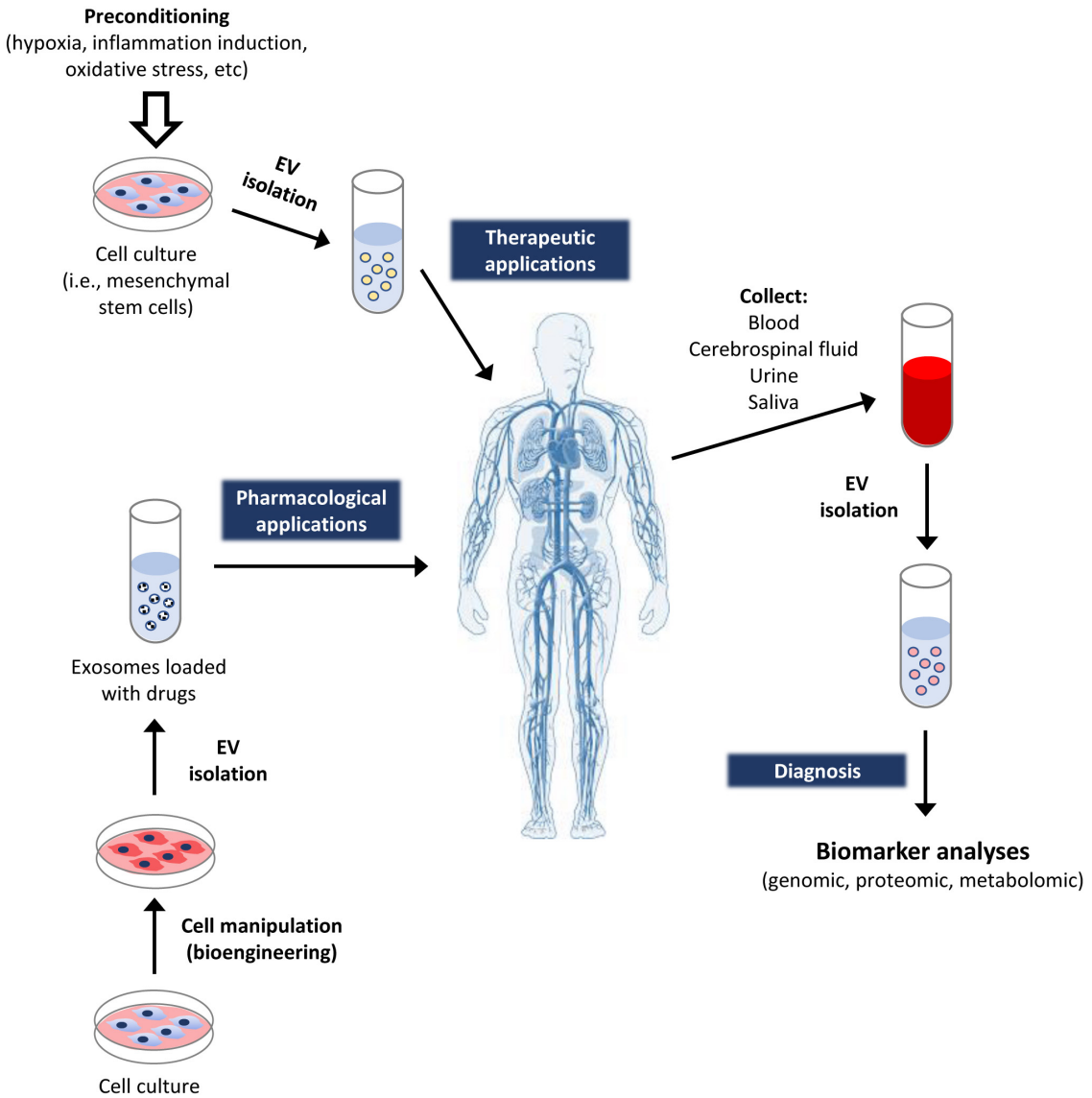

FIGURE 3 | Applications of extracellular vesicles in medicine. The EV obtained from cellular cultures may be applied to patients with specific therapeutic objectives. For instance, the ones derived from cells with regenerative capacity (like MSC) may be used for tissue regeneration. Additionally, the producing cells may be bioengineered to produce EV enriched in some cellular molecules (like specific RNA or proteins), or being loaded with specific drugs. This way, the EV work as vehicles for efficiently targeting the delivery of such molecules to patients. On the other hand, the exosomes can also be isolated from different fluids or tissues of healthy persons, as well as patients suffering different diseases. That allows to identify biomarkers in them, for subsequent diagnostic applications.

cancer (Di et al., 2018); and last, but not least (vi) be isolated from different cellular types with regenerative and/or anti-inflammatory capacity, with potential of being applied to repair damaged tissues (**Figure 3**).

Among the most used cellular types for such latter application are the MSC. Indeed, it has been demonstrated that the EV derived from them have an interesting potential for the treatment of cardiovascular diseases, renal, liver, and neural injuries, as well as skin wounds (Yamashita et al., 2018). Due to the interest and multiple studies available about the clinical applications of the exosomes derived from MSC, the main objective of the present work is to show a critical review about their therapeutic properties, including their specific applications for the treatment and healing of skin ulcers.

PROPERTIES AND THERAPEUTIC POTENTIAL OF MSC

The MSC were first described as having a morphology similar to fibroblasts, behaving as colony-forming unit-fibroblast (CFU-F), capable to differentiate into osteoblasts, in guinea-pig bone marrow and spleen (Friedenstein et al., 1970). Subsequently, it was found that such cells can differentiate into different cellular

types and tissues of mesenchymal origin, like bone, fat, and cartilage (Pittenger et al., 1999). Interestingly, it has been recently reported that such cells can be also induced to differentiate into cells of endodermic and ectodermic origin, like hepatocytes and neurons, respectively (Lee et al., 2018a; Marei et al., 2018).

The MSC have been isolated from different tissues, including bone marrow, fatty tissue, hair follicle, synovium, umbilical cord, placenta, and periodontal ligament, among others (Huang et al., 2011). Surprisingly, there is not a specific biochemical marker defining the MSC. Therefore, the scientific consensus, as we have previously described, is that they should not exhibit hematopoietic and endothelial markers, like CD-11b, CD-14, CD-31, CD-33, CD-34, CD-45, and CD-133 (Casado-Díaz et al., 2016). Thus, the International Society for Cellular Therapy (ISCT) has defined the minimum MSC features: (i) are plastic-adherent under standard culture conditions; (ii) express CD-73, CD-90, and CD-105, lacking the expression of CD-11b, CD-14, CD-19, CD-34, CD-45, CD-79a, and HLA-DR; and (iii) may differentiate into osteoblasts, adipocytes, or chondrocytes *in vitro* (Dominici et al., 2006). Likewise, it has been proposed that the MSC are involved in maintaining cellular homeostasis in the organism. That is accomplished through tissue regeneration and repair.

The MSC represent a convenient experimental model for studying cellular differentiation events. Likewise, to investigate how some physiological situations, drugs, and other compounds may modulate them. As a practical example, we have used such a model for genome-wide transcriptomic studies during adipogenesis, analyzing how natural products like the oleuropein polyphenol (adipogenesis inhibitor present in the olive oil, among other products) modulates it (Casado-Díaz et al., 2017a,b, 2019). On the other hand, their capacity to differentiate into different cellular types, as well as their anti-inflammatory and immunosuppressive activities (Regulski, 2017), have made them an interesting therapeutic tool in cellular therapy and regenerative medicine, as we have reviewed (Casado-Díaz et al., 2016). Such interesting therapeutic potential is mainly due to the following: (i) can be easily isolated and expanded *in vitro*; (ii) can be cryopreserved once isolated, without significant loss of their therapeutic potential; (iii) show intermediate and low levels of the MHC class I and II molecules, respectively, and therefore, they are hypoimmunogenic; and (iv) can be intravenously administered, efficiently reaching the damaged tissue via the bloodstream.

The interest on the therapeutic potential of the MSC has sparked multiple clinical studies about their applications on different pathologies. They include different types of tumors, multiple sclerosis, amyotrophic lateral sclerosis, stroke, acute and chronic heart failure, diabetes, rheumatoid arthritis and osteoarthritis, osteonecrosis, lumbar intervertebral disc degeneration, Crohn's disease, kidney and liver chronic disease, sepsis, spinal cord contusions, and critical limb ischemia, among others. Thus, searching for "mesenchymal stem cells" (other terms; no quotes) in the ClinicalTrials.gov database resource of the National Library of Medicine of the United States of America (USA)[3] showed more than 1000 studies at the time of writing.

[3]http://www.clinicaltrials.gov

MSC-DERIVED EXTRACELLULAR VESICLES FOR CELL-FREE THERAPIES

Surprisingly, patients inoculated with MSC to promote tissue regeneration showed < 1% of such cells in the damaged tissue after 1 week (Rani et al., 2015; Phinney and Pittenger, 2017). Yet, paradoxically, such strategy has produced positive results in the treatment of several pathologies, favoring tissue regeneration and functionality (Brown et al., 2019). Therefore, it has been suggested that the regenerative effect of the MSC is not mainly due to their capacity to proliferate and differentiate into the required cellular types in the damaged tissue. Instead, their main functionality would stem from their paracrine actions, through the production of different factors (Rani et al., 2015; Marote et al., 2016). Interestingly, such hypothesis is supported by several studies, demonstrating that conditioned media from MSC cultures have a similar regenerative capacity—or even higher—than the MSC themselves. For instance, that has been demonstrated in rodent models of acute myocardial infarction (Gnecchi et al., 2005; El Andaloussi et al., 2013). These results demonstrate the surprising therapeutic relevance of the MSC secretome. In view of these results, Caplan (one of the precursors of the MSC studies) has proposed to rename such stem cells as "medicinal signaling cells" (Caplan, 2010, 2017).

The secretome of the MSC has one free fraction, made of soluble factors and metabolites, as well as other encapsulated into MV, to which the EV belong. Interestingly, it has been found that the latter is the main responsible for the therapeutic properties of the conditioned media from MSC cultures (Kusuma et al., 2017). This way, those EV can regulate different physiological processes, like cellular proliferation, differentiation, and migration (Shimoda et al., 2017; Zou et al., 2018).

The therapeutic features of the MSC EV are mainly due to their immunomodulatory and immunosuppressive activities. This way, they can reduce the levels of cytokines, like interleukin 1 beta (IL-1b) and tumor-necrosis factor alpha (TNF-a), increasing the ones of the transforming growth-factor beta (TGF-b) (Chen et al., 2016). That can be exploited for the treatment of some pathologies, like those in which intense or chronic-inflammation processes may limit or jeopardize healing (Harting et al., 2018). Other relevant and interesting characteristic of the EV from the MSC is their antiaging and antifibrotic activities. Thus, the EV, secreted from both induced pluripotent stem cells (iPSC) and young MSC, reduce the cellular senescence associated to aging MSC cultures, by reducing the intracellular levels of reactive oxygen species (ROS) (Liu et al., 2019). On the other hand, the anti-fibrotic effect of EV can be applied to the treatment of fibrosis in organs such as the liver, heart, lung, and skin (Zhao et al., 2017; Davidson and Yellon, 2018; Mansouri et al., 2019; Rong et al., 2019).

The use of exosomes in therapy has relevant advantages, in relation to complete MSC (Keshtkar et al., 2018). Among them are the following: (i) can be isolated and stored at low temperatures (e.g., –80°C), until needed, without requiring the production of large amounts of cells at the time of inoculation, which is needed for cellular therapy; (ii) their contents are encapsulated and protected from degradation *in vivo*

(preventing some of the problems associated with small soluble molecules, such as cytokines, growth factors, transcription factors, and RNA, which are rapidly degraded); (iii) are quite stable, exhibiting a long average life; (iv) can be intravenously injected, reaching distant places, since the vesicles are small and circulate readily, whereas the MSC are too large, and thus may have difficulty circulating through thin capillaries; (v) can pass through the blood-brain barrier; and (vi) have reduced risks of unwanted side-effects, like immune rejection (as said above, they are hypoimmunogenic), cell dedifferentiation, or tumor formation, which can arise after applying exogenous cells (Jeong et al., 2011; Konala et al., 2016; Phinney and Pittenger, 2017; Mardpour et al., 2019).

It is currently estimated that more than 200 preclinic studies are being carried out with different animal models, with promising results (Elahi et al., 2019). The pathologies treated this way include immunologic, cardiovascular, renal, musculoskeletal, and neuronal ones, besides cancer and chronic skin ulcers (CSU), sometimes known as chronic cutaneous ulcers (CCU) (Rani et al., 2015; Marote et al., 2016; Elahi et al., 2019). In relation to the use of MSC-derived EV for skin ulcer healing—which is the main topic of this review—several studies have shown that they may contribute to accelerate skin wound healing and scar reduction. They include the ones derived from different sources, like adipose mesenchymal cells, human amniotic epithelial cells, endothelial progenitor cells (EPC) from human umbilical cord blood, human iPSC-derived MSC (hiPSC-MSC) and cardiosphere-derived cells, among others (Liu et al., 2018).

Clinical trials have recently started using EV from MSC. Thus, searching for "exosome mesenchymal stem cells" (other terms; no quotes) in ClinicalTrials.gov (see above) showed seven studies at the time of writing. One of them uses exosome identification as diagnostic tool. The other are related to their use in acute ischemic stroke, healing of large and refractory macular holes, β-cell mass regeneration in type 1 diabetes mellitus, dystrophic epidermolysis bullosa, and chronic ulcer wounds.

The properties of the EV derived from the MSC depend on the origin and culture conditions of such cells. Thus, differences have been described between the secretome of the human bone-marrow mesenchymal stem cells (BM-MSC), adipose-tissue stem cells (ATSC), and umbilical-cord perivascular cells (UCPC) (Pires et al., 2016). Cells grown under hypoxia produce exosomes with enhanced angiogenic, regenerative, and immunomodulating capacities (Li et al., 2015a; Han et al., 2019; Showalter et al., 2019). Besides, it has been recently described that even the type of culture as standard monolayer or as multilayers/globules (sometimes referred with the misleading names of 2D and 3D, respectively, since we live in a 3D world), may also modulate the properties of the exosomes produced by the MSC. Thus, human amnion-derived MSC grown in conditions to form aggregates or spheroids, produce more angiogenic and immunosuppressant factors than the ones grown in monolayers (Miceli et al., 2019). On the other hand, MSC pretreated with factors inducing the immune response, like interferon gamma (IFN-g) and TNF-a, generated EV with a higher immunosuppressing and/or immunomodulating capacity to direct the differentiation of M1 macrophages (pro-inflammatory) into the M2 (anti-inflammatory) phenotype (Domenis et al., 2018). Another study showed that EV derived from MSC at the latest stages of the osteoblastogenic induction had a higher capacity to induce osteoblastogenesis in undifferentiating MSC (Wang et al., 2018). Additionally, MSC manipulation, such as inducing the overexpression of miR-30b, enhanced the angiogenic capacity of their exosomes (Gong et al., 2017). In summary, the cell secretomes may be significantly modulated by the microenvironment, as well as the physiological and differentiating conditions of the producing MSC (Kusuma et al., 2017).

Therefore, the knowledge of all these modulating factors is of paramount relevance. That should allow to engineer MSC cultures for the desired objectives (Kusuma et al., 2017). Conversely, this scenario may complicate the large-scale production of EV for specific clinical applications. Thus, it may be difficult to generate homogeneous batches of EV. Both the cell origins and their physiological states may determine their contents, and thus their therapeutic properties (Rani et al., 2015). Therefore, new developments are needed to reach such objective for large-scale EV production and homogenization. That may require the use of genetic engineering of MSC. Fortunately, the knowledge of the human genome/transcriptomes to which we have contributed (Lario et al., 1997), together with new revolutionary technologies, like "clustered regularly-interspaced short-palindromic repeats" (CRISPR), should allow to reach such a goal (Amoasii et al., 2018; Lee et al., 2018b; Rees and Liu, 2018; Ryu et al., 2019). Yet, another putative handicap to overcome is that, although the EV are not cells, and therefore cannot generate tumors by themselves, their contents may induce neoplasia in cells of some patients. Curiously, the EV may have dual antagonic effects on tumoral cells. Thus, they can both activate or inhibit the proliferation and migration of tumoral cells (Zhou et al., 2018; Shojaei et al., 2019). It is therefore critical to determine the EV cargos, including their beneficial and putative unwanted side effects, before being routinely used in clinical therapies (Konala et al., 2016).

SKIN WOUND HEALING

The skin is the largest organ, accounting for 16% of the body weight, besides arguably being the most important as well, protecting the organisms from external aggressions, such as immaterial agents like sunlight [e.g., ultraviolet (UV) radiation], as well as physical ones, including both inorganic (e.g., abrasion) and organic or biological, like parasites (Kolarsick et al., 2011). The skin is made of three main layers: epidermis, dermis, and hypodermis. In turn, the epidermis has five sublayers (from outside to inside): corneum, lucidum, granulosum, spinosum, and basale. The epidermis is mainly made by keratinocytes (95%). They are proliferative in the stratum basale, differentiating and replacing the ones of top sublayers. Thus, they progressively lose they nuclei, take an ovoid shape, and eventually detach (Gantwerker and Hom, 2011). Such detachment helps to complete the physiological healing of skin wounds, besides being an effective way to get rid of ectoparasites, like some bacteria. The

epidermis also has intussusceptions (invaginations), harboring hair follicles associated to sebaceous glands (pilosebaceous units) and sweat glands. The pilosebaceous unit is one of the locations containing epithelial stem cells, differentiating into basal keratinocytes. Therefore, they are essential for skin re-epithelialization. On the other hand, the dermis is located below the epidermis, receiving the main blood supply of the skin. Additionally, it contains most of the dermic appendages (integumentary system), like apocrine and eccrine glands, as well as hair follicles. In the dermis, a superficial or papillary dermis and a deeper reticular dermis are distinguished. In addition, there are interdigitations called dermal papillae, located between the dermis and epidermis (Gantwerker and Hom, 2011). The main cells of the reticular dermis are the fibroblasts. They produce the extracellular matrix (ECM), mainly made by collagen.

There are four overlapping stages during skin wound healing: (i) hemostasis; (ii) inflammation; (iii) proliferation; and (iv) maturation/remodeling (**Figure 4**) (Gantwerker and Hom, 2011). The hemostasis is the first step, taking place a few seconds or minutes after the wound originates. The platelets produce a blood clot, preventing blood loss and entry of microorganisms. Besides, the platelets release different cytokines, hormones, and chemokines [e.g., PDGF, TGF-b, EGF, and fibroblast growth factor (FGF)], which are needed for the activation of the subsequent healing phases (Monaco and Lawrence, 2003), as described below. Then, the area of ulceration receives a stream of inflammatory cells during the second stage of wound healing. The first to arrive are the neutrophils, within the first 24 h after the wound is produced. These cells synthesize proteases and antimicrobial compounds, like ROS (Hart, 2002). After that, both the products generated by the neutrophils, as well as their initiation of apoptosis, attract macrophages and lymphocytes. They engulf and digest the remains of the matrix and cellular debris, as well as existing microorganisms, preventing infections. This way, the damaged zone gets cleaned. These events take place after about 48 h of wounding. The macrophages also release several cytokines at the end of this phase, which will activate regenerative processes in the next step (Robson et al., 2001; Hart, 2002).

New tissue is generated in such next proliferation phase. First, the re-epithelialization of the damaged skin takes place, due to the proliferation of the keratinocytes located at the edge of the wound. Additionally, an increase of VEGF induces angiogenesis from the blood vessels surrounding the wound. This way, the new generated tissue is vascularized. The fibroblasts also proliferate, producing a matrix of type III collagen, generating a granulation tissue. Some fibroblasts differentiate into myofibroblasts, with contractile function, effectively reducing

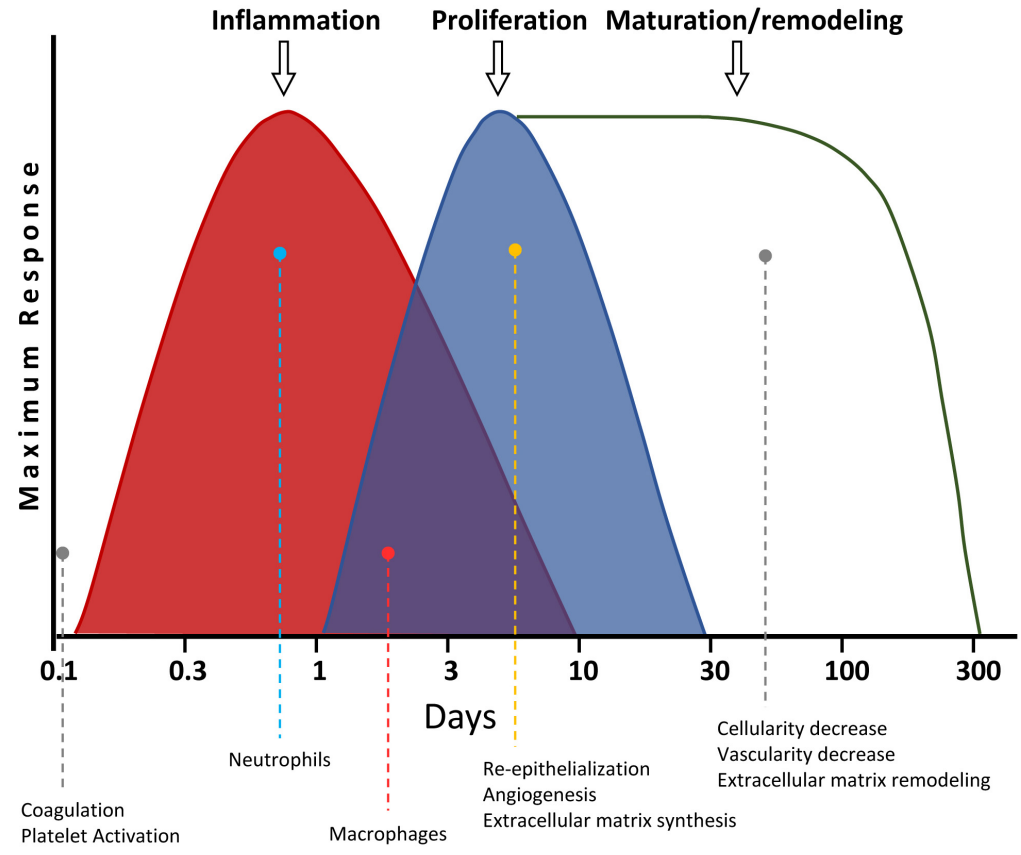

FIGURE 4 | Timeline of skin wound healing. The different phases are shown. The most relevant processes for each stage, as well as their overlapping with others, are graphically and quantitatively depicted for each step.

the wound size, contributing to the wound closing. Thus, the wound scar becomes smaller than the original damaged area (Velnar et al., 2009). Finally, in the last maturation/remodeling phase, the ECM of type III collagen is replaced by other of type I collagen. Besides, many of the cells from the previous phase undergo apoptosis. This way, both the dermis cellularity and the blood vessel density are reduced. This last step takes longer than the others. After that, the tissue reaches its final appearance of healing (Gantwerker and Hom, 2011). The correct sequence and timing of these phases is fundamental for a proper wound healing. Thus, for instance, if the inflammatory phase is not carried out appropriately and takes more than 3 weeks, the ulcer may become chronic (Szpaderska and DiPietro, 2005). Among the main risks for that are aging, diabetes, and recalcitrant infections. Likewise, an excess of fibrosis may generate hypertrophic scarring, which in the most extreme scenarios may degenerate into keloids (Velnar et al., 2009; Eming et al., 2014).

Unfortunately, the number of skin ulcers requiring frequent caring and cures by practitioners and nurses are growing, mainly in the most economically developed countries. That is due to the increased population aging and higher prevalence of diabetes (Wild et al., 2004). The latter is reaching epidemic proportions worldwide, with 463 million people living with such disease, and therefore having higher risk of skin ulcers (International Diabetes Federation [IDF], 2019). This way, open wounds are a problem for 3% of the population older than 65 years of age in the USA. Besides, the USA Government estimates that the elderly population will be over 55 million by 2020, and thus, the number of chronic wounds is expected to grow (Sen, 2019). This represents a very important health expenditure for the national health systems of such countries. In particular, foot ulcers are associated to diabetes, having a prevalence between 15 and 25%; and the management cost of these ulcers is $9 milliards to $13 milliards in the USA (Raghav et al., 2018).

Taking into account the previous data, it is important to prevent the appearance of CSU. Likewise, to develop new and more effective treatments, accelerating their healing. A new approach with great potential is the deployment of cellular therapies, using MSC in the ulcerated zone, to favor its regeneration and healing (Kucharzewski et al., 2019). Indeed, numerous studies about this approach have produced encouraging results. They included both preclinic trials with animal models, such as mouse, rat, dog, or pig, as well as clinic ones with humans (Nuschke, 2014; Li et al., 2015b; Maranda et al., 2016). Both autologous and allogenous MSC from different origins have been used, including bone marrow, adipose tissue, umbilical cord, and the stromal vascular fraction, among others (Teng et al., 2014). Interestingly, several works have demonstrated that conditioned media from MSC cultures have a similar—or even higher—regenerative capacity than such cells, when applied to wounds. Therefore, the regenerative capacity of the MSC should be mainly due to their paracrine activity, as indicated above (Walter et al., 2010; Yew et al., 2011). For instance, it has been found that such conditioned media is more effective than full MSC to heal wounds of diabetic mice (de Mayo et al., 2017).

Besides, the secretome of these cells has been separated into the fraction containing soluble factors and metabolites, on one side, as well as the one made by EV, on the other side. Interestingly, the latter is the main activator of wound healing, as previously described. Thus, EV derived of bone marrow MSC increased migration and proliferation of dermal fibroblasts, and angiogenesis in human umbilical-vein endothelial cells (HUVEC). However, the exosome-depleted conditioned media had not such effects (Shabbir et al., 2015). Also, it has been shown that conditioned media from human adipose-derived stem cell (ADSC) cultures stimulated both the human dermal-fibroblast migration and closure of ischemic wounds in a rat model. That is due to the presence of long ncRNA (lncRNA) of metastasis-associated lung-adenocarcinoma transcript 1 (MALAT-1) in EV (Cooper et al., 2018).

APPLICATION OF MSC EXTRACELLULAR VESICLES TO SKIN WOUND HEALING

The CSU are mainly characterized by an unfinished inflammation phase. As a consequence, the healing process does not end, stopping before an appropriate angiogenesis and tissue regeneration complete the physiological healing process. On the other hand, a defective wound healing, due to an increase in fibrosis, can cause hypertrophic scarring. Fortunately, the EV derived from the MSC have high immunomodulating, immunosuppressing, and angiogenic activities, as well as capacity to modulate the cellular proliferation and differentiation. Therefore, there are currently numerous researches evaluating the potential of these EV for the therapeutic treatment of the CSU and hypertrophic scarring. The works published at the time of writing were less than 50, and there is much to know about the practical clinical application of this therapeutic strategy. Yet, such published papers show that the EV derived from the MSC may positively modulate the different phases of the wound-healing process, as it has been proven by histological evaluations in animal models, including dogs (El-Tookhy et al., 2017).

Inflammation

The EV are partially responsible for the immunomodulatory and immunosuppressant activities of the MSC. The proteomic analyses of EV from such cells have shown that they contain some cytokines, chemokines, and chemokine receptors, related to the immune system. They include interleukin 10 (IL-10), hepatocyte growth factor (HGF), leukemia inhibitory factor (LIF), chemokine (C-C motif) ligand 2 (CCL-2), vascular endothelial growth factor C (VEGF-C), and chemokine (C-C motif) ligand 20 (CCL-20), with immunosuppressive and regenerative activities. Besides, the cargo of the EV derived from the MSC may contain chemokine (C-X-C motif) ligand 2, 8, and 16 (CXCL-2, CXCL-8, and CXCL-16, respectively), defensin alpha 1 (DEFA-1), homologous to the E6-associated protein (E6-AP) carboxyl terminus (HECT), and regulator of chromosome condensation 1 (RCC-1)-like domain (RLD)-containing E3 ubiquitin protein ligase 5 (HERC-5) and

interferon-induced transmembrane protein 2 (IFITM-2), which are chemoattractant proteins of immune cells. Therefore, the EV may activate a better protection against possible infections in damaged tissues (Mardpour et al., 2019). In fact, the treatment of cultures of peripheral-blood mononuclear cells with EV, derived from the MSC, reduced the production of the IL-1b and TNF-a inflammatory cytokines, while increasing TGF-b (Chen et al., 2016).

Interestingly, the effects of the EV derived from the MSC, on tissue inflammation, may be modulated by the environment in which the producing cells are growing. Thus, when they are kept in priming conditions, consisting of serum deprivation and cultured under hypoxic conditions (1% O_2), the EV derived from them were enriched in some specific metabolites. They include adenosine, arginine, aspartic acid, cholesterol, glutamine, nicotinamide, uridine diphosphate (UDP) *N*-acetylglucosamine (UDP-GlcNAc), 5'-deoxy-5'-methylthioadenosine (MTA), palmitic acid, and isoleucine. Curiously, such molecules have been associated to anti-inflammatory activities, M2 macrophage polarization, and induction of regulatory T lymphocytes (Showalter et al., 2019). Besides, the EV obtained from the MSC, after being exposed to inflammatory cytokines (IFN-g and TNF-a) for 40–48 h, inhibited the proliferation of B lymphocytes and natural killer (NK) cells, after being intaken by them (Di Trapani et al., 2016). Other authors have stimulated MSC with such inflammatory cytokines, showing that the anti-inflammatory activities of their EV were partially due to their effects on the cyclooxygenase-2 (COX-2)/PGE2 pathway (Harting et al., 2018). Thus, such EV contained abundant COX-2, involved in the biosynthesis of PGE2. Actually, it has been demonstrated that, after tissue injury, the latter promoted an anti-inflammatory effect, favoring the inflammation resolution *in vivo* (Loynes et al., 2018). Such strategy of using EV from preconditioned MSC (grown in inflammatory environments) has been used in the treatment of chronic inflammation and wound healing, in experimental models *in vitro* and *in vivo*, respectively (Ti et al., 2015).

The first macrophages arriving to a wound exhibit the "classically activated" M1 phenotype. Then, a change to "alternatively activated" M2 phenotype takes place, due to signals from the microenvironment. The pro-inflammatory responses of the M1 macrophages are activated through Toll-like receptors (TLR), as well as the activation of nuclear factor kappa-light-chain enhancer of activated B cells (NF-kB). That leads to pathogen phagocytosis, oxidative burst, and intracellular killing. The activation of the M2 macrophages leads the one of the signal transducer and activator of transcription 3 (STAT-3), or other transcription factors. They inhibit inflammation and promote tissue remodeling (Liu et al., 2014). Unfortunately, the high glucose concentrations arising with diabetes prevent the correct polarization of M1 macrophages toward the M2. That generates a chronic inflammation, preventing a correct healing (Bannon et al., 2013). Some researchers have shown that the EV obtained from MSC, previously activated with lipopolysaccharides (LPS) (LPS pre-Exo), have a higher anti-inflammatory activity, inducing the macrophage polarization toward the M2 phenotype. Thus, the treatment of skin wounds in diabetic animals with LPS pre-Exo reduced the inflammation and accelerated the skin wound healing. These effects were in part due to a high miRNA let-7b expression in the LPS pre-Exo. Such miRNA inhibited the Toll-like receptor 4 (TLR-4), and therefore the inflammatory response. In fact, these authors detected a reduction of the NF-kB activation, besides an increase of the STAT-3 in cultures of a human acute monocytic leukemia cell line (THP-1), treated with LPS pre-Exo (Ti et al., 2015).

The concentration of TNF-a and IL-1b increased, whereas the IL-10 levels decreased, in a model of burn injury in rats, as well as in macrophage cultures exposed to LPS. The treatment with EV derived from human umbilical-cord MSC (hucMSC), but not with the ones derived from human skin fibroblast cells, reduced the inflammation in both cases. That happens through the suppression of the TLR-4 signaling pathway (Li et al., 2016). Interestingly, these authors demonstrated that such effects are due to the presence of miR-181c in the hucMSC-derived EV. Such miRNA is a repressor of the TLR-4 expression (Zhang et al., 2015c; Li et al., 2016).

Angiogenesis

An appropriate regeneration requires the formation of new blood vessels, during the skin wound healing. That is a fundamental process for the delivery of oxygen, nutrients, and growth factors to the damaged tissues. A condition of hypoxia arises when the vascular tissue is damaged by a lesion. That activates the hypoxia-inducible factor-1 (HIF-1), which is a transcriptional activator, promoting the angiogenesis, by upregulating hundreds of target genes. Among them are the vascular endothelial growth factor A (VEGF-A) (Mole et al., 2009). It activates the endothelial cells of the surrounding blood vessels of the wound, generating new vessels. Other factors gear the growth of blood vessels, following the oxygen gradient (Okonkwo and Dipietro, 2017). Yet, unfortunately, the angiogenesis is reduced in the CSU of diabetics. That is partially due to the macrophages not polarizing toward M2. Since the latter are an important source of angiogenic factors, the chronic inflammation inhibits the angiogenesis in such patients. The EPC are mobilized from the bone marrow, to favor the angiogenesis after a tissular damage. But such cell population is decreased in diabetics (Okonkwo and Dipietro, 2017).

The angiogenic activity of the EV derived from the MSC has been investigated in numerous works, in relation to their application in the treatment of the CSU. Thus, HUVEC have been treated *in vitro* with EV obtained from MSC, derived from the adipose tissue. Interestingly, the results showed that the endothelial cells engulfed the EV, increasing the proliferation, migration, and angiogenesis events (Ren et al., 2019). These effects were accompanied by an upregulation of genes related to the proliferation (cyclin D1, cyclin D2, cyclin A1, and cyclin A2), angiogenesis [VEGF-A, platelet-derived growth factor subunit A (PDGF-A), EGF, and FGF 2 (FGF-2)], and migration [integrin beta 1 (ITGB-1) and CXCL-16]. The induction of the expression of these genes was associated to both, the activation of adrenocortical lipid-depletion with high leukemia incidence in mice due to AKV retrovirus (AKR) that develops thymomas (AKT), also known as protein kinase B (PKB), as well as the

extracellular-signal-regulated kinase (ERK) signaling pathways in HUVEC. Besides, the treatment of skin wounds in mice with these EV produced an increase of the vascularization and proliferation of endothelial cells. The consequence was a healing acceleration, in relation to untreated wounds (Ren et al., 2019). Additionally, the EV derived from the MSC isolated from bone marrow can be engulfed by the HUVEC, enhancing their angiogenic capacity (Shabbir et al., 2015). Interestingly, it has been found that such EV carry the transcription factor STAT-3. It is involved in numerous cellular processes, like proliferation, migration, and angiogenesis. Thus, the mechanisms of action of the EV derived from the MSC on angiogenesis might be mediated trough the AKT/ERK/STAT-3 signaling pathways (Shabbir et al., 2015; Ren et al., 2019).

Another source of EV derived from MSC is provided by hiPSC-MSC. They can be generated from different adult cell types, after genetic manipulation. The EV derived from hiPSC-MSC have capacity to promote skin wound healing, collagen biosynthesis, and vascularization at wound sites in rats. Besides, they induce angiogenesis in HUVEC *in vitro* (Zhang et al., 2015b).

The proangiogenic capacity of the EV for regenerative medicine can be enhanced by preconditioning the producing cells. It is known that hypoxia is an angiogenic inducer (Han et al., 2019). Thus, MSC derived from bone marrow have been preconditioned with deferoxamine (DFO) for 48 h. That is a classical hypoxia-mimetic agent, which activates genes induced by hypoxia (Templeton and Liu, 2003). The EV derived from such cells (DFO-Exos) increased the proliferation, migration, and angiogenesis of HUVEC, in relation to unconditioned ones. In those EV, it has been identified miR-126 as an important angiogenic factor, being highly expressed in DFO-Exos. Such miRNA reduced the expression of the phosphatase and tensin homolog (*PTEN*) gene and activated the phosphoinositide 3-kinase (PI3K)/AKT signaling pathways. This way, the angiogenesis was enhanced. DFO-Exos were applied to skin wounds in a rat model induced to suffer diabetes with streptozotocin. Interestingly, they were more effective inducing angiogenesis, and accelerating wound healing, than the EV obtained from unconditioned MSC (Ding et al., 2019).

Yet another possibility to generate EV with high angiogenic capacity is to use genetic engineering (bioengineering), to design secretory cells producing factors that activate angiogenesis. On the other hand, the increase of oxidative stress is one of the factors preventing the CSU healing, mostly in diabetics (Wei et al., 2009). Additionally, the nuclear factor erythroid 2 (E2)-related factor 2 (NRF-2) is translocated from the cytoplasm into the nucleus in oxidative-stress conditions. This way, such transcription factor induced the expression of genes encoding antioxidant enzymes (Kensler et al., 2007). Therefore, the effects of EV from ADSC overexpressing the gene encoding NRF-2 have been studied, including an animal model of diabetic foot ulcers (Li et al., 2018). Thus, the administration of EV derived from ADSC to EPC maintained in high glucose, reduced the senescence, oxidative stress, and expression of inflammatory cytokines. Such effects, besides the angiogenesis, were enhanced when the EV come from ADSC overexpressing the gene encoding NRF-2. Besides, such EV significantly increased the formation of granulation tissue, angiogenesis, and the levels of growth-factor biosynthesis in a streptozotocin-induced diabetic rat model. Additionally, they reduced the levels of inflammation and oxidative stress-related proteins, as well as the ulcerated area in wound beds (Li et al., 2018).

Different studies have been carried out to better understand the mechanisms activating the angiogenesis during CSU healing, after being treated with EV. That includes the involvement of several miRNA and the activation of the AKT, ERK, and STAT-3 signaling pathways (Shabbir et al., 2015; Ding et al., 2019; Ren et al., 2019). Additionally, it has been demonstrated that the EV can also enhance the angiogenesis, through the portmanteau of "Wingless" and "Int-1" called "wingless-related integration site" (Wnt)/b-catenin (or canonical Wnt) pathway (Zhang et al., 2015a). Its activation is important for the endothelial function and healing (Goodwin et al., 2006; McBride et al., 2014). The EV derived from the hucMSC favored the proliferation, migration, and angiogenic capacity of the EA.hy926 HUVEC-derived line. Besides, they promoted the angiogenesis in a rat model of skin-deep second-degree burn (Zhang et al., 2015a). Such effect was mediated by the Wnt family-member 4 (Wnt-4) present in the EV, which activated the Wnt/b-catenin signaling in endothelial cells. Thus, EV derived from hucMSC, with silenced Wnt-4, did not activate the nuclear translocation of b-catenin, losing their angiogenic capacity (Zhang et al., 2015a).

The previous reports showed a positive action of the EV on angiogenesis, and therefore, on CSU healing. Yet, such cellular vesicles exhibited a rapid clearance rate *in vivo*, with a relatively short half-life. Therefore, it would be convenient to increase their stability, once applied *in vivo* (Wang et al., 2019a). Different approaches have been carried out to reach such a goal, and increase the EV effectiveness. For instance, a thermosensitive, injectable, self-healing, and adhesive polysaccharide-based fluorinated ethylene-propylene (FEP) hydrogel scaffold has been developed. The EV derived from the MSC isolated from adipose tissue were loaded into that gel. Such structure is named as FEP@exosomes (FEP@exo), releasing the cellular vesicles in a pH-dependent manner. Interestingly, the FEP@exo strategy increased the proliferation, migration, and angiogenesis of the HUVEC *in vitro*, accelerating wound healing in a diabetic mouse model. Indeed, the FEP@exo stimulated the angiogenesis, formation of granulation tissue, collagen deposition, and re-epithelization of the skin. The efficiency of this scaffold dressing approach is thought to be due to several reasons: (i) maintaining a wet environment; (ii) absorbing wound secretions; (iii) acting as antimicrobial agent; (iv) protecting against the UV light; and (v) favoring angiogenesis, through the liberation of EV (Wang et al., 2019a).

Other approaches using matrices in the wound bed, for the storage, protection, and liberation of EV with angiogenic capacity, have also been reported. They include the use of chitosan hydrogel. Indeed, it has been found that the administration of such linear polysaccharide in open wounds favored their healing. Besides, it is biocompatible and biodegradable, with antimicrobial activity, being a good carrier for sustained release of materials, such as EV

(Ishihara et al., 2006). Researchers have used chitosan with exosomes derived from synovium-mesenchymal stem cells (SMSC), bioengineered to overexpress miR-126-3p (Tao et al., 2017). Such miRNA induced angiogenesis (Wang et al., 2008). The EV derived from the SMSC, expressing such miRNA (SMSC-126-Exos), exhibited interesting features. Thus, they induced the proliferation of human dermal-microvascular endothelial cell 1 (hDMEC-1) *in vitro*, as well as migration and capacity to generate tubular structures, through the activation of both the PI3K/AKT, as well as the mitogen-activated protein kinase (MAPK)/ERK pathways (Tao et al., 2017). Interestingly, the application of chitosan, loaded with SMSC-126-Exos, accelerated wound healing in rats with streptozotocin-induced diabetes. That was mainly due to enhanced angiogenesis. That demonstrates the exciting potential of EV enriched in proangiogenic factors for CSU healing, mainly using appropriate matrices (Tao et al., 2017).

Fibroblasts

The dermal fibroblasts are one of the most important cell lines involved in the normal wound-healing. Their main functions in such a physiological process are ECM production, collagen biosynthesis, wound contraction, re-epithelialization, and tissue remodeling (Darby et al., 2014). If the fibroblasts do not act properly, an excessive production of ECM may occur, leading to scarring (Eming et al., 2014). Indeed, numerous studies have shown that the effects of the EV from MSC in wound healing are, at least in part, due to their capacity to modulate the fibroblast biology. Thus, cultures of fibroblasts from normal donors and chronic wound patients have been treated with EV from bone-marrow MSC. Interestingly, they increased the cellular proliferation and migration (Shabbir et al., 2015). Indeed, such fibroblasts exhibited an activation of the AKT, ERK 1/2 (ERK-1/2), and STAT-3 pathways. The latter transcription factor is active inside the MSC EV, being responsible for the induction of genes involved in cell-cycle progression in fibroblast cultures. They include the avian-myelocytomatosis virus oncogene cellular-homolog (c-MYC), cyclins A1 and D2, HGF, growth factors [insulin-like growth factor 1 (IGF-1), nerve growth factor (NGF), and stromal-derived growth factor-1 (SDF-1)], and interleukin 6 (IL-6) cytokine (Shabbir et al., 2015). The EV derived from MSC obtained from adipose tissue have also been tested on fibroblast cultures. They are engulfed by the cells, increasing their proliferation and migration. The treatments with these EV produced several beneficial effects for wound healing. Thus, they induced the expression of several genes, including c-MYC, matrix metallopeptidase 9 (MMP-9), EGF, FGF-2, TGF-b, vascular endothelial growth factor receptor (VEGFR), VEGF-A, and PDGF-A. Likewise, they increase the amounts of several proteins involved in such physiological activity. Among them were the endothelial growth-factor receptor 2 (VEGFR-2), cyclin D1, fibronectin, collagen I and III, and elastin. These effects were also mediated by an increase of the activation of the AKT and ERK signaling pathways (Ren et al., 2019).

Overall, the results obtained so far show that the fibroblasts, when are treated with EV from MSC, have a higher capacity to produce different factors. They favor the angiogenesis and biosynthesis of proteins for the ECM. Thus, the ones used in an *in vivo* model of skin ulcers significantly increased the collagen deposition (Ren et al., 2019). Other study, carried out with the MSC EV obtained from adipose tissue, showed that cultures of human skin fibroblast, treated with these EV, increased the cell proliferation and migration. Likewise, they upregulated the expression of genes encoding the cluster of differentiation 34 (CD-34), collagen type 1, elastin, and keratinocyte growth factor (KGF), which are related to skin regeneration. Interestingly, genomic studies of such EV identified hsa-miR-4484, hsa-miR-619-5p, and hsa-miR-6879-5p as the most expressed miRNA. They can regulate the expression of different genes, like nucleophosmin 1 (NPM-1), programmed cell death 4 (PDCD-4), chemokine (C-C motif) ligand 5 (CCL-5), and nucleoporin 62 (NUP-62). They were related to proliferation and aging, being therefore involved in tissue regeneration (Choi et al., 2018).

The mechanisms of action of the EV on the fibroblasts are carried out through several ways, including: (i) miRNA content; (ii) capacity to activate the AKT/ERK/STAT-3 pathways; and (iii) activation of the Wnt/b-catenin pathway. In relation to the latter, the effects of the EV derived from the hucMSC on fibroblasts and wound healing in a deep second-degree burn injury in a rat model were mediated by their high Wnt-4 content, which is an activator of the Wnt/b-catenin pathway (Zhang et al., 2015a). On the other hand, the hucMSC EV obtained from the acellular gelatinous Wharton's jelly (structure envelope of the arteries and veins of the umbilical cord) (Meyer et al., 1983) have also been studied. Such EV enhance dermal fibroblast viability and migration *in vitro*, as well as skin wound healing in mice. It is interesting that these effects did not occur if the EV were lysed. Some authors have suggested that the EV must be intact when applied. The rationale is that intact EV allow the interaction between membranes and/or ensures that their cargos are delivered with enough concentration. This study also described that the effects of the EV were due, at least in part, to their high content of alpha-2-macroglobulin. Nevertheless, they did not identify the mechanisms by which this protein may act in wound healing (Bakhtyar et al., 2018).

Interestingly, EV derived from fetal dermal-mesenchymal stem cells (FDMSC) have been isolated from fetal skin. A potential advantage of such cells in regenerative medicine is their scarless wound-healing capability (Leavitt et al., 2016). Indeed, the EV derived from the FDMSC accelerated wound closure in a mouse full-thickness skin wound model. Besides, they increased the proliferation and migration of dermal fibroblasts *in vitro*. In addition, they induced the expression of genes encoding ECM proteins, such as collagen type I and III, fibronectin 1, elastin, and alpha-smooth muscle actin (a-SMA) (Wang et al., 2019b). These authors have shown that the effects of such EV on fibroblasts were mediated by activation of the Notch pathway. That was a consequence of the EV carrying the Notch ligand, known as jagged 1 (JAG-1) (Wang et al., 2019b). That is in agreement with the important roles assigned to the Notch-signaling pathway in wound healing (Chigurupati et al., 2007; Shi et al., 2015).

It is important to take into account that the fibroblasts may play a critical role in scar formation, during wound

healing. Indeed, an excessive production of ECM may favor such unwanted side effect. This can be prevented by applying EV (Zhao et al., 2017). Thus, the intravenous administration of EV, derived from human MSC from adipose tissue, in a mouse model, increased the expressions of collagen type I and III after 5 days of treatment, being reduced after 14 and 21 days of such administration. These results suggest that the EV may promote the early stages of wound healing, while inhibiting collagen biosynthesis—effectively reducing scar formation—at the later stages (Hu et al., 2016). More recent works of the same research team have shown that the administration of such EV promoted the ECM remodeling, as well as the scarless healing of cutaneous wounds. Yet, such effects were not found when using EV-free conditioned medium (Wang et al., 2017). These authors have demonstrated that the *in vivo* treatment with EV produced interesting results: (i) increase ratios of collagen type III:I, TGF-b 3:1 (TGF-b3:TGF-b1) and stromelysin-1 (also known as matrix metalloproteinase 3):tissue inhibitors of metalloproteinase/metallopeptidase inhibitor 1 (MMP-3:TIMP-1); and (ii) reduction of the differentiation of fibroblasts into myofibroblasts. Interestingly, such processes favored a proper remodeling of the ECM, being similar to the ones found in fetal wound healing, in which scars were not produced. Besides, *in vitro* studies have shown similar results when cultures of dermal fibroblasts were treated with EV. These effects were mediated by the MAPK/ER pathway. These results suggest that the activation of this signaling pathway by EV was, at least in part, responsible for scar reduction (Wang et al., 2017). Additionally, EV derived from the adipose tissue accelerated wound healing and reduced scar formation in full-thickness skin wounds, in a mouse model. Such authors also observed that the human dermal fibroblasts treated with such EV activated the biosynthesis of collagen type I and III, being the latter 50% higher than the former. On the other hand, they reported that the EV inhibited the biosynthesis of the a-SMA protein (Zhang et al., 2018). Those results are in agreement with the ones reported by other authors (Wang et al., 2017; Dalirfardouei et al., 2019). Therefore, the EV derived from the MSC of adipose tissue reduced scar formation, due to their effects on fibroblasts. Indeed, it has been found that such effects were mediated by the activation of the PI3K/AKT signaling pathway (Zhang et al., 2018).

On the other hand, the CSU associated to aging have been related, at least in part, to the beginning of senescence of dermal fibroblasts. That was due to both the chronic inflammatory status of this kind of ulcers, as well as a consequence of the aging effects (Harding et al., 2005; Wall et al., 2008). Fortunately, two interesting results have been recently reported. Thus, it has been found that: (i) the EV derived from embryonic stem cells of mice were enriched in mmu-miR-291a-3p; and (ii) such miRNA inhibited the senescence induced in human fibroblast cultures by replicative senescence, adriamycin-induced cellular senescence, or ionizing radiation-induced cellular senescence (Bae et al., 2019). Such latter effect was carried out through the repression of the gene encoding the transforming growth factor-beta receptor 2 (TGFBR-2). Its downregulation reduced the senescence in fibroblasts (Tsai et al., 2018; Bae et al., 2019). Besides, the treatment with mmu-miR-291a-3p accelerated *in vivo* skin wound healing in 12-month-old mice, but not in 8-week-old ones. Interestingly, the hsa-miR-372-3p and hsa-miR-371a-3p human miRNA (corresponding to mmu-miR-291a-3p in mouse) also had anti-senescence effects in fibroblasts. That opens the door to the use of EV enriched in such miRNA, for the treatment of skin ulcers associated to aging and diseases like diabetes (Bae et al., 2019).

Keratinocytes

The keratinocytes intervene in the re-epithelialization of skin. That is considered as one of the major processes in wound healing (Escámez et al., 2004). Such cells begin to migrate from the wound edge into the wound gap, at very early stages of healing. His migration is independent of the granulation-tissue formation and can be considered the first step in normal healing. That provides the basis for the subsequent stages. The keratinocyte proliferation and differentiation in the wound-healing process take place in both parallel and sequential manners (Braiman-Wiksman et al., 2007). Thus, these cells are hyperproliferative and mitotically active at the edge of chronic wounds. But they fail to migrate and create a hyperkeratotic tissue at the edge of the wound (Stojadinovic et al., 2012; Martin and Nunan, 2015).

The MSC-derived EV increased the skin re-epithelialization in full-thickness cutaneous wounds in animal models (Robson et al., 2001; Zhang et al., 2015a, 2018; Li et al., 2017; Tao et al., 2017; Ren et al., 2019; Wang et al., 2019b). However, there are few works analyzing the specific effects of such EV in keratinocytes. It has been found that the so-called "human, adult, low calcium, high temperature" (HaCaT) skin keratinocyte cells, internalized EV derived from adipose-tissue MSC. In addition, those EV promoted the proliferation and migration of HaCaT, with an upregulation of proliferative marker genes, such as cyclins A1, A2, D1, and D2, as well as fibronectin. Interestingly, the latter were involved in cell adhesion (Ren et al., 2019). They also increased the levels of PDGF-A, VEGF-A, FGF-2, EGF, and VEGFR-2. Such results suggest that the EV treatments may contribute to angiogenesis in wounds, by means of the paracrine pathways, as previously described. Thus, the effects of EV on HaCaT seem to be due to the activation of AKT and ERK signaling pathways (Ren et al., 2019). Additionally, the application of EV from iPSC-derived MSC (iMSC) increased the proliferation and migration of HaCaT cultures, as well as ERK-1/2 activation (Kim et al., 2018).

The AKT pathway has also been involved in the positive effects of the hucMSC-derived EV in keratinocytes. Thus, wounds of a deep second-degree burn-injury model in rat have been treated with such EV. A significant upregulation of the gene encoding the cytokeratin 19 (CK-19) was found after 1 week of treatment. That is an epithelial biochemical marker biosynthesized by basal cells, on the external root sheath of hair follicles (Michel et al., 1996). Interestingly, a complete epidermal structure, in the CK-19-positive area of the wounds, was formed after 2 weeks of application. This shows that the treatment with hucMSC-derived EV promoted the skin re-epithelization. On the other hand, the apoptosis of HaCaT cultures, subjected to heat stress (43°C for 40 min), decreased when they were treated with hucMSC-derived EV. In addition, both cell proliferation and

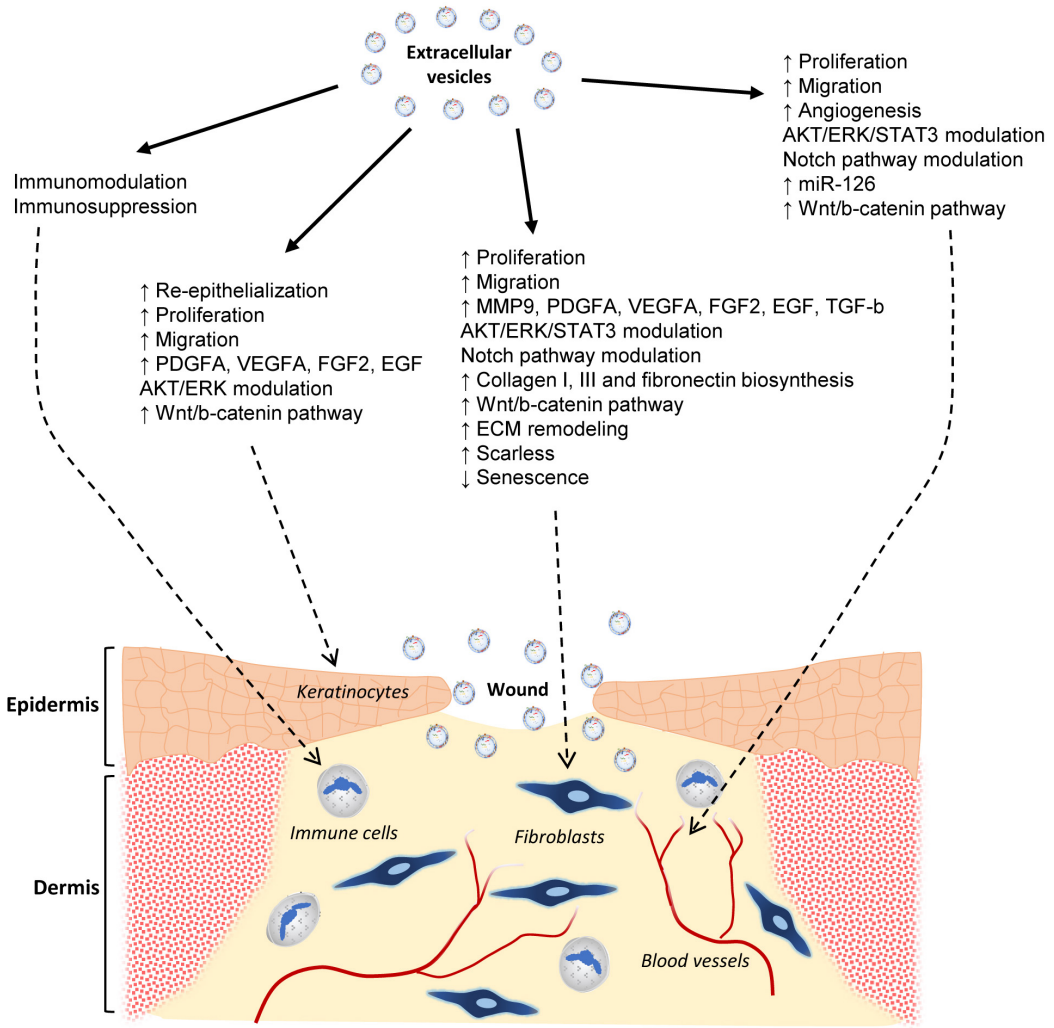

FIGURE 5 | Effects of MSC extracellular vesicles on wound healing. Graphical abstract of the current state-of-the-art knowledge of the EV actions on skin wound healing. The effects on different cell types involved in such a physiological process are shown. They include immune and endothelial cells, fibroblasts, and keratinocytes.

migration increased. These effects were mediated by both AKT and Wnt/b-catenin pathway activation, but in an independent manner. Such authors concluded that the activation of the AKT pathway can be induced by cytokines delivered by EV, such as the platelet-derived growth factor B-homodimer (PDGF-BB), granulocyte-colony stimulating factor (G-CSF or GCSF), VEGF, monocyte-chemoattractant protein 1 (MCP-1), as well as IL-6 and -8. On the other hand, b-catenin would be activated by the presence of Wnt-4 in the EV. The activation of both pathways would increase wound healing (Zhang et al., 2015a).

CONCLUDING REMARKS AND FUTURE PROSPECTS

The EV secreted by the cells play a significant role in both the intercellular communications, as well as the interactions with the cellular microenvironments. Such discoveries are fascinating and with great potential, allowing to exploit them to develop new and efficient therapeutic tools, for many pathologies. As described in this critical review, the properties of the EV depend on their cargos, which are confined and protected within a lipidic bilayer. That allows the EV to reach distant locations from the production site.

The EV obtained from MSC are characterized by having immunomodulatory and regenerative properties, similar to the ones of the producing cells. They can be used in cell-free therapies in regenerative medicine, and more specifically, in CSU treatments. The currently available publications show that the EV can modulate different stages of wound healing. They include inflammation, angiogenesis, proliferation, and ECM remodeling. This way, they can effectively accelerate and overall improve the wound healing process (**Figure 5**). Nevertheless, although the current results are certainly encouraging, further research is still

needed to optimize the EV applications, as routine clinical tools in CSU treatments. That includes their production, isolation, characterization, and ways of administration.

It is critical to determine the optimal source of MSC, if they should be bioengineered to produce the desired cargos in high amounts, as well as the putative requirement for cell immortalization. The latter is fundamental, since the cell senescence due to culture passages and time may alter the EV cargos, and, therefore, their properties. Also important is to determine the optimal culture conditions, depending on the experimental, clinical or therapeutic objectives to be reached, like wound healing. As described in this critical review, the cell preconditioning, for instance, in inflammatory or hypoxic environments, may significantly enhance and optimize the EV immunosuppressing or angiogenic capacities. Additionally, the methodology to isolate and purify the EV must be highly controlled and optimized. That is required to increase its efficiency, maintain the structure and functionality of such EV. Some events should be completely avoided. For instance, the putative contamination with other undesired particles, including cell components and culture media. The current methods of obtaining EV for skin wound healing are numerous. That makes difficult to properly compare them in many cases.

On the other hand, the characterization of the EV contents is also fundamental, to better understand their molecular mechanisms of action. Likewise, to predict putative unwanted side effects that their application may trigger. Numerous mechanisms of exosome action have been proposed in the available bibliography, depending on the specific study. For instance, they may involve the AKT, ERK, Notch, STAT-3, and Wnt/b-catenin signaling pathways, among others. Besides, different miRNA and other molecules may be involved. Interestingly, the current data show that similar skin wound healing results may be obtained from different pathways. Therebefore, many of the described mechanisms may be bound together, working in a coordinated, complementary, and interrelated way. That is not surprising, taking into account the exquisite integration of cellular functions allowing homeostasis and life itself. Nevertheless, a better understanding of their molecular bases is required. That is of paramount importance to optimize the EV cargo, which can be specifically designed by genetic engineering of the sourcing cells. It should also be taken into account that their contents may also be modulated by the tissue culture conditions. Besides, a better understanding of the molecules that can induce the acceleration of CSU healing should allow the future specific design of tailor-made particles. They could be similar—and even better—than the natural biological EV. Such a goal could be reached exploiting the tremendous power and flexibility of biotechnology and nanotechnology. These artificial constructs may become new drug carriers, with specific contents and targets. Actually, there are already exciting and promising results in the development of molecular origami based on DNA, RNA, and proteins, to carry drugs to specific cellular targets (Pugh et al., 2018). Finally, it is important to optimize the application of EV for the healing of skin wounds. Usually, they are subcutaneously applied in the wound edges. Sometimes, they are intravenously administered. That takes advantage of the property of these vesicles for targeting and concentrate in damaged tissues/cells. In other instances, the EV are liberated from a hydrogel placed over the wound. Therefore, it would be convenient to analyze the advantages and disadvantages, critically comparing the different application methodologies for each specific clinical goal. In principle, the use of EV embedded, in hydrogels or dressings with healing properties, has a great future potential for skin wound healing.

In conclusion, the currently available data on EV shed new light on this exciting topic and draw optimist prospects for their efficient exploitation in regenerative medicine, including the treatment of CSU. Nevertheless, further research is needed for a better understanding the molecular bases underlying these processes; and specifically on how the EV derived from MSC work on wound healing. Likewise, optimized methods for large-scale production of EV for human clinical applications must be developed. All such insights should have very positive impacts on regenerative medicine, as well as on the quality of life of the patients suffering different diseases. That includes the CSU in diabetics, among others. Indeed, some companies are focusing their investments efforts on the development of exosomes as therapeutics (Zipkin, 2019). And last but not least, that should also significantly reduce the overhead and cost of the private and public health and welfare systems worldwide.

AUTHOR CONTRIBUTIONS

AC-D designed the study. AC-D, GD, and JQ-G drafted, conducted reviews, literature analyses, edited, and approved the manuscript.

FUNDING

This work was supported by grants PI15/01857, PI18/01659, and CIBER "Fragilidad y Envejecimiento Saludable" (CIBERFES) of "Instituto de Salud Carlos III" (ISCIII), "Ministerio de Economía y Competitividad" (MINECO), Spain and European Union (EU).

REFERENCES

Amoasii, L., Hildyard, J. C. W., Li, H., Sanchez-Ortiz, E., Mireault, A., Caballero, D., et al. (2018). Gene editing restores dystrophin expression in a canine model of Duchenne muscular dystrophy. *Science* 362, 86–91. doi: 10.1126/science.aau1549

Andreu, Z., and Yáñez-Mó, M. (2014). Tetraspanins in extracellular vesicle formation and function. *Front. Immunol.* 5:442. doi: 10.3389/fimmu.2014.00442

Bae, Y.-U., Son, Y., Kim, C.-H., Kim, K. S., Hyun, S. H., Woo, H. G., et al. (2019). Embryonic stem cell-derived mmu-miR-291a-3p inhibits cellular senescence in human dermal fibroblasts through the TGF-β receptor 2 pathway. *J. Gerontol. A Biol. Sci. Med. Sci.* 74, 1359–1367. doi: 10.1093/gerona/gly208

Bakhtyar, N., Jeschke, M. G., Herer, E., Sheikholeslam, M., and Amini-Nik, S. (2018). Exosomes from acellular Wharton's jelly of the human umbilical cord promotes skin wound healing. *Stem Cell Res. Ther.* 9, 1–14. doi: 10.1186/s13287-018-0921-2

Bannon, P., Wood, S., Restivo, T., Campbell, L., Hardman, M. J., and Mace, K. A. (2013). Diabetes induces stable intrinsic changes to myeloid cells that contribute to chronic inflammation during wound healing in mice. *Dis. Model. Mech.* 6, 1434–1447. doi: 10.1242/dmm.012237

Basu, J., and Ludlow, J. W. (2016). Exosomes for repair, regeneration and rejuvenation. *Expert Opin. Biol. Ther.* 16, 489–506. doi: 10.1517/14712598.2016.1131976

Braiman-Wiksman, L., Solomonik, I., Spira, R., and Tennenbaum, T. (2007). Novel insights into wound healing sequence of events. *Toxicol. Pathol.* 35, 767–779. doi: 10.1080/01926230701584189

Brown, C., McKee, C., Bakshi, S., Walker, K., Hakman, E., Halassy, S., et al. (2019). Mesenchymal stem cells: cell therapy and regeneration potential. *J. Tissue Eng. Regen. Med.* 13, 1738–1755. doi: 10.1002/term.2914

Cañas, M. A., Fábrega, M. J., Giménez, R., Badia, J., and Baldomà, L. (2018). Outer membrane vesicles from probiotic and commensal *escherichia coli* activate NOD1-mediated immune responses in intestinal epithelial cells. *Front. Microbiol.* 9:498. doi: 10.3389/fmicb.2018.00498

Caplan, A. I. (2010). What's in a name? *Tissue Eng. Part A* 16, 2415–2417. doi: 10.1089/ten.tea.2010.0216

Caplan, A. I. (2017). Mesenchymal stem cells: time to change the name! *Stem Cells Transl. Med.* 6, 1445–1451. doi: 10.1002/sctm.17-0051

Casado-Díaz, A., Anter, J., Müller, S., Winter, P., Quesada-Gómez, J. M., and Dorado, G. (2017a). Transcriptomic analyses of adipocyte differentiation from human mesenchymal stromal-cells (MSC). *J. Cell. Physiol.* 232, 771–784. doi: 10.1002/jcp.25472

Casado-Díaz, A., Anter, J., Müller, S., Winter, P., Quesada-Gómez, J. M., and Dorado, G. (2017b). Transcriptomic analyses of the anti-adipogenic effects of oleuropein in human mesenchymal stem cells. *Food Funct.* 8, 1254–1270. doi: 10.1039/c7fo00045f

Casado-Díaz, A., Dorado, G., and Quesada-Gómez, J. M. (2019). Influence of olive oil and its components on mesenchymal stem cell biology. *World J. Stem Cells* 11, 1045–1064. doi: 10.4252/wjsc.v11.i12.1045

Casado-Díaz, A., Quesada-Gómez, J. M., and Dorado, G. (2016). "Stem cell research and molecular markers in medicine," in *Reference Module in Biomedical Sciences*, ed. M. En Caplan (Amsterdam: Elsevier), doi: 10.1016/B978-0-12-801238-3.99814-3

Chan, B. D., Wong, W. Y., Lee, M. M. L., Cho, W. C. S., Yee, B. K., and Kwan, Y. W. (2019). Exosomes in inflammation and inflammatory disease. *Proteomics* 19:e1800149. doi: 10.1002/pmic.201800149

Chargaff, E., and West, R. (1946). The biological significance of the thromboplastic protein of blood. *J. Biol. Chem.* 166, 189–197.

Chen, W., Huang, Y., Han, J., Yu, L., Li, Y., Lu, Z., et al. (2016). Immunomodulatory effects of mesenchymal stromal cells-derived exosome. *Immunol. Res.* 64, 831–840. doi: 10.1007/s12026-016-8798-6

Chigurupati, S., Arumugam, T. V., Son, T. G., Lathia, J. D., Jameel, S., Mughal, M. R., et al. (2007). Involvement of notch signaling in wound healing. *PLoS One* 2:e1167. doi: 10.1371/journal.pone.0001167

Choi, D. S., Kim, D. K., Kim, Y. K., and Gho, Y. S. (2013). Proteomics, transcriptomics and lipidomics of exosomes and ectosomes. *Proteomics* 13, 1554–1571. doi: 10.1002/pmic.201200329

Choi, E. W., Seo, M. K., Woo, E. Y., Kim, S. H., Park, E. J., and Kim, S. (2018). Exosomes from human adipose-derived stem cells promote proliferation and migration of skin fibroblasts. *Exp. Dermatol.* 27, 1170–1172. doi: 10.1111/exd.13451

Cocucci, E., and Meldolesi, J. (2015). Ectosomes and exosomes: shedding the confusion between extracellular vesicles. *Trends Cell Biol.* 25, 364–372. doi: 10.1016/j.tcb.2015.01.004

Colombo, M., Raposo, G., and Théry, C. (2014). Biogenesis, secretion, and intercellular Interactions of exosomes and other extracellular vesicles. *Annu. Rev. Cell Dev. Biol.* 30, 255–289. doi: 10.1146/annurev-cellbio-101512-122326

Cooper, D. R., Wang, C., Patel, R., Trujillo, A., Patel, N. A., Prather, J., et al. (2018). Human adipose-derived stem cell conditioned media and exosomes containing MALAT1 promote human dermal fibroblast migration and ischemic wound healing. *Adv. Wound Care* 7, 299–308. doi: 10.1089/wound.2017.0775

Dalirfardouei, R., Jamialahmadi, K., Jafarian, A. H., and Mahdipour, E. (2019). Promising effects of exosomes isolated from menstrual blood-derived mesenchymal stem cell on wound-healing process in diabetic mouse model. *J. Tissue Eng. Regen. Med.* 13, 555–568. doi: 10.1002/term.2799

Darby, I. A., Laverdet, B., Bonté, F., and Desmoulière, A. (2014). Fibroblasts and myofibroblasts in wound healing. *Clin. Cosmet. Investig. Dermatol.* 7, 301–311. doi: 10.2147/CCID.S50046

Davidson, S. M., and Yellon, D. M. (2018). Exosomes and cardioprotection – a critical analysis. *Mol. Aspects Med.* 60, 104–114. doi: 10.1016/j.mam.2017.11.004

de Mayo, T., Conget, P., Becerra-Bayona, S., Sossa, C. L., Galvis, V., and Arango-Rodríguez, M. L. (2017). The role of bone marrow mesenchymal stromal cell derivatives in skin wound healing in diabetic mice. *PLoS One* 12:e0177533. doi: 10.1371/journal.pone.0177533

Di, C., Zhang, Q., Wang, Y., Wang, F., Chen, Y., Gan, L., et al. (2018). Exosomes as drug carriers for clinical application. *Artif. Cells Nanomed. Biotechnol.* 46(Suppl. 3), S564–S570. doi: 10.1080/21691401.2018.1501381

Di Trapani, M., Bassi, G., Midolo, M., Gatti, A., Kamga, P. T., Cassaro, A., et al. (2016). Differential and transferable modulatory effects of mesenchymal stromal cell-derived extracellular vesicles on T, B and NK cell functions. *Sci. Rep.* 6, 1–13. doi: 10.1038/srep24120

Ding, J., Wang, X., Chen, B., Zhang, J., and Xu, J. (2019). Exosomes derived from human bone marrow mesenchymal stem cells stimulated by deferoxamine accelerate cutaneous wound healing by promoting angiogenesis. *Biomed. Res. Int.* 2019:9742765. doi: 10.1155/2019/9742765

Domenis, R., Cifù, A., Quaglia, S., Pistis, C., Moretti, M., Vicario, A., et al. (2018). Pro inflammatory stimuli enhance the immunosuppressive functions of adipose mesenchymal stem cells-derived exosomes. *Sci. Rep.* 8:13325. doi: 10.1038/s41598-018-31707-9

Dominici, M., Le Blanc, K., Mueller, I., Slaper-Cortenbach, I., Marini, F., Krause, D., et al. (2006). Minimal criteria for defining multipotent mesenchymal stromal cells. The international society for cellular therapy position statement. *Cytotherapy* 8, 315–317. doi: 10.1080/14653240600855905

El Andaloussi, S., Mäger, I., Breakefield, X. O., and Wood, M. J. A. (2013). Extracellular vesicles: biology and emerging therapeutic opportunities. *Nat. Rev. Drug Discov.* 12, 347–357. doi: 10.1038/nrd3978

Elahi, F. M., Farwell, D. G., Nolta, J. A., and Anderson, J. D. (2019). Preclinical translation of exosomes derived from mesenchymal stem/stromal cells. *Stem Cells* 38, 15–21. doi: 10.1002/stem.3061

El-Tookhy, O. S., Shamaa, A. A., Shehab, G. G., Abdallah, A. N., and Azzam, O. M. (2017). Histological evaluation of experimentally induced critical size defect skin wounds using exosomal solution of mesenchymal stem cells derived microvesicles. *Int. J. Stem Cells* 10, 144–153. doi: 10.15283/ijsc17043

Eming, S. A., Martin, P., and Tomic-Canic, M. (2014). Wound repair and regeneration: mechanisms, signaling, and translation. *Sci. Transl. Med.* 6:265sr6. doi: 10.1126/scitranslmed.3009337

Escámez, M. J., García, M., Larcher, F., Meana, A., Muñoz, E., Jorcano, J. L., et al. (2004). An in vivo model of wound healing in genetically modified skin-humanized mice. *J. Invest. Dermatol.* 123, 1182–1191. doi: 10.1111/j.0022-202X.2004.23473.x

Friedenstein, A. J., Chailakhjan, R. K., and Lalykina, K. S. (1970). The development of fibroblast colonies in monolayer cultures of guinea-pig bone marrow and spleen cells. *Cell Tissue Kinet.* 3, 393–403. doi: 10.1111/j.1365-2184.1970.tb00347.x

Fu, F., Jiang, W., Zhou, L., and Chen, Z. (2018). Circulating exosomal miR-17-5p and miR-92a-3p predict pathologic stage and grade of colorectal cancer. *Transl. Oncol.* 11, 221–232. doi: 10.1016/j.tranon.2017.12.012

Gantwerker, E. A., and Hom, D. B. (2011). Skin: histology and physiology of wound healing. *Facial Plast. Surg. Clin. North Am.* 19, 441–453. doi: 10.1016/j.fsc.2011.06.009

Gho, Y. S., and Lee, C. (2017). Emergent properties of extracellular vesicles: a holistic approach to decode the complexity of intercellular communication networks. *Mol. Biosyst.* 13, 1291–1296. doi: 10.1039/c7mb00146k

Gnecchi, M., He, H., Liang, O. D., Melo, L. G., Morello, F., Mu, H., et al. (2005). Paracrine action accounts for marked protection of ischemic heart by Akt-modified mesenchymal stem cells [2]. *Nat. Med.* 11, 367–368. doi: 10.1038/nm0405-367

Gong, M., Yu, B., Wang, J., Wang, Y., Liu, M., Paul, C., et al. (2017). Mesenchymal stem cells release exosomes that transfer miRNAs to endothelial cells and promote angiogenesis. *Oncotarget* 8, 45200–45212. doi: 10.18632/oncotarget.16778

Goodwin, A. M., Sullivan, K. M., and D'Amore, P. A. (2006). Cultured endothelial cells display endogenous activation of the canonical Wnt signaling pathway and express multiple ligands, receptors, and secreted modulators of Wnt signaling. *Dev. Dyn.* 235, 3110–3120. doi: 10.1002/dvdy.20939

Gupta, M. P., Tandalam, S., Ostrager, S., Lever, A. S., Fung, A. R., Hurley, D. D., et al. (2019). Non-reversible tissue fixation retains extracellular vesicles for in situ imaging. *Nat. Methods* 16, 1269–1273. doi: 10.1038/s41592-019-0623-4

Gurunathan, S., Kang, M., Jeyaraj, M., Qasim, M., and Kim, J. (2019). Review of the isolation, characterization, biological function, and multifarious therapeutic approaches of exosomes. *Cells* 8:307. doi: 10.3390/cells8040307

Han, Y., Ren, J., Bai, Y., Pei, X., and Han, Y. (2019). Exosomes from hypoxia-treated human adipose-derived mesenchymal stem cells enhance angiogenesis through VEGF/VEGF-R. *Int. J. Biochem. Cell Biol.* 109, 59–68. doi: 10.1016/j.biocel.2019.01.017

Hanson, P. I., and Cashikar, A. (2012). Multivesicular body morphogenesis. *Annu. Rev. Cell Dev. Biol.* 28, 337–362. doi: 10.1146/annurev-cellbio-092910-154152

Harding, C., Heuser, J., and Stahl, P. (1984). Endocytosis and intracellular processing of transferrin and colloidal gold-transferrin in rat reticulocytes: demonstration of a pathway for receptor shedding. *Eur. J. Cell Biol.* 35, 256–263.

Harding, K. G., Moore, K., and Phillips, T. J. (2005). Wound chronicity and fibroblast senescence–implications for treatment. *Int. Wound J.* 2, 364–368. doi: 10.1111/j.1742-4801.2005.00149.x

Hart, J. (2002). Inflammation. 2: its role in the healing of chronic wounds. *J. Wound Care* 11, 245–249. doi: 10.12968/jowc.2002.11.7.26416

Harting, M. T., Srivastava, A. K., Zhaorigetu, S., Bair, H., Prabhakara, K. S., Toledano Furman, N. E., et al. (2018). Inflammation-stimulated mesenchymal stromal cell-derived extracellular vesicles attenuate inflammation. *Stem Cells* 36, 79–90. doi: 10.1002/stem.2730

Hu, L., Wang, J., Zhou, X., Xiong, Z., Zhao, J., Yu, R., et al. (2016). Exosomes derived from human adipose mensenchymal stem cells accelerates cutaneous wound healing via optimizing the characteristics of fibroblasts. *Sci. Rep.* 6, 1–11. doi: 10.1038/srep32993

Huang, S., Leung, V., Peng, S., Li, L., Lu, F. J., Wang, T., et al. (2011). Developmental definition of MSCs: new insights into pending questions. *Cell. Reprogram.* 13, 465–472. doi: 10.1089/cell.2011.0045

International Diabetes Federation [IDF] (2019). *IDF Diabetes Atlas*, 9th Edn. Brussels: International Diabetes Federation. Available online at: https://www.diabetesatlas.org

Ishihara, M., Fujita, M., Obara, K., Hattori, H., Nakamura, S., Nambu, M., et al. (2006). Controlled releases of FGF-2 and paclitaxel from chitosan hydrogels and their subsequent effects on wound repair, angiogenesis, and tumor growth. *Curr. Drug Deliv.* 3, 351–358. doi: 10.2174/156720106778559047

Jeong, J.-O., Han, J. W., Kim, J.-M., Cho, H.-J., Park, C., Lee, N., et al. (2011). Malignant tumor formation after transplantation of short-term cultured bone marrow mesenchymal stem cells in experimental myocardial infarction and diabetic neuropathy. *Circ. Res.* 108, 1340–1347. doi: 10.1161/CIRCRESAHA.110.239848

Johnstone, R. M., Adam, M., Hammond, J. R., Orr, L., and Turbide, C. (1987). Vesicle formation during reticulocyte maturation. Association of plasma membrane activities with released vesicles (exosomes). *J. Biol. Chem.* 262, 9412–9420.

Juan, T., and Fürthauer, M. (2018). Biogenesis and function of ESCRT-dependent extracellular vesicles. *Semin. Cell Dev. Biol.* 74, 66–77. doi: 10.1016/j.semcdb.2017.08.022

Kensler, T. W., Wakabayashi, N., and Biswal, S. (2007). Cell survival responses to environmental stresses via the Keap1-Nrf2-ARE pathway. *Annu. Rev. Pharmacol. Toxicol.* 47, 89–116. doi: 10.1146/annurev.pharmtox.46.120604.141046

Keshtkar, S., Azarpira, N., and Ghahremani, M. H. (2018). Mesenchymal stem cell-derived extracellular vesicles: novel frontiers in regenerative medicine. *Stem Cell Res. Ther.* 9:63. doi: 10.1186/s13287-018-0791-7

Kim, J. H., Lee, J., Park, J., and Gho, Y. S. (2015). Gram-negative and gram-positive bacterial extracellular vesicles. *Semin. Cell Dev. Biol.* 40, 97–104. doi: 10.1016/j.semcdb.2015.02.006

Kim, S., Lee, S. K., Kim, H., and Kim, T. M. (2018). Exosomes secreted from induced pluripotent stem cell-derived mesenchymal stem cells accelerate skin cell proliferation. *Int. J. Mol. Sci.* 19:3119. doi: 10.3390/ijms19103119

Kolarsick, P. A. J., Kolarsick, M. A., and Goodwin, C. (2011). Anatomy and physiology of the skin. *J. Dermatol. Nurses Assoc.* 3, 203–213. doi: 10.1097/JDN.0b013e3182274a98

Konala, V. B. R., Mamidi, M. K., Bhonde, R., Das, A. K., Pochampally, R., and Pal, R. (2016). The current landscape of the mesenchymal stromal cell secretome: a new paradigm for cell-free regeneration. *Cytotherapy* 18, 13–24. doi: 10.1016/j.jcyt.2015.10.008

Kreimer, S., Belov, A. M., Ghiran, I., Murthy, S. K., Frank, D. A., and Ivanov, A. R. (2015). Mass-spectrometry-based molecular characterization of extracellular vesicles: lipidomics and proteomics. *J. Proteome Res.* 14, 2367–2384. doi: 10.1021/pr501279t

Kucharzewski, M., Rojczyk, E., Wilemska-Kucharzewska, K., Wilk, R., Hudecki, J., and Los, M. J. (2019). Novel trends in application of stem cells in skin wound healing. *Eur. J. Pharmacol.* 843, 307–315. doi: 10.1016/j.ejphar.2018.12.012

Kusuma, G. D., Carthew, J., Lim, R., and Frith, J. E. (2017). Effect of the microenvironment on mesenchymal stem cell paracrine signaling: opportunities to engineer the therapeutic effect. *Stem Cells Dev.* 26, 617–631. doi: 10.1089/scd.2016.0349

Lario, A., González, A., and Dorado, G. (1997). Automated laser-induced fluorescence DNA sequencing: equalizing signal-to-noise ratios significantly enhances overall performance. *Anal. Biochem.* 247, 30–33. doi: 10.1006/abio.1996.9933

Leavitt, T., Hu, M. S., Marshall, C. D., Barnes, L. A., Lorenz, H. P., and Longaker, M. T. (2016). Scarless wound healing: finding the right cells and signals. *Cell Tissue Res.* 365, 483–493. doi: 10.1007/s00441-016-2424-8

Lee, C. W., Chen, Y. F., Wu, H. H., and Lee, O. K. (2018a). Historical perspectives and advances in mesenchymal stem cell research for the treatment of liver diseases. *Gastroenterology* 154, 46–56. doi: 10.1053/j.gastro.2017.09.049

Lee, S. H., Kim, S., and Hur, J. K. (2018b). CRISPR and target-specific DNA endonucleases for efficient DNA knock-in in eukaryotic genomes. *Mol. Cells* 41, 943–952. doi: 10.14348/molcells.2018.0408

Li, L., Jin, S., and Zhang, Y. (2015a). Ischemic preconditioning potentiates the protective effect of mesenchymal stem cells on endotoxin-induced acute lung injury in mice through secretion of exosome. *Int. J. Clin. Exp. Med.* 8, 3825–3832.

Li, M., Zhao, Y., Hao, H., Han, W., and Fu, X. (2015b). Mesenchymal stem cell-based therapy for nonhealing wounds: today and tomorrow. *Wound Repair Regen.* 23, 465–482. doi: 10.1111/wrr.12304

Li, X., Guo, L., Liu, Y., Su, Y., Xie, Y., Du, J., et al. (2017). MicroRNA-21 promotes osteogenesis of bone marrow mesenchymal stem cells via the Smad7-Smad1/5/8-Runx2 pathway. *Biochem. Biophys. Res. Commun.* 493, 928–933. doi: 10.1016/j.bbrc.2017.09.119

Li, X., Liu, L., Yang, J., Yu, Y., Chai, J., Wang, L., et al. (2016). Exosome derived from human umbilical cord mesenchymal stem cell mediates MiR-181c attenuating burn-induced excessive inflammation. *EBioMedicine* 8, 72–82. doi: 10.1016/j.ebiom.2016.04.030

Li, X., Xie, X., Lian, W., Shi, R., Han, S., and Zhang, H. (2018). Exosomes from adipose-derived stem cells overexpressing Nrf2 accelerate cutaneous wound healing by promoting vascularization in a diabetic foot ulcer rat model. *Exp. Mol. Med.* 50:29. doi: 10.1038/s12276-018-0058-5

Liu, S., Mahairaki, V., Bai, H., Ding, Z., Li, J., Witwer, K. W., et al. (2019). Highly purified human extracellular vesicles produced by stem cells alleviate aging cellular phenotypes of senescent human cells. *Stem Cells* 37, 779–790. doi: 10.1002/stem.2996

Liu, Y., Wang, H., and Wang, J. (2018). Exosomes as a novel pathway for regulating development and diseases of the skin (Review). *Biomed. Rep.* 8, 207–214. doi: 10.3892/br.2018.1054

Liu, Y.-C., Zou, X.-B., Chai, Y.-F., and Yao, Y.-M. (2014). Macrophage polarization in inflammatory diseases. *Int. J. Biol. Sci.* 10, 520–529. doi: 10.7150/ijbs.8879

Loynes, C. A., Lee, J. A., Robertson, A. L., Steel, M. J. G., Ellett, F., and Feng, Y. (2018). PGE2 production at sites of tissue injury promotes an anti-inflammatory neutrophil phenotype and determines the outcome of inflammation resolution in vivo. *Sci. Adv.* 4:eaar8320. doi: 10.1126/sciadv.aar8320

Mansouri, N., Willis, G. R., Fernandez-Gonzalez, A., Reis, M., Nassiri, S., and Mitsialis, S. A. (2019). Mesenchymal stromal cell exosomes prevent and revert experimental pulmonary fibrosis through modulation of monocyte phenotypes. *JCI Insight* 4:e128060. doi: 10.1172/jci.insight.128060

Maranda, E., Rodriguez-Menocal, L., and Badiavas, E. (2016). Role of mesenchymal stem cells in dermal repair in burns and diabetic wounds. *Curr. Stem Cell Res. Ther.* 12, 61–70. doi: 10.2174/1574888x11666160714115926

Mardpour, S., Hamidieh, A. A., Taleahmad, S., Sharifzad, F., Taghikhani, A., and Baharvand, H. (2019). Interaction between mesenchymal stromal cell-derived extracellular vesicles and immune cells by distinct protein content. *J. Cell. Physiol.* 234, 8249–8258. doi: 10.1002/jcp.27669

Marei, H. E. S., El-Gamal, A., Althani, A., Afifi, N., Abd-Elmaksoud, A., Farag, A., et al. (2018). Cholinergic and dopaminergic neuronal differentiation of human adipose tissue derived mesenchymal stem cells. *J. Cell. Physiol.* 233, 936–945. doi: 10.1002/jcp.25937

Marote, A., Teixeira, F. G., Mendes-Pinheiro, B., and Salgado, A. J. (2016). MSCs-derived exosomes: cell-secreted nanovesicles with regenerative potential. *Front. Pharmacol.* 7:231. doi: 10.3389/fphar.2016.00231

Martin, P., and Nunan, R. (2015). Cellular and molecular mechanisms of repair in acute and chronic wound healing. *Br. J. Dermatol.* 173, 370–378. doi: 10.1111/bjd.13954

McBride, J. D., Jenkins, A. J., Liu, X., Zhang, B., Lee, K., Berry, W. L., et al. (2014). Elevated circulation levels of an antiangiogenic SERPIN in patients with diabetic microvascular complications impair wound healing through suppression of Wnt signaling. *J. Invest. Dermatol.* 134, 1725–1734. doi: 10.1038/jid.2014.40

Meyer, F. A., Laver-Rudich, Z., and Tanenbaum, R. (1983). Evidence for a mechanical coupling of glycoprotein microfibrils with collagen fibrils in Wharton's jelly. *Biochim. Biophys. Acta* 755, 376–387. doi: 10.1016/0304-4165(83)90241-6

Miceli, V., Pampalone, M., Vella, S., Carreca, A. P., Amico, G., and Conaldi, P. G. (2019). Comparison of immunosuppressive and angiogenic properties of human amnion-derived mesenchymal stem cells between 2D and 3D culture systems. *Stem Cells Int.* 2019:7486279. doi: 10.1155/2019/7486279

Michel, M., Török, N., Godbout, M. J., Lussier, M., Gaudreau, P., and Royal, A. (1996). Keratin 19 as a biochemical marker of skin stem cells in vivo and in vitro: keratin 19 expressing cells are differentially localized in function of anatomic sites, and their number varies with donor age and culture stage. *J. Cell Sci.* 109(Pt 5), 1017–1028.

Mistry, D. S., Chen, Y., and Sen, G. L. (2012). Progenitor function in self-renewing human epidermis is maintained by the exosome. *Cell Stem Cell* 11, 127–135. doi: 10.1016/j.stem.2012.04.022

Mole, D. R., Blancher, C., Copley, R. R., Pollard, P. J., Gleadle, J. M., Ragoussis, J., et al. (2009). Genome-wide association of hypoxia-inducible factor (HIF)-1alpha and HIF-2alpha DNA binding with expression profiling of hypoxia-inducible transcripts. *J. Biol. Chem.* 284, 16767–16775. doi: 10.1074/jbc.M901790200

Monaco, J. A. L., and Lawrence, W. T. (2003). Acute wound healing: an overview. *Clin. Plast. Surg.* 30, 1–12. doi: 10.1016/S0094-1298(02)00070-6

Nuschke, A. (2014). Activity of mesenchymal stem cells in therapies for chronic skin wound healing. *Organogenesis* 10, 29–37. doi: 10.4161/org.27405

Okonkwo, U. A., and Dipietro, L. A. (2017). Diabetes and wound angiogenesis. *Int. J. Mol. Sci.* 18, 1–15. doi: 10.3390/ijms18071419

Pan, B. T., and Johnstone, R. M. (1983). Fate of the transferrin receptor during maturation of sheep reticulocytes in vitro: selective externalization of the receptor. *Cell* 33, 967–978. doi: 10.1016/0092-8674(83)90040-5

Phinney, D. G., and Pittenger, M. F. (2017). Concise review: MSC-derived exosomes for cell-free therapy. *Stem Cells* 35, 851–858. doi: 10.1002/stem.2575

Pires, A. O., Mendes-Pinheiro, B., Teixeira, F. G., Anjo, S. I., Ribeiro-Samy, S., Gomes, E. D., et al. (2016). Unveiling the differences of secretome of human bone marrow mesenchymal stem cells, adipose tissue-derived stem cells, and human umbilical cord perivascular cells: a proteomic analysis. *Stem Cells Dev.* 25, 1073–1083. doi: 10.1089/scd.2016.0048

Pittenger, M. F., Mackay, A. M., Beck, S. C., Jaiswal, R. K., Douglas, R., and Mosca, J. D. (1999). Multilineage potential of adult human mesenchymal stem cells. *Science* 284, 143–147. doi: 10.1126/science.284.5411.143

Pugh, G. C., Burns, J. R., and Howorka, S. (2018). Comparing proteins and nucleic acids for next-generation biomolecular engineering. *Nat. Rev. Chem.* 2, 113–130. doi: 10.1038/s41570-018-0015-9

Raghav, A., Khan, Z. A., Labala, R. K., Ahmad, J., Noor, S., and Mishra, B. K. (2018). Financial burden of diabetic foot ulcers to world: a progressive topic to discuss always. *Ther. Adv. Endocrinol. Metab.* 9, 29–31. doi: 10.1177/2042018817744513

Rani, S., Ryan, A. E., Griffin, M. D., and Ritter, T. (2015). Mesenchymal stem cell-derived extracellular vesicles: toward cell-free therapeutic applications. *Mol. Ther.* 23, 812–823. doi: 10.1038/mt.2015.44

Raposo, G., Nijman, H. W., Stoorvogel, W., Leijendekker, R., Harding, C. V., Melief, C. J. M., et al. (1996). B lymphocytes secrete antigen-presenting vesicles. *J. Exp. Med.* 183, 1161–1172. doi: 10.1084/jem.183.3.1161

Ratajczak, J., Miekus, K., Kucia, M., Zhang, J., Reca, R., Dvorak, P., et al. (2006). Embryonic stem cell-derived microvesicles reprogram hematopoietic progenitors: evidence for horizontal transfer of mRNA and protein delivery. *Leukemia* 20, 847–856. doi: 10.1038/sj.leu.2404132

Rees, H. A., and Liu, D. R. (2018). Base editing: precision chemistry on the genome and transcriptome of living cells. *Nat. Rev. Genet.* 19, 770–788. doi: 10.1038/s41576-018-0059-1

Regulski, M. J. (2017). Mesenchymal stem cells: "Guardians of Inflammation". *Wounds* 29, 20–27.

Ren, S., Chen, J., Duscher, D., Liu, Y., Guo, G., Kang, Y., et al. (2019). Microvesicles from human adipose stem cells promote wound healing by optimizing cellular functions via AKT and ERK signaling pathways. *Stem Cell Res. Ther.* 10:47. doi: 10.1186/s13287-019-1152-x

Robson, M. C., Steed, D. L., and Franz, M. G. (2001). Wound healing: biologic features and approaches to maximize healing trajectories. *Curr. Probl. Surg.* 38, 72-140. doi: 10.1067/msg.2001.111167

Rong, X., Liu, J., Yao, X., Jiang, T., Wang, Y., and Xie, F. (2019). Human bone marrow mesenchymal stem cells-derived exosomes alleviate liver fibrosis through the Wnt/β-catenin pathway. *Stem Cell Res. Ther.* 10:98. doi: 10.1186/s13287-019-1204-2

Ryu, S.-M., Hur, J. W., and Kim, K. (2019). Evolution of CRISPR towards accurate and efficient mammal genome engineering. *BMB Rep.* 52, 475–481. doi: 10.5483/bmbrep.2019.52.8.149

Sen, C. K. (2019). Human wounds and its burden: an updated compendium of estimates. *Adv. Wound Care* 8, 39–48. doi: 10.1089/wound.2019.0946

Shabbir, A., Cox, A., Rodriguez-Menocal, L., Salgado, M., and Van Badiavas, E. (2015). Mesenchymal stem cell exosomes induce proliferation and migration of normal and chronic wound fibroblasts, and enhance angiogenesis In Vitro. *Stem Cells Dev.* 24, 1635–1647. doi: 10.1089/scd.2014.0316

Shi, Y., Shu, B., Yang, R., Xu, Y., Xing, B., Liu, J., et al. (2015). Wnt and Notch signaling pathway involved in wound healing by targeting c-Myc and Hes1 separately. *Stem Cell Res. Ther.* 6:120. doi: 10.1186/s13287-015-0103-4

Shimoda, A., Tahara, Y., Sawada, I., Sasaki, Y., and Akiyoshi, K. (2017). Glycan profiling analysis using evanescent-field fluorescence-assisted lectin array: importance of sugar recognition for cellular uptake of exosomes from mesenchymal stem cells. *Biochem. Biophys. Res. Commun.* 491, 701–707. doi: 10.1016/j.bbrc.2017.07.126

Shojaei, S., Hashemi, S. M., Ghanbarian, H., Salehi, M., and Mohammadi-Yeganeh, S. (2019). Effect of mesenchymal stem cells-derived exosomes on tumor microenvironment: tumor progression versus tumor suppression. *J. Cell. Physiol.* 234, 3394–3409. doi: 10.1002/jcp.27326

Showalter, M. R., Wancewicz, B., Fiehn, O., Archard, J. A., Clayton, S., Wagner, J., et al. (2019). Primed mesenchymal stem cells package exosomes with metabolites associated with immunomodulation. *Biochem. Biophys. Res. Commun.* 512, 729–735. doi: 10.1016/j.bbrc.2019.03.119

Stojadinovic, O., Gordon, K. A., Lebrun, E., and Tomic-Canic, M. (2012). Stress-induced hormones cortisol and epinephrine impair wound epithelization. *Adv. Wound Care* 1, 29–35. doi: 10.1089/wound.2011.0320

Szpaderska, A. M., and DiPietro, L. A. (2005). Inflammation in surgical wound healing: friend or foe? *Surgery* 137, 571–573. doi: 10.1016/j.surg.2005.01.006

Tao, S.-C., Guo, S.-C., Li, M., Ke, Q.-F., Guo, Y.-P., and Zhang, C.-Q. (2017). Chitosan wound dressings incorporating exosomes derived from microrna-126-overexpressing synovium mesenchymal stem cells provide sustained release of exosomes and heal full-thickness skin defects in a diabetic rat model. *Stem Cells Transl. Med.* 6, 736–747. doi: 10.5966/sctm.2016-0275

Templeton, D. M., and Liu, Y. (2003). Genetic regulation of cell function in response to iron overload or chelation. *Biochim. Biophys. Acta Gen. Subj.* 1619, 113–124. doi: 10.1016/S0304-4165(02)00497-X

Teng, M., Huang, Y., and Zhang, H. (2014). Application of stems cells in wound healing-an update. *Wound Repair Regen.* 22, 151–160. doi: 10.1111/wrr.12152

Théry, C., Witwer, K. W., Aikawa, E., Alcaraz, M. J., Anderson, J. D., and Andriantsitohaina, R. (2018). Minimal information for studies of extracellular

vesicles 2018 (MISEV2018): a position statement of the international society for extracellular vesicles and update of the MISEV2014 guidelines. *J. Extracell. Vesicles* 7:1535750. doi: 10.1080/20013078.2018.1535750

Ti, D., Hao, H., Tong, C., Liu, J., Dong, L., Zheng, J., et al. (2015). LPS-preconditioned mesenchymal stromal cells modify macrophage polarization for resolution of chronic inflammation via exosome-shuttled let-7b. *J. Transl. Med.* 13:308. doi: 10.1186/s12967-015-0642-6

Tsai, C.-W., Chiang, I.-N., Wang, J.-H., and Young, T.-H. (2018). Chitosan delaying human fibroblast senescence through downregulation of TGF-β signaling pathway. *Artif. Cells Nanomed. Biotechnol.* 46, 1852–1863. doi: 10.1080/21691401.2017.1394873

Valadi, H., Ekström, K., Bossios, A., Sjöstrand, M., Lee, J. J., and Lötvall, J. O. (2007). Exosome-mediated transfer of mRNAs and microRNAs is a novel mechanism of genetic exchange between cells. *Nat. Cell Biol.* 9, 654–659. doi: 10.1038/ncb1596

van der Pol, E., Böing, A. N., Harrison, P., Sturk, A., and Nieuwland, R. (2012). Classification, functions, and clinical relevance of extracellular vesicles. *Pharmacol. Rev.* 64, 676–705. doi: 10.1124/pr.112.005983

Velnar, T., Bailey, T., and Smrkolj, V. (2009). The wound healing process: an overview of the cellular and molecular mechanisms. *J. Int. Med. Res.* 37, 1528–1542. doi: 10.1177/147323000903700531

Wall, I. B., Moseley, R., Baird, D. M., Kipling, D., Giles, P., Laffafian, I., et al. (2008). Fibroblast dysfunction is a key factor in the non-healing of chronic venous leg ulcers. *J. Invest. Dermatol.* 128, 2526–2540. doi: 10.1038/jid.2008.114

Walter, M. N. M., Wright, K. T., Fuller, H. R., MacNeil, S., and Johnson, W. E. B. (2010). Mesenchymal stem cell-conditioned medium accelerates skin wound healing: an in vitro study of fibroblast and keratinocyte scratch assays. *Exp. Cell Res.* 316, 1271–1281. doi: 10.1016/j.yexcr.2010.02.026

Wang, L., Hu, L., Zhou, X., Xiong, Z., Zhang, C., Shehada, H. M. A., et al. (2017). Exosomes secreted by human adipose mesenchymal stem cells promote scarless cutaneous repair by regulating extracellular matrix remodelling. *Sci. Rep.* 7, 1–12. doi: 10.1038/s41598-017-12919-x

Wang, M., Wang, C., Chen, M., Xi, Y., Cheng, W., Mao, C., et al. (2019a). Efficient angiogenesis-based diabetic wound healing/skin reconstruction through bioactive antibacterial adhesive ultraviolet shielding nanodressing with exosome release. *ACS Nano* 13, 10279–10293. doi: 10.1021/acsnano.9b03656

Wang, S., Aurora, A. B., Johnson, B. A., Qi, X., McAnally, J., Hill, J. A., et al. (2008). The endothelial-specific microRNA miR-126 governs vascular integrity and angiogenesis. *Dev. Cell* 15, 261–271. doi: 10.1016/j.devcel.2008.07.002

Wang, X., Jiao, Y., Pan, Y., Zhang, L., Gong, H., and Qi, Y. (2019b). Fetal dermal mesenchymal stem cell-derived exosomes accelerate cutaneous wound healing by activating Notch signaling. *Stem Cells Int.* 2019:2402916. doi: 10.1155/2019/2402916

Wang, X., Omar, O., Vazirisani, F., Thomsen, P., and Ekström, K. (2018). Mesenchymal stem cell-derived exosomes have altered microRNA profiles and induce osteogenic differentiation depending on the stage of differentiation. *PLoS One* 13:e0193059. doi: 10.1371/journal.pone.0193059

Wei, W., Liu, Q., Tan, Y., Liu, L., Li, X., and Cai, L. (2009). Oxidative stress, diabetes, and diabetic complications. *Hemoglobin* 33, 370–377. doi: 10.3109/03630260903212175

Wild, S., Roglic, G., Green, A., Sicree, R., and King, H. (2004). Global prevalence of diabetes: estimates for the year 2000 and projections for 2030. *Diabetes Care* 27, 1047–1053. doi: 10.2337/diacare.27.5.1047

Wolf, P. (1967). The nature and significance of platelet products in human plasma. *Br. J. Haematol.* 13, 269–288. doi: 10.1111/j.1365-2141.1967.tb08741.x

Xiao, J., Pan, Y., Li, X. H., Yang, X. Y., Feng, Y. L., Tan, H. H., et al. (2016). Cardiac progenitor cell-derived exosomes prevent cardiomyocytes apoptosis through exosomal miR-21 by targeting PDCD4. *Cell Death Dis.* 7:e2277. doi: 10.1038/cddis.2016.181

Yamashita, T., Takahashi, Y., and Takakura, Y. (2018). Possibility of exosome-based therapeutics and challenges in production of exosomes eligible for therapeutic application. *Biol. Pharm. Bull.* 41, 835–842. doi: 10.1248/bpb.b18-00133

Yáñez-Mó, M., Siljander, P. R. M., Andreu, Z., Zavec, A. B., Borràs, F. E., Buzas, E. I., et al. (2015). Biological properties of extracellular vesicles and their physiological functions. *J. Extracell. Vesicles* 4:27066. doi: 10.3402/jev.v4.27066

Yew, T.-L., Hung, Y.-T., Li, H.-Y., Chen, H.-W., Chen, L.-L., Tsai, K.-S., et al. (2011). Enhancement of wound healing by human multipotent stromal cell conditioned medium: the paracrine factors and p38 MAPK activation. *Cell Transplant.* 20, 693–706. doi: 10.3727/096368910X550198

Yi, M., Wu, Y., Long, J., Liu, F., Liu, Z., Zhang, Y.-H., et al. (2019). Exosomes secreted from osteocalcin-overexpressing endothelial progenitor cells promote endothelial cell angiogenesis. *Am. J. Physiol. Cell Physiol.* 317, C932–C941. doi: 10.1152/ajpcell.00534.2018

Zhang, B., Wang, M., Gong, A., Zhang, X., Wu, X., Zhu, Y., et al. (2015a). HucMSc-exosome mediated-Wnt4 signaling is required for cutaneous wound healing. *Stem Cells* 33, 2158–2168. doi: 10.1002/stem.1771

Zhang, J., Guan, J., Niu, X., Hu, G., Guo, S., Li, Q., et al. (2015b). Exosomes released from human induced pluripotent stem cells-derived MSCs facilitate cutaneous wound healing by promoting collagen synthesis and angiogenesis. *J. Transl. Med.* 13:49. doi: 10.1186/s12967-015-0417-0

Zhang, L., Li, Y.-J., Wu, X.-Y., Hong, Z., and Wei, W.-S. (2015c). MicroRNA-181c negatively regulates the inflammatory response in oxygen-glucose-deprived microglia by targeting Toll-like receptor 4. *J. Neurochem.* 132, 713–723. doi: 10.1111/jnc.13021

Zhang, W., Bai, X., Zhao, B., Li, Y., Zhang, Y., Li, Z., et al. (2018). Cell-free therapy based on adipose tissue stem cell-derived exosomes promotes wound healing via the PI3K/Akt signaling pathway. *Exp. Cell Res.* 370, 333–342. doi: 10.1016/j.yexcr.2018.06.035

Zhao, B., Zhang, Y., Han, S., Zhang, W., Zhou, Q., Guan, H., et al. (2017). Exosomes derived from human amniotic epithelial cells accelerate wound healing and inhibit scar formation. *J. Mol. Histol.* 48, 121–132. doi: 10.1007/s10735-017-9711-x

Zhou, J., Tan, X., Tan, Y., Li, Q., Ma, J., and Wang, G. (2018). Mesenchymal stem cell derived exosomes in cancer progression, metastasis and drug delivery: a comprehensive review. *J. Cancer* 9, 3129–3137. doi: 10.7150/jca.25376

Zhu, L., Kalimuthu, S., Gangadaran, P., Oh, J. M., Lee, H. W., Baek, S. H., et al. (2017). Exosomes derived from natural killer cells exert therapeutic effect in melanoma. *Theranostics* 7, 2732–2745. doi: 10.7150/thno.18752

Zipkin, M. (2019). Exosome redux. *Nat. Biotechnol.* 37, 1395–1400. doi: 10.1038/s41587-019-0326-5

Zou, X. Y., Yu, Y., Lin, S., Zhong, L., Sun, J., Zhang, G., et al. (2018). Comprehensive miRNA analysis of human umbilical cord-derived mesenchymal stromal cells and extracellular vesicles. *Kidney Blood Press. Res.* 43, 152–161. doi: 10.1159/000487369

Conflict of Interest: The authors declare that the research was conducted in the absence of any commercial or financial relationships that could be construed as a potential conflict of interest.

frontiers in Bioengineering and Biotechnology

REVIEW
published: 31 March 2020
doi: 10.3389/fbioe.2020.00239

Current Status and Future Prospects of Genome-Scale Metabolic Modeling to Optimize the Use of Mesenchymal Stem Cells in Regenerative Medicine

Þóra Sigmarsdóttir[1,2†], Sarah McGarrity[2,3†], Óttar Rolfsson[3], James T. Yurkovich[4] and Ólafur E. Sigurjónsson[1,2]*

[1] The Blood Bank, Landspitali – The National University Hospital of Iceland, Reykjavik, Iceland, [2] School of Science and Engineering, Reykjavik University, Reykjavik, Iceland, [3] Faculty of Medicine, School of Health Sciences, University of Iceland, Reykjavik, Iceland, [4] Institute for Systems Biology, Seattle, WA, United States

OPEN ACCESS

Edited by:
Martin James Stoddart, AO Research Institute Davos, Switzerland

Reviewed by:
Ngan F. Huang, Stanford University, United States
Ron June, Montana State University, United States

***Correspondence:**
Ólafur E. Sigurjónsson
oes@ru.is

† These authors have contributed equally to this work

Specialty section:
This article was submitted to Tissue Engineering and Regenerative Medicine, a section of the journal Frontiers in Bioengineering and Biotechnology

Received: *11 July 2019*
Accepted: *09 March 2020*
Published: *31 March 2020*

Citation:
Sigmarsdóttir Þ, McGarrity S, Rolfsson Ó, Yurkovich JT and Sigurjónsson ÓE (2020) Current Status and Future Prospects of Genome-Scale Metabolic Modeling to Optimize the Use of Mesenchymal Stem Cells in Regenerative Medicine. Front. Bioeng. Biotechnol. 8:239. doi: 10.3389/fbioe.2020.00239

Mesenchymal stem cells are a promising source for externally grown tissue replacements and patient-specific immunomodulatory treatments. This promise has not yet been fulfilled in part due to production scaling issues and the need to maintain the correct phenotype after re-implantation. One aspect of extracorporeal growth that may be manipulated to optimize cell growth and differentiation is metabolism. The metabolism of MSCs changes during and in response to differentiation and immunomodulatory changes. MSC metabolism may be linked to functional differences but how this occurs and influences MSC function remains unclear. Understanding how MSC metabolism relates to cell function is however important as metabolite availability and environmental circumstances in the body may affect the success of implantation. Genome-scale constraint based metabolic modeling can be used as a tool to fill gaps in knowledge of MSC metabolism, acting as a framework to integrate and understand various data types (e.g., genomic, transcriptomic and metabolomic). These approaches have long been used to optimize the growth and productivity of bacterial production systems and are being increasingly used to provide insights into human health research. Production of tissue for implantation using MSCs requires both optimized production of cell mass and the understanding of the patient and phenotype specific metabolic situation. This review considers the current knowledge of MSC metabolism and how it may be optimized along with the current and future uses of genome scale constraint based metabolic modeling to further this aim.

Keywords: MSCs, metabolism, personalized/precision medicine, metabolomics, metabolic modeling, tissue engineering

INTRODUCTION

In recent years, there has been increasing interest in the possibilities offered by regenerative medicine (Maienschein, 2011; Sampogna et al., 2015), a field which seeks solutions for the restoration of the structure and functions of organs and tissues that have become permanently damaged. While regenerative medicine has enjoyed success in some areas, treatment can result in

danger to patients or in therapeutic inefficiency (Neman et al., 2012; Campana et al., 2014; Goldberg et al., 2017; Moreira et al., 2017; Cunningham et al., 2018; Solarte et al., 2018) that have pushed researchers to continuously search for novel approaches to address limitations.

One important area of regenerative medicine is the use of stem cells to enhance available therapeutic applications and to further the development of new ones (Mahla, 2016). In particular, mesenchymal stem cells, or mesenchymal stromal cells (MSCs) (Rosenbaum et al., 2008; Ullah et al., 2015; Fitzsimmons et al., 2018), are of interest. MSCs are multipotent cell types with stem cell-like abilities that can be isolated from various adult and neonatal tissues (Nombela-Arrieta et al., 2011; Alberts et al., 2014). MSCs maintain proliferation abilities while possessing the ability to undergo trilineage differentiation (adipogenic, chondrogenic, and osteogenic differentiation) and remarkable immunomodulatory capabilities (Rosenbaum et al., 2008; Lin et al., 2013). These properties offer the possibility of furthering treatment options for various ailments, such as metabolic and autoimmune diseases like multiple sclerosis (Bonab et al., 2012), Alzheimer's disease (Rosenbaum et al., 2008; Mahla, 2016), diabetes (Ullah et al., 2015; Fitzsimmons et al., 2018), Crohn's disease (Duijvestein et al., 2010), and cancer (Qin et al., 2016).

For the past decade, MSCs metabolism has received growing interest due to mounting evidence suggesting that the manipulation of metabolism allows enhanced therapeutic uses of these cells (e.g., cell retention, cell survival, immunoregulation, differentiation) in cell-based medicine and tissue engineering (Chen et al., 2008; Croitoru-Lamoury et al., 2011; Pattappa et al., 2011; Buravkova et al., 2013; Beegle et al., 2015; Shum et al., 2016; Li et al., 2017; Meyer et al., 2018; Vigo et al., 2019; Zhu and Thompson, 2019). Cellular metabolism is an intricate and complex network of pathways, enzymatic reactions, metabolites, and co-factors with numerous effects on the cell and its immediate surroundings. Due to the complexity of metabolism and its effects, research into the possibilities of manipulating metabolism in these cells has been slow.

The advent of high-throughput -omic technologies (Henry et al., 2010; Resendis-Antonio, 2013) has allowed for the detailing of genome-scale metabolic networks (Yurkovich and Palsson, 2016). This holistic systems biology approach acknowledges that biological systems are made up of a network of networks (Reed and Palsson, 2003; Resendis-Antonio, 2013; Bordbar et al., 2014). Genome-scale models (GEMs) of metabolism (Rocha et al., 2008) provide a framework for the computation of the genotype-phenotype relationship in which various types of -omics data can be integrated along with organism-specific network reconstructions to generate tissue, cell, or organism specific *in silico* models (Feist et al., 2009; Chang et al., 2010; Agren et al., 2014; Fouladiha et al., 2015). These models can then be constrained by experimental measurements and computed in order to explore possible therapeutic applications, making use of the newest RNA sequencing and metabolomic data or *in vitro* experimentation. Such models will aid further understanding of MSCs metabolism under various external or internal conditions. Thus far, metabolic modeling has not been applied to the study of MSCs, but this area offers great possibilities for enhancing both research and therapeutic application of these cells.

In this review, we describe how the study of human MSC (hMSC) metabolism can be used to answer the fundamental question: "How can GEMs be used to optimize MSC therapeutics?" First, we describe the biology of MSCs, their differentiation and immunomodulation properties and their applications and limitations in regenerative medicine. Next, we detail how metabolism affects or can be used to manipulate these functions. We then discuss how mathematical modeling of hMSC metabolism can aid in developing pre-clinical and clinical experiments. Finally, we give our vision for the future of using metabolic modeling to study hMSCs and how the resulting insights could prove transformative for the field of regenerative medicine.

BIOLOGY OF MESENCHYMAL STEM CELLS (MSCs)

Mesenchymal stromal cells comprise non-hematopoietic cells originating from the mesodermal germ layer and are capable of both self-renewal and multilineage differentiation into various tissues of mesodermal origin (Gazit et al., 2014). These multipotent cells can be isolated both from various adult tissues (e.g., skin, peripheral blood, bone marrow) and neonatal tissues (e.g., Wharton's jelly, umbilical cord blood) (Nombela-Arrieta et al., 2011; Alberts et al., 2014). Despite the historical lack of consensus on methods for isolation, expansion, and characterization of hMSCs, the International Society for Cellular Therapy (ISCT) has produced minimal criteria to define hMSCs (Rosenbaum et al., 2008; Lin et al., 2013). The cells must be able to:

- Adhere to plastic and develop as fibroblast colony-forming units and differentiate into cells of mesodermal origin (i.e., osteocytes, chondrocytes, and adipocytes). See **Figure 1**.
- Express the surface markers CD73, CD90, and CD105 during *in vitro* culture expansion
- Lack expression of CD11b, CD14, CD34, CD45, CD19, and HLA-DR surface markers during *in vitro* culture expansion

It is likely that this definition will continue to evolve to account for new findings.

Differentiation of MSCs

One of the identifying characteristics of MSCs is their ability to differentiate into cells of mesodermal origin (Nombela-Arrieta et al., 2011; Gazit et al., 2014). In addition to this hallmark trilineage differentiation, there have also been reports of differentiation toward other cell types of the ectodermal and endodermal origins, including tenocytes, cardiomyocytes, skeletal myocytes, smooth muscle cells, and neurons (Tatard et al., 2007; Galli et al., 2014; Ullah et al., 2015; Youngstrom et al., 2016). The actual functionality of the end product in this transdifferentiation is still debated.

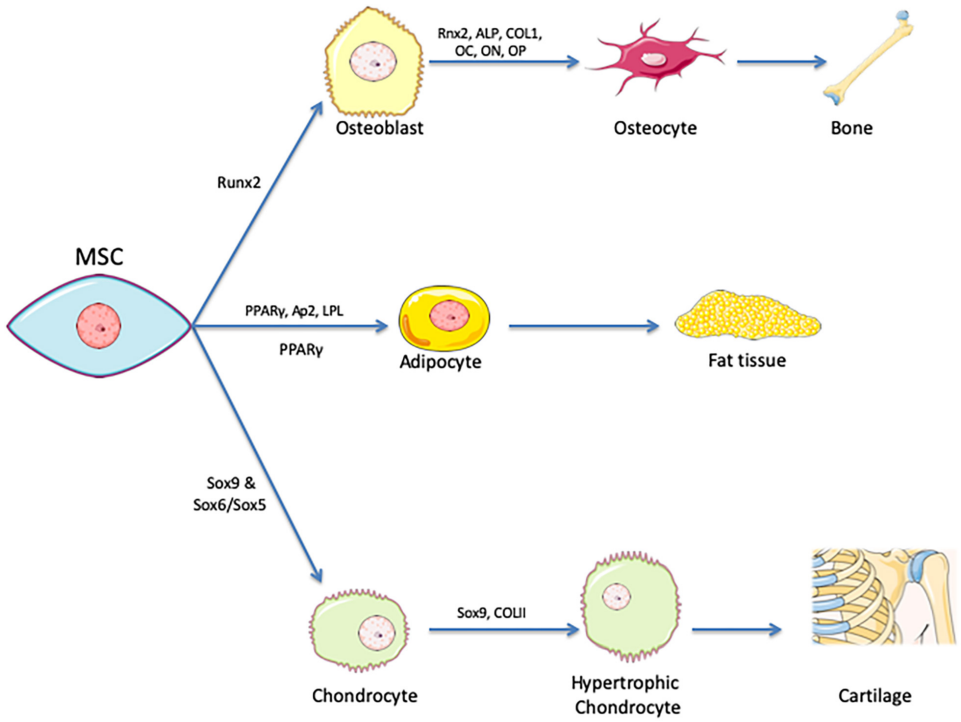

FIGURE 1 | Tri-lineage encompasses differentiation of MSCs. Mesenchymal stem cells are identified by their ability to differentiate into chondrocytes, adipocytes, and osteoblasts that in turn develop into cartilage, fat tissue and bone. PPARγ is the master regulator of adipogenesis, Runx2 for osteogenesis and Sox9 for chondrogenesis. Various expression markers are used as indicators of successful differentiation.

Differentiation of MSCs is primarily induced through media supplementation (and, in some instances, mechanical stimulation), with different supplements being required for the various differentiations. Adipogenesis, for example, is induced through supplementation with dexamethasone, indomethacin, insulin, and isobutyl methyl xanthine. Osteogenic differentiation is induced by dexamethasone, ascorbic acid, β-glycerophosphate, and sometimes bone morphogenic protein 2 (BMP-2) (Ullah et al., 2015). The completion of differentiation is verified by checking the expression of characteristic cell type markers, such as lipoprotein lipase (LPL) for adipogenesis and alkaline phosphatase (ALP) activity for osteogenesis (Ullah et al., 2015). More detailed lists of differentiation-promoting components and the most characteristic markers used to measure level of differentiation are shown in **Table 1**.

Differentiation is controlled by an interlinked set of regulatory molecules forming complex signaling pathways. These pathways are somewhat distinct between differentiation lineages, although there are important areas of overlap. This phenomenon is demonstrated by the inverse relationship that exists between pathways relating to adipogenic and osteogenic differentiation (**Figure 2**). Most differentiation pathways revolve around regulation of peroxisome proliferator-activated receptor (PPAR), which is the master regulator of adipogenesis, and runt-related transcription factor 2 (RUNX2), which is the master regulator of osteogenesis (Muruganandan et al., 2009; Neve et al., 2011; James, 2013; Hu et al., 2018). Further details on the most relevant reported signaling pathways and molecules for each type of differentiation are provided in **Table 1**.

Immunomodulation of MSCs

Beyond their potential for differentiation, hMSCs have remarkable immunomodulatory properties; they possess the ability to inhibit or promote the immune response of the host's body though mediated immunosuppression. These mechanisms include direct inhibitory effects and other indirect regulatory effects. This regulatory response involves inhibition of B and T cell proliferation, cytokine production inhibition, decreased natural killer (NK) cell activation, and dendritic cell maturation (**Figure 3**; Deng et al., 2005; Ma and Chan, 2016; Cunningham et al., 2018; Wang et al., 2018).

The immunomodulatory response of hMSCs is activated by inflammatory cytokines (e.g., IFN-γ, IL-1α, IL-1β, and TNF-α) that are secreted by T cells and other antigen-presenting cells (Ren et al., 2008; Németh et al., 2009). In response to their activation, MSCs secrete soluble immune factors capable of affecting both the innate and adaptive immune systems by mediating the subsequent regulatory responses of target cells (**Figure 4**; Kaundal et al., 2018; Wang et al., 2018). The immunoregulatory effects mediated in each instance are dependent on one or more of these secreted factors.

Indoleamine 2,3-dioxygenase (IDO) is one of the well-known paracrine factors released by hMSCs and has been shown to promote kidney allograft tolerance (Lan et al., 2010). It

TABLE 1 | Summary of various inducing components, expression markers, and signaling pathways related to differentiation.

Cell type resulting from differentiation	Differentiation-inducing components	Culturing time	Relevant expression markers	Most relevant reported signaling pathways and molecules	References
Adipocytes	Dexamethasone Indomethacin Insulin Isobutylmethyl xanthine	14–21 days, with 2 phases (determination and terminal differentiation)	ap2 LPL PPARγ	β-catenin dependent Wnt (anti) Hedgehog (anti) NELL-1 (anti) BMP (pro)	James, 2013
Cardiomyocytes	5-azacytidine	28 days	α-MHC α-cardiac actin ANP cTnT Desmin	miR1-2 + Wnt/β-catening (pro) HDAC TGF-β VR-1 5-aza	Solchaga et al., 2011; Guo et al., 2018
Chondrocytes	Ascorbate 2-phosphate Dexamethasone Insulin Linoleic acid Selenious pyruvate Selenium TGF-βIII Transferrin	21 days, with 2 phases (pre – induction and terminal differentiation)	*Phase 1:* Collagen types I and II *Phase 2:* L-Sox5 Sox6 Sox9	*Phase 1 expression dependent upon:* TGF-β1,2 and 3 *Phase 2 expression dependent upon:* BMP2 IGF-I TGF-β1 Wnt/β-catenin (pro) PTHrp (anti)	Mackay et al., 1998; Antonitsis et al., 2008; Li and Dong, 2016
Hepatocytes	*Phase 1:* bFGF EGF Nicotinamide *Phase 2:* Dexamethasone Insulin Oncostatin M Selenium Transferrin	2 phases: differentiation (7 days) and maturation			Ullah et al., 2015
Neuronal cells	bFGF BME EGF FGF HGF Insulin LMX1A* NGF Retinoic acid Valproic acid				Ullah et al., 2015
Osteocytes	β-glycerophosphate Ascorbic acid BMP-2 Dexamethasone	21–35 days	ALP COL1 OC ON OP RUNX2	β-catenin dependent Wnt (pro) BMP (pro) Hedgehog (pro) NELL-1 (pro) TGF-β1 + Wnt/β-catening (anti)	Neve et al., 2011; James, 2013
Pancreocytes	Actavin A Nicotinaminde Sodium butyrate Taurine				Ullah et al., 2015
Skeletal/smooth muscle	NICD TGF-β				Ullah et al., 2015

Note that this is not an exhaustive list.

suppresses proliferation and activity of NK and T cells by its metabolic activity – converting tryptophan into kynurenine. In humans, IDO synthesis has been reported as a response of MSCs to pro-inflammatory cytokine production that suppresses the inflammatory response (Bernardo and Fibbe, 2013; Mbongue et al., 2015; Gao et al., 2016; Kaundal et al., 2018; Wang et al., 2018).

Another reported soluble factor with immunoregulatory effects is the unstable oxidative molecule nitric oxide (NO), which is generated by NO synthase. Inducible NO synthase (iNOS) is responsible for the immunomodulatory effect of NO. Increased secretion of NO results in modulation of both the proliferation and function of T cells. At very high concentrations, it can lead to the apoptosis of immune cells (Bernardo and Fibbe, 2013; Gao et al., 2016; Kaundal et al., 2018; Wang et al., 2018). A list of the known soluble paracrine factors secreted by hMSCs that are involved in immunoregulation is provided in **Table 2**, along with their related effects.

Homing Effects of MSCs

Mesenchymal stromal cells secrete paracrine factors that promote tissue repair. In response to physical tissue damage, MSCs secrete factors that allow them to navigate to the site of injury, referred to as homing (Ullah et al., 2015). An example of a homing molecules used by MSCs are the chemokine receptors CXCR4 and CXCR7, which both bind to stromal cell-derived factor (SDF-1) on endothelial cells; this is a critical step in facilitating homing of MSCs to various tissues (Ullah et al., 2019). Homing is generally considered to be beneficial for tissue repair (Ullah et al., 2015) due to the interaction of the cells with the host tissue via secretion of trophic and paracrine factors (Ullah et al., 2015; Moreira et al., 2017). Engrafting or migration of hMSCs in experimental settings relies in part on this phenomenon in combination with the direct delivery of cells.

The homing effect and subsequent migration of hMSCs has been observed. However, the mechanisms behind it are not well understood. Only a small percentage of systemically administered cells manage to reach target tissue and remain there (De Becker and Riet, 2016; Moreira et al., 2017). For the most part, this low success rate has been ascribed to low expression levels of homing molecules, loss of expression of homing molecules during *in vitro* expansion, and cultural heterogeneity of the hMSCs. Cells derived from different sources seem to express different profiles of the homing molecules (De Becker and Riet, 2016; Moreira et al., 2017).

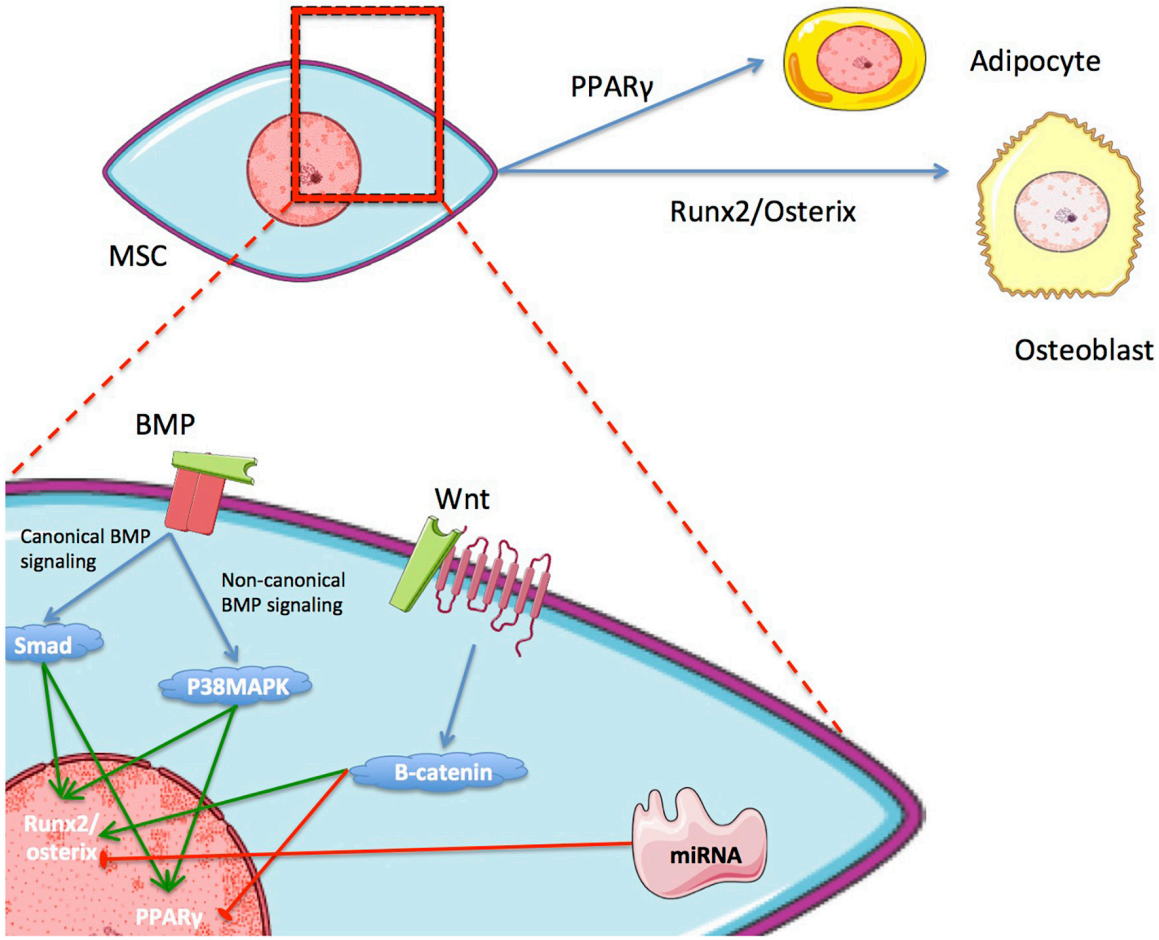

FIGURE 2 | The inverse relationship of the main metabolic pathways in OD and AD. Differentiation toward one lineage can inhibit differentiation toward the other.

MSCs as a Novel Tool in Regenerative Medicine

Regenerative medicine is considered a novel frontier in medical research (Maienschein, 2011; Sampogna et al., 2015). It combines the knowledge and application of various fields such as tissue engineering, cell transplantation, stem cell biology, biomechanics, prosthetics, nanotechnology, and biochemistry to replace or restore human cells, tissues, or organs to their normal functions (Sampogna et al., 2015). A variety of regenerative medicine therapies are available (see Lonner et al., 2000; Blais et al., 2013; Zhang X. et al., 2013; Trushina and Mielke, 2014; Björnson et al., 2016; Moreira et al., 2017), but their success has been limited by functional obstacles that increase the risk of harm to patients and reduce their efficacy as a therapeutic (Neman et al., 2012; Campana et al., 2014; Goldberg et al., 2017; Cunningham et al., 2018; Solarte et al., 2018). Despite recent progress, there is obvious room for improvements regarding both the safety and efficacy of therapies for patients. The multipotency, high proliferation potential, paracrine effect, and immunomodulatory activity of hMSCs (Rosenbaum et al., 2008; Ullah et al., 2015; Fitzsimmons et al., 2018) have led to development of MSCs as a tool for use in regenerative medicine. Thus, MSCs are considered ideal candidates for immunotherapy and tissue engineering.

Recent advancements have allowed researchers to overcome initial obstacles in the use of MSCs. Numerous clinical trials have assessed their safety and found that transfusions using these cells are safe (Neman et al., 2012; Zhao et al., 2016). Various studies have developed isolation and culture approaches along with various possible mechanisms of delivery. These studies have shown that long-term culture of MSCs is possible without losing the cells functional, phenotypical, or morphological features (Bernardo et al., 2007).

Further, MSCs are becoming readily available for biomedical research. There is growing interest in the use of placental- and umbilical cord-derived hMSCs due to the relatively high availability of discarded tissue associated with births (Moreira et al., 2017); however, the variance in phenotypic properties (if any) between hMSCs derived from different sources is an important open question. Bone marrow- (BM-) and adipose tissue-derived (Ad-) hMSCs are the most favored stem cell

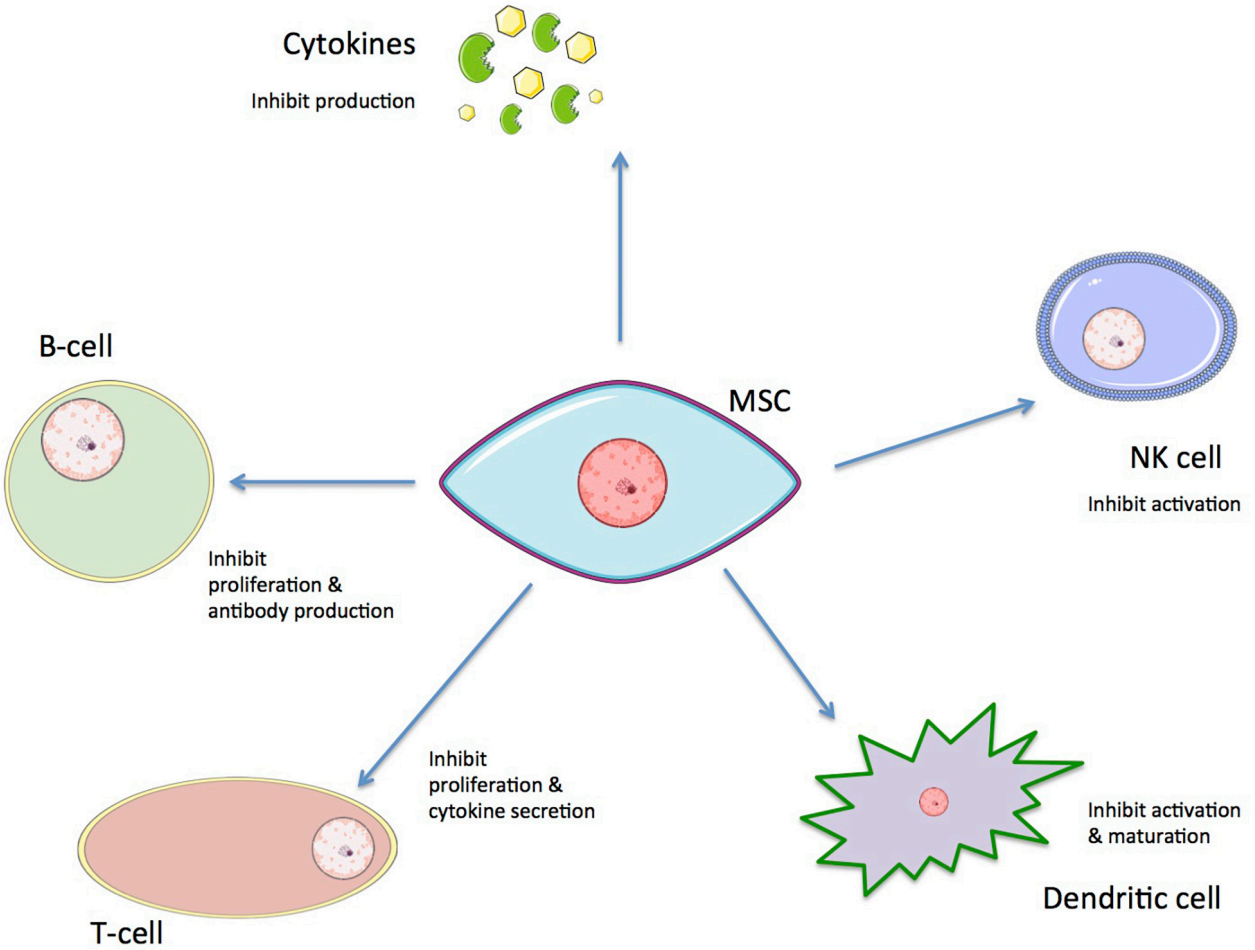

FIGURE 3 | The immunoregulatory effects of hMSCs on immune cells.

types in both tissue engineering and cell-based medicine for a variety of reasons, despite the invasive procedures required for tissue collection (Fitzsimmons et al., 2018): (1) the total cell number that can be harvested each time is higher than with other stem cells; (2) the frequency of cells of interest is higher than with other stem cells; and (3) Ad-hMSC harvesting can be performed as part of some elective cosmetic surgeries (e.g., liposuction) (Fitzsimmons et al., 2018). Ad-hMSCs have been shown to have increased capacity for adipogenic differentiation *in vitro*, while BM-hMSCs have increased capacity for osteogenic and chondrogenic differentiation (Liu et al., 2007). Through a comparative study on the immunomodulatory abilities of cells derived from the same donor bit different tissues, Valencia et al. (2016) determined that Ad-hMSCs have a higher capacity for inhibiting dendritic cell differentiation than do BM-hMSCs, while BM-hMSCs displayed a higher capacity for inhibition of NK cell cytotoxic activity; these results have been corroborated by several independent groups (Ivanova-Todorova et al., 2009; Blanco et al., 2016). These observations—whether relating to proliferation potential or direct therapeutic application abilities—highlight the importance of choosing the optimal cell source for a particular clinical circumstance.

Efficacy of Cell Engraftment vs. Paracrine Factors

For the last several decades, the therapeutic potential of hMSCs has been focused on cell transplantation, adding hMSCs to a recipient donor site for repair via regeneration, differentiation, and immunomodulation (Lukomska et al., 2019). Co-culturing in animal studies has shown that hMSCs can induce tissue regeneration to some extent in the heart (Rose et al., 2008), kidneys (Qian et al., 2008), and liver (Cho et al., 2009) through infiltration and replacement in damaged or injured tissue by multipotent hMSCs (see **Figure 5**). Increasing attention, however, has lately been given to the immunomodulatory and suppressive capabilities of hMSCs, especially with regards to their paracrine factors (Németh et al., 2009; Cunningham et al., 2018; Kaundal et al., 2018). Currently, approximately 10% of the clinical trials registered in the United States are using MSCs to study immunological disease. Through their ability to decrease inflammation and general inhibitory functions, hMSCs have been utilized as contributing factors for various immune disorders for

TABLE 2 | A list of inflammatory cytokines that activate immunoregulatory state of hMSCs, major known soluble paracrine factors secreted by hMSCs, and a summary of their biological functions.

Immunosuppressive factors secreted by MSCs	Summary of biological function	Activating inflammatory cytokines
CCL2	Promotion of monocyte migration. Suppression of activation and mitigation of TH17 cells.	IFN-γ, IL-1α, IL-1β, TNF-α
Galectins	Suppression of the immunomodulatory effects of T cells.	
IDO	Suppression of the effects and proliferation of immune cells.	
IL-10	Suppression of immune cell apoptosis.	
NO	Promotion of immune cell apoptosis. Suppression of proliferation and modulation of T cells.	
PGE2	Suppression of NK cell cytolytic activity and T cell proliferation.	
TSG6	Overall anti-inflammatory effect.	
TGF-β	Inhibition of mast cell degranulation, NK cell activation and proliferation, and Treg induction.	

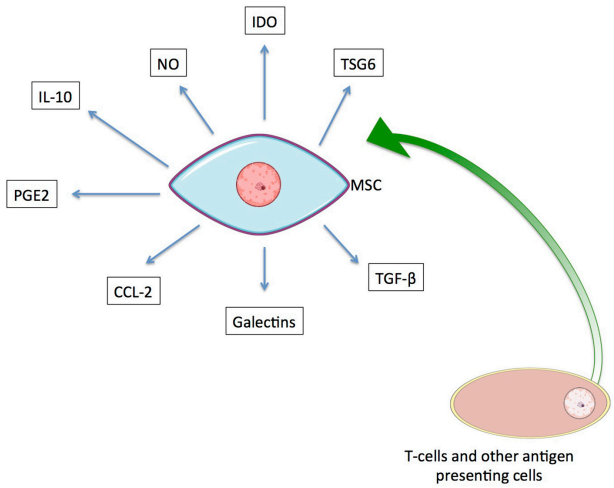

FIGURE 4 | The immunoregulatory secretome of hMSCs. Known soluble factors secreted by MSCs upon activation by T cells and other antigen presenting cells are shown.

symptom relief. Such disorders include type 1 and type 2 diabetes (Moreira et al., 2017), acute graft versus host disease (GvHD) (Gao et al., 2016), arthritis (Burke et al., 2016), allograft rejection (Munir and McGettrick, 2015), and Crohn's disease (Ibraheim et al., 2018). The possible immunomodulatory effects of hMSCs have been found to be dependent upon the source of the hMSCs as well as their immediate microenvironment (Bortolotti et al., 2015). The microenvironment is dependent upon the individual inflammatory profile of the host, which is potentially related to any disease pathogenesis present. This variability leads to varied cytokine profiles that are, at least in part, responsible for the difficulties of using MSC therapy effectively in both preclinical and clinical situations (Kaundal et al., 2018). Some of these challenges may be overcome by personalizing each case (i.e., tailoring each therapy to the inflammatory environment of the recipient patient).

There has been a recent paradigm shift away from the primary aim of hMSC transplantation being tissue repair by engraftment toward the use of hMSCs to promote healing via their secretion of paracrine factors. In many therapeutic contexts, it is now recognized that MSCs exert their healing effects through paracrine signaling and cell-to-cell contact, not by replacing cells (Fitzsimmons et al., 2018). There are a few notable examples using hSMCs as paracrine-mediated treatment currently in development (Amorin et al., 2014; Hofer and Tuan, 2016; Archambault et al., 2017; Moreira et al., 2017; Cunningham et al., 2018; Ibraheim et al., 2018; Solarte et al., 2018). The reported success of these studies indicates that the MSC secretome exerts beneficial effects that may be exploited by therapeutic applications.

Existing Challenges and Problems

Despite the initial successes demonstrated in animal and early clinical trials regarding the safety and efficacy of hMSCs, a number of challenges, problems, and unanswered questions remain. In order for *in vitro* cultured MSCs to engraft after implantation or to secrete their beneficial factors, they must be able to survive. The transplantation procedure itself exerts various direct mechanical and chemical stresses on the cells, and the treated tissue offers a comparatively much harsher environment than the standard culture surroundings that cells experience *in vitro*. In tissues *in vivo*, there are various negatively impacting stressors, such as hypoxia, inflammation, decreased energy/nutritional availability, and high acidity. Various strategies to enhance survival and overcome these adverse conditions have been developed, including preconditioning, genetic modification, and supportive biomaterials as a delivery device (Baldari et al., 2017; Moreira et al., 2017).

It is possible that donor variability and differences in isolation site have an effect on experimental outcomes, though the extent of these effects is not yet well understood. This uncertainty may be exacerbated by heterogeneity in the origins of MSCs used in tests (Bortolotti et al., 2015; Lukomska et al., 2019). Further, there is a lack of knowledge of the optimal dose and frequency required for hMSC transplantation (Lee, 2018; Lukomska et al., 2019). In addition, generating high doses of hMSCs requires cellular expansion on a large scale. Despite being proven to retain their characteristics over long term expansion (Bernardo et al., 2007), MSCs eventually become senescent (Turinetto et al., 2016). Senescent cells have undergone functional changes. Firstly, differentiation potential usually decreases due to accumulation of oxidative stress and dysregulation of key differentiation

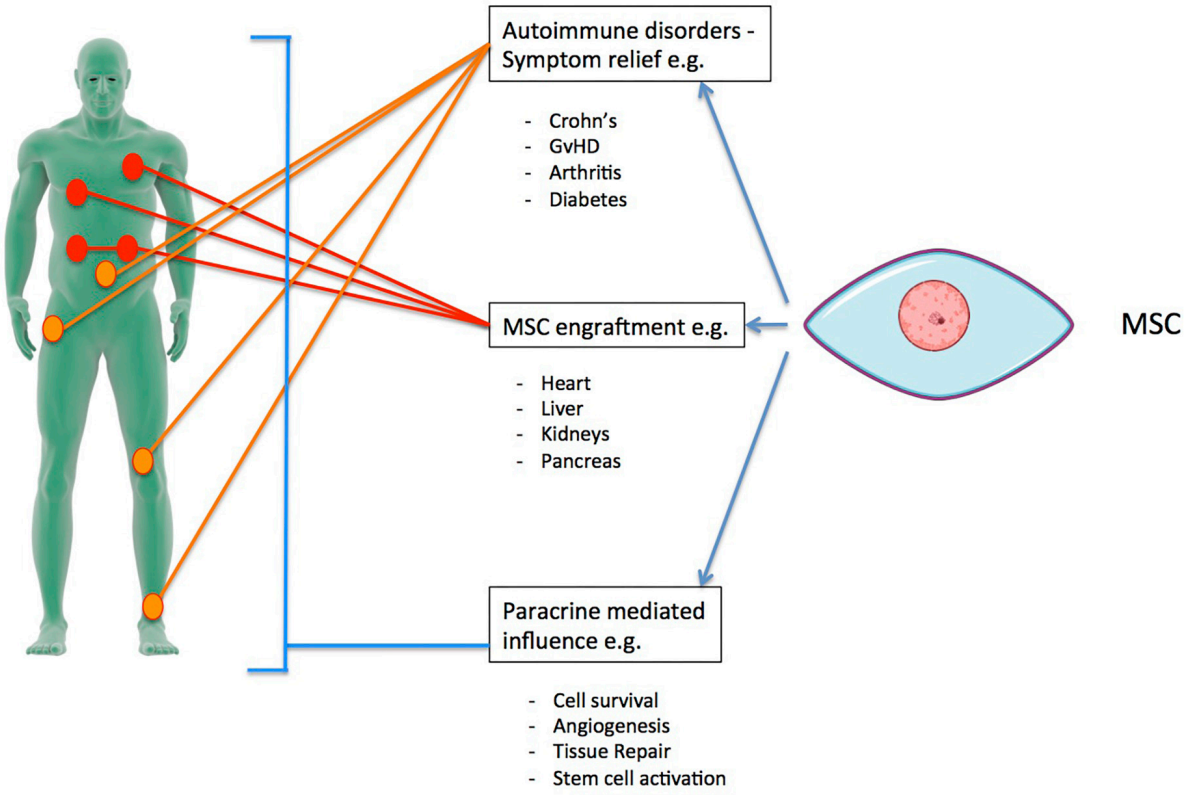

FIGURE 5 | Examples of therapeutic applications for hMSCs, including organs where cell transplants have been used for engraftment, some autoimmune disorders where the immunoregulatory and differentiation abilities of hMSCs have been utilized, and some of the paracrine factor-mediated influences that can be used in a therapeutic setting.

regulatory factors. Secondly, both migratory- and homing-related abilities of hMSCs are reduced as they move into senescence. Finally, the secretome of hMSCs becomes compromised in senescence. Many of the factors that are present in the senescent MSC secretome can exacerbate an inflammatory response at a systemic level and so promote either migration or proliferation of cancer cells (Turinetto et al., 2016).

In many cases of MSC transplantation, there is little to no integration of the transplanted cells, and cells that are retained are observed to have a short survival time in some cases (Li et al., 2016; Lukomska et al., 2019). Even though more than two thousand patients have received either autologous or culture expanded allogeneic MSCs, long-lasting observations are lacking in many cases (Lukomska et al., 2019). This lack of data indicates that more progress is difficult. Tumor support due to the immunosuppressive effects of MSCs and the related possibility of tumorigenicity of such a therapy has been reported (Barkholt et al., 2013). There have also been reports of BM-hMSC-induced liver fibrosis (Russo et al., 2006). These issues must be addressed by long-term studies regarding safety of use.

While the use of hMSCs holds great promise in regenerative medicine, the hurdles and unanswered questions outlined in this section still linger. perhaps the greatest barrier preventing widespread and successful implementation of hMSCs as tools to enhance and develop therapeutics is the critical gap in knowledge of hMSC metabolism. During differentiation, we can observe a metabolic shift in hMSCs from using only glycolysis to a mix of glycolysis, oxidative phosphorylation, and beta fatty acid oxidation to produce energy. However, in order to have immunomodulatory effects (via paracrine factors) on a host's immune system, hMSCs must be mainly in a glycolytic state. Further, it is not well understood to what extent energy metabolism is mixed at different stages of differentiation (early versus late) or whether it is dependant upon the type of differentiation the cells are undergoing. An understanding of how cell source and age affects differentiation and if different states affect the survival and function and, therefore, usability of cells *in vivo*. In the following section, we delve into some of these gaps and discuss how acquiring a deep understanding of underlying mechanisms can help unlock the therapeutic potential of hMSCs in regenerative medicine.

METABOLISM OF MSCs

MSC Function Is Linked to Metabolism

The proliferation, differentiation, and immunomodulatory functions of hMSCs are linked to cellular metabolism

(dos Santos et al., 2010; Estrada et al., 2012; Beegle et al., 2015). Emerging evidence suggests that hMSCs are metabolically heterogeneous and that these differing metabolic states impact both differentiation ability and capacity for immunomodulation (Agathocleous and Harris, 2013; Liu et al., 2019). To date, studies have focused primarily on BM-hMSCs and Ad-hMSCs.

There is strong evidence suggesting that, in their undifferentiated state (while undergoing proliferation), hMSCs rely primarily on glycolysis for energy production. This phenotype has been demonstrated in BM-hMSCs, which show a preference for glycolysis during proliferation (Pattappa et al., 2011; Buravkova et al., 2013; Shum et al., 2016; Zhu and Thompson, 2019) but shift to a more oxidative phosphorylation (OxPhos)-dependent metabolism during osteogenic and adipogenic differentiation (OD, AD) (Meleshina et al., 2016; Shum et al., 2016). Similar findings have been reported for Ad-hMSCs (Meleshina et al., 2016; Meyer et al., 2018). Proliferating Ad-hMSCs were found to have a preference for glycolysis even under aerobic conditions, while during OD the cells increased both glycolysis and mitochondrial metabolism, including the processes of OxPhos and fatty acid β-oxidation. However, when Ad-hMSCs underwent AD, they showed a decreased capacity for the pentose phosphate pathway (PPP) and glycolysis, while mitochondrial enzyme activities increased, indicating an increased capacity for oxidative phosphorylation and β-oxidation (Meleshina et al., 2016; Meyer et al., 2018).

The ability of BM-hMSCs to differentiate has also been shown to be affected by mitochondrial functions (Zhang Y. et al., 2013; Li et al., 2017). Consistent with reports that proliferating hMSCs have a glycolytic phenotype, undifferentiated cells have high levels of hypoxia-inducible factor 1 (HIF-1), a transcriptional regulator central to regulation of genes that are involved in hypoxic responses. It is also a crucial physiological regulator of anaerobic metabolism (Gaspar and Velloso, 2018). Cells undergoing OD downregulate HIF-1. Downregulation of HIF-1 seems to be required for the activation of mitochondrial OxPhos, an oxygen-dependent pathway (Shum et al., 2016).

The mitochondria of hMSCs seem to be primarily inactive while cells remain in their proliferation stage, during which metabolic pathways related to glycolysis and its associated signaling pathways required for adenosine triphosphate (ATP) generation and general anabolitic activity are most active (see **Table 3**). Glycolytic metabolism also seems to be a requirement for hMSCs to be able to sustain immunosuppressive factor secretion (Liu et al., 2019). Secretion of immunomodulatory factors is only possible when hMSCs have been activated, such as by IFN-γ (Waterman et al., 2010). Liu et al. (2019) utilized IFN-γ treatment to cause immune polarization in hMSCs leading to remodeling of metabolic pathways toward glycolysis (reducing TCA cycle metabolism), a requirement for sustained immunosuppressive factor secretion. The activated cells were measured to have increased lactate levels, glucose consumption, and acidification rate. Increased expression of glucose transporter 1 and hexokinase isoform 2 (key enzymes in glycolysis), along with reduced electron transport and OxPhos, was also observed. These are all indicators of increased glycolytic activity (Liu et al., 2019). MSCs with a glycolytic phenotype are also able to sustain IDO production and the exposure to IFN-γ inhibited activity of the mitochondrial electron transport chain (complexes I or III), blocking OxPhos and reducing mitochondria-related reactive oxygen species (mROS). This reduces the effects of mROS that are key to metabolic remodeling in differentiation. Liu et al. (2019) further showed that Akt/mTOR signaling pathway activation is required to induce metabolic reconfiguration, specifically IDO and Prostaglandin E2 (PGE2) production. PGE2 increases in response to increased aerobic glycolysis. The immune response of hMSCs treated with IFN-γ is altered if the metabolic reconfiguration induced by Akt/mTOR is disrupted.

TABLE 3 | List of common signals in metabolism and the major metabolic pathways effected.

Signal	Metabolic pathways regulated by the signal
AMPK	Inhibition of glycolysis and fatty acid synthesis. Promotion of fatty acid oxidation.
Hedgehog	Stimulation of glycolysis.
HIF	Redirection of energy metabolism from OXPhos to glycolysis.
mTOR	Stimulation of glycolysis, lipid synthesis, protein synthesis, and pyrimidine synthesis.
Myc	Stimulation of glycolysis, glutaminolysis, and nucleotide synthesis.
PI3K	Stimulation of glucose uptake, fatty acid synthesis, and glycolysis.
Ras	Stimulation of glucose uptake and PPP. Regulation of glutaminolysis.
Sirtuins	Regulation of TCA cycle, glycolysis, and fatty acid oxidation.

The effect of interferon regulation on hMSC metabolism can be varied. IFN-γ has also been used to inhibit proliferation and alter AD, OD, and neural differentiation (ND) by activating IDO (Croitoru-Lamoury et al., 2011). The kynurenine pathway (KP), along with IDO1 and IDO2, is expressed in hMSCs and highly regulated by both IFN-γ and IFN-β. IFN-γ licensing of hMSCs results in inhibited proliferation via activation of the KP and subsequently IDO, and inhibits the cell potential for OD and AD. In contrast to IFN-γ licensing, IFN-β treatment managed to increase expression of adipogenic markers (Croitoru-Lamoury et al., 2011).

IFN-β has been shown to enhance immunomodulatory functions of hMSCs in other reports. Vigo et al. (2019) demonstrated IFN-γ induced expression of secretory leukocyte protease inhibitor (SLPI) and hepatocyte growth factor (HGF), soluble mediators that are involved in both immune and regenerative functions of hMSCs. Simultaneously, IFN-β induced the activity of mTOR, increasing the glycolytic capacity of the cells. This energy metabolic modification improved the cells' ability to control T cell proliferation, yet another indication of a link between high glycolytic capacity and immunomodulatory capabilities (Vigo et al., 2019).

Overall reports discussing hMSC metabolism seem to, for the most part, agree that during proliferation the cells primarily generate ATP through glycolysis. However, upon initiation of differentiation, cells seem to turn toward mitochondrial metabolism, with reported increases in metabolism and

biogenesis indicating the importance of mitochondrial activity when it comes to hMSC functionality (Shum et al., 2016).

There is not much known about whether amino acid metabolism is affected during functional progression of hMSCs or what effects they induce if modified through metabolic changes. For example, El Refaey et al. (2015) studied the aromatic amino acids tryptophan and tyrosine, finding that oxidation (via cell senescence) disrupted their anabolic effects on BM-MSCs. By using mouse BM-MSCs, they were able to examine effects of oxidized dityrosine and kynurenine of proliferation and differentiation and found that these oxides inhibited BM-MSC proliferation, ALP expression and activity and expression of osteogenic markers. Yue et al. (2018) studied fatty acid related gene expression and compositions of fatty acids during adipogenesis of bovine Ad-MSCs and found that lipid-related gene expression and fatty acid composition changed noticeably during the early stages of differentiation (e.g., there was increased expression of *de novo* lipogenesis-related genes, and thus *de novo* lipogenesis produced fatty acid elongation and desaturation) before returning to normal (e.g., proportions of saturated fatty acids, monounsaturated fatty acids, and polyunsaturated fatty acids returned to initial levels in later stages). Their conclusion was that *de novo* lipogenesis and desaturation comprised the major fatty acid flux during adipogenic differentiation of bovine Ad-MSCs.

Ornithine decarboxylase (ODC) and polyamine biosynthesis are important in the proliferation of stem cells (Tsai et al., 2015). The role of ODC regarding differentiation has not been fully explored but is considered to be diverse. Through the study of inhibition of ODC's irreversible inhibitor, α-difluoromethylornithine, Tsai et al. (2015) hypothesized that inhibition of ODC and the accompanying depletion of exogenous polyamines might be correlated with the osteogenic induction of BM-hMSCs, and demonstrated (in BM-hMSCs) that decreases in the expression of PPAR- γ and ODC along with an accompanying reduction in polyamines, are responsible for enhanced osteogenesis.

MSC Functionality Is Greatly Impacted by Mitochondrial Activity

As suggested in section "MSC Function Is Linked to Metabolism," active mitochondria are necessary for successful differentiation. Accumulating evidence indicates that mitochondrial enzymes and regulatory pathways are of great importance for MSCs in proliferative and differentiating states (Chen et al., 2008; Buravkova et al., 2013; Li et al., 2017). Mitochondria have been found to be crucial for sufficient ATP production to support OD, in addition to other mechanisms. Active mitochondria support OD by promoting β-catenin acetylation and, therefore, its activity. β-catenin is an important signaling pathway in osteogenesis (Shares et al., 2018). In osteogenesis, a mechanism of OD induction is to induce mitochondrial OxPhos by replacing glucose with galactose. This switch also stimulates β-catenin signaling and β-catenin acetylation. Increased β-catenin acetylation is the mechanism of osteogenesis driven by mitochondrial OxPhos (Shares et al., 2018). This acetylation increases during osteogenesis (BM-hMSCs). Active mitochondria may also support other osteogenic pathways by providing acetyl groups.

Other enzymatic activity has been confirmed that further supports the importance of mitochondrial activation for MSC functionality. Creatine kinase (CK) activity, which is involved in buffering and recovery of ATP, has been reported in Ad-hMSCs. It stimulates glycogenolysis by increasing cytoplasmic concentration of inorganic phosphate. Activity of CK was found in both differentiated and proliferating Ad-hMSCs, with more mitochondrial CK activity in AD cells. This further supports the theory of a shift toward oxidative metabolism/mitochondrial metabolism during differentiation of MSCs (Meyer et al., 2018).

Through the reversible mitochondrial nicotinamide adenine dinucleotide phosphate (NADP)-dependent reaction of isocitrate dehydrogenase (NADP-IDH), an anaplerotic pathway exists that forms isocitrate from glutamine through a process called glutaminolysis. Through this pathway, glutamine can compensate for the lack of glucose for both ATP production and anabolic precursor supply (Smolková and Ježek, 2012). This pathway is active in MSCs during OD, indicating yet another important role that mitochondria play when it comes to provision of sufficient ATP to ensure successful differentiation.

Reactive oxygen species (ROS) are known to serve as signaling molecules capable of regulating biochemical pathways that are a part of normal cell function. They are particularly important in metabolism and inflammatory signaling (Forrester et al., 2018). Regulation of mROS levels also contributes to determination of differentiation outcome. For a long time, these molecules were considered to be harmful to cells, inducing organismal death and dysfunction, but more recent reports suggest that excess mROS impair OD and promote AD by inhibiting Hedgehog signaling (a pathway essential for bone development and maintenance) (Li et al., 2017).

Possible Ways to Achieve Metabolic Manipulation

Since functionality and survival of hMSCs is affected by changes in their metabolism, there is the potential to enhance the efficacy of hMSC therapies through manipulation of metabolism. hMSCs can effectively reconfigure metabolism to respond to the biochemical demands of tissue repair, be it secretion of immunomodulatory factors or integration and differentiation toward tissue specific cell types (Mylotte et al., 2008; Zhu et al., 2014; Yuan et al., 2019). Currently, the most extensively studied subtypes are BM-hMSCs and Ad-hMSCs, but even these subtypes have not been exhaustively studied. Evidence indicating the importance of both the enzymes and mitochondrial pathways support its significance for proliferation and differentiation of hMSCs (Chen et al., 2008; Buravkova et al., 2013; Li et al., 2017). In addition, several critical MSC functions are not only influenced by internal cellular mechanisms, but also by external ones (mechanical and biochemical) such as the composition of its microenvironment (Bloom and Zaman, 2014). Previous work has explored various ways of affecting the mechanisms controlling MSC metabolic function (see **Figure 6**).

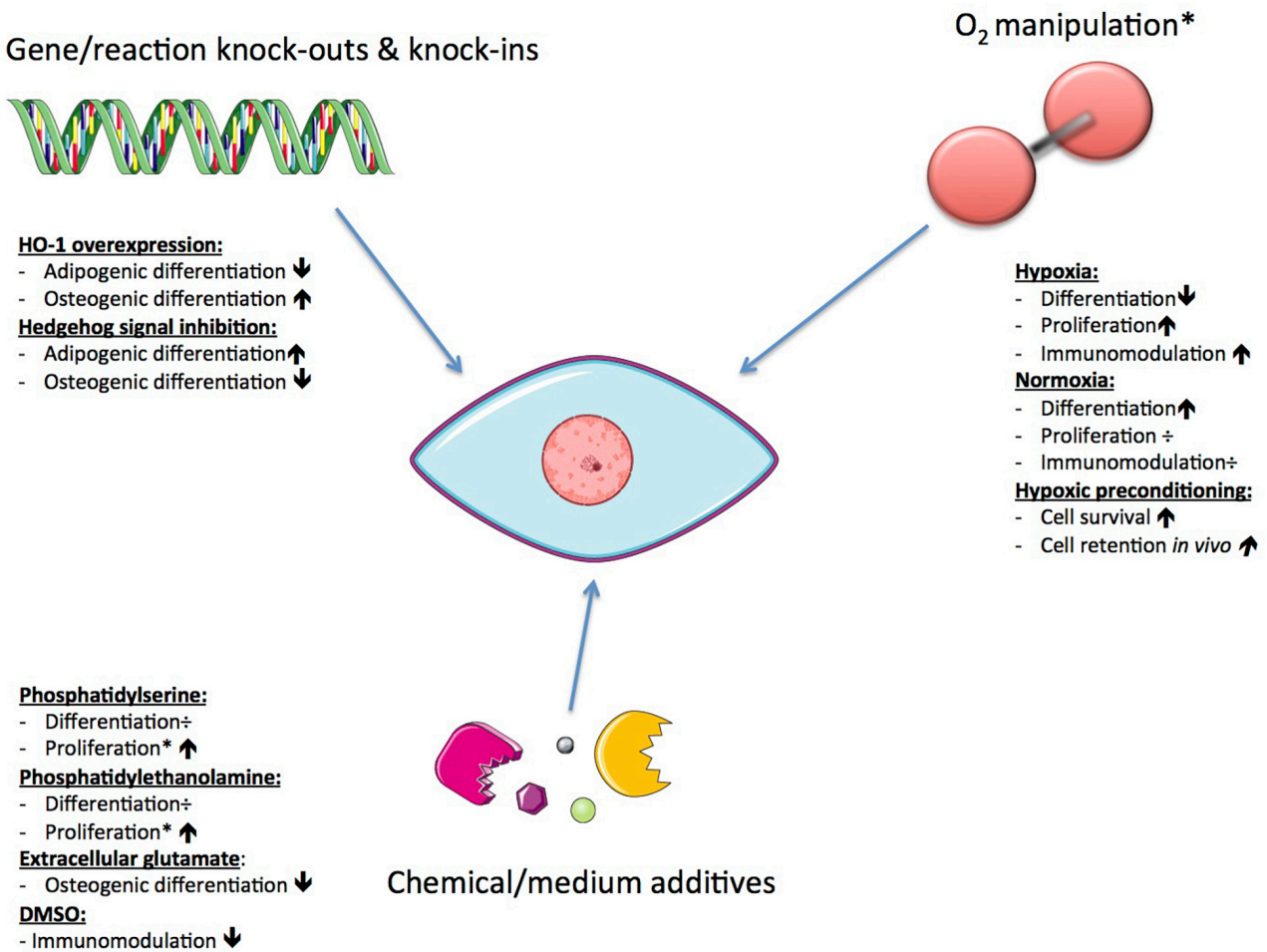

FIGURE 6 | Possible ways to achieve metabolic manipulation of hMSCs. The resulting effects may vary depending on the original cell source.

One such approach is to alter the functional capacity of MSCs through oxygen manipulation, due to the importance of mitochondria and mROS discussed above. Muñoz et al. (2014) investigated the effect of oxygen levels on metabolic phenotypes of hMSCs. Oxygen is a ubiquitous regulator of cellular metabolic activity and of the survival, function, and differentiation of hMSCs. Using both normoxic and hypoxic conditions, they found contrasting metabolic profiles for hMSCs during proliferation versus OD. The key difference was found in the coupling of glycolysis to the TCA cycle, glutaminolysis, and malate-aspartate shuttle. In response to low oxygen levels, undifferentiated hMSCs showed increased consumption of both glucose and glutamine that activated the malate-aspartate shuttle in order to accommodate increased cytosolic production of nicotinamide adenine dinucleotide + hydrogen (NADH) and transport glutamate and reducing equivalents into the mitochondrial matrix for oxidation (Muñoz et al., 2014). Low oxygen also activates HIF-1, reducing pyruvate dehydrogenase activity so that transport of glucose derived carbons into the TCA cycle decreases (Estrada et al., 2012). These metabolic characteristics allow increased proliferation under hypoxic circumstances, allowing cells to survive in an ischemic environment.

Similar findings were reported for proliferation of cells grown under hypoxia (dos Santos et al., 2010). For cells in OD, hypoxia induces a more significant block of carbon flow from glycolysis into the TCA cycle, compared to undifferentiated cells. This is demonstrated by a greater rise in lactate levels. The carbon flow blockage results in lower citrate levels and less production of reduced cofactors [e.g., NADH and flavin adenine dinucleotide ($FADH_2$)] involved in OxPhos. The lower citrate levels indicate a more pronounced metabolic uncoupling of glycolysis and TCA cycle for cells in OD compared to undifferentiated cells (Muñoz et al., 2014). This observation of a tight coupling of glycolysis and TCA cycle in cells undergoing OD compared to proliferating hMSCs suggests a stronger dependence on oxygen during OD (Muñoz et al., 2014). This dependency has been shown independently (Buravkova et al., 2013). Permanent oxygen deprivation resulted in the attenuation of cellular ATP levels, leading to diminished mitochondrial ATP production and stimulation of glycolytic ATP production. The attenuated cellular ATP levels stimulated a proliferation state of the hMSCs and

reduced the differentiation capacity, indicating that low ATP levels (arising from glycolysis only) are sufficient to maintain the cells' uncommitted state (Buravkova et al., 2013). Hypoxia has also been used to precondition MSCs to enhance their survival and cell retention *in vivo* via induction of metabolic changes (Beegle et al., 2015).

Reactive oxygen species are known to play a role in the mediation of both pathophysiological and physiological signal transduction (Forrester et al., 2018). The subcompartments in cells (e.g., peroxisome and mitochondria) that produce ROS are often associated with metabolism. Mitochondria-related ROS are able to influence metabolic processes on their own, and so have an effect on differentiation and immunomodulation of hMSCs. Studies have shown that by using mitochondrial-targeted antioxidants, AD may be inhibited; however, as mentioned in section "MSC Functionality Is Greatly Impacted by Mitochondrial Activity," excess mROS impair OD and promote AD by inhibiting Hedgehog signaling (Li et al., 2017). The role of mROS in chondrogenic differentiation (CD) is less well known (Li et al., 2017). Takarada-Iemata et al. (2011) found that through sustained exposure to glutamate, a significant decrease in osteoblastic marker expression could be induced. This happened in association with a reduction of intracellular glutathione (GSH) levels, but without affecting adipogenic marker expression. This finding suggests that extracellular glutamate preferentially suppresses osteoblastogenesis over adipogenesis in MSCs through the cysteine/glutamate antiporter (Takarada-Iemata et al., 2011).

The effects of other chemical stimuli have also been reported. In contrast to the inhibiting effects of extracellular glutamate on OD, it was reported that by inducing overexpression of heme oxygenase-1 (HO-1) OD of BM-hMSCs may be enhanced and adipogenesis decreased (although no mechanism was determined) (Barbagallo et al., 2010). HO-1 is a nuclear factor erythroid 2-related factor 2 (Nrf2)-regulated gene that plays a critical role in preventing vascular inflammation. It also has important antioxidant, anti-inflammatory, antiproliferative, and antiapoptotic effects in vascular cells (Araujo et al., 2012). Recent reports suggest that frozen or cryopreserved hMSCs are therapeutically less effective than freshly harvested MSCs (François et al., 2012). It seems that dimethyl sulfoxide (DMSO), a commonly used cryopreservative solution, decreases metabolic and immunosuppressive properties of hMSCs, while valproic acid (VPA) pre-treatment enhances both (François et al., 2012). Moreover, the T cell suppressive capacity of hMSCs *in vivo* is related to the cells' glycolytic and respiratory capacity, in contrast to their IDO dependence *in vitro*. This observation, therefore, leads to speculation that hMSCs may only be able to induce immunoregulatory effects when undifferentiated.

Metabolism in MSCs is a complex and dynamic system. We have outlined several gaps in the collective knowledge of MSC metabolism that are actively being addressed by the community. As we gain insights into questions regarding the primary energy-generating pathway(s) utilized during differentiation, we will move closer to manipulating these systems. However, we will need a holistic perspective that integrates knowledge at the various biological levels of MSC differentiation.

MATHEMATICAL MODELING OF HUMAN METABOLISM

A bottom-up systems biology approach allows for a mechanistic understanding of a system (Westerhoff and Palsson, 2004). Such mathematical models can predict potential interventions, potentially providing insights into how to successfully manipulate MSCs for therapeutic applications. Over the last few decades, many individual components of MSC biology have been studied in detail. However, to predict a cell's phenotype, it is necessary to understand all of the systemic interactions of environmental and cellular components that contribute to that phenotype (Bordbar et al., 2014). A combination of high-throughput -omics technologies, enabling the collection of large data sets, and improved computational modeling methods to holistically analyze that data have made systems biology possible (Henry et al., 2010; Resendis-Antonio, 2013).

The first step in modeling metabolism at the genome-scale is to reverse engineer the network structure (Reed and Palsson, 2003; Resendis-Antonio, 2013; Bordbar et al., 2014; Yurkovich and Palsson, 2016). This reconstruction process starts with collecting all annotated components of the genome and experimental evidence of biochemical reactions for the organism of interest (Thiele and Palsson, 2010). Further constraints are placed on the network based on biochemical knowledge—including stoichiometric constraints (e.g., mass and charge balance of reactions), thermodynamic constraints, and enzymatic capacity constraints (Reed and Palsson, 2003; Rocha et al., 2008; Oberhardt et al., 2009; Thiele and Palsson, 2010)—eventually resulting in a genome-scale model (GEM) of metabolism (see **Figure 7**). Transcriptomic and proteomic data is then used to select which of these reactions are active in a given phenotype, based on the presence of the enzyme that catalyzes the reaction. Metabolomic data may be used to constrain which metabolites should be produced or consumed by the cell being modeled (Bordbar et al., 2017). The resulting GEM can then be used with a variety of computational approaches, such as flux balance analysis (FBA), to determine the flux state (i.e., pathway usage) of the entire metabolic network (see **Figure 8**).

This ability to integrate information from multiple types of -omic data with previously acquired detailed biochemical data makes metabolic modeling a powerful technique to answer biological questions regarding how phenotypes occur due to genetic mutation or environmental perturbations (Thiele and Palsson, 2010). As further data is obtained, the model will more closely represent the intended physiological conditions. An updated model may produce novel hypotheses which can suggest new experimental directions. Establishing this feedback between experimental design and computational evaluation is valuable and enables a better understanding of how cells—including MSCs—organize their metabolic system in response to shifts in environment and functional demands (Reed and Palsson, 2003; Resendis-Antonio, 2013). Furthermore, the ability to contextualize models based on information at various levels from genomic to environmental has the potential to allow models

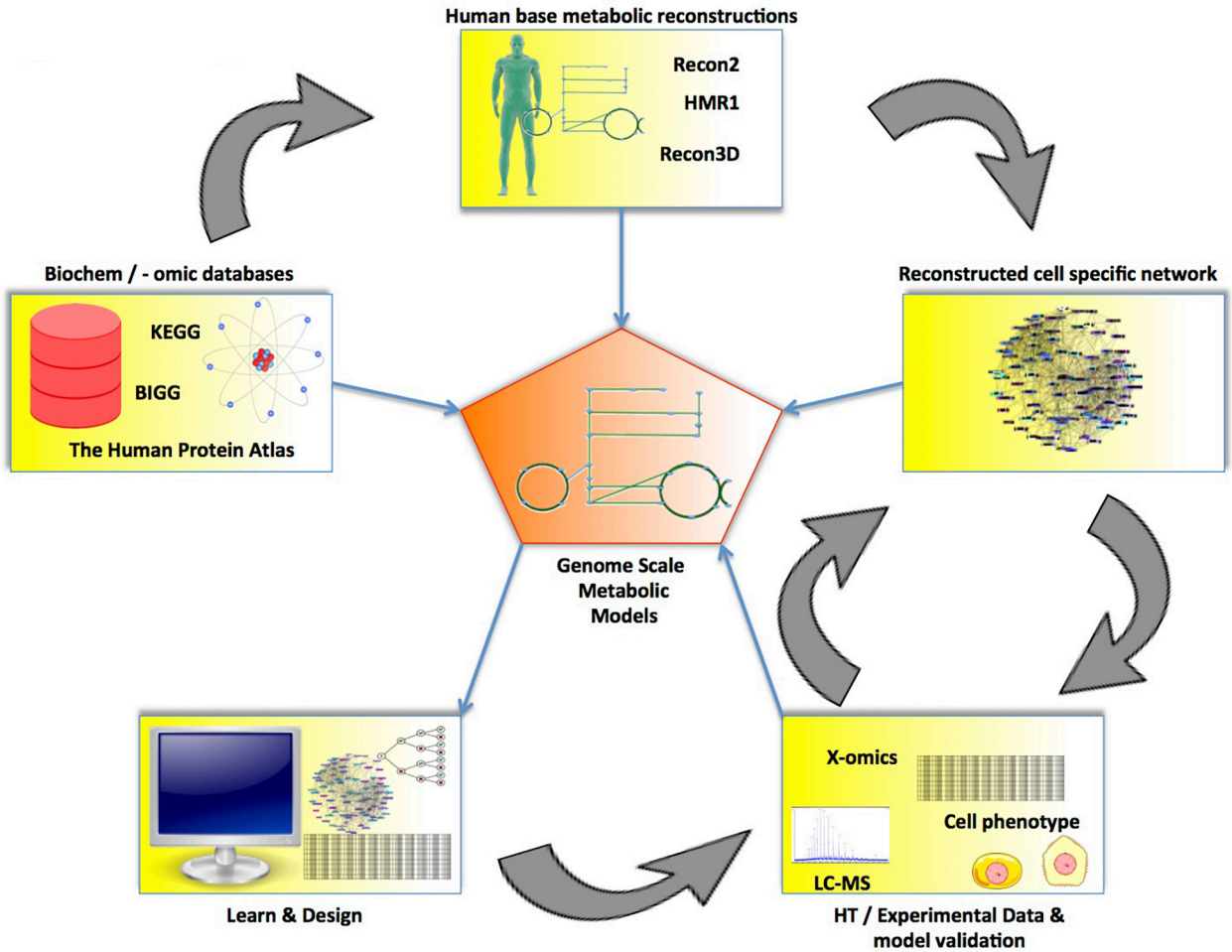

FIGURE 7 | The process of reconstructing a genome-scale metabolic model (GEM). Using a base human metabolic reconstruction along with experimental data and biochemical databases (e.g., KEGG or BiGG), a constraint-based model can be created. From this model, a GEM is derived, from which cellular functions can be studied. Newly acquired knowledge from the GEM can be used to create cell experiments to further validate or improve the model. The validated GEMs can then be used to further study cells for use in regenerative medicine.

to inform personalization of medicine, for example by predicting potential genetic markers of a successful MSC donor.

Existing Human Models

Genome Annotation Efforts Led to the First Human Metabolic Reconstructions

Various community-driven efforts have led to several reconstructions of the global human metabolic network (Romero et al., 2004; Duarte et al., 2007; Ma et al., 2007; Agren et al., 2012; Thiele et al., 2013; Mardinoglu et al., 2014). Compiling data on all reactions that have been linked to genes annotated in the human genome from various databasesas having metabolic activity is a substantial task, and important to the quality of subsequent work (Kanehisa et al., 2016; Norsigian et al., 2020). This production of annotated human genomes allowed, for the first time, metabolic networks that cover the entire human metabolic repertoire to be produced. Between 2005 and 2012, the first four human metabolic reconstructions were produced; humanCyc (Romero et al., 2004), Recon1 (Duarte et al., 2007), Edinburgh Human Metabolic Network (EHMN) (Ma et al., 2007), and Human Metabolic Reconstruction (HMR) (Agren et al., 2012). Each of these networks expanded on the previous work, including more reactions and better links between reactions and genes, allowing for improved analysis of expression data. Further improvements were made in Recon2 (Thiele et al., 2013) and HMR2 (Mardinoglu et al., 2014) and their updates (Smallbone et al., 2013; Quek et al., 2014; Sahoo et al., 2014, 2015; Swainston et al., 2016). By expanding the extent of the reaction coverage, increasing the detail of the available gene-to-reaction links, and placing more emphasis on the inclusion of good thermodynamic and stoichiometric information, better possibilities for accurate simulations were afforded; thus, these models represent significant steps forward. In addition, tools such as PathwayBooster and Path2Models have allowed the utilization of data bases such as KEGG in the automated reconstruction of new or custom built networks.

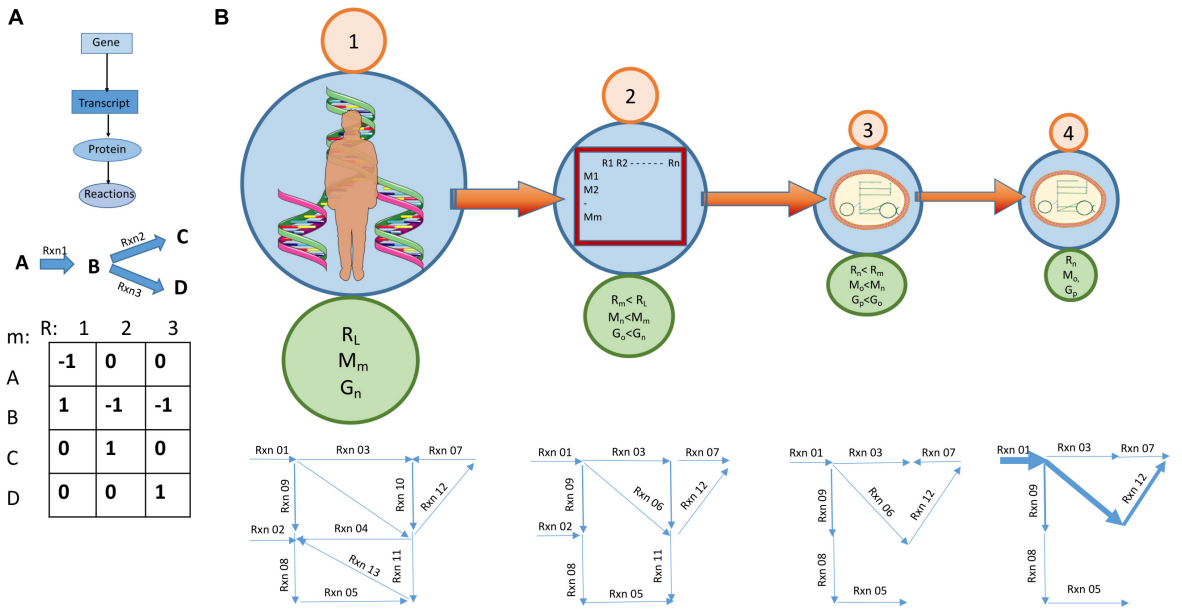

FIGURE 8 | Going from a large base model to a cell specific GEM. **(A)** Genome scale metabolic models build on the gene-protein reaction association and represent a set of reactions as a matrix with linked genes. Synthesis of metabolites is designated by a positive number and breakdown with a negative number. **(B)** Going from a large base model to a cell/condition specific model. (1) A relevant base model is chosen. This model is a summary of known metabolic reactions and forms a species specific metabolic reconstruction. This base model usually has the highest count of genes, reactions and metabolites. (2) A process aiming at reducing the size of the model starts. By considering biochemical and biophysical constraints, e.g., thermodynamic feasibility, some reactions stop being reversable and the reconstruction becomes a model. Other constraints applied at this stage relate to stoiciometricity and enzyme capacity. The number of genes, reactions and metabolites is reduced. (3) Data about transcripts and proteins present in a cell type and the availability of nutrients in medium lead to the removal of yet more reactions. A cell specific model is created. (4) Metabolomic data specific to the condition the cell is supposed to represent allows the magnitude of reactions to be predicted. Some will have higher flux rates than others. More reactions may be removed at this stage. The model now becomes condition specific.

The Latest Human Metabolic Reconstructions Contain New Dimensions of Information

Recon3D is the latest update of the Recon family of human metabolic network reconstructions (Brunk et al., 2018). The key novel attribute of this reconstruction is that it includes information regarding protein and metabolite structures. In addition, the number of reactions included in the reconstruction has almost doubled from the previous version, to 13,453 total reactions. The inclusion of three-dimensional (3D) structural information has allowed Recon3D to be used to show that deleterious mutations map to specific areas of the genome. By using this information, improved predictions of cancer-related mutations may be made compared to previous Recon models, which include a less detailed mapping of genes. The 3D aspect of the protein and metabolite information in Recon3D has also been used to investigate the metabolic effects of various drugs; this analysis revealed that drug effect signatures often contained disparate functional domains and metabolites, indicating that many drug effects are due to compensatory downstream metabolic effects (Brunk et al., 2018). Recon3D has been constructed in such a way as to allow for integration with the AGORA platform for modeling the gut microbiome by using a consistent set of identifiers (Magúsdóttir et al., 2017). As it becomes increasingly clear that the microbiome plays an important part in human health, being able to include cometabolism by human and microbial cells is a very useful feature (Magúsdóttir et al., 2017). A global network reconstruction can then provide the starting point for the production of tissue-, cell-, or condition-specific GEMs.

Current State-of-the-Art Applications

Generic Human Metabolic Reconstructions Can Be Analyzed to Gain General Metabolic Insights

A base GEM may be utilized to produce general predictions about whole human metabolism, providing useful insights into both human health and predictions of currently unknown human metabolic functions.

The various human models have been used to predict biomarkers for inborn errors of metabolism (the accuracy of previous predictions feeds into improving these models) (Kell and Goodacre, 2014). Inborn errors of metabolism (IEMs) are a collection of hereditary metabolic defects found in most of the main human metabolic pathways. These defects are usually screened for in infants by way of biofluid metabolomics (i.e., metabolomics analysis of either dried blood samples or urine). Early recognition and treatment of IEMs is very important. The current method detects specific biomarkers that have altered concentrations due to known genomic mutations. Identifying good biomarkers is key to successful early diagnosis. With the advent of the human metabolism genome-scale network model, a novel computational approach was developed that could systematically predict altered or affected metabolic biomarkers.

This possible use of GEMs has the potential to extend the information that can be inferred from the data, enabling accurate diagnosis for each individual patient, further insight of hot spots in human metabolism with respect to IEMs, and discovery of novel IEMs (expanding the range of disease-associated metabolites). By making use of the GEM, gene-protein-reaction (GPR) metabolic pathways relevant to a specific genotype-phenotype pair can become more feasible, meaning that disease-specific biological insights can be derived (Shlomi et al., 2009; Sahoo et al., 2012; Mandal et al., 2018; Mussap et al., 2018).

By analyzing reactions in Recon1 that were defined as being present due to genome annotation or literature data, but that were not predicted to be active, and then adding surrounding reactions to activate them, predictions have been made about previously unknown human metabolic functions such as that of iduronic acid following glycan degradation, N-acetylglutamate in amino acid metabolism, and the human activity of gluconokinase (Rolfsson et al., 2011; Paglia et al., 2016). Such information will improve future metabolic studies both computationally and in the laboratory.

Reconstructions can be made specific by integrating -omics data

Once a base GEM has been selected, there are a variety of methods available to make the model specific to a particular cell type and circumstance by integrating transcriptomic, proteomic, and metabolomics data. These context-specific models are able to provide more detailed insights into human metabolism in a particular cell type, and comparison of models is particularly useful. Previous context-specific human models have produced useful insights into healthy and diseased metabolism.

A cell's metabolic capabilities are defined by which enzymes it expresses. Transcriptomic and proteomic data provide information about the enzymes expressed under certain circumstances. Both of these data types correlate to enzyme activity, although not perfectly (Munir and McGettrick, 2015; Ibraheim et al., 2018). Several methods to prune a GEM based on expression data, mostly transcriptomics, have been developed. Although there are numerous technical differences, all seek to balance the retention of reactions known to be or likely to be present in a particular cell type, based on expression data or prior knowledge, while removing extraneous reactions. GIMME (Moreira et al., 2017), iMAT and INIT (Antonitsis et al., 2008; Vigo et al., 2019), and MBA, Fastcore, and mCADRE (Ullah et al., 2015; Archambault et al., 2017; Fitzsimmons et al., 2018) are all commonly used (Rosenbaum et al., 2008; Neman et al., 2012).

Another way to make models more context specific is to use metabolomic data collected by mass spectrometry or NMR to constrain what the model takes up or secretes to realistic values. By either measuring changes in the concentration of various metabolites in the medium over time or by comparing the relative values of metabolites at different times, the rate of uptake or secretion of a range of metabolites is determined. These rates can be applied to the model as additional constraints that will restrict the model predictions to those consistent with the metabolic dataset (Bordbar et al., 2017). These additional constraints help to predict different sets of active and inactive intracellular reactions based on extracellular data. This process may follow a protocol such as Metabotools. This protocol has been used to obtain metabolic insights into the metabolic differences between different leukemic cell lines (Aurich et al., 2015, 2016; von Bomhard et al., 2016).

Models can also be used to analyze isotope labeling data and this data can, in turn, contribute better constraints to improve the model. Cells may be fed on medium containing glucose or glutamine labeled with heavy isotopes of carbon or nitrogen. The proportions of various metabolites labeled with these heavy isotopes in cells that are sampled and analyzed at different time points after this treatment allows inferences to be made about the production of the labeled metabolites. Sholmi et al. used this technique to elucidate the differences in the TCA cycle during the cell cycle. Further information may be obtained if the cells are fractionated into different organelles before analysis (Ahn et al., 2017). For example, the subcellular localization of glutamine metabolism in cancer has been elucidated using this technique (Lee et al., 2019).

Using the model building algorithm (MBA) (Jerby et al., 2010), which generates tissue-specific models, a focused model for cancer metabolism has been created containing a core set of reactions known to be common for 60 variant cancer cell lines. Using this model and the knowledge that uncontrolled cell growth and altered metabolism are characterizing hallmarks for cancer cells, it was possible to identify two different types of drug targets (Hanahan and Weinberg, 2011; Dougherty et al., 2017). The first target type was growth-supporting genes (found via *in silico* gene deletion screens) that resulted in identification of 52 metabolic drug targets; 8 of these currently correspond to cancer therapeutics. In addition, a set of genes were identified in the healthy cell model network that were downregulated in the cancer model. By inhibiting the genes more highly expressed in cancer cells, targeting could be achieved (Dougherty et al., 2017).

More specific cancer models have also been produced. For example, a model has been created for hepatocellular carcinoma by Agren et al. (2014). They evaluated the presence of proteins in 27 patients and from that reconstructed personalized GEMs for six. These reconstructions were then used to identify anticancer drugs by observing the inhibition of reactions around each metabolite in a network and the subsequent effects on cellular growth within the models. By conceptualizing drugs as structural analogs to metabolites, and so capable of interfering with target enzymes and enzymatic activity, 101 antimetabolites were predicted as possible drug targets (Agren et al., 2014). Similar approaches have been applied to breast cancer undergoing epithelial-to-mesenchymal transition in order to identify targets to reduce this pro-metastatic process (Halldorsson et al., 2017).

Comparing Models of Cells in Different Circumstances Can Produce Useful Insights Into Metabolism

Many constraint-based metabolic analyses have historically relied upon an objective function, which is defined as a metabolic objective of a cell; flux through this reaction is either maximized or minimized to compute the flux state (i.e., pathway usage) across the entire network. For metabolic states that do not

have as well-defined objective functions as cancer does (i.e., gross cellular growth), algorithms that are able to create tissue- or cell-specific models without a specific objective function are needed. An algorithm often used for this purpose is the metabolic transformation algorithm (MTA) (Yizhak et al., 2013), an algorithm that uses GEMs to predict genetic perturbations that are able to shift a diseased metabolic state toward a healthy one. This algorithm has been used to determine reactions capable of shifting "old" muscle into "young" (providing potential targets that can help reducing metabolic shifts related to aging) and to determine key reactions that, when removed from a GEM modeling Alzheimer's disease, resulted in a network reconstruction more similar to that of a healthy state (Stempler et al., 2014; Wone et al., 2018).

Obesity has been addressed through the use of the human metabolic reconstruction by identifying pathways implicated in the disease process. As with many diseases, pinpointing a specific genetic or environmental marker as a cause for obesity, making the determination of progression, and deciding on a "treatment" a difficult task. Using the HMR and transcriptomic data from both healthy and obese individuals, a GEM with the objective function defined as acetyl-CoA production and formation of lipid droplets was produced. Through this analysis, two possible drug targets were identified by considering reactions with significantly changed flux values, and a potential biomarker for obesity was identified through reporter metabolites, which is an algorithm allowing the analysis of transcriptomic data in the light of the metabolic network structure to predict highly affected metabolites (Bordbar et al., 2011; Väremo et al., 2013; Levian et al., 2014; Dougherty et al., 2017).

Drug toxicity levels and side effects over both short and long periods of usage can also be identified in an easier and more cost-efficient manner using GEMs. It is possible to make predictions on system-wide perturbations using previously determined information on how protein structural analysis can be used to determine off-target binding of drugs, in combination with metabolic networks, as was done by Chang et al. (2010).

Metabolic Models Can Be Used to Uncover Changes Over Time

Biological systems often change dynamically over time. Analyzing how these changes occur can be challenging but is being addressed through the integration of time-course experimental data. One approach, dynamic flux balance analysis (dFBA) {ref 10.1016/j.celrep.2017.07.04}, integrates time-course measurements of the major inputs and outputs of the system to provide more accurate flux predictions. dFBA provides a continuous prediction based on these changing inputs and outputs (e.g., end products of pathways). This method has been applied to murine embryonic stem cells and revealed changes to mitochondrial metabolism and one carbon metabolism during priming (Shen et al., 2019). more recently, time-course -omic measurements have been integrated with metabolic models. One such method, unsteady-state flux balance analysis (uFBA), integrates absolutely quantified time-course metabolomic data to model cellular dynamics. uFBA was used to explore how temporal dynamics impact the cellular metabolism of stored red blood cells, which led to the proposal of better storage solutions that could potentially increase the storage time and quality of this key medical product. Such methods may be applied to other cell types and phenotypes in the future where dynamics play a key role. In MSCs, for example, key metabolic shifts that occur during trilineage differentiation may be examined and compared as a function of time.

A Metabolic Model of MSCs Has Already Predicted Better Ways to Expand MSC Cultures

A GEM of MSCs, iMSC1255, was recently created to improve understanding of the function of MSC metabolism. This model is based upon publicly available transcriptomic data sets from proliferating, early passage bone marrow MSCs. The data was used with the mCADRE algorithm to generate a tissue-specific version of the global human model Recon1, which was then manually curated by comparison to proteomic data and the literature to ensure that all desirable reactions were included to account for known MSC metabolic functions (Wang et al., 2012). Further metabolic constraints were added based on the composition of the commonly used medium alpha MEM, which meant that the modeled cells were able to take up metabolites known to be available in alpha MEM. This model was compared to previous models created with the same algorithm for adipose, bone marrow, and blood (using tissue-based, rather than cell-based, models). These previous models were shown to be less specific than iMSC1255. iMSC1255 was also shown to be able to produce amino acid uptake and secretion and growth rate predictions consistent with data available in the literature (Fouladiha et al., 2015).

iMSC1255 has subsequently been used to computationally predict metabolic interventions to optimize proliferation and chondrogenic differentiation of MSCs. By analyzing the maximum growth rate predicted FBA with and without allowing the uptake of a range of nutrients, it was proposed that supplementing the MSC medium with the phospholipids phosphoethanolamine and phosphoserine would improve proliferation. This was confirmed experimentally (Fouladiha et al., 2018). This paper also describes how MTA was used along with transcriptomic data from chondrocytes to determine likely metabolic changes during chondrocyte differentiation. This analysis suggested that mitochondrial transport reactions are key to chondrocyte differentiation, a finding that has yet to be experimentally confirmed. Further, the authors also examined the effects of hypoxia on proliferating MSCs by assessing the range of possible metabolic activities when the models use different levels of oxygen and glucose availability. The predicted metabolic changes to lactate and glucose uptake and secretion, G6P isomerase, and pyruvate transport were generally correct, with the exception of superoxide dismutase, according to the literature (Fouladiha et al., 2018). This study showed that a model of MSC metabolism can provide useful insights into their proliferation under different circumstances. This will allow the optimization of MSC growth that may be useful for large scale production of MSC-based therapeutics. Follow-up work has begun to examine the potential of GEMs to predict changes necessary for successful differentiation (Fouladiha et al., 2018).

By expanding upon such techniques, including by using models constrained with metabolic data from differentiating cells, this can be built upon.

LOOKING AHEAD

Since 2007, when the very first global GEM for humans was reconstructed (Duarte et al., 2007), researchers have been exploring the clinical application possibilities of GEMs. Some of the possible ways GEMs can be of use in furthering the clinical application of cell-based medicine include: (1) trials with *in silico* metabolic engineering (gene knock-outs and knock-ins); (2) identifying biomarkers of diseases; (3) predicting drug targets and therapeutic windows; and (4) optimization of cellular functions without the cost of wet lab experimentation. Some success has already been reported, as mentioned in section "Current State-of-the-Art Applications."

Manipulation of the Metabolic State

Building on the various uses of existing cell- or tissue-specific human GEMs and the most up-to-date version of the human reconstruction (Brunk et al., 2018), the potential use of GEMs to explore methods to maintain or manipulate a desired metabolic state for hMSCs (in order to provide a specific function or desired effect) has been the subject of work done by Fouladiha et al. They demonstrated the potential of GEMs to gain insight into how MSCs may be manipulated by means of nutrient supplementation (Fouladiha et al., 2018). By adding nutrients into the growth medium or manipulating oxygen concentration *in silico*, the number of experiments needed to optimize growth conditions may be reduced. This may be an interesting avenue to explore for each cell type and cell state, since different responses may be observed. Such testing is more feasible to explore *in silico* than *in vitro*. Even though time and money will have to be spent on reconstruction of the GEMs themselves, the savings in experimental time and material costs afforded by the use of validated reconstructions will likely outweigh these costs. Promising *in silico* outcomes can then be taken further, being validated or explored *in vitro* and later *in vivo*. Positive results would further validate the models and perhaps further that particular avenue of cell-based medicine or that particular use of the cells in regenerative medicine.

Exploration of Metabolic Differences

One potential use for GEMs would be to explore the different metabolic capacities of hMSCs from different sources. There have been some reports, albeit limited, explaining possible differences in the proliferative, differentiation, and immunomodulatory abilities of hMSCs isolated from various tissues (Liu et al., 2007; Hass et al., 2011; Secunda et al., 2015; Tachida et al., 2015). As hMSCs are isolated from disparate microenvironments, some with large differences in their surroundings, their optimal survival conditions and, possibly, utilization potential may differ. For example, by comparing models created using transcriptomics data from a study of MSCs from various sources such as ArrayExpress (EMBL-EBI, 2014; Athar et al., 2019) and then subjecting them to comparative flux analysis, different metabolic patterns may be discovered and linked to previously reported functional differences, such as the ability to form hematopoietic cells. Results could be verified or supplemented with data from independent proteomics experiments such as can be found via PRIDE Archive (Billing et al., 2016).

The creation and study of GEMs of MSCs undergoing each of the three classical differentiation (adipo-, osteo- and chondrogenic) could be approached in various ways. uFBA could be used as a framework to examine MSC metabolomics data collected at different timepoints during each of the differentiation lineages (Bordbar et al., 2017). The study of other stem cell types over time has already provided useful insights into differentiation from a transcriptional viewpoint. uFBA would allow a better understanding of the metabolic changes to be reached (Bordbar et al., 2017).

Experimental Cost Reduction via *in silico* Result Prediction

As expansion and differentiation of MSCs is a time-consuming and potentially expensive process, it would be desirable to be able to predict in advance the success of cells from a particular donor. For example, a signature pattern of gene features could be tested before donation. To this end, a model of successful and unsuccessful cells created with Recon3D could be used to analyze the genes relevant to an ideally differentiated model *in silico* (Strober et al., 2019). Single and combined gene deletion to find genes essential to each form of differentiation would be useful as a secondary way of finding a genetic signature for successful differentiation. This process could provide a means of reducing the necessary number of *in vitro* analyses.

It would also be desirable to confirm adequate differentiation by measuring a few metabolites before attempting implantation. The reporter metabolites algorithm (Çakır, 2015; Schultz and Qutub, 2016) applied to a model of well- differentiated MSCs would determine exometabolomic biomarkers that are indicative of successful levels of differentiation.

Multi-Cell Models

Community models or multi-cell models are another avenue to be explored as a potential use for GEMs to enhance the use of hMSCs in regenerative medicine. These models can provide insight into the metabolic functions of possible interacting organisms or the various cell types residing within the same organism (Levy and Borenstein, 2013; Dougherty et al., 2017). Given that hMSCs are intended to be integrated into a host system for clinical application (Han et al., 2012; Levy and Borenstein, 2013; Burke et al., 2016; Archambault et al., 2017; Goldberg et al., 2017; Moreira et al., 2017; Cunningham et al., 2018; Hu et al., 2018; Ibraheim et al., 2018; Solarte et al., 2018), this could provide useful insights.

Recently, more attention has been given to the hMSC secretome and its possible therapeutic effect; this might be well explored through the use of multi-cellular GEMs. The secretome of hMSCs might be manipulated via some of the previously mentioned methods, and the effect of composition changes on

the targeted organism, cell, and/or environment observed. This could help to find novel directions in which to expand the use of hMSCs in regenerative medicine.

Age Related Exploration

Yet another aspect that could more easily be explored through the use of GEMs covering hMSCs is the effect of donor age. This is not the same as cell senescence, but effects due to age have been observed in hMSCs lines through *in vitro* experiments (Choudhery et al., 2014; Narbonne, 2018). This appears in the way that cells are able to perform with regard to proliferation speed, differentiation ability, and immunomodulation. There have been numerous attempts to return functionality to stem cells from aged donors, with some degree of success (Neves et al., 2017). However, with the application of GEMs, the significant changes and the reasons behind them may be more systematically documented and attempts to return function performed in a more cost-effective and time-saving manner.

Overall, the use of GEMs to further the use of hMSCs in regenerative medicine is increasing, but, as of yet, is a relatively unexplored avenue that holds a lot of promise. We anticipate that *in silico* metabolic modeling will help to elucidate the differentiation process of hMSCs, ultimately providing crucial insights into novel therapies in the field of regenerative medicine.

AUTHOR CONTRIBUTIONS

ÞS and SM were the main authors of the manuscript. All additional authors (ÓR, JY, and ÓS) also contributed to the writing and editing of the manuscript.

FUNDING

This research was supported by the Icelandic Research Fund (grant number 217005) and by the Institute for Systems Biology's Translational Research Fellows Program (JY).

REFERENCES

Agathocleous, M., and Harris, W. A. (2013). Metabolism in physiological cell proliferation and differentiation. *Trends Cell Biol.* 23, 484–492. doi: 10.1016/j.tcb.2013.05.004

Agren, R., Bordel, S., Mardinoglu, A., Pornputtapong, N., Nookaew, I., and Nielsen, J. (2012). Reconstruction of genome-acale active metabolic networks for 69 human cell types and 16cancer types using INIT. *PLoS Comput. Biol.* 8:e1002518. doi: 10.1371/journal.pcbi.1002518

Agren, R., Mardinoglu, A., Asplund, A., Kampf, C., Uhlen, M., and Nielsen, J. (2014). Identification of anticancer drugs for hepatocellular carcinoma through personalized genome-scale metabolic modeling. *Mol. Syst. Biol.* 10:721. doi: 10.1002/msb.145122

Ahn, E., Kumar, P., Mukha, D., Tzur, A., and Shlomi, T. (2017). Temporal fluxomics reveals oscillations in TCA cycle flux throughout the mammalian cell cycle. *Mol. Syst. Biol.* 13:953. doi: 10.15252/msb.20177763

Alberts, B., Bray, D., Hopkin, K., Johnson, A., Lewis, J., Raff, M., et al. (2014). "Chapter 13: how cells obtain energy from food," in *Essential Cell Biology*, ed. K. Mesa (New York, NY: Garland Science), 419–437.

Amorin, B., Alegretti, A. P., Valim, V., Pezzi, A., Laureano, A. M., da Silva, M. A. L., et al. (2014). Mesenchymal stem cell therapy and acute graft-versus-host disease: a review. *Hum. Cell* 27, 137–150. doi: 10.1007/s13577-014-0095-x

Antonitsis, P., Ioannidou-Papagiannaki, E., Kaidoglou, A., Charokopos, N., Kalogeridis, A., Kouzi-Koliakou, K., et al. (2008). Cardiomyogenic potential of human adult bone marrow mesenchymal stem cells in vitro. *Thorac. Cardiovasc. Surg.* 56, 77–82. doi: 10.1055/s-2007-989328

Araujo, J. A., Zhang, M., and Yin, F. (2012). Heme oxygenase-1, oxidation, inflammation, and atherosclerosis. *Front. Pharmacol.* 3:119. doi: 10.3389/fphar.2012.00119

Archambault, J., Moreira, A., McDaniel, D., Winter, L., Sun, L., and Hornsby, P. (2017). Therapeutic potential of mesenchymal stromal cells for hypoxic ischemic encephalopathy: a systematic review and meta-analysis of preclinical studies. *PLoS One* 12:e0189895. doi: 10.1371/journal.pone.0189895

Athar, A., Füllgrabe, A., George, N., Iqbal, H., Huerta, L., Ali, A., et al. (2019). ArrayExpress update - from bulk to single-cell expression data. *Nucleic Acids Res.* 47, D711–D715. doi: 10.1093/nar/gky964

Aurich, M. K., Fleming, R. M. T., and Thiele, I. (2016). MetaboTools: a comprehensive toolbox for analysis of genome-scale metabolic models. *Front. Physiol.* 7:327. doi: 10.3389/fphys.2016.00327

Aurich, M. K., Paglia, G., Rolfsson, Ó., Hrafnsdóttir, S., Magnúsdóttir, M., Stefaniak, M. M., et al. (2015). Prediction of intracellular metabolic states from extracellular metabolomic data. *Metabolomics* 11, 603–619. doi: 10.1007/s11306-014-0721-3

Baldari, S., Di Rocco, G., Piccoli, M., Pozzobon, M., Muraca, M., and Toietta, G. (2017). Challenges and strategies for improving the regenerative effects of mesenchymal stromal cell-based therapies. *Int. J. Mol. Sci.* 18:2087. doi: 10.3390/ijms18102087

Barbagallo, I., Vanella, A., Peterson, S. J., Kim, D. H., Tibullo, D., Giallongo, C., et al. (2010). Overexpression of heme oxygenase-1 increases human osteoblast stem cell differentiation. *J. Bone Miner. Metab.* 28, 276–288. doi: 10.1007/s00774-009-0134-y

Barkholt, L., Flory, E., Jekerle, V., Lucas-Samuel, S., Ahnert, P., Bisset, L., et al. (2013). Risk of tumorigenicity in mesenchymal stromal cell-based therapies–bridging scientific observations and regulatory viewpoints. *Cytotherapy* 15, 753–759. doi: 10.1016/j.jcyt.2013.03.005

Beegle, J., Lakatos, K., Kalomoiris, S., Stewart, H., Isseroff, R. R., Nolta, J. A., et al. (2015). Hypoxic preconditioning of mesenchymal stromal cells induces metabolic changes, enhances survival, and promotes cell retention in vivo. *Stem Cells* 33, 1818–1828. doi: 10.1002/stem.1976

Bernardo, M. E., and Fibbe, W. E. (2013). Mesenchymal stromal cells: sensors and switchers of inflammation. *Cell Stem Cell* 13, 392–402. doi: 10.1016/j.stem.2013.09.006

Bernardo, M. E., Zaffaroni, N., Novara, F., Cometa, A. M., Avanzini, M. A., Moretta, A., et al. (2007). Human bone marrow derived mesenchymal stem cells do not undergo transformation after long-term in vitro culture and do not exhibit telomere maintenance mechanisms. *Cancer Res.* 67, 9142–9149. doi: 10.1158/0008-5472.can-06-4690

Billing, A. M., Ben Hamidane, H., Dib, S. S., Cotton, R. J., Bhagwat, A. M., Kumar, P., et al. (2016). Comprehensive transcriptomic and proteomic characterization of human mesenchymal stem cells reveals source specific cellular markers. *Sci. Rep.* 6:21507. doi: 10.1038/srep21507

Björnson, E., Borén, J., and Mardinoglu, A. (2016). Personalized cardiovascular disease prediction and treatment—a review of existing strategies and novel systems medicine tools. *Front. Physiol.* 7:2. doi: 10.3389/fphys.2016.00002

Blais, M., Parenteau-Bareil, R., Cadau, S., and Berthod, F. (2013). Concise review: tissue-engineered skin and nerve regeneration in burn treatment. *Stem Cells Transl. Med.* 2, 545–551. doi: 10.5966/sctm.2012-0181

Blanco, B., Herrero-Sánchez, M. D. C., Rodríguez-Serrano, C., García-Martínez, M. L., Blanco, J. F., Muntión, S., et al. (2016). Immunomodulatory effects of bone marrow versus adipose tissue-derived mesenchymal stromal cells on NK cells: implications in the transplantation setting. *Eur. J. Haematol.* 97, 528–537. doi: 10.1111/ejh.12765

Bloom, A. B., and Zaman, M. H. (2014). Influence of the microenvironment on cell fate determination and migration. *Physiol. Genomics* 46, 309–314. doi: 10.1152/physiolgenomics.00170.2013

Bonab, M. M., Sahraian, M. A., Aghsaie, A., Karvigh, S. A., Hosseinian, S. M., Nikbin, B., et al. (2012). Autologous mesenchymal stem cell therapy in progressive multiple sclerosis: an open label study. *Curr. Stem Cell Res. Ther.* 7, 407–414. doi: 10.2174/157488812804484648

Bordbar, A., Feist, A. M., Usaite-Black, R., Woodcock, J., Palsson, B. O., and Famili, I. (2011). A multi-tissue type genome-scale metabolic network for analysis of whole-body systems physiology. *BMC Syst. Biol.* 5:180. doi: 10.1186/1752-0509-5-180

Bordbar, A., Monk, J. M., King, Z. A., and Palsson, B. O. (2014). Constraint-based models predict metabolic and associated cellular functions. *Nat. Rev. Genet.* 15, 107–120. doi: 10.1038/nrg3643

Bordbar, A., Yurkovich, J. T., Paglia, G., Rolfsson, O., Sigurjónsson, Ó. E., and Palsson, B. O. (2017). Elucidating dynamic metabolic physiology through network integration of quantitative time-course metabolomics. *Sci. Rep.* 7:46249. doi: 10.1038/srep46249

Bortolotti, F., Ukovich, L., Razban, V., Martinelli, V., Ruozi, G., Pelos, B., et al. (2015). In vivo therapeutic potential of mesenchymal stromal cells depends on the source and the isolation procedure. *Stem Cell Rep.* 4, 332–339. doi: 10.1016/j.stemcr.2015.01.001

Brunk, E., Sahoo, S., Zielinski, D. C., Altunkaya, A., Dräger, A., Mih, N., et al. (2018). Recon3D enables a three-dimensional view of gene variation in human metabolism. *Nat. Biotechnol.* 36, 272–281. doi: 10.1038/nbt.4072

Buravkova, L. B., Rylova, Y. V., Andreeva, E. R., Kulikov, A. V., Pogodina, M. V., Zhivotovsky, B., et al. (2013). Low ATP level is sufficient to maintain the uncommitted state of multipotent mesenchymal stem cells. *Biochim. Biophys. Acta* 1830, 4418–4425. doi: 10.1016/j.bbagen.2013.05.029

Burke, J., Hunter, M., Kolhe, R., Isales, C., Hamrick, M., and Fulzele, S. (2016). Therapeutic potential of mesenchymal stem cell based therapy for osteoarthritis. *Clin. Transl. Med.* 5:27. doi: 10.1186/s40169-016-0112-7

Çakır, T. (2015). Reporter pathway analysis from transcriptome data: metabolite-centric versus reaction-centric approach. *Sci. Rep.* 5:14563. doi: 10.1038/srep14563

Campana, V., Milano, G., Pagano, E., Barba, M., Cicione, C., Salonna, G., et al. (2014). Bone substitutes in orthopaedic surgery: from basic science to clinical practice. *J. Mater. Sci. Mater. Med.* 25, 2445–2461. doi: 10.1007/s10856-014-5240-2

Chang, R. L., Xie, L., Xie, L., Bourne, P. E., and Palsson, B. Ø. (2010). Drug off-target effects predicted using structural analysis in the context of a metabolic network model. *PLoS Comput. Biol.* 6:e1000938. doi: 10.1371/journal.pcbi.1000938

Chen, C.-T., Shih, Y.-R. V., Kuo, T. K., Lee, O. K., and Wei, Y.-H. (2008). Coordinated changes of mitochondrial biogenesis and antioxidant enzymes during osteogenic differentiation of human mesenchymal stem cells. *Stem Cells* 26, 960–968. doi: 10.1634/stemcells.2007-0509

Cho, K.-A., Ju, S.-Y., Cho, S. J., Jung, Y.-J., Woo, S.-Y., Seoh, J.-Y., et al. (2009). Mesenchymal stem cells showed the highest potential for the regeneration of injured liver tissue compared with other subpopulations of the bone marrow. *Cell Biol. Int.* 33, 772–777. doi: 10.1016/j.cellbi.2009.04.023

Choudhery, M. S., Badowski, M., Muise, A., Pierce, J., and Harris, D. T. (2014). Donor age negatively impacts adipose tissue-derived mesenchymal stem cell expansion and differentiation. *J. Transl. Med.* 12:8. doi: 10.1186/1479-5876-12-8

Croitoru-Lamoury, J., Lamoury, F. M. J., Caristo, M., Suzuki, K., Walker, D., Takikawa, O., et al. (2011). Interferon-γ regulates the proliferation and differentiation of mesenchymal stem cells via activation of indoleamine 2,3 dioxygenase (IDO). *PLoS One* 6:e14698. doi: 10.1371/journal.pone.0014698

Cunningham, C. J., Redondo-Castro, E., and Allan, S. M. (2018). The therapeutic potential of the mesenchymal stem cell secretome in ischaemic stroke. *J. Cereb. Blood Flow Metab.* 38, 1276–1292. doi: 10.1177/0271678X18776802

De Becker, A., and Riet, I. V. (2016). Homing and migration of mesenchymal stromal cells: how to improve the efficacy of cell therapy? *World J. Stem Cells* 8, 73–87. doi: 10.4252/wjsc.v8.i3.73

Deng, W., Han, Q., Liao, L., You, S., Deng, H., and Zhao, R. C. H. (2005). Effects of allogeneic bone marrow-derived mesenchymal stem cells on T and B lymphocytes from BXSB mice. *DNA Cell Biol.* 24, 458–463. doi: 10.1089/dna.2005.24.458

dos Santos, F., Andrade, P. Z., Boura, J. S., Abecasis, M. M., da Silva, C. L., and Cabral, J. M. S. (2010). Ex vivo expansion of human mesenchymal stem cells: a more effective cell proliferation kinetics and metabolism under hypoxia. *J. Cell. Physiol.* 223, 27–35. doi: 10.1002/jcp.21987

Dougherty, B. V., Moutinho, T. J., and Papin, J. (2017). "Accelerating the drug development pipeline with genome-scale metabolic network reconstructions," in *Systems Biology*, eds J. Nielsen and S. Hohmann (Hoboken, NJ: John Wiley & Sons, Ltd), 139–162. doi: 10.1002/9783527696130.ch5

Duarte, N. C., Becker, S. A., Jamshidi, N., Thiele, I., Mo, M. L., Vo, T. D., et al. (2007). Global reconstruction of the human metabolic network based on genomic and bibliomic data. *Proc. Natl. Acad. Sci. U.S.A.* 104, 1777–1782. doi: 10.1073/pnas.0610772104

Duijvestein, M., Vos, A. C. W., Roelofs, H., Wildenberg, M. E., Wendrich, B. B., Verspaget, H. W., et al. (2010). Autologous bone marrow-derived mesenchymal stromal cell treatment for refractory luminal Crohn's disease: results of a phase I study. *Gut* 59, 1662–1669. doi: 10.1136/gut.2010.215152

El Refaey, M., Watkins, C. P., Kennedy, E. J., Chang, A., Zhong, Q., Ding, K.-H., et al. (2015). Oxidation of the aromatic amino acids tryptophan and tyrosine disrupts their anabolic effects on bone marrow mesenchymal stem cells. *Mol. Cell. Endocrinol.* 410, 87–96. doi: 10.1016/j.mce.2015.01.034

EMBL-EBI (2014). *Array Express: E-GEOD-57151 - Epigenetic and In Vivo Comparison of Diverse Mesenchymal Stromal Cell Sources Reveals an Endochondral Signature for Human Hematopoietic Niche Formation*. Hinxton: European Bioinformatics Institute.

Estrada, J. C., Albo, C., Benguría, A., Dopazo, A., López-Romero, P., Carrera-Quintanar, L., et al. (2012). Culture of human mesenchymal stem cells at low oxygen tension improves growth and genetic stability by activating glycolysis. *Cell Death Differ.* 19, 743–755. doi: 10.1038/cdd.2011.172

Feist, A. M., Herrgard, M. J., Thiele, I., Reed, J. L., and Palsson, B. O. (2009). Reconstruction of biochemical networks in microbial organisms (supplementary table 1). *Nat. Rev. Microbiol.* 7, 129–143. doi: 10.1038/nrmicro1949

Fitzsimmons, R. E. B., Mazurek, M. S., Soos, A., and Simmons, C. A. (2018). Mesenchymal stromal/stem cells in regenerative medicine and tissue engineering. *Stem Cells Int.* 2018:8031718. doi: 10.1155/2018/8031718

Forrester, S. J., Kikuchi, D. S., Hernandes, M. S., Xu, Q., and Griendling, K. K. (2018). Reactive oxygen species in metabolic and inflammatory signaling. *Circ. Res.* 122, 877–902. doi: 10.1161/CIRCRESAHA.117.311401

Fouladiha, H., Marashi, S.-A., and Shokrgozar, M. A. (2015). Reconstruction and validation of a constraint-based metabolic network model for bone marrow-derived mesenchymal stem cells. *Cell Prolif.* 48, 475–485. doi: 10.1111/cpr.12197

Fouladiha, H., Marashi, S.-A., Shokrgozar, M. A., Farokhi, M., and Atashi, A. (2018). Applications of a metabolic network model of mesenchymal stem cells for controlling cell proliferation and differentiation. *Cytotechnology* 70, 331–338. doi: 10.1007/s10616-017-0148-6

François, M., Copland, I. B., Yuan, S., Romieu-Mourez, R., Waller, E. K., and Galipeau, J. (2012). Cryopreserved mesenchymal stromal cells display impaired immunosuppressive properties as a result of heat-shock response and impaired interferon-γ licensing. *Cytotherapy* 14, 147–152. doi: 10.3109/14653249.2011.623691

Galli, D., Vitale, M., and Vaccarezza, M. (2014). Bone marrow-derived mesenchymal cell differentiation toward myogenic lineages: facts and perspectives. *Biomed Res. Int.* 2014:762695. doi: 10.1155/2014/762695

Gao, F., Chiu, S. M., Motan, D. A. L., Zhang, Z., Chen, L., Ji, H.-L., et al. (2016). Mesenchymal stem cells and immunomodulation: current status and future prospects. *Cell Death Dis.* 7:e2062. doi: 10.1038/cddis.2015.327

Gaspar, J. M., and Velloso, L. A. (2018). Hypoxia inducible factor as a central regulator of metabolism – implications for the development of obesity. *Front. Neurosci.* 12:813. doi: 10.3389/fnins.2018.00813

Gazit, Z., Pelled, G., Sheyn, D., Kimelman, N., and Gazit, D. (2014). "Chapter 19 - mesenchymal stem cells," in *Essentials of Stem Cell Biology*, eds R. Lanza and A. Atala (Cambridge, MA: Academic Press), 255–266. doi: 10.1016/B978-0-12-409503-8.00019-6

Goldberg, A., Mitchell, K., Soans, J., Kim, L., and Zaidi, R. (2017). The use of mesenchymal stem cells for cartilage repair and regeneration: a systematic review. *J. Orthop. Surg. Res.* 12:39. doi: 10.1186/s13018-017-0534-y

Guo, X., Bai, Y., Zhang, L., Zhang, B., Zagidullin, N., Carvalho, K., et al. (2018). Cardiomyocyte differentiation of mesenchymal stem cells from bone marrow: new regulators and its implications. *Stem Cell Res. Ther.* 9:44. doi: 10.1186/s13287-018-0773-9

Halldorsson, S., Rohatgi, N., Magnusdottir, M., Choudhary, K. S., Gudjonsson, T., Knutsen, E., et al. (2017). Metabolic re-wiring of isogenic breast epithelial cell lines following epithelial to mesenchymal transition. *Cancer Lett.* 396, 117–129. doi: 10.1016/j.canlet.2017.03.019

Han, Z., Jing, Y., Zhang, S., Liu, Y., Shi, Y., and Wei, L. (2012). The role of immunosuppression of mesenchymal stem cells in tissue repair and tumor growth. *Cell Biosci.* 2:8. doi: 10.1186/2045-3701-2-8

Hanahan, D., and Weinberg, R. A. (2011). Hallmarks of cancer: the next generation. *Cell* 144, 646–674. doi: 10.1016/j.cell.2011.02.013

Hass, R., Kasper, C., Böhm, S., and Jacobs, R. (2011). Different populations and sources of human mesenchymal stem cells (MSC): a comparison of adult and neonatal tissue-derived MSC. *Cell Commun. Signal.* 9:12. doi: 10.1186/1478-811X-9-12

Henry, C. S., DeJongh, M., Best, A. A., Frybarger, P. M., Linsay, B., and Stevens, R. L. (2010). High-throughput generation, optimization and analysis of genome-scale metabolic models. *Nat. Biotechnol.* 28, 977–982. doi: 10.1038/nbt.1672

Hofer, H. R., and Tuan, R. S. (2016). Secreted trophic factors of mesenchymal stem cells support neurovascular and musculoskeletal therapies. *Stem Cell Res. Ther.* 7:131. doi: 10.1186/s13287-016-0394-0

Hu, L., Yin, C., Zhao, F., Ali, A., Ma, J., and Qian, A. (2018). Mesenchymal stem cells: cell fate decision to osteoblast or adipocyte and application in osteoporosis treatment. *Int. J. Mol. Sci.* 19:360. doi: 10.3390/ijms19020360

Ibraheim, H., Giacomini, C., Kassam, Z., Dazzi, F., and Powell, N. (2018). Advances in mesenchymal stromal cell therapy in the management of Crohn's disease. *Expert Rev. Gastroenterol. Hepatol.* 12, 141–153. doi: 10.1080/17474124.2018.1393332

Ivanova-Todorova, E., Bochev, I., Mourdjeva, M., Dimitrov, R., Bukarev, D., Kyurkchiev, S., et al. (2009). Adipose tissue-derived mesenchymal stem cells are more potent suppressors of dendritic cells differentiation compared to bone marrow-derived mesenchymal stem cells. *Immunol. Lett.* 126, 37–42. doi: 10.1016/j.imlet.2009.07.010

James, A. W. (2013). Review of signaling pathways governing MSC osteogenic and adipogenic differentiation. *Scientifica* 2013:684736. doi: 10.1155/2013/684736

Jerby, L., Shlomi, T., and Ruppin, E. (2010). Computational reconstruction of tissue-specific metabolic models: application to human liver metabolism. *Mol. Syst. Biol.* 6:401. doi: 10.1038/msb.2010.56

Kanehisa, M., Sato, Y., Kawashima, M., Furumichi, M., and Tanabe, M. (2016). KEGG as a reference resource for gene and protein annotation. *Nucleic Acids Res.* 44, D457–D462. doi: 10.1093/nar/gkv1070

Kaundal, U., Bagai, U., and Rakha, A. (2018). Immunomodulatory plasticity of mesenchymal stem cells: a potential key to successful solid organ transplantation. *J. Transl. Med.* 16:31. doi: 10.1186/s12967-018-1403-0

Kell, D. B., and Goodacre, R. (2014). Metabolomics and systems pharmacology: why and how to model the human metabolic network for drug discovery. *Drug Discov. Today* 19, 171–182. doi: 10.1016/j.drudis.2013.07.014

Lan, Z., Ge, W., Arp, J., Jiang, J., Liu, W., Gordon, D., et al. (2010). Induction of kidney allograft tolerance by soluble CD83 associated with prevalence of tolerogenic dendritic cells and indoleamine 2,3-dioxygenase. *Transplantation* 90, 1286–1293. doi: 10.1097/TP.0b013e3182007bbf

Lee, S. H. (2018). The advantages and limitations of mesenchymal stem cells in clinical application for treating human diseases. *Osteoporos. Sarcopenia* 4:150. doi: 10.1016/j.afos.2018.11.083

Lee, W. D., Mukha, D., Aizenshtein, E., and Shlomi, T. (2019). Spatial-fluxomics provides a subcellular-compartmentalized view of reductive glutamine metabolism in cancer cells. *Nat. Commun.* 10:1351. doi: 10.1038/s41467-019-09352-1

Levian, C., Ruiz, E., and Yang, X. (2014). The pathogenesis of obesity from a genomic and systems biology perspective. *Yale J. Biol. Med.* 87, 113–126.

Levy, R., and Borenstein, E. (2013). Metabolic modeling of species interaction in the human microbiome elucidates community-level assembly rules. *Proc. Natl. Acad. Sci. U.S.A.* 110, 12804–12809. doi: 10.1073/pnas.1300926110

Li, J., and Dong, S. (2016). The signaling pathways involved in chondrocyte differentiation and hypertrophic differentiation. *Stem Cells Int.* 2016:2470351. doi: 10.1155/2016/2470351

Li, L., Chen, X., Wang, W. E., and Zeng, C. (2016). How to improve the survival of transplanted mesenchymal stem cell in ischemic heart? *Stem Cells Int.* 2016:9682757. doi: 10.1155/2016/9682757

Li, Q., Gao, Z., Chen, Y., and Guan, M.-X. (2017). The role of mitochondria in osteogenic, adipogenic and chondrogenic differentiation of mesenchymal stem cells. *Protein Cell* 8, 439–445. doi: 10.1007/s13238-017-0385-7

Lin, C.-S., Xin, Z.-C., Dai, J., and Lue, T. F. (2013). Commonly used mesenchymal stem cell markers and tracking labels: limitations and challenges. *Histol. Histopathol.* 28, 1109–1116. doi: 10.14670/HH-28.1109

Liu, T. M., Martina, M., Hutmacher, D. W., Hui, J. H. P., Lee, E. H., and Lim, B. (2007). Identification of common pathways mediating differentiation of bone marrow- and adipose tissue-derived human mesenchymal stem cells into three mesenchymal lineages. *Stem Cells* 25, 750–760. doi: 10.1634/stemcells.2006-0394

Liu, Y., Yuan, X., Muñoz, N., Logan, T. M., and Ma, T. (2019). Commitment to aerobic glycolysis sustains immunosuppression of human mesenchymal stem cells. *Stem Cells Transl. Med.* 8, 93–106. doi: 10.1002/sctm.18-0070

Lonner, J. H., Hershman, S., Mont, M., and Lotke, P. A. (2000). Total knee arthroplasty in patients 40 years of age and younger with osteoarthritis. *Clin. Orthop. Relat. Res.* 380, 85–90. doi: 10.1097/00003086-200011000-00012

Lukomska, B., Stanaszek, L., Zuba-Surma, E., Legosz, P., Sarzynska, S., and Drela, K. (2019). Challenges and controversies in human mesenchymal stem cell therapy. *Stem Cells Int.* 2019:9628536. doi: 10.1155/2019/9628536

Ma, H., Sorokin, A., Mazein, A., Selkov, A., Selkov, E., Demin, O., et al. (2007). The Edinburgh human metabolic network reconstruction and its functional analysis. *Mol. Syst. Biol.* 3:135. doi: 10.1038/msb4100177

Ma, O. K.-F., and Chan, K. H. (2016). Immunomodulation by mesenchymal stem cells: interplay between mesenchymal stem cells and regulatory lymphocytes. *World J. Stem Cells* 8, 268–278. doi: 10.4252/wjsc.v8.i9.268

Mackay, A. M., Beck, S. C., Murphy, J. M., Barry, F. P., Chichester, C. O., and Pittenger, M. F. (1998). Chondrogenic differentiation of cultured human mesenchymal stem cells from marrow. *Tissue Eng.* 4, 415–428. doi: 10.1089/ten.1998.4.415

Magúsdóttir, S., Heinken, A., Kutt, L., Ravcheev, D. A., Bauer, E., Noronha, A., et al. (2017). Generation of genome-scale metabolic reconstructions for 773 members of the human gut microbiota. *Nat. Biotechnol.* 35, 81–89. doi: 10.1038/nbt.3703

Mahla, R. S. (2016). Stem cells applications in regenerative medicine and disease therapeutics. *Int. J. Cell Biol.* 2016:6940283. doi: 10.1155/2016/6940283

Maienschein, J. (2011). Regenerative medicine's historical roots in regeneration, transplantation, and translation. *Dev. Biol.* 358, 278–284. doi: 10.1016/j.ydbio.2010.06.014

Mandal, R., Chamot, D., and Wishart, D. S. (2018). The role of the human metabolome database in inborn errors of metabolism. *J. Inherit. Metab. Dis.* 41, 329–336. doi: 10.1007/s10545-018-0137-8

Mardinoglu, A., Agren, R., Kampf, C., Asplund, A., Uhlen, M., and Nielsen, J. (2014). Genome-scale metabolic modelling of hepatocytes reveals serine deficiency in patients with non-alcoholic fatty liver disease. *Nat. Commun.* 5:3083. doi: 10.1038/ncomms4083

Mbongue, J. C., Nicholas, D. A., Torrez, T. W., Kim, N.-S., Firek, A. F., and Langridge, W. H. R. (2015). The role of indoleamine 2, 3-dioxygenase in immune suppression and autoimmunity. *Vaccines* 3, 703–729. doi: 10.3390/vaccines3030703

Meleshina, A. V., Dudenkova, V. V., Shirmanova, M. V., Shcheslavskiy, V. I., Becker, W., Bystrova, A. S., et al. (2016). Probing metabolic states of differentiating stem cells using two-photon FLIM. *Sci. Rep.* 6:21853. doi: 10.1038/srep21853

Meyer, J., Salamon, A., Mispagel, S., Kamp, G., and Peters, K. (2018). Energy metabolic capacities of human adipose-derived mesenchymal stromal cells in vitro and their adaptations in osteogenic and adipogenic differentiation. *Exp. Cell Res.* 370, 632–642. doi: 10.1016/j.yexcr.2018.07.028

Moreira, A., Kahlenberg, S., and Hornsby, P. (2017). Therapeutic potential of mesenchymal stem cells for diabetes. *J. Mol. Endocrinol.* 59, R109–R120. doi: 10.1530/JME-17-0117

Munir, H., and McGettrick, H. M. (2015). Mesenchymal stem cell therapy for autoimmune disease: risks and rewards. *Stem Cells Dev.* 24, 2091–2100. doi: 10.1089/scd.2015.0008

Muñoz, N., Kim, J., Liu, Y., Logan, T. M., and Ma, T. (2014). Gas chromatography–mass spectrometry analysis of human mesenchymal stem cell metabolism during proliferation and osteogenic differentiation under different oxygen tensions. *J. Biotechnol.* 169, 95–102. doi: 10.1016/j.jbiotec.2013.11.010

Muruganandan, S., Roman, A. A., and Sinal, C. J. (2009). Adipocyte differentiation of bone marrow-derived mesenchymal stem cells: cross talk with the osteoblastogenic program. *Cell. Mol. Life Sci.* 66, 236–253. doi: 10.1007/s00018-008-8429-z

Mussap, M., Zaffanello, M., and Fanos, V. (2018). Metabolomics: a challenge for detecting and monitoring inborn errors of metabolism. *Ann. Transl. Med.* 6:338. doi: 10.21037/atm.2018.09.18

Mylotte, L. A., Duffy, A. M., Murphy, M., O'Brien, T., Samali, A., Barry, F., et al. (2008). Metabolic flexibility permits mesenchymal stem cell survival in an ischemic environment. *Stem Cells* 26, 1325–1336. doi: 10.1634/stemcells.2007-1072

Narbonne, P. (2018). The effect of age on stem cell function and utility for therapy. *Cell Med.* 10:2155179018773756. doi: 10.1177/2155179018773756

Neman, J., Hambrecht, A., Cadry, C., and Jandial, R. (2012). Stem cell-mediated osteogenesis: therapeutic potential for bone tissue engineering. *Biologics* 6, 47–57. doi: 10.2147/BTT.S22407

Németh, K., Leelahavanichkul, A., Yuen, P. S. T., Mayer, B., Parmelee, A., Doi, K., et al. (2009). Bone marrow stromal cells attenuate sepsis via prostaglandin E(2)-dependent reprogramming of host macrophages to increase their interleukin-10 production. *Nat. Med.* 15, 42–49. doi: 10.1038/nm.1905

Neve, A., Corrado, A., and Cantatore, F. P. (2011). Osteoblast physiology in normal and pathological conditions. *Cell Tissue Res.* 343, 289–302. doi: 10.1007/s00441-010-1086-1

Neves, J., Sousa-Victor, P., and Jasper, H. (2017). Rejuvenating strategies for stem cell-based therapies in aging. *Cell Stem Cell* 20, 161–175. doi: 10.1016/j.stem.2017.01.008

Nombela-Arrieta, C., Ritz, J., and Silberstein, L. E. (2011). The elusive nature and function of mesenchymal stem cells. *Nat. Rev. Mol. Cell Biol.* 12, 126–131. doi: 10.1038/nrm3049

Norsigian, C. J., Pusarla, N., McConn, J. L., Yurkovich, J. T., Dräger, A., Palsson, B. O., et al. (2020). BiGG models 2020: multi-strain genome-scale models and expansion across the phylogenetic tree. *Nucleic Acids Res.* 48, D402–D406. doi: 10.1093/nar/gkz1054

Oberhardt, M. A., Palsson, B. Ø., and Papin, J. A. (2009). Applications of genome-scale metabolic reconstructions. *Mol. Syst. Biol.* 5:320. doi: 10.1038/msb.2009.77

Paglia, G., Sigurjónsson, Ó. E., Bordbar, A., Rolfsson, Ó., Magnusdottir, M., Palsson, S., et al. (2016). Metabolic fate of adenine in red blood cells during storage in SAGM solution. *Transfusion* 56, 2538–2547. doi: 10.1111/trf.13740

Pattappa, G., Heywood, H. K., de Bruijn, J. D., and Lee, D. A. (2011). The metabolism of human mesenchymal stem cells during proliferation and differentiation. *J. Cell. Physiol.* 226, 2562–2570. doi: 10.1002/jcp.22605

Qian, H., Yang, H., Xu, W., Yan, Y., Chen, Q., Zhu, W., et al. (2008). Bone marrow mesenchymal stem cells ameliorate rat acute renal failure by differentiation into renal tubular epithelial-like cells. *Int. J. Mol. Med.* 22, 325–332. doi: 10.3892/ijmm_00000026

Qin, J., Zhao, Y., Wang, Y., Betzler, C., Popp, F., Sen Gupta, A., et al. (2016). Therapeutic potential of mesenchymal stem cells in gastrointestinal cancers - current evidence. *Gastrointest. Cancer Targets Ther.* 2016, 41–47.

Quek, L.-E., Dietmair, S., Hanscho, M., Martínez, V. S., Borth, N., and Nielsen, L. K. (2014). Reducing recon 2 for steady-state flux analysis of HEK cell culture. *J. Biotechnol.* 184, 172–178. doi: 10.1016/j.jbiotec.2014.05.021

Reed, J. L., and Palsson, B. Ø. (2003). Thirteen years of building constraint-based in silico models of *Escherichia coli*. *J. Bacteriol.* 185, 2692–2699. doi: 10.1128/JB.185.9.2692-2699.2003

Ren, G., Zhang, L., Zhao, X., Xu, G., Zhang, Y., Roberts, A. I., et al. (2008). Mesenchymal stem cell-mediated immunosuppression occurs via concerted action of chemokines and nitric oxide. *Cell Stem Cell* 2, 141–150. doi: 10.1016/j.stem.2007.11.014

Resendis-Antonio, O. (2013). "Constraint-based modeling," in *Encyclopedia of Systems Biology*, eds W. Dubitzky, O. Wolkenhauer, K.-H. Cho, and H. Yokota (New York, NY: Springer), 494–498. doi: 10.2147/GICTT.S54121

Rocha, I., Förster, J., and Nielsen, J. (2008). "Design and application of genome-scale reconstructed metabolic models," in *Microbial Gene Essentiality: Protocols and Bioinformatics Methods in Molecular BiologyTM*, Vol. 416, eds A. L. Osterman and S. Y. Gerdes (Totowa, NJ: Humana Press), 409–431. doi: 10.1007/978-1-59745-321-9_29

Rolfsson, O., Palsson, B. Ø., and Thiele, I. (2011). The human metabolic reconstruction recon 1 directs hypotheses of novel human metabolic functions. *BMC Syst. Biol.* 5:155. doi: 10.1186/1752-0509-5-155

Romero, P., Wagg, J., Green, M. L., Kaiser, D., Krummenacker, M., and Karp, P. D. (2004). Computational prediction of human metabolic pathways from the complete human genome. *Genome Biol.* 6:R2. doi: 10.1186/gb-2004-6-1-r2

Rose, R. A., Jiang, H., Wang, X., Helke, S., Tsoporis, J. N., Gong, N., et al. (2008). Bone marrow-derived mesenchymal stromal cells express cardiac-specific markers, retain the stromal phenotype, and do not become functional cardiomyocytes in vitro. *Stem Cells* 26, 2884–2892. doi: 10.1634/stemcells.2008-0329

Rosenbaum, A. J., Grande, D. A., and Dines, J. S. (2008). The use of mesenchymal stem cells in tissue engineering. *Organogenesis* 4, 23–27. doi: 10.4161/org.6048

Russo, F. P., Alison, M. R., Bigger, B. W., Amofah, E., Florou, A., Amin, F., et al. (2006). The bone marrow functionally contributes to liver fibrosis. *Gastroenterology* 130, 1807–1821. doi: 10.1053/j.gastro.2006.01.036

Sahoo, S., Aurich, M. K., Jonsson, J. J., and Thiele, I. (2014). Membrane transporters in a human genome-scale metabolic knowledgebase and their implications for disease. *Front. Physiol.* 5:91. doi: 10.3389/fphys.2014.00091

Sahoo, S., Franzson, L., Jonsson, J. J., and Thiele, I. (2012). A compendium of inborn errors of metabolism mapped onto the human metabolic network. *Mol. Biosyst.* 8, 2545–2558. doi: 10.1039/c2mb25075f

Sahoo, S., Haraldsdóttir, H. S., Fleming, R. M. T., and Thiele, I. (2015). Modeling the effects of commonly used drugs on human metabolism. *FEBS J.* 282, 297–317. doi: 10.1111/febs.13128

Sampogna, G., Guraya, S. Y., and Forgione, A. (2015). Regenerative medicine: historical roots and potential strategies in modern medicine. *J. Microsc. Ultrastruct.* 3, 101–107. doi: 10.1016/j.jmau.2015.05.002

Schultz, A., and Qutub, A. A. (2016). Reconstruction of tissue-specific metabolic networks using CORDA. *PLoS Comput. Biol.* 12:e1004808. doi: 10.1371/journal.pcbi.1004808

Secunda, R., Vennila, R., Mohanashankar, A. M., Rajasundari, M., Jeswanth, S., and Surendran, R. (2015). Isolation, expansion and characterisation of mesenchymal stem cells from human bone marrow, adipose tissue, umbilical cord blood and matrix: a comparative study. *Cytotechnology* 67, 793–807. doi: 10.1007/s10616-014-9718-z

Shares, B. H., Busch, M., White, N., Shum, L., and Eliseev, R. A. (2018). Active mitochondria support osteogenic differentiation by stimulating β-catenin acetylation. *J. Biol. Chem.* 293, 16019–16027. doi: 10.1074/jbc.RA118.004102

Shen, F., Cheek, C., and Chandrasekaran, S. (2019). Dynamic network modeling of stem cell metabolism. *Methods Mol. Biol.* 1975, 305–320. doi: 10.1007/978-1-4939-9224-9_14

Shlomi, T., Cabili, M. N., and Ruppin, E. (2009). Predicting metabolic biomarkers of human inborn errors of metabolism. *Mol. Syst. Biol.* 5:263. doi: 10.1038/msb.2009.22

Shum, L. C., White, N. S., Mills, B. N., de Mesy Bentley, K. L., and Eliseev, R. A. (2016). Energy metabolism in mesenchymal stem cells during osteogenic differentiation. *Stem Cells Dev.* 25, 114–122. doi: 10.1089/scd.2015.0193

Smallbone, K., Messiha, H. L., Carroll, K. M., Winder, C. L., Malys, N., Dunn, W. B., et al. (2013). A model of yeast glycolysis based on a consistent kinetic characterisation of all its enzymes. *FEBS Lett.* 587, 2832–2841. doi: 10.1016/j.febslet.2013.06.043

Smolková, K., and Ježek, P. (2012). The role of mitochondrial NADPH-dependent isocitrate dehydrogenase in cancer cells. *Int. J. Cell Biol.* 2012:273947. doi: 10.1155/2012/273947

Solarte, V. A., Bayona, S. B., Aranguren, L. S., Sossa, C. L., Meana, A., Lloves, J. M., et al. (2018). Function and therapeutic potential of mesenchymal stem cells and their acellular derivatives on non-healing chronic skin ulcers. *J. Stem Cell Res. Ther.* 8:423. doi: 10.4172/2157-7633.1000423

Solchaga, L. A., Penick, K. J., and Welter, J. F. (2011). Chondrogenic differentiation of bone marrow-derived mesenchymal stem cells: tips and tricks. *Methods Mol. Biol.* 698, 253–278. doi: 10.1007/978-1-60761-999-4_20

Stempler, S., Yizhak, K., and Ruppin, E. (2014). Integrating transcriptomics with metabolic modeling predicts biomarkers and drug targets for Alzheimer's disease. *PLoS One* 9:e105383. doi: 10.1371/journal.pone.0105383

Strober, B. J., Elorbany, R., Rhodes, K., Krishnan, N., Tayeb, K., Battle, A., et al. (2019). Dynamic genetic regulation of gene expression during cellular differentiation. *Science* 364, 1287–1290. doi: 10.1126/science.aaw0040

Swainston, N., Smallbone, K., Hefzi, H., Dobson, P. D., Brewer, J., Hanscho, M., et al. (2016). Recon 2.2: from reconstruction to model of human metabolism. *Metabolomics* 12:109.

Tachida, Y., Sakurai, H., Okutsu, J., Suda, K., Sugita, R., Yaginuma, Y., et al. (2015). Proteomic comparison of the secreted factors of mesenchymal stem cells from bone marrow, adipose tissue and dental pulp. *J. Proteomics Bioinform.* 8, 266–273. doi: 10.4172/jpb.1000379

Takarada-Iemata, M., Takarada, T., Nakamura, Y., Nakatani, E., Hori, O., and Yoneda, Y. (2011). Glutamate preferentially suppresses osteoblastogenesis than adipogenesis through the cystine/glutamate antiporter in mesenchymal stem cells. *J. Cell. Physiol.* 226, 652–665. doi: 10.1002/jcp.22390

Tatard, V. M., D'Ippolito, G., Diabira, S., Valeyev, A., Hackman, J., McCarthy, M., et al. (2007). Neurotrophin-directed differentiation of human adult marrow stromal cells to dopaminergic-like neurons. *Bone* 40, 360–373. doi: 10.1016/j.bone.2006.09.013

Thiele, I., and Palsson, B. Ø. (2010). A protocol for generating a high-quality genome-scale metabolic reconstruction. *Nat. Protoc.* 5, 93–121. doi: 10.1038/nprot.2009.203

Thiele, I., Swainston, N., Fleming, R. M. T., Hoppe, A., Sahoo, S., Aurich, M. K., et al. (2013). A community-driven global reconstruction of human metabolism. *Nat. Biotechnol.* 31, 419–425. doi: 10.1038/nbt.2488

Trushina, E., and Mielke, M. M. (2014). Recent advances in the application of metabolomics to Alzheimer's disease. *Biochim. Biophys. Acta Mol. Basis Dis.* 1842, 1232–1239. doi: 10.1016/j.bbadis.2013.06.014

Tsai, Y.-H., Lin, K.-L., Huang, Y.-P., Hsu, Y.-C., Chen, C.-H., Chen, Y., et al. (2015). Suppression of ornithine decarboxylase promotes osteogenic differentiation of human bone marrow-derived mesenchymal stem cells. *FEBS Lett.* 589, 2058–2065. doi: 10.1016/j.febslet.2015.06.023

Turinetto, V., Vitale, E., and Giachino, C. (2016). Senescence in human mesenchymal stem cells: functional changes and implications in stem cell-based therapy. *Int. J. Mol. Sci.* 17:1164. doi: 10.3390/ijms17071164

Ullah, I., Subbarao, R. B., and Rho, G. J. (2015). Human mesenchymal stem cells - current trends and future prospective. *Biosci. Rep.* 35:e00191. doi: 10.1042/BSR20150025

Ullah, M., Liu, D. D., and Thakor, A. S. (2019). Mesenchymal stromal cell homing: mechanisms and strategies for improvement. *iScience* 15, 421–438. doi: 10.1016/j.isci.2019.05.004

Valencia, J., Blanco, B., Yáñez, R., Vázquez, M., Herrero Sánchez, C., Fernández-García, M., et al. (2016). Comparative analysis of the immunomodulatory capacities of human bone marrow- and adipose tissue-derived mesenchymal stromal cells from the same donor. *Cytotherapy* 18, 1297–1311. doi: 10.1016/j.jcyt.2016.07.006

Väremo, L., Nookaew, I., and Nielsen, J. (2013). Novel insights into obesity and diabetes through genome-scale metabolic modeling. *Front. Physiol.* 4:92. doi: 10.3389/fphys.2013.00092

Vigo, T., La Rocca, C., Faicchia, D., Procaccini, C., Ruggieri, M., Salvetti, M., et al. (2019). IFNβ enhances mesenchymal stromal (stem) cells immunomodulatory function through STAT1-3 activation and mTOR-associated promotion of glucose metabolism. *Cell Death Dis.* 10:85.

von Bomhard, A., Elsässer, A., Ritschl, L. M., Schwarz, S., and Rotter, N. (2016). Cryopreservation of endothelial cells in various cryoprotective agents and media - vitrification versus slow freezing methods. *PLoS One* 11:e0149660. doi: 10.1371/journal.pone.0149660

Wang, M., Yuan, Q., and Xie, L. (2018). Mesenchymal stem cell-based immunomodulation: properties and clinical application. *Stem Cells Int.* 2018:3057624. doi: 10.1155/2018/3057624

Wang, Y., Eddy, J. A., and Price, N. D. (2012). Reconstruction of genome-scale metabolic models for 126 human tissues using mCADRE. *BMC Syst. Biol.* 6:153. doi: 10.1186/1752-0509-6-153

Waterman, R. S., Tomchuck, S. L., Henkle, S. L., and Betancourt, A. M. (2010). A new mesenchymal stem cell (MSC) paradigm: polarization into a pro-inflammatory MSC1 or an Immunosuppressive MSC2 phenotype. *PLoS One* 5:e10088. doi: 10.1371/journal.pone.0010088

Westerhoff, H. V., and Palsson, B. O. (2004). The evolution of molecular biology into systems biology. *Nat. Biotechnol.* 22, 1249–1252. doi: 10.1038/nbt1020

Wone, B. W. M., Kinchen, J. M., Kaup, E. R., and Wone, B. (2018). A procession of metabolic alterations accompanying muscle senescence in *Manduca sexta*. *Sci. Rep.* 8:1006. doi: 10.1038/s41598-018-19630-5

Yizhak, K., Gabay, O., Cohen, H., and Ruppin, E. (2013). Model-based identification of drug targets that revert disrupted metabolism and its application to ageing. *Nat. Commun.* 4:2632. doi: 10.1038/ncomms3632

Youngstrom, D. W., LaDow, J. E., and Barrett, J. G. (2016). Tenogenesis of bone marrow-, adipose-, and tendon-derived stem cells in a dynamic bioreactor. *Connect. Tissue Res.* 57, 454–465. doi: 10.3109/03008207.2015.1117458

Yuan, X., Logan, T. M., and Ma, T. (2019). Metabolism in human mesenchymal stromal cells: a missing link between hMSC biomanufacturing and therapy? *Front. Immunol.* 10:977. doi: 10.3389/fimmu.2019.00977

Yue, Y., Zhang, L., Zhang, X., Li, X., and Yu, H. (2018). De novo lipogenesis and desaturation of fatty acids during adipogenesis in bovine adipose-derived mesenchymal stem cells. *In Vitro Cell. Dev. Biol. Anim.* 54, 23–31. doi: 10.1007/s11626-017-0205-7

Yurkovich, J. T., and Palsson, B. O. (2016). Solving puzzles with missing pieces: the power of systems biology. *Proc. IEEE* 104, 2–7. doi: 10.1109/JPROC.2015.2505338

Zhang, X., Zhang, L., Xu, W., Qian, H., Ye, S., Zhu, W., et al. (2013). Experimental therapy for lung cancer: umbilical cord-derived mesenchymal stem cell-mediated interleukin-24 delivery. *Curr. Cancer Drug Targets* 13, 92–102. doi: 10.2174/1568009611309010092

Zhang, Y., Marsboom, G., Toth, P. T., and Rehman, J. (2013). Mitochondrial respiration regulates adipogenic differentiation of human mesenchymal stem cells. *PLoS One* 8:e77077. doi: 10.1371/journal.pone.0077077

Zhao, Q., Ren, H., and Han, Z. (2016). Mesenchymal stem cells: immunomodulatory capability and clinical potential in immune diseases. *J. Cell. Immunother.* 2, 3–20. doi: 10.1016/j.jocit.2014.12.001

Zhu, H., Sun, A., Zou, Y., and Ge, J. (2014). Inducible metabolic adaptation promotes mesenchymal stem cell therapy for ischemia: a hypoxia-induced and glycogen-based energy prestorage strategy. *Arterioscler. Thromb. Vasc. Biol.* 34, 870–876. doi: 10.1161/ATVBAHA.114.303194

Zhu, J., and Thompson, C. B. (2019). Metabolic regulation of cell growth and proliferation. *Nat. Rev. Mol. Cell Biol.* 20, 436–450. doi: 10.1038/s41580-019-0123-5

Conflict of Interest: The authors declare that the research was conducted in the absence of any commercial or financial relationships that could be construed as a potential conflict of interest.

frontiers in Bioengineering and Biotechnology

ORIGINAL RESEARCH
published: 17 April 2020
doi: 10.3389/fbioe.2020.00327

Angiogenic Potential of Tissue Engineered Cartilage From Human Mesenchymal Stem Cells Is Modulated by Indian Hedgehog and Serpin E1

*Yannick Nossin[1], Eric Farrell[2], Wendy J. L. M. Koevoet[1], Rodrigo A. Somoza[3,4], Arnold I. Caplan[3,4], Bent Brachvogel[5,6] and Gerjo J. V. M. van Osch[1,7]**

[1] Department of Otorhinolaryngology, Head and Neck Surgery, Erasmus MC, University Medical Center, Rotterdam, Netherlands, [2] Department of Oral and Maxillofacial Surgery, Erasmus MC, University Medical Center, Rotterdam, Netherlands, [3] Department of Biology, Skeletal Research Center, Case Western Reserve University, Cleveland, OH, United States, [4] Center for Multimodal Evaluation of Engineered-Cartilage, Case Western Reserve University, Cleveland, OH, United States, [5] Department of Pediatrics and Adolescent Medicine, Experimental Neonatology, Faculty of Medicine, University of Cologne, Cologne, Germany, [6] Faculty of Medicine, Center for Biochemistry, University of Cologne, Cologne, Germany, [7] Department of Orthopedics, Erasmus MC, University Medical Center, Rotterdam, Netherlands

OPEN ACCESS

Edited by:
Sandra Hofmann, Eindhoven University of Technology, Netherlands

Reviewed by:
Susanne Grässel, University of Regensburg, Germany
Adetola Adesida, University of Alberta, Canada

***Correspondence:**
Gerjo J. V. M. van Osch
g.vanosch@erasmusmc.nl

Specialty section:
This article was submitted to Tissue Engineering and Regenerative Medicine, a section of the journal Frontiers in Bioengineering and Biotechnology

Received: *16 October 2019*
Accepted: *25 March 2020*
Published: *17 April 2020*

Citation:
Nossin Y, Farrell E, Koevoet WJLM, Somoza RA, Caplan AI, Brachvogel B and van Osch GJVM (2020) Angiogenic Potential of Tissue Engineered Cartilage From Human Mesenchymal Stem Cells Is Modulated by Indian Hedgehog and Serpin E1. Front. Bioeng. Biotechnol. 8:327. doi: 10.3389/fbioe.2020.00327

With rising demand for cartilage tissue repair and replacement, the differentiation of mesenchymal stem cells (BMSCs) into cartilage tissue forming cells provides a promising solution. Often, the BMSC-derived cartilage does not remain stable and continues maturing to bone through the process of endochondral ossification *in vivo*. Similar to the growth plate, invasion of blood vessels is an early hallmark of endochondral ossification and a necessary step for completion of ossification. This invasion originates from preexisting vessels that expand via angiogenesis, induced by secreted factors produced by the cartilage graft. In this study, we aimed to identify factors secreted by chondrogenically differentiated bone marrow-derived human BMSCs to modulate angiogenesis. The secretome of chondrogenic pellets at day 21 of the differentiation program was collected and tested for angiogenic capacity using *in vitro* endothelial migration and proliferation assays as well as the chick chorioallantoic membrane (CAM) assay. Taken together, these assays confirmed the pro-angiogenic potential of the secretome. Putative secreted angiogenic factors present in this medium were identified by comparative global transcriptome analysis between murine growth plate cartilage, human chondrogenic BMSC pellets and human neonatal articular cartilage. We then verified by PCR eight candidate angiogenesis modulating factors secreted by differentiated BMSCs. Among those, Serpin E1 and Indian Hedgehog (IHH) had a higher level of expression in BMSC-derived cartilage compared to articular chondrocyte derived cartilage. To understand the role of these factors in the pro-angiogenic secretome, we used neutralizing antibodies to functionally block them in the conditioned medium. Here, we observed a 1.4-fold increase of endothelial

cell proliferation when blocking IHH and 1.5-fold by Serpin E1 blocking compared to unblocked control conditioned medium. Furthermore, endothelial migration was increased 1.9-fold by Serpin E1 blocking and 2.7-fold by IHH blocking. This suggests that the pro-angiogenic potential of chondrogenically differentiated BMSC secretome could be further augmented through inhibition of specific factors such as IHH and Serpin E1 identified as anti-angiogenic factors.

Keywords: angiogenesis, microarray, SerpinE1, IHH, VEGFa, BMSC, chondrogenesis, secretome

INTRODUCTION

Mesenchymal Stem Cells (BMSCs) are multipotent progenitor cells that can be isolated from a large variety of tissues such as bone marrow, synovium, adipose tissue and umbilical cord and can be differentiated *in vitro* toward the chondrogenic lineage (Pittenger et al., 1999; Somoza et al., 2014). Expression of Collagen Type X and Alkaline Phosphatase show a chondrocyte phenotype that resembles that of the chondrocytes found in the hypertrophic zone in the *in vivo* growth plate (Yoo et al., 1998; Zimmermann et al., 2008; Hellingman et al., 2010; Farrell et al., 2011) during endochondral ossification. Moreover, BMSC-derived cartilage constructs that are implanted subcutaneously in mice or rat, promote the transition of cartilage to bone via the invasion of blood vessels into the constructs (Pelttari et al., 2006; Cui et al., 2007; Scotti et al., 2010; Marino, 2011; Staines et al., 2013; Walzer et al., 2014; Thompson et al., 2015). This is driven by the formation of new vessels from preexisting vessels (known as angiogenesis), which is mainly induced and directed by secreted factors (Otrock et al., 2007; Rocha et al., 2014). Soluble factors secreted by BMSC-derived cartilage are proposed to have a pro-angiogenic capacity (Rocha et al., 2014) by stimulating the proliferation of endothelial cells and their migration into the cartilage template (Otrock et al., 2007) to promote subsequent vessel formation. This process requires a finely tuned interplay between pro- and anti-angiogenic factors to form fully functional vessels (Iruela-Arispe and Dvorak, 1997).

In this study, we identified soluble factors in the secretome of chondrogenically differentiated bone marrow-derived BMSCs that can modulate angiogenesis. We first confirmed the effect of the secretome of chondrogenically differentiated BMSCs on angiogenic capacity using a set of different angiogenesis assays: the chicken chorioallantoic membrane assay (CAM) and commonly used *in vitro* assays for migration and proliferation using Human Umbilical Vein Endothelial Cells (HUVEC). We then used global transcriptome comparison of existing data sets from murine growth plate cartilage (Iruela-Arispe and Dvorak, 1997), healthy human articular cartilage and healthy human chondrogenic BMSCs (Somoza et al., 2018) to identify expressed factors which may be secreted by chondrogenic BMSC constructs to mediate angiogenic effects in these assays. Finally, we studied the role of these factors in CAM and HUVEC proliferation and migration assays by applying neutralizing antibodies. Here, we show that IHH and Serpin E1 act as anti-angiogenic factors, as they are secreted by chondrogenically differentiated BMSCs and prevent endothelial cell proliferation and migration into BMSC derived cartilage constructs.

MATERIALS AND METHODS

Chondrogenic Differentiation of BMSCs and Generation of Conditioned Medium

Mesenchymal stem cells were isolated from seven human bone marrow samples aspirated from patients undergoing total hip arthroplasty after informed consent (MEC-2004-142 and MEC-2015-644). In total, seven donors were used, 4 female and 3 male (age range from 20 to 63–71) were used. Cells were plated at a density of 2,300 cells/cm^2 in expansion medium, α-MEM (Gibco, Dublin, Ireland) containing 10% FCS (Gibco, Basel, Switzerland), supplemented with 1 ng/mL FGF2 (BioRad, Hercules, CA, United States), 10 mM ascorbic acid-2-phosphate (Fluka, Charlotte, NC, United States), 1.5 μg/mL fungizone (Gibco) and 50 μg/mL gentamicin (Gibco) at 37°C and 5% CO_2). After 24 h, non-adherent cells were removed and adherent cells were expanded in the above-mentioned medium. At confluence, cells were passaged, and seeded at 2,300 cells/cm^2. For generation of pellets, BMSCs at passage three were utilized (≈3 population doublings in passage 2 and 3 population doublings in passage 3. Population doublings in passage 1 are unknown as we do not know the exact number of MSCs in the fresh bone marrow biopsy).

Cartilage was obtained from seven patients (4 males, 3 females, ages between 63 and 86) undergoing total knee replacement surgery for osteoarthritis with implicit consent of the use of leftover material after surgery (after approval by the local ethics committee; MEC-2004-322). Full thickness cartilage was harvested, treated with 2 mg/mL protease in physiological saline solution (Sigma-Aldrich, St. Louis, MO, United States) for 90 min and subsequently digested overnight in basal medium [DMEM, 4.5 g/L glucose with 10% fetal calf serum (FCS), 50 μg/mL gentamicin, and 1.5 μg/mL fungizone (all Invitrogen, Carlsbad, CA, United States)] supplemented with 0.12 U collagenase B (Roche Diagnostics, Almere, the Netherlands). The next day, the resulting cell number was determined using a hemocytometer. The primary chondrocytes were then seeded at a density of 7,500 cell/cm^2 in T175 culture flasks for expansion with the above-mentioned basal medium. For generation of stable cartilage pellets, chondrocytes at passage 1 were utilized.

Pellet cultures of BMSCs and primary chondrocytes were formed by seeding 2.0×10^5 cells in 0.5 mL in a 15 mL

conical polypropylene tube and centrifuging for 8 min at 300 g. Pellets from both cell sources were cultured for 21 days in chondrogenic medium, high-glucose DMEM supplemented with 50 μg/mL gentamicin (Invitrogen), 1.5 μg/mL fungizone (Invitrogen), 1 mM sodium pyruvate (Invitrogen), 40 μg/mL proline (Sigma, Kawasaki, Kanagawa Prefecture, Japan), 1:100 v/v insulin-transferrin-selenium (ITS; BD Biosciences, San Jose, CA, United States), 10 ng/mL Transforming Growth Factor β1 (R&D Systems), 10 mM ascorbic acid-2-phosphate (Sigma), and 100 nM dexamethasone (Sigma). The medium was renewed twice a week. At day 21, medium was renewed and 24 h later the pellets were washed three times with PBS and then incubated with basal medium (UCM) consisting of phenol-red free DMEM (Gibco) supplemented with 0.1% w/v BSA (Sigma) and 10 mM ascorbic acid-2-phosphate (Fluka) for 24 h to produce conditioned medium (CM) for downstream experiments. This CM was collected, cell debris removed by centrifugation at 300xg for 8 min and stored at −80°C. Pellets were digested in 350 μL RNABee (Tel-Test. Inc., Pearland, TX, United States) and stored at −80°C for subsequent RNA-isolation, cDNA synthesis and gene expression analysis. In addition, pellets were fixed in 4% formalin at room temperature overnight and then processed for histological analysis.

Gene Expression Analysis

To isolate RNA, the pellets in RNABee were homogenized with an Eppendorf- Micro-pestle (Eppendorf, Hamburg, Germany). Total RNA isolation was performed according to manufacturer's protocol utilizing the RNeasy Column system (Quiagen, Hilden, Germany). The RNA concentration was determined using a NanoDrop® spectrophotometer (Isogen Life Science, Utrecht, the Netherlands). 0.5 μg RNA was used for cDNA synthesis following the protocol of the manufacturer of the RevertAid First Strand cDNA kit (Thermo Fisher Scientific, Waltham, MA, United States). Gene expression was analyzed by real-time Reverse Transcription Quantitative Polymerase Chain Reaction (RT-qPCR) on a StepOnePlus™ System using SYBR Green (Applied Biosystems, Foster City, CA, United States) or Taqman (Thermo Fisher Scientific, Waltham, MA, United States) assays. Primers for Syber Green RT-qPCR analysis *(ENPP2, IHH, NDNF, RAMP1, SRPX1, ADM, SERPIN E1*) were purchased as assays-on-demand from BioRad. Sequences of additional primers and probes for Taqman and Syber PCR analysis are Alkaline Phosphatase, Biomineralization Associated (*ALPL) (Fw:* GGC AATAGCAGGTTCACGTACA; Rev: CGATAACAGTCTTGC CCCACTT; Probe: CCGGTATGTTTCGTGCAGCCATCCT); Collagen Type II Alpha 1 Chain (COL2A1) (Fw: GGCAAT AGCAGGTTCACGTACA; Rev: CGATAACAGTCTTGC CCCACTT; Probe: CCGGTATGTTTCGTGCAGCCATCCT); Collagen Type X Alpha 1 Chain (COL10A1) (Fw; CAAGG CACCATCTCCAGGAA; Rev: AAAGGGTATTTGTGGC AGCATATT; Probe: TCCAGCACGCAGAATCCATCTGA); Glyceraldehyde-3-Phosphate Dehydrogenase (GAPDH) (Fw: GTCAACGGATTTGGTCGTATTGGG; Rev: TGCCATGGGT GGAATCATATTGG; Probe: TGGCGCCCCAACCAGCC); Hypoxanthine Phosphoribosyltransferase 1 (HPRT1) (Fw: TAT GGACAGGACTGAACGTCTTG; Rev: CACACAGAGGGC TACAATGTG; Probe: AGATGTGATGAAGGAGATGGGAG GCCA); Ribosomal Protein S27 (RPS27) (Fw: TGGCTGTCCT GAAATATTATAAGGT; Rev: CCCCAGCACCACATTCATCA); Vascular Endothelial Growth Factor A (VEGFA) (Fw: CTT GCCTTGCTGCTCTACC; Rev: CACACAGGATGGCTTG AAG). The best housekeeper index (BKI) was calculated from *GPDH, RSP27* and *HPRT* and used for the $2^{-\Delta CT}$ method.

Histology

Fixed pellets were embedded in 1% agarose and then further in paraffin using standard procedures. Six μm sections were cut and further processed by deparaffinizing and rehydrating. At least three pellets per condition were sectioned.

Glycosaminoglycan Staining

Deposition of glycosaminoglycan (GAG) was determined by thionine staining. Paraffin sections were stained for 5 min in 0.4% thionine in 0.01 M of aqueous sodium acetate, resulting in a selective staining for glycosaminoglycans (Bulstra et al., 1993).

Immunohistochemical Staining for Collagen Type II and Collagen Type X

Following deparaffinization and rehydration, sections were treated with 1% w/v hyaluronidase to increase antibody penetration and antigen retrieval was performed using 0.1% w/v pronase, both were sequentially incubated for 30 min at 37°C. Following this, the sections were blocked using normal goat serum (Southern Biotech, Birmingham, AL, United States). Sections were incubated with either mouse monoclonal antibody against collagen type II 0.4 μg/mL (Developmental Studies Hybridoma Bank, Cat.# II-II6B3) for 60 min or collagen type X 5 μg/mL (Thermo Fisher Scientific, Clone X53, Cat.# 14-9771-82) in PBS 1%BSA overnight. Both were incubated with a biotinylated goat anti-mouse antibody for 30 min followed by an incubation with ALP-conjugated streptavidin. Staining was revealed by incubation with a New Fuchsin substrate (Chroma, Kongen, Germany). Corresponding isotype controls for both antibodies were used (0.4 and 5 μg/mL of an isotype immunoglobulin G1 monoclonal antibody, respectively).

Global Gene Expression Analysis

Candidate Angiogenesis Modulating Factor Selection From Previously Published Microarrays

The aim of this analysis was to identify known secreted angiogenic factors released from chondrogenic pellets. We first compared data from different zones of the murine growth plate (proliferative, pre-hypertrophic and hypertrophic) via paired *t*-test and selected factors with a cut off value of 3-fold change in the expression of genes. The selected list of uniquely expressed factors where then overlapped with different online resources from Uniprot, Geneontology and the Matrisome Project (Hynes and Naba, 2012) utilizing the Funrich software[1] (Pathan et al., 2015) to select for secreted genes associated with the regulation of angiogenesis. The selected murine genes were then used as input for comparison with a human microarray to select those genes

[1]http://www.funrich.org/

differentially expressed between chondrogenically differentiated BMSCs and newly formed articular cartilage with a criterion of either being expressed in one condition and not the other or having a 3-fold difference.

For comparison of the different growth plate zones, we used a dataset previously generated and described by Belluoccio et al. (2010). In brief, femoral growth plates were isolated from long bones of two 14 days old female Swiss White mouse. Using microdissection of frozen sections, ≈2,000 chondrocytes (per layer) were isolated from the proliferative (PR), pre-hypertrophic (PH) and hypertrophic (H) layer of the growth plate. Total RNA was extracted using PicoPure RNA isolation kit (Arcturus Bioscience, San Diego, CA, United States), treated with DNase, linearly amplified using MessageAmp aRNA kit (Thermo Fisher Scientific) labeled with Cy3/Cy5 fluorophores, then hybridized to 44k whole genome oligo microarrays (G4122A; Agilent Technologies, Santa Clara, CA, United States) and scanned on an Axon 4000B scanner. Features were extracted using GenePix Pro software (version 4.1; Axon Instruments, San Jose, CA, United States). The microarray data have been validated by qPCR on amplified RNA (Belluoccio et al., 2010).

To compare the murine data with a human model similar to the one used in this study, we overlapped the dataset with a list of genes we previously determined with microarray analysis. In this dataset, the transcriptome of human neonatal articular cartilage from femoral and tibial plateau of 1 month old cadaveric specimens (n = 2) was compared with chondrogenically differentiated BMSCs of two healthy adult volunteer donors (Somoza et al., 2018). In brief, RNA was isolated after homogenization with RNeasy mini columns (Quiagen), total RNA was linearly amplified and biotin labeled using Illumina TotalPrep™ kits (Life Technologies) and whole-genome expression analysis was carried out using Illumina (CA) Human Ref-8v3 or Human HT-12 v4 BeadArrays™. The cRNA was hybridized to Illumina BeadChips™, processed and read using a BeadStation™ array reader according to the manufacturer's instructions (Illumina). Values of less than 130 relative fluorescence units were considered to be non-specific background signals.

Angiogenesis Assays

Commercially derived pooled Human Umbilical Vein Endothelial Cell (HUVEC) (Lonza, Basel, Switzerland) were seeded at a density of 5×10^3 cells/cm^2 in culture flasks and cultured in endothelial growth medium (EGM-2 Promocell, Heidelberg, Germany). Medium was renewed every 2–3 days. When they neared confluency, cells were detached with 0.05% Trypsin-EDTA (Gibco) and used for angiogenesis assays. For angiogenesis assays, HUVECs between passages 8 and 10 were used.

Endothelial Cell Migration Assay

Migration assays were performed by seeding HUVEC (5×10^4 cells/well) in 24-well Transwell inserts (8 μm pore size, Corning Life Sciences) in serum-free medium containing 0.05% BSA (Merk). The CM from chondrogenically differentiated BMSCs was placed in the lower compartment of different wells and diluted 1:1 with Endothelial Basal Medium (EBM-2, Promocell). EBM and non-conditioned medium are used as negative controls and Endothelial Growth Medium (EGM-2) (EBM-2 supplemented with EGF, FGF2, IGF-1, VEGFa, AA, Heparin, Hydrocortisone, and FBS) (Promocell) is used as positive control. After 10 h of incubation at 37°C 5% CO_2, the cells on the membrane were fixed with 4% formaldehyde/PBS and the non-migrated cells from the upper surface of the membrane were removed with a cotton swab. We confirmed that no cell proliferation took place during the 10 h incubation, based on cell count. The migrated cells on the lower surface of the membrane were then stained with DAPI and then quantified by fluorescence microscopy and image analysis through ImageJ utilizing the included particle analysis macro. Five non-overlapping pictures were taken and analyzed per well for three independent experiments (Schindelin et al., 2012).

Endothelial Proliferation

To measure proliferation, 2.5×10^3 HUVEC/cm^2 were seeded in 48-well plates. After 24 h, medium was replaced with endothelial basal medium to synchronize the cells. After 8 h, cells were stimulated with either CM, EGM-2 as positive control or EBM-2 as negative control for 24 h. With the stimulus, 10 μM dEdU (BaseClick, Neuried, Germany) was added to stain DNA of replicating cells to allow assessment of proliferation. After 24 h, the cells were washed three times with phosphate-buffered saline and fixed with 4% formalin for 5 min. The EdU label was then revealed according the protocol provided by the manufacturer. The cells were counterstained with DAPI and imaged using fluorescence microscopy. Utilizing the particle analysis macro in ImageJ, we determined the amount of positively stained cells for DAPI and EdU and the percentage of cells positive for EdU was calculated.

Chick Chorioallantoic Membrane (CAM) Assay

Fertilized chicken eggs laid the day before (purchased from Drost Loosdrecht B.V.) were incubated sideways at 37°C and 65% humidity for 3 days before rupturing the air sack located at the blunt side of the egg, as well as opening a small hole on the top to deflate the air-sack and lower the fluid level. After 3 days of incubation, part of the shell was removed and filters containing concentrated CM were placed on top of the CAM. Therefore, CM harvested from chondrogenically differentiated BMSCs was concentrated utilizing the Amicon® Ultra-2 mL Centrifugal Filters (Merck, Kenilworth, NJ, United States) and a sterile filter disks with a diameter of 5 mm were soaked with 5 μL of the concentrated CM and placed on the membrane. As a negative control, concentrated basal medium was utilized and 100 ng FGF2 was used as positive control (Schindelin et al., 2012). After 3 days of incubation, the CAM was fixed with 4% Formalin/PBS solution and the removed from the egg. Induction of vessel formation was assessed by taking pictures of each filter on the membrane, and the blinded pictures were ranked by three independent observers. A total of 45 images were ranked (45 being the highest and one the lowest rank). The inter-observer correlation was tested and the final rank determined by averaging the ranks per image.

Antibody Blocking

To evaluate the effect of the selected factors, we neutralized their effect in CM by incubating with the corresponding antibodies for 30 min before utilization in the different assays. Blocking antibodies against VEGF-A (Cat. # AF-293-SP) and Serpin E1 (Cat.# MAB1786-SP, Clone # 242816) were obtained from R&D-Systems (Minneapolis, MN, United States) and utilized at 0.5 μg/mL according to the manufacturers *in vitro* testing protocol. The IHH neutralizing antibody (Cat.# 5E1) was purchased from DSHB (Iowa City, IA, United States) and used at 5 μg/mL according to the manufacturers specifications.

Data Analysis and Statistics

The statistical analyses of gene expression data were performed on three replicates for each of the seven BMSC and seven chondrocyte donors. Since in some conditions certain genes were not expressed and a Shapiro-Wilk test revealed the absence of a normal distribution we chose a non-parametric analysis. Technical triplicates per donor were averaged and the differences between conditions were statistically tested by a Mann–Whitney *U*-test. The *in vitro* angiogenesis tests were performed in two batches of BMSC CM; for each batch, the media of three donors were pooled. These batches were tested in triplicate in independent experiments. Due to the continuous nature of the data it was depicted as a bar graph and for statistical evaluation of the data, a linear mixed model was utilized with a Bonferroni *post hoc* test. For the CAM assay, the inter-observer correlation was tested through a Spearman-correlation test. Per sample the rank of two observers was averaged and then per condition graphed as a boxplot with whiskers. The conditions were compared using the average rank of three observers with a Kruskal-Wallis one-way analysis of variance with ensuing Bonferroni *post hoc* test. For the *in vitro* and *in vivo assays* positive controls were included in the experiments to be able to exclude possible technical failures. These positive controls were omitted from statistical analyses as they are not biologically meaningful for the conclusions. Statistical analysis

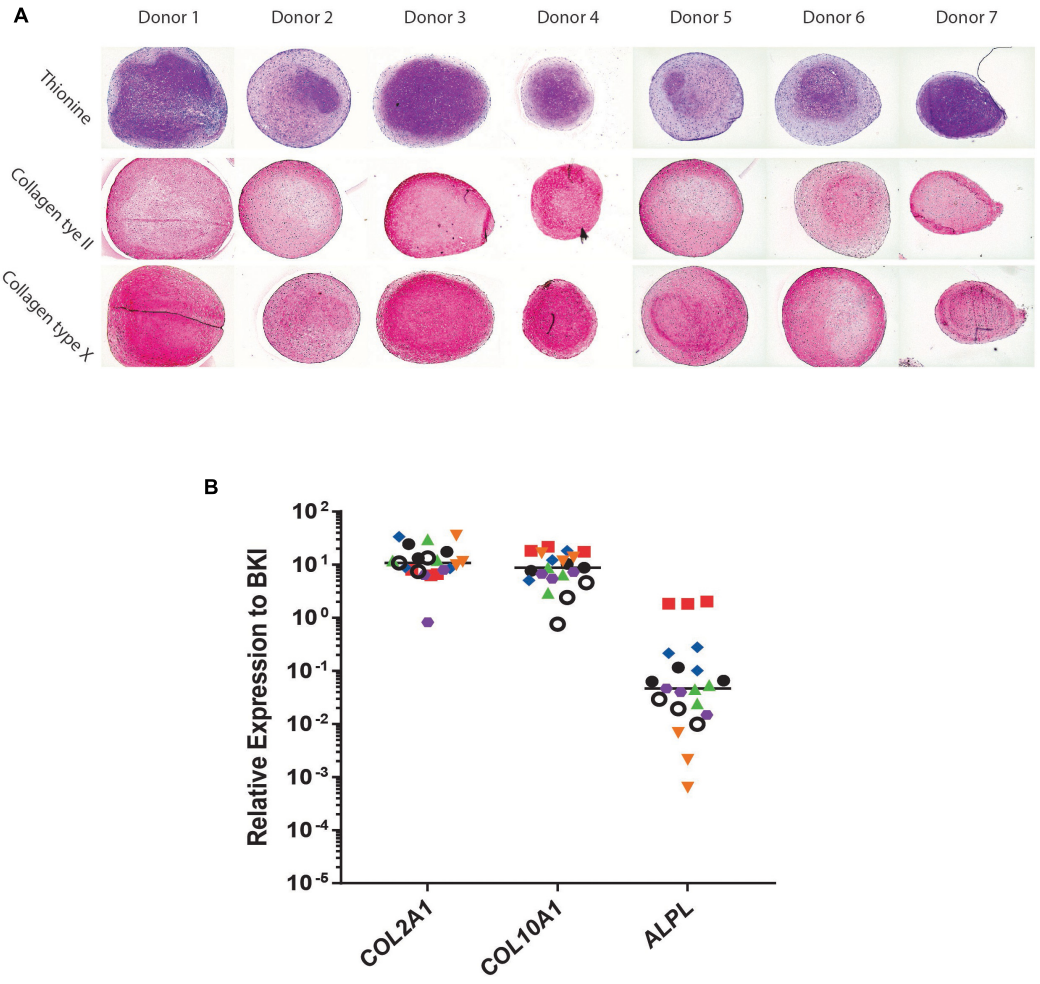

FIGURE 1 | Chondrogenic differentiation of bone marrow derived mesenchymal stem cells (BMSC). **(A)** Histological and Immunohistological staining of day 21 chondrogenically differentiated BMSC-pellets of the donors for Collagen type II, Thionine and Collagen type X. **(B)** qPCR Gene-expression analysis of chondrocyte and hypertrophy marker genes in day 21 chondrogenically differentiated BMSCs. Raw average Ct value for COL2A1 = 20.54; COL10A1 = 20.99; ALPL = 28.19.

was performed using SPSS11 for Windows (IBM, Armonk, NY, United States).

RESULTS

Conditioned Medium From Chondrogenically Differentiated BMSCs Induces Angiogenesis

Conditioned medium was generated from day 21 chondrogenically differentiated BMSC-pellets and its angiogenic potential was evaluated. Cells of all donors used were successfully differentiated toward a chondrocyte-like phenotype as shown by thionine and type II collagen staining (**Figure 1A**). The BMSC-pellets also underwent hypertrophy as shown by deposition of type X collagen protein (**Figure 1A**). Further, gene expression analysis showed clear collagen type II, collagen type X and alkaline phosphatase expression in chondrogenic BMSC pellets.

To assess the effects of CM on specific aspects of angiogenesis, we performed an endothelial cell migration assay utilizing a modified Boyden chamber assay. At a concentration of 50%, the CM induced a 9.2 (±4.5) fold increase (p = 0.00004) in the number of cells migrating compared to the non-CM

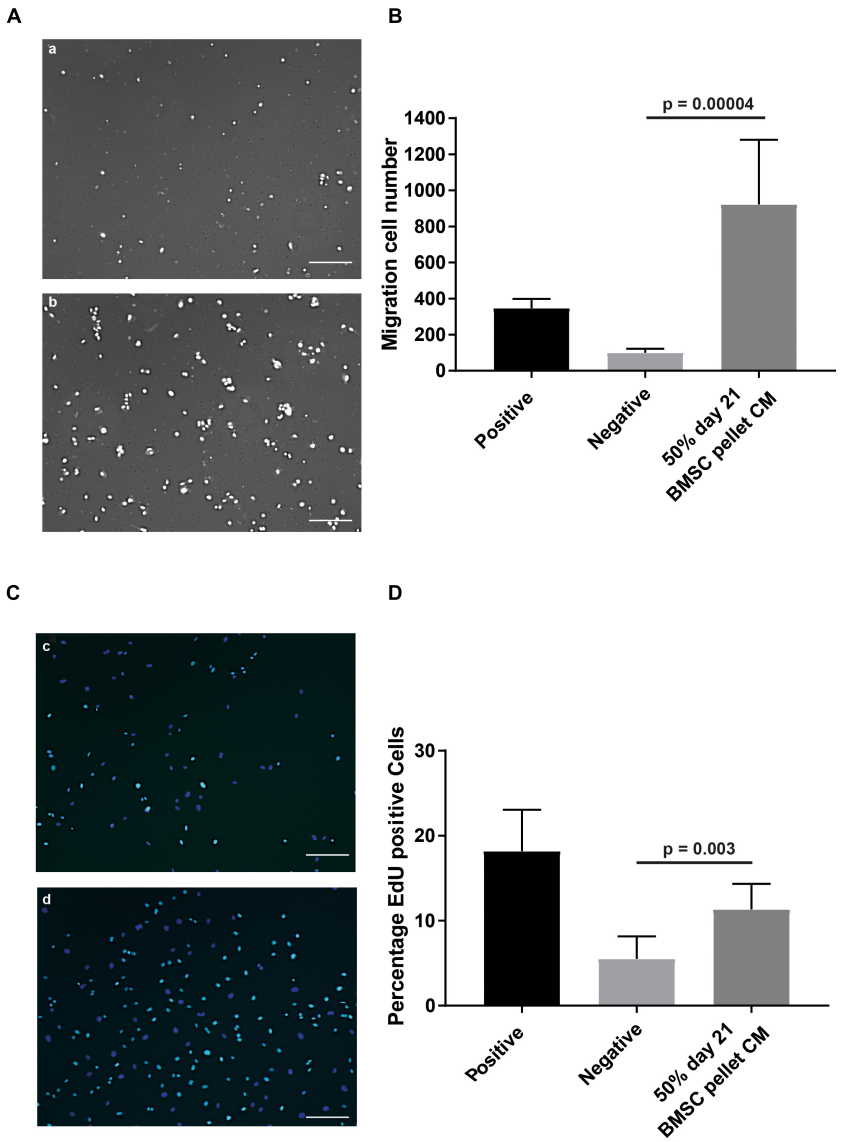

FIGURE 2 | *In vitro* angiogenesis assays confirmed pro-angiogenic potential of CM of chondrogenically differentiated BMSCs in pellets. **(A)** Modified Boyden chamber endothelial migration assay images; (a) Negative control, 50% endothelial basal medium and 50% non-CM; (b) positive control, endothelial growth medium. **(B)** Quantification of amount of migrated cells stimulated by the CM. **(C)** Endothelial proliferation assay; (c) negative control; (d) positive control showing in cyan positive EdU staining, counterstained with DAPI (blue). **(D)** Quantification of difference in actively proliferating HUVECs after 24 h. Both experiments were performed in two batches each pooling 3 donors; n = 3. Scalebar = 200 μm, Statistical analyses were performed with mixed-linear model with Bonferroni *post hoc* test.

(**Figures 2A,B**). To evaluate the effect of CM on endothelial cell proliferation the EdU incorporation in an *in vitro* HUVEC proliferation assay, was assessed. Exposure to CM resulted in 2.1 (±0.4) fold (p = 0.003) increase in EdU incorporation, indicating factors secreted by chondrogenically differentiated BMSCs increase endothelial cell proliferation (**Figures 2C,D**).

Next, we tested the BMSC-derived CM in an *in vivo* chick chorioallantoic membrane (CAM) assay in which it induced an increase in angiogenesis compared to non-CM controls (**Figure 3A**). The observed vessels had a high degree of directionality toward the stimulus containing filter-disks as ranked by three independent observers (p = 0.001; **Figure 3B**). These results confirm that the secretome of chondrogenically differentiated BMSCs can induce angiogenesis.

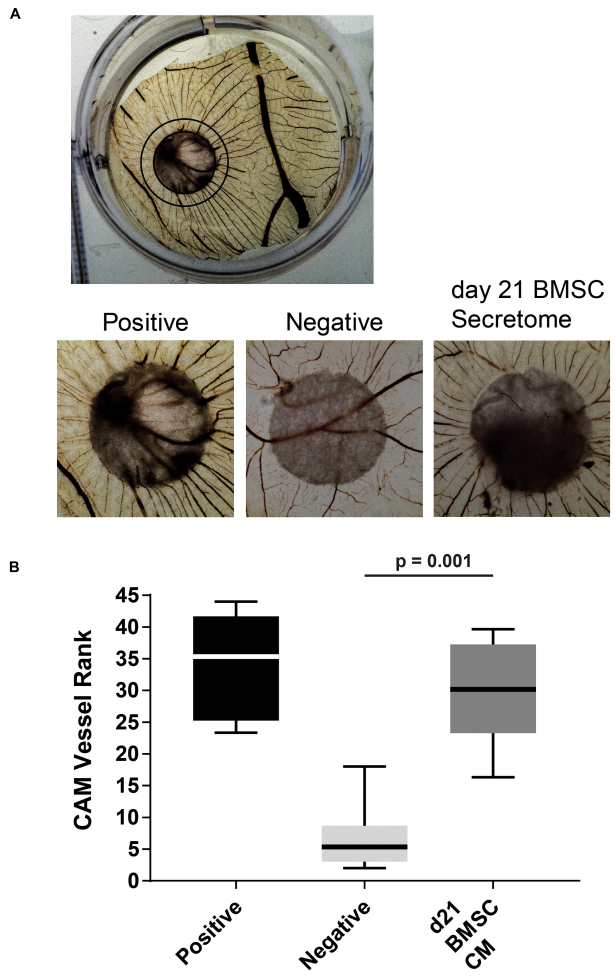

FIGURE 3 | *In vivo* CAM assay illustrated the pro-angiogenic potential of chondrogenically differentiated BMSC secretome. **(A)** Overview of treated CAM [Black circle depicts approximate range of influence of placed filter (center)]. Magnifications of chick chorioallantoic membrane incubated for 72 h with CM soaked 5 mm filter disks. Filter circles were placed on a vessel free area on day 7 of the chick development. **(B)** Boxplot depicting the ranking of the angiogenic potential (lowest = 1 highest = 45: average of 3 independent observers; box = interquartile range, whiskers + 1–99%). N = 6 per condition.

Selection of Eight Candidate Secreted Angiogenesis Regulating Factors From Microarray Datasets

To identify angiogenic factors in the secretome of hypertrophically differentiated chondrogenic cells we analyzed the expression of genes in data sets of growth plate cartilage, chondrogenic BMSC and neonatal cartilage. The different zones of the growth plate represent different phenotypical stages from cartilage to bone. We utilized microarray data comparing the three different zones (proliferative, pre-hypertrophic, and hypertrophic) of murine growth plate (Belluoccio et al., 2010) to determine which genes are differentially regulated in these zones. 1,328 genes showed a 3-fold difference in expression between two of the zones and among these 174 correspond to known secreted factors and 26 of these genes are described to regulate angiogenesis based according to online resource analysis (Uniprot, GeneOntology matrisome project database, Pubmed; **Figure 4**). We then compared the remaining 26 genes to a human microarray dataset that compared day 21 chondrogenically differentiated human BMSC pellets to neonatal articular cartilage (Somoza et al., 2018). Genes that were not differentially expressed in the human BMSC pellets and neonatal cartilage were discarded which led to the identification of eight genes: *ENPP2, IHH, NDNF, RAMP1, SPRX2, VEGFa, ADM, SERPIN E1* (**Figure 4**).

We then determined the gene expression levels of the final eight factors via qPCR, comparing our transient cartilage model (chondrogenically differentiated BMSC pellets) and a stable cartilage model of culture expanded articular chondrocytes differentiated as pellets following the same protocol used for BMSCs. *IHH* and *SERPINE1* were expressed significantly higher in BMSC-derived than in articular chondrocyte pellets (**Table 1**), confirming the data obtained from both microarrays. While the expression of *ENPP2, NDNF, SPRX2, VEGFa,* and *ADM,* showed no significant differences between transient and stable cartilage. *RAMP1* appeared to have a low expression in both the murine and human microarrays and was undetectable by PCR. This led us to select IHH and SERPINE1 as the most relevant factors for further follow-up.

Blocking IHH and Serpin E1 Increases Angiogenic Potential of Transient Cartilage Secretome

To confirm the role of IHH and Serpin E1 present in BMSC CM on angiogenesis, we conducted the *in vitro* angiogenesis assays in the presence of neutralizing antibodies against IHH and Serpin E1. In addition, we used a neutralizing antibody against the major bioactive pro-angiogenic factor VEGF. In the endothelial migration assay, blocking Serpin E1 led to a significant increase in migration of endothelial cells of 1.9 (±0.6) (p = 0.001) fold and 2.7 (±1.1) (p = 0.0000002) fold when blocking IHH (**Figure 5A**). Interestingly, the angiogenic potential of the CM was not influenced by the presence of the VEGFa blocking antibody. Similar behavior was observed in the proliferation assay where blocking Serpin E1 led to 1.5 (±0.4) (p = 0.03) fold

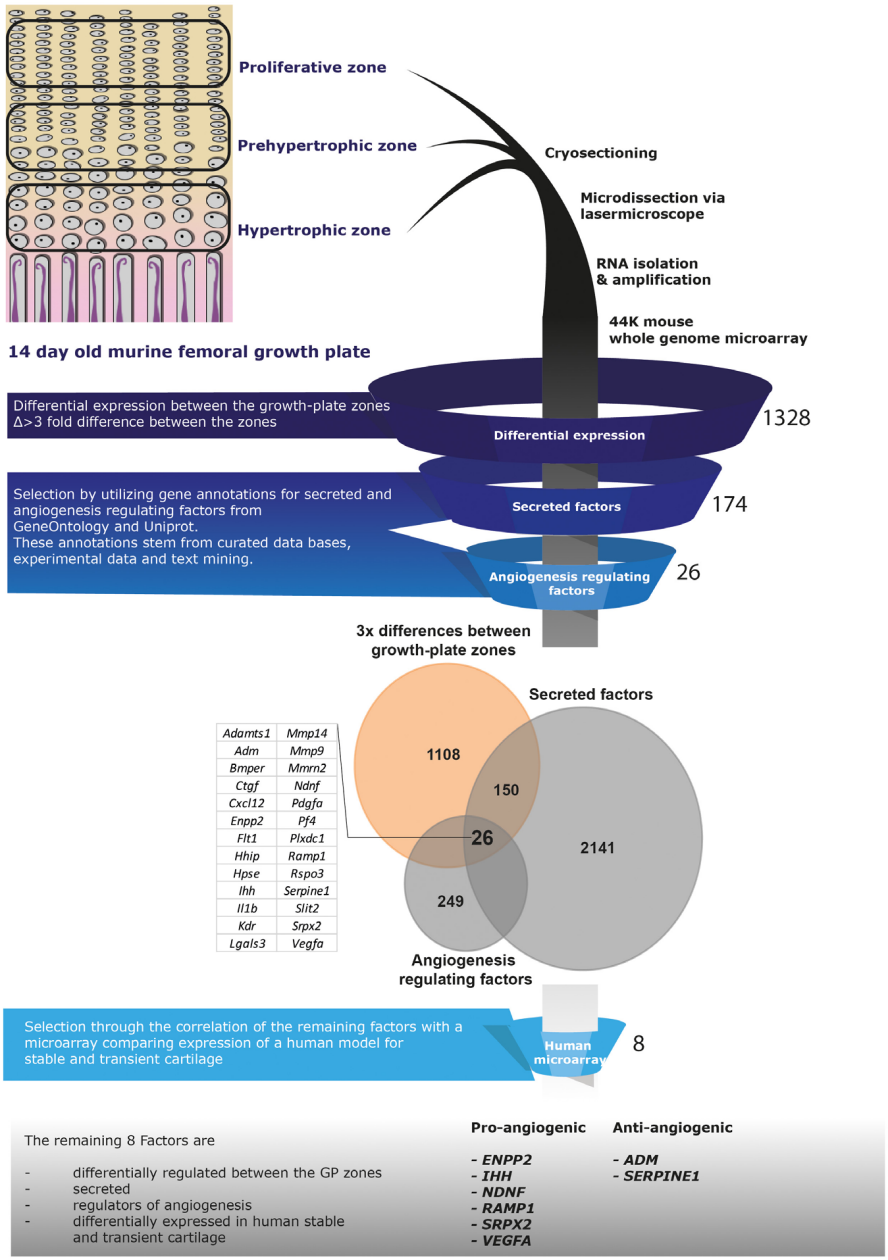

FIGURE 4 | Selection pipeline for factors of interest. Diagram of the selection process of factors of interest starting from a growth plate microarray going through the selection of secreted, angiogenesis regulating factors via online resources ending at the comparison to a human dataset including neonatal cartilage and chondrogenically differentiated BMSC data. Twenty-six factors were identified being differentially expressed between the growth plate zones, secreted and regulate angiogenesis (Venn-diagram). From these, 8 factors appeared differentially expressed between human chondrogenically differentiated BMSC and neonatal articular cartilage.

increase, blocking IHH increased endothelial cell proliferation by 1.4 (±0.3) fold, albeit not significant (p = 0.2), and no observed effect of the VEGFa blocking antibody (**Figure 5B**).

Blocking either IHH or Serpin E1 in the CAM assay did not increase the number of vessels or their directionality (**Figures 5C,D**). Blocking VEGFa showed a statistically significant (p = 0.006), reduction in the pro-angiogenic capacity of the chondrogenically differentiated BMSC secretome.

DISCUSSION

In this study, we identified soluble factors in BMSC-derived cartilage secretome that modulate angiogenesis. We first confirmed that the secretome of BMSC-derived cartilage is pro-angiogenic. Through a detailed analysis of multiple microarray datasets, Serpin E1 and IHH were identified as potential modulators of the angiogenic effect in our BMSC

TABLE 1 | Selection of IHH and SERPINE1 via microarray and PCR analysis.

	Microarray		QPCR
	P. vs. PH & H	NAC vs. d21 BMSC	d21 chon vs. d21 BMSC
ADM	4.60	0.40	0.23
ENPP2	14.42	0.43	2.07
IHH	13.62	2.73	34.45*
NDNF	3.84	12.14	1.68
RAMP1	3.48	2.91	Not expressed
SERPINE1	5.05	10.45	7.37*
SRPX2	0.26	2.63	2.48
VEGFA	11.27	0.63	1.35

*Expression of the 8 selected factors. (A) Expression pattern (increase or decrease) of the factors of interest comparing growth plate zones with neonatal articular cartilage (NAC) with chondrogenically differentiated BMSC and further with the gene expression pattern of the transient cartilage used in this study compared to a model of stable cartilage derived from 21 d differentiated chondrocytes (chon, chondrocyte derived pellet). *Significant difference in gene-expression analysis p = 0.001 tested with a Mann Whitney U-test. P, proliferative zone; PH, pre-hypertrophic zone; H, hypertrophic zone.*

CM. Experiments where IHH and Serpin E1 were blocked demonstrated a further enhancement of the angiogenic potential of the chondrogenic BMSC CM. This indicated that IHH and Serpin E1 contribute as anti-angiogenic modulators to the process of angiogenesis. Despite the fact that the role of recombinant IHH and Serpin E1 in angiogenesis is already established in the literature (Isogai et al., 2001; Devy et al., 2002; Chinchilla et al., 2010; Wu et al., 2015), to our knowledge this is the first study where their presence and role have been identified in the context of the secretome of a transient human cartilage model.

Serpin E1 has been shown to be both pro (Devy et al., 2002; Wu et al., 2015) and anti-angiogenic (Isogai et al., 2001; Devy et al., 2002; Stefansson et al., 2003) under different conditions. This is dependent, for example, on the presence of fibronectin or vitronectin as well as on its own concentration. As Serpin E1 is part of the plasminogen activator system, it may further regulate angiogenesis through the inhibition of the activation of serine proteases. This effect has been studied in cancer and shows an upregulation of the plasminogen activator as well as Serpin E1. This may protect the fibrin-rich ECM to provide a scaffold for endothelial cell invasion (Pepper, 2001). This clear anti-angiogenic capacity might be explained by the previously described mechanism in which Serpin E1 in the presence of vitronectin prevents the interaction of Integrin αvβ3 with KDR (Isogai et al., 2001). The anti-angiogenic capacity of Serpin E1 is further supported by *in vivo* CAM data showing recombinant Serpin E1 preventing FGF2 induced angiogenesis (Stefansson et al., 2001). An additional possibility for Serpin E1 to influence angiogenesis is through the plasminogen system and its influence on fibrin which has been linked to angiogenesis during endochondral ossification (DeSimone and Reddi, 1992; Yuasa et al., 2015). By targeting Serpin E1 in a bone defect, fibrinolysis may increase depending on the presence of plasminogen activator and hence create an enhanced environment for vessel invasion and subsequent bone-repair (Yuasa et al., 2015).

IHH is known to be important in the transitioning from cartilage to bone through signaling in the pre-and hypertrophic zones in the growth plate (Chung et al., 2001). As a recombinant protein, it is slightly pro-angiogenic (Chinchilla et al., 2010; Chapouly et al., 2019) while during endochondral ossification, it has been described in a murine *in vivo* model to negatively impact vessel expansion and persistence (Colnot et al., 2005). Blocking the function of IHH in the context of our transient cartilage model resulted in a clear increase in the migration and a slight increase in the proliferation of endothelial cells, supporting the anti-angiogenic effect of IHH. This provides an *in vitro* confirmation the results shown by Colnot et al. (2005) where an anti-angiogenic effect of IHH using a conditional IHH knock-out mouse model was observed. In addition to the role of IHH in the PTHrP feedback loop and in osteoblast formation (Ohba, 2016), this suggests a role in modulating angiogenesis during endochondral ossification.

We demonstrated the pro-angiogenic effect through different *in vitro* as well as *in vivo* angiogenesis assays. Our data is at odds with the findings of Bara et al. (2014) who used chondrogenically differentiated equine BMSC pellet CM (conditioned for 96 h) on a Matrigel-tube formation assay with HUVECs to conclude the secretomes anti-angiogenic capacity. The difference observed might be attributed to differences in cell source, generation of CM or choice of assays. For our study, we used human endothelial cells for the *in vitro* assays and to evaluate *in vivo* angiogenesis, we have performed the CAM assay. Taken together, there is a strong indication that the CM is pro-angiogenic while the Matrigel tube-formation assay, focuses on the network organization of cells which is not indicative for angiogenesis (Simons et al., 2015). The CAM assay comes with the limitation that human secreted factors are used to induce avian blood vessel formation. Furthermore, this assay provides a rather qualitative assessment of the angiogenesis modulating capacity of a factor. This might have (partly) caused the absence of an observed effect of blocking Serpin E1 or IHH in this assay. It is also possible that further improvement of the already pro-angiogenic signal might have not been achievable (i.e., we reached the limits of possible blood vessel formation in the CAM using our CM). We did, however, observe a significant reduction of the pro-angiogenic effect of the secretome when using a VEGFa blocking antibody, indicating that modulation of angiogenesis induced by CM from BMSC in the CAM assay is possible. Interestingly, the inhibition of angiogenesis using VEGFa blocking antibodies was absent in the *in vitro* angiogenesis assays. The blocking antibody was checked for its function against recombinant VEGF where a diminished pro-angiogenic effect *in vitro* was observed. This suggests that VEGFa in the CM does not primarily act on endothelial cell migration or proliferation but could influence other sub-processes of angiogenesis (Shin et al., 2016). Furthermore, it was previously shown that the BMSC derived cartilage secretome contains VEGF (Farrell et al., 2009).

Initially, we expected to identify pro-angiogenic proteins by selecting factors upregulated in the pre-hypertrophic and

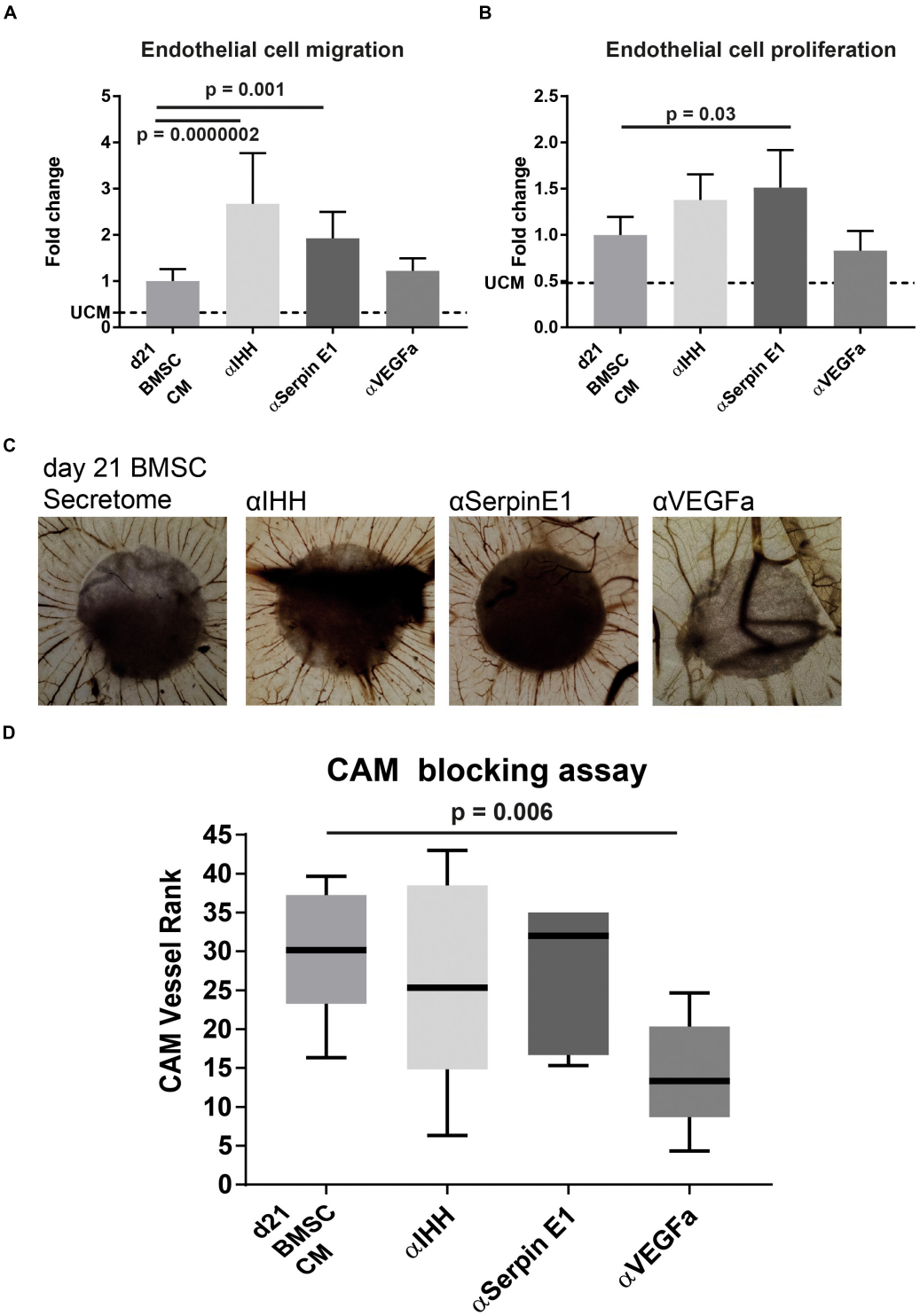

FIGURE 5 | Blocking IHH or Serpin E1 increased angiogenic potential of CM of chondrogenically differentiated BMSC *in vitro* and showed no effect *in vivo* CAM assay. **(A)** Quantification of endothelial cell migration assay comparing the impact of pre-incubation of CM with blocking antibodies for factors of interest. Values are normalized to the BMSC-CM condition. UCM depicts the un-conditioned medium. **(B)** Quantification of endothelial cell proliferation assay comparing the impact of pre-incubation of CM with blocking antibodies for factors of interest. Values are normalized to the BMSC-CM condition. UCM depicts the un-conditioned medium. **(C)** Images of chick chorioallantoic membrane incubated for 72 h with CM (blocked for 30 min) soaked 5 mm filter disks. Filter circles were placed on a vessel free area on day 7 of the chick development. **(D)** Boxplot depicting the ranking of the angiogenic potential (lowest = 1 highest = 45: average of 3 independent observers: box = interquartile range, whiskers + 1–99%). *N* = 5 per condition. A & B were performed in two batches each pooling 3 donors; *n* = 3. Significance was determined by mixed-linear model with Bonferroni *post hoc* test.

hypertrophic zone of the growth plate and in transient cartilage generated by BMSCs. However, our two top hits were anti-angiogenic in our assays. In order to identify possible factors that are not categorized in gene ontology tools as "angiogenesis regulating" we removed this criterion from our search and ran the *in silico* analysis again. The previously described selection pipeline was repeated for both the growth plate and the human BMSC-derived cartilage microarray datasets, excluding the extra criterion of "known angiogenic factors." Comparing the expression profiles, the lists of differentially expressed secreted factors lead to the identification of 16 genes encoding for secreted factors: *MMP10, HPSE, TOR3A, PENK, SRGN, LOX, IGFBP3, MMP11, COL10A1, IGFBP5, COL5A2, GAS6, POSTN, F13A1, SPON2, EPDR1*. These were uniquely upregulated in transient cartilage generated by BMSCs compared to neonatal articular cartilage and in the pre-/hypertrophic zone of the GP compared to the proliferative zone. One or more of these 16 factors might hold the explanation for the partially VEGFa independent pro-angiogenic potential shown by the CM.

This study focused on the angiogenic potential of BMSC-derived cartilaginous constructs, which are known to undergo endochondral ossification after subcutaneous implantation (Scotti et al., 2010; Farrell et al., 2011; Staines et al., 2013; Thompson et al., 2015). This process is dependent on the invasion of blood vessels, likely due to the pro-angiogenic capacity of the secretome (Gerber et al., 1999; Yang et al., 2012; Grosso et al., 2017). The set-up of our study had some limitations. Since we have pooled conditioned medium of three donors, not considering the sex of the donor we cannot exclude sex-dependent differences. Moreover, BMSC were obtained from patient with osteoarthritis. Although chondrogenically differentiated BMSC derived from healthy and OA donors have both demonstrated to undergo endochondral ossification when implanted *in vivo* (Yang et al., 2015) – which was also demonstrated in other mammals (Janicki et al., 2011; Sheehy et al., 2015) – we cannot fully exclude that the disease might have affected the angiogenic potential of the cells. Finally, it is well known that undifferentiated BMSC have a pro-angiogenic capability (Du et al., 2016) as well. Whether or not the factors secreted by chondrogenically differentiated BMSC are similar or different to undifferentiated BMSC remains to be investigated.

The work presented in this article shows that the secretome from chondrogenically differentiated human bone marrow derived BMSCs is pro-angiogenic. We further show that IHH and Serpin E1 are uniquely upregulated factors during chondrogenesis and endochondral ossification that act in an anti-angiogenic fashion in this context. This might be useful in articular cartilage repair approaches by taking advantage of the anti-angiogenic capacity demonstrated by IHH & Serpin E1. Furthermore, identification of a unique pro-angiogenic secreted factor to target would also offer potential solutions for the generation of stable articular cartilage. On the other hand, chondrogenic differentiation of adult human BMSCs provides a pro-angiogenic secretome that may be used to enhance bone regeneration and repair, which could be further enhanced by reducing the effect of IHH & Serpin E1.

DATA AVAILABILITY STATEMENT

The human datasets for this article is available in the GEO-Microarray database (GSE140861). The murine growth-plate microarray data is available in the GEO-Microarray database (GSE144362).

ETHICS STATEMENT

The studies involving human participants were reviewed and approved by the Medical Ethical Committee Erasmus MC. The patients/participants provided their written informed consent to participate in this study.

AUTHOR CONTRIBUTIONS

YN was involved in the conception and design, collection of data, data analysis, interpretation, and manuscript drafting and editing. EF was involved in the conception, data analysis, interpretation, manuscript drafting, and editing. WK was involved in the collection of data and editing of materials and methods. RS and AC was involved in the data analysis and interpretation of the human microarray dataset, and manuscript editing. BB was involved in the data analysis and interpretation of the murine microarray dataset, and manuscript editing. GO was involved in the conception and design, data analysis and interpretation, and manuscript drafting and editing. All authors approved the final version of the manuscript.

FUNDING

This project has received funding from the European Union's Horizon 2020 Research and Innovation Programme under the Marie Skłodowska-Curie grant agreement no. 721432 CarBon. This research was funded in part by a grant from the NIH/NIBIB: 1P41EB021911 CWRU Center for Multimodal Evaluation of Engineered Cartilage.

ACKNOWLEDGMENTS

We are grateful to Steve Allen, Jan de Swart, and Gabrielle Doeswijk for sharing their expertise on fertilized chicken eggs. Further we want to thank Shorouk Fahmy Garcia, Andrea Lolli, Enrique Andres Sastre, and Janneke Witte-Bouma for ranking the CAM images. This work was performed within the framework of the Erasmus Postgraduate School Molecular Medicine and Medical Delta Regenerative Medicine 4D program.

REFERENCES

Bara, J. J., McCarthy, H. E., Humphrey, E., Johnson, W. E., and Roberts, S. (2014). Bone marrow-derived mesenchymal stem cells become antiangiogenic when chondrogenically or osteogenically differentiated: implications for bone and cartilage tissue engineering. *Tissue Eng. Pt. A* 20, 147–159. doi: 10.1089/ten.tea.2013.0196

Belluoccio, D., Etich, J., Rosenbaum, S., Frie, C., Grskovic, I., Stermann, J., et al. (2010). Sorting of growth plate chondrocytes allows the isolation and characterization of cells of a defined differentiation status. *J. Bone Miner. Res.* 25, 1267–1281. doi: 10.1002/jbmr.30

Bulstra, S. K., Drukker, J., Kuijer, R., Buurman, W. A., and van der Linden, A. J. (1993). Thionin staining of paraffin and plastic embedded sections of cartilage. *Biotech. Histochem.* 68, 20–28. doi: 10.3109/10520299309105572

Chapouly, C., Guimbal, S., Hollier, P. L., and Renault, M. A. (2019). Role of hedgehog signaling in vasculature development, differentiation, and maintenance. *Int. J. Mol. Sci.* 20:3076. doi: 10.3390/ijms20123076

Chinchilla, P., Xiao, L., Kazanietz, M. G., and Riobo, N. A. (2010). Hedgehog proteins activate pro-angiogenic responses in endothelial cells through non-canonical signaling pathways. *Cell Cycle* 9, 570–579. doi: 10.4161/cc.9.3.10591

Chung, U. I., Schipani, E., McMahon, A. P., and Kronenberg, H. M. (2001). Indian hedgehog couples chondrogenesis to osteogenesis in endochondral bone development. *J. Clin. Invest.* 107, 295–304. doi: 10.1172/jci11706

Colnot, C., de la Fuente, L., Huang, S., Hu, D., Lu, C., St-Jacques, B., et al. (2005). Indian hedgehog synchronizes skeletal angiogenesis and perichondrial maturation with cartilage development. *Development* 132, 1057–1067. doi: 10.1242/dev.01649

Cui, J. H., Park, S. R., Park, K., Choi, B. H., and Min, B. H. (2007). Preconditioning of mesenchymal stem cells with low-intensity ultrasound for cartilage formation in vivo. *Tissue Eng.* 13, 351–360. doi: 10.1089/ten.2006.0080

DeSimone, D. P., and Reddi, A. H. (1992). Vascularization and endochondral bone development: changes in plasminogen activator activity. *J. Orthop. Res.* 10, 320–324. doi: 10.1002/jor.1100100303

Devy, L., Blacher, S., Grignet-Debrus, C., Bajou, K., Masson, V., Gerard, R. D., et al. (2002). The pro- or antiangiogenic effect of plasminogen activator inhibitor 1 is dose dependent. *FASEB J.* 16, 147–154. doi: 10.1096/fj.01-0552com

Du, W. J., Chi, Y., Yang, Z. X., Li, Z. J., Cui, J. J., Song, B. Q., et al. (2016). Heterogeneity of proangiogenic features in mesenchymal stem cells derived from bone marrow, adipose tissue, umbilical cord, and placenta. *Stem Cell Res. Ther.* 7:163.

Farrell, E., Both, S. K., Odorfer, K. I., Koevoet, W., Kops, N., O'Brien, F. J., et al. (2011). In-vivo generation of bone via endochondral ossification by in-vitro chondrogenic priming of adult human and rat mesenchymal stem cells. *BMC Musc. Disord* 12:31. doi: 10.1186/1471-2474-12-31

Farrell, E., van der Jagt, O. P., Koevoet, W., Kops, N., van Manen, C. J., Hellingman, C. A., et al. (2009). Chondrogenic priming of human bone marrow stromal cells: a better route to bone repair? *Tissue Eng. Pt. C Methods* 15, 285–295. doi: 10.1089/ten.tec.2008.0297

Gerber, H. P., Vu, T. H., Ryan, A. M., Kowalski, J., Werb, Z., and Ferrara, N. (1999). VEGF couples hypertrophic. *Nat. Med.* 5, 623–628. doi: 10.1038/9467

Grosso, A., Burger, M. G., Lunger, A., Schaefer, D. J., Banfi, A., and Di Maggio, N. (2017). It takes two to tango: coupling of angiogenesis and osteogenesis for bone regeneration. *Front. Bioeng. Biotechnol.* 5:68. doi: 10.3389/fbioe.2017.00068

Hellingman, C. A., Koevoet, W., Kops, N., Farrell, E., Jahr, H., Liu, W., et al. (2010). Fibroblast growth factor receptors in in vitro and in vivo chondrogenesis: relating tissue engineering using adult mesenchymal stem cells to embryonic development. *Tissue Eng. Pt. A* 16, 545–556. doi: 10.1089/ten.TEA.2008.0551

Hynes, R. O., and Naba, A. (2012). Overview of the matrisome–an inventory of extracellular matrix constituents and functions. *Cold Spring Harb. Perspect. Biol.* 4:a004903. doi: 10.1101/cshperspect.a004903

Iruela-Arispe, M. L., and Dvorak, H. F. (1997). Angiogenesis: a dynamic balance of stimulators and inhibitors. *Thromb. Haemost.* 78, 672–677. doi: 10.1055/s-0038-1657610

Isogai, C., Laug, W. E., Shimada, H., Declerck, P. J., Stins, M. F., Durden, D. L., et al. (2001). Plasminogen activator inhibitor-1 promotes angiogenesis by stimulating endothelial cell migration toward fibronectin. *Cancer Res.* 61, 5587–5594.

Janicki, P., Boeuf, S., Steck, E., Egermann, M., Kasten, P., and Richter, W. (2011). Prediction of in vivo bone forming potency of bone marrow-derived human mesenchymal stem cells. *Eur. Cell Mater.* 21, 488–507.

Marino, R. (2011). Growth plate biology: new insights. *Curr. Opin. Endocrinol. Diabetes Obes.* 18, 9–13. doi: 10.1097/MED.0b013e3283423df9

Ohba, S. (2016). Hedgehog signaling in endochondral ossification. *J. Dev. Biol.* 4:20. doi: 10.3390/jdb4020020

Otrock, Z. K., Mahfouz, R. A., Makarem, J. A., and Shamseddine, A. I. (2007). Understanding the biology of angiogenesis: review of the most important molecular mechanisms. *Blood Cells Mol. Dis.* 39, 212–220. doi: 10.1016/j.bcmd.2007.04.001

Pathan, M., Keerthikumar, S., Ang, C. S., Gangoda, L., Quek, C. Y., Williamson, N. A., et al. (2015). FunRich: an open access standalone functional enrichment and interaction network analysis tool. *Proteomics* 15, 2597–2601. doi: 10.1002/pmic.201400515

Pelttari, K., Winter, A., Steck, E., Goetzke, K., Hennig, T., Ochs, B. G., et al. (2006). Premature induction of hypertrophy during in vitro chondrogenesis of human mesenchymal stem cells correlates with calcification and vascular invasion after ectopic transplantation in SCID mice. *Arthritis Rheum.* 54, 3254–3266. doi: 10.1002/art.22136

Pepper, M. S. (2001). Role of the matrix metalloproteinase and plasminogen activator-plasmin systems in angiogenesis. *Arterioscler. Thromb. Vasc. Biol.* 21, 1104–1117. doi: 10.1161/hq0701.093685

Pittenger, M. F., Mackay, A. M., Beck, S. C., Jaiswal, R. K., Douglas, R., Mosca, J. D., et al. (1999). Multilineage potential of adult human mesenchymal stem cells. *Science* 284, 143–147. doi: 10.1126/science.284.5411.143

Ribatti, D., Nico, B., Vacca, A., and Presta, M. (2006). The gelatin sponge-chorioallantoic membrane assay. *Nat. Protoc.* 1, 85–91. doi: 10.1038/nprot.2006.13

Rocha, B., Calamia, V., Casas, V., Carrascal, M., Blanco, F. J., and Ruiz-Romero, C. (2014). Secretome analysis of human mesenchymal stem cells undergoing chondrogenic differentiation. *J. Proteome Res.* 13, 1045–1054. doi: 10.1021/pr401030n

Schindelin, J., Arganda-Carreras, I., Frise, E., Kaynig, V., Longair, M., Pietzsch, T., et al. (2012). Fiji: an open-source platform for biological-image analysis. *Nat. Methods* 9, 676–682. doi: 10.1038/nmeth.2019

Scotti, C., Tonnarelli, B., Papadimitropoulos, A., Scherberich, A., Schaeren, S., Schauerte, A., et al. (2010). Recapitulation of endochondral bone formation using human adult mesenchymal stem cells as a paradigm for developmental engineering. *Proc. Natl. Acad. Sci. U.S.A.* 107, 7251–7256. doi: 10.1073/pnas.1000302107

Sheehy, E. J., Mesallati, T., Vinardell, T., and Kelly, D. J. (2015). Engineering cartilage or endochondral bone: a comparison of different naturally derived hydrogels. *Acta Biomater.* 13, 245–253. doi: 10.1016/j.actbio.2014.11.031

Shin, M., Beane, T. J., Quillien, A., Male, I., Zhu, L. J., and Lawson, N. D. (2016). Vegfa signals through ERK to promote angiogenesis, but not artery differentiation. *Development* 143, 3796–3805. doi: 10.1242/dev.137919

Simons, M., Alitalo, K., Annex, B. H., Augustin, H. G., Beam, C., Berk, B. C., et al. (2015). State-of-the-art methods for evaluation of angiogenesis and tissue vascularization: a scientific statement from the american heart association. *Circ. Res.* 116, e99–e132.

Somoza, R. A., Correa, D., Labat, I., Sternberg, H., Forrest, M. E., Khalil, A. M., et al. (2018). Transcriptome-wide analyses of human neonatal articular cartilage and human mesenchymal stem cell-derived cartilage provide a new molecular target for evaluating engineered cartilage. *Tissue Eng. Pt. A* 24, 335–350. doi: 10.1089/ten.tea.2016.0559

Somoza, R. A., Welter, J. F., Correa, D., and Caplan, A. I. (2014). Chondrogenic differentiation of mesenchymal stem cells: challenges and unfulfilled expectations. *Tissue Eng. Pt. B Rev.* 20, 596–608. doi: 10.1089/ten.TEB.2013.0771

Staines, K. A., Pollard, A. S., McGonnell, I. M., Farquharson, C., and Pitsillides, A. A. (2013). Cartilage to bone transitions in health and disease. *J. Endocrinol.* 219, R1–R12. doi: 10.1530/JOE-13-0276

Stefansson, S., McMahon, G. A., Petitclerc, E., and Lawrence, D. A. (2003). Plasminogen activator inhibitor-1 in tumor growth, angiogenesis and vascular remodeling. *Curr. Pharm. Des.* 9, 1545–1564. doi: 10.2174/1381612033454621

Stefansson, S., Petitclerc, E., Wong, M. K., McMahon, G. A., Brooks, P. C., and Lawrence, D. A. (2001). Inhibition of angiogenesis in vivo by plasminogen activator inhibitor-1. *J. Biol. Chem.* 276, 8135–8141.

Thompson, E. M., Matsiko, A., Farrell, E., Kelly, D. J., and O'Brien, F. J. (2015). Recapitulating endochondral ossification: a promising route to in vivo bone regeneration. *J. Tissue Eng. Regen. Med.* 9, 889–902. doi: 10.1002/term.1918

Walzer, S. M., Cetin, E., Grubl-Barabas, R., Sulzbacher, I., Rueger, B., Girsch, W., et al. (2014). Vascularization of primary and secondary ossification centres in the human growth plate. *BMC Dev. Biol.* 14:36. doi: 10.1186/s12861-014-0036-7

Wu, J., Strawn, T. L., Luo, M., Wang, L., Li, R., Ren, M., et al. (2015). Plasminogen activator inhibitor-1 inhibits angiogenic signaling by uncoupling vascular endothelial growth factor receptor-2-alphaVbeta3 integrin cross talk. *Arterioscler. Thromb. Vasc. Biol.* 35, 111–120. doi: 10.1161/atvbaha.114.304554

Yang, W., Both, S. K., van Osch, G. J., Wang, Y., Jansen, J. A., and Yang, F. (2015). Effects of in vitro chondrogenic priming time of bone-marrow-derived mesenchymal stromal cells on in vivo endochondral bone formation. *Acta Biomater.* 13, 254–265. doi: 10.1016/j.actbio.2014.11.029

Yang, Y. Q., Tan, Y. Y., Wong, R., Wenden, A., Zhang, L. K., and Rabie, A. B. (2012). The role of vascular endothelial growth factor in ossification. *Int. J. Oral. Sci.* 4, 64–68.

Yoo, J. U., Barthel, T. S., Nishimura, K., Solchaga, L., Caplan, A. I., Goldberg, V. M., et al. (1998). The chondrogenic potential of human bone-marrow-derived mesenchymal progenitor cells. *J. Bone Joint Surg. Am.* 80, 1745–1757.

Yuasa, M., Mignemi, N. A., Nyman, J. S., Duvall, C. L., Schwartz, H. S., Okawa, A., et al. (2015). Fibrinolysis is essential for fracture repair and prevention of heterotopic ossification. *J. Clin. Invest.* 125:3723. doi: 10.1172/jci84059

Zimmermann, P., Boeuf, S., Dickhut, A., Boehmer, S., Olek, S., and Richter, W. (2008). Correlation of COL10A1 induction during chondrogenesis of mesenchymal stem cells with demethylation of two CpG sites in the COL10A1 promoter. *Arthritis Rheum.* 58, 2743–2753. doi: 10.1002/art.23736

Conflict of Interest: The authors declare that the research was conducted in the absence of any commercial or financial relationships that could be construed as a potential conflict of interest.

frontiers in Bioengineering and Biotechnology

ORIGINAL RESEARCH
published: 30 June 2020
doi: 10.3389/fbioe.2020.00658

Enhanced Chondrogenic Capacity of Mesenchymal Stem Cells After TNFα Pre-treatment

Chantal Voskamp[1], *Wendy J. L. M. Koevoet*[2], *Rodrigo A. Somoza*[3], *Arnold I. Caplan*[3], *Véronique Lefebvre*[4], *Gerjo J. V. M. van Osch*[1,2] *and Roberto Narcisi*[1]*

[1] Department of Orthopaedics, Erasmus MC, University Medical Center, Rotterdam, Netherlands, [2] Department of Otorhinolaryngology, Erasmus MC, University Medical Center, Rotterdam, Netherlands, [3] Department of Biology and Skeletal Research Center, Case Western Reserve University, Cleveland, OH, United States, [4] Division of Orthopedic Surgery, Department of Surgery, Children's Hospital of Philadelphia, Philadelphia, PA, United States

Mesenchymal stem cells (MSCs) are promising cells to treat cartilage defects due to their chondrogenic differentiation potential. However, an inflammatory environment during differentiation, such as the presence of the cytokine TNFα, inhibits chondrogenesis and limits the clinical use of MSCs. On the other hand, it has been reported that exposure to TNFα during *in vitro* expansion can increase proliferation, migration, and the osteogenic capacity of MSCs and therefore can be beneficial for tissue regeneration. This indicates that the role of TNFα on MSCs may be dependent on the differentiation stage. To improve the chondrogenic capacity of MSCs in the presence of an inflamed environment, we aimed to determine the effect of TNFα on the chondrogenic differentiation capacity of MSCs. Here, we report that TNFα exposure during MSC expansion increased the chondrogenic differentiation capacity regardless of the presence of TNFα during chondrogenesis and that this effect of TNFα during expansion was reversed upon TNFα withdrawal. Interestingly, pre-treatment with another pro-inflammatory cytokine, IL-1β, did not increase the chondrogenic capacity of MSCs indicating that the pro-chondrogenic effect is specific for TNFα. Finally, we show that TNFα pre-treatment increased the levels of SOX11 and active β-catenin suggesting that these intracellular effectors may be useful targets to improve MSC-based cartilage repair. Overall, these results suggest that TNFα pre-treatment, by modulating SOX11 levels and WNT/β-catenin signaling, could be used as a strategy to improve MSC-based cartilage repair.

Keywords: mesenchymal stem cells, tumor necrosis factor-alpha, cartilage, regenerative medicine, SOXC transcription factors, chondrogenesis, tissue engineering

OPEN ACCESS

Edited by:
Martin James Stoddart, AO Research Institute, Switzerland

Reviewed by:
Anna Lange-Consiglio, University of Milan, Italy
Travis Klein, Queensland University of Technology, Australia
Susanne Grässel, University of Regensburg, Germany

***Correspondence:**
Roberto Narcisi
r.narcisi@erasmusmc.nl

Specialty section:
This article was submitted to Tissue Engineering and Regenerative Medicine, a section of the journal Frontiers in Bioengineering and Biotechnology

Received: *27 February 2020*
Accepted: *27 May 2020*
Published: *30 June 2020*

Citation:
Voskamp C, Koevoet WJLM, Somoza RA, Caplan AI, Lefebvre V, van Osch GJVM and Narcisi R (2020) Enhanced Chondrogenic Capacity of Mesenchymal Stem Cells After TNFα Pre-treatment. Front. Bioeng. Biotechnol. 8:658. doi: 10.3389/fbioe.2020.00658

INTRODUCTION

Cartilage has a limited repair capacity and, if left untreated after damage, it will often undergo progressive, irreversible degeneration. The treatment of cartilage defects still remains challenging and novel regenerative medicine strategies are needed. Mesenchymal stem cells (MSCs) are promising cells for cell-based cartilage regeneration approaches (Caplan, 1991; Caplan and Dennis, 2006) because ease of isolation, chondrogenic potential (Johnstone et al., 1998; Pittenger et al., 1999) and anti-inflammatory properties (Kinnaird et al., 2004; Caplan and Dennis, 2006; Ren et al., 2008; van Buul et al., 2012). These properties can be affected by factors present in the microenvironment,

such as pro-inflammatory cytokines. TNFα is one of the pro-inflammatory cytokines that can be present in symptomatic cartilage defects (Tsuchida et al., 2014), osteoarthritic cartilage and synovium (Chu et al., 1991; Kapoor et al., 2011; Tsuchida et al., 2014), and that contributes to the pathophysiology of osteoarthritis (reviewed by Fernandes et al., 2002; Goldring and Otero, 2011).

Exposure to TNFα during MSC chondrogenesis *in vitro* reduces the chondrogenic capacity (Wehling et al., 2009), increasing the expression of aggrecanases and decreasing expression of proteoglycans (Markway et al., 2016). However TNFα is known to be involved in several biological processes such as apoptosis, proliferation and cell survival (Brenner et al., 2015; Cheng et al., 2019). In addition, there is also evidence that TNFα can promote tissue regeneration since it can increase osteogenesis (Daniele et al., 2017) and MSC proliferation and migration (Bocker et al., 2008; Bai et al., 2017; Shioda et al., 2017). It has been shown that MSCs primed with TNFα *in vitro* survive better than control MSCs when transplanted *in vivo* (Giannoni et al., 2010). Overall these data suggest that the effect of TNFα may depend on the dynamics of exposure and that its effect may be beneficial for MSC-based tissue regeneration. Specifically, the effect on chondrogenesis of TNFα administration during MSC expansion has been incompletely investigated whether in the presence or absence of an inflamed environment during the subsequent phase of cell differentiation.

In order to increase the chondrogenic capacity of MSCs under inflammatory conditions, we hypothesized that TNFα administration during cell expansion (pre-treatment) would have a beneficial effect on the subsequent chondrogenesis performed in the presence of TNFα. Here we demonstrated that TNFα pre-treatment increases MSC chondrogenesis regardless of the presence of TNFα during differentiation and that the effect of TNFα on the chondrogenic capacity is reversible. This pro-chondrogenic effect could not be obtained by pre-treatment with interleukin 1β (IL-1β) another pro-inflammatory cytokine involved in local inflammation in the joint (Goldring and Otero, 2011). Finally, to identify a possible TNFα target pathway in the pre-treated MSCs, we investigated the levels of the SOXC protein (SOX4 and SOX11), this group of SRY-related transcription factors was previously described to be stabilized by TNFα and involved in cartilage primordia and growth plate formation (Kato et al., 2015; Bhattaram et al., 2018). In addition, we also analyzed active β-catenin levels, since SOXC can increase β-catenin protein levels (Bhattaram et al., 2014) and WNT/β-catenin signaling can increase the chondrogenic potential of MSCs (Narcisi et al., 2015).

MATERIALS AND METHODS

MSC Isolation and Expansion

MSCs were isolated from human bone marrow aspirates from patients (17–73 years old, **Table S1**) undergoing total hip replacement after informed consent and with approval of the ethics committee (MEC 2015-644: Erasmus MC, Rotterdam). Patients with radiation therapy in the hip area, hematologic disorders and mental retardation or dementia were excluded from our study population. MSCs were isolated by plastic adherence and the day after seeding the non-adherent cells were washed away with PBS with 1% fetal calf serum (Gibco, selected batch 41Q2047K). They were cultured in alpha-MEM (Invitrogen), with 10% fetal calf serum, 1.5 μg/ml fungizone (Gibco), 50 μg/ml gentamicin (Invitrogen), 1 ng/ml FGF2 (AbD Serotec), and 0.1 mM ascorbic acid-2-phosphate (Sigma-Aldrich). After 10–12 days, the MSCs were trypsinized and re-seeded at a density of 2,300 cells/cm^2. MSCs in our study were selected based on their capacity to chondrogenically differentiate, their MSC morphology (small elongated and spindle-shaped cells) and expansion capacity (cells with less than 0.15 doublings/day were excluded). To investigate whether exposure to TNFα during expansion prior to chondrogenic differentiation (pre-treatment) could inhibit the negative effect of TNFα, MSCs were pre-treated with different concentrations of TNFα (0, 1, 10, or 50 ng/ml TNFα, PeproTech) for different exposure times 24 h, 4–6 days (1 passage) or 8–10 days (2 passages), and then chondrogenically differentiated in the presence of 0 or 1 ng/ml TNFα. When indicated, MSCs were first treated with TNFα for 1 passage (4 days) followed by removal of TNFα for 1 passage (4 days) and subsequently chondrogenically differentiated in the presence of 1 ng/ml TNFα. To investigate the effect of IL-1β pre-treatment on the chondrogenic differentiation, MSCs were pre-treated for 1 passage with different concentrations of IL-1β (0, 0.1, 1, 10, and 50 ng/ml, PeproTech), followed by chondrogenic differentiation in the absence of IL-1β. MSCs from different donors are indicated as donor 1, 2, 4, 5, 6, 7, 8, or 9.

Chondrogenic Differentiation

To obtain a 3D pellet culture, 2 x 10^5 MSCs were centrifuged at 300 g for 8 min in polypropylene tubes. To induce chondrogenesis, the pelleted cells were cultured in DMEM-HG (Invitrogen), 1% ITS (B&D), 1.5 μg/ml fungizone (Invitrogen), 50 μg/ml gentamicin (Invitrogen), 1 mM sodium pyruvate (Invitrogen), 40 μg/ml proline (Sigma-Aldrich), 10 ng/ml TGFβ1 (R&D Systems), 0.1 mM ascorbic acid 2-phosphate (Sigma-Aldrich), and 100 nM dexamethasone (Sigma-Aldrich), referred to as chondrogenic medium (Johnstone et al., 1998). After 24 h, the medium was renewed with chondrogenic medium with or without 1 ng/ml TNFα, as indicated. Afterwards the medium was renewed two times per week for a period of 4 weeks.

COL2A1 Reporter Assays

Cultures of human bone marrow-derived MSCs from healthy de-identified adult volunteer donors (31–33 years old, **Table S1**) were established as previously described (Lennon and Caplan, 2006) after informed consent. The bone marrow was collected using a procedure reviewed and approved by the University Hospitals of Cleveland Institutional Review Board (IRB# 09-90-195). MSCs from different donors are indicated as donor 3 or 10. Lentiviral constructs for the *COL2A1* promoter were placed upstream of the Gaussia luciferase reporter gene. MSCs were transduced with the *COL2A1* reporter lentivirus as previously

described for a *SOX9* reporter (Correa et al., 2018). MSCs with the *COL2A1* luciferase reporter were expanded as indicated above. At different time points during chondrogenesis, medium of MSCs with the *COL2A1* reporter was harvested 48 h after the last medium renewal. Per condition, 50 μl of the medium was transferred to a white 96-well plate and 20 μM coelenterazine substrate (NanoLight technology) was injected into the wells. The Gaussia Luciferase (Gluc) activity was measured using a GloMax-96 Microplate Luminometer (Promega) in technical duplicates.

CD Marker Analysis

Per condition, 2 x 10^5 MSCs were re-suspended in 500 μl FACSFlow solution (BD Biosciences) and stained with antibodies against human CD45-APC (368515, BioLegend), CD90-APC (FAB2067A, R&D Systems), CD73-PE (550257, BD Biosciences), or CD105-FITC (FAB10971F, R&D Systems), following the manufacturer's guidelines. Afterwards, the cells were fixed using 2% formaldehyde (Fluka) and were filtered through 70-μM filters. Unstained cells were used as a negative control. Samples were analyzed by flow cytometry using a BD Fortessa machine (BD Biosciences). The data were analyzed using FlowJo V10 software.

Apoptosis Analysis

Per condition, 5 x 10^5 MSCs were re-suspended in 1x Binding Buffer and stained with Annexin V and Propidium Iodide using manufacturer's instructions (all products from eBioscience, San Diego, USA). Samples were analyzed by flow cytometry using a BD Fortessa machine (BD Biosciences) and analyzed using FlowJo V10 software.

(Immuno)Histochemistry

After 4 weeks of chondrogenic induction, pellets were fixed with 3.8% formaldehyde, embedded in paraffin and sectioned (6 μm). Glycosaminoglycans (GAG) were stained with 0.04% thionine solution and collagen type-2 was immunostained using a collagen type-2 primary antibody (II-II 6B3, Developmental Studies Hybridoma Bank). Antigen retrieval was performed with 0.1% Pronase (Sigma-Aldrich) in PBS for 30 min at 37°C, followed by incubation with 1% hyaluronidase (Sigma-Aldrich) in PBS for 30 min at 37°C to improve antibody penetration. The slides were pre-incubated with 10% normal goat serum (Sigma-Aldrich) in PBS with 1% bovine serum albumin (BSA; Sigma-Aldrich). Next, the slides were incubated for 1 h with collagen type-2 primary antibody, and then with a biotin-conjugated secondary antibody (HK-325-UM, Biogenex), alkaline phosphatase-conjugated streptavidin (HK-321-UK, Biogenex), and the New Fuchsine chromogen (B467, Chroma Gesellschaft). An IgG1 isotype antibody (X0931, Dako Cytomation) was used as negative control.

DNA and Glycosaminoglycan (GAG) Quantification

After chondrogenic induction for 28 days, pellets were digested using 250 μl digestion solution containing in 1 mg/ml Proteinase K, 1 mM iodoacetamide, 10 μg/ml Pepstatin A in 50 mM Tris, 1 mM EDTA buffer (pH 7.6; all Sigma-Aldrich) for 16 h at 56°C. Next, Proteinase K was inactivated at 100°C for 10 min. To determine the DNA content, 50 μl cell lysate was treated with 100 μl heparin solution (8.3 IU/ml) and 50 μl RNase (0.05 mg/ml) solution for 30 min at 37°C. Next 50 μl ethidium bromide (25 μg/ml) was added and the samples were analyzed on a Wallac 1420 Victor2 plate reader (Perkin-Elmer) using an excitation of 340 nm and an emission of 590 nm. In case the amount of DNA was lower than 1 μg per ml, 50 μl cell lysate was treated with 50 μl heparin solution and 25 μl RNase for 30 min at 37°C. After incubation, 30 μl CYQUANT GR solution (Invitrogen) was added and samples were analyzed on a SpectraMax Gemini plate reader using an excitation of 480 nm and an emission of 520 nm. DNA sodium salt from calf thymus was used as a standard (Sigma-Aldrich). GAG content was determined using the 1,9-dimethylmethylene blue (DMB) assay, as previously described (Farndale et al., 1986). In short, 100 μl cell lysate, containing up to 5 μg GAG, was incubated with 200 μl DMB solution and analyzed using an extinction of 590 nm and 530 nm. Chondroitin sulfate sodium salt from shark cartilage was used as a standard (Sigma-Aldrich).

mRNA Expression Analysis

After chondrogenic induction for 14 or 28 days, pellets were lysed in RNA-Bee (TEL-TEST) and manually homogenized. RNA was extracted using chloroform and purified using the RNeasy Kit (Qiagen), following manufacturer's guidelines. RNA was reverse-transcribed with a RevertAid First Strand cDNA synthesis kit (MBI Fermentas). Real-time polymerase chain reactions were performed with TaqMan Universal PCR MasterMix (Applied Biosystems) or SYBR Green MasterMix (Fermentas) using a CFX96TM PCR detection system (Bio-Rad). Primers are listed in **Table S2** and the genes *GAPDH*, *RPS27A*, and *HPRT1* were used as housekeeping genes. The best housekeeping index (BHI) was calculated using the formula $(Ct^{GAPDH*}\ Ct^{RPS27a*}\ Ct^{HPRT1})^{1/3}$. Relative mRNA levels were calculated using the formula $2^{-\Delta\Delta Ct}$.

Adipogenic Differentiation

To induce differentiation toward the adipogenic lineage, 2 x 10^4 cells/cm^2 were seeded and cultured in DMEM HG (Invitrogen) with 10% fetal calf serum (Gibco), 1.5 μg/ml fungizone (Invitrogen), 50 μg/ml gentamicin (Invitrogen), 1.0 μM dexamethasone (Sigma-Aldrich), 0.2 mM indomethacin (Sigma-Aldrich), 0.01 mg/ml insulin (Sigma-Aldrich) and 0.5 mM 3-isobutyl-l-methyl-xanthine (Sigma-Aldrich) for 14 days. In order to visualize intracellular lipid accumulation, cells were fixed in 3.8% formaldehyde, treated with 0.3% Oil red O solution (Sigma-Aldrich) for 10 min and then washed with distilled water. In addition, *PPARG* mRNA expression was analyzed as indicated above.

Osteogenic Differentiation

To induce differentiation toward the osteogenic lineage, 3 x 10^3 cells/cm^2 were seeded and cultured in DMEM HG (Invitrogen) with 10% fetal calf serum (Gibco), 1.5 μg/ml fungizone

(Invitrogen), 50 μg/ml gentamicin (Invitrogen), 10 mM β-glycerophosphate (Sigma-Aldrich), 0.1 μM dexamethasone (Sigma-Aldrich), and 0.1 mM ascorbic acid-2-phosphate (Sigma-Aldrich) for 14–18 days. For the detection of calcium deposits (Von Kossa staining), cells were fixed in 3.8% formaldehyde, hydrated with distilled water, treated with 5% silver nitrate solution (Sigma-Aldrich) for 60 min in the presence of bright light and then washed with distilled water followed by counterstaining with 0.4% thionine (Sigma-Aldrich). In addition, *ALPL* mRNA expression was analyzed as indicated above.

Western Blot

To test for SMAD2 activation, MSC monolayers were pre-treated for 4 days with 0 or 50 ng/ml TNFα in standard MSC growth medium, followed by serum starvation overnight (16 h) in DMEM-HG (Invitrogen) containing 1% ITS (B&D), 1.5 μg/ml fungizone (Invitrogen), 50 μg/ml gentamicin (Invitrogen), 1 mM sodium pyruvate (Invitrogen), 40 μg/ml proline (Sigma-Aldrich) and 0 or 50 ng/ml TNFα. Next, MSCs were stimulated for 30 min with 0 or 10 ng/ml TGFβ1 in the presence or absence of 1 ng/ml TNFα. To assess the SOXC proteins (SOX11 and SOX4), and (active) β-catenin levels, MSCs were pre-treated for 4 days with 0 or 50 ng/ml TNFα in standard MSC medium. Twenty-four hours prior to harvest, the medium was renewed with standard MSC growth medium containing 0 or 50 ng/ml TNFα. Western blot were made using MSC lysates prepared using M-PER lysis buffer containing 1% Halt Protease Inhibitor and 1% Halt Phosphatase Inhibitor (Thermo Scientific). Total protein concentration was determined using a BCA assay (Thermo Scientific). Eight to ten micrograms of protein was electrophoresed on a 4–12% gradient SDS-PAGE gel. Proteins were transferred to a nitrocellulose membrane (Millipore) by semi-wet transfer, followed by blocking with 5% milk powder dissolved in Tris-buffered saline containing 0.1% Tween (TBST) for 3 h. Membranes were incubated overnight at 4°C with primary antibody according to **Table S3** in 5% BSA in TBST, followed by incubation at room temperature for 1.5 h with peroxidase-conjugated anti-rabbit secondary antibody (Cell Signaling, 7074S) in 5% dry milk in TBST. Proteins were detected using the SuperSignal Wester Pico Complete Rabbit IgG detection kit (ThermoFisher scientific) following manufacturer's instructions.

Statistical Analysis

Data were analyzed using SPSS software (IBM SPSS statistics 25). Normal distribution was tested using the Kolmogorov-Smirnov test. Since the Kolmogorov-Smirnov test showed that the *COL2A1* reporter data was not normally distributed a Mann-Whitney *U*-test was applied to analyze these data. All other data were normally distributed and a linear mixed model, with the different conditions considered as fixed parameters and the donors as random parameters was applied. Bonferroni *post-hoc* tests were performed to correct for multiple comparisons. *P*-values less than 0.05 were considered statistically significant.

RESULTS

MSCs Pre-treated With TNFα Had an Increased Chondrogenic Potential When Subsequently Maintained Under Stimulation by TNFα During Differentiation

To study if TNFα exposure during MSCs expansion (pre-treatment) could inhibit the negative effect of TNFα during chondrogenic differentiation, MSCs were pre-treated with different concentrations of TNFα and incubation time prior to chondrogenic differentiation in the presence of 1 ng/ml TNFα (**Figure S1A**). First, we confirmed that the presence of 1 ng/ml TNFα during the chondrogenic phase reduced the ability of MSCs to differentiate (**Figures S1B–D**; condition 0/0 vs. 0/1). Pre-treatment for 1 passage increased GAG deposition in MSC pellets after chondrogenic induction in the presence of TNFα (**Figure S1C**), with the larger effect occurring when the pre-treatment was performed with 10 and 50 ng/ml TNFα (**Figure S1C**; condition 0/1 vs. 10/1 and 50/1). Pre-treatment with TNFα for 24 h and 2 passages did not have a clear effect on chondrogenesis (**Figures S1B,D**; 0/1 vs. 1/1, 10/1 and 50/1). Given these observations, we performed the rest of the experiments using TNFα pre-treatment for 1 passage (**Figure 1A**).

Next, we analyzed MSCs from four other donors and observed that chondrogenic pellets of MSCs pre-treated for 1 passage with 50 ng/ml TNFα had a higher GAG content after 28 days of chondrogenic induction in the presence of TNFα compared to MSCs without TNFα pre-treatment (**Figure 1B** and **Figure S2A**; 0/1 vs. 50/1, $p = 0.003$), while no effect on DNA content was observed (**Figure S2A**). Moreover, GAG staining demonstrated an increased GAG content in the TNFα pre-treated MSCs at day 28 (**Figure 1C**; 0/1 vs. 50/1). Staining for collagen type-2 did not show differences (**Figure 1D**). No increase in GAG content was observed after pre-treatment for 1 passage with 10 ng/ml TNFα (**Figures 1B,C**). In order to determine whether the effect of 50 ng/ml TNFα is due to an acceleration of chondrogenic differentiation, first a non-destructive luciferase-based method was validated as a proxy for endogenous *COL2A1* expression in pellet cultures (**Figure S3**) and then applied to assess *COL2A1* promoter activation at day 3 and day 7 of chondrogenic differentiation. However, no significant differences were observed in *COL2A1* promoter activation at day 3 and day 7 (**Figure S4A**) of chondrogenesis, suggesting that TNFα pre-treatment did not increase the rate of chondrogenesis during the first week of differentiation. Subsequent analysis performed by RT-PCR on *SOX9*, *COL2A1,* and *ACAN* showed no significant differences at day 14 and 28 during chondrogenesis between the conditions (**Figures S4A,B**).

Overall, these data indicate that pre-treatment of MSC monolayers with 50 ng/ml TNFα significantly increases the chondrogenic potential of MSCs when exposed to 1 ng/ml TNFα during differentiation, but without prompting the onset of chondrocyte marker expression. For this reason,

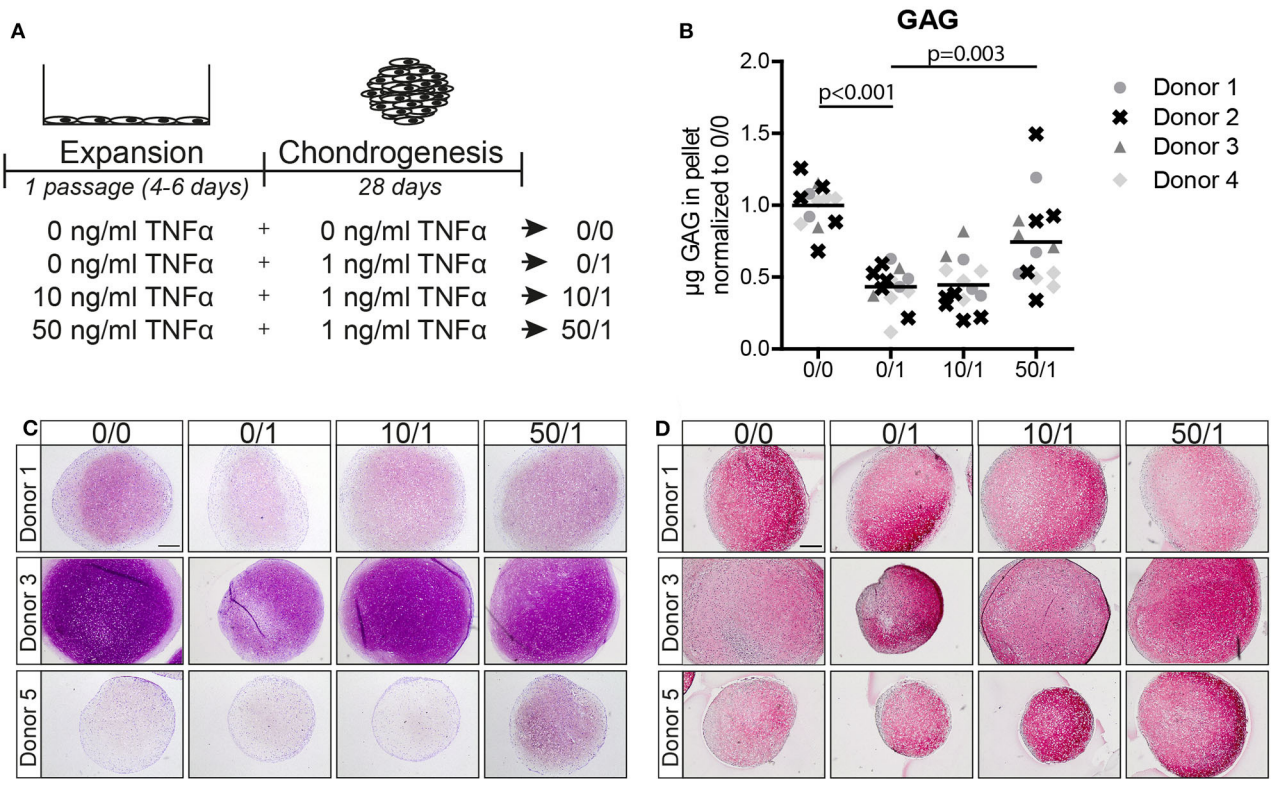

FIGURE 1 | Pre-treatment of MSC monolayers with 50 ng/ml TNFα reduced the inhibitory effect of the cytokine in subsequent chondrogenic conditions. **(A)** Schematic overview of the experiment. **(B)** GAG content of MSC pellets after 28 days of chondrogenic induction. $N = 4$ donors with 2–5 pellets per donor. **(C,D)** Representative images of pellets stained for GAG with **(C)** thionine and **(D)** COL2A1 after 28 days of chondrogenic induction. $N = 5$ donors with 2–3 pellets per donor. Scale bar represents 250 µm.

the following experiments were performed using 50 ng/ml TNFα pre-treatment.

Pre-treatment With TNFα Increased the Chondrogenic Potential of MSCs Regardless the Presence of the Cytokine During Chondrogenic Differentiation

Next, we tested whether the effect of TNFα pre-treatment on the chondrogenic potential of MSCs was dependent on the presence of the cytokine during the differentiation phase. MSCs were pre-treated during expansion with 0 and 50 ng/ml TNFα, followed by chondrogenic induction in the absence of TNFα (**Figure 2A**). Biochemical assays determined that chondrogenic pellets of MSCs pre-treated with TNFα had a higher GAG concentration ($p = 0.011$; **Figure 2B** and **Figure S2B**) and DNA content (**Figure S2B**). Histological staining confirmed increased GAG accumulation (**Figure 2C**), while no clear effect on collagen type-2 content was observed after chondrogenic induction (**Figure 2D**). To further investigate the effect of TNFα pre-treatment on the speed of chondrogenic induction in the absence of TNFα, we determined *COL2A1* promoter activation over time using a *COL2A1* luciferase reporter system. Analysis on 3-day pellet cultures indicated that TNFα pre-treated MSCs had enhanced luciferase activity, while no differences between the conditions were observed at day 7 (**Figure 2E**). These data suggest that TNFα pre-treatment accelerates chondrogenic differentiation probably via an early induction of *COL2A1* expression among other genes. These data indicate that TNFα pre-treatment increases the chondrogenic potential of the MSCs regardless of the presence of TNFα during chondrogenesis.

To better understand the effect of the TNFα pre-treatment on MSCs and the specificity for the chondrogenic lineage, we determined if TNFα increased apoptosis, expansion, and multilineage differentiation potential. No clear effect on apoptotic rates was observed after 24 h or 5 days of exposure to TNFα (**Figures S5A,B**), but a slight increase in MSC expansion capacity was detected after pre-treatment for 1 passage (1.4-fold difference; **Figure S5C**). Adipogenically induced MSCs pre-treated with TNFα showed less lipid accumulation compared to control MSCs ($p = 0.039$; **Figure S5D**) and a reduced *PPARG* expression, which codes for a transcription factor involved in the adipogenic differentiation process (**Figure S5E**). No statistically significant effect of TNFα pre-treatment on the osteogenic differentiation capacity was observed although, on average, mineralization and *ALPL* expression slightly increased

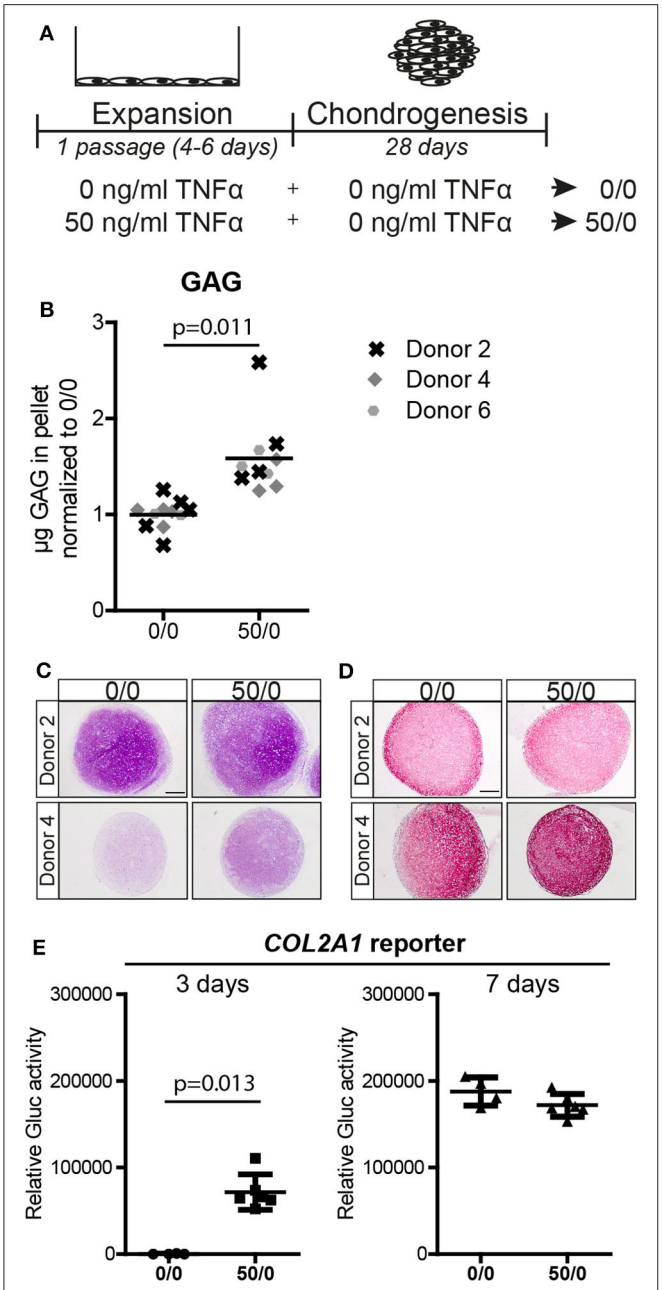

FIGURE 2 | Pre-treatment with 50 ng/ml TNFα increased the chondrogenic potential**. (A)** Schematic overview of the experiment. **(B)** GAG content of MSC pellets after 28 days of chondrogenic induction. $N = 3$ donors with 2–4 pellets per donor. **(C,D)** Representative images of pellets stained for **(C)** GAG with thionine and **(D)** COL2A1 after 28 days of chondrogenic induction. $N = 4$ donors with 2–3 pellets per donor. Scale bar represents 250 µm. **(E)** Relative secreted Gaussia Lucificerase (Gluc) activity of medium from MSC pellets containing the *COL2A1* promoter reporter after 3 and 7 days of chondrogenic induction. Values represent the mean ± SD with 4–6 pellets.

(**Figures S5F,G**). Overall, these data suggest that TNFα pre-treatment specifically enhances the chondrogenic potential of the MSCs.

IL-1β Pre-treatment Did Not Increase the Chondrogenic Potential of MSCs

We then investigated whether the effect of pre-treatment on the chondrogenic potential of MSCs was specific for TNFα or whether IL-1β another pro-inflammatory cytokine can have a similar effect (**Figure 3A**). No differences in GAG deposition were observed after pre-treatment with different concentrations of IL-1β, based on histology (**Figure 3B**), indicating that in contrast to TNFα, IL-1β pre-treatment for 1 passage does not increase the chondrogenic potential of the MSCs. These data suggest distinct effects of TNFα and IL-1β pretreatments on MSCs.

The Effect of TNFα Pre-treatment on the Chondrogenic Capacity and Expression of MSC Marker CD105 Was Reversible

To study whether the effect of TNFα is reversible, MSCs were pre-treated with TNFα for one passage followed by TNFα withdraw for one additional passage and subsequently subjected to chondrogenic differentiation (**Figure 4A**). Interestingly, GAG staining and biochemical assays showed that the positive effect of TNFα on the amount of GAG was lost after TNFα withdrawal ($p < 0.001$; **Figures 4B,C** and **Figure S2C**). No consistent effect on DNA content and collagen type-2 expression was observed after chondrogenic induction (**Figure 4D** and **Figure S2C**). To further characterize the MSCs after TNFα pre-treatment, we analyzed the expression of the MSC markers CD73, CD90, and CD105 (Dominici et al., 2006) together with the negative MSC marker CD45 (hematopoietic marker). In the control condition without TNFα pre-treatment, more than 97% of the MSCs expressed CD73 and CD105, on average 77% of the cells expressed CD90 (**Figure 4E**), while no cells expressed CD45 (data not shown). TNFα administration had no effect on the expression of CD73 and CD90, but it significantly decreased the number of CD105 positive MSCs ($p = 0.013$; **Figure 4E**), indicating that TNFα can modulate the MSC phenotype. Interestingly, the number of CD105 positive cells returned back to control levels after TNFα withdrawal for one passage ($p = 0.020$; **Figure 4E**). These data indicate that the effect of TNFα pre-treatment on MSC chondrogenic capacity and phenotype is reversible.

TNFα Pre-treatment Increased SOX11 and Active β-Catenin Expression in MSCs

To elucidate how TNFα pre-treatment increases the chondrogenic differentiation capacity of MSCs we first evaluated effects on the TGFβ1 signaling pathway, since exposure to TNFα reduced the expression of the TGFβ co-receptor CD105 (**Figure 4E**). MSCs were then stimulated by 10 ng/ml TGFβ1 for 30 min in the presence or absence of 1 ng/ml TNFα. TGFβ1 increased pSMAD2 levels, however the levels were not altered by TNFα pre-treatment (0/1 vs. 50/1 and 0/0 vs. 50/0; **Figures S6A,B**). These data suggested that TNFα pre-treatment does not alter the canonical TGFβ1/SMAD2 signaling pathway in MSCs.

We next studied the effect of TNFα pre-treatment on SOXC proteins, SOX11 and SOX4 in MSCs. The level of SOX11 protein

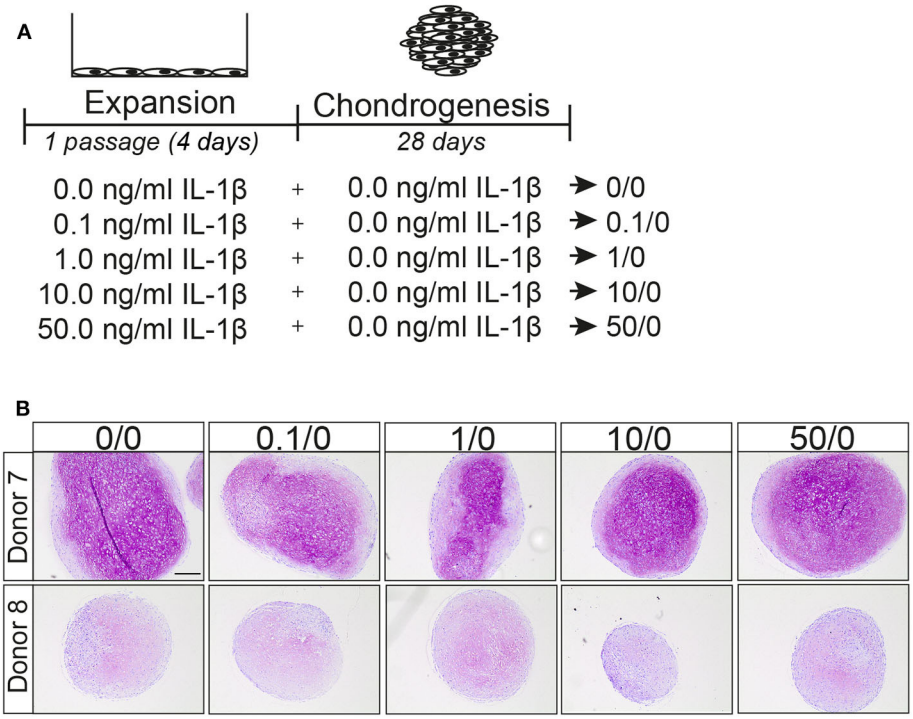

FIGURE 3 | IL-1β pretreatment did not increase the chondrogenic differentiation capacity of MSCs. **(A)** Schematic overview of experiment. **(B)** GAG staining with thionine of MSCs pellets after 28 days culture in chondrogenic medium. Representative image of MSC pretreated for 1 passage with different concentrations IL-1β. $N = 2$ donors with 3 pellets per donor. Scale bar represents 250 μm.

was significantly increased (6.5-fold; $p < 0.001$; **Figure 5A**), while no significant effect was observed for SOX4 ($p = 0.983$; **Figure 5A**). Finally, since SOXC proteins can stabilize β-catenin (Bhattaram et al., 2014), we analyzed the level of active β-catenin in the TNFα pre-treated MSCs. Interestingly, the amount of active β-catenin was increased after TNFα pre-treatment in MSCs (2.0-fold; $p = 0.003$; **Figure 5A**). This suggests that TNFα pre-treatment increased canonical WNT signaling in MSCs, possibly via SOXC stabilization, and thereby enhanced the chondrogenic potential (**Figure 5B**).

DISCUSSION

In this study, we demonstrated that TNFα pre-treatment of MSCs in monolayers reduced the inhibitory effect of TNFα during chondrogenic differentiation by boosting the chondrogenic capacity of these cells. This pro-differentiation effect was both temporal and specific for the chondrogenic lineage and possibly mediated by SOX11 and WNT signaling.

SOX11 is a SOXC protein which TNFα is known to stabilize in fibroblast-like synoviocytes (Bhattaram et al., 2018). SOXC genes play a crucial role in mesenchymal progenitor cell fate during skeletal development (reviewed in Lefebvre and Bhattaram, 2016). In addition, SOXC proteins are known to synergize with canonical WNT signaling via stabilization of β-catenin (Bhattaram et al., 2014). WNT signaling has been shown before to play a role in stem cell fate (ten Berge et al., 2008). We previously showed that induction of WNT signaling during monolayer increases the expansion and chondrogenic potential of MSCs (Narcisi et al., 2015, 2016). A link between SOX11 and WNT signaling has been suggested before in a study with rat MSCs where Sox11 overexpression also increased the β-catenin level and resulted in improved cartilage defect repair (Xu et al., 2019). The results of the current study suggest that SOX11 may play a role during chondrogenesis of human MSCs. Furthermore, we show that the expression of SOX11 in MSCs can be modulated by TNFα.

MSCs are a heterogeneous population of cells with known intra and inter-donor phenotypic and potency variability. This is what we also observed in our study where we used MSCs from both healthy donors and from patients undergoing total hip replacements. In addition, MSCs from patients with a broad age range were used for which we cannot exclude a possible effect of unknown underlying conditions. The differences in the chondrogenic capacity of MSCs in our study could be due to differences in cell subpopulations, since the bone marrow houses MSC subpopulations with different chondrogenic capacities (Sivasubramaniyan et al., 2018). In addition the age of the donor can have an effect on the chondrogenic capacity of MSCs (Payne et al., 2010). Although differences in chondrogenic potential were observed between MSCs from different patients, a similar effect after TNFα stimulation was detected in all cases, indicating that

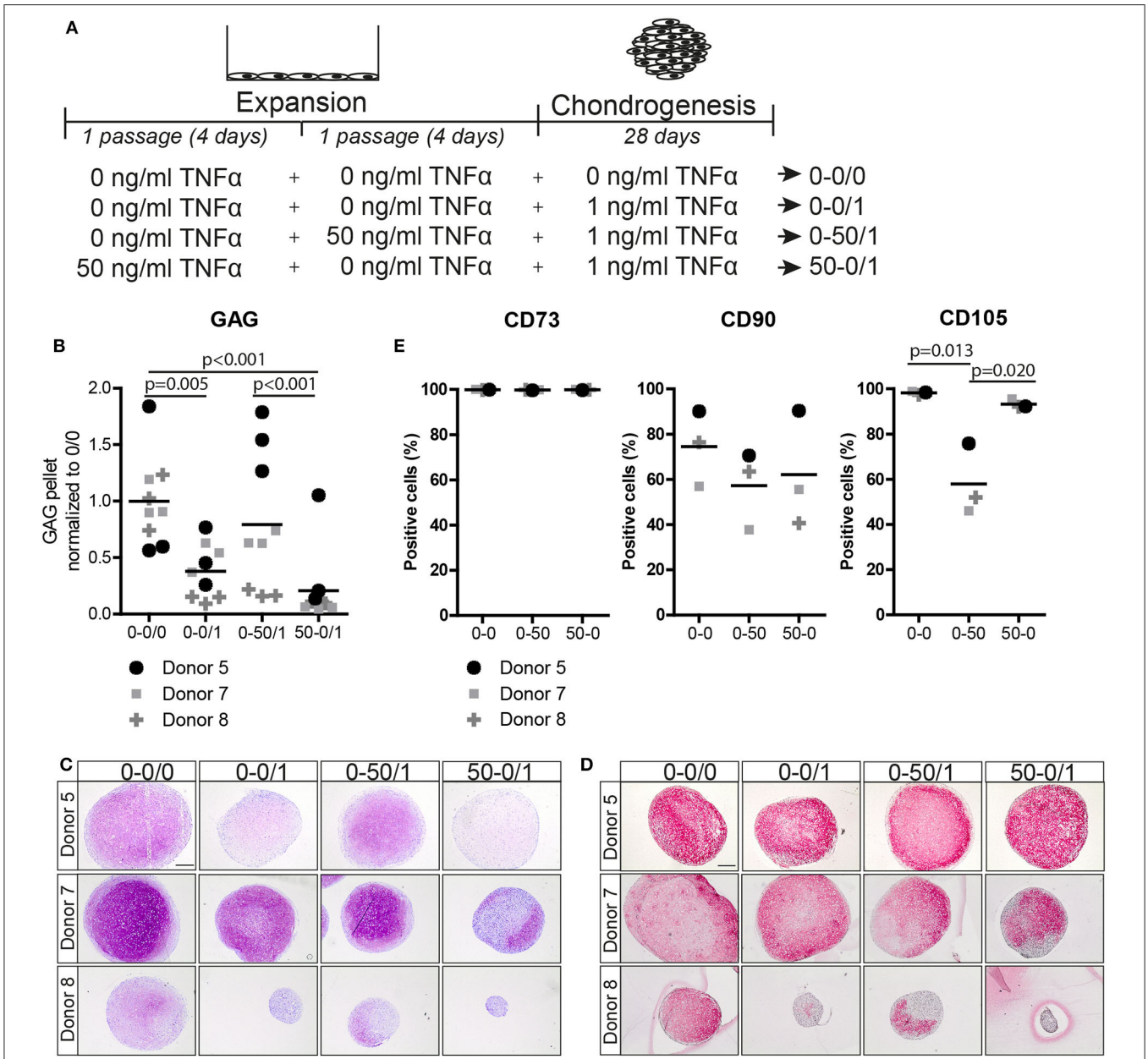

FIGURE 4 | The effect of TNFα pre-treatment on chondrogenesis and MSC marker expression was reversible after TNFα withdraw**. (A)** Schematic overview of the experiment. **(B)** GAG content of MSC pellets after 28 days of chondrogenic induction. *N* = 3 donors with 3 pellets per donor. **(C,D)** Representative images of pellets stained for **(C)** GAG with thionine and **(D)** COL2A1 after 28 days of chondrogenic induction. *N* = 3 donors with 3 pellets per donors. Scale bar represents 250 μm. **(E)** Flow cytometry analysis of surface markers CD73, CD90, and CD105. The values represent the percentage of positive cells for the indicated surface marker, *N* = 3 donors.

TNFα increases the chondrogenic potential of MSCs regardless of their chondrogenic capacity before TNFα pre-treatment.

Immunophenotyping of MSC is often used to characterize the cells (Dominici et al., 2006), even though it is a topic of discussion. We here demonstrated a clear difference in the expression of CD105, a surface marker commonly associated with the MSC phenotype (Haynesworth et al., 1992; Dominici et al., 2006), after pre-treatment with TNFα. In line with our previous work (Cleary et al., 2016), we further confirmed that CD105 is not a good marker to predict the chondrogenic potential of bone marrow-derived MSCs and, on the contrary, its expression was inversely associated with the chondrogenic capacity of MSCs. In addition, we show that the expression of CD105 can be strongly influenced by inflammatory environmental changes. This could be an explanation for contradictory published results regarding CD105 and MSCs

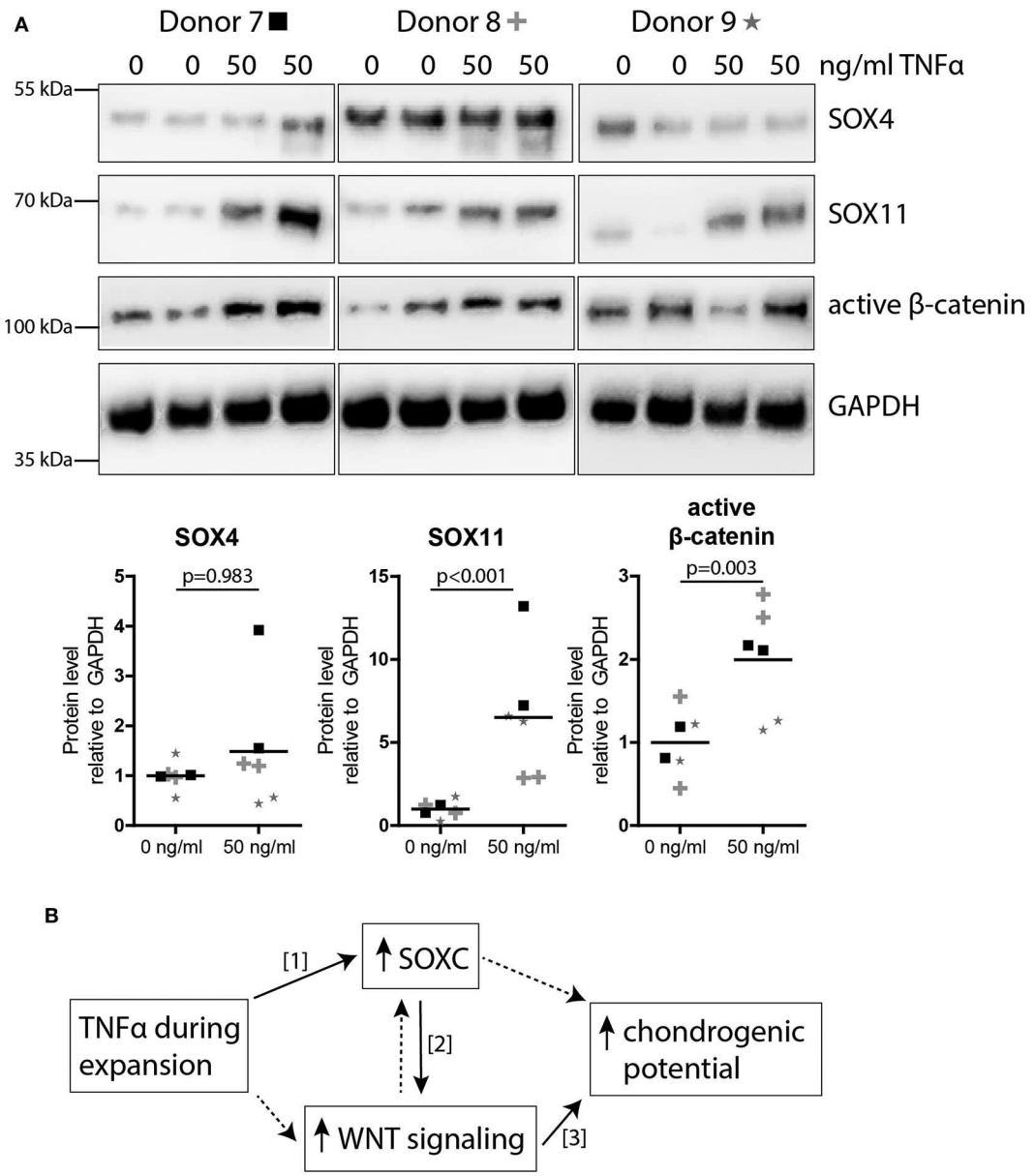

FIGURE 5 | TNFα pre-treatment increased SOXC and active β-catenin expression in MSCs**. (A)** Western blot for SOXC (SOX11 and SOX4, pan-SOXC antibody) and non-phospho (active) β-catenin (Ser33/37Thr41). Below: quantification of western blot results relative to GAPDH and normalized to 0 ng/ml TNFα pre-treatment. *N* = 3 donors with biological duplicates per donor. **(B)** Possible working mechanism of TNFα pre-treatment on the chondrogenic potential of MSC. Solid lines show known interactions, [1] Bhattaram et al. *Arthritis Rheumatol* 2018. [2] Bhattaram et al. *J Cell Biol* 2014. [3] Narcisi et al. *Stem Cell Reports* 2015. Dotted lines indicate unknown interactions.

(Majumdar et al., 2000; Kastrinaki et al., 2008; Jiang et al., 2010; Asai et al., 2014; Cleary et al., 2016). In addition, a reduced adipogenic differentiation was observed after TNFα pre-treatment. It is known that TNFα can reduce the adipogenic differentiation in 3T3-L1 pre-adipocytes by preventing *Pparg* and *Cebpa* expression (Cawthorn et al., 2007), which is in line with the reduction of *PPARG* gene expression levels that we found after TNFα pre-treatment. In agreement with other studies (Daniele et al., 2017), we observed that TNFα pre-treatment slightly increased the osteogenic differentiation capacity of MSCs. Overall, these data suggest that TNFα pre-treatment changes the immunophenotype and multipotency of MSCs.

In this study, we tested three different concentrations and incubation times and found that pre-treatment with 50 ng/ml TNFα for 1 passage (4–6 days) increased the chondrogenic capacity in a more reproducible way than the other conditions. Since a previous study indicated that 50 ng/ml TNFα can induce apoptosis in MSC (Cheng et al., 2019), we investigated apoptosis.

No large effect on apoptosis was observed after addition of TNFα. Given the fact that our apoptosis rates are relatively low, we assume that the pro-chondrogenic effect of TNFα on MSCs in not due to an increased apoptotic rate. In addition TNFα can activate several transduction pathways, among which are the NF-κB, ERK, and JNK pathways (Lu et al., 2016; Bai et al., 2017). Since a 24-h pre-treatment was not sufficient to observe an effect on chondrogenesis, we assume that the effect of TNFα on the chondrogenic capacity of MSCs was not mediated via direct induction of these pathways, since they are already activated after 24 h (van Buul et al., 2012). In addition, TNFα pre-treatment for 2 passages (8–10) did not increase the chondrogenic potential suggesting that long-term exposure to TNFα during expansion does not improve the chondrogenic capacity of MSCs. Moreover, no increase in chondrogenic differentiation was observed after pre-treatment with 0.1, 1, 10, and 50 ng/ml IL-1β for 1 passage. Similar to TNFα, IL-1β is involved in joint inflammation (Goldring and Otero, 2011). This suggests that TNFα induces the pro-chondrogenic effect in MSCs via an intracellular pathway that is not activated by IL-1β. As far as we know, no previous research has investigated whether IL-1β can increase SOXC and WNT levels in human MSCs. Overall, these data indicate that not all pro-inflammatory cytokines can increase the chondrogenic potential of MSCs and that the effect seems to be specific for TNFα.

As previously reported, TNFα exposure during the chondrogenic differentiation phase reduces chondrogenesis of MSCs (Markway et al., 2016). Although the TNFα concentrations used during chondrogenic differentiation in this *in vitro* study are higher than the TNFα concentrations in post-traumatic and OA joints (4–24 pg/ml, Sward et al., 2012; Tsuchida et al., 2014; Imamura et al., 2015; Alonso et al., 2020), our data indicate that *in vitro* pre-treatment with 50 ng/ml TNFα can be beneficial for cartilage regeneration in an inflamed environment. In addition we found an association between TNFα pre-treatment and SOX11 and β-catenin activation in MSCs, therefore regulation of these pathways might improve cartilage repair in the presence of TNFα. Overall, the results of our study suggest that exposure to TNFα during the expansion phase of MSCs could improve cartilage regeneration approaches.

DATA AVAILABILITY STATEMENT

The datasets generated for this study are available on request to the corresponding author.

ETHICS STATEMENT

The studies involving human participants were reviewed and approved by the Erasmus MC ethics committee (MEC 2015-644) and the University Hospitals of Cleveland Institutional Review Board (IRB# 09-90-195). Written informed consent to participate in this study was provided by the participants or the participants' legal guardian/next of kin.

AUTHOR CONTRIBUTIONS

CV: conception and design, collection of data, data analysis and interpretation, manuscript writing and final approval of manuscript. WK: collection of data, data analysis and interpretation, and final approval of manuscript. RS: data analysis and interpretation and final approval of manuscript. AC and VL: data interpretation and final approval of manuscript. GO and RN: conception and design, data analysis and interpretation, manuscript writing and final approval of manuscript. All authors contributed to the article and approved the submitted version.

FUNDING

This research was financially supported by the Dutch Arthritis Foundation (ReumaNederland; 16-1-201), the TTW Perspectief grant from NWO (William Hunter Revisited; P15-23) and NIH/NIBIB P41 EB021911.

ACKNOWLEDGMENTS

The authors would like to thank Sascha Schmidt and Janneke Witte-Bouma for technical assistance with the Gaussia luciferase activity measurements and the FACS sorting facility at the Erasmus MC for support with the BD Fortessa machine. The monoclonal antibody II-II 6B3 deposited by Linsenmayer, T. F. was obtained from the Developmental Studies Hybridoma Bank created by the NICHD of the NIH and maintained at The University of Iowa, Department of Biology, Iowa City, IA 52242. This study is part of the Medical Delta RegMed4D program.

SUPPLEMENTARY MATERIAL

The Supplementary Material for this article can be found online at: https://www.frontiersin.org/articles/10.3389/fbioe.2020.00658/full#supplementary-material

REFERENCES

Alonso, B., Bravo, B., Mediavilla, L., Gortazar, A. R., Forriol, F., Vaquero, J., et al. (2020). Osteoarthritis-related biomarkers profile in chronic anterior cruciate ligament injured knee. *Knee* 27, 51–60. doi: 10.1016/j.knee.2019.12.007

Asai, S., Otsuru, S., Candela, M. E., Cantley, L., Uchibe, K., Hofmann, T. J., et al. (2014). Tendon progenitor cells in injured tendons have strong chondrogenic potential: the CD105-negative subpopulation induces chondrogenic degeneration. *Stem Cells* 32, 3266–3277. doi: 10.1002/stem.1847

Bai, X., Xi, J., Bi, Y., Zhao, X., Bing, W., Meng, X., et al. (2017). TNF-alpha promotes survival and migration of MSCs under oxidative stress via NF-kappaB pathway to attenuate intimal hyperplasia in vein grafts. *J. Cell. Mol. Med.* 21, 2077–2091. doi: 10.1111/jcmm.13131

Bhattaram, P., Muschler, G., Wixler, V., and Lefebvre, V. (2018). Inflammatory cytokines stabilize SOXC transcription factors to mediate the transformation of fibroblast-like synoviocytes in arthritic disease. *Arthritis Rheumatol.* 70, 371–382. doi: 10.1002/art.40386

Bhattaram, P., Penzo-Méndez, A., Kato, K., Bandyopadhyay, K., Gadi, A., Taketo, M. M., et al. (2014). SOXC proteins amplify canonical WNT signaling to

secure nonchondrocytic fates in skeletogenesis. *J. Cell. Biol.* 207, 657–671. doi: 10.1083/jcb.201405098

Bocker, W., Docheva, D., Prall, W. C., Egea, V., Pappou, E., Rossmann, O., et al. (2008). IKK-2 is required for TNF-alpha-induced invasion and proliferation of human mesenchymal stem cells. *J. Mol. Med.* 86, 1183–1192. doi: 10.1007/s00109-008-0378-3

Brenner, D., Blaser, H., and Mak, T. W. (2015). Regulation of tumour necrosis factor signalling: live or let die. *Nat. Rev. Immunol.* 15, 362–374. doi: 10.1038/nri3834

Caplan, A. I. (1991). Mesenchymal stem cells. *J. Orthop. Res.* 9, 641–650. doi: 10.1002/jor.1100090504

Caplan, A. I., and Dennis, J. E. (2006). Mesenchymal stem cells as trophic mediators. *J. Cell. Biochem.* 98, 1076–1084. doi: 10.1002/jcb.20886

Cawthorn, W. P., Heyd, F., Hegyi, K., and Sethi, J. K. (2007). Tumour necrosis factor-alpha inhibits adipogenesis via a beta-catenin/TCF4(TCF7L2)-dependent pathway. *Cell. Death Differ.* 14, 1361–1373. doi: 10.1038/sj.cdd.4402127

Cheng, S., Li, X., Jia, Z., Lin, L., Ying, J., Wen, T., et al. (2019). The inflammatory cytokine TNF-alpha regulates the biological behavior of rat nucleus pulposus mesenchymal stem cells through the NF-kappaB signaling pathway *in vitro*. *J. Cell. Biochem.* 120, 13664–13679. doi: 10.1002/jcb.28640

Chu, C. Q., Field, M., Feldmann, M., and Maini, R. N. (1991). Localization of tumor necrosis factor alpha in synovial tissues and at the cartilage-pannus junction in patients with rheumatoid arthritis. *Arthritis Rheum.* 34, 1125–1132. doi: 10.1002/art.1780340908

Cleary, M. A., Narcisi, R., Focke, K., van der Linden, R., Brama, P. A. J., van Osch, G. J. V. M., et al. (2016). Expression of CD105 on expanded mesenchymal stem cells does not predict their chondrogenic potential. *Osteoarthr. Cartil.* 24, 868–872. doi: 10.1016/j.joca.2015.11.018

Correa, D., Somoza, R. A., and Caplan, A. I. (2018). Nondestructive/Noninvasive imaging evaluation of cellular differentiation progression during *In Vitro* mesenchymal stem cell-derived chondrogenesis. *Tissue Eng Part A*. 24, 662–671. doi: 10.1089/ten.TEA.2017.0125

Daniele, S., Natali, L., Giacomelli, C., Campiglia, P., Novellino, E., Martini, C., et al. (2017). Osteogenesis is improved by low tumor necrosis factor alpha concentration through the modulation of Gs-coupled receptor signals. *Mol. Cell. Biol.* 37, e00442–16. doi: 10.1128/MCB.00442-16

Dominici, M., Le Blanc, K., Mueller, I., Slaper-Cortenbach, I., Marini, F., Krause, D., et al. (2006). Minimal criteria for defining multipotent mesenchymal stromal cells. The international society for cellular therapy position statement. *Cytotherapy* 8, 315–317. doi: 10.1080/14653240600855905

Farndale, R. W., Buttle, D. J., and Barrett, A. J. (1986). Improved quantitation and discrimination of sulphated glycosaminoglycans by use of dimethylmethylene blue. *Biochim. Biophys. Acta* 883, 173–177. doi: 10.1016/0304-4165869 0306-5

Fernandes, J. C., Martel-Pelletier, J., and Pelletier, J. P. (2002). The role of cytokines in osteoarthritis pathophysiology. *Biorheology* 39, 237–246.

Giannoni, P., Scaglione, S., Daga, A., Ilengo, C., Cilli, M., Quarto, R., et al. (2010). Short-time survival and engraftment of bone marrow stromal cells in an ectopic model of bone regeneration. *Tissue Eng. A* 16, 489–499. doi: 10.1089/ten.tea.2009.0041

Goldring, M. B., and Otero, M. (2011). Inflammation in osteoarthritis. *Curr. Opin. Rheumatol.* 23, 471–478. doi: 10.1097/BOR.0b013e328349c2b1

Haynesworth, S. E., Goshima, J., Goldberg, V. M., and Caplan, A. I. (1992). Characterization of cells with osteogenic potential from human marrow. *Bone* 13, 81–88. doi: 10.1016/8756-3282(92)90364-3

Imamura, M., Ezquerro, F., Marcon Alfieri, F., Vilas Boas, L., Tozetto-Mendoza, T. R., Chen, J., et al. (2015). Serum levels of proinflammatory cytokines in painful knee osteoarthritis and sensitization. *Int. J. Inflam.* 2015:329792. doi: 10.1155/2015/329792

Jiang, T., Liu, W., Lv, X., Sun, H., Zhang, L., Liu, Y., et al. (2010). Potent *in vitro* chondrogenesis of CD105 enriched human adipose-derived stem cells. *Biomaterials* 31, 3564–3571. doi: 10.1016/j.biomaterials.2010.01.050

Johnstone, B., Hering, T. M., Caplan, A. I., Goldberg, V. M., and Yoo, J. U. (1998). *In vitro* chondrogenesis of bone marrow-derived mesenchymal progenitor cells. *Exp. Cell. Res.* 238, 265–272. doi: 10.1006/excr. 1997.3858

Kapoor, M., Martel-Pelletier, J., Lajeunesse, D., Pelletier, J. P., and Fahmi, H. (2011). Role of proinflammatory cytokines in the pathophysiology of osteoarthritis. *Nat. Rev. Rheumatol.* 7, 33–42. doi: 10.1038/nrrheum.2010.196

Kastrinaki, M.C., Andreakou, I., Charbord, P., and Papadaki, H. A. (2008). Isolation of human bone marrow mesenchymal stem cells using different membrane markers: comparison of colony/cloning efficiency, differentiation potential, and molecular profile. *Tissue Eng. C Methods* 14, 333–339. doi: 10.1089/ten.tec.2008.0173

Kato, K., Bhattaram, P., Penzo-Mendez, A., Gadi, A., and Lefebvre, V. (2015). SOXC transcription factors induce cartilage growth plate formation in mouse embryos by promoting noncanonical WNT signaling. *J. Bone Miner. Res.* 30, 1560–1571. doi: 10.1002/jbmr.2504

Kinnaird, T., Stabile, E., Burnett, M. S., Lee, C. W., Barr, S., Fuchs, S., et al. (2004). Marrow-derived stromal cells express genes encoding a broad spectrum of arteriogenic cytokines and promote *in vitro* and *in vivo* arteriogenesis through paracrine mechanisms. *Circ. Res.* 94, 678–685. doi: 10.1161/01.RES.0000118601.37875.AC

Lefebvre, V., and Bhattaram, P. (2016). SOXC genes and the control of skeletogenesis. *Curr. Osteoporos. Rep.* 14, 32–38. doi: 10.1007/s11914-016-0296-1

Lennon, D. P., and Caplan, A. I. (2006). Isolation of human marrow-derived mesenchymal stem cells. *Exp. Hematol.* 34, 1604–1605. doi: 10.1016/j.exphem.2006.07.014

Lu, Z.Y., Chen, W.C., Li, Y.H., Li, L., Zhang, H., Pang, Y., et al. (2016). TNF-α enhances vascular cell adhesion molecule-1 expression in human bone marrow mesenchymal stem cells via the NF-κB, ERK and JNK signaling pathways. *Mol. Med. Rep.* 14, 643–648. doi: 10.3892/mmr.2016.5314

Majumdar, M. K., Banks, V., Peluso, D. P., and Morris, E. A. (2000). Isolation, characterization, and chondrogenic potential of human bone marrow-derived multipotential stromal cells. *J. Cell. Physiol.* 185, 98–106. doi: 10.1002/1097-4652(200010)185:1<98::AID-JCP9>3.0.CO;2-1

Markway, B. D., Cho, H., Anderson, D. E., Holden, P., Ravi, V., Little, C. B., et al. (2016). Reoxygenation enhances tumour necrosis factor alpha-induced degradation of the extracellular matrix produced by chondrogenic cells. *Eur. Cell. Mater.* 31, 425–439. doi: 10.22203/eCM.v031a27

Narcisi, R., Arikan, O. H., Lehmann, J., Ten Berge, D., and van Osch, G. J. V. M. (2016). Differential effects of small molecule WNT agonists on the multilineage differentiation capacity of human mesenchymal stem cells. *Tissue Eng. A* 22, 1264–1273. doi: 10.1089/ten.tea.2016.0081

Narcisi, R., Cleary, M. A., Brama, P. A., Hoogduijn, M. J., Tuysuz, N., ten Berge, D., et al. (2015). Long-term expansion, enhanced chondrogenic potential, and suppression of endochondral ossification of adult human MSCs via WNT signaling modulation. *Stem Cell Rep.* 4, 459–472. doi: 10.1016/j.stemcr.2015.01.017

Payne, K. A., Didiano, D. M., and Chu, C. R. (2010). Donor sex and age influence the chondrogenic potential of human femoral bone marrow stem cells. *Osteoarthr. Cartil.* 18, 705–713. doi: 10.1016/j.joca.2010.01.011

Pittenger, M. F., Mackay, A. M., Beck, S. C., Jaiswal, R. K., Douglas, R., Mosca, J. D., et al. (1999). Multilineage potential of adult human mesenchymal stem cells. *Science* 284, 143–147. doi: 10.1126/science.284.5411.143

Ren, G., Zhang, L., Zhao, X., Xu, G., Zhang, Y., Roberts, A. I., et al. (2008). Mesenchymal stem cell-mediated immunosuppression occurs via concerted action of chemokines and nitric oxide. *Cell Stem Cell* 2, 141–150. doi: 10.1016/j.stem.2007.11.014

Shioda, M., Muneta, T., Tsuji, K., Mizuno, M., Komori, K., Koga, H., et al. (2017). TNFalpha promotes proliferation of human synovial MSCs while maintaining chondrogenic potential. *PLoS ONE* 12:e0177771. doi: 10.1371/journal.pone.0177771

Sivasubramaniyan, K., Ilas, D. C., Harichandan, A., Bos, P. K., Santos, D. L., de Zwart, P., et al. (2018). Bone marrow-harvesting technique influences functional heterogeneity of mesenchymal stem/stromal cells and cartilage regeneration. *Am. J. Sports Med.* 46, 3521–3531. doi: 10.1177/0363546518804807

Sward, P., Frobell, R., Englund, M., Roos, H., and Struglics, A. (2012). Cartilage and bone markers and inflammatory cytokines are increased in synovial fluid in the acute phase of knee injury (hemarthrosis)–a cross-sectional analysis. *Osteoarthr. Cartil.* 20, 1302–1308. doi: 10.1016/j.joca.2012.07.021

ten Berge, D., Brugmann, S. A., Helms, J. A., and Nusse, R. (2008). Wnt and FGF signals interact to coordinate growth with cell fate specification during limb development. *Development* 135, 3247–3257. doi: 10.1242/dev.023176

Tsuchida, A. I., Beekhuizen, M., t Hart, M. C., Radstake, T. R., Dhert, W. J., Saris, D. B., et al. (2014). Cytokine profiles in the joint depend on pathology, but are different between synovial fluid, cartilage tissue and cultured chondrocytes. *Arthritis Res. Ther.* 16:441. doi: 10.1186/s13075-014-0441-0

van Buul, G. M., Villafuertes, E., Bos, P. K., Waarsing, J. H., Kops, N., Narcisi, R., et al. (2012). Mesenchymal stem cells secrete factors that inhibit inflammatory processes in short-term osteoarthritic synovium and cartilage explant culture. *Osteoarthr. Cartil.* 20, 1186–1196. doi: 10.1016/j.joca.2012.06.003

Wehling, N., Palmer, G. D., Pilapil, C., Liu, F., Wells, J. W., Muller, P. E., et al. (2009). Interleukin-1beta and tumor necrosis factor alpha inhibit chondrogenesis by human mesenchymal stem cells through NF-kappaB-dependent pathways. *Arthritis Rheum.* 60, 801–812. doi: 10.1002/art.24352

Xu, L., Shunmei, E., Lin, S., Hou, Y., Lin, W., He, W., et al. (2019). Sox11-modified mesenchymal stem cells accelerate cartilage defect repair in SD rats. *Cell. Tissue Res.* 376, 247–255. doi: 10.1007/s00441-018-02979-4

Conflict of Interest: The authors declare that the research was conducted in the absence of any commercial or financial relationships that could be construed as a potential conflict of interest.

frontiers in Bioengineering and Biotechnology

ORIGINAL RESEARCH
published: 05 October 2020
doi: 10.3389/fbioe.2020.502213

Comparative Effect of MSC Secretome to MSC Co-culture on Cardiomyocyte Gene Expression Under Hypoxic Conditions *in vitro*

Nina Kastner[1], Julia Mester-Tonczar[1], Johannes Winkler[1], Denise Traxler[1], Andreas Spannbauer[1], Beate M. Rüger[2], Georg Goliasch[1], Noemi Pavo[1], Mariann Gyöngyösi[1] and Katrin Zlabinger[1]*

[1] Department of Cardiology, Medical University of Vienna, Vienna, Austria, [2] Department of Blood Group Serology and Transfusion Medicine, Medical University of Vienna, Vienna, Austria

Introduction: Despite major leaps in regenerative medicine, the regeneration of cardiomyocytes after ischemic conditions remains to elucidate. It is crucial to understand hypoxia induced cellular mechanisms to provide advanced treatment options, including the use of stem cell paracrine factors for myocardial regeneration.

Materials and Methods: In this study, the regenerative potential of hypoxic human cardiomyocytes (group Hyp-CMC) *in vitro* was evaluated when co-cultured with human bone-marrow derived MSC (group Hyp-CMC-MSC) or stimulated with the secretome of MSC (group Hyp-CMC-S_{MSC}). The secretome of normoxic MSC and CMC, and the hypoxic CMC was analyzed with a cytokine panel. Gene expression changes of *HIF-1*α, proliferation marker *Ki-67* and cytokinesis marker *RhoA* over different reoxygenation time periods of 4, 8, 24, 48, and 72 h were analyzed in comparison to normoxic CMC and MSC. Further, the proinflammatory cytokine IL-18 protein expression change, metabolic activity and proliferation was assessed in all experimental setups.

Results and Conclusion: *HIF-1*α was persistently overexpressed in Hyp-CMC-S_{MSC} as compared to Hyp-CMC (except at 72 h). Hyp-CMC-MSC showed a weaker *HIF-1*α expression than Hyp-CMC-S_{MSC} in most tested time points, except after 8 h. The *Ki-67* expression showed the strongest upregulation in Hyp-CMC after 24 and 48 h incubation, then returned to baseline level, while a temporary increase in *Ki-67* expression in Hyp-CMC-MSC at 4 and 8 h and at 48 h in Hyp-CMC-S_{MSC} could be observed. *RhoA* was increased in normoxic MSCs and in Hyp-CMC-S_{MSC} over time, but not in Hyp-CMC-MSC. A temporary increase in IL-18 protein expression was detected in Hyp-CMC-SMSC and Hyp-CMC. Our study demonstrates timely dynamic changes in expression of different ischemia and regeneration-related genes of CMCs, depending from the culture condition, with stronger expression of *HIF-1*α, *RhoA* and IL-18 if the hypoxic CMC were subjected to the secretome of MSCs.

Keywords: human cardiomyocytes, hypoxia, regeneration, cell therapy, MSC secretome

Abbreviations: αSMA, α-sarcomeric-Actinin; MSC, Mesenchymal stem cells; cMHC, Cardiac Heavy Chain Myosin; CMC, Cardiomyocytes; cTNT, Cardiac Troponin T; HIF-1α, Hypoxia-inducible factor 1α; HPRT, Hypoxanthin guanine phosphoribosyltransferase; Hyp, Hypoxic; P/S, Penicillin/Streptomycin; RT-qPCR, Reverse transcriptase quantitative polymerase chain reaction.

OPEN ACCESS

Edited by:
Martin James Stoddart, AO Research Institute, Switzerland

Reviewed by:
Sveva Bollini, University of Genoa, Italy
Michela Pozzobon, University of Padua, Italy

****Correspondence:***
Mariann Gyöngyösi
mariann.gyongyosi@meduniwien.ac.at

Specialty section:
This article was submitted to Tissue Engineering and Regenerative Medicine, a section of the journal Frontiers in Bioengineering and Biotechnology

Received: *01 October 2019*
Accepted: *04 September 2020*
Published: *05 October 2020*

Citation:
Kastner N, Mester-Tonczar J, Winkler J, Traxler D, Spannbauer A, Rüger BM, Goliasch G, Pavo N, Gyöngyösi M and Zlabinger K (2020) Comparative Effect of MSC Secretome to MSC Co-culture on Cardiomyocyte Gene Expression Under Hypoxic Conditions in vitro. Front. Bioeng. Biotechnol. 8:502213. doi: 10.3389/fbioe.2020.502213

INTRODUCTION

Myocardial ischemia leads to permanent cell damage after 20 to 60 min (Silbernagl and Lang, 2000), depending on the *in vitro* and *in vivo* conditions. Cardiovascular diseases account for approximately a third of all deaths (Benjamin et al., 2017) globally and though long-term survival has improved over the last decades, regenerative treatment options for lost myocytes still remain limited (Puymirat et al., 2017). In 2001 the first approaches of human regenerative therapy have been tested with myoblasts, leading to further cell transplantation trials (Menasché et al., 2001). Since then several different regeneration possibilities have been explored in heart failure treatment, such as re-activation of endogenous cardiomyocyte proliferation via cell reprograming, activation of vascularization with growth factors and immunomodulation (Cahill et al., 2017). The initial research focus was on replacement of cardiomyocytes (CMC) by stem cell delivery, however, since the hypothesis of stem cells differentiating into cardiomyocytes was refuted, the focus shifted to stimulation of endogenous cardiac repair (Orlic et al., 2001; Murry et al., 2004). Extracellular vesicles and paracrine factors released by stem cells may influence and improve cardiac repair, since they carry proliferative and growth factors (Cahill et al., 2017).

Mesenchymal stem cells (MSC) are adult stem cells that are multipotent and can differentiate into adipocytes, osteoblasts and chondrocytes (Beresford et al., 1992; Pittenger et al., 1999). Transdifferentiation of MSCs to CMCs is still heavily debated (Szaraz et al., 2017; Guo et al., 2018). The first discovery of MSC was in bone marrow (Prockop, 1997), however, they have been found in most post-natal tissues (da Silva Meirelles et al., 2006). Bone marrow (Kern et al., 2006; Pendleton et al., 2013), adipose tissue (Zuk et al., 2002; Kern et al., 2006), the umbilical cord (Sarugaser et al., 2005; Beeravolu et al., 2017) and the placenta (Pelekanos et al., 2016) are the most commonly used sources for MSC isolation. The International Society of Cellular Therapy has defined certain criteria for characterization of isolated MSC, consisting of ability to differentiate into adipocytes, osteoblast and chondrocytes *in vitro*, plastic adhesion and expression of CD105 + , CD90 + , CD73 + , CD45-, CD34-, CD14- or CD11b-, CD79α - or CD19- and HLA-DR- (Dominici et al., 2006).

The first use of bone marrow derived cells in clinical trials for heart regeneration was by Assmus et al. (2002) by injecting a variety of cell types residing in bone morrow. Selected bone marrow-derived MSC were first studied in cardiac research in mice by Yoon et al. in 2005 (Yoon et al., 2005). The majority of first-generation clinical trials, however, focused on injection of unselected bone-marrow origin mononuclear cells or hematopoietic stem cells, rather than MSC (Gyöngyösi et al., 2015). In 2014 one of the first clinical trial with bone marrow derived MSC was completed by Karantalis et al. (2014; Karantalis et al., 2014). The general understanding was that stem cells can modulate cell behavior and proliferation of the cardiomyocytes, however, the mechanism was not fully understood, which lead to the hypothesis of stem cell differentiation to CMC (Yoon et al., 2005). Recently, the hypothesis shifted to the reparative effect of paracrine factors that contain proliferation-inducing factors, including transcription, growth, angiogenic and immunosuppressive factors (Thum et al., 2005; Safari et al., 2016; Shafei et al., 2017). Paracrine factors are theorized to induce re-entry into the cell cycle of CMCs, however, the regulation mechanism has not been fully understood (Shafei et al., 2017). The benefit of using just excreted secretome and not cells themselves is the lowered risk of an immune reaction when using allogenic MSC. It is considered to be safe to use MSC due to the low expression of MHC molecules, however, in recent years several studies have encountered anti-donor immune responses non-etheless (Lohan et al., 2017).

In contrast to the initial assumption, that intracoronary infusion of bone-marrow cells induces myocardial regeneration in reperfused acute myocardial infarction, patient individual data-based meta-analysis has revealed no significant benefit of this treatment, and the research has focused on other cell types and interventions (Gyöngyösi et al., 2015).

In this study we aimed to simulate the reperfused acute myocardial infarction *in vitro* and evaluated the effect of MSCs or their secretome on the temporary hypoxic CMC. We have supposed that just using secretome of MSC (instead of cells) has a similar or better benefit for CMC survival and proliferation. Accordingly, we have evaluated the expression of the angiogenic marker *HIF-1α*, the cytokinesis marker *RhoA* and the proliferation marker *Ki-67*, and the proliferation/metabolic activity (EZ4U kit, MTT assay, BrdU assay) of the CMCs and proinflammatory cytokine IL-18 protein levels.

MATERIALS AND METHODS

Study Design

The protein expression and proliferation of hypoxic human CMC (Hyp-CMCs) was tested in co-culture with human MSCs directly (Hyp-CMC-MSC) or in culture with secretome of human MSCs (Hyp-CMC-S_{MSC}) via 3 μm transwells (Greiner Bio-One International GmbH, Austria). Additionally, unstimulated hypoxic CMCs were evaluated. CMCs (PromoCell GmbH, Germany) were cultured in 6-well plates (TPP, Switzerland) and used for experiments at 95% confluency. Human MSCs (EK1193/2015) were kindly provided from the Department of Blood Group Serology and Transfusion Medicine, Medical University of Vienna (Rüger et al., 2018). The setup of the study is summarized in **Figure 1**.

CMCs were cultured in Basal Medium (PromoCell GmbH, Germany) supplemented with Growth Medium SupplementMix, (PromoCell GmbH, Germany) with final concentrations of FBS 0.05 mL/mL, Epidermal Growth Factor (recombinant) 0.5 ng/mL, Basic Fibroblast Growth Factor (recombinant human) 2 ng/mL and insulin (recombinant human) 5 μg/mL. $5{\cdot}10^4$ CMC were seeded into each well of 6-well plate and medium was changed 24 h before to M199 (Sigma-Aldrich, Germany) supplied with 1% P/S (Sigma-Aldrich, Germany). M199 + 1% P/S was changed again right before conduction of the experiment.

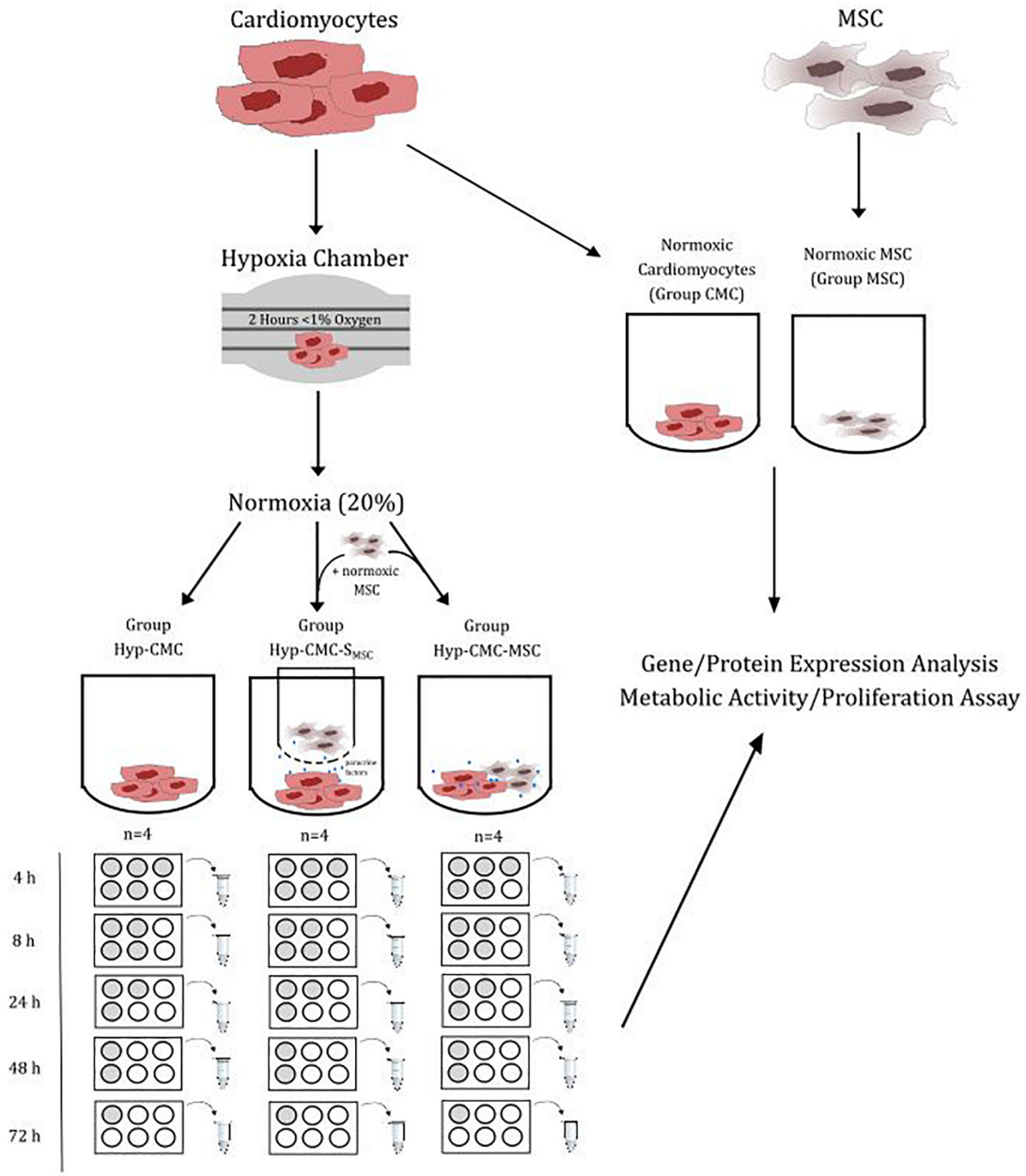

FIGURE 1 | Overview of the study design setup. CMC were exposed to < 1% oxygen level for 2 h. After restoration of the normoxic condition, the CMCs were separated in three groups: Unstimulated hypoxic CMC (Hyp-CMC), CMC stimulated with MSC secretome (Hyp-CMC-S_{MSC}) and CMC stimulated directly with MSC (Hyp-CMC-MSC). The samples of each setup were analyzed after the respective reoxygenation period. Additionally, normoxic CMC (CMC) and normoxic MSC (MSC) were analyzed. Each setup was evaluated using gene/protein analysis and a proliferation assay. MSC – Mesenchymal stem cells. CMC – cardiomyocytes. Hyp – hypoxic.

MSCs were cultured in Dulbecco's Modified Eagle Medium DMEM HG 4.5 g/L glucose (Sigma-Aldrich, Germany) supplemented with 10% Fetal Bovine Serum FBS (Biochrom GmbH, Germany) and 1% Penicillin/Streptomycin. Medium was exchanged to M199 + 1% P/S 24 h before MSCs were used in experiments.

CMCs were exposed to a gas mixture of nitrogen and oxygen via a hypoxia chamber (Billups-Rothenberg Inc., United States) for 2 h and an oxygen level of under 1%. M199 + 1% P/S was again changed right after, inducing normoxic conditions (simulating myocardial reperfusion). Afterward Hyp-CMC were classified to one of the three experimental groups, unstimulated CMC (Hyp-CMC), directly stimulated with MSC (Hyp-CMC-MSC) and indirectly stimulated with MSC secretome (Hyp-CMC-S_{MSC}). Unstimulated CMC were lysed after the respective time period without further processing. Directly stimulated

CMCs were co-cultured with MSC by adding $5{\cdot}10^4$ MSC into the well right after hypoxia and then also lysed after the respective follow-up time period. Indirectly stimulated CMC were co-cultured with MSC by transferring a transwell with $5{\cdot}10^4$ pre-seeded MSC to the well right after hypoxia and then also lysed after the respective time period. Additionally, $5{\cdot}10^4$ unstimulated MSC were seeded into two wells of a 6-well-plate and lysed after 24 h culturing in serum free M199 medium. Tested time periods after reoxygenation were 4, 8, 24, 48, and 72 h. Additionally, samples were evaluated directly after hypoxia and before hypoxia as control. Each setup was carried out with $n = 4$.

RNA Isolation and cDNA Synthesis

Cells were lysed with 350 µL RLT Buffer (QIAGEN GmbH, Germany) per well with 1% β-mercaptoethanol (Sigma-Aldrich, Germany). RNA was automatically isolated from cell lysates with the QIACube (QIAGEN GmbH, Germany) using QIAgen miRNeasy Kit (QIAGEN GmbH, Germany). Isolated RNA was measured with a NanoDrop™ 3300 Fluorospectrometer (Thermo Fisher Scientific, United States) and diluted, respectively, with RNAse free water (QIAGEN GmbH, Germany) to a final concentration of 41.67 ng/µL. Further 2 µL gDNA Wipeout Buffer (QIAGEN GmbH, Germany) was added to 12 µL sample, equaling 500 ng RNA, and incubated at 42°C for two minutes. Reverse Transcriptase MM, QuantiScript RT Buffer and RT Primer Mix from the QuantiTect Reverse Transcription Kit (QIAGEN GmbH, Germany) were then added to the samples, which were then incubated at 42°C for 15 min for cDNA synthesis. The Reverse Transcriptase was then inactivated via incubation at 95°C for 3 min.

Gene Expression Analysis via qPCR

cDNA samples were diluted to a concentration of 2.5 ng/µL with RNAse free water. The PCR plate was stored on a cooling block and 4 µL sample equaling 10 ng RNA, 10 µL QuantiTect SYBR Green PCR MM (QIAGEN GmbH, Germany), 2 µL Primer (10 µM) forward, 2 µL Primer (10 µM) reverse and 2 µL RNAse free water was added. Following primer were designed with PrimerBlast from NCBI and obtained from Microsynth Austria GmbH, Austria: *HIF-1α* fwd ACC TGA GCC TAA CAG TCC CAG TG, *HIF-1α* rev TTC TTT GCC TCT GTG TCT TCA GCA A (Tm = 63°C, 104 bp); *Ki-67* fwd CCA CAC TGT GTC GTC GTT TG, *Ki-67* rev CCG TGC GCT TAT CCA TTC A (Tm = 59°C, 123 bp); *RhoA* fwd CCC AAT GTG CCC ATC ATC CT, *RhoA* rev TGG TTT TAC TGG CTC CTG CT (Tm = 60°C, 102 bp); *HPRT* fwd CCC AGC GTC GTG ATT AGT GA, *HPRT* rev ATC TCG AGC AAG CCG TTC AG (Tm = 60°C, 141 bp). The PCR plate was briefly centrifuged at 300 × *g* when all components were added. The PCR was carried out in the QuantStudio 5 PCR cycler (Applied Biosystems by Thermo Fisher Scientific, United States) and the according software Analysis Software v1.4.1. The setup consisted of a 15-min hold stage at 95°C at the beginning, followed by 40 cycles of 94°C for 15 s (Denaturation), 60°C for 30–60 s (Annealing) and 72°C for 30 s (Elongation). Data was collected in the Elongation Step. After the PCR stage, a melt curve was obtained. Gene expression was analyzed using the $2^{(-\Delta\Delta Ct)}$ method.

Characterization of CMCs and MSCs via Immunofluorescence Staining

Normoxic MSCs and normoxic CMCs were characterized with an immunofluorescence staining of specific markers.

CMCs were indirectly labeled with α-Sarcomeric-Actinin, BNP, Connexin 43 and Troponin-T, heavy chain cardiac Myosin, Nkx2.5 (Abcam plc., United Kingdom). CMCs were characterized for each experiment setup (CMC, Hyp-CMC, Hyp-CMC-SMSC and Hyp-CMC-MSCS). CMSs were seeded into 96-well plates (TPP, Switzerland) and 48-well plates (TPP, Switzerland). Experiments as described in 2.1 and subsequent staining was performed when 80% confluency was reached. CMCs were fixed in 4% paraformaldehyde (Merck, Germany) for 15 min. After removing the fixative solution, the CMCs were washed two times with PBS. Primary antibody solutions were prepared by appropriately diluting the respective antibodies in permeabilization buffer, consisting of 3% non-fat dry milk (Sigma Aldrich, St. Louis, MO, United States) with 0.1% Triton X-100 (Sigma Aldrich, St. Louis, MO, United States) in PBS. CMCs were incubated with the respective antibody solution for 2 h and were then washed twice with PBS. Then the secondary antibody solution with Goat-anti-Rabbit 488, Goat-anti-Mouse FITC, Donkey-anti-Goat 488 (Abcam plc., United Kingdom), in permeabilization buffer was added to the cells for 2 h. A 1:2500 Hoechst in PBS working solution was added for 20 min without discarding the secondary antibody solution. CMCs were then counterstained for 10 min with a 1:40 Phalloidin (Thermo Fisher Scientific, United States) working solution in PBS after washing with PBS twice. CMCs were again washed two times with PBS and then and stored at 4°C in 100 µL PBS per well.

MSCs were seeded into 8-well-slips, pre-coated with 0.1% porcine gelatin (Sigma-Aldrich, Germany). Staining was performed when 80% confluency was reached. MSCs were therefore fixed with 2.5% formalin (Merck, Germany) for 15 min and permeabilized with methanol (Fisher Chemical, United Kingdom) for three minutes. 0.1% Tween-20 (Sigma-Aldrich, Germany) in PBS was added as blocking buffer for 15 min. MSC were directly labeled with CD105, CD90, CD44, and CD29 (EXBIO Praha a.s., Czechia) with the, respectively, diluted antibody for an hour. A 1:5000 Hoechst (Sigma-Aldrich, Germany) in PBS working solution was added for five minutes. The slip was mounted with fluoroshield mounting medium (Abcam, United Kingdom) and stored at 4°C.

Images were taken on the Olympus IX83 Inverted Microscope (OLYMPUS EUROPA SE & CO. KG, Germany) using cellSens imaging software.

EZ4U Proliferation Assay

Evaluation of proliferation was additionally performed with an EZ4U Proliferation Assay (Biomedica Medizinprodukte GmbH, Austria), which is based on the reduction of tetrazolium salt to colored formazan that can then be measured and is

directly proportional to the mitochondrial oxidative capacity of the living cells. The substrate was prepared according to manufacturer protocol and was then added to the respective wells 4 h before readout of the time-point. The readout was performed with the Tecan Sunrise plate reader (Tecan Group, Switzerland) at the wavelength of 450 nm, 620 nm as reference wavelength.

MTT Assay

Evaluation of metabolic activity was performed with an MTT Assay (Thermo Fisher Scientific, United States) according to the manufacturer protocol using DSMO. The readout was performed with the Tecan Sunrise plate reader (Tecan Group, Switzerland) at the wavelength of 540 nm as indicated by the manufacturer.

BrdU Assay

Cell cycle progression was measured with a BrdU Assay (Exalpha Biologicals Inc., United States), which relies on [3H] thymidine incorporation as cells enter S phase. The protocol was performed according to the manufacturer protocol. The readout was performed with the Tecan Sunrise plate reader (Tecan Group, Switzerland) at the wavelength of 450 nm and 550 as reference as indicated by the manufacturer.

Cytokine Evaluation of CMC and MSC Secretome

A cytokine analysis was performed with the Proteome Profiler Human Cytokine Array Kit (R&D systems, United States). Samples of cell secretome (2 mL serum-free M199 medium) were taken from a 6-well plate with approximately $5{\cdot}10^4$ cells of the respective cell type (MSC, CMC, Hyp-CMC). 1 mL of the samples was used for the analysis. The assay was performed according to the manufacturer protocol. Readout was performed by adding 1 mL Novex^{TM} ECL Chemiluminescent Substrate Reagent Kit (Thermo Fisher Scientific, United States) 1:1 according to manufacturer protocol and imagining in the membranes on the ChemiSmart-3600 (Peqlab Biotechnologie GmbH, Germany) after 3 min of incubation. The images were then analyzed with the fiji software to evaluate the intensity of the signal.

IL-18 ELISA

An IL-18 ELISA BMS672 (affymetrix eBioscience, United States) was performed with cell lysates to determine protein expression. Cells were lysed for 10 min with trypsin after the respective regeneration time and stored at −80°C. The ELISA was then performed according to the manufacturer protocol. The standard curve was fitted with a 4-parameter logarithmic curve fit.

Statistical Analysis

Statistical analysis was conducted in Prism 5 for Windows v5.01 (GraphPad Software, Inc.) using one-way ANOVA (Kruskal-Wallis test) and groups were compared with the Dunn's Multiple Comparison Test.

RESULTS

Characterization of MSC Showed Characteristic Stem Cell Markers and CMC Showed Characteristic Cardiac Lineage Associated Markers

As seen in **Figures 2A–F**, CMCs showed positive expression of all cardiac lineage associated markers BNP (**Figure 2B**), Connexin 43 (**Figure 2C**), cTNT (**Figure 2D**), cMHC (**Figure 2E**), and Nkx2.5 (**Figure 2D**), indicating a CMC phenotype. Further, αSMA was weakly expressed. Connexin 43 was mainly expressed in gap junctions, cTNT as shown in **Figure 2D** showed structural features of CMCs. BNP and cMHC was expressed consistently throughout the cells (**Figures 2A,E**).

In hypoxia treated CMCs, the expression of αSMA and BNP could not be detected or only weakly in all experimental setups, all other marker showed expression throughout all groups and timepoints (**Supplementary Figures 1–5**).

Immunofluorescence staining of naïve MSCs showed positive expression of specific stem cell markers CD29, CD44, CD90 and CD105 (**Figures 2G–J**). CD105 occasionally showed weaker expression, CD29, CD44, and CD90 were expressed throughout all cells (**Figure 2J**).

Cytokine Analysis of Secretome of Unstimulated Normoxic CMC and MSC and Hyp-CMC Revealed Specific Cytokine Release

The cytokine array was carried out to determine secretome content and to characterize important key factors. Secrectome analysis for cytokines revealed an expression of CCL5/RANTES (534 ± 15.0) and CXCL12/SDF-1 (3682 ± 238.5) in secretome of Hyp-CMC (**Figures 3A,D**). In secretome of normoxic CMC (group CMC), there was no detectable cytokine expression (**Figure 3F**). Secretome of normoxic MSC (group MSC) showed cytokine expression for CD40L (78 ± 2.0), IL-17 (1050 ± 63.0), IL-17E (888.5 ± 120.5), and CXCL12/SDF-1 (648.5 ± 67.5) (**Figures 3B,E**). Evaluation of all experimental setups and time points was out of the scope of this study.

EZ4U Assay Showed Elevated CMC Metabolic Activity in Long-Term Regeneration When Stimulated With MSC Secretome

The EZ4U assay (**Figure 3C**) showed an increased metabolic activity in Hyp-CMC-MSC after 4 h (0.249) and 8 h (0.407), followed by rapid decrease with OD values of 0.016 (24 h), 0.010 (48 h), and 0.014 (72 h). Metabolic activity of Hyp-CMC and Hyp-CMC-S_{MSC} increased first 24 h after reoxygenation and remained undulant high in Hyp-CMC-S_{MSC} at 48 and 72 h (OD values: 0.284 – 0.092 – 0.295, respectively), while it decreased in Hyp-CMC (OD values: 0.218 – 0.251 – 0.032, respectively).

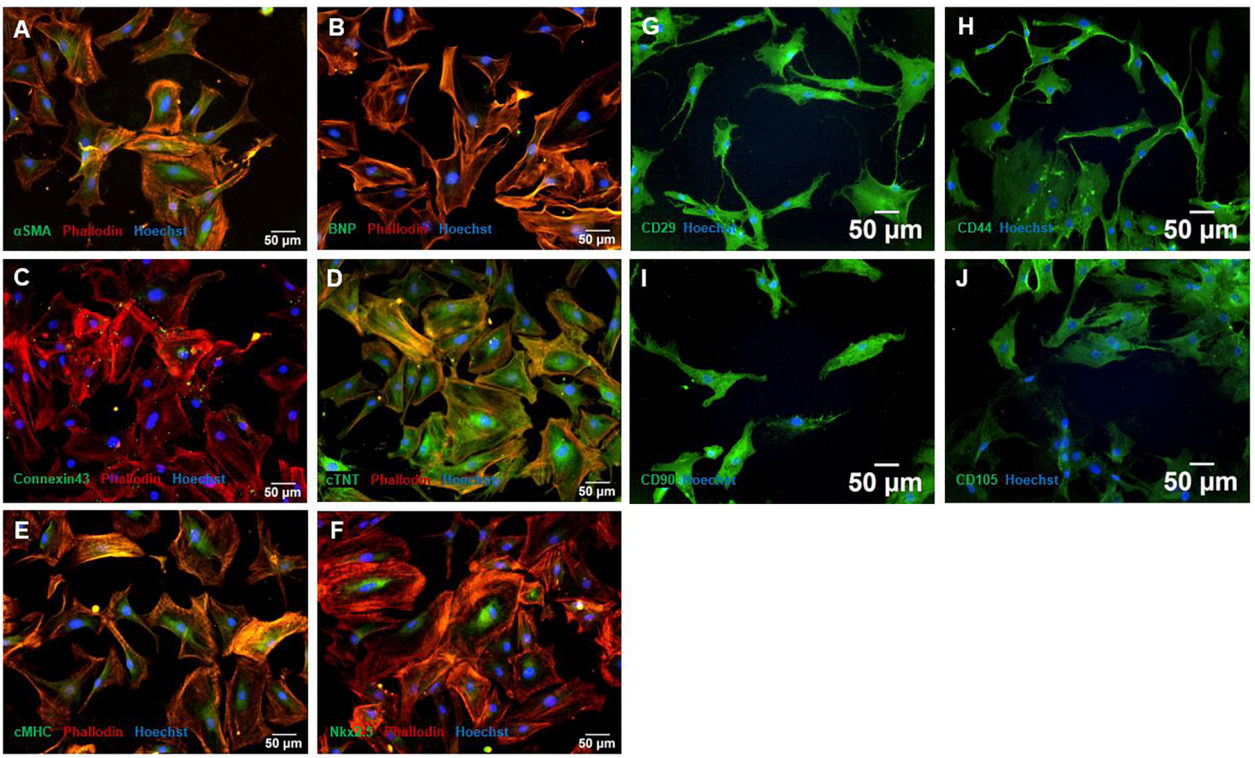

FIGURE 2 | Characterization with immunofluorescence staining of MSC and CMC. CMC showed typical cardiac lineage marker expression of αSMA **(A)**, BNP **(B)**, Connexin 43 **(C)**, cTNT **(D)**, cMHC **(E)**, and Nkx2.5 **(F)**. MSC showed the expression of characteristic stem cell markers CD29 **(G)**, CD44 **(H)**, CD90 **(I)**, and CD105 **(J)**. Cells were counterstained with Hoechst. MSC – Mesenchymal stem cells. CMC – cardiomyocytes. cTNT – Cardiac Troponin T. cMHC - Cardiac Heavy Chain Myosin. αSMA - α-sarcomeric-Actinin.

MTT and BrdU Assay Showed no Significant Differences in Proliferation and Metabolic Activity Between Groups

As shown in **Figure 4B**, metabolic activity asses with MTT varied between time points and throughout the experimental groups of Hyp-CMC, Hyp-CMC-MSC and Hyp-CMC-$S_{MSC,}$ with a drop after 24 h in all groups. The group comparison did not reveal significant differences between the groups. The proliferation asses with a BrdU assay (**Figure 4A**) also showed no significant difference between the groups, however, a trend toward higher proliferation in Hyp-CMC-S_{MSC} was observed.

HIF-1α, Ki-67, and RhoA Expression Showed Elevated CMC Proliferation When Stimulated With MSC Secretome

HIF-1α gene expression (**Figure 5A**), *Ki-67* gene expression (**Figure 5B**) and *RhoA* gene expression (**Figure 5C**) showed significant differences among the experimental groups.

HIF-1α gene expression showed a trend toward downregulation in directly stimulated CMCs (Hyp-CMC-MSC) in comparison to Hyp-CMC-S_{MSC}, reaching significance at 72 h. When comparing Hyp-CMC-MSC with Hyp-CMC-S_{MSC}, the secretome treatment showed a significantly ($p < 0.05$) higher *HIF-1α* expression at 4, 48, and 72 h. Hyp-CMC-S_{MSC} showed a trend toward upregulation of *HIF-1α* expression as compared with the Hyp-CMC in all follow-ups.

Hyp-CMC showed a significant upregulation of *Ki-67* expression at 24 h when compared to the other treatment groups and remained high at 48 h before decreasing after 72 h. Similar trend toward increase in expression of *Ki-67* in both stimulated groups (Hyp-CMC-SMSC and Hyp-CMC-S_{MSC}) were observed with less extent at 8 and 48 h, with decrease to almost baseline levels at 72 h.

RhoA gene expression showed a slight upregulation in Hyp-CMC-S_{MSC} after 4 and 8 h and a trend toward downregulation in Hyp-CMC-MSC. Hyp-CMC-S_{MSC} *RhoA* expression then showed a significant upregulation when compared to Hyp-CMC-MSC. Hyp-CMC-MSC showed a significant downregulation in Hyp-CMC-MSC from 24–72 h when compared to normoxic CMC. Hyp-CMC showed a slight downregulation at all timepoints.

IL-18 Protein Concentration Showed Different Inflammatory Cytokine Signaling Throughout Reoxygenation Time Points and Type of Stimulation

As demonstrated in **Figure 4C**, Il-18 protein concentration varied between time points and throughout the experimental groups of Hyp-CMC, Hyp-CMC-MSC, and Hyp-CMC-$S_{MSC,}$

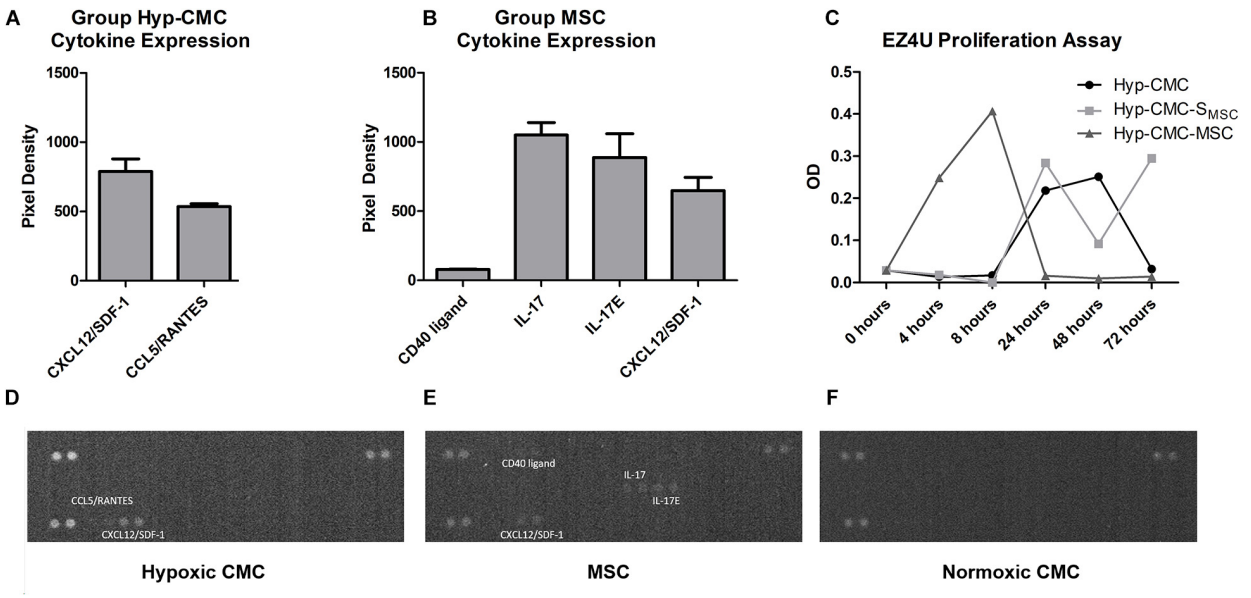

FIGURE 3 | Cytokine expression and EZ4U proliferation assay readout in unstimulated hypoxic and normoxic CMC and normoxic MSC. **(A** and **D)** Cytokine expression of Hyp-CMC secretome, showing detectable readout of CXCL12/SDF-1 and CCL5/RANTES. **(B** and **E)** Cytokine expression of normoxic MSC secretome, with detectable readout of CD40 ligand, IL-17, IL-17E, and CXCL12/SDF-1. **(C)** EZ4U proliferation assay of the control CMC and MSC and of the samples taken from each of the three experiment groups unstimulated hypoxic CMC (group Hyp-CMC), CMC stimulated with MSC secretome (group Hyp-CMC-S_{MSC}) and CMC stimulated directly with MSC (group Hyp-C-MSC) after the respective tested time period of 4, 8, 24, 48, and 72 h. **(F)** No detectable cytokine expression in normoxic CMC. MSC – Mesenchymal stem cells. CMC – cardiomyocytes. Hyp – hypoxic.

with an increase at 8 and 24 h with a drop after 48 h. The group comparison did not reveal significant differences between the groups.

DISCUSSION

Here we show, that MSC secretome might provide a better treatment option after hypoxic events when compared to direct MSC cell therapy, based on our *in vitro* analysis. *In vitro* co-culture of human CMCs subjected to ischemia followed by normoxia (simulating ischemia/reperfusion) with human MSCs did not reveal substantial changes in *HIF-1α*, *Ki-67* and *RhoA* expression, which is line with the clinical observation that even a direct contact of ischemic injured CMC with reparative MSCs does not induce robust angiogenic or proliferative processes of the CMCs (Gyöngyösi et al., 2015). Subjecting the ischemia-affected CMC to secretome, time-dependent increase of *HIF-1α* and *RhoA* expression could be detected, indicating that cell-free therapy might be considered as a more viable option for cardiac regeneration (Pavo et al., 2014; Roura et al., 2017). In contrast to our study simulating acute myocardial ischemia and reperfusion, recent studies demonstrated that MSC show cardioprotective effects and can trigger cell-cycle progression in murine cardiomyocytes in diverse other conditions, such as chronic ischemia, or cardiomyopathies (Ezquer et al., 2015; Huang et al., 2019).

HIF-1α is considered as a hypoxic marker, that is linked with cell survival when and after enduring hypoxic conditions. It serves as a modulator of various pathways that allow the cell to switch metabolism, accommodate to pH variations and activate cell protective mechanisms (Weidemann and Johnson, 2008). When *HIF-1α* is upregulated, the cell has a better chance of avoiding apoptosis or necrosis, which is favorable for cardiac repair (Semenza, 2014). As *HIF-1α* showed to be generally more strongly expressed in CMCs stimulated with MSC secretome (Hyp-CMC-S_{MSC}) than in CMCs stimulated with MSCs directly (Hyp-CMC-MSC), the assumption of better cell survival hints benefits of a treatment with solely excreted secretome.

Expression of *Ki-67* is linked to proliferation, since *Ki-67* is upregulated during mitosis and the G_2 phase (Sobecki et al., 2017). Interestingly, the strongest upregulation of *Ki-67* expression was measured in unstimulated Hyp-CMCs, indicating an impairment of proliferation by the stimulation at 24 and 48 h. However, *Ki-67* has been described to vary in expression throughout cell types, presenting a more graded proliferation marker, rather than a binary proliferation marker (Miller et al., 2018). Additionally, *Ki-67* was also discovered to be upregulated in cardiomyocyte endoreduplication, without a correlation with *de novo* cardiomyogenesis (Zebrowski and Engel, 2013; Drenckhahn et al., 2015; Alvarez et al., 2019). Therefore, the expression of a cytokinesis marker (*RhoA*) and a proliferation and metabolic assay (EZ4U) was additionally performed to validate *Ki-67* expression due to proliferation.

The EZ4U assay showed a similar relation of proliferation like *Ki-67* in Hyp-CMC, as proliferation peaked after 24 and 48 h. Additionally, in Hyp-CMC-MSC, proliferation peaked

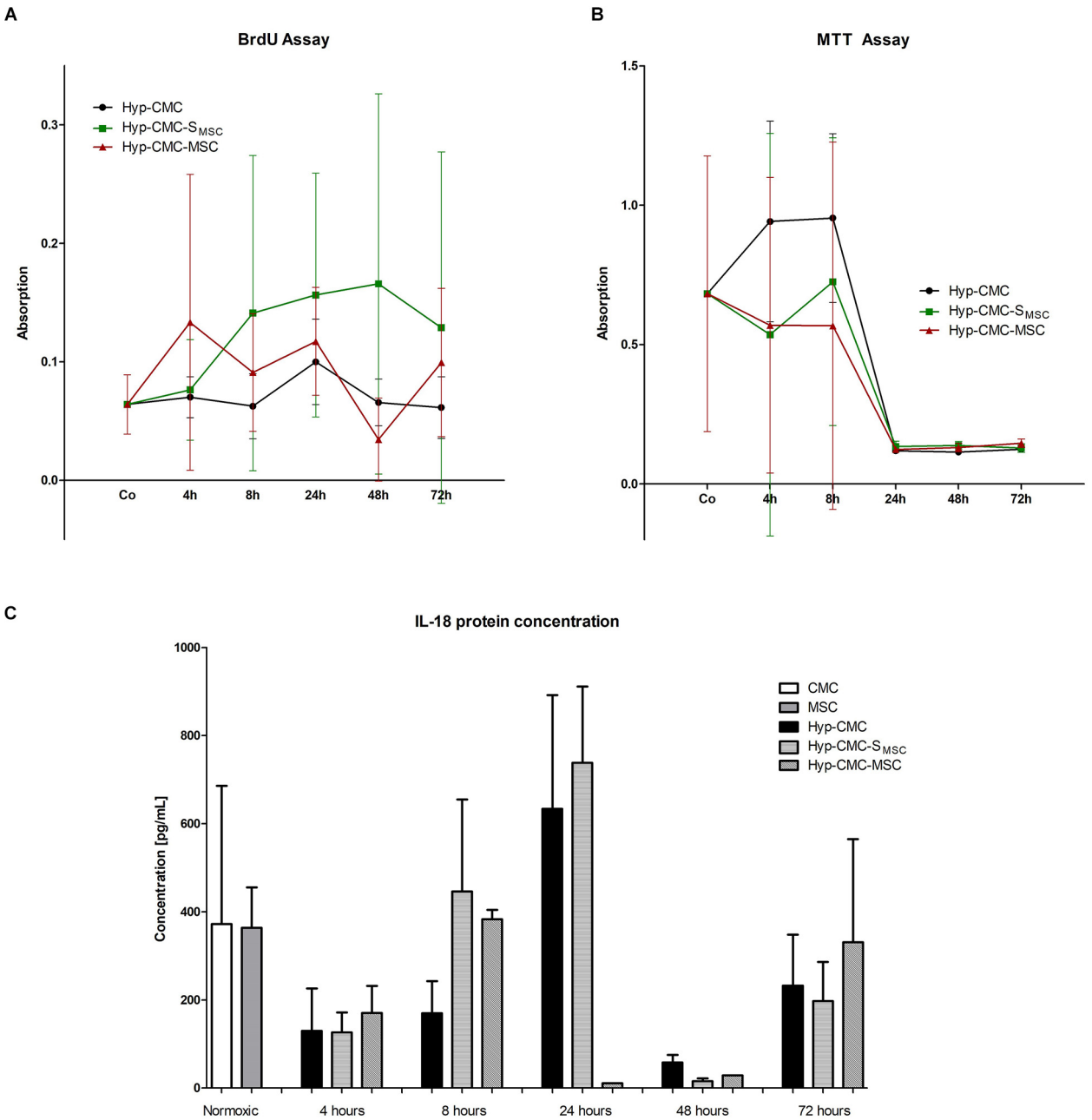

FIGURE 4 | (A–C) BrdU and MTT assay, IL-18 protein concentration analysis with ELISA of the three experimental groups: unstimulated hypoxic CMC (group Hyp-CMC), CMC stimulated with MSC secretome (group Hyp-CMC-S_{MSC}) and CMC stimulated directly with MSC (group Hyp-CMC-MSC) after the respective reoxygenation period of 4, 8, 24, 48, and 72 h. IL-18 protein concentration of CMC and MSC were also evaluated as control. Each stimulation method and respective time point was analyzed with one-way ANOVA (Kruskal-Wallis test) and groups were compared with the Dunn's Multiple Comparison Test. $^{*}p < 0.05$, $^{**}p < 0.01$, $n = 2$ technical replicates (Il-18), $n = 6$ technical replicates (BrdU and MTT). MSC – Mesenchymal stem cells. CMC – cardiomyocytes. Hyp – hypoxic.

after 4 and 8 h, showing similarities to *Ki-67* expression. In Hyp-CMC-S_{MSC} *Ki-67* expression and proliferation evaluated with the EZ4U assay showed a similar course, however, the peak of *Ki-67* expression after 48 h showed a time delay in the EZ4U assay after 72 h. The BrdU assay and the MTT assay showed no significant changes when CMCs were stimulated in comparison to Hyp-CMC, however, a trend to higher proliferating cells in group hyp-CMC-S_{MSC} was observed. *RhoA* expression showed a generally low expression in Hyp-CMC-MSC and a generally high expression in Hyp-CMC-S_{MSC}. Further, Hyp-CMC showed a moderate *RhoA* expression throughout all reoxygenation periods. Since *RhoA* is highly expressed during anaphase, telophase and especially cytokinesis (Chircop, 2014), the readout of expression changes can be attributed to cell division and proliferation, rather

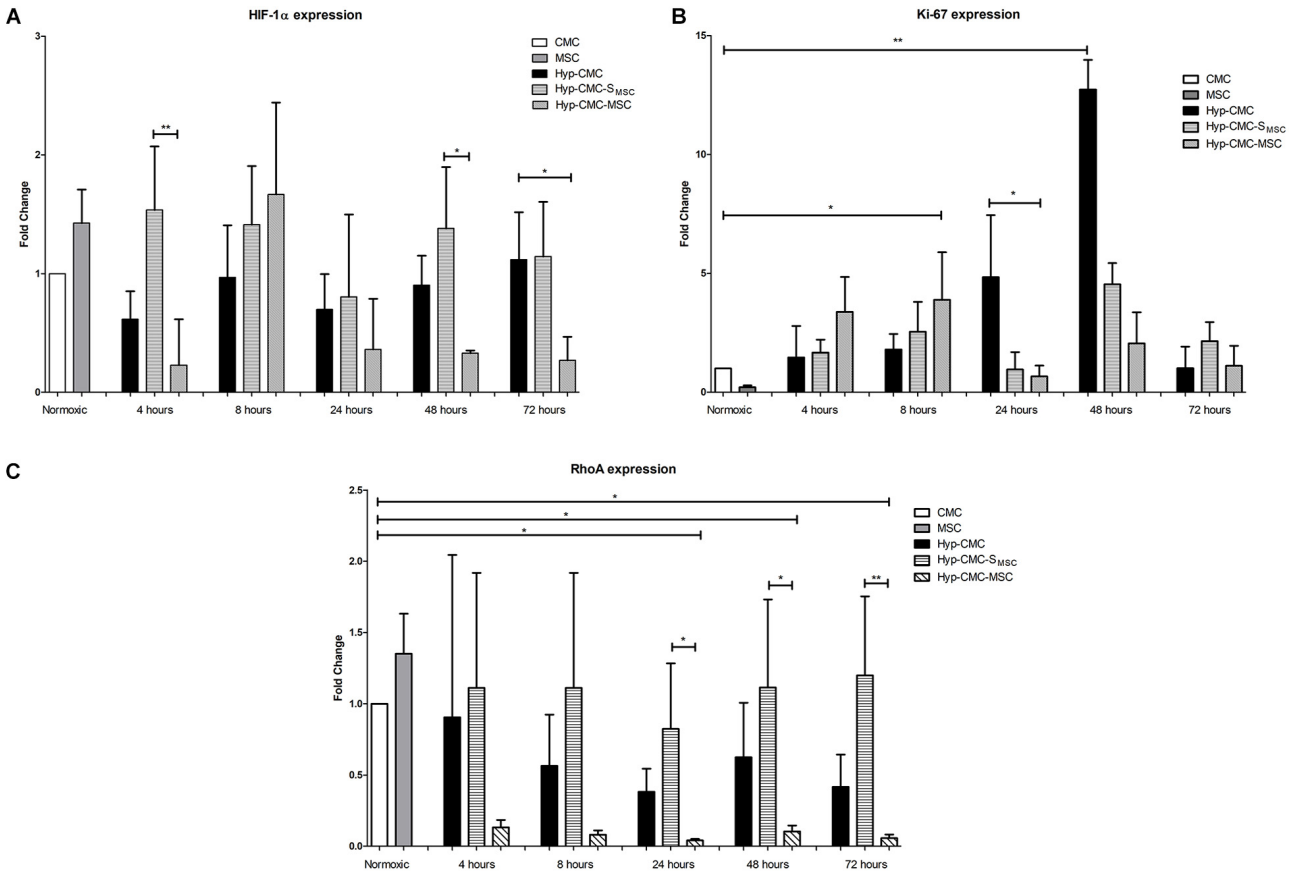

FIGURE 5 | Gene expression analysis of **(A)** *HIF-1α*, **(B)** *Ki-67*, and **(C)** *Rho-A* with RT-qPCR of the control CMC and MSC and of the samples taken from each of the three experimental groups: unstimulated hypoxic CMC (group Hyp-CMC), CMC stimulated with MSC secretome (group Hyp-CMC-S_{MSC}) and CMC stimulated directly with MSC (group Hyp-CMC-MSC) after the respective reoxygenation period of 4, 8, 24, 48, and 72 h. Values are relative to normoxic gene expression. *HPRT* was used as reference gene. The expression of each stimulation method was compared to the control group of the respective time point with one-way ANOVA (Kruskal-Wallis test) and groups were compared with the Dunn's Multiple Comparison Test. $^{*}p < 0.05$, $^{**}p < 0.01$, $n = 4$ technical replicates. MSC – Mesenchymal stem cells. CMC – cardiomyocytes. Hyp – hypoxic.

than CMC endoreduplication. When comparing *RhoA* and *Ki-67* expression, some discrepancies can be observed, especially in unstimulated CMC (Hyp-CMC), which show a high *Ki-67* expression after 24 and 48 h. This may be attributed due to higher endoreduplication, as it has been described that CMC without any stimulation do not significantly replicate after ischemia (Van Amerongen and Engel, 2008). When reviewing expression changes of *HIF-1α, Ki-67,* and *RhoA* and the proliferation assay, the general pro-survival and proliferation inducing effect of MSC secretome can be concluded.

The secretome analysis further revealed pro-inflammatory cytokine release (CD40L, IL-17, IL-17E, and CXCL12/SDF-1) in MSC secretome, which were completely missing in normoxic CMC secretome. CD40 ligand are expressed on non-inflammatory cells in inflammatory states and induce a wide variety of immunological signaling, like T-cell induction (Elgueta et al., 2009). CXCL12/SDF-1 has been described as a crucial factor for stem cell recruitment after hypoxic cardiac injury, but adverse effects on remodeling processes have also been associated with its upregulated release (Mühlstedt et al., 2016). Similarly, the effect of IL-17 and its variant IL-17E in myocardial infarction has revealed contradictory data on outcome; however, a general understanding that IL-17 induces CMC apoptosis leading to iNOS and free radical release subsequently leading to leukocyte accumulation and cardiac repair at the target site (Carreau et al., 2011; Pietrowski et al., 2011; Mora-Ruíz et al., 2019). Hyp-CMC secretome also revealed cytokine expression of CCL5/RANTES and CXCL12/SDF-1. CCL5/RANTES signaling recruits leukocytes to the site and generally act pro-inflammatory, however, there has been some contradicting data, whether higher concentrations of CCL5/RANTES show a positive or negative effect after acute myocardial infarction (Badacz et al., 2019). Additionally, IL-18 protein concentration, linked with the regulation of cardiomyocyte hypertrophy and extracellular matrix remodeling (O'Brien et al., 2014), was generally slightly higher or equally high in Hyp-CMC-S_{MSC} in relation to the control.

Study limitations. The study was carried out *in vitro* on CMCs that showed a not fully mature characteristic. The lack of beating in serum-free culture medium indicates that (even

though stated by the manufacturer) the cells were not fully mature (Boheler et al., 2002). Immature CMCs show a higher self-regeneration possibility than adult CMCs, which may influence the results (Hesse et al., 2018). Additionally, CMCs in culture only tolerated 2 h of hypoxia, before becoming severely apoptotic, making accurate analysis unattainable. Therefore, a short hypoxia time was chosen for the experiments. Further in the group stimulated with MSCs directly (Hyp-CMC-MSC), the separation of CMCs and MSCs for gene expression analysis could not be carried out. However, the gene expression in MSC were analyzed separately. The cells showed a *HIF-1α* upregulation and *Ki-67* downregulation when compared to the same normoxic control (CMC), which concludes that there is indeed a different gene regulation in MSC which influences the measurements in directly co-cultured samples.

A further deep analysis of the molecular processes was out of scope of this work. For example, investigations on oxidative stress due to ischemic damage and antioxidative enzymes (Kurian et al., 2016; González-Montero et al., 2018; Peoples et al., 2019), as well as ATP consumption (Casey and Arthur, 2000; Wu et al., 2008; McDougal and Dewey, 2017) have already been investigated and published several times; we did not intend to repeat literature data. We did not measure cardiac function recovery parameters in *in vitro* cell culture, albeit cardiac markers, such as troponin T could indicate a cardiac injury, and restoration of ischemic cardiac injury. We further did not include western blot analysis for measuring protein expression, as protein concentrations were too low to obtain a reliable result.

In conclusion the treatment with MSC secretome showed to be a comparable and even better treatment option in most parameter setups and show potential for usage as regenerative therapy after myocardial ischemia.

DATA AVAILABILITY STATEMENT

The datasets generated for this study are available on request to the corresponding author.

ETHICS STATEMENT

Human bone marrow MSC (EK1193/2015) were used to perform this study, isolated by BR, MSc. All donors provided written informed consent.

AUTHOR CONTRIBUTIONS

NK, KZ, JW, JM-T, DT, and MG: planning of the study. NK: conducting of the experiments. NK, JM-T, AS, and KZ: analysis. MG: funding acquisition. MG, BR, and NP: resources. NK and KZ: writing. NP, GG, MG, KZ, and NK: review and editing. All authors reviewed and contributed to the article and approved the submitted version.

FUNDING

Open access funding provided by Medical University of Vienna.

SUPPLEMENTARY MATERIAL

The Supplementary Material for this article can be found online at: https://www.frontiersin.org/articles/10.3389/fbioe.2020.502213/full#supplementary-material

REFERENCES

Alvarez, R. J., Wang, B. J., Quijada, P. J., Avitabile, D., Ho, T., Shaitrit, M., et al. (2019). Cardiomyocyte cell cycle dynamics and proliferation revealed through cardiac-specific transgenesis of fluorescent ubiquitinated cell cycle indicator (FUCCI). *J. Mol. Cell. Cardiol.* 127, 154–164. doi: 10.1016/j.yjmcc.2018.12.007

Assmus, B., Schächinger, V., Teupe, C., Britten, M., Lehmann, R., Döbert, N., et al. (2002). Transplantation of progenitor cells and regeneration enhancement in acute myocardial infarction (TOPCARE-AMI). *Circulation* 106, 3009–3017.

Badacz, R., Podolec, J., Przewlocki, T., Siedlinski, M., Jozefczuk, E., Oleksy, H., et al. (2019). The role of chemokine ccl5/rantes and metalloproteinase-9 as inflammatory modulators in symptomatic internal carotid artery stenosis. *J. Physiol. Pharmacol.* 70, 545–555. doi: 10.26402/jpp.2019.4.06

Beeravolu, N., McKee, C., Alamri, A., Mikhael, S., Brown, C., Perez-Cruet, M., et al. (2017). Isolation and characterization of mesenchymal stromal cells from human umbilical cord and fetal placenta. *J. Vis. Exp.* 122:55224. doi: 10.3791/55224

Benjamin, E. J., Blaha, M. J., Chiuve, S. E., Cushman, M., Das, S. R., Deo, R., et al. (2017). Heart disease and stroke statistics-2017 update: a report from the american heart association. *Circulation* 135, e146–e603. doi: 10.1161/CIR.0000000000000485

Beresford, J. N., Bennett, J. H., Devlin, C., Leboy, P. S., and Owen, M. E. (1992). Evidence for an inverse relationship between the differentiation of adipocytic and osteogenic cells in rat marrow stromal cell cultures. *J. Cell Sci.* 102(Pt 2), 341–351.

Boheler, K. R., Czyz, J., Tweedie, D., Yang, H.-T., Anisimov, S. V., and Wobus, A. M. (2002). Differentiation of pluripotent embryonic stem cells into cardiomyocytes. *Circ. Res.* 91, 189–201. doi: 10.1161/01.RES.0000027865.61704.32

Cahill, T. J., Choudhury, R. P., and Riley, P. R. (2017). Heart regeneration and repair after myocardial infarction: translational opportunities for novel therapeutics. *Nat. Rev. Drug Discov.* 16, 699–717. doi: 10.1038/nrd.2017.106

Carreau, A., Kieda, C., and Grillon, C. (2011). Nitric oxide modulates the expression of endothelial cell adhesion molecules involved in angiogenesis and leukocyte recruitment. *Exp. Cell Res.* 317, 29–41. doi: 10.1016/j.yexcr.2010.08.011

Casey, T. M., and Arthur, P. G. (2000). Hibernation in noncontracting mammalian cardiomyocytes. *Circulation* 102, 3124–3129. doi: 10.1161/01.CIR.102.25.3124

Chircop, M. (2014). Rho GTPases as regulators of mitosis and cytokinesis in mammalian cells. *Small GTPases* 5:e29770. doi: 10.4161/sgtp.29770

da Silva, Meirelles, L., Chagastelles, P. C., and Nardi, N. B. (2006). Mesenchymal stem cells reside in virtually all post-natal organs and tissues. *J. Cell Sci.* 119, 2204–2213. doi: 10.1242/jcs.02932

Dominici, M., Le Blanc, K., Mueller, I., Slaper-Cortenbach, I., Marini, F., Krause, D. S., et al. (2006). Minimal criteria for defining multipotent mesenchymal stromal cells. the international society for cellular therapy position statement. *Cytotherapy* 8, 315–317. doi: 10.1080/14653240600855905

Drenckhahn, J.-D., Strasen, J., Heinecke, K., Langner, P., Yin, K. V., Skole, F., et al. (2015). Impaired myocardial development resulting in neonatal cardiac hypoplasia alters postnatal growth and stress response in the heart. *Cardiovasc. Res.* 106, 43–54. doi: 10.1093/cvr/cvv028

Elgueta, R., Benson, M. J., De Vries, V. C., Wasiuk, A., Guo, Y., and Noelle, R. J. (2009). Molecular mechanism and function of CD40/CD40L engagement in the immune system. *Immunol. Rev.* 229, 152–172. doi: 10.1111/j.1600-065X.2009.00782.x

Ezquer, F., Gutiérrez, J., Ezquer, M., Caglevic, C., Salgado, H. C., and Calligaris, S. D. (2015). Mesenchymal stem cell therapy for doxorubicin cardiomyopathy: hopes and fears. *Stem Cell Res. Ther.* 6:116. doi: 10.1186/s13287-015-0109-y

González-Montero, J., Brito, R., Gajardo, A. I., and Rodrigo, R. (2018). Myocardial reperfusion injury and oxidative stress: therapeutic opportunities. *World J. Cardiol.* 10, 74–86. doi: 10.4330/wjc.v10.i9.74

Guo, X., Bai, Y., Zhang, L., Zhang, B., Zagidullin, N., Carvalho, K., et al. (2018). Cardiomyocyte differentiation of mesenchymal stem cells from bone marrow: new regulators and its implications. *Stem Cell Res. Ther.* 9:44. doi: 10.1186/s13287-018-0773-779

Gyöngyösi, M., Wojakowski, W., Lemarchand, P., Lunde, K., Tendera, M., Bartunek, J., et al. (2015). Meta-Analysis of Cell-based CaRdiac stUdiEs (ACCRUE) in patients with acute myocardial infarction based on individual patient data. *Circ. Res.* 116, 1346–1360. doi: 10.1161/CIRCRESAHA.116.304346

Hesse, M., Welz, A., and Fleischmann, B. K. (2018). Heart regeneration and the cardiomyocyte cell cycle. *Pflugers Arch.* 470, 241–248. doi: 10.1007/s00424-017-2061-2064

Huang, P., Wang, L., Li, Q., Xu, J., Xu, J., Xiong, Y., et al. (2019). Combinatorial treatment of acute myocardial infarction using stem cells and their derived exosomes resulted in improved heart performance. *Stem Cell Res. Ther.* 10, 1–12. doi: 10.1186/s13287-019-1353-1353

Karantalis, V., DiFede, D. L., Gerstenblith, G., Pham, S., Symes, J., Zambrano, J. P., et al. (2014). Autologous mesenchymal stem cells produce concordant improvements in regional function, tissue perfusion and fibrotic burden when administered to patients undergoing coronary artery bypass grafting – the PROMETHEUS trial. *Circ. Res.* 114, 1302–1310. doi: 10.1161/CIRCRESAHA.114.303180

Kern, S., Eichler, H., Stoeve, J., Klüter, H., and Bieback, K. (2006). Comparative analysis of mesenchymal stem cells from bone marrow, umbilical cord blood, or adipose tissue. *Stem Cells* 24, 1294–1301. doi: 10.1634/stemcells.2005-2342

Kurian, G. A., Rajagopal, R., Vedantham, S., and Rajesh, M. (2016). The role of oxidative stress in myocardial ischemia and reperfusion injury and remodeling: revisited. oxid. *Med. Cell. Longev.* 2016:1656450. doi: 10.1155/2016/1656450

Lohan, P., Treacy, O., Griffin, M. D., Ritter, T., and Ryan, A. E. (2017). Anti-Donor immune responses elicited by allogeneic mesenchymal stem cells and their extracellular vesicles: are we still learning? *Front. Immunol.* 8:1626. doi: 10.3389/FIMMU.2017.01626

McDougal, A. D., and Dewey, C. F. J. (2017). Modeling oxygen requirements in ischemic cardiomyocytes. *J. Biol. Chem.* 292, 11760–11776. doi: 10.1074/jbc.M116.751826

Menasché, P., Hagège, A. A., Scorsin, M., Pouzet, B., Desnos, M., Duboc, D., et al. (2001). Myoblast transplantation for heart failure. *Lancet* 357, 279–280. doi: 10.1016/S0140-6736(00)03617-3615

Miller, I., Min, M., Yang, C., Tian, C., Gookin, S., Carter, D., et al. (2018). Ki67 is a graded rather than a binary marker of proliferation versus quiescence. *Cell Rep.* 24, 1105–1112.e5. doi: 10.1016/j.celrep.2018.06.110

Mora-Ruíz, M. D., Blanco-Favela, F., Chávez Rueda, A. K., Legorreta-Haquet, M. V., and Chávez-Sánchez, L. (2019). Role of interleukin-17 in acute myocardial infarction. *Mol. Immunol.* 107, 71–78. doi: 10.1016/j.molimm.2019.01.008

Mühlstedt, S., Ghadge, S. K., Duchene, J., Qadri, F., Järve, A., Vilianovich, L., et al. (2016). Cardiomyocyte-derived CXCL12 is not involved in cardiogenesis but plays a crucial role in myocardial infarction. *J. Mol. Med.* 94, 1005–1014. doi: 10.1007/s00109-016-1432-1

Murry, C. E., Soonpaa, M. H., Reinecke, H., Nakajima, H., Nakajima, H. O., Rubart, M., et al. (2004). Haematopoietic stem cells do not transdifferentiate into cardiac myocytes in myocardial infarcts. *Nature* 428, 664–668. doi: 10.1038/nature02446

O'Brien, L. C., Mezzaroma, E., Van Tassell, B. W., Marchetti, C., Carbone, S., Abbate, A., et al. (2014). Interleukin-18 as a therapeutic target in acute myocardial infarction and heart failure. *Mol. Med.* 20, 221–229. doi: 10.2119/molmed.2014.00034

Orlic, D., Kajstura, J., Chimenti, S., Jakoniuk, I., Anderson, S. M., Li, B., et al. (2001). Bone marrow cells regenerate infarcted myocardium. *Nature* 410, 701–705. doi: 10.1038/35070587

Pavo, N., Zimmermann, M., Pils, D., Mildner, M., Petrási, Z., Petneházy, Ö, et al. (2014). Long-acting beneficial effect of percutaneously intramyocardially delivered secretome of apoptotic peripheral blood cells on porcine chronic ischemic left ventricular dysfunction. *Biomaterials* 35, 3541–3550. doi: 10.1016/j.biomaterials.2013.12.071

Pelekanos, R. A., Sardesai, V. S., Futrega, K., Lott, W. B., Kuhn, M., and Doran, M. R. (2016). Isolation and expansion of mesenchymal stem/stromal cells derived from human placenta tissue. *J. Vis. Exp.* 112:54204. doi: 10.3791/54204

Pendleton, C., Li, Q., Chesler, D. A., Yuan, K., Guerrero-Cazares, H., and Quinones-Hinojosa, A. (2013). Mesenchymal stem cells derived from adipose tissue vs bone marrow: in vitro comparison of their tropism towards gliomas. *PLoS One* 8:e58198. doi: 10.1371/journal.pone.0058198

Peoples, J. N., Saraf, A., Ghazal, N., Pham, T. T., and Kwong, J. Q. (2019). Mitochondrial dysfunction and oxidative stress in heart disease. *Exp. Mol. Med.* 51:162. doi: 10.1038/s12276-019-0355-7

Pietrowski, E., Bender, B., Huppert, J., White, R., Luhmann, H. J., and Kuhlmann, C. R. W. (2011). Pro-Inflammatory effects of interleukin-17A on vascular smooth muscle cells involve NAD(P)H- oxidase derived reactive oxygen species. *J. Vasc. Res.* 48, 52–58. doi: 10.1159/000317400

Pittenger, M. F., Mackay, A. M., Beck, S. C., Jaiswal, R. K., Douglas, R., Mosca, J. D., et al. (1999). Multilineage potential of adult human mesenchymal stem cells. *Science* 284, 143–147. doi: 10.1126/SCIENCE.284.5411.143

Prockop, D. J. (1997). Marrow stromal cells as stem cells for nonhematopoietic tissues. *Science* 276, 71–74. doi: 10.1126/SCIENCE.276.5309.71

Puymirat, E., Simon, T., Cayla, G., Cottin, Y., Elbaz, M., Coste, P., et al. (2017). Acute myocardial infarction. *Circulation* 136, 1908–1919. doi: 10.1161/CIRCULATIONAHA.117.030798

Roura, S., Gálvez-Montón, C., Mirabel, C., Vives, J., and Bayes-Genis, A. (2017). Mesenchymal stem cells for cardiac repair: are the actors ready for the clinical scenario? *Stem Cell Res. Ther.* 8:238. doi: 10.1186/s13287-017-0695-y

Rüger, B. M., Buchacher, T., Giurea, A., Kubista, B., Fischer, M. B., and Breuss, J. M. (2018). Vascular morphogenesis in the context of inflammation: self-organization in a fibrin-based 3D culture system. *Front. Physiol.* 9:679. doi: 10.3389/fphys.2018.00679

Safari, S., Malekvandfard, F., Babashah, S., Alizadehasl, A., Sadeghizadeh, M., and Motavaf, M. (2016). Mesenchymal stem cell-derived exosomes: a novel potential therapeutic avenue for cardiac regeneration. *Cell. Mol. Biol. (Noisy-le-grand).* 62, 66–73.

Sarugaser, R., Lickorish, D., Baksh, D., Hosseini, M. M., and Davies, J. E. (2005). Human Umbilical Cord Perivascular (HUCPV) Cells: a source of mesenchymal progenitors. *Stem Cells* 23, 220–229. doi: 10.1634/stemcells.2004-2166

Semenza, G. L. (2014). Hypoxia-inducible factor 1 and cardiovascular disease. *Annu. Rev. Physiol.* 76, 39–56. doi: 10.1146/annurev-physiol-021113-170322

Shafei, A. E. S., Ali, M. A., Ghanem, H. G., Shehata, A. I., Abdelgawad, A. A., Handal, H. R., et al. (2017). Mesenchymal stem cell therapy: a promising cell-based therapy for treatment of myocardial infarction. *J. Gene Med.* 19:e2995. doi: 10.1002/jgm.2995

Silbernagl, S., and Lang, F. (2000). *Color Atlas of Pathophyiology*. Stuttgart: Georg Thieme Verlag.

Sobecki, M., Mrouj, K., Colinge, J., Gerbe, F., Jay, P., Krasinska, L., et al. (2017). Cell-cycle regulation accounts for variability in Ki-67 expression levels. *Cancer Res.* 77, 2722–2734. doi: 10.1158/0008-5472.CAN-16-0707

Szaraz, P., Gratch, Y. S., Iqbal, F., and Librach, C. L. (2017). In vitro differentiation of human mesenchymal stem cells into functional cardiomyocyte-like cells. *J. Vis. Exp.* 126:55757. doi: 10.3791/55757

Thum, T., Bauersachs, J., Poole-Wilson, P. A., Volk, H. D., and Anker, S. D. (2005). The dying stem cell hypothesis: immune modulation as a novel mechanism for progenitor cell therapy in cardiac muscle. *J. Am. Coll. Cardiol.* 46, 1799–1802. doi: 10.1016/j.jacc.2005.07.053

Van Amerongen, M. J., and Engel, F. B. (2008). Features of cardiomyocyte proliferation and its potential for cardiac regeneration: stem Cells Review Series. *J. Cell. Mol. Med.* 12, 2233–2244. doi: 10.1111/j.1582-4934.2008.00439.x

Weidemann, A., and Johnson, R. S. (2008). Biology of HIF-1α. *Cell Death Differ.* 15, 621–627. doi: 10.1038/cdd.2008.12

Wu, F., Zhang, E. Y., Zhang, J., Bache, R. J., and Beard, D. A. (2008). Phosphate metabolite concentrations and ATP hydrolysis potential in normal and ischaemic hearts. *J. Physiol.* 586, 4193–4208. doi: 10.1113/jphysiol.2008.154732

Yoon, J., Min, B. G., Kim, Y.-H., Shim, W. J., Ro, Y. M., and Lim, D.-S. (2005). Differentiation, engraftment and functional effects of pre-treated mesenchymal stem cells in a rat myocardial infarct model. *Acta Cardiol.* 60, 277–284. doi: 10.2143/AC.60.3.2005005

Zebrowski, D. C., and Engel, F. B. (2013). The cardiomyocyte cell cycle in hypertrophy, tissue homeostasis, and regeneration. *Rev. Physiol. Biochem. Pharmacol.* 165, 67–96. doi: 10.1007/112_2013_12

Zuk, P. A., Zhu, M., Ashjian, P., De Ugarte, D. A., Huang, J. I., Mizuno, H., et al. (2002). Human adipose tissue is a source of multipotent stem cells. *Mol. Biol. Cell* 13, 4279–4295. doi: 10.1091/mbc.e02-02-0105

Conflict of Interest: The authors declare that the research was conducted in the absence of any commercial or financial relationships that could be construed as a potential conflict of interest.

Advantages of publishing in Frontiers

OPEN ACCESS
Articles are free to read for greatest visibility and readership

FAST PUBLICATION
Around 90 days from submission to decision

HIGH QUALITY PEER-REVIEW
Rigorous, collaborative, and constructive peer-review

TRANSPARENT PEER-REVIEW
Editors and reviewers acknowledged by name on published articles

Frontiers
Avenue du Tribunal-Fédéral 34
1005 Lausanne | Switzerland

Visit us: www.frontiersin.org
Contact us: info@frontiersin.org | +41 21 510 17 00

REPRODUCIBILITY OF RESEARCH
Support open data and methods to enhance research reproducibility

DIGITAL PUBLISHING
Articles designed for optimal readership across devices

FOLLOW US
@frontiersin

IMPACT METRICS
Advanced article metrics track visibility across digital media

EXTENSIVE PROMOTION
Marketing and promotion of impactful research

LOOP RESEARCH NETWORK
Our network increases your article's readership